

GEOTECHNICAL, GEOLOGICAL AND EARTHQUAKE ENGINEERING

ASSESSING AND MANAGING EARTHQUAKE RISK

**Geo-scientific and Engineering Knowledge
for Earthquake Risk Mitigation:
developments, tools, techniques**

CARLOS SOUSA OLIVEIRA, ANTONI ROCA
AND XAVIER GOULA
EDITORS

 Springer

CD-Rom
included

ASSESSING AND MANAGING EARTHQUAKE RISK

GEOTECHNICAL, GEOLOGICAL AND EARTHQUAKE ENGINEERING

Volume 2

Series Editor

*Atila Ansal, Kandilli Observatory and Earthquake Research Institute,
Boğaziçi University, Istanbul, Turkey*

Editorial Advisory Board

*Julian Bommer, Imperial College London, U.K.
Jonathan D. Bray, University of California, Berkeley, U.S.A.
Kyriazis Pitilakis, Aristotle University of Thessaloniki, Greece
Susumu Yasuda, Tokyo Denki University, Japan*

The titles published in this series are listed at the end of this volume

ASSESSING AND MANAGING EARTHQUAKE RISK

Geo-scientific and Engineering Knowledge
for Earthquake Risk Mitigation:
developments, tools, techniques

edited by

CARLOS SOUSA OLIVEIRA

*DECivil/ICIST, Instituto Superior Técnico,
Lisbon, Portugal*

ANTONI ROCA

*Institut Cartogràfic de Catalunya,
Barcelona, Spain*

and

XAVIER GOULA

*Institut Cartogràfic de Catalunya,
Barcelona, Spain*

 Springer

A C.I.P. Catalogue record for this book is available from the Library of Congress.

ISBN-13 978-1-4020-3524-1 (HB)
ISBN-13 978-1-4020-3608-8 (e-book)

Published by Springer,
P.O. Box 17, 3300 AA Dordrecht, The Netherlands.

www.springer.com

02-1207-200ts

Printed on acid-free paper

All Rights Reserved
© 2006, 2008 Springer

No part of this work may be reproduced, stored in a retrieval system, or transmitted in any form or by any means, electronic, mechanical, photocopying, microfilming, recording or otherwise, without written permission from the Publisher, with the exception of any material supplied specifically for the purpose of being entered and executed on a computer system, for exclusive use by the purchaser of the work.

This book is dedicated to our families for their support and for the many hours we have taken from them.

PREFACE BY BRUCE A. BOLT

Population growth, modern economic developments, real-time communication, and industrial interdependence among countries have sharpened the impact of natural disasters. Never before have such calamities and miseries been given intense global publicity. The result is a realization that much can be done through rational study and foresight to mitigate these risks to life and social well being. This conclusion is particularly true for the risk due to great earthquakes.

This book is particularly valuable in that it presents novel disciplinary approaches to both the mitigation of earthquake risk and post-earthquake management of the disasters. The editors have been successful in attracting a list of distinguished and experienced expositors who present a broad range of critical problems on estimating seismic risk, reacting to it, and reducing it, and on assessing and repairing the damage. Often in encyclopedic treatments that utilize separate authors in separate chapters there is substantial unevenness in the clarity and accessibility of the presentations. In this book, appropriate guidance by the Editors on the scope and presentation has ensured that the text is suitable for students and professionals with geological, engineering, and architectural backgrounds, as well as, at least in part, managers of earthquake emergency agencies. The emphasis is on examples from Europe. This aspect is helpful to the audience whose knowledge of seismic risk has been restricted to the professional problems in North America, emphasized in many previous textbooks.

Aspects of the presentation that will be found particularly useful are the description of the latest methods for use of the Internet and digital early warning systems. Many Chapters highlight the present wide availability of relatively inexpensive communication systems that allow rapid damage assessment and response. Such systems were available, for example, in the 1999 Chi Chi earthquake, Taiwan, but not in the 2004 Sumatra tragedy.

Another attractive element is the discussion of the role of insurance in encouraging the adoption of seismic building codes, as well as in pooling capital to allow the spreading of public losses. The book also contains guidelines for probability assessments, often not explained in available textbooks on earthquake risk. Many readers will also find helpful the discussions of the synthesis of modern probability hazard estimation with vulnerability calculations in order to predict risk. Because seismic risk assessment involves uncertainty and judgment and often foreshadows significant expense, the subject must be approached in a critical way so that controversy is not hidden and uncertainties can be incorporated explicitly into the mitigation of the dangers.

Bruce A. Bolt[†]

Professor of Seismology Emeritus, University of California, Berkeley, USA

Editor's note:

Since the writing of the preface, Prof. Bruce A. Bolt has passed away. The editors wish to express their great respect for him for all his work in the field of Seismology. He was a master and a friend for us.

PREFACE BY ALFONSO LÓPEZ ARROYO

A new book, on any scientific matter, raises two main previous questions to the reader: one related with the interest of its subject matter at the time of publication (its opportunity); and a second one that refers to the value of the contents.

I have no doubt that the book now presented comes on time, as it includes chapters on all problems identified along many years as crucial in the study of earthquake risk and on the development of measures to reduce damage from it.

It may be worth to note that the order accepted in the book for the first three parts corresponds both, with that to be followed in the applications and, also, with the historical development of the earthquake studies from Greek and Latin philosophers to present times.

The inclusion of a part on managing the earthquake risk adds a further interest to the book, as contributions towards the solution of this problem are not common in the earthquake bibliography. Such management of risk includes actions of quite different types. This is well described in Part IV which gives several practical examples that may guide the application to problems related to several scenarios.

The scenarios shown in Part V might guide the approach to other practical cases.

As a final comment, I consider the book an excellent approach to the solution and management of problems related with the action of earthquakes.

Alfonso López Arroyo
Past-President of the Spanish Association of Earthquake Engineering

EDITORS' NOTE

The joint participation of the editors in the execution of several EU projects in the last five years such as EuroSeisTest, EuroSeisMod, EuroSeisRisk, ISARD and Risk-UE, and in the organisation of different scientific sections on International Meetings, as the European Geophysical Society Assemblies in the period 1999-2003 has triggered the idea of this Book. The large number of recent damaging earthquakes in the neighbouring of European region has pushed us to assemble this volume, hoping to contribute for formation and information of professionals, students and public in general, necessary for the mitigation of such an important risk.

The present book could not be finalized without the participation and interest of many individuals. We would like to acknowledge, first of all, the authors and friends involved in the preparation of their chapters, not only for their contribution but also for the many discussions on different aspects of the book's content. We would also like to acknowledge the two institutions where the editors develop their professional activity, the Instituto Superior Técnico in Lisbon (Carlos Sousa Oliveira) and the Institut Cartogràfic de Catalunya in Barcelona (Antoni Roca and Xavier Goula), for their support and logistics made available, and to Springer for promoting this Project. Last but not least, we would like to thank our dear friends María José Mejón and Teresa Susagna for their highly valuable support and help in the many phases of the book preparation and edition processing.

We thank Petra van Steenbergen and Mieke van der Fluit (first at Kluwer) and Maria Jonckheere, all from Springer, for their support and permanent motivation.

Carlos Sousa Oliveira, Antoni Roca and Xavier Goula

Lisbon and Barcelona, March 2005

TABLE OF CONTENTS

<i>Preface by Bruce A. Bolt</i>	vii
<i>Preface by Alfonso López Arroyo</i>	ix
<i>Editors' Note</i>	xi
Chapter 1. Assessing and managing earthquake risk. An introduction	
<i>C. S. Oliveira, A. Roca and X. Goula</i>	
1.1. Organization of the Book.....	1
1.2. Natural Hazards. Earthquakes.....	2
1.3. Earthquake prediction and prevention.....	5
1.4. Construction practices and urban planning.....	6
1.4.1. <i>New constructions and existing building stock</i>	6
1.4.2. <i>Building codes</i>	6
1.4.3. <i>Insurance</i>	7
1.4.4. <i>Urban planning</i>	7
1.5. Emergency planning and managing.....	8
1.5.1. <i>Planning</i>	8
1.5.2. <i>Managing disaster recovery</i>	8
1.6. Reinforcing and reconstruction of the building stock.....	10
1.7. Philosophies and policies.....	10
1.8. Lessons learned from recent earthquakes.....	11
1.9. Political considerations.....	11
1.10. Education and mass media risk communication.....	12
1.11. Definitions of some basic concepts.....	12
PART I: EARTHQUAKE HAZARD AND STRONG MOTION	
Chapter 2. Overview on earthquake hazard assessment - methods and new trends	
<i>C. S. Oliveira and A. Campos-Costa</i>	
2.1. Introduction.....	15
2.2. Historical evolution of methods.....	15
2.2.1. <i>Generalities</i>	15
2.2.2. <i>Methods</i>	16
2.3. Fundamentals of seismic hazard analysis.....	19
2.3.1. <i>Deterministic versus probabilistic methods</i>	19
2.3.2. <i>Cornell method using seismogenetic sources</i>	21
2.3.3. <i>Empirical method (extreme value distributions of the catalogue events)</i>	27

2.3.4. <i>Hybrid methods</i>	28
2.4. Methodology for seismic risk scenario assessment	28
2.4.1. <i>Hazard consistent analysis</i>	28
2.4.2. <i>Disaggregating</i>	29
2.5. New contributions to the earthquake process.....	31
2.5.1. <i>Hazard algorithms</i>	31
2.5.2. <i>The occurrence process</i>	32
2.5.3. <i>Attenuation of strong ground motion</i>	34
2.6. Data to support hazard modelling.....	36
2.6.1. <i>Type of existing data</i>	36
2.6.2. <i>Quality in earthquake catalogues</i>	38
2.6.3. <i>Incorporation of uncertainties</i>	39
2.7. Results and illustrations.....	40
2.7.1. <i>Some examples. international initiatives</i>	40
2.7.2. <i>Analysis of uncertainty</i>	42
2.8. PSHA and the design of civil engineering constructions.....	43
2.9. Final tendencies of the future development and considerations.....	46
2.9.1. <i>New questions</i>	46
Chapter 3. Observation, characterization and prediction of strong ground motion	
<i>X. Goula and T. Susagna</i>	
3.1. Introduction.....	47
3.2. Strong ground motion measurements.....	47
3.2.1. <i>Instrumentation and major networks</i>	47
3.2.2. <i>Analysis of strong motion records</i>	50
3.2.3. <i>Data from moderate earthquakes</i>	51
3.2.4. <i>Dissemination of strong ground motion data</i>	53
3.3. Explanatory variables of ground motion.....	54
3.3.1. <i>Characterization of the seismic source</i>	54
3.3.2. <i>Location of the site with respect to the earthquake</i>	55
3.3.3. <i>Characterization of the local effects</i>	56
3.4. Predictive methods of ground motion.....	58
3.4.1. <i>Empirical methods</i>	58
3.4.2. <i>Components of nonempirical methods</i>	59
3.5. Definition of seismic action.....	62
3.5.1. <i>Peak ground acceleration (PGA) and response spectrum</i>	62

3.5.2. Smoothed acceleration response spectrum from Eurocode 8.....	63
3.5.3. Implications in the use of fixed spectral forms anchored to the peak ground acceleration.....	64
3.5.4. Demand spectrum or acceleration-displacement response spectrum (adrs).....	65
Chapter 4. Local site effects and microzonation	
<i>A. Roca, C. S. Oliveira, A. Ansal and S. Figueras</i>	
4.1. Introduction.....	67
4.2. Importance of local site effects on observed earthquake damage.....	68
4.3. Zoning, microzoning and resulting maps: a tool for predicting local site effects.....	71
4.4. Geological, geotechnical and geophysical approaches for soil characterization	73
4.5. Nonlinear effects	75
4.6. Numerical methods for estimating local effects.....	78
4.6.1. Linear methods.....	78
4.6.2. Non-linear methods	81
4.7. Experimental methods for estimating local site effects.....	82
4.7.1. Observations from earthquakes.....	82
4.7.2. Microtremor measurements.....	84
4.8. Topographic effects.....	86
4.9. Liquefaction and induced effects.....	87
4.10. Final considerations.....	89
Chapter 5. Site-city interaction	
<i>P. -Y. Bard, J. L. Chazelas, Ph. Guéguen, M. Kham and J. F. Semblat</i>	
5.1. Introduction.....	91
5.2. Experimental evidence.....	92
5.2.1. In situ observations.....	92
5.2.2. Centrifuge modelling.....	94
5.3. Modelling simple interaction.....	96
5.3.1. Model and calibration: the Volvi experiment	96
5.3.2. Application to Mexico-city.....	98
5.4. Multiple interaction.....	100
5.4.1. 2D case.....	100
5.4.2. Hint on 3D results.....	106
5.5. A simple energetic model.....	108

5.5.1. An index for site-city interaction.....	108
5.5.2. Example values and discussion.....	110
5.6. Concluding comments.....	112
PART II: VULNERABILITY ASSESSMENT	
Chapter 6. Vulnerability assessment of dwelling buildings	
<i>A. H. Barbat, S. Lagomarsino and L. G. Pujades</i>	
6.1. Introduction.....	115
6.2. Methodologies for vulnerability assessment.....	116
6.3. Vulnerability index method based on the EMS-98 macroseismic scale.....	119
6.3.1. EMS-98 Based vulnerability curves	119
6.3.2. Evaluation of the vulnerability index.....	124
6.4. Capacity spectrum method.....	129
6.4.1. Example.....	131
6.5. Final remarks.....	134
Chapter 7. Vulnerability assessment of historical buildings	
<i>S. Lagomarsino</i>	
7.1. Introduction.....	135
7.2. The observed vulnerability in historical buildings.....	139
7.2.1. Damage and vulnerability assessment of churches.....	139
7.2.2. Vulnerability curves of palaces and churches.....	141
7.3. The vulnerability assessment methodology.....	142
7.3.1. Basis of the macroseismic approach (level 0).....	143
7.3.2. Statement of the mechanical approach (levels 0 and 1).....	145
7.4. Macroseismic vulnerability assessment of churches (level 2).....	149
7.5. A mechanical model for capacity spectrum method on monuments (level 2)..	150
7.5.1. Examples and applications.....	156
7.6. Final remarks.....	158
Chapter 8. Experimental techniques for assessment of dynamic behaviour of buildings	
<i>M. Navarro and C. S. Oliveira</i>	
8.1. Introduction.....	159
8.2. Brief characterisation of dynamic properties of buildings.....	160
8.2.1. Linear behaviour.....	160
8.2.2. Influence of amplitude on motion - non-linear behaviour.....	162
8.3. Dynamic testing.....	163

8.3.1. <i>Equipment - velocity versus acceleration transducer</i>	163
8.3.2. <i>Sources of excitation</i>	163
8.4. Techniques for identification of natural periods and evaluation of damping ratio	165
8.4.1. <i>Natural period</i>	165
8.4.2. <i>Damping ratio</i>	166
8.5. Comparison of methods. Calibration with analytical techniques.....	168
8.5.1. <i>Characteristics of a prototype isolated building</i>	168
8.5.2. <i>Simulation of response</i>	169
8.5.3. <i>Microtremors</i>	169
8.5.4. <i>Earthquake records</i>	170
8.5.5. <i>Comparison of methods</i>	170
8.6. Correlation of natural frequencies and damping with geometry of buildings ..	173
8.6.1. <i>Generalities</i>	173
8.6.2. <i>Values for different regions and structural types (low amplitude motions)</i>	174
8.6.3. <i>Amplitude dependence of natural periods</i>	176
8.6.4. <i>Amplitude dependence of damping ratios</i>	180
8.7. Relation between building damage and soil predominant frequencies.....	180
8.8. Final considerations.....	182
Chapter 9. Vulnerability and risk assessment of lifelines	
<i>K. Pitilakis, M. Alexoudi, S. Argyroudis, O. Monge and C. Martin</i>	
9.1. Introduction.....	185
9.2. Social and economic consequences of lifeline damages.....	187
9.3. Advancement in risk management of lifelines.....	188
9.4. Basic features of lifelines.....	189
9.5. Overview of seismic risk assessment methodology for lifelines.....	190
9.5.1. <i>Inventory</i>	190
9.5.2. <i>Typology</i>	192
9.5.3. <i>Global value of lifeline systems</i>	193
9.5.4. <i>Interactions</i>	195
9.5.5. <i>Seismic hazard</i>	196
9.5.6. <i>Vulnerability</i>	197
9.5.7. <i>Performance criteria and analysis</i>	204
9.6. Losses, mitigation.....	206

9.6.1. Losses estimation.....	206
9.6.2. Mitigation.....	207
9.7. Earthquake risk reduction policy.....	211
PART III: SYSTEM ANALYSIS AND RISK	
Chapter 10. Damage scenarios and damage evaluation	
<i>M. Erdik and Y. Fahjan</i>	
10.1. Introduction.....	213
10.2. Earthquake hazard.....	214
10.2.1. Examples: earthquake hazard in Istanbul.....	216
10.3. Elements at risk.....	217
10.3.1. Standardizing and classifying building data.....	219
10.4. Earthquake vulnerabilities.....	220
10.4.1. Primary physical vulnerabilities.....	221
10.4.2. Secondary physical vulnerabilities.....	221
10.4.3. Socio-economic vulnerabilities.....	222
10.4.4. Intensity-based building vulnerabilities.....	222
10.4.5. Spectral displacement-based vulnerabilities.....	223
10.4.6. Capacity and demand spectrum.....	225
10.4.7. Casualty vulnerabilities.....	227
10.4.8. Lifeline vulnerabilities.....	228
10.5. Urban earthquake risk results.....	232
10.5.1. Methodologies and software.....	232
10.5.2. Example urban earthquake loss assessments from Istanbul.....	234
Chapter 11. Urban system exposure to natural disasters: an integrated approach	
<i>P. Masure and C. Lutoff</i>	
11.1. Introduction.....	239
11.2. Characterisation of the urban system.....	240
11.2.1. The city as an open system: urban components and elements interdependency.....	240
11.2.2. Characterising the urban components: a global approach to the city...	241
11.2.3. An analytic approach of the urban elements at risk.....	242
11.2.4. Urban data collection and organisation into the GIS.....	244
11.3. Valuation and classification of elements at risk.....	247
11.3.1. Reference values, measure units, and indicators.....	247
11.3.2. Value assessment of the elements at risk.....	249

11.3.3. <i>Classifying elements at risk and identifying the “critical issues” of the urban system</i>	252
11.4. Analysis of vulnerability factors and element interdependency.....	254
11.4.1. <i>Analysing dysfunction and defences of the urban system</i>	254
11.4.2. <i>Identification of sensitive elements or configurations</i>	255
11.5. Validation phase with the local actors.....	256
11.6. Conclusion.....	258
11.6.1. <i>A complete vulnerability assessment</i>	258
11.6.2. <i>A tool for earthquake scenario generation and impact assessment</i>	259
11.6.3. <i>A guide for preventive planning and risk reduction priorities</i>	259
Chapter 12. Response of hospital systems	
<i>L. G. Pujades, A. Roca, C. S. Oliveira and S. Safina</i>	
12.1. Introduction.....	261
12.2. The seismic behaviour of hospitals.....	261
12.3. Response of the hospital network to an emergency: general aspects.....	262
12.3.1. <i>Demand: the casualties</i>	263
12.3.2. <i>Hospitals: potential and effective capacity</i>	264
12.3.3. <i>Transportation, hospital access and communication system</i>	265
12.3.4. <i>Time discretization, rescue and mortality</i>	265
12.3.5. <i>Managing casualties queues</i>	267
12.4. Simplified model: seismic analysis of a regional system.....	269
12.4.1. <i>Hospital response</i>	269
12.4.2. <i>Response of the system</i>	270
12.4.3. <i>The demand: the earthquake scenario (T=0)</i>	272
12.4.4. <i>Capacity: the degradation of the system</i>	272
12.4.5. <i>Time evolution of the system</i>	275
12.5. Case study.....	277
12.5.1. <i>Hazard</i>	277
12.5.2. <i>Feasible seismic performance</i>	278
12.5.3. <i>Target hospital and transportation time</i>	278
12.5.4. <i>Seismic response of the hospitals and of the hospital system: preliminary analysis</i>	279
12.5.5. <i>Global characterization of the system and the hospitals</i>	282

PART IV: MANAGING EARTHQUAKE RISK**Chapter 13. Building against earthquakes***F. Mañá, L. Bozzo and J. Irizarry*

13.1. Introduction.....	287
13.2. Architectural design.....	287
13.2.1. Principle of order.....	288
13.2.2. Principle of inclusiveness.....	290
13.2.3. Principle of shear strength.....	292
13.2.4. Principle of monolithism.....	293
13.2.5. Principle of structural design with a low level of stress.....	295
13.2.6. Principle of free deformation.....	295
13.2.7. Principle of lightness.....	297
13.2.8. Principle of non-resonance.....	298
13.2.9. Principle of ductility.....	299
13.3. Code design and construction details.....	301
13.4. Actual trends for seismic design.....	305
13.5. Final remarks.....	308

Chapter 14. Industrial facilities*B. Mohammadioun and L. Serva*

14.1. Introduction.....	309
14.2. Seismic hazard—some recent developments in engineering seismology	309
14.3. Design earthquakes in IAEA safety guides.....	311
14.3.1. Design earthquakes and associated topics for NPP siting according to the IAEA ns-g-3.3 guide.....	311
14.3.2. Repository sites for nuclear waste disposal.....	314
14.4. Earthquake-resistant design.....	315
14.4.1. IAEA safety guides for the seismic design of nuclear power plants.....	315
14.4.2. IAEA safety guides for waste disposal and repository sites.....	316
14.5. Approach for exclusion criteria and minimum seismic design for NPP's, followed by a description of practice in some countries.....	316
14.6. A proposed approach for other critical facilities.....	319
14.6.1. Mitigation of major risks: the Seveso directive.....	319
14.6.2. Seismic risk mitigation.....	320

Chapter 15. Early warning and rapid damage assessment*M. Erdik and Y. Fahjan*

15.1. Background and introduction.....	323
15.1.1. Basic components of early warning and rapid response system.....	323
15.2. Early warning.....	324
15.2.1. Rapid assessment of earthquake magnitude and location.....	325
15.2.2. Direct (engineering) early warning: PGA and CAV threshold.....	325
15.3. Rapid post-earthquake damage assessment.....	325
15.3.1. Shake Maps.....	326
15.3.2. Peak acceleration maps.....	326
15.3.3. Peak velocity maps.....	327
15.3.4. Spectral response maps.....	327
15.4. Earthquake early warning and rapid response systems.....	328
15.4.1. Urgent earthquake detection and alarm systems (UREDAS) in Japan..	328
15.4.2. Seismic alert system of Mexico city.....	328
15.4.3. Istanbul earthquake rapid response and the early warning system	329
15.4.4. Earthquake rapid reporting and early warning systems in Taiwan	332
15.4.5. Early warning system for Bucharest.....	334
15.4.6. Rapid response and disaster management system in Yokohama, Japan	336

Chapter 16. Technical emergency management*A. Goretti and G. Di Pasquale*

16.1. Introduction.....	339
16.2. Immediate occupancy and damage survey.....	340
16.3. Basis of methodology.....	345
16.3.1. Building safety evaluation in Italy.....	349
16.3.2. Building safety evaluation in Japan.....	351
16.3.3. Building rapid evaluation in California.....	352
16.3.4. Building safety evaluation in Greece.....	353
16.4. Time and space evolution.....	354
16.5. Procedures and forms.....	356
16.6. Statistics and predictive models.....	359
16.7. Special buildings.....	361
16.7.1. Hospitals.....	361
16.7.2. Churches.....	363
16.8. Training and preparedness.....	364

16.9. Short term countermeasures.....	365
Chapter 17. Civil protection management	
<i>E. Galanti, A. Goretti, B. Foster and G. Di Pasquale</i>	
17.1. Introduction.....	369
17.2. Civil protection organization.....	371
17.3. SEMS, California.....	373
17.4. Augustus method, Italy.....	375
17.5. Molise 2002 earthquake.....	378
Chapter 18. Earthquake risk and insurance	
<i>R. Spence and A. Coburn</i>	
18.1. Insurance and earthquakes.....	385
18.1.1. Catastrophe reinsurance.....	386
18.1.2. Catastrophe modelling.....	387
18.1.3. Insurance and earthquake risk mitigation	387
18.2. Losses and insurance exposure in recent events.....	388
18.3. Modelling of earthquake risks for insurance.....	390
18.3.1. Underwriting results.....	390
18.3.2. Capital adequacy.....	391
18.3.3. Reinsurance.....	391
18.3.4. Portfolio management.....	392
18.3.5. Underwriting policies.....	392
18.3.6. Modelling attributes for insurance applications.....	392
18.3.7. Rewarding mitigation activities.....	393
18.3.8. Limitations to the role of private insurance.....	393
18.4. Modelling earthquake risk for the Turkish catastrophe insurance pool.....	394
18.4.1. The hazard model.....	395
18.4.2. Building stock inventory.....	395
18.4.3. The vulnerability model.....	397
18.4.4. The earthquake loss model.....	398
18.4.5. Comparison of the model result with observed damage.....	400
18.5. Conclusion.....	401
Chapter 19. Strengthening and repairing earthquake damaged structures	
<i>A. G. Costa</i>	
19.1. Introduction.....	403
19.2. Historical survey.....	403

19.3. Defining the constructions.....	404
19.4. Observation and surveyed damages.....	406
19.5. Material mechanical characterization.....	408
19.5.1. Introduction.....	408
19.5.2. Tests on stone masonry constructions.....	408
19.5.3. Tests on steel structures.....	411
19.5.4. Test on reinforced concrete structures	411
19.5.5. Dynamic characterization of structures	413
19.6. Numerical analysis.....	414
19.6.1. Introduction.....	414
19.6.2. Selecting the analysis program.....	414
19.6.3. Numerical analyses.....	416
19.7. Strengthening solutions and application conditions.....	418
19.7.1. Introduction.....	418
19.7.2. Stone masonry structures.....	419
19.7.3. Steel structures.....	422
19.7.4. Reinforced concrete structures.....	423
19.7.5. Another examples of strengthening techniques.....	424
19.8. Conclusions.....	425
Chapter 20. Advanced techniques in modelling, response and recovery	
<i>L. Chiroiu, B. Adams and K. Saito</i>	
20.1. Introduction.....	427
20.2. Remote sensing and geomatic technologies.....	428
20.2.1. Optical imagery.....	429
20.2.2. Radar imagery.....	430
20.3. Applications for earthquake risk management.....	432
20.3.1. Building inventory development.....	432
20.3.2. Mapping ground surface displacement.....	435
20.3.3. Urban damage assessment.....	435
20.3.4. Loss estimation.....	440
20.4. Case studies.....	440
20.4.1. Marmara (Turkey) earthquake, August 17th, 1999.....	440
20.4.2. Bhuj (India) earthquake, January 26th, 2001.....	442
20.4.3. Boumerdes (Algeria) earthquake, May 21st, 2003.....	444
20.4.4. Bam (Iran) earthquake, December 26th, 2003.....	445

20.5. Conclusions.....	447
PART V: CASE STUDIES, INITIATIVES AND EXPERIENCES	
Chapter 21. Seismic loss scenarios based on hazard disaggregation. Application to the metropolitan region of Lisbon, Portugal	
<i>A. Campos Costa, M. L. Sousa, A. Carvalho and E. Coelho</i>	
21.1. Introduction.....	449
21.2. Assessment of probability-based seismic loss scenarios.....	450
21.2.1. Seismic hazard disaggregation.....	450
21.2.2. Application to the metropolitan area of Lisbon.....	451
21.3. A seismic loss methodology integrated in a geographic information system.....	453
21.3.1. Overview.....	453
21.3.2. Input data.....	455
21.3.3. Procedures and results.....	455
21.3.4. Seismic risk analysis.....	460
21.4. Conclusions.....	461
Chapter 22. Loss scenarios for regional emergency plans: application to Catalonia, Spain	
<i>T. Susagna, X. Goula, A. Roca, L. Pujades, N. Gasulla and J. J. Palma</i>	
22.1. Introduction.....	463
22.2. Risk assessment.....	463
22.2.1. Seismic hazard assessment.....	464
22.2.2. Vulnerability assessment.....	465
22.2.3. Loss estimation.....	466
22.2.4. Damage estimation at hospitals.....	469
22.2.5. Loss estimation in lifelines.....	470
22.3. Damage scenario mapping: a tool for emergency preparedness.....	471
22.3.1. Methodology.....	472
22.3.2. Damage scenario for an earthquake similar to an historical one.....	472
22.3.3. Criteria of activation of the plan of seismic emergencies in Catalonia (SISMICAT).....	474
Chapter 23. RISK-UE project: An advanced approach to earthquake risk scenarios with application to different European towns	
<i>P. Mouroux and B. Le Brun</i>	
23.1. Introduction.....	479
23.2. Previous case studies.....	480

Table of contents

xxv

23.2.1. HAZUS	480
23.2.2. RADIUS.....	486
23.3. The RISK-UE project.....	491
23.3.1. Objectives.....	491
23.3.2. Organisation of the RISK-UE project.....	493
23.3.3. Definition of the methodology developed in RISK-UE	493
23.3.4. Application of the methodology to the seven cities.....	500
23.4. Comparison between HAZUS, RADIUS and RISK- UE	507
23.5. Final conclusions.....	507
References.....	509
Figures acknowledgements.....	543

CHAPTER 1 ASSESSING AND MANAGING EARTHQUAKE RISK. AN INTRODUCTION

C. S. Oliveira¹, A. Roca² and X. Goula²

1. Instituto Superior Técnico, Lisbon, Portugal

2. Institut Cartogràfic de Catalunya, Barcelona, Spain

1.1. Organization of the Book

This book compiles in a single volume different aspects directly related to earthquake mitigation. It is intended to initiate graduate and undergraduate students in the field of earthquake damage assessment and mitigation as well as to provide updated information for professionals dealing with these matters. In particular, it is addressed to students in applied Geosciences who need to have some skills in more engineering oriented topics and also for Engineering students that need to have some background on Engineering Seismology.

Students and professionals with initial academic background in Geology, Geophysics, Geotechnical and Civil Engineering, System Analysis, Geography or Architecture are in optimal position to acquire from this book a good background in earthquake risk assessment and management.

This volume also shows how geo-scientific and engineering knowledge is transferred to Civil Protection and insurance agents, and how the close collaboration between geoscientists, engineers and emergency managers can contribute to more efficient earthquake mitigation.

Following this chapter, the book is organized into five main parts:

Part I (*Earthquake hazard and strong motion*) deals with the concepts involved in the seismic process from source to site, including the most recent advances in the techniques of hazard analysis (Chapter 2), strong motion representation (Chapter 3) and microzonation (Chapter 4). Chapter 5 deals with the problem of interaction of buildings with neighbouring media.

Part II (*Vulnerability assessment*) is devoted to the analysis of vulnerability of dwelling buildings (Chapter 6), historical buildings (Chapter 7) and lifelines (Chapter 9), while (Chapter 8) is dedicated to experimental methods for determining the fundamental frequency of buildings.

Part III (*System analysis and Risk*) looks at the seismic risk problem from an individual level (Chapter 10) to an integrated system level (Chapter 11), with hospital networks as an example (Chapter 12).

Part IV (*Managing earthquake risk*) develops the main concepts of mitigation, through construction and control practices (Chapters 13 and 14), early warning and rapid damage assessment (Chapter 15), emergency management (Chapters 16 and 17), insurance (Chapter 18) and reinforcing the building stock (Chapter 19). Chapter 20 describes some new available technologies.

Finally, Part V (*Case studies, initiatives and experiences*) presents in Chapters 21 to 23 examples of applications in which the scale of work and the methodologies are different, allowing comparisons among various seismic scenario situations.

An extensive list of references corresponding to all chapters, assembled at the end of the book, will help the reader interested in further details on the covered topics.

1.2. Natural Hazards. Earthquakes

The so called “natural” disasters, that is, those related to phenomena of Nature, have caused throughout the centuries great convolutions in the process of human development. Even though advances in science and technology have produced a great deal of knowledge on the causes of those disasters, human deaths in the world per million inhabitants are only slightly decreasing with time, but the economic losses have dramatically increased in the last decades. The rise in world population and the complexity of societal organisation, among others, are factors that may explain this unfortunate fact. Inadequate non-sustainable use of the territory and present day inadequate construction practices, especially in developing countries, are clear causes of the too frequent “natural” disasters.

In general, it can be stated that society has become more vulnerable. Natural disasters reveal the fact that our economic development is unacceptably brittle, too vulnerable to the normal behaviour of Nature.

Therefore, when we speak about natural hazards we refer to those events that are triggered by or related to phenomena of Nature.

Man-made accidents dominate the entire panorama of death toll around the world. For example, the number of deaths from road accidents in the world for 2003 (2.2 millions) is still larger than the total number of deaths from earthquake activity during the 20th century (1.5 millions). However, the number of worldwide victims from earthquakes is high when compared with other natural hazards, as shown in Figure 1.1.

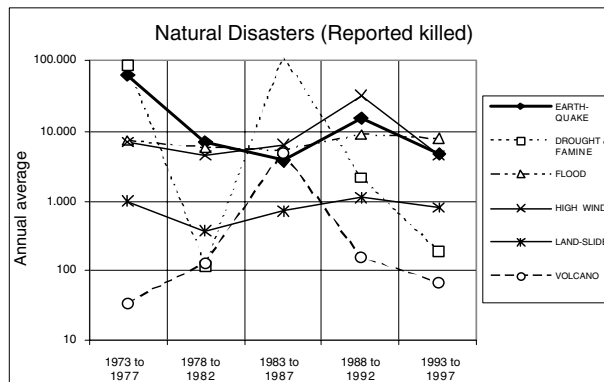


Fig. 1.1. Comparison since 1973 by periods of 5 years of reported deaths by earthquake, drought and famine, floods, high winds, landslide and volcano (Oliveira, 2003)

Table 1.1 reports the world’s largest earthquakes since 1900 with respect to number of deaths (larger than or equal to 10 000), also showing the region of occurrence and the corresponding magnitudes. Both, from Figure 1.2 and Table 1.1 it is interesting to note that this period of time is characterized by an annual average of 15 000 deaths with two main fluctuations (modal values), the largest in the period 1900 to 1940 and another with a larger value in the decade of 1970-80.

Figure 1.2 shows the number of total deaths from the greatest earthquakes that occurred in the XX century. Although the number of victims has a tendency to decrease with time, the economic losses are increasing significantly (see Chapter 18 of this book).

Table 1.1. World earthquakes since 1900 with number of deaths greater than 10 000

Year	Region	Deaths	Magnitude	Year	Region	Deaths	Magnitude
1905	India	19000	8.6	1960	Agadir, Morocco	12000	5.9
1906	Chile	20000	8.6	1962	Iran	12000	7.3
1907	Central Asia	12000	8.1	1968	Iran	10000	7.3
1908	Italy	70000	7.5	1970	Yunnan, China	10000	7.5
1915	Italy	29980	7.5	1970	Peru	67000	7.7
1917	Indonesia	15000	-	1972	Nicaragua	10000	6.2
1918	China	10000	7.3	1976	Guatemala	23000	7.5
1920	China	220000	8.5	1976	Tangshan, China	242000	7.8
1923	Japon	142807	7.9	1978	Tabas, Iran	25000	7.4
1927	China	80000	8	1985	Mexico	10000	8.1
1932	China	70000	7.6	1988	USSR (Armenia)	25000	6.8
1933	China	10000	7.4	1990	Manjil, Iran	40000	7.7
1934	India	10700	8.4	1999	Izmit, Turquia	30000	7.4
1935	Pakistan	30000	7.5	2001	Gujará, India	20000	7.7
1939	Chile	28000	8.3	2003	Bam, Iran	26796	6.6
1939	Turkey	32700	8	2004	NW Sumatra	300000	8.9
1948	Ashkhabad	19800	7.3				

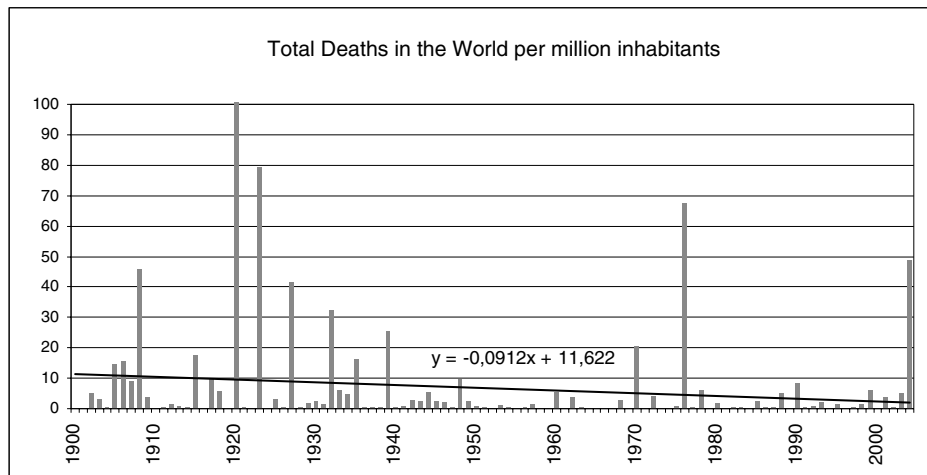


Fig. 1.2. List of “notable” “Great” earthquakes of the 20th century by number of deaths per million world inhabitants (data from Coburn and Spence, 2002; Samardjieva and Badal, 2002 and USGS web site)

The number of victims and the economic losses from earthquakes are strongly dependent on the seismic magnitude and focal distances to urban areas. Moreover, the relation between economic losses and number of victims is dependent on social and economic factors associated to the level of development of the affected country. This can be seen in Figure 1.3, which shows the human losses as a function of magnitude for the major earthquakes in the 20th century. For the same range of magnitudes a larger number of victims occur in less developed countries. On the other hand the larger economic losses occur in the most developed countries, as seen in Figure 1.4.

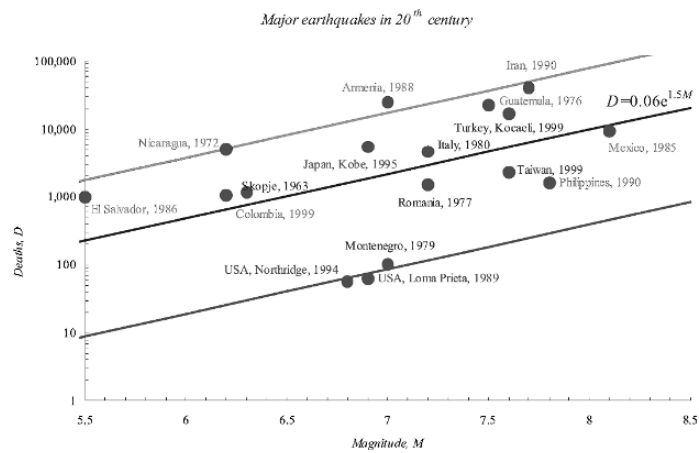


Fig. 1.3. Human losses as a function of magnitude (Vacareanu et al., 2004)

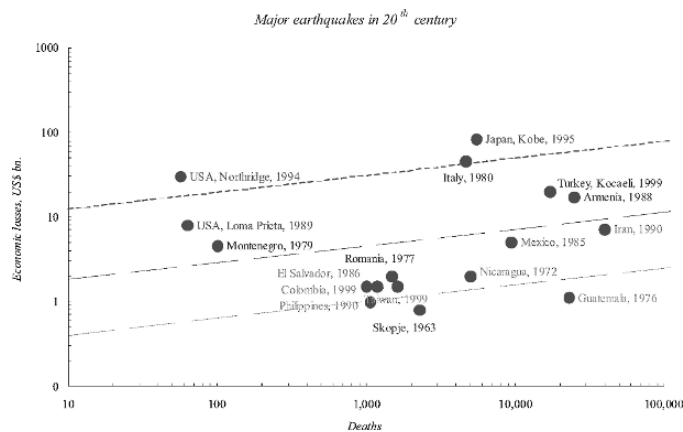


Fig. 1.4. Economic versus human losses caused by earthquakes (Vacareanu et al., 2004)

1.3. Earthquake prediction and prevention

The seismic phenomena have been largely studied by seismologists, comprising a large number of disciplines, approaches and knowledge. From the beginning of time, prediction of natural phenomena and, in particular, earthquakes has been one of the objectives of human kind. However, the complexity of the rupture processes at the origin of earthquakes does not yet allow science to produce earthquake predictions in a reasonable term period that would satisfy our needs: to know the time, location and size of the next important event within narrow and accurate windows. Furthermore there are some present scientific tendencies that point to the nonlinearity of the phenomenon, with the consequence that what is commonly understood as prediction may not be possible.

Even in the case of a hypothetical precise prediction at short term (days or weeks) which would allow saving human lives by moving the population to safer places, economic losses would not be avoided because of the impossibility of protecting structures and the economic fabric at such short notice.

In recent years, with the development of rapid transmission and treatment of data, it has been possible to design early-warning systems, which, after the occurrence of an earthquake, produce information about the possible arrival of strong seismic waves. In some cases, when the source is distant enough from urban areas, a few tens of seconds can be used to trigger security systems of some critical facilities (see Chapter 15).

In any case, it is more and more possible to produce information about the possible effects and their geographical distribution by an early scenario simulation (see Chapter 10), in order to speed up the intervention of emergency services acting to rescue the populations (see Chapters 16 and 17).

On the other hand, prediction in the medium and long term (tens to hundreds of years) is routinely used for assessing the seismic hazard at regional or local levels and for specific sites with critical facilities, evaluating the more exposed zones and quantifying the possible seismic actions (see Chapters 2, 3, 4, 5 and 14). This constitutes the first step of the strategy of *prevention*. In fact this is, at the moment, the only way to prepare for earthquakes.

An adequate strategy of prevention should include three main principles: (i) acknowledgement of the seismic phenomenon and its consequences in the built environment; (ii) assessment of the risk in both the seismic hazard and vulnerability of all components of the built environment; (iii) awareness of the importance of these assessments and putting in practice different actions in order to mitigate the estimated risks. Among these principles, the first two are of scientific and technical nature and they are developed in great extension in the first parts of the book (Chapters 2 to 12). The third one has an important political component and the technical aspects are introduced below and developed in Chapters 13 to 20.

1.4. Construction practices and urban planning

The most efficient way to mitigate earthquake risks is through an adequate construction practice and urban planning. In both cases for most countries, codes, either for construction and urban planning, define the minimum requirements or recommendations for a “good performance” in the face of a possible seismic action that may occur during the life-time of a given construction.

1.4.1. NEW CONSTRUCTIONS AND EXISTING BUILDING STOCK

New construction should reflect the knowledge and good practices of present day developments. This means that a society, wherever its makeup, should not build without the necessary resources to provide safe structures. Seismology, Geology and Engineering have all the means to do that at a reasonably low price compared to the price without using them. Quality control has to be practiced in a very strict way in order that everything built from now onwards can be considered safe in all senses as a heritage of security for the next generations. To accomplish these requirements extensive campaigns for policy changes should be promoted especially in countries with poorer knowledge and capacities. Simple, easy to apply and efficient techniques have to be implemented.

1.4.2. BUILDING CODES

Building codes and “good building practice” has been throughout the decades the only effective way to mitigate earthquake damage (see Chapter 13). Historically they were developed upon the construction knowledge accumulated by generations that suffer the action of earthquakes. The developments of science and technology through the 20th century, especially in the last 20 years, has led to complete new formulations of building codes, adapted to proven construction standards. Present codes are instruments of great use in all countries and should constitute the most important form of quality control in earthquake resistant construction.

The philosophy of codes has changed in recent years creating a more stringent concept of life-save and introducing the concept of minimization of certain types of losses, via the concept of performance. This last criterion depends very much on the type and importance of a facility. Vision 2000 (SEAOC, 1995) introduces this philosophy and tries to apply it to common construction (the housing stock), to important structures (schools, places of large concentration of population), and to very important structures (hospitals, decision centres, etc.). Another category of facilities should have a very special treatment due to the critical consequences in case of partial failure (critical structures, power plants, etc.). Figure 1.5 shows the performance stage for different frequencies of events (probability of occurrence).

The philosophy of codes has changed quite significantly in the last 50 years. The first generation of codes in the 1950's took as their main goal the preservation of lives only, for a low probability of occurrence. But the latest generation follows very much the “performance criteria” as referred in Figure 1.5, requiring the verification of “performance” for different levels of ground motion. Chapter 2 discusses this subject

under the concept of acceptable probability of occurrence of that risk, i.e. what is acceptable or unacceptable risk for the community and how far can we go with codes.

As far as legal character of codes there are various statuses among countries and among regions. In many countries in Europe codes are mandatory rules (Spain, France, Italy, etc.), while in the USA great differences do exist from state to state, in many cases codes are not more than recommendations.

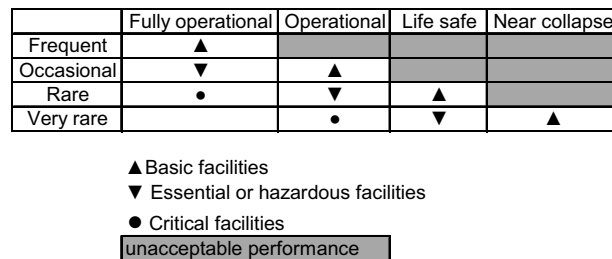


Fig. 1.5. Performance of construction in function of probability of occurrence

Freeman (2004), analysing the performance of properly designed and constructed buildings, concluded that there are several reasons to explain why so many buildings survived with relatively little or no damage, given the large strong motion observed near those buildings. Those reasons for better performance are due to some conservatism in design, to excess of vertical capacity which increases lateral resisting forces, and to the experience of engineering design that can anticipate the potential for weak links and, consequently, provide alternative loading systems.

1.4.3. INSURANCE

Insurances (public and private), differentiating the premium, may contribute to control the quality of design and construction. Several models for the application of insurance are available and practiced throughout the world (see Chapter 18). Essentially, one can have centralized bodies as practiced in Spain by the Consorcio de Compensación de Seguros (Nájera, 1999), or a moderate centralized scheme such as the Solidarity Fund created in the EU in the aftermath of the large Central Europe floods of summer 2002. But the most practiced case is the existence of individual national or international companies with pools through international re-insurance. All these schemes could help to increase the public awareness towards seismic risk, creating a culture of risk prevention. It should be mentioned that for large installations it is already current practice to have expert judgement on these matters (see Chapter 14). It is now necessary to extend this policy to the more common types of buildings. Private and public interference in these issues is a matter of political environment, but should stay outside the basic problem of quality control.

1.4.4. URBAN PLANNING

Urban planning is an important component of earthquake risk mitigation. One can say that, in extremis, engineering and scientific/technical knowledge can overcome all difficult natural environments. But this may imply important costs in design and

construction and be always a less equilibrated solution. Urban planning should define better uses of the territory in view of all possible threats, setting limits to the types of construction, layouts and size or defining more detailed seismic action for that environment, envisaging the possibility of excluding high level hazard zones. Urban planning may establish the degree of intervention in an existing block of buildings, the need for reinforcing, etc.

But a great deal of application comes from integration into urban planning of land use restrictions related to other effects beyond the direct ground motion, such as the influence of known active faults, the induced phenomena of liquefaction and landslides, but also the tsunami flooding, flooding from dam failure, etc.

An example of an important development of rules related to municipal urban planning has been carried out in France by the Plans for Prevention of Risk (PPR), whose strategy is published in *Commissariat General du Plan* (1997). An important number of municipalities have developed their own local Plan during the last few years.

1.5. Emergency planning and managing

Civil Protection bodies are the agencies of larger public impact and visibility, responsible for the actions of earthquake risk mitigation. Emergency preparedness is the direct consequence of a good definition of hazard, vulnerability and risk assessment. Planning rescue operations, including transportation of injured, managing homeless problems, providing basic services, etc., and managing post-events in all their ramifications is of most importance for reducing the suffering of the affected populations and in returning disrupted lives to a normal standard. Chapters 16 and 17 elaborate on these multiple issues and Chapter 21 to 23 present several case studies dealing with cities, metropolitan areas and large regions for scenario evaluations.

1.5.1. PLANNING

Planning requires a prior definition of the seismic scenario or collection of seismic scenarios. For each one, the effect of the simulated motion is treated and transformed into variables to be used in the planning of all operations. Planning should consider the zones more prone to different incidences, and prepare logistic and field exercises to simulate situations that may happen in the case of a real earthquake.

1.5.2. MANAGING DISASTER RECOVERY

Managing an earthquake disaster has two essential components: the one right after the earthquake (the following few hours) and the one in its sequence (few days or weeks). The first one deals with all the operational measures to be taken in relation to the planning established, which includes a fast assessment of damage evaluation. Chapters 10, 15 and 20 devote a great deal of their contents to this subject. The second component has to do with the actions to be taken in order to lead to resumption of normal life (see Chapters 16 and 17) Detailed field surveys for precise evaluation of damage distribution are among the actions to be taken for deciding building occupation and urgent building intervention.

Rapid damage assessment after the occurrence is an essential part of the emergency process. Indeed, knowledge of the areas more affected by the earthquake should be consolidated in the shortest time possible. This requires a fast and accurate assessment of what has occurred, where and what type of problems should be addressed. For instance, the suffering of the populations can be slightly mitigated if information is given with precision, injured population is recovered at the earliest possible time, the homeless are transported to temporary shelters. The rapid damage assessment tool should help in determining which areas are more affected, the blocks of higher damage constraints in emergency road circuitry, buildings with higher concentration of victims, structures in danger of collapse due to some aftershock activity and needing immediate shoring, etc.

At other levels, insurance companies may start understanding the part of their portfolio that has been affected, lifeline agents can check the degree of interruption of operation of networks (telephone, gas, electricity, etc.), industrial agents can start the inventory of impacts in their activities, etc. All them are in better position for defining policies for intervention.

Modern technological developments can provide Civil Protection and other managing and security bodies with new forms of mitigation such as the seismic Early Warning systems (EWS). These systems are essentially of two types. The most widely accepted EWS takes advantage of real time modern seismology and deals with the lead time one can gain after the onset of an event by identifying from the first seconds of the P-wave the size of the S-wave which will arrive at a later stage. If the distance that the waves travel to a site is sufficiently large, one can gain tens of seconds and be able to send information prior to the arrival of the large S-amplitudes (Allen and Kanamori, 2003). Depending on the gained time, this technique will allow launching of important actions, such as shutdown of industries, closing networks, stopping dangerous activities, or preparing for active control of constructions. These new ideas are already being practiced in several locations as test cases, the most known one being the system for stopping the Sinkansan train in Japan. Chapter 15 will present the most recent advances dealing with these technologies which require well coordinated efforts between instrumental seismology, communication science and technology and engineering knowledge on how to use the information.

A second type of Early Warning Systems is used for tsunami alerts. In this case, the time to send the alert may be much larger depending on the distance that ocean waves travel. An alert of this type has already existed for many years in the Pacific Ocean (<http://www.prh.noaa.gov/ptwc>), for waves travelling during several hours to reach the target, but in other situations the times are less than half an hour. To be effective in these cases, good EWS should also be implemented with the most modern technological knowledge.

The December 26, 2004 M9.0 NW Sumatra earthquake, with more than 300 000 deaths, is the most tragic example of a tsunami effect in modern times. It is clear that the use of an EWS conjugated with adequate preparedness would have saved a large number of lives. Even though not directly addressed in this book, this topic is of most significant relevance in mitigating earthquake risk and should be analysed in great detail.

1.6. Reinforcing and reconstruction of the building stock

Reinforcing the most vulnerable construction and upgrading critical facilities is the best way to prepare society for future earthquake events. If an earthquake occurs, reconstruction should be practiced following the most well known principles and techniques. Reinforcing is a large burden to be taken up by various generations but cost-benefit analysis may indicate that, in the long run, it is the best policy to follow. Chapter 19 deals with this matter and presents practical situations using new scientific technologies, with particular emphasis on action in the case of low rise old masonry buildings. A construction that can resist seismic action to an adequate level will survive the earthquake, probably keeping its operational integrity. Damage may occur in some cases but casualties are reduced tremendously. Even in the worst cases, the housing facilities can be used right away, avoiding an enormous amount of homeless.

A programme for reinforcing has to be planned carefully in order to optimize resources and establish priorities through time. For instance, schools and hospitals are in the first line of priorities, followed by certain networks (lifelines). Housing, construction of cultural value, etc. are matters of a different kind. The first has to deal with private/public ownership, the second with the level of cultural value attributed. But, in all cases, an accurate evaluation of (i) the seismic vulnerability, (ii) the probability of surpassing some damage limit state, (iii) the cost of the intervention and (iv) the benefit produced has to be assessed.

Policies on rent, incentives, market expectations, architectural/historical values, insurance, land-use regulation, etc., play decisive roles on decision-making about this issue.

1.7. Philosophies and policies

Philosophies and public policies arise from human attitudes that evolve rapidly with the course of events. Historical documentation reveals the influence of earthquake impacts on the ways in which communities respond to mitigate their actions. Looking only at the last decade, one recognizes that the philosophy of modern codes is changing rapidly toward more adequate response to the problems that arise. We can cite many examples of structures that suffered no damage in circumstances where they would previously have been severely harmed.

Similar arguments can be brought in relation to public policies. Nowadays, the California law requires retrofit of special structures to be made within a certain limited time period.

“Field-Acts” and “Bills” have been the legal instruments in California to fulfil some of these compulsory requirements. The oldest “Alquist-Priolo Earthquake Fault Zone Act”, signed into Law December 22, 1972, concerns the location of schools and is more than 30 years old. The recent “Seismic Hazards Mapping Act” of 1990 defines land-use areas and the “California State Bill” of 1953, dedicated to hospitals, was updated in 1995 after the Northridge 1994 earthquake.

Retrofitting in certain seismic environments is being initiated. In Europe policies tend to change only after momentous events. The most recent case is in Italy, with the new legislation “Nuova Ordinanza, 3274” of 20/03/2003, which revises many sensible points of acceptable risk. This movement towards an updated legislation is the political response to the impact of the Molise (Italy) 2002 earthquake.

1.8. Lessons learned from recent earthquakes

In the past decade, many lessons were learned from earthquakes. In fact, not only large and diverse types of events occurred but also the monitoring of the seismic process has become very detailed. These circumstances allowed a better understanding of many of the parameters entering in the characterization of, for instance, ground motion (see Chapter 3), site effects (see Chapter 4), damage quantification (see Chapter 10) and the impact of earthquakes in more qualified terms. Also, emergency responses in terms of its achievements (see Chapters 16 and 17) were characterized in a more effective form, with clear identification of zones of success and zones of failure.

So, in almost all topics new information can be used for better characterization of the whole process and for calibrating the different models developed throughout the years.

1.9. Political considerations

Our scientific and technical knowledge has improved considerably in the last decade. This is clearly shown by many technological achievements, by the number of scientists devoted to these subjects with an excellent research production provided through a large and diverse number of research programmes and national and international initiatives, and by a huge amount of publications (books, specialized journals, frequent international conferences, meetings, workshops, etc.). These scientific achievements have led to an increase in efforts towards the assessment of hazard and vulnerability but, only very recently, has political awareness gained some visibility, in particular in the wealthier earthquake prone countries.

It is clear that much is still needed to understand seismic phenomena and the technical needs of varied types of constructions and facilities. But, on the other hand, a great effort has to be made to provide public information which will contribute to an increase in decision-makers' awareness, so that they can support public and private actions leading to the mitigation of risk. The final word in prevention is to develop programmes and initiatives, by using the tools developed in scientific/technical circles, to avoid “damage” and “collapse” of individual constructions and to avoid the stoppage of “operation status” or “collapse” of network systems. These steps can be taken prior to an earthquake occurrence, by reinforcing the most vulnerable constructions, and consequently, reducing their probability of failure.

Bachmann (2004) asks the engineering community if it is doing the right things, and what policies it is pursuing to achieve a substantial reduction of seismic risk. He advocates that, to reduce casualties significantly in the third world countries, the best policy is to apply simple construction technologies that have been well known for a long time to withstand earthquake action.

As for new construction in developing countries, the scientific and technological advances of recent codes are good enough to prevent large problems if quality is assured. In the cases with large ancient housing stocks, the policy of retrofitting and the use of modern control systems depend very much on the hazard level. Simple and cost-effective techniques are not yet sufficiently developed to be accepted by these communities in general.

1.10. Education and mass media risk communication

This important topic is perhaps the one that might be the most effective to increase public awareness of the risks one faces in zones of high potential for earthquake activity. Increasing the number of people who can understand the risks associated to their lives and can learn how to cope with them in a conscientious way is the most effective form of reducing disaster impact (Bolt, 2004).

Prior-to-the-event awareness may press decision makers to take the most adequate decisions on time, such as launching policies for the reinforcement of the most vulnerable/risky structures.

An integrated information system for disaster management is a comprehensive way to cope with emergency post-event, using simulators for training disaster scenarios, e-learning as a form to divulgate concepts, actions, and a data-archive to bring together all available post-event information.

Recent initiatives emphasize the need for increasing the quality of communication, so the Euro-Mediterranean Forum on disaster reduction and a project on communication on Natural Risks in the frame of the Western Mediterranean region published a Decalogue of recommendations:

<http://www.rinamed.net>

http://www.proteccioncivil.org/informes/formediterraneo2003/declaration_madrid.htm.

1.11. Definitions of some basic concepts

Seismic process – Deals with the occurrence of an earthquake event and the process of wave propagation from the source to the site. At the origin, one is interested in characterizing the Time of occurrence, the location of the source (Space – focus, fault structure) and the Size of the phenomenon (magnitude, rupture properties and its kinematics, etc.). For the wave propagation, besides the source rupture, one needs to know the outer structure of the Earth from the source to the site.

Ground motion – The movement of the Earth surface caused by the wave passage. This movement involves the complexity of source mechanism, especially if we are in the near-field (at a distance comparable to the dimensions of the rupture), the characteristics of the medium travelled, and the geometric characteristics and mechanical properties of the geological stratum around the site under analysis.

Hazard assessment – Gives the probability that a certain parameter of ground motion (MMI, PGA, Spectra) or, in a more general case, of the seismic process, will be surpassed within a lifetime period.

Site effects – Changes in the ground motion propagating near the site, in amplitude, frequency content and duration, relatively to the motion at a “hard” lower layer, due to the geometric characteristics and mechanical properties of surface layers surrounding the site, especially for cases of soft layers and complex geometries. For strong motions the nonlinear behaviour of soil layers may take place, altering them significantly.

Other geotechnical problems – Liquefaction, landslide, lateral spreading, compaction: in certain geotechnical conditions other phenomena may take place as a consequence of the wave passage, causing mass movements of small to large extension.

Site-city interaction – Possibility of a “global” interaction between all the buildings of a city and its subsoil.

Tsunami – Sea wave caused at the earthquake source due to the vertical component of the fault rupture offset, or due to some important sequential mass movement at the seabed. When arriving at the coastal shoreline this wave becomes of large height hitting the land or acting as a rapid tide with important “run-up and run-down” if it enters a harbour or large river mouth.

Vulnerability – Degree (level) of performance of a system (engineering structure, network, social group, etc.) under a certain level of seismic action. A more vulnerable system is the one that, for a given action, cannot perform so well as another one.

Fragility – Similar to vulnerability but where the performance is viewed in a statistical way.

Damage (victims, casualties) – “physical damage”: deaths, injures (severe, light, etc.), homeless, damage to buildings, economical impact; “indirect damage”: social impact; “immaterial damage”: psychological impact, etc.

Damage scenario – Geographical distribution of damage for a given earthquake event or a set of events.

Risk – The convolution of hazard with vulnerability for a group of structures, a region, etc. This means the product of probability of occurrence of a certain level of ground motion by the vulnerability of a group of structures, multiplied by their number, and extended to all possible levels of ground motion.

Zonation. Microzonation – Identification of geographical areas having homogeneous similar behaviour under seismic action. Depending on the scale of work, we may consider only the regional differences derived from seismic sources and path, as the case of a gross scale, or consider site effects if working at a detail scale. Microzoning may include also other effects beyond the traditional seismic action parameters, such as landslide, liquefaction, etc.

Networks (lifelines) – Systems of transportation (car traffic, water, gas, electricity, communications, etc.) spread in a region, subjected to different levels of ground motion during a given event.

Essential (critical) facilities – Installations or equipment whose performance during an earthquake is decisive under various different functions: to serve in the emergency operation, to avoid leakage of dangerous products, or due to have a large concentration of population. These facilities, due to their importance should be kept functional under severe or extreme conditions, depending on the expected consequences of failure.

Urban system analysis – An integrated system subsuming all possible consequences of the earthquake impact in an urban centre. Direct, indirect, economic, commercial, business, social, etc., consequences of the earthquake are weighted for a global index value.

Performance – The form a system responds to a given earthquake action in terms of measurement of the functions assigned to that system.

Mitigation – Policies for reduction of consequences of earthquake activity within a lifetime period.

Codes – The most practical and efficient form of designing a structure to withstand seismic action, by defining the minimum requirements (compulsory in some societies and recommendations in others) as far as structural performance. Also codes can be extended to urban and land-use definitions as far as types, sizes, etc. of constructions that can be built in face of existing hazards.

Structural reinforcement – The form of mitigation which considers that vulnerable constructions should undergo reinforcement of their structural system in order to decrease that vulnerability. Recent technological advances have enlarged the spectrum of action for better performance, by using base-isolation techniques, damping devices or dynamic control of structures.

Emergency – Set of actions to be launched when the earthquake occurs. These should optimize the time of intervention (rescue, hospital treatment, etc.) in the most efficient way to minimize the suffering of the populations. Emergency to be fully effective at the needed time requires a great deal of preparation in a great variety of fields of human activity. Preparedness means preparation for the intervention.

Alert – Possibility of expecting a certain level of impact in a region hit by an earthquake, preparing the emergency system for action.

CHAPTER 2
OVERVIEW ON EARTHQUAKE HAZARD ASSESSMENT - METHODS AND NEW TRENDS

C. S. Oliveira¹ and A. Campos-Costa²

1. Instituto Superior Técnico, Lisbon, Portugal

2. Laboratório Nacional de Engenharia Civil, Lisbon, Portugal

2.1. Introduction

A general overview of the methods for assessing seismic hazard at a site or a set of sites is made, explaining the algorithms and discussing their limitations and advantages. An analysis of the variables intervening in the process is done and their uncertainties discussed. Implications of hazard towards risk assessment are also briefly analysed together with structure reliability concepts to help in defining the levels of the seismic action. Finally, a few examples illustrate the importance of the concepts developed, which will be applied in different chapters of the book.

The Probabilistic Seismic Hazard Analysis (PSHA) has become the most widely used method for assessing seismic hazards for “input”, not only considered in the design of structures, but also in various aspects of public and financial policies dealing with seismic mitigation. National hazard maps, directly based on PSHA, have been the basis for national codes and design standards and also a basis for site-dependent studies.

During the 1990's, a period elected by the United Nations for the International Decade for Natural Disasters Reduction (IDNDR), concerted efforts have been made to develop projects that analyse the seismic hazard affecting diverse regions around the World. Supranational organisations, namely, the European and the International Associations for Earthquake Engineering (EAEE, IAEE), the International Association of Seismology and Physics of the Earth's Interior (IASPEI), the European Seismological Commission (ESC), etc., played a very important role. As described later, the case of the Global Seismic Hazard Project (GSHAP) was very peculiar, corresponding to an effort to join experts of neighbouring countries in several meetings to discuss in detail the methods and data for solving border problems.

The idea to have a European seismic regulation with a common format, the EC8 (Eurocode 8, 2003), has also triggered an ample discussion on the definition of seismic actions. To respond to the necessities put forward by the National Document of Application (NDA), a document where each country defines its hazard according to specific criteria, some countries are reviewing their studies of hazard or developing new initiatives, which led in the short term to a modern and integrated vision of the seismic hazard in Europe.

2.2. Historical evolution of methods

2.2.1. GENERALITIES

During the 1980's, interest in methodologies to compute the seismic hazard grew to a significant degree, as has been well described in the compilation of world-wide

regulations made by IASPEI (McGuire, 1993) concerning seismic design. Among the applications that have used hazard concepts, essential initiatives are the studies toward the definition of seismic action in connection with codes and with the safety of important structures and the methodologies for damage scenarios which include criteria for risk evaluation of insurance companies. In the case of critical structures, hazard studies based on probabilistic concepts were accepted, for the first time, as a complementary method to the deterministic evaluations.

In recent years, the computation of seismic hazard at a site experienced a sophisticated evolution producing more accurate results. In the present calculation one describes in a more precise way the location of a seismic source in a region, expresses in a more adequate form the recurrence law of events in that region, and represents in a more comprehensive formulation the strong motion that can occur at that site. The result of hazard is the probability of exceeding, within a given period of time or exposure, a set of parameters characterizing that motion. More recently, through the techniques of expert opinion, uncertainties have been incorporated and, consequently, the level of confidence in the final result can be better quantified.

The use of modern techniques of Geographical Information Systems (GIS) to model the hazard has not only revolutionized completely the computation algorithms, but also made it easier to introduce the data, to update the information available, and to present/display the final graphical results. Sensitivity studies of the parameters involved in the calculation can be approached in a friendly way with the aid of GIS.

In regions with high seismic risk, working groups of experts in different fields, from Geology to Seismology and Earthquake Engineering, were formed with the objective of capturing all the available knowledge to define the best estimate of the seismic actions for periods of 10, 20, 30, etc., years. The examples of Southern California and the Bay Area in the U.S.A., of Japan, of Italy, etc., are important to follow.

2.2.2. METHODS

Seismic hazard study, as it stands nowadays, was initiated with the pioneering theoretical work of Cornell (1968). This work established, within a probabilistic framework, the bases to define the seismic actions at a site, considering as stochastic processes both the occurrence of events in the seismic sources and the attenuation of the strong ground motion, Figure 2.1. This led to the probability distribution function, $G(U \leq u) = 1 - P(U > u)$, of a given parameter U , representative of strong ground motion at the site for a given *time interval* or *exposure time*, T . As will be described later, this method uses the catalogue of events to define a Poisson occurrence process within the seismic sources and the attenuation laws derived for the region under analysis.

In parallel, European experts developed another probabilistic methodology based on the statistics of the extreme values of strong ground motion parameters at the site, deduced from events in the past (Gumbel, 1958). This method analyzes the catalogue of events and fits the data to a distribution of extreme values. Esteva (1968) developed a complementary approach adding the Baye's theorem to update the predictions on the base of the new recorded information.

Prior to these developments, seismic action was obtained directly from maximum felt

intensities (IMM or MSK) or, for critical structures such as nuclear power plants, was defined in a deterministic framework considering the largest possible earthquake in a seismic source and the upper values given by the attenuation law. These two concepts are still present nowadays in several instances.

In the middle of the 1970's, diverse schools in the U.S.A. and around the World developed their hazard algorithms and applied them to different seismic regions (see Oliveira, 1974, for an account of the most used methods and algorithms). The group of the Stanford University applied their models in Central America, and the group of the Massachusetts Institute of Technology applied them in the Eastern U.S.A. The group of the University of Illinois developed more elaborated algorithms, including the fault rupture concept. Experts from the Universidad Nacional Autonoma de Mexico used Bayesian methods. In Eastern Europe, maps of historical maximum intensities were developed, and the group of Moscow (International Institute of Earthquake Prediction and Mathematical Geophysics) developed detailed and sophisticated prediction, hazard, and risk models. The use of extreme value statistics was developed by different groups in Western Europe.

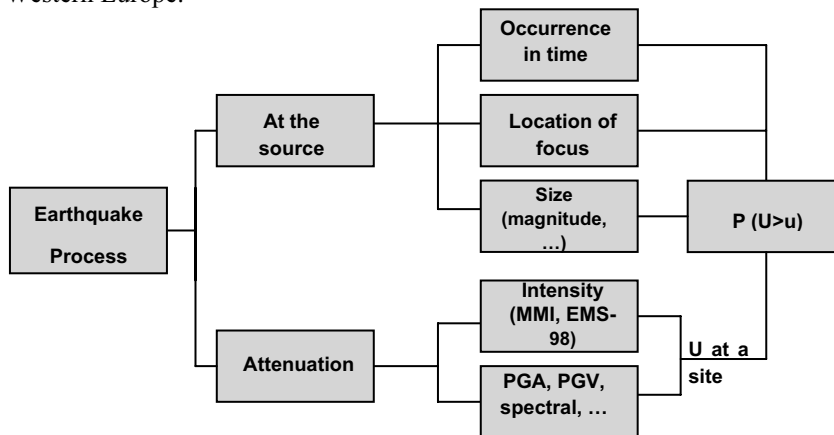


Fig. 2.1. Schematic procedure to analyze the seismic hazard

The concept of hazard analysis for a set of sites was essential to design vital communication systems and lifelines or extended structures, and was the object of a specific analytical treatment (Panoussis, 1974; Taleb-Agha and Whitman, 1975; Keilis-Borok et al., 1974).

Because hazard results for a given site depend to a large extent on the values attributed to many parameters, in such a way that different authors could obtain completely different predictions of ground motion, progress during the 1980's was not so much in the development of new mathematical methods or numerical algorithms, but more on the definition of the quality of the data used. Among others, the EC project "Review of Historical Seismicity in Europe" RHISE (1989-1993) dealt with the essentials of the issue. The quality-data problem weakened the defenders of the probabilistic methodologies in favour of the deterministic defenders. Much later, in the 1990's, these two schools of thought were somehow merged into a more unified approach which is accepted nowadays by almost the entire scientific community, including the one dealing with codes for nuclear installations.

The combination of methodologies, the analysis of sensitivity of few parameters, and the determination of the uncertainties throughout the process of the seismic hazard, have led to the use of logical techniques of decision trees (Schwartz and Coppersmith, 1984; EPRI, 1989) and of MonteCarlo simulation (Bernreuter and Chung, 1979, Bernreuter, 1981 and Bernreuter et al., 1989) to incorporate explicitly and systematically the uncertainties and the different expert interpretations. Expert opinion techniques became popular to deal with topics of great subjectivity due to uncertainties, and were introduced in hazard estimations.

Essentially, there are two types of uncertainties in these models, (i) inherent uncertainties, which are part of the process and cannot be reduced without further technological advancements, and (ii) epistemic uncertainties, which can be reduced by acquisition of more and better qualified data.

Because of the fast growth of seismological data, better characterisation of the seismic sources, and attenuation of the waves, the window of uncertainty of the complete hazard process became narrower and the most critical aspects were identified. From these aspects, it was important to promote the qualification of the historical data, to advance on the paleo- and arqueo-seismology, and to develop strong motion networks. These new sources of information open up the possibilities of reducing epistemic uncertainties, either in the occurrence model (i.e., increasing the confidence for longer return periods (RPs), using Markov models for the time occurrences, etc.) or by proportioning more sophisticated attenuation functions to compute the seismic hazard in terms of PGA, PGV, and spectral contents for both the horizontal and vertical components.

From the end of the 1980's to the first part of the 1990's, the concept of *characteristic earthquake* has gained consensus among various researchers. The concept, initially proposed by Cluff (1978), considers that for great magnitudes the occurrence process deviates from the law of Gutenberg-Richter, due to the presence of asperities in the plan of the fault. These earthquakes are specific of each fault and can only be analysed if the period of observation is sufficiently long to include the characteristic event. To improve the knowledge of the seismic hazard, Allen (1995) presents a series of geologic observations obtained in recent earthquake occurrences supporting this concept.

Modern code maps defining the seismic action to be used in the design of engineered structures are essentially supported on hazard studies for the territory. Also, detailed hazard analysis constitutes the bases to establish ground motion for important structures. The essential problem when dealing with probability distributions is the selection of the probability value to be used. A RP of 475 years has been used in many codes as the accepted level for the *near-collapse* situation of common structures, whereas a RP of 5000 years is used for some *critical structures*. This issue will be discussed later under reliability concepts.

At the beginning of the 1990's, the need to study damage scenarios that simulate the effects of earthquakes on the urban regions (management of emergencies, portfolio insurance losses) and the need to have artificial time histories gave rise to the development of the concept of *seismic scenario*, consistent with hazard studies. The idea, originally proposed by Ishikawa and Kameda (1988), was further extended leading to the concept of *seismic disaggregation* (Bazzurro and Cornell, 1999). Also, joint

probabilities of more than one variable, such as PGA and duration, have been developed.

Very recently, a few books were published containing chapters with material on hazard analysis. They constitute very good references for a detailed analysis of the various issues involved in PSHA, some of which are discussed in this Chapter. Among them we should mention McGuire (2004), Lee et al. (2003), and Chang and Scawthorn (2003).

2.3. Fundamentals of seismic hazard analysis

As already referred to in section 2.2, there are several methodologies to determine the seismic hazard at a site or groups of sites. Table 2.1 summarizes the main issues related to these methodologies, adding to Figure 2.1 various procedures which will be discussed at a later stage.

Table 2.1. Methodologies to compute seismic hazard

Occurrence	Propagation - Attenuation	Convolution	Sensitivity studies
Source areas	Statistical methods	Deterministic	Alternative procedures Uncertainty analysis
Mechanisms	Simulation methods	Analytical	
Active Faults	Physical methods	Extreme values	
Probable Faults	Inclusion of site effects	Bayesian	
Blind faults			

The fundamental of PSHA starts by defining the occurrence and attenuation models. The first one is based on tectonic/geological/seismological information, which leads to the setting of the seismic sources, Figure 2.2, for which a process in time-space-size is built. The second model is obtained from various sources of information dealing with the complex process of source mechanism/propagation of seismic waves till reaching the site under analysis. Computation of PSHA requires the “convolution” of the first two processes, and can be done according to various schemes. Finally, due to lack of high quality data and to the intrinsic nature of the processes under analysis, alternative models should be essayed, uncertainties in parameter estimates should be quantified, and an analysis of sensitivity makes sense.

2.3.1. DETERMINISTIC *VERSUS* PROBABILISTIC METHODS

It is an unquestionable fact that earthquakes are produced in faults (at least those that are located in the Earth crust, which are the most destructive for man). Deterministic methods try to characterize the maximum event that can be produced at a fault and propagate the wave field generated by that event to the site. All variables are treated in a deterministic framework, usually seeking the upper estimative. They are based on the hypothesis that future seismicity of a region behaves with a pattern similar to that observed in the past (including the geological registry), which seems to be a guarantee that no earthquakes with larger effects will happen in the future. Deterministic methods

would therefore rely essentially on a good knowledge of fault activity. On the other hand, and in face of the ignorance on geologic data, this methodology has been frequently interpreted in a restricted way. At the opposite, in some cases historical and instrumental seismicity are considered as the only sources of the information available (Martín Martín, 1989).

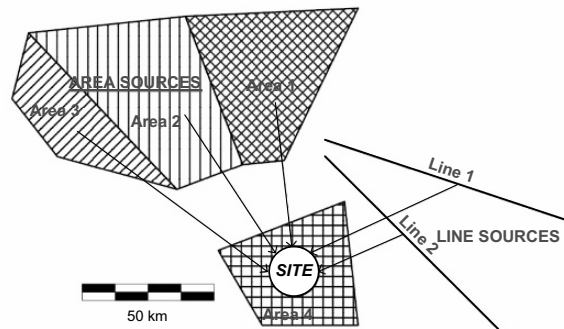


Fig. 2.2. Type of seismic sources contributing to hazard analysis

In general, these techniques have been used in hazard studies of special structures, such as nuclear power plants (NPP), thermal plants, large dams, gas deposits, etc., where specifications to the earthquake design include the so-called Safe Shutdown Earthquake (SSE). This level of ground motion, which is considered as the largest possible to occur, is associated to a *limit state* that tries to avoid the collapse of the structure (NRC, 1973, 1977, 1997a, 1997b and 1977c; EC8, 2003). Deterministic methods are also used to define maps of maximum felt Intensities, with the objective to establish the seismic zonation of a territory.

Deterministic methods depend totally on existing data, which might be incomplete and uncertain. In a probabilistic context, the seismic phenomena consider a series of events whose occurrence is random in space, time, and size. Each process is assigned with a probability function. The most common methodologies of probabilistic nature to treat the occurrence process are referred to in Table 2.2.

The existing limitations to model the earthquake generation and the propagation of seismic waves have led the specialists in Tectonics, Seismology, and Engineering Seismology to use probabilistic methods to analyze the seismic processes of occurrence and strong motion. These methods present the great advantage of introducing a probability value associated to the parameters that characterize the ground motion at a site.

Nevertheless, the probabilistic methods also have some important limitations. For example in the cases when it is necessary to extrapolate the results to much larger return periods than the time interval covered by the available data, which means to extrapolate the validity of the probability distributions to larger time periods and higher magnitudes, where the existing information usually does not exist. Other cases are when the observed process of occurrence does not satisfy the hypotheses of the used models: the Poisson distribution, the stationarity of the process, etc. (Martín Martín, 1989).

Table 2.2. Characterization of the occurrence process

Space	Time interval	Size
Source zones	Process without Memory (Poisson)	Magnitude
Geometry		Intensity ↔ Magnitude
Volume	Process with Memory (Markov)	Statistical Distribution
Area		(upper and lower truncations)
Point	Statistical Distribution (Semi-Markov)	Characteristic Earthquake
Statistical Distribution		
Uniform Distribution		
Empirical Distribution		
Other		
Space – Time – Size: Process with Memory		

Examples of the application of probabilistic methods are the definition of seismic zones for codes and the studies of seismic risk related to the insuring activity. Probabilistic methodologies are also commonly accepted to define design ground motion in the case of NPP or other special structures for the Operating Basis Earthquake (OBE) or similar limit states. In these cases, the design ground motion should insure the functionality of these facilities.

The new philosophy followed by organizations such as the Nuclear Regulatory Commission (NRC) of the U.S.A., which in the past required the exclusive use of deterministic methods for the SSE, nowadays recommend the parallel application of the deterministic and probabilistic methodologies, so that the design earthquake or earthquakes obtained by the first methodology must be consistent with that obtained by the second one for a frequency of occurrence in the order of 10^{-5} per year (NRC, 1973, 1977, 1997a, 1997b and 1997c).

2.3.2. CORNELL METHOD USING SEISMOGENETIC SOURCES

The theoretical background of Probability Seismic Hazard Analysis (PSHA) was developed by Cornell (Cornell, 1968, 1971; Merz and Cornell, 1973) and includes the modelling of those uncertainties through probabilistic methods.

From a mathematical point of view, the PSHA can be formulated as follows (Campos-Costa and Pinto, 1997): let the site seismic intensity U be a random variable dependent on a set of random variables given in the vector \mathbf{x} . The probability $P(U > u)$ that the site seismic intensity does exceed a certain level u can be computed applying the Total Probability Theorem, expressed as:

$$P(U > u) = \int P(U > u | \mathbf{x}) \cdot f_{\mathbf{x}}(\mathbf{x}) \cdot d\mathbf{x} \tag{2.1}$$

where $P(U > u | \mathbf{x})$ indicates the conditional probability of occurring an intensity greater than a certain level u , given that a sample vector \mathbf{x} had occurred; $f_{\mathbf{x}}(\mathbf{x})$ is the joint probability density function (*pdf*) of the random variables \mathbf{x} .

Considering that the site seismic intensity is reasonably described by n uncorrelated variables $x_1, x_2 \dots x_n$, the integral equation 2.1 can be simplified to:

$$P(U > u) = \int \dots \int P(U > u | x_1, \dots, x_n) \cdot f_1(x_1) \cdot \dots \cdot f_n(x_n) \cdot dx_1 \cdot \dots \cdot dx_n \quad (2.2)$$

Uncertainties in the quantification of seismic intensity at a given site are caused by (i) the randomness of the variables related to the amount of energy released, (ii) the randomness of the epicentral location in each source zone, and (iii) the uncertainties in the variables associated to the physical phenomena of propagation and attenuation of the energy released from the source to the site.

Typically, PSHA uncertainties are modelled by (i) the probability distribution of the magnitude m , (ii) the probability distribution of the location of events within each idealized source zone (that location can be transformed to a random variable distance R from the source to the site), and (iii) the random functional descriptions known as attenuation laws.

Furthermore, as generally assumed, the random variables magnitude M and epicentral distance R are statistically independent. Then, the computation of $P(U > u)_i$, taking into account each seismic source i separately, is given by:

$$P(U > u)_i = \int_R \int_{m_{oi}}^{m_{ui}} P(U > u | m, R) \cdot f_M(m)_i \cdot f_R(R)_i \cdot dm \cdot dR \quad (2.3)$$

In this particular case, $P(U > u | m, R)$ gives the conditional probability of exceeding the intensity level u at a site, given that an earthquake of magnitude m and distance R has occurred in a seismic source zone i ; $f_M(m)_i$ represents the *pdf* associated to the likelihood of the magnitude of events ($m_{oi} < m < m_{ui}$) occurring in zone i , and $f_R(R)_i$ represents the *pdf* used to reflect the randomness of epicentral location of earthquakes inside each source i . m_{oi} and m_{ui} are lower and upper values of $f_M(m)_i$.

If, as usually, $f_R(R)_i$ is assumed uniformly distributed, eq (2.3) becomes:

$$P(U > u)_i = \int_R \int_{m_{oi}}^{m_{ui}} P(U > u | m, R) \cdot f_M(m)_i \cdot dm \cdot dR \quad (2.4)$$

On the other hand, if PSHA is performed for some spectral description of site intensity, instead of a unique ground motion parameter intensity U , and the values of spectral ordinates are uncorrelated, eq (2.4) can be generalized for the j ordinate in the form:

$$P(S_j > s_j)_i = \int_R \int_{m_{oi}}^{m_{ui}} P(S_j > s_j | m, R) \cdot f_M(m)_i \cdot dm \cdot dR \quad (2.5)$$

where $P(S_j > s_j | m, R)$ gives the conditional probability of exceeding, at the site, the spectral ordinate s_j at a frequency (or period) f_j , given that an earthquake of magnitude m has occurred at a distance R in the seismic source zone i .

Spectral ordinates of a PSHA constitute what is generally called the Uniform Risk Spectra, *URS*. As mentioned before, those spectral ordinates have the same probability

of being exceeded, in a given exposure time T , due to the seismicity of the seismic source i .

In PSHA, the procedures for estimating the values m_0 , m_u , and other parameters associated to $f_m(m)$ are generally called modelling earthquake *magnitude recurrence*, whereas the idealization of attenuation relationships and the associated estimates of $P(U>u|m,R)$ are referred to as modelling the *attenuation of seismic intensity*. The next two sections will be devoted to those topics.

2.3.2.1. The occurrence model

As pointed out, the density probability function $f_M(m)_i$ in eq. (2.3) only refers to the relative number of events as a function of magnitude, in the source zone i and in a specified period of time, ranging from a minimum positive value m_0 to a maximum value m_u . In other words, that probability can be interpreted as conditional, regarding the occurrence of an earthquake in source zone i with magnitude between those limits. The integral of $f_M(m)_i$ from m_0 to m_u must be always equal to 1. On the other hand, the term $P(U>u|m,R)$ in the same expression is obviously conditional on the occurrence of an earthquake with a given magnitude and focal distance.

Consequently, values of $P(U>u)_i$ (given by eq. 2.3) also translate the probability of exceeding the intensity u , conditioned by the occurrence of an earthquake in seismic source i , with magnitude between the limits m_0 and m_u ; so far nothing was said about the probability of the occurrence of this event.

However, it is clearly recognized that the occurrence of earthquakes is a time dependent stochastic process, meaning that the probability $P(U>u)_i$ should always be combined with a model of earthquake occurrence in time.

The simplest relation for the occurrence of earthquakes is the so called Gutenberg-Richter law of magnitudes (Richter, 1958):

$$\log N(m) = a - b \cdot m \quad (2.6)$$

where $N(m)$ is the number of events per year having magnitudes greater than m , and a and b are constants defined by the regression analysis. The slope of the Gutenberg-Richter magnitude-frequency defines the "b value" parameter. This expression is equivalent to an exponential distribution of the random variable M .

This relation can be improved by introducing various important corrections such as the lower and upper magnitude values, defined as the truncation parameters related, respectively, to the minimum and maximum values of magnitude, obtained by different methods in the region under analysis. For instance, the upper one is related to the tectonic environment and structural geology capable of generating the largest possible magnitude. Uncertainties in all parameters, including lower and upper truncation values, can be introduced in the general equations defining the recurrence of earthquake activity in a region. For details with the probability laws associated to these various situations see McGuire (2004).

If events with magnitude less than or equal to m_0 are assumed to have no engineering significance and if the existence of a regional maximum probable magnitude m_u is recognized, then the cumulative distribution of magnitudes of the earthquakes with

epicentres inside source i is easily derived as:

$$F_M(m)_i = P(M < m | m_0 < M \leq m_u)_i = \frac{1 - e^{-\beta_i(m-m_0)}}{1 - e^{-\beta_i(m_u-m_0)}} \quad (2.7)$$

where $\beta = b \ln(10)$.

Other recurrence magnitude models have been used in PSHA, such as the bilinear law (Shah et al., 1973) or the quadratic law (Merz and Cornell, 1973).

The bilinear law is used to reduce the bias due to incomplete small magnitude data, because, in such cases, a single line overestimates the frequency of large magnitudes and, consequently, the hazards tend to be overestimated (Araya and Kiureghian, 1988). The quadratic law predicts fewer events of high magnitude than the bilinear law. Its use in the PSHA is significant for high intensity levels, with hazard curve falling off faster than in the case of the bilinear law (Araya and Kiureghian, 1988).

Other more complex expressions can be found in McGuire (2004) for the common cases of unequal periods of completeness.

Eq. (2.7) gives the final distribution to be introduced in eq. (2.3) to eq. (2.5) in order to compute the contribution to the final seismic hazard of the earthquakes occurring in the seismic source i . This distribution is truncated for values between m_0 and m_u , meaning that the integral between those limits equals 1.

Although not always a valid assumption, the most simple and commonly used stochastic idealisation of time occurrences is the well-known Poisson process. The validity of such a model is based on three assumptions (Araya and Kiureghian, 1988):

- An event can occur at random and at any time.
- The number of occurrences in non-overlapping intervals is independent.
- The probability of occurrence of an event in a small interval Δt is proportional to Δt and is given by $\nu \Delta t$, where ν is the mean rate of occurrence of events (assumed as constant). Furthermore, the probability of two or more occurrences in Δt is negligible.

The first two assumptions imply the basic property of Poisson processes known as the “lack of memory”. That is, any occurrence at an instant in time is not affected by past occurrences nor does it affect any future events. Other more sophisticated models of occurrence include Markov and semi-Markov models, exhibiting memory, clusters, etc. The difficulties of application of these models are due to the scarcity of good data, either related to the quality of catalogue data, or to the extension of coverage of data.

2.3.2.2. The attenuation model: Functional form

Another important issue of the PSHA is the complex phenomenology of propagation and attenuation of the energy released in the source that reaches a particular site (see Chapter 3 for a detailed description).

Typically, the decreasing of intensities of seismic strong ground motion with distance, from the source to the site, is attributed to two main causes: geometric and viscoelastic attenuation. The first one is related to the fact that seismic waves cross a greater volume of earth crust as the distance from the source increases. The second one is the result of

the inelastic behaviour of the materials that compose the propagation medium.

In PSHA, attenuation is generally considered as a random phenomenon and that is reflected in the mathematical procedures by the conditional probability $P(U > u | m, R)$.

Araya and Kiureghian (1988) suggested the general formula to represent attenuation:

$$U = Z_U \cdot f(M, R, \mathbf{p}) \quad (2.8)$$

where U is the strong motion parameter to be predicted; Z_U is a random variable representing the uncertainty in U ; R and M were already defined; and \mathbf{p} is a vector representing a set of parameters that can characterise the earthquake source (type of faults - normal, reverse, strike - and kinematics, directivity, etc.), the wave propagation path, and the local site conditions (topography and soil effects).

Typically, U is taken as the maximum peak ground acceleration (PGA), velocity (PGV), or displacement (PGD). Moreover, the random variable Z , accounting for the scatter in the registered data and representing the uncertainty in the predicted values, is usually assumed to be Log-normally distributed.

Multi-regression analysis is used to fit semi-empirical attenuation relationships to strong ground motion data registered during earthquakes at stations distancing from the source from few kilometres to few hundred kilometres, and for events of several magnitudes.

A lot of research has been done in this field, and many empirical relations have been proposed, which are generally valid for broad regions from where the data were originated and in the domain covered by the epicentre distances and magnitudes used in the regression analysis. However, instrumental data covers only few regions in the world and the attenuation models estimated for one region must be applied to other regions with similar local soil conditions.

Several frequency-dependent attenuation relationships, with PSV, PSA, or SA response variables, have been published that allow carrying out seismic hazard analysis in terms of spectral ordinates, at different periods, all with the same hazard level (URS) (Trifunac and Lee, 1989; Abrahamson and Silva, 1997; Ambraseys et al., 1996; Boore et al., 1997; Joyner and Boore, 1981; Sabetta and Pugliese, 1996). Borzi, et al. (1998) and Faccioli et al. (2004) derived attenuation relationships for Europe related to displacement spectral ordinates. These displacement spectra are very important for long period structures.

One functional (logarithmic) form of eq. (2.8) is defined as (Reiter, 1990):

$$\ln(U) = \ln(b_I) + \ln(f_1(M)) + \ln(f_2(R)) + \ln(f_3(M, R)) + \ln(f_4(P_i)) + \ln(\varepsilon) \quad (2.9)$$

where U is the strong motion parameter to be estimated (dependant variable), a lognormal distributed random variable; $f_1(M)$ is a function of the independent magnitude variable M , the earthquake source size. There are several magnitude definitions; the most common still is the Richter magnitude, but more recently the moment magnitude (M_w) is preferred because it is directly related to the seismic moment of the earthquake and does not saturate; $f_2(R)$ depends on the variable R , the seismicogenic area source to site distance; $f_3(M, R)$ is a possible joint function between M and R ; $f_4(P_i)$ are functions representing possible source and site effects: for example, different style of faulting may generate in the near field different ground motions values

(Abrahamson and Shedlock, 1997); and ε is an error term representing the uncertainty in U . These relationships are valid for a specific site classification (hard rock, soft rock, etc.).

2.3.2.3. Final computation

To include the stochastic model in the hazard analysis, let v_i be the estimate of the annual mean rate of occurrence of earthquakes with magnitude greater than m_0 in a given seismic source zone i . Thus the mean rate of occurrence of intensity greater than u at a site, defined as ω_i , will be the simple product:

$$\omega_i = v_i \cdot P(U > u)_i \quad (2.10)$$

Under the validity of the assumptions of a stochastic Poisson model for time occurrences, the probability that a reference intensity level u is exceeded at least once within a specified time interval T , due to the seismicity of a source zone i , is given by:

$$P(U_T > u)_i = 1 - e^{-\omega_i T} \quad (2.11)$$

Final estimates of the probability due to the random seismicity in the entire region covered by n source zones, is based on the property of the aggregation of n independent Poisson processes.

Thus, assuming that the time occurrence processes are independent among source zones, the occurrence rate of a global Poisson process can be determined by summing all contributions ω_i :

$$P(U_T > u) = 1 - e^{-T \cdot \sum_{i=1}^n \omega_i} \quad (2.12)$$

Of course, the applicability of this last expression depends also on the validity of the assumptions assumed for the Poisson process outlined above, extended to the entire region covered by all the seismic sources. The probability density function (*pdf*) corresponding to $h(U)$ is assumed as the hazard density function.

When the reference time interval equals one year ($T = 1$), eq. (2.12) gives the annual probability of exceedance. In this context, the return period $RP(u)$ is defined as the inverse of the annual probability of u being exceeded at least once, that is:

$$RP(u) = \frac{1}{1 - e^{-\sum_{i=1}^n \omega_i}} \quad (2.13)$$

The assumed independence of events in a Poisson process implies some contradiction with the generally accepted physical phenomenology for earthquake occurrences. In fact, if an earthquake is the consequence of a sudden release of gradually accumulated strains in the earth crust, it is obvious that time sequences of such events could not strictly be considered Poissonian. However, the reasonability of the Poisson law to represent the occurrence process of large events depends, sometimes, on the adequate elimination of aftershocks and foreshocks from the time sequence of events.

In what concerns the evaluation of uniform risk spectra (*URS's*), eq. (2.12) can be generalized to (Campos-Costa and Pinto, 1997):

$$P(S_j^T > s_j) = 1 - e^{(-T \cdot \sum_{i=1}^n \omega_{j,i})} \tag{2.14}$$

where, in this case, S_j is the spectral component of seismic ground motion for frequency j and $\omega_{j,i}$ is:

$$\omega_{j,i} = v_i \cdot P(S_j > s_j)_i \tag{2.15}$$

The concept of RP , the reciprocal of the annual probability of occurrence, is very important and can be related to the probability of non-exceedance for a given time interval (exposure time) T , as:

$$1 - P(S_j^T > s_j) = \left(1 - \frac{1}{RP}\right)^T \tag{2.16}$$

For instance, the probability of exceedance of 10% during a period T of 50 years corresponds to a $RP = 475$ years. For other relations see Fig. 2.3. Caution should however be exercised on the meaning of RP , because it may be wrongly inferred that the seismic action (PGA, etc.) corresponding to a given RP occurs at regular time intervals equal to the RP . In fact, the probability of exceedance of that variable in a time period equal to the RP is only 33% and not 100%.

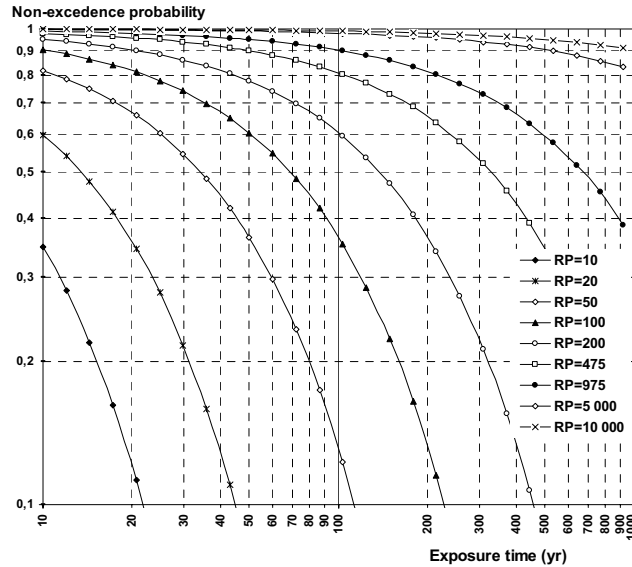


Fig. 2.3. Conversion of probability of exceedance in T (exposure time) into RP

2.3.3. EMPIRICAL METHOD (EXTREME VALUE DISTRIBUTIONS OF THE CATALOGUE EVENTS)

The development of this method is directly based on statistical analysis of ground motion parameter values at a site corresponding to the sequence of earthquake events occurring through time. It requires the compilation of earthquakes with the time of occurrence, epicentral location and magnitude, and the use of an attenuation law. The

series obtained at the site (PGA, PGV, etc.) is then treated as an extreme value distribution (Gumbel distribution), by taking the largest value in a time period, normally the year. Three distribution types are usually used (Borges and Castanheta, 1968), type I, type II, and type III (Weibull, *in* Gumbel, 1958); the former two with a single parameter, and the third one with two. The numerical procedures could include nonlinear least square analysis, the method of moments, and the Maximum Likelihood estimative. The extreme values of some parameters, like the magnitude and hypocentral intensity, in special if they belong to historical events, have the advantage to be determined with greater exactitude than the intermediate values (Martín Martín, 1984). A by-product of this method is the study of the Historical Maximum Intensities, which consists of assigning the maximum intensity to different locations of a region, in agreement with the information of the historical catalogue of the observed seismicity. As already indicated when using intensities, the Historical Maximum Intensities will always have to be calibrated with the results of any other method for seismic hazard.

Mucciarelli et al. (2000) developed an algorithm that compares, in a systematic way, the results of this method with the *source method*. The results show great differences among them, depending on the used level of intensity and the number of available observations. This is a question of greater importance that deserves further research.

2.3.4. HYBRID METHODS

A sub-product from the *source* and *empirical methods* is a *hybrid method*, consisting of the simulation of a catalogue of seismic occurrences according to certain pre-established laws that reproduce the historical and instrumental processes of the region. The *hybrid method* is applied to the time series obtained at the site. An advantage of this method, as opposed to the simple *empirical method*, is that it can consider a set of series instead of a single one, and may incorporate any type of information of tectonic, geologic, or seismological nature.

Simulation of catalogues has been tried by several authors. Among them, the studies by Costa (1989) modelling a three-dimensional markovian process deserves a special reference. The model, developed to represent Seismic Stochastic Processes of the Iberian Peninsula (PESPI), is characterized by three levels of interdependence between time, space and size of the occurrence process.

There is a wide variety of methods concerning the wave field produced at the fault rupture and its propagation to the site. Some of them are discussed in Chapter 3.

Bayesian methods are particularly useful in hazard analysis, as they can incorporate information of different nature (subjective or not) on the seismic process, to combine the results obtained with various methods, and update the estimations of the parameters from *a-priori* distributions (Costa, 1989, mentioning Esteva, 1968).

2.4. Methodology for seismic risk scenario assessment

2.4.1. HAZARD CONSISTENT ANALYSIS

The concept of Hazard Consistent Analysis can be used to define seismic scenarios

needed to perform risk studies and to deal with the problem of artificial generation of the strong motion time-histories. In this case, it is necessary to determine the probability distributions of variables such as M and R . Using the Ishikawa approach (Ishikawa et al., 1988), the expected values of magnitude M and focal distance R could be assessed by the Bayes theorem, as:

$$E(M|U > u) = \frac{\int_m \int_r m \cdot P(U > u|m, R) \cdot f_M(m) \cdot f_R(r) \cdot dm \cdot dR}{\int_m \int_r P(U > u|m, R) \cdot f_M(m) \cdot f_R(r) \cdot dm \cdot dR} \quad (2.17)$$

$$E(R|U > u) = \frac{\int_m \int_r r \cdot P(U > u|m, R) \cdot f_M(m) \cdot f_R(r) \cdot dm \cdot dR}{\int_m \int_r P(U > u|m, R) \cdot f_M(m) \cdot f_R(r) \cdot dm \cdot dR} \quad (2.18)$$

where $E(M|U > u)$ and $E(R|U > u)$ express the conditional expected values of magnitude and focal distance, given that a certain level of U , that is u , is exceeded. This level is related to a certain probability of exceedance by the hazard curve.

Another way to assess the most probable pair of parameters (M , R) is to perform the probabilistic disaggregating of magnitude and distance (McGuire, 1995).

2.4.2. DISAGGREGATING

To derive a potential design earthquake, or simply a hazard dominating scenario event at a site, from a probabilistic seismic hazard analysis, it is important to perform the hazard disaggregation. Although this analysis has been recently developed, it was already extensively discussed and applied (e.g., Chapman, 1995; Frankel 1995; Cramer and Petersen, 1996; McGuire, 1995; Bazzurro and Cornell, 1999; Harmsen et al., 1999).

Seismic hazard disaggregation consists in the assessment of the hazard contributions in a space of bins of the random variables of the process.

The most used bin space is bi-dimensional; that is, the relative contribution to the hazard is studied in terms of elementary bins of magnitude M , and source-to-site distance R . Therefore, hazard disaggregation represents the conditional probability that, given the exceedance of a specified ground motion level (hazard value), which combination of M and R (McGuire, 1995) contributes more to that level of ground motion.

Bazzurro and Cornell (1999) suggest that the results of hazard disaggregation can be summarised into central statistics, like means or modes. They improved the disaggregation procedure by evaluating hazard contributions in terms of M , ϵ and latitude and longitude, instead of R . ϵ is a measure of the deviation of ground motion from the predicted (median) motion variable. Disaggregation permits a direct display on a map of the source areas dominating the hazard, along with the knowledge of the most likely magnitude values. This way one can get a better definition of the specific earthquake that presents the largest contribution to the hazard at a given site. One should keep in mind, according to the current state-of-the-art of seismotectonic studies,

that usually (i) earthquakes are not uniformly distributed in space (inside gross source zones) and that (ii) the source zones are frequently designed larger than geodynamic evidences. To cope with this statistical significance of the random variables involved in PSHA analysis, the inclusion of the randomness of epicentre location inside gross source zones is the only way for selecting a meaningful regional seismic risk scenario based on the hazard disaggregation.

Let i be a given site which is affected by a seismogenic region characterized by a truncated probability density function (*pdf*) of magnitude $f_M(m)$ and a global annual rate of events λ , taking all earthquakes with magnitudes $m_0 \leq m \leq m_u$. Additionally, consider that earthquake epicentres are not uniformly distributed, but can be characterized by a spatial density function $f_S(x,y)$ expressing the spatial distribution of relative frequency of events with magnitudes $m_0 \leq m \leq m_u$ in such a way that integration over the area A of the seismogenic region is unit, $\int_A f_S(x,y) = 1$.

Following Cornell's approach, the mean annual frequency of exceedance $\omega(U > u_i)$ of a specified level u at the site i , due to earthquake events occurring inside A , is given by eq. (2.10), which can be written in terms of elementary area $dA(x,y)$ as:

$$\omega(U > u_i) = \lambda \cdot \int_A \int_M f_S(x,y) \cdot f_M(m) \cdot P(U > u_i | m, R_i) \cdot dm \cdot dA \quad (2.19)$$

where the function $P(U > u_i | m, R_i)$ reflects the randomness associated to the attenuation of seismic ground motion intensity, idealised by the conditional probability that the intensity U of ground motion exceeds a specified level u_i at the site, given an earthquake, of magnitude m at the epicentral distance R , in which R_i is the distance of zone point (x,y) to the considered site. λ is similar to previous ν , the annual mean rate of occurrences with intensity greater than m_0 .

Let the integrand of eq. (2.19) be represented by:

$$\ell(m, x, y | U > u_i) = f_S(x, y) \cdot f_M(m) \cdot P(U > u_i | m, R_i) \quad (2.20)$$

Note that $\ell(m, x, y | U > u_i)$ is not exactly a probability density function but, as stated by Chapman (1995), can be defined as a "joint hazard density" for the frequency of exceeding motion level inside gross source zones inside gross source zones u_i .

For the general case in which there are n statistically independent seismic sources, it is possible to rewrite eq. (2.20) as:

$$\ell(m, x, y | U > u_i) = \sum_k^n f_S(x, y) \cdot f_M(m)_k \cdot P(U > u_i | m, R_i)_k \quad (2.21)$$

where subscript k refers to the k^{th} source zone. Similarly to what was done in section 2.4.1., it is possible to determine the joint hazard function of only the geographic random variables $g(x,y)$. This can be obtained by a marginal hazard function adequately normalized:

$$g(x,y) = \frac{\int_A \ell_M(x,y | u_i)}{\int_A \ell_M(x,y | u_i) \cdot dA} \quad (2.22)$$

The function $g(x,y)$ is now a *pdf*, and can be plotted for several pairs of geographic

coordinates x,y and for several seismic intensity levels u . It reflects the geographic relative contribution of all the seismic area affecting the site. Being a marginal density function, those contributions are independent of the magnitude of events but, as stated before, they are always conditional on the exceedance of a seismic intensity level u at the site.

This distribution may be used in the consistent selection of seismic hazard scenarios, since each event is associated with an objective likelihood and a pair of geographical coordinates x, y . In the application cases, mean or modal values are generally used. For example, the epicentre of a seismic scenario is defined as the location of the modal value of pdf in eq. (2.21), i.e., the modal event for a specified motion parameter value u_i occurs at:

$$(\tilde{x}, \tilde{y}): g(\tilde{x}, \tilde{y}) = \max [g(x,y)] \tag{2.23}$$

Moreover, for a complete definition of a seismic scenario, a magnitude must be chosen for the modal event which geographical position is defined in eq. (2.23), e.g., by assigning the expected value of magnitude, also referred to as hazard-consistent magnitude and given by:

$$E(M | (\tilde{x}, \tilde{y})) = \frac{\int \ell(m, \tilde{x}, \tilde{y} | u_i) \cdot m \cdot dm}{\int_M \ell(m, \tilde{x}, \tilde{y} | u_i) \cdot dm} \tag{2.24}$$

Chapter 21 presents an application of the disaggregation concept to Portugal.

2.5. New contributions to the earthquake process

2.5.1. HAZARD ALGORITHMS

The seismic source zones could be modelled like volumes, areas, or lines, Figure 2.2. The first numerical algorithms consider area zones divided in polygons, whose numerical integration had to be approached considering circular elements centred at the site under analysis. Another characteristic of the initial development was the adoption of upper and lower truncation limits in the law of Gutenberg-Richter. Der Kiureghian and Ang (1977) developed the concept of preferred direction of the rupture, which considers the possibility of having shorter epicentral distances due to the geometry of the rupture. After these developments, no great progress took place in theoretical terms. With the advent of strong motion networks, small advances in the distribution of the magnitude (parabolic functions, characteristic event, etc.) and on the attenuation laws have produced an enormous amount of information. But the initial software versions, EQRISK (McGuire, 1976), STASHA (Guidi, 1979), and SEISRISK-III (Bender et al., 1987), continue as the essential basis of the most recent ones, namely, CRISIS (Ordaz 1991), EZ-Frisk (Risk Engineering, Inc, 1997), Geodeco, SpA (1998), and OpenSHA (Field et al., 2003). This latter software is composed by different modules that the user can modify at his interest.

Parallel to the appearance of the newer and more commercial oriented computer applications, some authors have developed their own algorithms. To mention only the

Portuguese contributions, Campos-Costa (1993), based on EQRISK, has introduced a series of new routines applicable to hazard consistent studies; Correia (1996) has formulated the joint probability of the magnitude and the epicentral distance; and Coelho and Marcelino (1997) evaluated the potential of rupture of a segment of a given fault, quantifying the slip associated to that fault in probabilistic terms.

Throughout these years, the evolution of the integration procedures, including the numerical algorithms to calculate the space portion, has been almost null. This is due to the fact that, if attenuation has circular symmetry as currently assumed, concentric segments around the site have the same contribution to the seismic hazard.

However, three new contributions in this subject should be mentioned. Budnitz et al. (1997) discussed the propagation of the uncertainty related to the methods of integration. A novel algorithm of space analysis uses a transformation of variables, reducing any parallelogram to a normalized square (Estêvão and Oliveira, 1999). Another approach to the seismic source concept with homogeneous seismic activity (uniform spatial distribution) is the *semi-zonified source model*. This methodology, proposed by Frankel (1995), assumes a spatially smoothed seismicity with no need to delineate seismic sources.

2.5.2. THE OCCURRENCE PROCESS

Earthquakes are phenomena of chaotic nature that can shake a region or an area in random form. As far as space and time are concerned, their occurrences are somehow distributed in grouped form, demonstrating the pattern of the released energy. In regions with high energy concentration, such as the zones of accretion (oceanic mountain ranges), subduction, collision, etc., the occurrence behaviour can be characterized during relatively short periods of time (decades, centuries). On the contrary, regions with low or very low concentration of energy, like passive margins, or shields, require longer periods of observation (several thousands to tens or hundreds of thousands of years, and even more) to have a complete representation of the processes.

When the accumulated energy reaches the rupture level, Nature is ready to initiate the unloading of this energy, which will take place for reasons unknown for the present state of our knowledge. The rupture mechanism is a very complex process that depends on a large number of parameters, difficult to observe and measure. This mechanism depends on the friction between the rocks that contact throughout the plane of the fault (known "asperities"), as well as on other circumstances such as the presence of viscous material, water, etc. When ready to rupture, any small overload can trigger the process, which evolves in a rather unknown way rupturing throughout the fault plane, or redistributing loads to other neighbouring faults which may also rupture. An example of this stress transfer has probably happened during the earthquake of Azores-Faial of July 9, 1998 (Malheiro et al., 1999).

Although a great amount of information has been obtained in the last years, much randomness still exists in the seismic process, which reflects the analytical modelling development taking place. The models "with memory", more suitable to full represent the reality, try to capture the process where energy is accumulated and suddenly released, but require much data to calibrate the various defining parameters. In this type of analysis it is necessary enlarge the region under analysis and models should have a

regional character, instead of local, to correlate events in both time and space.

Models with memory, such as Markov models, never had a great development due to the absence of representative data. Kiremidjian and Anagnos (1984) were the first authors to try these techniques, applying them to California; but the results obtained were never transferred to the professional field. To study the earthquake occurrence in the Iberian Peninsula, Costa (1989) and Rodrigues (1999) used a semi-Markov technique, and proposed a very complex model to be explored together with real time data.

The *characteristic earthquake* concept, whose occurrence takes place when the accumulated energy exceeds the capacity of “asperities” of great size, can also be considered in this line of reasoning. In this situation, there is not a finite fractal dimension and the recurrence law of Gutenberg-Richter is not valid in the long term (at least, for events of magnitude compatible with the size of the asperities). Nevertheless, the smallest events would still behave like part of a stationary process. The law of seismic recurrence can also be seen as a fractal distribution.

Data have shown that the linearity proposed by eq. (2.6) is not possible, suggesting other functional forms. The *characteristic earthquake* is the most important deviation of that principle, because it considers that events of a certain magnitude occur separately, at equal recurrence time intervals, altering the general trend of the basic Gutenberg-Richter law (Figure 2.4).

Figure 4 a) presents an example of incompleteness of data. The upper curve gives the Gutenberg-Richter fitting for the entire world for the period 1900-2004, while the lower curve includes only data of damaging events. The same trend is observed for regions or local active areas. The *characteristic earthquake* is specific of a fault or fault system, Figure 4 b).

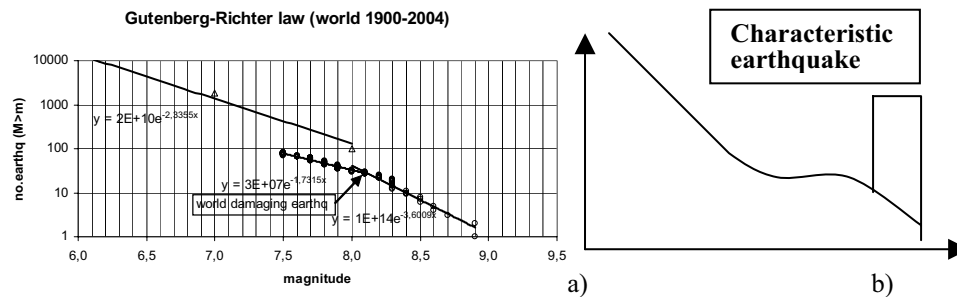


Fig 2.4. Gutenberg-Richter law and the *characteristic earthquake*

Recently, new algorithms are being developed to identify occurrence patterns of earthquakes from regional or global data, which will probably allow a better and more complete idea of the process of energy release. The new developments include the application of techniques of artificial intelligence, like neuronal networks (Alves, 1994), genetic models, etc.; and techniques of operation research, like fractal analysis (Turcotte, 1997), chaotic dynamic systems, auto-regressive models, Markov chains, processes with deformation (Ribeiro, 1997, Bak et al., 1994), etc.

According to Ribeiro (1997), it is possible to consider that faults have a fractal

distribution, each one with a characteristic event and, consequently, from its dimensions, with a Maximum magnitude. Nevertheless, it would not be possible to attribute a RP, unless the geologic record would allow dating coseismic evidences as they appear in liquefaction or in slip displacements at the fault plane.

The concepts of active fault, probable fault, and extinct fault (Mallard, 1991) still remain open for discussion; although the idea to consider that a fault is active if it has been activated during the neotectonic epoch, and more precisely during the quaternary, approximately in the last two million years (Allen, 1975, NCR, 1997a). On the other hand, in regions with low to moderate seismicity, where the maximum earthquakes have large return periods, or in the case of critical facilities like nuclear power plants where it is necessary to design for earthquakes with RPs larger than 10^5 years, it is necessary to know and to analyze a geologic record that contemplates, at least, a time window of the same order.

Empirical correlations are used to assign a maximum magnitude to a given fault based on the length of the potential rupture, the total length of the fault trace, or the area of the rupture zone. When faults cannot be clearly identified, the maximum magnitude is deduced in most cases either from the earthquake catalogue, from the recurrence rate (extrapolating the Gutenberg-Richter relationship), or from paleo-seismicity studies.

2.5.3. ATTENUATION OF STRONG GROUND MOTION

Under this concept a great variety of problems should be analyzed, related to the functional form of eq. (2.9) between the parameters of the earthquake in the source to those that characterize the severity of the strong motion at a given site. This functional form can be adapted from another location that has similar tectonic environment or has been obtained specifically for the region under analysis. Since attenuation has been identified as the most critical component for the process of estimating the strong ground motion, concerted efforts in this field have been made recently (see Chapter 3 for more details).

Even though historically, one started using the attenuation of the Intensity (MMI, EMS-98, etc.) due to the little instrumental information available, with the advent of digital instruments to measure the strong motion, the panorama has been changing rapidly. In early nineteen seventies only a few world-wide records were available, but in our days it is possible to have access to a large amount of information. In relation to the data available the following commentaries can be made:

- The precise data of the strong motion, as far as attenuation of Intensity or other parameters, exhibit a very large dispersion whose causes have still not yet been well identified.
- Unfortunately, the existing data do not cover all the rank of magnitudes and distances; this is why, in the interval of interest, there are many regions with an insufficient number of data points to support a good fitting.
- The attenuation laws are very dependent of the amplitude of the movement; and if small amplitude coming from events with low magnitude are used, (obtained with instrumentation of hi-resolution, such as from the seismological networks or from weak motion), it is very important that this effect can be reflected in the apparent observed

nonlinear behaviour of the propagation of the seismic waves.

The universal attenuation laws that govern the seismic process are not clear. Regional peculiarities are not enough to explain the differences observed from the mean values. Other variables such as the direction (azimuth) with respect to the source, the directionality in the propagation of the rupture, the stress drop at the source, the existence of multiple events originated at different points within the fault plane, etc., are also very important. Site effects contribute as well to the large uncertainties in data.

The existence of these large uncertainties (Figure 2.5) led to various problems in the process of fitting to an attenuation model (Paula and Oliveira, 1996): (i) the form of the equation, (ii) the type of adjustment, (iii) the numerical algorithm, (iv) the use of average values and the separated consideration of a standardized general error, (v) the use of the 84% (or another) percentile or the pure deletion of the standardized error, etc.

Selection of strong motion parameters or intensity measurements to use in the attenuation laws depends on the type of information to be processed and on the availability of data. Obviously, countries with better strong motion data will prefer to work with PGA, PGV or spectral content. But in any case, the comparison of instrumental with intensity data should always be essayed.

The physical wave propagation modelling is becoming an important tool for the analysis of attenuation (Suhadolc and Panza, 1985). Present models that consider the properties of the source and the directions of propagation including fault rupture, and the Earth structure, can reproduce phase arrivals and corresponding amplitudes up to a few Hertz. The complete spectral shape still is far from being well-known due to the disturbances generated by the small changes of the elastic medium. In order to simulate the strong motion time histories, the use of an empirical Green function obtained from small magnitude earthquakes has been tried with some success. Other techniques, such as the use of neuronal networks have been tried (Frade and Graça, 1999) to obtain correlations among the various parameters characterizing the whole process of strong motion.

The recording of several earthquakes in regions of well known Earth layers, such as the case of the San Andreas Fault system and on the Eastern US, has shown that for certain epicentral distance ranges, the amplitude of motion tends to be kept in a plateau, independently of increased distance. This effect, due to a strong reflection at the Moho for certain angles, introduces novelty that needs to be considered in the attenuation law, Figure 2.6. Data dispersion present in Figure 2.5 may partially be due to this effect.

The effect of radiation of seismic waves due to the mechanism at the fault trace and the directivity originated from the rupture kinematics have been emphasized in recent events (Kobe, 1995, Kocaeli, 1999), and should not be ignored in the attenuation model if the system of faults under study is well characterized. For these cases, the circular model needs to be linked to large uncertainties that cover these issues.

In modern studies performance design analysis of engineering structures dominated by long period motions, such as long bridges, tall buildings, extended pipes, base-isolation structures, needs a good knowledge of the spectral content in regions of long periods and of peak ground displacements (PGD), instead of PGA, PGV or spectral content in the central frequencies. This question requires a hazard analysis for PGD. The *fling*

caused by the wave passage with permanent displacement near the trace of a ruptured fault, is another topic of importance when dealing with sites in the neighbourhood of the fault. Some hazard computations at specific sites include directly the soil column with all the uncertainties carried out by these columns.

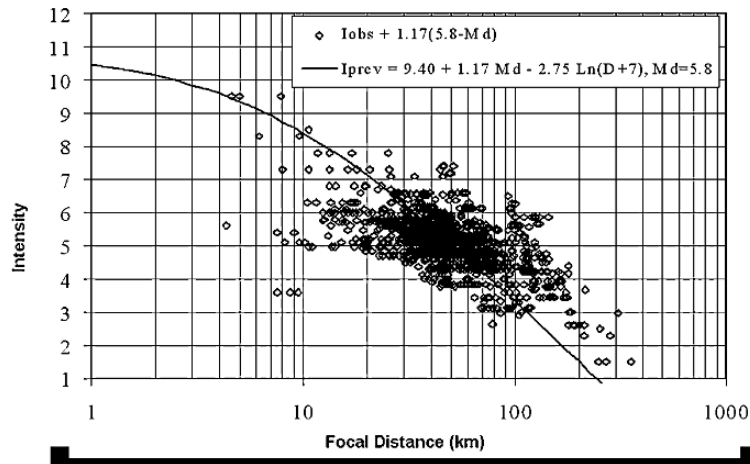


Fig. 2.5. Dispersion in the attenuation law (Paula and Oliveira, 1996)

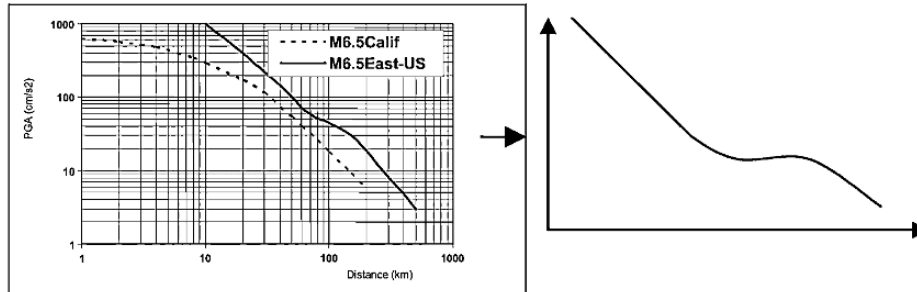


Fig. 2.6. Effect of strong reflection at the Moho in the attenuation law. (adapted from Bolt and Abrahamson, 2003)

2.6. Data to support hazard modelling

Several types of data are needed to perform hazard analysis. The degree of confidence on the final estimates depends on the accuracy of existing data and on the quality of modelling.

2.6.1. TYPE OF EXISTING DATA

Studies of seismic hazard on a seismic zone in an individual basis must use all the available data. Table 2.3 summarizes the type, utility, and quality of these data; and in

Table 2.4 emphasizes the importance of the type of data in the characterization of the seismicity of a region.

Table 2.3. Type, utility, and quality of available data

Field of knowledge	Time period	Type of information. Quality
Neotectonic	10 ⁷ to 10 ⁴ years	Long term plate tectonic motion
Paleoseismology	10 ⁵ to 10 ² years	Registry of strong events
Archeoseismology	6 × 10 ³ to 10 ³ years	Registry of strong events. Intensity
History (depends!)	Xth to XXth century	Intensity, epicentre, other data
Historical seismicity	1920 to 1970	Idem, with moderate precision
Instrumental seismicity	1970 to 1990	Idem, with higher precision
Recent seismicity	1990 up to now	Data with very high precision
Other data	Satellite, aerial images ...	
	Geodesy (GPS)	
	Radar(InSAR, PSInSAR)	
	Geomagnetism	
	Gravimetry	
	Electric field	

Table 2.4. Importance of the type of data

Historical seismicity ⇒ Interpretation ⇒ Intensities, isosseismals, damage distribution
Neotectonic ⇒ Identification of lineaments, blind structures, faults and their activity, mechanism and rupture length, recurrence, deformation in the long term
Instrumental seismicity ⇒ lineaments, mechanisms; recurrence, attenuation
Geodesy, inSAR, etc. ⇒ lineaments, mechanisms, rapid deformations, quality in all determinations
Paleoseismology ⇒ active faults, magnitude, intensity, recurrence

As may be seen, very exact data were obtained only for the last few years due to the launching of sophisticated instrumentation. On the other hand, historical seismicity can inform on longer recurrence intervals but their data are cruder.

In a broad sense, the level of precision is opposite to the time interval that represents the data, although this depends on the analyzed variables. In general, strong earthquakes are separated by long quiescence intervals, in which it is not possible to collect data. For this case, slow deformations and the evolution of strong events are the more important sources of information to predict the maximum values of the seismic parameters.

All the available data are important not only to characterize the occurrence process (interval, magnitude, and location of the event) but also to establish the attenuation laws, the effect site analysis, etc. Data bases are growing everywhere nowadays, and to verify the uniformity of the Earth processes it is advisable to compare data recorded in similar conditions. The pioneering work of Johnston (1996a and 1996b) on the

determination of the Seismic Moment in the stable Continental Region of North America is a good example of this procedure. Nevertheless, in many regions few data are available due to the absence of instrumentation or investigation studies. In that case, the best thing is to look for laws obtained in similar seismotectonic environments, such as the recurrence law of Gutenberg-Richter (value of b, \dots) and the attenuation models. In regions of lower seismicity within intraplate locations it may be even more difficult to identify fault structures, such as the Umbria-Marchè (Italy) region, with epicentres dispersed in the horizontal plane, where it is difficult to visualize fault plane structures.

2.6.2. QUALITY IN EARTHQUAKE CATALOGUES

In the last decade, a great effort has been made to qualify the data presented in seismic catalogues especially that concerns the historical parts. Many authors are presenting data always referring to the written sources. Two types of catalogues are available: (i) descriptive catalogues, containing all the information, and (ii) parametric catalogues, where the data are already interpreted. The former type of data requires extra time for interpretation, but, in the second one, the quality of the presented parameter values may not be known.

Historical information also varies from region to region, depending on the seismic activity of any particular epoch but also on the development of such region.

More recently, the emphasis on data qualification has become a major issue. For example, the completeness of catalogues for events of low magnitude; the compatibility of maximum magnitudes with the historical data; and the neotectonic evidence, obtained through paleoseismicity and archeoseismology information, which enhances the occurrence of large events in epochs prior to historical data, are considered in most studies for important structures. The significance of these latter developments has been emphasised since large events have occurred in regions apparently without historical seismic evidence. The earthquakes of Kobe (1995), Athens (1999) and Bam (2003) have occurred in geological structures which did not exhibit activity for more than one thousand years.

The case of China shows good descriptions a few centuries before Christ, while in California the oldest historical records are only two centuries old. For Europe, initiatives have been taken promoting the quality of data in historical catalogues (Project EBECED, Albini and Stucchi, 1997).

The first period of instrumental seismicity, from early 1890 up to 1950, has been revisited in order to use historical records obtained in the first seismographs to recalculate magnitude values with much higher accuracy and, in a few cases, to obtain focal mechanisms. Several examples of large events in the decade of 1910-1920 illustrate the characterization of parameter values of historical earthquakes (Benavente, 1909), where magnitude values were fixed in the interval 5.8–6.3, while all previous studies indicate values in the range 6–7.5.

A “Quality Factor” should always be linked to parameters such as location, depth, and magnitude. In this respect, a revision of intensity data of historical events has brought an increase of quality in data treatment by using large amounts of information, which are important to emphasize inconsistencies or systematic anomalous behaviour in

certain locations. This might be caused by site-effects due to surface geology or topography, by radiation patterns in the near field, or by focusing energy due to the presence of heterogeneities or specific wave packages.

Archeoseismicity is an added value from recent advancements in dating with great precision archeological artefacts. This new tool is essential for assessing pre-historical events. Old civilizations, such as the Greek and Roman in Europe, the Babylonian in the Middle East, the Chinese, the Arabic and the Spanish–American can also give important information on archeoseismicity through the re-evaluation of damage caused by earthquakes.

Both digital modelling of Terrain and of bathymetry detail, coupled with aerial photographs and satellite pictures, have enhanced the visualization of geologic surface discontinuities, indicating areas for better geological characterization. This may function as a screening for setting higher priority areas for monitoring.

Movements at the plate level, detected from the SAR and other techniques, may point to areas of higher stress concentration. Long-term international slippage, which is related to the integrated energy dissipation, is also a good indicator of overall slip concentration.

2.6.3. INCORPORATION OF UNCERTAINTIES

As already stated, uncertainties are present in all components of the hazard analysis process, from basic input data to lack of knowledge. The modelling can take into consideration some of these uncertainties by introducing additional random variables, such as upper limits of magnitude values, the attenuation law about the mean curve, or the geographical source distribution. Alternative models for data interpretation and for analytical expressions can be computed using logic trees (Frankel, 1995). One simple example is the consideration of various source models, corresponding to different schools of thought in the tectonic interpretation. Another example considers fault segmentation, under different hypothesis of rupture. For the mathematical modelling, alternatives are the *source* and the *empirical methods*. In each one, a certain probability of acceptance may be assigned by expert opinion. Final hazard calculations combine the various alternatives in a weighted average (mean, mode, or median) hazard value.

Unfortunately, only a few design practitioners have an in-depth understanding of the limitations of PSHA applicability and sensitivity to the assumptions in underlying parameters. Discussion among specialists will go on for many years to come.

The influence of uncertainty in policy decisions derived from PSHA is that it may not provide uniform protection against seismic risk in the entire territory. Risk assessment may be over-conservative in some places and not conservative enough in other places (Wang, 2004). The use of PSHA for generating artificial ground motion records is not compatible with the physics of the earthquake phenomenon. Seismic consistent concept or disaggregation is better suited for this purpose.

The PSHA method based on a Poisson model is not compatible with the lack of stationarity observed in long periods of records. This problem is aggravated for the case of low seismicity areas, where large errors can be committed, especially if we are trying to extrapolate to much larger RPs than the span of the catalogue.

The duality between deterministic and probabilistic models is that the latter ones do not allow defining an upper limit or worst-case scenario, and implying a prior decision on the level of accepted probability of exceedance. Deterministic approaches evaluate the maximum expected ground motion at a site, resulting from the strongest potential earthquake at the nearer possible distance. They are generally more conservative, but do not take into account uncertainties or an estimate of the frequency of occurrence, which is needed by decision makers for planning purposes.

2.7. Results and Illustrations

2.7.1. SOME EXAMPLES. INTERNATIONAL INITIATIVES

Most of the studies of the seismic hazard made in various countries and regions, were developed to provide more suitable support for the definition of code maps codes; and also to visualize, on regional or country scales, the areas of greater interest with respect to earthquake damage scenarios, etc.

An example of an old study made in mid 1980's was the Canadian Hazard Map which gave rise to the definition of 6 zones, Figure 2.7 (*in* Atkinson, 2004). In this study, as in many others at the epoch, source zones were mainly based on seismicity pattern, particularly of the instrumental period, with weak link to geological active structures which at the time were poorly known in several instances. New approaches (*in* Atkinson, 2004) updated this map using more refined source areas and algorithms.

The compilation of McGuire (IASPEI, 1993) on the geographical distribution of the seismic hazard in the world is a good documentary reference on the methods for calculation of the seismic hazard in different countries. Nevertheless, due to the uncertainties associated to these predictions, all the countries continue updating their studies.

Similar efforts were made by IASPEI with the GSHAP Project which was launched in early 1990 and was completed in 1999 (Giardini et al. 1999). This Project, aiming at obtaining hazard estimation for the entire World, had the great virtue of putting together experts from different countries speaking the same language and sharing the same concerns. A good outcome was the necessity of solving border problems in neighbouring countries where hazard discontinuities should not be caused just by country borders. However, the results obtained should be viewed with caution because the specificities of each region could not be totally contemplated and the working scale was not too detailed.

The more detailed and continuously updated work comes from the Working Group on California Earthquake Probabilities (WGCEP), where a large spectrum of experts participate (Neotectonics, Seismology, Engineering Seismology) which have been using the most reliable data and techniques as presented in the previous sections to produce hazard estimates with a tendency to reduce uncertainties. The first publication (WGCEP, 1988) goes back to 1988 dealing only with occurrence probabilities of large earthquakes in the San Andreas Fault, and since then, this study was extended to Southern California (WGCEP, 1995), San Francisco (WGCEP, 2002). The main results are expressed in the form of the probability of exceedance of a PGA, for a period of 30 years starting when the report was issued (Figure 2.8).

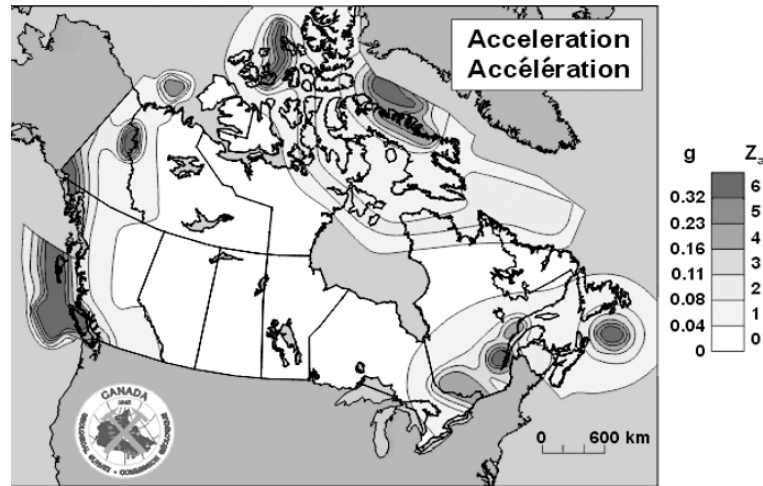


Fig. 2.7 Canadian Acceleration zoning map: 1985 NBCCPGA with 10% exceedance per 50 years - 500 year return period (*in Atkinson, 2004*)

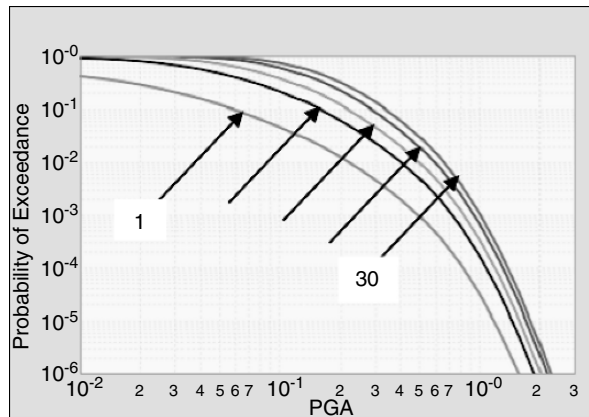


Fig. 2.8. Seismic hazard for San Francisco (WGCEP, 2002) for 1, 5, 10, 20 and 30 yrs

One of the recent examples in Europe is France. The French Ministries of Equipment and Environment have undertaken the revision of seismic zonation of metropolitan France and French West Indies in order to satisfy the Eurocode 8 requirements. This revision is based on a probabilistic seismic hazard assessment carried out to obtain and justify the seismic hazard maps in terms of spectral accelerations at four return periods: 100, 475, 975 and 1975 years (Figure 2.9). The probabilistic model developed by GEOTER takes into account all seismic and geologic data available in France up to the moment of the study (Martin et al., 2002). It allows considering the epistemic and aleatory uncertainties associated to the input hypothesis and data interpretation. Propagation of these uncertainties is based on the logic tree method coupled to a Monte Carlo process. Results are therefore explained in terms of statistical values of spectral accelerations resulting from a weighting process. Maps of median and mean PSHA

values will allow the revision of seismic zones where Eurocode will be enforced.

2.7.2. ANALYSIS OF UNCERTAINTY

The dispersion of results obtained using different approaches (seismic sources, models of attenuation, etc.) are quite significant, as shown in Table 2.5, where Peak Ground Acceleration for the city of Faro (south of Portugal) were obtained by several authors. The studies of Estevão and Oliveira (1999) consider the influence of the focal depth in a zone next to Faro. The interval of values (almost at a relation 1:3) indicated the large existing uncertainty.

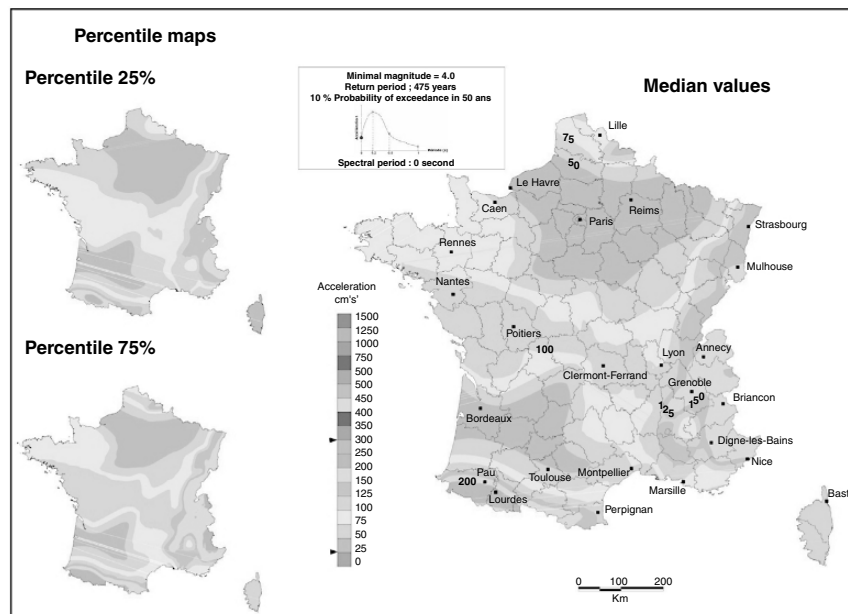


Fig. 2.9. Maps of median and different percentiles of Peak Ground Acceleration (cm/s^2), horizontal component, for a $\text{RP}=475$ years on France (Martin et al., 2002)

Larger uncertainties were already present in the studies made in 1977 for Portugal, Figure 2.10 – a site near Lisbon. In this case several alternative models and work hypotheses were used such as 2 algorithms, 3 source models, 2 catalogue epochs (prior to 1900 and post 1900), 2 attenuation laws. Mean and $\text{mean}+2\sigma$, computed at an equal weighted basis, are presented in Figure 2.10. Great differences are observed in the hazard estimates, representing both stochastic and epistemic uncertainties. Mean values, used for the definition of seismic code in Portugal (RSA, 1985), are still used nowadays, even though uncertainty range has been diminishing significantly through the last 30 years.

Table 2.5. Influence of the method of computation and type of seismic sources used to determine the seismic hazard in the towns of Faro, South of Portugal and Lisbon (RP of 10^3 years; units in cm/s^2)

Faro			Lisbon		
Oliveira, 1977	Campos-Costa, 1993	Sousa and Oliveira, 1997	Estêvão and Oliveira, 1999 Source 1	Source 2	Source 3
177	220	300	188	265	472

2.8. PSHA and the design of civil engineering constructions

The traditional design process of civil engineering constructions is carried out taking into account a set of requirements that must be fulfilled during the design lifetime of the structure, usually taken as 50 years for common buildings.

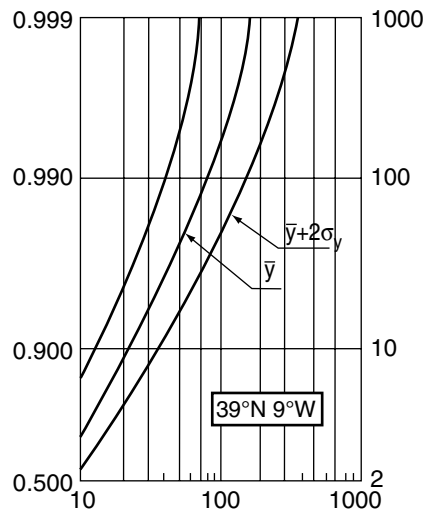


Fig. 2.10. Common uncertainties in hazard analysis (mean values and mean $\pm 2\sigma$) (Oliveira, 1987)

Those requirements are mathematically reflected in design codes by *limit state equations* which, ultimately, are deemed to protect human life and to mitigate the social-economic impact arising from load environment. Usually, two *limit states* are considered: the service or operational limit state and the ultimate limit state. Such *limit state equations* must take into account the lack of knowledge about the actual structural behaviour and load intensities that the construction will undergo during its lifetime.

Uncertainties are reflected in code design practice by a set of partial safety factors affecting the characteristic values of the design control variables (structural resistances and structural actions effects) in what is generally referred as *Level 1* reliability analysis (Borges and Castanheta, 1968). The values of safety factors are, in principle, calibrated for a target reliability level for each limit state: for the case of *ultimate limit state*, corresponding to a scenario where the structural collapse may occur, it is generally accepted that the reliability level to be achieved corresponds to an annual probability of

exceedance of 10^{-4} to 10^{-7} (i.e. similar to having 1 over 10 000 to 10 000 000 structures, depending on their importance, with possible collapse during each year).

Safety factors for design of structures at *Level 1* can be calibrated using sophisticated *Reliability Analysis* leading to *Level 3* analysis, where target probabilities are computed to attain certain limit states.

This apparently high level of safety of the civil engineering constructions (comparing to other construction industries such as aeronautic and automotive) comes from several specific issues, related to: (i) the social risk aversion effect in relation to collapse of houses and other civil engineering constructions; (ii) direct and indirect economic impact of a catastrophic events affecting large urban areas (risk accumulation effect); and (iii) the unpredictable, and/or uncontrolled, nature of natural phenomena underlying the catastrophe (natural hazard effect).

Thus, the characterization of seismic action, based on PSHA, is a necessary condition, although not sufficient for the definition of the design seismic action to be used either in design of structures (*Level 1*) or in the calibration of safety factors in *Level 3*; and essential for design purposes, such as building construction, civil protection management, insurance policies, etc.

In the regions around the world exhibiting the highest seismic hazard, the modern seismic design practice of civil engineering structures is based on the capacity design rules which imply that structural systems can develop sustainable hysteretic behaviour to a certain extent under rare and severe seismic actions (generally associated to 475 years return period). The high level of safety required for important structures implies that the probabilistic characterization of seismic action should involve very long return periods.

The criteria of accepting that structures can be damaged to a certain degree under extreme actions, such as intense earthquakes, is related to the fact that otherwise structural systems for civil engineering constructions would have a great amount of resistance not effective for daily use, as those actions are rare, thus becoming economically inefficient. In that sense, a capacity designed structure, can be considered smart structure because it automatically adjust structural characteristics, in response to the change in external disturbance and environments, toward structural safety and serviceability as well as the elongation of structural service life.

However, recent earthquakes have shown that indirect economic impacts associated to structural damage (business interruption) are significant even for moderate events. This is the case of the 1994 Northridge M6.4 earthquake which caused 30 000 million of Euros losses. Consequently, the design for ductility under extreme actions, based on capacity design rules, is being criticized since then, research in the domain of the seismic protection systems for use in civil engineering has been intensified towards a more advanced approach of design known as performance based design.

The probabilistic approach to seismic hazard characterisation is very compatible with current trends in earthquake engineering and the recent developments of performance-based design. Examples are given in the SEAOC Vision 2000 (1996), FEMA 273, and EERI (1998). (See Figure 1.7, Chapter 1). In the performance-based design an explicit prediction of the structural performance at different levels of ground motion are set,

according to performance objectives.

In general terms, we should specify a given level of intensity, related to a *RP* to perform the design process. It is generally accepted, for common building construction, that the seismic intensity corresponding to the 475 years *RP* is an adequate level to check the non-collapse criteria. Also, for the operational criteria, the 95 year *RP* is commonly accepted. This means that some level of risk is present in every situation. Independently of the design process and design level it is important to be able to evaluate the probability that those limit states, for a given life-time, are surpassed.

The concept of risk and the methods for its evaluation are adequate approaches for analysing the problem, which in mathematical terms are expressed by the total probability theorem, in the form of

$$P[D > d_L] = \int_I P[D > d_L | I] \cdot h(I) \cdot dI \tag{2.25}$$

where D is an appropriate response control variable of the system, d_L is the quantification of given “Limit State” expressed in terms of that control variable and, $h(I)$, is the hazard density function. The conditional probability $P[D > d_L | I]$ reflects the uncertainty of the response fragility of the structural system (Figure 2.11). Bazzurro and Cornel (1999), McGuire (2004) and Pinto et al. (2004) have recently addressed this problem in the context of reliability analysis applied to the definition of seismic action.

These may range from a continuous function keeping the structure operational for relatively small, frequent ground motions; to limiting damage below the life safety threshold in severe, less frequent ground motions; and to preventing collapse for very severe, infrequent ground motions. Each performance objective is associated with an annual probability of occurrence (Figure 2.11).

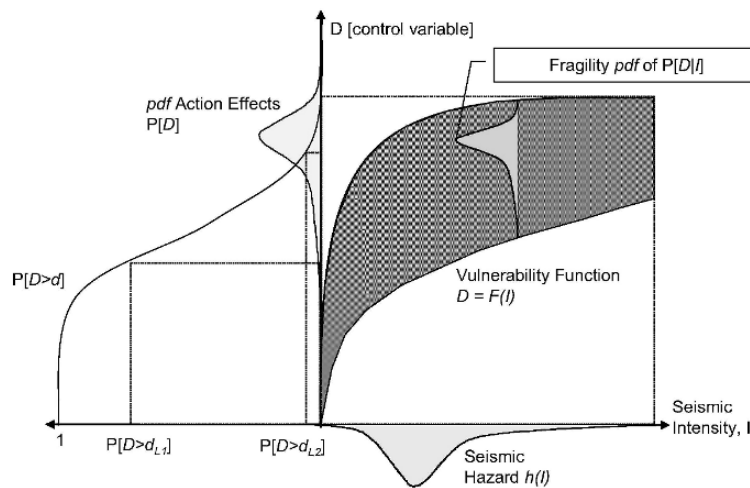


Fig. 2.11. Schematic representation for computing the probability $P[D > dL]$

This Figure pretends to synthesize the whole reliability procedure from *hazard* $h(I)$ to the quantification of the probability of Limit State, through the use of *vulnerability function* and the associated *fragility*. This probability of Limit State is the one that

counts and should be the basis for definition of input motion and the corresponding RP. In that sense, the generalized use of 475 and 95 years RP, independently of low, medium or high seismically active regions, should be criticised if limit state values (d_{Li}) are kept constant. It must be recognized that the steepest of hazard function (smaller variance of hazard function) (Campos-Costa, 1994, Pinto et al., 2004 and Duarte et al., 1992) plays an important role in the definition of RP to be used in lower levels of seismic design. On the other hand, the bi-modal hazard function generated by the presence of *characteristic earthquakes* will also be important in this regard.

2.9. Final tendencies of the future development and considerations

2.9.1. NEW QUESTIONS

Although much progress has taken place in the study of the seismic hazard which includes, naturally, the analysis of the uncertainty (representativeness of the data, incompleteness of the seismic catalogue, and period of return for great and small intervals), there still are a large number of open questions that cause much preoccupation among specialists in the matter, some of which are cited below.

- The definition of the levels of seismic hazard (criteria for the selection of the period of reference return). The analysis of the seismic hazard based on evolution of events throughout time, so that it reflects the observed occurrences, and the permanent concern of specialists.
- Software PSHA should allow the inclusion of all new advances in the entire process of earthquake source-propagation-site, such as time-dependent occurrences, alternative approaches by logic tree techniques and specific source-propagation models.
- Bayesian methods have had relatively little acceptance in studies of the seismic hazard (Esteva, 1968); nevertheless, they can be very useful to make a continuous update with new incoming information such as strong motion data, occurrence of new events, etc., consequently reducing the interval of uncertainties.
- Hazard maps in terms of displacement spectra are a need for studies for long period structures such as tall buildings, long bridges, buried pipelines and base-isolated structures.

**CHAPTER 3
OBSERVATION, CHARACTERIZATION AND PREDICTION OF STRONG
GROUND MOTION**

X. Goula and T. Susagna
Institut Cartogràfic de Catalunya. Barcelona, Spain

3.1. Introduction

A seismic risk mitigation strategy has two main technical legs: to construct performing buildings and other structures using an aseismic design and to prepare emergency plans using realistic seismic scenarios. Both technical actions need a precise definition of the seismic action of potentially damaging earthquakes by means of measurable parameters related to shear stresses and strains affecting structures, which are ground motion acceleration and displacement.

An important challenge for seismic risk mitigation is thus to develop methodologies for seismic hazard analysis, and to assess vulnerability of structures and cost functions in terms of ground motion parameters.

In recent decades much progress was made in the study of strong ground motion produced by earthquakes and its application to earthquake engineering. New data and analysis have given us more and more accurate and reliable empirical estimations of strong ground motion for future earthquakes. In parallel, the development of theoretical methods led to the proposition of new explanatory models of the seismic strong ground motions.

In this chapter, after remarking on new advances in instrumentation and its capacity to measure and disseminate strong ground motion data, we describe the main parameters and factors useful in characterizing ground motion. The main components of these more useful predictive methods of ground motion for future earthquakes are analysed. Finally, different formal aspects concerning the definition of seismic actions from the predicted strong ground motion are discussed.

3.2. Strong ground motion measurements

3.2.1. INSTRUMENTATION AND MAJOR NETWORKS

The development of instrumentation with digital recording, in the 1980's, allowed a considerable improvement in the quality of accelerograms and therefore a greater reliability in their interpretation. Let us mention some of the most important improvements:

- Quality of the record, when suppressing the manipulations of the old analogue records (photographic process, digitisation, filtering processes, etc.).
- Activation of the detection system for small ground motions (< 0.01 g), with the consequent availability of a greater number of records.
- Great dynamic range, increasing the resolution for small ground motions.

- Greater reliability in the lower frequency content of the record when eliminating possible drifts in the record system that, in the old analogue instruments, was necessary to correct by numerical methods.
- Greater reliability in the content of high frequencies provided by the new force-balance sensors.

This situation has been further improved in recent years with the appearance of converters A/D of 24 bits, with which the dynamic range has extended enormously, allowing the recording not only of strong motions, but also of weak motions, until now the dominion of seismographs; thus for example it is possible to record ground motions of 10^{-6} or $10^{-7}g$ for accelerographs whose maximum scale is $1g$. Actually, the resolution in many cases is determined by the background noise of the site.

3.2.1.1. Major Networks of accelerometers

In the last few years dense networks of accelerometers have been implemented. This has been possible thanks to advances in telecommunications that allow us to centralize the data in real time.

A clear example can be found in the Kyushin Net (K-net) network in Japan (Kinoshita, 2003) with about 1000 homogenous instruments (see Figure 3.1). It was created after the earthquake of Kobe of 1995, with some basic characteristics:

- Systematic observation of the ground motion.
- Uniform distribution of the stations (with a stations spacing of about 25 km).
- Dissemination of the data via Internet in few days after the event occurrence.
- Information on the soil column at each station's site, obtained by means of down-hole measurement, to provide the users with a useful tool for interpreting soil effects.

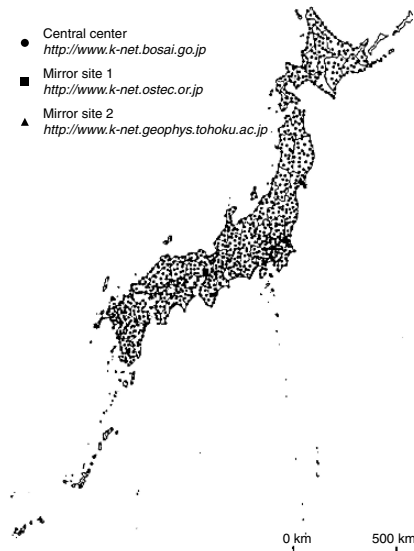


Fig. 3.1. Locations of the K-net network in Japan (Kinoshita, 2003)

Another region dense with instrumentation is Taiwan where several networks of accelerometers have been installed with different purposes: study of rupture process of seismic faults, evaluation of soil-structure interaction, rapid earthquake information, and monitoring buildings and bridges.

In Figure 3.2 we can see the distribution of the 640 free-field accelerometers (as of the end of 2000) belonging to the Central Weather Bureau (CWB), the official centre in charge of monitoring earthquakes in Taiwan (Shing et al., 2003). CWB also has 56 instruments in buildings and bridges. In order to produce an early warning after the occurrence of an earthquake, CWB has 80 instruments that continuously transmit data, via telephone, to the CWB headquarters. For the analysis of rupture process, dense arrays of accelerometers have been implemented. This is the case of SMART-1 that was created in the 1980's with 43 accelerographs installed in three concentric circles of radii 200 m, 1 km and 2 km, respectively, of radio and SMART-2, settled in the 1990's.

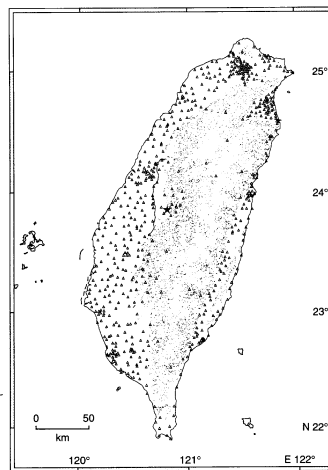


Fig. 3.2. Distribution of the 640 free-field accelerometers of the CWB (Shing et al., 2003)

In U.S.A. the California Strong Motion Instrumentation Program (CSMIP) was established in 1972 by California Legislation to obtain valuable earthquake data for the engineering and scientific communities through a state-wide network of strong motion instruments. The program has installed more than 900 stations, including 650 ground-response stations, 170 buildings, 20 dams and 60 bridges.

In 1997, a joint project, TriNet, between the CSMIP, Caltech and USGS at Pasadena was funded by the Federal Emergency Management Agency through the California Office of Emergency Services. The goals of the project are to record and rapidly communicate ground shaking information in southern California, and to analyse the data for the improvement of seismic codes and standards (Hauksson et al., 2003).

In 2001, the California Office of Emergency Services started to improve the California Integrated Seismic Network (CISN), a state-wide system that includes the TriNet system. Five organizations have collaborated to form the CISN in order to further the

goals of earthquake monitoring. The founding members of the CISN include: California Geological Survey Caltech Seismological Laboratory, Berkeley Seismological Laboratory, USGS Menlo Park, and the USGS Pasadena. The California Governor's Office of Emergency Services is an ex-officio participant in the CISN.

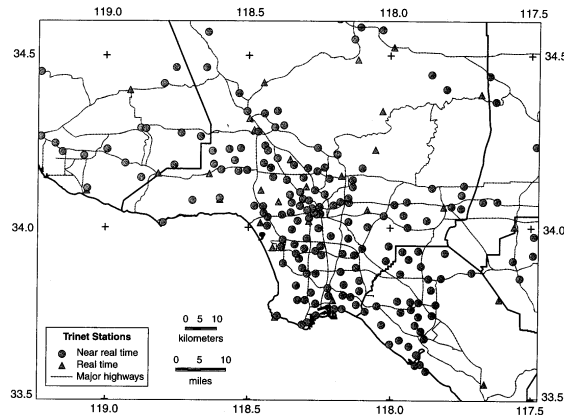


Fig. 3.3. TriNet strong-motion and broadband stations in the greater Los Angeles area. (Hauksson et al., 2003)

3.2.1.2. Broad Band seismographic stations

The improvements of the accelerometers also have been accompanied by the appearance of Broad-Band seismographs (velocity sensors), that allow with a great resolution the record of very low frequencies (<0.05 Hz), completing therefore the records of acceleration for weak motions and long periods, useful for structures sensible to such periods, and for the definition of seismological parameters (Hauskov and Alguacil, 2004).

3.2.2. ANALYSIS OF STRONG MOTION RECORDS

Until the 1980's strong ground motion databases contained accelerograms obtained from analogue records corresponding to earthquakes that occurred in California and some countries of the Mediterranean area.

For many years, these data were the base of the development of empirical methods of determination of the seismic actions that still today are used in the building regulations in many countries.

However, to some extent, all these data suffered from some common problems:

- Due to the high values of activation of the recording system ($PGA=0.01g$) only records of the strongest ground motions were obtained and, consequently, the resulting datasets are biased because of the lack of records of weak and moderate acceleration ground motions.
- Very often, only one part of the accelerogram was recorded, because the system was activated only by the more energetic part of the signal (S or surface waves).

- The process of digitisation of the signal gave rise to significant distortions of the frequency content. In the low frequencies, due to the problems associated to the base line shift, a high pass filter was necessary, resulting in either excessive cuts of important information, or insufficient cuts, resulting in an over-estimation of the content in low frequencies, which is mainly seen in the displacement time histories obtained by a double integration.
- Due to the fact that the natural frequencies of the accelerometers used to be 25 Hz or even lower, the content in high frequencies was difficult to be reliably estimated because of its dependence on the recovery process and the signal sampling frequency.

From the end of the 1980's databases have become richer with much data of greater quality, coming from a much larger number of digital instruments of the new networks. Let us mention some examples of earthquakes that produced a huge quantity of records: Loma Prieta (California), 1989, of $M=6.9$; Landers (California), 1992, of $M=7.3$; Northridge (California), 1994, of $M=6.7$; Kobe (Japan), 1995, of $M=6.9$; Chi-chi (Taiwan), 1999 of $M_w=7.6$; Kocaeli (Turkey), 1999 of $M_w=7.4$; Bam (Iran), 2003 of $M_w=6.8$. On the contrary it is important to notice the fact that, even recently, some damaging earthquakes occurred in regions that still have a poor coverage of accelerographs as, for example, Dominican Republic, September 2003, of $M_w=6.5$ or Al Hoceima (Morroco), February 2004 of $M_w=6.5$.

The extensive amount of data obtained in all of these events has shown a great variability of the recorded ground motion. These data have contributed, as it will be seen later, to the knowledge of the different factors that take part in the resulting characteristics of earthquake ground motion, mainly:

- The complexity of the time and space distributions of the rupture in the fault plane.
- The irregularities in the rupture that give rise to records of acceleration incoherent in time and with high variability in the values of peak ground acceleration.
- The phenomena of directivity and fling, amplifying the ground motion (lower frequency band) in the direction of the propagation of the rupture.
- The local effects, amplification of the ground motion for different frequencies, depending on the geologic and topographic characteristics of the recording site.

3.2.3. DATA FROM MODERATE EARTHQUAKES

The new instrumentation and the increase of the number of installed instruments allowed to obtain earthquake records of moderate magnitude, between 5.0 and 6.0, with non-negligible damaging capacity; moreover, weak ground motions that until a few years ago were not recorded, because they lay below the resolution of the old accelerometers and over the values of saturation of the seismographs, are now available.

Let us mention, as an example, some of the earthquakes of moderate magnitude recently recorded in the Mediterranean zone, some of them in areas in which accelerograms were not available until now.

- The series of Adra (Spain), with two earthquakes of $m_b=5.0$, occurred on 23-12-1993 and the 4-01-1994 in strike-slip faults, with normal component. They produced moderate damages (I=VI-VII) in the epicentral region. Records were obtained, with maximum values of acceleration of 0.025 g and 0.03 g in Adra for the first and the second event, located at 6 km and 30 km, respectively from this town (Martín et al., 1996).
- The earthquake of Eastern French Pyrenees of $M_L=5.0$, occurred on 18-02-1996 in a strike-slip fault, with some vertical component. It produced weak damages in the region of San Pau de Fenollet (I=VI). A record of peak ground acceleration of 0.04 g was obtained within 8 km of the epicentre and maximum values of 0.004 g and 0.002 g at 70 km of distance (ICC, 1997).
- The earthquake of Konitsa (Greece) of the 5-08-1996, of $M=5.6$ was recorded at 15 km from the epicentre with a value of maximum acceleration of 0.4 g in the low part of the city of Konitsa (on soft soil), and of 0.17 g in the high part (on rock). These acceleration values agree with the observed larger damages in the low part of the city (Papaioannou et al., 1997).
- The series of earthquakes of Umbria-Marche in Italy, with two earthquakes of magnitudes 5.6 and 5.8, occurring within a 9 hours interval from the 26-09-1997. They caused significant damages (I>VIII) mainly throughout a NW direction, which corresponds to the direction of propagation of the two ruptures (in opposite senses), with mechanisms of normal fault. In the epicentral zone, values of 0.3 g in a lacustrine zone (Colfiorito) and of 0.5 g in the direction of the rupture (in Nocera-Umbra), at about 20 km of the epicentre were recorded (ENEL, 1998).
- The earthquake of Mula (Spain) occurred on 2-02-1999 with a magnitude of 5.0. It caused moderate damages (I=VII) in the epicentral area, near Mula. Records of acceleration in several localities were obtained, with a value of 0.012 g at a distance of 20 km of the epicentre (IGN, 1999b).
- The Nice (France) earthquake of magnitude 4.7 in February 2001, produced accelerograms with maximum values of 0.04 g at about 30 km from the epicentre, which was located offshore. Some records were obtained at up to 300 km of distance (RAP, www-rap.obs.ujf-grenoble.fr).
- The earthquake in central Pyrenees 16-05-2002 with a magnitude of 4.7 produced records of a maximum value of 0.045 g at an epicentral distance around 12 km. Damages corresponding to intensity VII-VIII in the epicentral area were reported (RAP, www-rap.obs.ujf-grenoble.fr).

The analysis of this new set of observations allows us to point out the following:

- For the earthquakes of the Western Mediterranean region, Adra, 1993-1994; Eastern French Pyrenees, 1996; Mula, 1999; Nice, 2001 and Central Pyrenees, 2002 weak acceleration values rather lower than 0.05 g, have been observed. As it can be seen in Figure 3.4, the recorded values are lower than those obtained by average curves of attenuation proposed by Sabetta and Pugliese (1996), Ambraseys et al. (1996) or Sadigh et al. (1997).

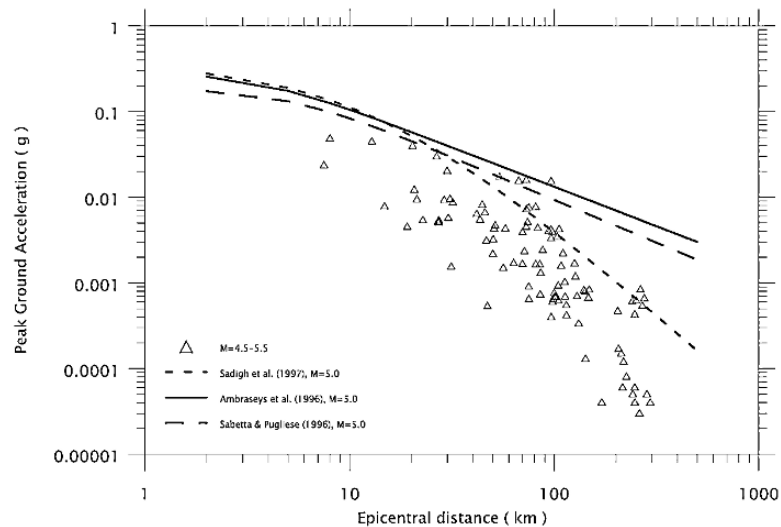


Fig. 3.4. Peak ground acceleration recorded from recent western Mediterranean earthquakes compared to some average curves proposed by different authors (Tapia, personal communication)

- For the earthquakes of the Central and Eastern parts of the Mediterranean region, significant values of acceleration (0.4g) have been observed, as was the case of the city of Konitsa (Greece); these large acceleration values are associated with soil amplification. For the earthquakes of Umbria-Marche, recorded values of 0.3 g and 0.5 g in Nocera-Umbra seem to be related to effects of local amplification and also to the directivity effects.

Therefore, the differences seen between the attenuation behaviour in the two regions for moderate (between 5 and 6) magnitude events are probably related to the particularities of the tectonic characteristics of the two regions. Increasing the recordings in the future and detailed analysis of the data will yield a better interpretation of these observations (Tapia et al., 2005).

Sections 3.3 and 3.4 present a more detailed description concerning the variables that affect the characteristics of the seismic ground motion. An overview of the models currently used for predicting ground motion will also be given.

3.2.4. DISSEMINATION OF STRONG GROUND MOTION DATA

Until the 1980's the necessary data for the study and prediction of seismic actions were only available through a few national and international agencies that some times did not made their data easily available to the public. The more known strong motion databases were those of the National Geophysical Data Center (NOAA, USA) and the European database (ENEA/ENEL, CEA, Imperial College).

In the last few years, the possibility of data storage in supports of great capacity (CD-ROM; DVD-ROM), the advances in communications (Internet) and the protocols of dissemination of the data (FTP, autodrm, etc.) have made possible an easy access of these data.

In USA, the Consortium of Organizations for Strong-Motion Observation Systems (COSMOS) Virtual Data Center www.db.cosmos-eq.org is a portal to other servers where the data is stored and maintained, usually by the owner of the data. Several International contributing members are associated to this virtual data centre. Data can easily be downloaded.

In Japan, different agencies belonging to essential infrastructures, as for example Ports and Airports (PARI, 2003) are providing strong motion data.

In Europe, several networks produced collections of their own records; an example of these facilities is the CD-ROM published by the IGN (IGN, 1999a) with accelerograms recorded in Spain between 1984 and 1997 or the availability of the French Accelerographic Network (RAP, www-rap.obs.ujf-grenoble.fr) data on the Internet. The European Strong-Motion Database www.isesd.cv.ic.ac.uk provides an interactive, fully relational database and databank with more than 3,000 uniformly processed and formatted European strong-motion records and associated earthquake, station and waveform-parameters. The user can search the database and databank interactively and download selected strong-motion records and associated parameters. Information about European organizations involved in strong-motion recordings is also available.

3.3. Explanatory variables of ground motion

The parameters or variables that explain ground motion or seismic action in one site can be grouped in three categories:

- Size and characteristics of the source of the earthquake.
- Position of the site with respect to the source.
- Local characteristics of the site.

For a probabilistic definition of ground motion (SSHAC, 1995) the incorporation of a new variable to a model is justified when an important reduction of the dispersion of the computed ground motion is obtained and when its probabilistic distribution can be proposed. In general a relation between the number and type of used variables and the associated uncertainties exists.

3.3.1. CHARACTERIZATION OF THE SEISMIC SOURCE

The magnitude is the most used variable to measure the size of an earthquake. Multiple scales exist and it is therefore important to maintain coherence with use of the same scale throughout all the study of seismic risk. The magnitude can be defined in different ways:

- The instrumental magnitude is defined on an instrumental record and it is computed from the maximum amplitude and epicentral distance, in a logarithmic scale. M_L , m_b and M_s represent different scales according to the considered distances and waves.
- The Moment magnitude, M_w (Hanks and Kanamori, 1979) is different from the instrumental one as it is related to a physical parameter of the seismic source, the

seismic moment, although actually the seismic moment is not observed directly, but computed from indirect observations (usually seismic records and seldom geodesic or geologic measurements).

- For earthquakes previous to the instrumental period the magnitude can be deduced from the macroseismic observations (intensity), using empirical correlations.

For engineering applications the use of local magnitude, M_L is frequent, according to the original definition of Richter (1935), using records limited in distance to a few hundreds of kilometres. In recent years the Moment magnitude, M_w , has been used for moderate and large earthquakes. It correlates well with M_L for magnitudes between 3 and 6 and it is practically the same magnitude as obtained from surface waves, M_s , for large earthquakes, presenting the advantage of not showing saturation for values higher than 8.0.

As previously mentioned it is important to use the same magnitude scale throughout a study. Therefore, it is recommended to use unified criteria, in particular in the Euro-Mediterranean zone, where many regional and national agencies are involved.

Another characteristic of the source that affects the ground motion is the tectonic regime of the zone where the earthquake occurs (intraplate, zone of subduction, limit of plates, etc.). This characteristic usually is not specified in the available models, so the model must be adapted to the type of study region.

Another characteristic that affects the seismic ground motion is the earthquake focal mechanism (strike-slip, normal or inverse). It is not often used as an explanatory variable. Nevertheless, some relations of attenuation developed recently show that the values of the maximum acceleration (PGA) can be 20-30% greater for inverse faults than for strike-slip faults, for the same magnitude and focal distance (Abrahamson and Somerville, 1996; Boore et al., 1997). These differences can be explained by simple geometric reasons (Cocco, 1998).

The depth of the seismic source is also often not included explicitly as an explanatory variable in current practice, although it can play an important role in the observed ground motion.

3.3.2. LOCATION OF THE SITE WITH RESPECT TO THE EARTHQUAKE

The variable commonly used is distance. There are several ways to define distance:

- For small and moderate size the magnitude earthquake of the rupture is negligible in relation to the distance between the site and the earthquake. In these cases the hypocentral (focal) or the epicentral distance is used. The use of one or another must be consistent with the representation of the earthquake occurrence in source zones of two or three dimensions and the attenuation relationships used in the evaluation of the hazard.
- If the size of the rupture is not negligible in relation to the distance to the site, other definitions like the minimum distance to the rupture or its projection in the surface are used. As in the previous case, consistency with the other steps of the evaluation of the seismic hazard must be maintained.

Another characteristic in addition to the distance is the azimuth of the location with respect to the direction of propagation of the rupture. The physical phenomenon known as directivity causes larger ground motion in the direction of propagation of the rupture. The phenomenon is observed specially for low frequencies (<0.5 Hz) and it is not considered in most of the models of attenuation functions, being implicit in the dispersion of the data and therefore in the nonexplained dispersion. On the contrary, most theoretical models consider directivity. Observations of important space variations of seismic ground motion due to directivity exist, among others, in the earthquakes of Landers (California) of the 28 of June of 1992, Mw 7.3 (Bernard and Herrero, 1994); in the earthquake of Northridge of the 17 of January of 1994, Mw 6.7 (Wald et al., 1996) and in the earthquake of Kobe of the 16 of January of 1995, Mw 6.9; the directivity effects of all these event have been analyzed by Cocco, 1998. See an example in Figure 3.5.

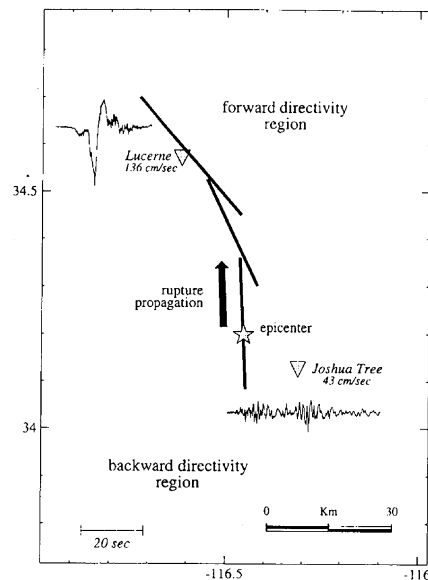


Fig. 3.5. Example of directivity of the rupture during the earthquake of Landers of 1992 (Cocco, 1998)

3.3.3. CHARACTERIZATION OF THE LOCAL EFFECTS

Almost all recent destructive earthquakes have shown the importance of amplification of the seismic ground motion due to local effects in distribution of the damage. Perhaps the most dramatic case happened on the 19 of September of 1985 in Mexico City due to an earthquake with epicentre 300 km away, in the zone of Guerrero in the Pacific coast; the waves of long period were amplified by lacustrine sediments of great thickness on which a great part of the city is founded.

Important amplifications also occurred in the Bay area of San Francisco due to the Loma Prieta earthquake of 1989; or in the most recent cases in the city of Los Angeles with the earthquake of Northridge of 1994 or in the city of Kobe in 1995, in which,

aside from having important other effects due to the rupture, as it has been previously seen, large amplifications were observed in the ground motion records leading to great damages.

On the other hand, measurements have been made in different places around the world and in many cases amplification factors are larger than 5 and even 10 in some frequencies. In the Mediterranean area such effects have been observed in cities like Thessaloniki and Corinth in Greece, Lisbon in Portugal, Nice and Grenoble in France, central Italy, etc. The cause of these amplifications is the presence of soft soils with different thicknesses as well as other aspects of the local topography (see chapter 4).

The local effects are better treated in studies at local level, for which it is important to have data relative to the dynamic properties of soils. Nevertheless, some variables that control the amplification and that have been used in predictive models of attenuation of the ground motion can be described. A synthesis of those studies can be found in Joyner and Boore (1988). Most studies only consider if the site is located on rock or in soft soil. Some studies have taken into account the thickness of sediments in a simplified way, considering only two categories: lower or higher than 30m (Sabetta and Pugliese, 1996), Figure 3.6, or the shear wave velocities in the first 30m (Boore et al., 1993, 1994).

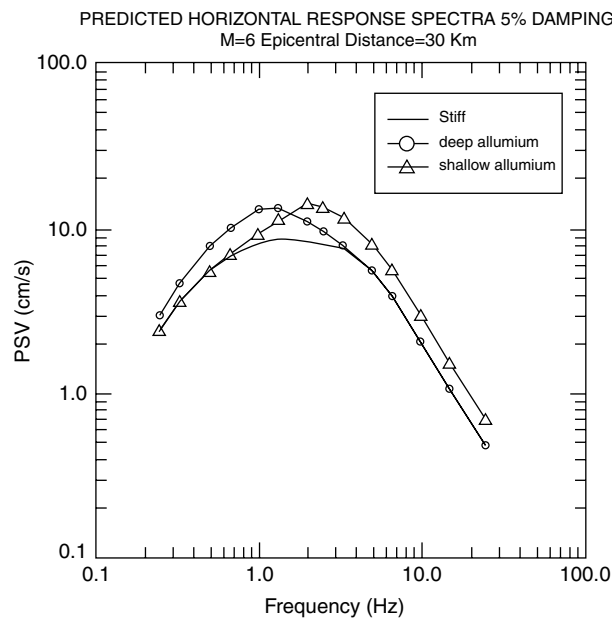


Fig. 3.6. Dependency of the horizontal synthetic spectra on site geology (Sabetta and Pugliese, 1996)

An important aspect is selection of the reference site or the type of hard rock contained in it. It is necessary to know the shear wave velocity of the site material. In most cases hard rock is considered to be those consistent materials with velocity higher than 750 m/s. In the case of larger velocities, for example 2800 m/s, which corresponds to rocks of the Palaeozoic age that have remained unaltered, effects of amplification can be observed in consistent or rocky ground sites ($v=750$ m/s). In any case it is important to choose the type of site of reference that is consistent with the used model of attenuation.

3.4. Predictive methods of ground motion

A brief description of some common components that appear in the predictive models (not only based on data) follows. The sequential consideration of the different components presented below gives rise to a so-called prediction model. We will understand by *method* a way or general procedure to make the prediction, whereas we will use the term *model* for a particular application of a method that allows calculation of the seismic ground motion.

3.4.1. EMPIRICAL METHODS

Empirical methods can be divided into methods using instrumental data and methods based on macroseismic data:

3.4.1.1. Methods that use instrumental recordings

For some specific studies it can be enough to have records of earthquakes of similar size, same type of fault and equal distance to the site.

For studies that require a definition of ground motion for different values of magnitude and distances it is usual to establish a regression analysis to fit a functional form to a set of available spectra. The details about those methods can be found in Joyner and Boore (1988), Boore et al. (1993, 1994), Sabetta and Pugliese (1996), among others. Differences in the results are mainly due to the data used, to the election of the explanatory variables and to the selected functional forms (Figure 3.7).

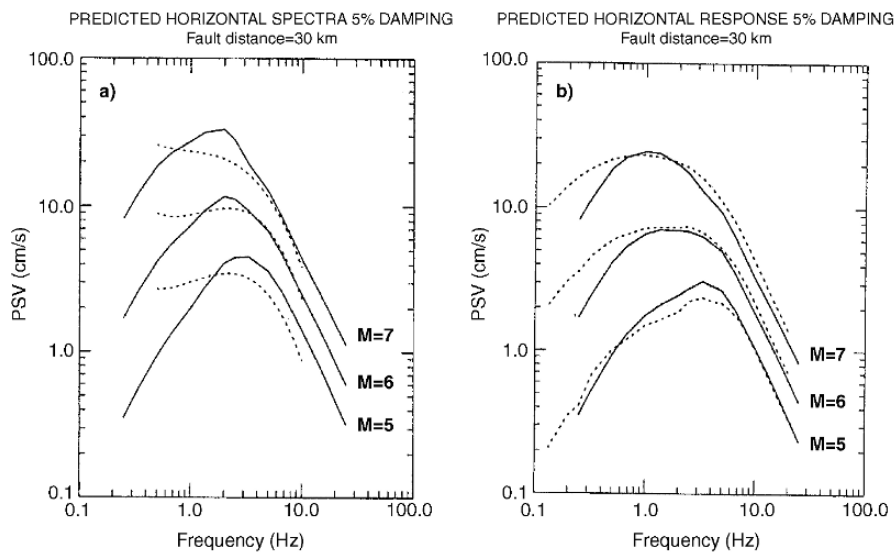


Fig. 3.7. a) Comparison of mean horizontal spectra from recent attenuation relationships: Boore et al. (1993, 1994) for a soft soil site, with Sabetta and Pugliese (1996) for a shallow alluvium site; b) Comparison of mean horizontal spectra from recent attenuation relationships: Sadigh (1993) for a rock site with Sabetta and Pugliese (1996) for a stiff site. (From Sabetta and Pugliese, 1996)

Most of these methods consider the type of soil of the recording site and the regressions are made classifying the type of soil in a simple way. In general, those methods are limited by the lack of data in some ranges of distance and magnitude, in particular for short distances and large magnitudes and also for distances larger than 100 km, (weak motions, until recently located below the threshold of the accelerograph). The introduction of new data and theoretical concepts has to help to eliminate possible bias in the deduced values.

3.4.1.2. *Methods that use macroseismic data*

In regions of moderate seismicity with a long series of macroseismic information available, macroseismic intensity is a useful variable to determine the laws of occurrence of earthquakes. In these cases, the ground motion at one site can be approached by the intensity deduced by attenuation laws adjusted from site intensity data observed during regional past earthquakes. Then, the seismic risk analysis can be carried out completely with the variable intensity, from the definition of the earthquake occurrence, through the expression of hazard maps, to the use of damage probability matrices defined for the different intensity degrees to obtain the estimation of losses.

3.4.2. COMPONENTS OF NONEMPIRICAL METHODS

In some cases, the use of empirical methods is not appropriate, usually because of lack of data in the region of study and the poor reliability in the use data from other regions. Alternatively the ground motion can be defined from hybrid methods that combine the functional forms deduced from fault mechanism and wave propagation theory, with parameters determined by regional data or analogy with other regions or experiences.

3.4.2.1. *General aspects*

Prediction in retrospective sense. Risk studies try to define the statistical distribution of future seismic action as a function of magnitude and distance. The objective of many seismological studies is the "retrospective prediction" of the distribution of ground motion for a given earthquake, for which instrumental records are available. The intention is to know the details of the seismic source, is to say its geometry and the time and space evolution of the rupture. The methods used to generate synthetic records can be predictive for future earthquakes. However, many simulations would be needed in order to archive the required statistical significance. As more data and more sophisticated computing resources are available, the more reliable will be the results.

Complexity of the ground motion. It seems clear from the observation of accelerograms that seismic ground motions present a great complexity, especially in the high frequencies. The simple model formed by a fault with uniform sliding in a homogenous medium does not give rise to a complexity in the motion (these models are useful only for study of the long period components). A good model must reproduce complexity and randomness in the motion. Figure 3.8 shows an example of this complexity.

Some methods try to model the Earth complexity, whereas others classified as phenomenological look for functional forms derived from physical models, with parameters that can be considered by adjustment to the data. A fundamental idea in those methods is that the dynamic processes are too complex to be modelled in a deterministic way especially for a future earthquake.

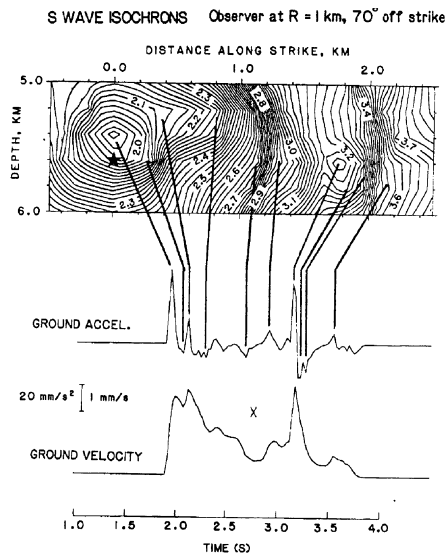


Fig. 3.8. Example of an acceleration record simulated for a time distribution of the rupture shown in the upper part for an observer located at 1 km of distance and an azimuth of 70° . The distribution of isochrons is shown together with the amplitude of the ground motion (Cocco, 1998)

3.4.2.2. Parts of the problem.

The current methods divide the problem in three parts: seismic source, path and local effects.

Seismic Source. The seismic source is described by the time and space distribution of the rupture (or slip) in the fault plane. This information is never available for future earthquakes and therefore methods to obtain the radiation of the source are needed. Some methods use a point source to represent the rupture of the fault, valid for ranks of distance larger than the size of the fault, whereas others consider the rupture as a sum of sub-events on a finite fault.

- Point Source. The called "stochastic" models are member of the group of models that consider a point source. In these methods the radiation is described in terms of spectra, whose amplitude is given by relatively simple functions, of smoothed shape and whose phase is almost-random, so that the ground motion duration is related to the size of the source and to the distance between source and site. In most methods, the spectral amplitude follows seismological models with a physical basis. So it is the case of the well-known model of Brune (1970, 1971) also known as the ω^2 -model, characterized by a corner frequency f_c , and later modified with another cut-off frequency f_{max} (see an example in Figure 3.9 from Catalan et al. (1999).

The most well known stochastic model in literature is that proposed by Boore (1983). However, the possible spatial variation of the movement along the fault is not taken into account, when considering it a point source. Later developments have allowed us to explain these variations considering a time-window, whose form contains the information of the rupture process (Cocco, 1998).

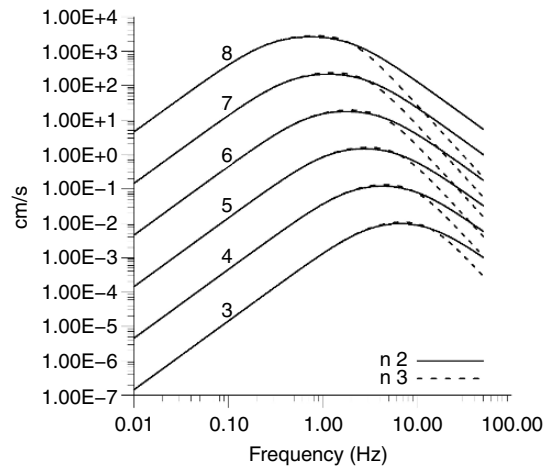


Fig. 3.9. Acceleration Spectra corresponding to a modified Brune Model for different magnitudes considering an epicentral distance of 60 km. Attenuation of amplitudes for high frequencies with $n=2$ and $n=3$, for some dependency of frequency (Catalan et al., 1999)

- Extensive Source. The seismic ground motion produced by an extensive source can be calculated combining the motions produced by sub-events distributed on the fault plane. The sub-events can be defined in several ways:
 - Using actual records of small earthquakes, so that they contain the same information about the path and site as the record of the great earthquake (e.g. Irikura, 1983).
 - By generation of a random distribution of slips with certain properties (e.g. Bernard and Herrero, 1994).
 - Using a fractal distribution of the size and a random position of sub-events (e.g. Zeng et al., 1994).

Path. The energy emitted by the source is modified throughout the path followed by the waves until they reach the site. This modification can be modelled by two types of approaches:

- Green Function. Some methods use empirical Green functions from records of small earthquakes that have followed the same path, as it has been mentioned also for treating the extensive source (e.g. Irikura, 1983). Others calculate the Green functions for stratified media (Bouchon and Aki, 1977) from the complete modelling of the wave field. The main problem in computation is the difficulty in knowing enough details about the internal Earth structure, and from the details one has to generate the high frequencies contents (short wavelengths).
- Simplified methods. Quite often the path effect is parameterised in the frequency domain by the product of two factors: the geometrical spreading and the anelastic attenuation. The first of them is modelled for a homogenous medium by a diminution of the wave amplitude proportional to r^{-1} (spherical wavefronts) or r^{-2}

for distances superior to 100 km (cylindrical wavefronts). The second one has less importance for the frequencies of interest at the regional distances.

Local Effects. As seen in Section 3.3.3 the consideration of the possible amplification of ground motion due to specific local conditions, say, effects of soft soils and steep topography, is absolutely necessary. In general the effects are considered through the estimation of the transfer function, that is, the spectral relation between a record in a given site and a record placed in a reference location, usually hard rock. Also the increase of the duration of the ground motion can be of importance. Observations of these effects in recent earthquakes and a more complete overview of the methods are developed in Chapter 4.

3.5. Definition of Seismic Action

The seismic action on a structure is defined by the time-history series corresponding to the acceleration or accelerogram or its spectral representation, in the frequency domain. For non-linear dynamic analysis, an accelerogram representative of the action to be considered is needed.

In many cases the structural analysis needs only the maximum value of the acceleration (peak ground acceleration or PGA) and a few ordinates of the linear response spectrum for some frequencies of interest, in most cases between 0.2 and 20 Hz.

One of the ways to obtain a representation of the seismic action is to analyse the hazard in terms of Peak Ground Acceleration (PGA) and to use a spectral form obtained independently to convert PGA in a response spectrum. One example of this procedure is the development of a smoothed acceleration response spectrum from Eurocode 8 (EC8, 2003), described in section 3.5.2.

Recently, the use of variable spectrum forms to define seismic zonation has been extended since the first proposal in the USA (Frankel et al., 1996).

Seismic action can be defined in several forms depending on the method used to evaluate the seismic damage of a structure or to design a future one. In the methods based on forces acting on the structure, the seismic action is defined in terms of the acceleration spectra, but recent methods based on displacements and the performance of the structure rely on demand spectra to represent the seismic action.

3.5.1. PEAK GROUND ACCELERATION (PGA) AND RESPONSE SPECTRUM

The Peak Ground Acceleration or PGA is defined as the absolute maximum value of the representative temporary series of the ground acceleration. It is useful to define lateral forces and shear stresses in procedures that use equivalent static forces like the specified ones in the Seismic Codes. When being controlled by the spectral value corresponding to the greater frequency, its value is very sensible to the processes that can alter the spectral content at high frequencies, such as the site conditions or the instrumental transfer function. Moreover, PGA is not easily related with a given frequency range of interest, depending on the distance to the source of the earthquake. The frequencies that control the value of PGA are often not in the rank of interest of the structural answer. For example, the maximum values of the acceleration can exceed 5 g in the case of the

record of explosions at short distances, but for frequencies near 400 Hz. For the above reasons the PGA is not recommended for the definition of the seismic action of design, being more representative of the complete response spectrum.

The response spectrum describes the answer of a damped linear oscillator to a seismic excitation. The more used measurement is the PSA (T) or spectral maximum acceleration defined by:

$$PSA(T) = (2\pi/T)^2 S_d(T), \quad (3.1)$$

where $S_d(T)$ is the maximum displacement of the mass of a damped linear oscillator with an undamped natural period T , relative to the point of anchorage to the ground. In most applications a damping of 5% is used. The response spectrum is useful to calculate directly the answer for most structures, since these can be modelled by the linear oscillator.

Despite its extended use, the response spectrum shows some disadvantages:

- A non-linear analysis needs a more complex representation.
- In spite of calculating a PSA for any frequency, a not-null value does not imply that the ground motion contains energy to this frequency. Thus, for example, if the excitation of the oscillator is made to frequencies lower than 5 Hz, the answer to higher frequencies will simply reproduce the ground acceleration.
- The Response Spectrum does not have the same properties as the Fourier Spectrum, when a value of not-null damping is used. In this case the spectral relations can give rise to erroneous interpretations.
- The spectrum is computed generally for a horizontal seismic action without taking care of the direction.
- Importance of the spectrum corresponding to the vertical component of the motion is usually not given and it is a current practice to deduce it from the horizontal spectrum applying a factor of 2/3. If vertical actions are considered important for a given structure or building, the vertical response spectrum must be computed independently.

3.5.2. SMOOTHED ACCELERATION RESPONSE SPECTRUM FROM EUROCODE 8

For the horizontal components of the seismic action, the Eurocode 8 (EC8, 2003) defines the elastic response spectrum, $S_a(T)$, using the following expressions:

$$0 \leq T \leq T_B \quad S_a(T) = pga \left[1 + \frac{T}{T_B} (B_C - 1) \right] \quad (3.2)$$

$$T_B \leq T \leq T_C \quad S_a(T) = pga B_C \quad (3.3)$$

$$T_C \leq T \leq T_D \quad S_a(T) = pga \left(\frac{T_C}{T} \right) B_C \quad (3.4)$$

$$T_D \leq T \leq 4 \text{ sec} \quad S_a(T) = pga \left(\frac{T_C T_D}{T^2} \right) B_C \quad (3.5)$$

where:

- $S_a(T)$ = ordinate of the elastic response spectrum,
- T = vibration period of a linear single degree of freedom system,
- pga = peak ground acceleration (PGA),
- B_C = factor defined as $S_{a \max} / pga$,
- T_B, T_C = limits of the constant spectral acceleration branch,
- T_D = beginning of the constant displacement response range.

A diagram for the Eurocode 8 (EC8, 2003) elastic response spectrum, $S_e(T)$, is shown in Figure 3.10.

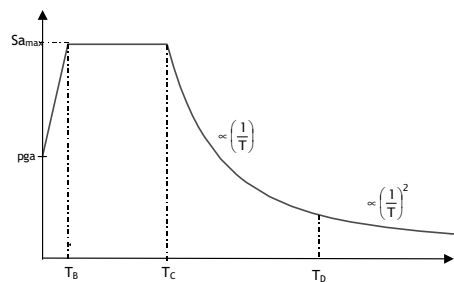


Fig. 3.10. Diagram for the Eurocode 8 (EC8, 2003) acceleration response spectrum formulation

Eurocode 8 offers the possibility of two types of response spectra that depends on the maximum surface wave magnitude of the earthquakes that are expected to affect the selected site. If it is higher than 5.5, spectrum type 1 is used, but when it is lower than 5.5, the type 2 spectrum should be used (see Figure 3.11).

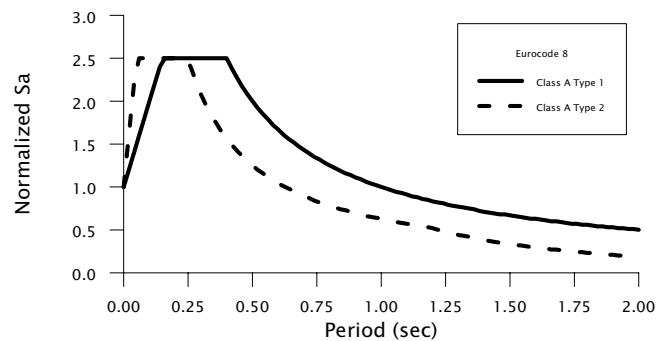


Fig. 3.11. Response spectra of Eurocode 8 for two types of magnitudes in case of soil class A

3.5.3. IMPLICATIONS IN THE USE OF FIXED SPECTRAL FORMS ANCHORED TO THE PEAK GROUND ACCELERATION

It has been a common practice to use a fixed spectral form scaled ("anchored") to a given PGA. According to what has been discussed in the previous sections, the use of

PGA to scale spectral forms and the use of the above described practices present some important problems.

Some of the consequences of the different methods and values of variables on the spectra are summarized as follows:

- Peak ground acceleration is a very sensitive parameter to the recording conditions (geology and instrument), it is not associated to a frequency in particular and its value is difficult to predict due to the random character of the complexity of the rupture that generates the incoming waves.
- The great earthquakes produce a greater proportion of low-frequencies, in relation to smaller earthquakes and, for this reason, the PSA(fr)/PGA relation will grow with the magnitude of the event.

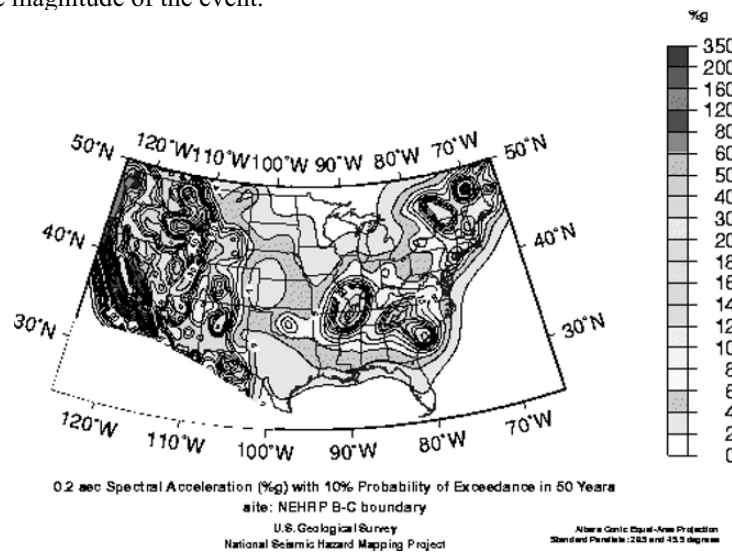


Fig. 3.12. Spectral accelerations for 5 Hz in %g with a 10% probability of being surpassed in 50 years in the U.S.A (Frankel et al., 1996)

Recently, there have been proposals, in particular in the U.S.A., to use variable spectrum forms to define the seismic zonation (Frankel et al., 1996). In Figure 3.12 there is an example of a map with the results of a Probabilistic Seismic Hazard Assessment for one spectral value.

3.5.4. DEMAND SPECTRUM OR ACCELERATION-DISPLACEMENT RESPONSE SPECTRUM (ADRS)

The demand spectrum is the 5% damped acceleration response spectrum expressed in an acceleration-displacement (AD) diagram. In the AD diagram, ordinates are expressed in terms of spectral acceleration, S_a , while abscissas are expressed as spectral displacement, S_d . The demand spectrum represents the spectral acceleration and spectral displacement that the seismic event demands on the structure. It is also often called acceleration-displacement response spectra or ADRS. The conversion from the 5%

damped acceleration response spectrum (S_a , T) to a demand spectrum (S_a , S_d) only requires a definition of the spectral displacements using the following transformation:

$$S_d = S_a \left[\frac{T^2}{4\pi^2} \right] \quad (3.6)$$

A smoothed demand spectrum or ADRS diagram is shown in Figure 3.13. Each point in the demand spectrum represents the spectral acceleration, S_a , and the spectral displacement, S_d , corresponding to a vibration period, T . As can be seen the structural period in the acceleration displacement response spectra diagram can be represented by a line passing through the origin (Mahaney et al., 1993). The slope of this line is inversely proportional to the structural period, that is, as the structural period increases, the slope of the line decreases.

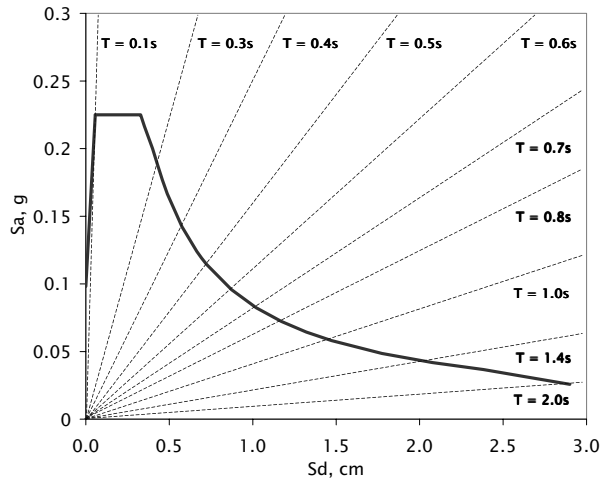


Fig. 3.13. Smoothed form of the demand spectrum or ADRS diagram

Having analytical formulation for smoothed demand spectra can be very useful when they are used for the performance evaluation of large building stocks by allowing programming of the methods to be performed automatically. The acceleration response spectrum obtained can be smoothed using code-like formulations. The analytical formulations for smoothed acceleration response spectra can be then used to obtain the analytically expressed smoothed demand spectra.

Acknowledgements

The analysis of data from recent western Mediterranean moderate earthquakes is based on the ongoing PhD Thesis works from Mar Tapia and we are grateful to her for the help provided.

We are also grateful to Drs. Antoni Roca and Carlos Sousa Oliveira for fruitful discussions during the elaboration of the Chapter.

CHAPTER 4
LOCAL SITE EFFECTS AND MICROZONATION

A. Roca¹, C. S. Oliveira², A. Ansal³ and S. Figueras¹

1. *Institut Cartogràfic de Catalunya, Barcelona, Spain*

2. *Instituto Superior Técnico, Lisbon, Portugal*

3. *Boğaziçi University, Istanbul, Turkey*

4.1. Introduction

Seismic waves generated at the earthquake source propagate through different geological formations until they reach the surface at a specific site. The travel paths of these seismic waves in the uppermost geological layers strongly affect their characteristics, producing different effects on the earthquake motion at the ground surface. In general, thicker layers of soft, unconsolidated deposits tend to amplify selectively different wave frequencies. These complex physical phenomena are known as *soil effects*. On the other hand, the local topography can also modify the characteristics of the incoming waves, leading to the so called topographic effects. *Soil* and *topographic effects* are considered under the general denomination of *local site effects*. Beyond these effects and under certain circumstances, *induced effects* may occur for large amplitude incoming waves, among which are slope instabilities (landslides) and liquefaction.

Within a more generalized scope, active faulting should also be considered as, in case of fault ruptures. In addition permanent differential displacements and near fault effects are other important issues to be recognized.

In many past and recent earthquakes it has been observed that the local site conditions - soil and topographic effects, as well as induced effects - have a great influence on the damage distribution. It is therefore very important to take into account and predict these possible local site effects when assessing the earthquake hazard at regional and local scale.

Seismic microzonation is the generic name for subdividing a region into individual areas having different potentials for hazardous earthquake effects, defining their specific seismic behaviour for engineering design and land-use planning. Seismic microzoning, including approaches for assessing local ground response, slope instability and liquefaction, has become a useful tool for cost effective earthquake risk mitigation. There is a demand from international, national, regional and municipal administrations for microzoning urban areas generating maps to be taken into account in urban planning, in seismic codes and in civil protection preparedness procedures.

Various approaches are currently applied for microzonation studies. Experimental techniques, together with theoretical approaches involving ground motion modelling under different hypotheses, are used to classify urban areas in various zones of different earthquake response characteristics.

Several review and synthesis papers on the different methods used for geological and geotechnical site characterisation and microzoning have been published (e.g. Bard, 1994; Kudo, 1995; Pitilakis and Anastasiadis, 1998; Bard, 1999; Mulas, 2002; Kawase,

2003; Pitilakis, 2004; among others) and many conferences, symposia and workshops have been organised under this subject. Some special volumes and technical books have been also devoted to this topic (e.g. Priolo et al., 2001; Roca and Oliveira, 2002; Ansal et al., 2004, among others).

Guidelines or recommendations for seismic microzoning have been produced in different countries (e.g. AFPS, 1995; ISSMGE, 1999; DRM, 2004a). The guideline manual from Mayer-Rosa and Jiménez (2000) includes a state-of-the-art and a useful collection of case studies with emphasis in ground amplification while the manual for zonation ISSMGE (1999) points out mainly earthquake induced phenomena such as slope instability and liquefaction. The DRM (2004a, 2004b) study presents a comprehensive treatment of the microzonation based on case studies along with a manual for establishing a microzonation code in Turkey. Microzoning results are being slowly incorporated into recent earthquake construction codes (e.g. Eurocode 8, 2004).

This chapter is an account for readers who are not very familiar with the topic. The purpose of this brief and comprehensive review is to describe and clarify the goals, terminology and concepts involved in seismic microzoning and to present and discuss the main numerical and experimental techniques used in current research and application-related studies, pointing out their limitations, advantages and disadvantages. The societal value of these studies and the need of including them in the framework of seismic regulations are also discussed.

4.2. Importance of local site effects on observed earthquake damage

There can be significant differences in local site conditions due to variations in geological formations, thickness and properties of soil and rock layers, depth of bedrock and water table, surface and underground topography. These variations would have significant effects on the characteristics of earthquake motions on the ground surface. There are large numbers of instrumental field observations obtained during recent earthquakes reflecting the effects of local site conditions.

As reported by many researchers (Borcherdt and Gibbs, 1976; Iglesias, 1988; Gazetas et al., 1990; Seed et al., 1991; Ansal et al., 1993; Lekkas, 1996; Jennings, 1997; Ishihara, 1997; Guéguen et al., 1998; Pergalani et al., 1999; Tertulliani, 2000; Hartzell et al., 2001, Ansal et al., 2001a; Özel et al., 2002) local site conditions could play a dominant role in damage distribution as well as in the recorded strong motion records (Aki, 1993, 1998; Bard, 1994; Reinoso and Ordaz, 1997; Shome et al., 1998).

In addition, one of the controlling factors on building damage, not very related to the local site conditions, is the surface manifestation and type of faulting that took place during the earthquakes. As an example it was possible to observe the diverse effects of fault ruptures during the 1999 Kocaeli, Turkey earthquakes as shown in Figure 4.1. The house located a few meters away from the fault trace with permanent lateral displacements around 4m appears to be intact as shown in Figure 4.1a. However, in the case the fault trace goes through a building, total collapse may take place as shown in Figure 4.1b.

Likewise as shown in Figure 4.1c, even though the lateral displacements were on the order of 4m, the building survived without experiencing total collapse. It is also interesting to see that the building located right next to the normal fault with vertical displacements on the order of 2m (Figure 4.1d) survived the earthquake with minor damages.



Fig. 4.1. Effects of fault rupture on buildings

Figure 4.2 shows different urban areas with different degrees of damage distribution during the 1999 Kocaeli earthquake. Damages to buildings in the near field in Golcük and Adapazarı show varying degrees of damage distribution most likely due to the diverse effects of local site conditions.



Fig. 4.2. Variation of building damage in different zones in the near field during 1999 Kocaeli, Turkey earthquake

Geologic structures such as basins and sediment filled valleys and topographical features may also have very important effects on the variation of the earthquake ground motions. Local site effects on basins and valleys and topographical effects have been

investigated by many researchers (Murphy and Hewlett, 1975; Bard and Bouchon, 1980a, 1980b, 1985; Geli et al., 1988; Faccioli, 1991; Zhao and Valliappan, 1993; Wen et al., 1995; Rassem et al., 1995; Gao, et al., 1996; Chávez-García et al., 1996; Reinoso et al., 1997; Chin-Hsiung et al., 1998; Su et al., 1998; Wald and Graves, 1998; Kawase, 1998; Amirbekian and Bolt, 1998; Athanasopoulus et al., 1999; Paolucci et al., 2000; Sokolov et al., 2001; Chávez-García and Faccioli, 2000).

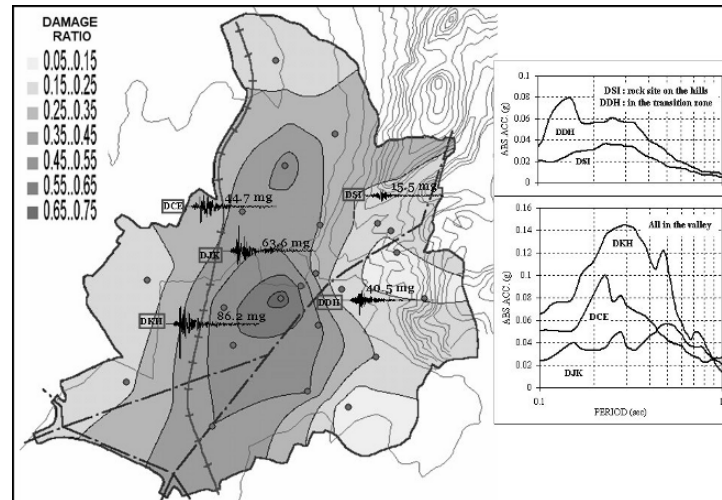


Fig. 4.3. The variation of damage in Dinar after the 1995 earthquake in comparison with the aftershock records from the temporary KOERI network (Durukal et al., 1998)

An example from the recent past, 1995 Dinar (Turkey) Earthquake can be given to demonstrate the importance of local site conditions. The variation of damage distribution in Dinar after the 1995 Earthquake, as shown in Figure 4.3 given by Ansal et al. (2001a), has been determined based on detailed damage survey conducted by the Turkish General Directorate of Disaster Affairs. It appears logical to assume that there would hardly be significant variations in engineering and in the quality of construction in Dinar. Therefore this large variation of the earthquake damage observed may be explained with respect to variations in earthquake characteristics due to different local site conditions. The recorded ground motions during an aftershock ($M_L=4.1$) located on the same fault zone clearly demonstrate the differences in ground motion characteristics. The peak ground and peak spectral accelerations were 0.086g and 0.14g at DKH station located on the alluvium sediments in the valley while it was only 0.015g and 0.04 g at DSI station located on the rock outcrop.

The other important issue concerning local site conditions is related to the landslides induced during and after earthquakes. Especially landslides in residential districts may cause extensive damage and large numbers of casualties. A devastating example of such a landslide that took place during the 1995 Hyogoken-Nanbu earthquake is shown in Figure 4.4.

All of the above mentioned earthquake induced damages and recorded ground motion characteristics clearly indicate the importance of local site conditions during

earthquakes. Thus one logical mitigation measure requires detailed investigation and realistic assessment of the local site conditions.



Fig. 4.4. Large landslide in Kobe, Japan caused by the 1995 Hyogoken-Nanbu earthquake, causing the destruction of a large number of houses located on the slopes

4.3. Zoning, microzoning and resulting maps: a tool for predicting local site effects

The general concept of zoning refers to the process of subdividing a region into sectors with similar behaviour with respect to a given set of parameters. Zoning always relates to a specific application, and, in most cases, is linked to engineering design or land-use planning purposes. Seismic *zonation* and *microzonation* refer to the working scale, regional and local, respectively. They are the basic tools for earthquake damage mitigation on the side of ground motion and ground induced effects, (Mayer-Rosa and Jimenez, 2000; Roca et al., 1999).

Zoning parameters have been treated in chapters 2 and 3 of this book. They are essentially physical variables defining the characteristics of ground shaking such as: macroseismic intensity, peak ground acceleration, velocity and displacement (PGA, PGV and PGD), Fourier and response spectra, duration, etc.

The current output from microzoning studies dealing with soil and topographic amplifications consists of maps defining sectors of different earthquake response, and are referred to a specific parameter or function such as:

- ΔI , increment of macroseismic intensity, I , with respect to the I values of the corresponding national or regional hazard map. An important point is to know if the intensities given in the hazard map correspond to rock site or to the “predominant” - most frequently observed - soil site.

- Δ_{PGA} , increment of the peak ground acceleration at each specific point of the territory with respect to the values for a neighbouring rock site. Similar representations can be done with Δ_{PGV} and Δ_{PGD} .
- T_p , predominant period, defined as the period for which the maximum soil amplifications occur. The fundamental or natural period, T_1 , corresponding to the first mode of vibration of the soil system, is used by several authors as microzoning parameter. However, it should be considered that T_p is a more significant parameter than T_1 as far as their relation to damage in most standard dwelling buildings.
- Transfer function - soil to rock spectral ratio - gives a more complete representation of local effects, as it covers the entire spectral domain.
- A site specific response spectrum is another useful function to characterise ground behaviour for engineering purposes.

In order to obtain these parameters a large amount of territorial information (topographic, geological, geophysical, geotechnical, hydrological, etc.) is needed. In many cases, given the lack of available data, a microzoning project must include surveys for obtaining some of this basic information. In this way, intermediate results and maps issued during the process of a seismic microzoning project can be of a high value themselves for their possible use in other applications. Examples of these intermediate products are maps with geotechnical information, water table, potential active faults, topography and underground local characteristics (i.e. ICC, 2000; SGP, 1988). Given the large amount of data that has to be managed, a Geographical Information System (GIS) is a valuable tool to be used for microzoning and also for risk assessment and for the generation of damage scenarios.

The results of microzoning studies can be integrated in various applications corresponding to different levels: i) National codes which define the minimum requirements for earthquake protection can benefit from zonation maps; ii) Regional and municipal regulations may detail and modify National codes with results from microzoning; and iii) Site-specific studies are needed for the design and construction of important engineering structures, as well as for performing safety analysis of existing important vulnerable structures.

In addition the issue of fault traces, which deserves specific treatment in a microzoning study, are strongly linked with the concept of “active” fault. Whenever the geological study has identified such a feature, a “free-distance” from the fault trace should be kept for special consideration where compulsory measures should be applied, restricting the land-use or requiring more stringent ground motion conditions.

Each one of these levels of application requires a specific mapping scale and the corresponding grade or “grain of information”. Various existing guidelines recommend intervals for these levels (AFPS, 1995, ISSMGE, 1999; Mayer-Rosa and Jiménez, 2000; DRM, 2004a, b). Usual mapping scales range from 1:2,000,000 – 1:250,000 for national or regional hazard assessment to 1:10,000 - 1:5,000 for local effects evaluation at municipality level or to 1:500 for site specific studies.

Sections 4.4 and 4.5 are devoted to the characterisation of soil properties in the linear and nonlinear regime, while Sections 4.6 and 4.7 will present the current numerical and experimental methods to predict earthquake ground response. Finally, in sections 4.8 and 4.9 the topographic, liquefaction and induced effects are presented.

4.4. Geological, Geotechnical and Geophysical approaches for soil characterization

As mentioned before, local soil characterisation plays a decisive role in determining their behaviour under seismic excitation. Detailed geometry of layers and evaluation of linear and nonlinear properties of all types of soils are necessary for an appropriate analysis. These include, in the first place, a description of the geological environment and lithology, then density, the presence of water content, and finally the various moduli of elasticity and damping ratio as a function shear strain. The detail of the analysis depends on the objectives and on the capacity to gather information.

The geological description and interpretation of data contained in detailed geological maps constitutes the first and most basic information necessary to perform a microzoning study. The existence of down-hole data complements the geological information. The more convenient situation as far as gathering the best information on soil strata would be to have the deeper down-hole information for the larger geographical extension. The detail of this information depends on existing available data and on the capabilities to perform survey analysis.

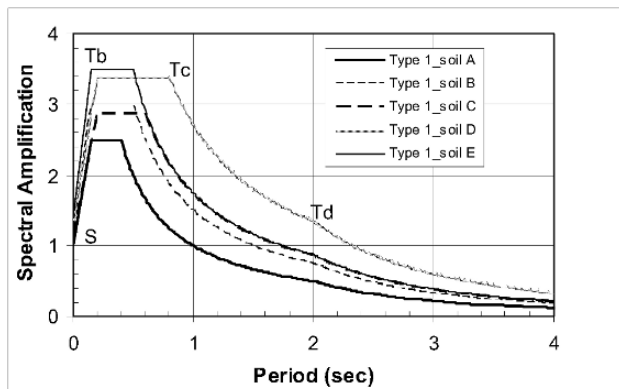
Soil classification used in most modern construction codes is essentially based on this data as the cases of the EC-8, the European Eurocode 8 (2004) and the NEHRP (2000) cases. Table 4.1 presents the soil classes of the recently approved EC-8, according to main mechanical characteristics of the surface layers; the proposed spectra for the different types of soils defined and for earthquakes of magnitude equal to or larger than 5.5 are shown in Figure 4.5.

The evaluation of local conditions including surface geology to determine the geometry and mechanical characteristics of “layers” can be performed in different ways, essentially using seismological methods, either geophysical and/or geotechnical. The surface geophysical methods include reflection, refraction profiles, spectral analysis of surface waves, electric, electro-magnetic fields and microgravimetry (Montesinos et al., 2003). New digital technology instrumentation and powerful software have enhanced the scope of applications and the accuracy of estimations. Among these techniques we cite the use of dense arrays for better inversion procedures including tomography. The most recent array techniques use the Frequency-Wave number (F-K) algorithm (Kagawa, 1996) applied to surface waves caused by impact sources and ambient noise, and the Spatial Autocorrelation Method (SPAC) for ambient noise (Estrella and González, 2003; Pascalis et al., 2004).

The geotechnical methods include evaluation of wave velocity in particular layers through cross-hole, down-hole techniques, etc., through the execution of borehole logs to perform associated testing.

Table 4.1. Classification of soil types according to main mechanical characteristics of the surface layers according to Eurocode 8

Ground class	Description of stratigraphic profile	Parameters		
		$V_{s,30}$ (m/s)	N_{SPT} (bl/30cm)	c_u (kPa)
A	Rock or other rock-like geological formation, including at most 5 m of weaker material at the surface	> 800	-	-
B	Deposits of very dense sand, gravel, or very stiff clay, at least several tens of m in thickness, characterised by a gradual increase of mechanical properties with depth	360 – 800	> 50	> 250
C	Deep deposits of dense or medium-dense sand, gravel or stiff clay with thickness from several tens to many hundreds of m.	180 – 360	15 - 50	70 – 250
D	Deposits of loose-to-medium cohesionless soil (with or without some soft cohesive layers), or of predominantly soft-to-firm cohesive soil	< 180	< 15	< 70
E	A soil profile consisting of a surface alluvium layer with $V_{s,30}$ values of class C or D and thickness varying between about 5 m and 20 m, underlain by stiffer material with $V_{s,30} > 800$ m/s			
S ₁	Deposits consisting – or containing a layer at least 10 m thick – of soft clays/silts with high plasticity index (PI > 40) and high water content	< 100 (indicative)	-	10 – 20
S ₂	Deposits of liquefiable soils, of sensitive clays, or any other soil profile not included in classes A –E or S ₁			



EC8-00 TYPE 1	S	T _b	T _c	T _d
soil A $V_s > 800$ m/s	1,00	0,15	0,4	2,0
soil B $360 < V_s < 800$ m/s	1,10	0,15	0,5	2,0
soil C $180 < V_s < 360$ m/s	1,35	0,20	0,6	2,0
soil D $V_s < 180$ m/s	1,35	0,20	0,8	2,0
soil E ($h < 20$ m)	1,40	0,15	0,4	2,0

- S : spectral value for period zero
 T_B, T_C : period limits (sec) for constant spectral acceleration branch
 T_D : period value defining the beginning of the constant displacement response range of the spectrum.

Fig. 4.5. Eurocode 8 Type 1 elastic response spectra for the 5 subsoil classes, for magnitude equal to or larger than 5.5

Many different methods are available today throughout the specialised literature. Pitilakis and Anastasiadis (1998) present a good summary of those methods, their efficiency, and the degree of uncertainty in property retrieval and on costs of operations.

The average shear wave velocity $V_{s,30}$ in Table 4.1 is computed according to the following expression:

$$V_{s,30} = \frac{30}{\sum_{i=1,N} \frac{h_i}{V_i}} \quad (4.1)$$

where h_i and V_i denote the thickness (in m) and shear-wave velocity (at shear strain level of 10^{-6} or less) of the i -th formation or layer, in a total of N , existing in the top 30 metres. The site will be classified according to the value of $V_{s,30}$ if this is available, otherwise the value of N_{SPT} will be used taking into account the several physical properties that can be obtained from simple *in-situ* tests.

One special important situation departing from the previous soil classification that considers the top 30 m as sufficient to characterize site effects, is the case of thick layers of soft material, in some cases with more than 1 km, corresponding to very old river basins existing for instance in Central Europe. These cases require special treatment because modes with very large periods may be present, modifying considerably the spectral shape in the long period range for large magnitude events.

For microzoning purposes, data from boreholes associated to construction logs have been collected in GIS systems for posterior analysis. This policy is of maximum interest as it can be used for an updating of information at a given area. Contour lines with soil layers shear velocities, thickness, SPT, etc. will help visualising the space variations on soil properties. Results of modelling can easily be also added for comparison.

4.5. Nonlinear effects

Soil behaviour and consequently site effects depend very much on the amount of soil distortion provoked by the wave passage. The behaviour of various types of soils is markedly nonlinear for high amplitude motions and this effect cannot be ignored when dealing with any kind of microzoning. Extrapolation of results obtained from micro-earthquakes and microtremor recordings should be considered carefully in some geological environments where nonlinear effects can appear even at low PGA values (at the rock level). Some simple test of linearity – nonlinearity can be carried out taking as input data the geotechnical dynamical properties of the soils obtained experimentally or deduced from available correlations.

Nonlinearity is well observed in laboratory testing of samples adequately taken from the field, but great uncertainty still exists even though great advances were recently achieved in sampling and testing techniques. Many parameters control the nonlinear behaviour of different soils for increasing amplitude of shear levels. These can be reduced to the changes of modulus of elasticity and damping values (Figure 4.6), which differ from soil to soil and depend on other characteristics such as effective overburden stresses.

Table 4.2 presents a summary of techniques for soil characterisation and numerical modelling corresponding to different levels of soil distortion. In all cases full *in-situ* monitoring for earthquake events is recommended.

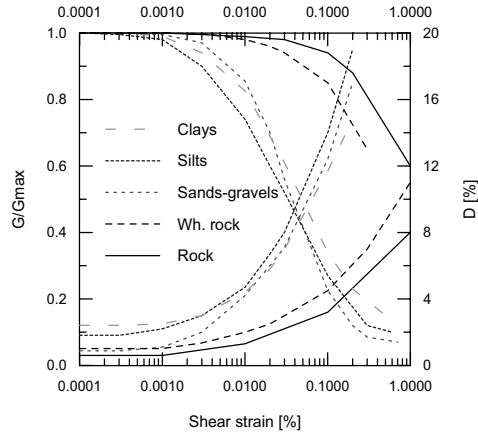


Fig. 4.6 Modulus reduction (G) and damping curves (D) with shear strain amplitude for typical soils (Cid et al., 2001)

Table 4.2. Summary of techniques for soil characterization and the corresponding levels of soil shear strain

Shear strain ($\gamma\%$)	10^{-5}	10^{-4}	10^{-3}	10^{-2}	10^{-1}
Application	Linear	Weak events	Moderate events	Large events	Very large events
Type of test	<i>In-situ</i> prospection	Resonant column	Triaxial	Large Shear testing	
Modelling	Linear elastic	Linear-equivalent	Nonlinear simplified	Nonlinear 1-D; 2-D	Full soil constitutive relationships

Well instrumented sites allow clear identification of nonlinearity when high quality strong motion recordings are obtained, by simply comparing the Fourier spectral ratio of soil to rock site motion for different amplitudes (strong versus weak motion, for instance).

Figueras et al. (1992), analysing records from the SMART-1 accelerometric array in Taiwan, showed a very different behaviour for small and large acceleration events. In the left part of Figure 4.7 the undamped response spectra obtained on rock (thick line) and on different soil sites (thin lines) for a weak motion (top) corresponding to an earthquake of magnitude 5.3 at 30 km distance to recording sites, and for a stronger motion (bottom) corresponding to an earthquake of magnitude 6.2 at 6 km distance.

The response spectra on soils are amplified, in all the frequency range, in the case of the lower input motion while for the stronger event a reduction in the amplitude of the high frequencies is observed (nonlinear behaviour). In the lower frequencies, the amplification observed on soil is much larger for the stronger motion. The same phenomena can be seen in the time histories (right): For the smaller event, peak accelerations (PGA) of 44.09, 47.16 and 48.69 cm/s^2 are observed at sites on rock, on

medium deep soil and deeper soil, respectively. This corresponds to peak ground displacements (PGD) of 0.91, 1.39 and 1.57 mm, respectively. For stronger ground motion (bottom) the acceleration obtained on rock is 181.50 cm/s^2 and on two soil sites it is reduced to 148.64 and 108.06. The PGD on rock is 5.5 mm and on soil sites 27.77 and 40.81 mm (this means that amplification of the PGD reaches a factor of 7) as displacements are related with the low frequency band of the spectra.

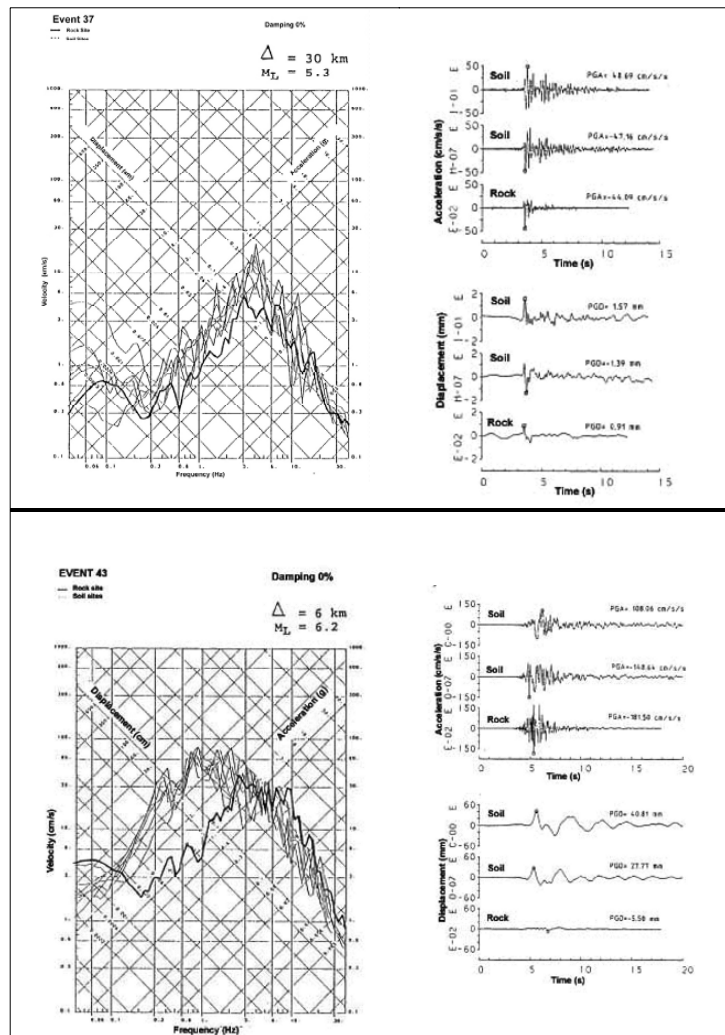


Fig. 4.7. Fourier spectra, accelerograms and displacement time histories obtained on rock and soil sites at the SMART-1 array, showing a very different behaviour depending on the input acceleration. Top: magnitude 5.3 event at 30 km distance. Bottom: magnitude 6.2 event at 6 km distance (Figueras et al., 1992)

4.6. Numerical methods for estimating local effects

The geological environment around a site is in general very complex both in geometry and in material characteristics. Current situations include basins with three-dimensional geometry filled with soft, unconsolidated materials with diverse properties, anisotropy and inhomogeneities (Figure 4.8).

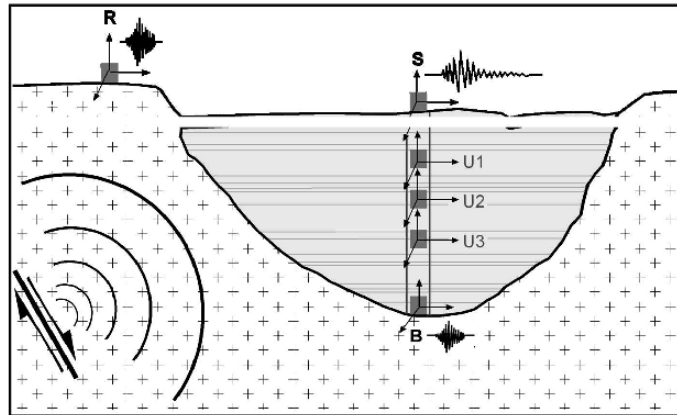


Fig. 4.8. Sketch of a sedimentary basin with instruments on rock outcrop, basement, boreholes and surface soils

Understanding of the entire process of wave propagation through this real medium is not an easy task, not only due to the complexity of the geological model, but also due to the complex nature of the multiple waves propagating inside the structure that will result in the ground shaking at each point on the surface. In addition to that, in case of large amplitude motions, as mentioned before, nonlinear behaviour of soils has to be considered. In order to analyse these phenomena and approach the prediction of the characteristics of ground motion at the surface, simplifications both in the wave field description as well as in the geological structure have to be made.

Numerical modelling with linear and nonlinear soil properties require quite sophisticated methods in 1-D, 2-D or in 3-D. While linear modelling might be easier to handle, but must include all kind of possible propagating waves, for the nonlinear analysis even the 1-D model requires a good characterisation of the mechanical properties of the soil layers.

4.6.1. LINEAR METHODS

4.6.1.1. 1D Models

The simplest approach to the problem is to consider a single horizontal layer with infinite length and uniform characteristics, overlaying a rigid semi-infinite body. This layer, exhibiting average characteristics of the soil in the basin, has a shear velocity V_1 , density ρ_1 , and thickness H (m). An estimation of the fundamental frequency of the basin is given by $f_0 = V_s/(4H)$. The amplitude of surface motion for the case of vertical incident SH waves can be computed with the impedance contrast between the two media, $C = (\rho_2 V_2)/(\rho_1 V_1)$ ($i=1$: soil medium; $i=2$: lower medium).

A less simple model consists of a series of horizontal infinite parallel layers over a bottom half space. The existence of various types of waves propagating inside the basin, even for the simplified horizontal layered case (inclined SH+SV; surface Rayleigh and Love waves; etc.) causes myriad solutions that can be observed at the surface. Also the problem of reflection/refraction (Thomson, 1950 and Haskell, 1953) at each boundary requires a great deal of expertise in order to adapt the models to more realistic situations where energy is absorbed.

This problem has been addressed by many researchers, considering not only the linear behaviour of the material, but also introducing the concept of nonlinearity. A later numerical approximation by Kennet and Kerry (1979) is known as the reflectivity method or the matrix propagation method. The structure is considered as a pile of homogeneous horizontal layers over the bedrock (half space). Each layer is characterised by its reflection and transmission coefficients. Figure 4.9 presents the transfer functions obtained with application of the Kennet method to different 1D structures.

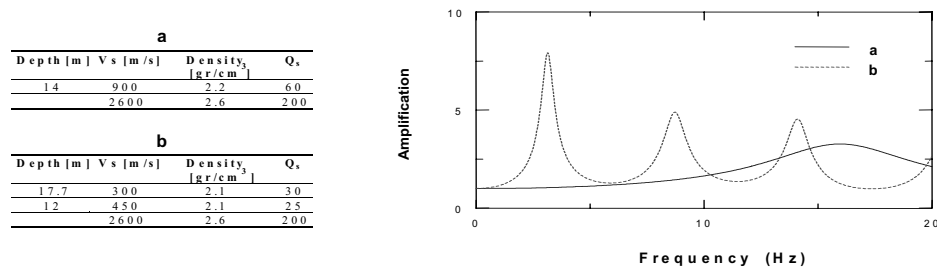


Fig. 4.9. 1D structural models and corresponding transfer functions computed with 1D lineal method. a) one sedimentary layer over a bottom halfspace; b) two sedimentary layers above a halfspace (Figueras, 1994)

4.6.1.2. 2D-3D Models

A step forward to solve the non-horizontal geometry of the layers is first to develop a 2-D model of the basin using more elaborate mechanical algorithms, such as Finite-Element (Paolucci, 1999; Gomes et al., 1999), Finite-Difference (Kamiyama et al., 1999; Moczo, 1989), discrete element methods (Sincranian and Oliveira, 2002) and Discrete wave-number methods (Bouchon, 1985). While 1-D methods give in general a good account for the soil response in many situations, these 2-D methods are needed to analyze edge-effects in some geometric layouts, in particular, for steep or abrupt lateral contrasts as those present in some alluvial valleys. One of the most used methods for 2-D computations is the Discrete wave-number, algorithm by Aki and Larner (1970), developing an idea of Lord Rayleigh (1896), considering the diffraction of plane waves at irregular discontinuities. This method has been further improved by Bard and Bouchon (1980a, b), Bard and Gariel (1986) and Sánchez-Sesma et al. (1989), among others. An example taken from the Volvi Valley (Greece) is shown in Figure 4.10, where the response in the time domain can be seen for a Ricker 1Hz wave propagation in the basin using the 1-D linear Kennett method and 2D finite-differences method. In the 2D modelling case the effects can be seen for wave conversions, wave diffractions and the creation of surface waves.

Complex models: Even though the theoretical basis is quite similar, different approaches have been developed, with increased degree of detail: 2-D, 3-D with various mechanical behaviour (visco-elastic, nonlinear), etc. Essentially four methods have been developed: i) analytic, which have closed form solutions for simple geometries; ii) ray method good for high frequency; iii) modal superposition of the Earth, adapted to the low frequency spectra; iv) boundary-integral methods (Sánchez-Sesma and Campillo, 1991); v) finite element or finite differences methods including linear and nonlinear properties (Moczo et al., 2000). All these methods need a great deal of calibration, but they are very useful for studying sensitivity of parameter values, etc.

Hybrid methods (Panza, 1993; Fäh, 1994) use the mode superposition of the Earth composed by concentric sphere layers to propagate the seismic motion from the source to a neighbourhood boundary around the site, and then use finite elements to propagate this motion from the boundary to the site considering the local soil 2-D characteristics. This method, initially developed for a lateral homogeneous Earth, has been extended to situations allowing for some lateral heterogeneity. It has the great advantage of simulating the entire wave field (P, S, surface, converted P-S waves, etc., if a large number of modal functions are taken into account), and consequently, simulating in a more realistic way the motion entering the region of more soft layers around the site. If used together with nonlinear soil characteristics, this method can be of great importance in merging the better description of wave field from source to near site, with the geotechnical approaches dealing with nonlinear effects of surface layers.

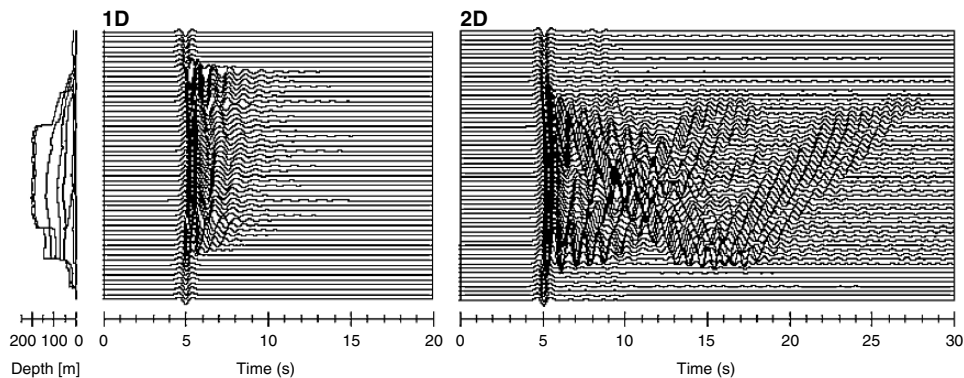


Fig. 4.10. Comparison between lineal 1D (Kennett) and 2D (finite-difference) numerical simulation of the propagation of a Ricker 1Hz wavelet along a sedimentary basin (EuroseisRisk project)

4.6.1.3. Empirical Green's Function method

The empirical Green's Function method is based in the principle that one can obtain the dynamic response of a given space (Earth) at a certain site for a unit impulse applied at another location, if there is a small event located at that location, for which the wave propagation was recorded at the site. From this point onwards the principle of superposition holds and can be generated for a wide range of situations. Convolution of the source function with the Green's function can produce a wave passage at that particular site. Of course there are many limitations of this method, even though it can

well represent the “path and the site effect” under certain circumstances: it should cover a wide range of spectral contents and cannot be extrapolated for energies high above the ones recorded.

There are other semi-empirical approaches such as Tsurugi et al. (2000) consisting of trying to remove source and path effect from moderate magnitude earthquake records.

4.6.2. NON-LINEAR METHODS

The geotechnical community has a long history of developing nonlinear methods. There are very simple methods, in geometry of soil strata, in the nonlinear approximation and in the type of propagating wave, which are commonly used in current applications, as well as quite sophisticated methods dealing with complex geometries, complex nonlinear representations and various types of waves. For a thorough review of the different concepts related to nonlinear soil mechanics see Prevost (1993).

The simplest case to analyse is a soil column under a quasi-linear behaviour, subjected to a vertical incidence of a shear wave. Even for this situation there are few models to compute the response of a soil column. For this case, knowledge of the variation of modulus of elasticity and of damping with shear strain is required for each layer composing the soil column. The simplest method (Seed and Idriss, 1969) considers that the soil behaves linearly but the modulus of elasticity and the damping change as a function of the level of distortion introduced by the amplitude of input. The SHAKE algorithm is essentially based on these ideas (Schnabel et al., 1972).

Another way to consider the nonlinear soil behaviour is the so-called method of characteristics (CHARSOIL) developed by Streeter et al. (1974) which is a 1-D finite differences method that propagates shear waves in different soil stratification and evaluates the soil response considering elastic, visco-elastic and non-linear behaviour; in this case the Ramberg-Osgood curve is used. Figueras (1994) introduced the water table parameter in the Charsoil algorithm in order to evaluate pore water pressure in modelling of the strong ground motion recorded on the SMART-1 accelerometer array in Taiwan.

The most recent algorithms include 3-D nonlinear analyses based on the most complete constitutive laws of all materials present in the basin or other topographic situations under analysis. The influence of the boundaries where ground motion is applied still constitutes a great complexity, partially solved within these problems through the consideration of absorbing boundaries or coupling to boundary methods. ® ABACUS is one among the few commercial software packages available for these analyses, already used in conjunction with the study of volcanic hills (Sinclairian and Oliveira, 2002). Another method was developed at École de Ponts et Chaussées, Paris (Aubry et al., 1986; Aubry and Modaressi, 1996).

The nonlinear analysis of soil deposits is of major importance in the evaluation of liquefaction potential, compaction, lateral spreading and landslides, and indispensable for the estimation of their effects.

4.7. Experimental methods for estimating local site effects

4.7.1. OBSERVATIONS FROM EARTHQUAKES

The most direct way to investigate seismic local effects is to analyse the response of the different soil conditions which are present in the study area to real, strong, moderate and small, seismic events. The following methods are currently being used:

4.7.1.1. *Macroseismic observations*

This is a direct method of observation of effects after an earthquake. Observed damage mainly on buildings but also in other systems (structures and lifelines) can be mapped according to pre-established scales for damage classification. One of the last attempts to improve the estimation of intensity was the new European Macroseismic Scale, EMS-98 (Grünthal, 1998). Damage observations are extremely useful information that serves critically to calibrate any microzonation method.

Guidoboni et al. (2003) show the interest of this type of analysis studying the damage distribution in the city of Palermo, Italy, for three past earthquakes that occurred in 1726, 1823 and 1940. Dividing up the study area using a grid of 100 m×100 m elements they showed a systematic amplification of effects in some of the grid elements which they interpreted in terms of near-surface geology. Instrumental records obtained from a M5.6 earthquake that occurred off the Palermo coast in 2002 validated the macroseismic results.

4.7.1.2. *Strong ground motion recording*

When dense networks of strong motion recorders are installed in a specific area, the direct use of the records after a moderate or strong earthquake gives the most reliable evaluation of site effects. These records include most of the information of the site, including nonlinear effects. However, complete sets of records from dense networks are unfortunately scarce and only in a very few cases was it possible to draw zoning maps from them. This is the case of the work carried out by Iglesias (1991) comparing maximum horizontal acceleration patterns observed in Mexico City for recent earthquakes with the observed damage in former events. Even though the comparison was quite satisfactory there were still some discrepancies observed at several sites, probably due to the complex nature of wave propagation in the Mexico City valley related to source location.

Duration of ground motion clearly increases in central valleys in comparison with rock sites, as the example of Volvi, Greece (Beauval et al., 2004) and of São Sebastião, Azores (Montesinos et al., 2003).

4.7.1.3. *Experiments based on weak earthquake ground motion recording*

Fortunately, in a given place, moderate-to-strong earthquakes do not occur very often and, consequently, strong motion records can not be obtained in a short time period. Records from small events are used instead to characterize local effects. The most direct technique to investigate the effect of soft sediments consists of computing the spectral ratio between two seismic records from a given earthquake, one obtained at the surface and the other at a certain depth in a borehole (Sensors S and B in Figure 4.8); this is the so called SBSR, *Surface - to - Borehole Spectral Ratio*.

Strong motion networks in different countries have operative sets of accelerometers installed in boreholes at different depths. Records of an earthquake obtained in the Ashigara Valley (Japan) in rock site and different soil (surface and borehole) sites are shown in Figure 4.11, as an example of the clear amplification of the ground motion, and the increase on the record duration, from depth to the surface.

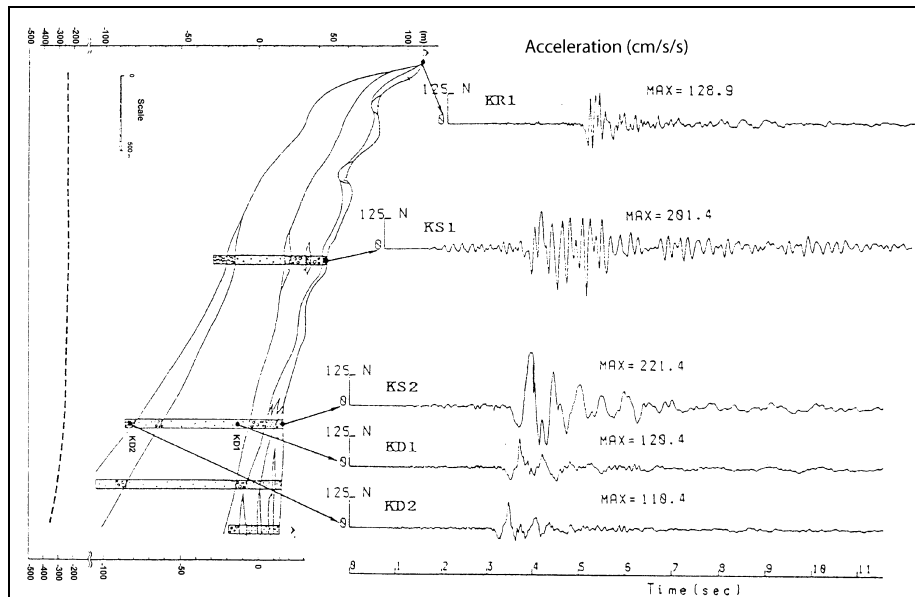


Fig. 4.11. Records of a $M=5.1$ event in the Ashigara Valley (Japan). Recorded on rock site (KR1) and different soil sites, KD1 and KD2 are boreholes at 30 and 80m depth (Kudo, 1991)

However, considering the high cost of these experiments, this method can be applied only at very specific sites and can not be used massively as a microzonation technique.

In the *Standard Spectral Ratio (SSR)* method, introduced by Borchardt (1970), instead of using the borehole sensor needed when applying SBSR, the Fourier spectrum of a given earthquake recorded at the site to be investigated (site S in Figure 4.8) is divided by that of a nearby reference site on bedrock (site R). Provided that the two sites have similar source and path effects and that the reference site has negligible site response, the obtained soil-to-rock spectral ratio gives a reliable estimation of earthquake soil response. Steidl et al. (1996) pointed out that the choice of the reference site might be critical, since rock sites might have their own site response and then a deconvolution would be needed to obtain an estimate to the bedrock record.

Alternate non-reference techniques have been developed. One of these methods, the so-called *Horizontal- - to -- vertical spectral ratio (HVSR)*, is based on the computation of the spectral ratio between the horizontal and vertical (H/V) spectra of the S-wave window at each site. This method was introduced by Lermo and Chávez-García (1993) to characterize site response. The basic assumption is that only the horizontal

components are influenced by the local structure. Lermo and Chávez-García (1993) found, for three different sites in Mexico, that both frequencies and amplitudes of resonant peaks were similar in the SSR and the HVSR. Theodulidis and Bard (1995) concluded that the HVSR shape appears to be well correlated with surface geology but the absolute level of amplification does not coincide with the absolute level of measured HVSR, which seems to be dependent on the incident wave type. Theodulidis et al. (1995) have applied H/V spectral ratio method to strong motion records from Greece and Taiwan obtaining reasonable results.

A number of other techniques have been proposed, among them those based on the inversion of *coda wave* and analysis of the coda decay (Phillips and Aki, 1986). One of the main drawbacks of these techniques is that in populated areas the ambient noise induced coda records are very difficult to obtain. Consequently, these methods have not been widely used for microzoning purposes.

4.7.2. MICROTREMOR MEASUREMENTS

One of the main practical problems associated to the methods that are based on weak or strong earthquake ground motion recording is that several earthquakes have to be recorded simultaneously on rock and on soils sites, imposing long periods of observation, even more when the seismic activity is moderate. Recording seismic events under different soil conditions for microzoning purposes is a slow and costly task. Microtremor measurements, instead, are easy and affordable to be carried out.

The first to use *microtremors* as a good source for the study of local effects was Kanai (1957) considering that the context of microtremors was white noise. The origin of this noise, also known as *ambient noise* or *cultural noise*, is still under debate, but a large portion might be due to surface waves and essentially of Rayleigh nature. While for frequencies below 0.5 Hz *microseism* is caused by oceanic waves or other perturbations of meteorological origin at large distances, for shorter periods (frequencies larger than 1 Hz) microtremors are essentially due to human activities such as traffic. The nature of surface waves, as an important part of microtremors, constitutes the basis of the experimental methods to determine the natural periods and amplifications of the soil strata.

The following techniques based on microtremor recordings are currently being used:

An analogous technique to that of the SSR described above uses spectral ratios between microtremor recordings at different soil sites and at the reference rock site (*sediment-to-bedrock noise ratio, NSR*). The main problem of this technique is the possible different origin of the noise recorded at the site under investigation and at the reference site. The identification of a common wave train for the stations involved is very difficult. Kagami et al. (1986), Field et al. (1990) and Seo et al. (1991) among others applied this method to different areas with successful results within given frequency bands. However, Gutierrez and Singh (1992) and Lermo and Chavez-Garcia (1994) among others report dissimilarities between spectral amplitudes of strong motion and microtremor records.

A technique using horizontal-to-vertical spectral ratios of microtremors (instead of earthquakes as in the HVSR technique) was first applied by Nogoshi and Igarashi (1970, 1971) and later popularised by Nakamura (1989b). This technique, usually called

the Nakamura's horizontal- to -vertical noise ratio (HVNR) or, simply, the *H/V* or *QTS*, *Quasi-Transfer Spectra*, is very frequently used for microzonation studies. Even though it is not completely supported by a sound theoretical basis, it has been shown as useful in some places.

Problems, possibilities and limitations of this method have been discussed by many authors (Lermo and Chávez Garcia, 1994; Lachet and Bard, 1994; Mucciarelli, 1998; among others). It should be considered that Nakamura's method gives a good account of the fundamental frequency at the site but do not give confident values of the corresponding amplification factor (Nakamura, 2000). In some soil conditions the largest amplifications occur not at the fundamental frequency but at higher modes. In simple situations, such as the case of a relatively homogeneous layer of soft, low velocity, soil lying over the rock basement (high impedance contrast), Nakamura's method is very efficient for determining the fundamental frequency which, in this case coincides with the predominant frequency (frequency for which the maximum amplification occurs). But when one tries to determine the fundamental frequency of more complex multilayer systems Nakamura's method gives low values as it provides an estimation of the fundamental frequency (produced by the deeper structure), which is not the frequency for which the maximum soil amplification takes place. This problem has been encountered in several cases, e.g. comparing modelling results with microtremor measurements in the city of Barcelona (Cid et al., 2001) as illustrated in Figure 4.12. While in zone III and I Nakamura measurements do not differ much from the predominant frequencies obtained from modelling, in zone II Nakamura's measurements account for the "fundamental frequency", first peak on the transfer function obtained numerically, which is a lower frequency than that where the maximum amplifications occur. The consideration of predominant frequency as one important parameter for microzonation should be taken with caution, as discussed in Chapter 8, because performance of buildings will depend not only on source / path of seismic waves, but also on the inelastic response of soil and structure.

The composition of noise wavefield is still a very controversial topic. The project SESAME (Bard, 2004) (<http://SESAME-FP5.obs.ujf-grenoble.fr>) offers several advancements in this field by comparing analytical developments with in-situ measurements. It contains a great proportion of surface waves in relation to body waves but the proportion of Rayleigh to Love waves is very questionable. Following Bard (2004), "the origin of *H/V* peak is multiple: Rayleigh wave ellipticity, Airy phase of fundamental Love wave mode, and partly fundamental resonance of S body waves", also a checklist of the main problems that may or may not influence the final results of *H/V* method is provided.

It can be concluded that the use of simple experimental methods without comparison with modelling results are not reliable unless they are based on strong motion records produced by several earthquakes. Both numerical and experimental methods should be complementarily applied in microzoning projects.

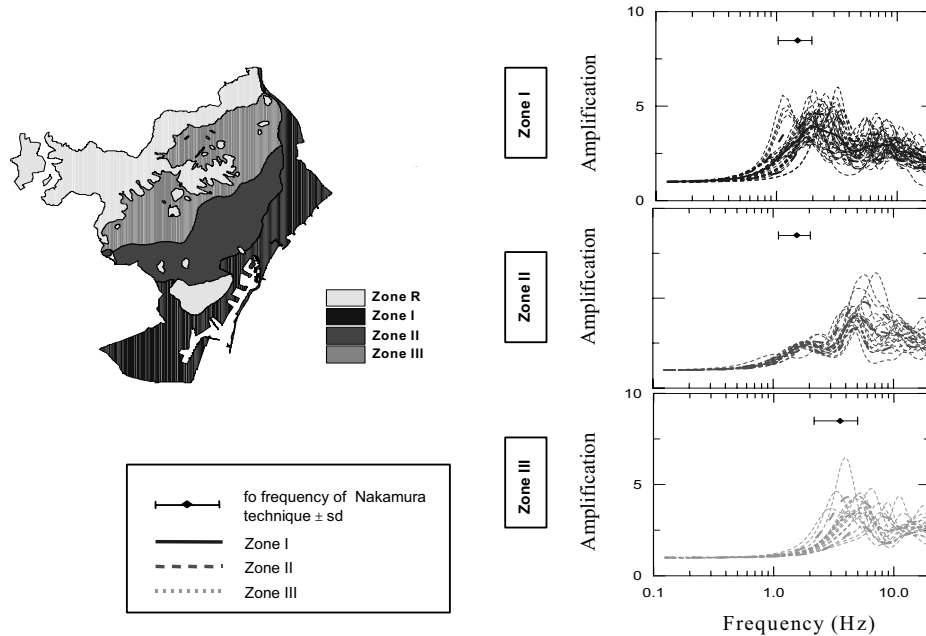


Fig. 4.12. Three plots with the transfer functions obtained at different points in three zones of Barcelona are shown together with the mean frequency (with standard deviation brackets) measured in each zone

4.8. Topographic effects

The influence of topography on the seismic signal is well known. It has been observed in past earthquakes such as the 1971 San Fernando, 1985 Central Chilean, 1989 Loma Prieta, 1994 Northridge and 1999 Athens events, among others, that concentrated patterns of damage and unusually high amplitude recorded ground motion near the crests of ridges are present (Celebi, 1987; Spudich et al., 1996; Bouckovalas and Koutretzis, 2001). Buildings located at hill tops suffer much more intensive damage than those located at the base.

Research on topographic effects has generally focussed on numerical studies of two-dimensional ridges or canyons (Geli et al., 1988; Zhang et al., 1998; Bouckovalas and Papadimitriou, 2004) and on empirical studies based on instrumental deployments that are in general limited to low amplitude recordings of aftershocks (Celebi, 1987; Pedersen et al., 1994). The main results from topographic effects studies pointed out by Brune (1984), Sanchez-Sesma (1983, 1985) are: i) amplification of SH waves near the crests of canyons; ii) the presence of a shear fundamental resonance in a 3-5 Hz frequency band; iii) dependence on the radiation wave field, angle of incidence and canyon dimensions.

Chávez-García et al. (1996; 1997) present a new comparison between numerical and empirical approaches; they use on one hand a generalised inversion technique and on the other the experimental HVSR (Horizontal-to-Vertical Spectral Ratio) technique explained in the previous section. They conclude by recommending the use of the HVSR, Nakamura, technique, which is in principle oriented to the study of the influence of soil conditions on ground motion, as a good approach to analyse also topographic effects. An overview of the subject of topographic effects can be found in Bard (1998) and Alvarez Rubio (1999). The Guidelines AFPS (1995) from the French Association for Earthquake Engineering give a simple way to calculate the topographic amplification coefficient and have been extensively used elsewhere. At present many countries and regions of the world have available high precision digital terrain models (DTM) which are very useful to predict the effect of topography on earthquake ground motions. However, one of the main problems in the identification of such effects is still the difficulty to distinguish between the topographic or geological origin of the observed ground amplifications. The various available techniques have to be applied simultaneously in order to reach satisfactory results.

4.9. Liquefaction and induced effects

Liquefaction is defined as the transformation of a granular material from a solid to a liquefied state as a consequence of increased pore water pressure and reduced effective stress (Martin et al., 1975; Marcuson 1978, Castro and Poulos, 1977). Increased pore water pressure is induced by the tendency of granular materials to compact when subjected to cyclic shear deformations. The change of state occurs most readily in loose to moderately dense granular soils, such as silty sands and sands and gravels capped by or containing seams of impermeable sediment. As liquefaction occurs, soil stratum softens, allowing large cyclic deformations to occur. In loose materials softening is also accompanied by a loss of shear strength that may lead to a large shear deformations or even flow failure under moderate to high shear stresses, such as beneath a foundation or a sloping ground. In moderately dense to dense materials, liquefaction leads to transient softening and increased cyclic shear strains, but a tendency to dilate during shear inhibits major strength loss and large ground deformations. A condition of cyclic mobility or cyclic liquefaction may develop following liquefaction of moderately dense materials. Beneath gently sloping to flat ground, liquefaction may lead to ground oscillation or lateral spread as a consequence of either flow deformation or cyclic mobility. Loose soils also compact during liquefaction and reconsolidation, leading to ground settlement. Sand boils may also erupt as excess pore water pressure dissipates. (Youd et al., 2001)

Figure 4.13 is a clear example of the liquefaction phenomenon as observed by the tilted buildings and excessive settlements in Adapazarı during the 1999 Kocaeli earthquake.

Foundation material did not support the shearing stresses developed during the passage of seismic waves causing the partial sinking of the building which led to overturning in some buildings with very shallow foundation depths and excessive settlements in others. These phenomenon observed throughout parts of Adapazarı did not occur in buildings supported by piles or in buildings with basements.

One possible approach is microzonation mapping in terms of the liquefaction susceptibility that may be based on the method developed by Youd et al. (2001). In this approach safety factors need to be calculated along the whole depth of the borehole for all liquefiable soil layers, based on the available SPT-N blow counts using the surface peak ground accelerations calculated from site response analysis.



Fig. 4.13. Evidence of liquefaction related damages during the 1999 Kocaeli earthquake

In order to evaluate the severity of induced liquefaction on the ground surface the method developed by Iwasaki et al. (1978) could be used. Iwasaki et al. (1978) quantified the severity of possible liquefaction at any site by introducing a factor called the liquefaction potential index, P_L , defined as

$$P_L = \int F(z)w(z)dz \quad (4.2)$$

where z is the depth below the ground water surface, measured in meters; $F(z)$ is a function of the liquefaction resistance factor, F_L , where $F(z)=1-F_L$ but if $F_L > 1.0$, $F(z)=0$; and $w(z)=10-0.5z$.

For the purpose of demonstrating the proposed approach, the liquefaction susceptibility microzonation map was produced for the Gölcük region in western Turkey. Based on the results reported by Iwasaki et al. (1978), three zones (A, B, and C) were identified with respect to liquefaction potential index. Zone A is where the liquefaction potential index is $P_L > 15$, zone B is the intermediate zone where the liquefaction potential index is $5 > P_L > 15$, and zone C is the safest zone where the liquefaction potential index is $P_L < 5$. The microzonation map for liquefaction susceptibility determined by this approach is shown for the Gölcük region with respect to surface geology in Figure 4.14 (Ansal et al., 2004).

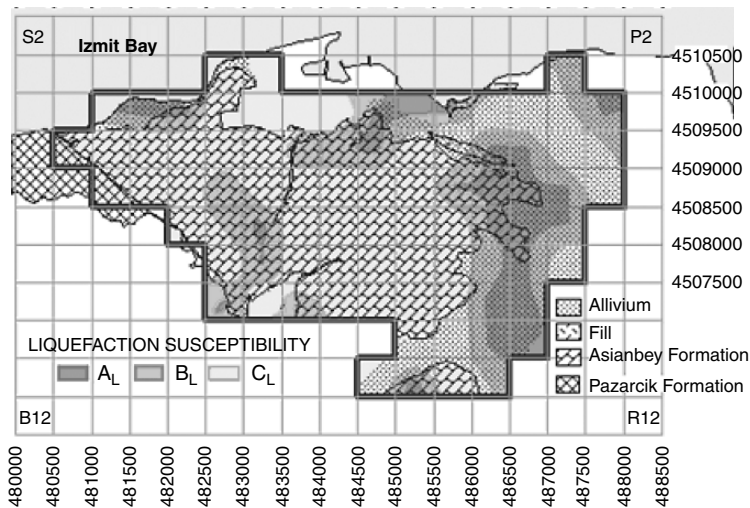


Fig. 4.14. Comparison of liquefaction susceptibility map with geological formations (Ansal et al., 2004)

4.10. Final Considerations

Seismic microzoning is clearly a powerful tool towards reducing earthquake risk in urban areas.

- Different experimental and modelling techniques are currently used for microzoning. However, it is still necessary to assess the limits of validity of those methods through comparison of results obtained in different areas using various techniques and also to calibrate them with real strong earthquake data. Comparison of experimental methods dealing with low amplitude in-situ measurements (such as wave velocity) and laboratory testing (resonant column, etc.) is of great importance.
- For this purpose it is recommended that the information from the various studies which are being carried out throughout the world should be collected and analysed under homogeneous criteria.
- More research in these fields is necessary in order to reduce the uncertainties that are present in the current studies and to satisfy the needs of society for having better established seismic codes.

Once microzoning analysis is well established its results should be incorporated in seismic regulations, both at the land-use and structural engineering levels (at the local level such as EC-8), especially in zones with dense population as in urban areas.

There still are microzonation methods of very different scope: some require simple techniques with one or two-parameters, others are very sophisticated with various parameters and detailed in-situ and laboratory measurements. Studies comparing these two different approaches in the light of cost-benefit analyses should be encouraged.

CHAPTER 5
SITE-CITY INTERACTION

P. -Y. Bard^{1,2}, J. L. Chazelas³, Ph. Guéguen^{1,2}, M. Kham^{1,2} and J. F. Semblat²

1. *University Joseph Fourier, Grenoble, France*

2. *Laboratoire Central des Ponts-et-Chaussées, Paris, France*

3. *Laboratoire Central des Ponts-et-Chaussées, Nantes, France*

5.1. Introduction

Structural and geotechnical engineers have been aware for a long time of soil-structure interaction (SSI) phenomena, which modify the seismic response of massive or tall buildings erected on soft soils. On their side, seismologists have known for a long time that it is not a good idea to install seismological stations close to trees. During the last decades, it has also become clear how large the effects of surface heterogeneities, commonly called "site effects" (SE, concerning soft soils as well as topographic features), can be. On this basis, it is legitimate to wonder whether a large building on a soft soil can contaminate the ground motion in its immediate vicinity (phenomenon hereafter abbreviated as "CGMB", Contamination of Ground Motion by Buildings). Going one step further, we may ask about the overall effect of such contamination in a densely urbanized area. The aim of this chapter is to present an overview of the results that substantiate the plausibility of this kind of "global" interaction between all the buildings of a city and its subsoil, which we call hereafter "site-city interaction" (SCI).

Despite the abundant literature on SSI and SE, their overlapping domains of CGMB and SCI have received surprisingly little attention. This could mean that the issues addressed here may be irrelevant. However, if SCI effects turn out to be significant, one immediate consequence is that erecting or destroying a building, or a group of buildings, could modify seismic hazard for the neighbourhood, which in turn could lead to significant conceptual changes, especially concerning microzoning studies, land-use planning, and insurance policies. Another goal of the present chapter is to try to convince the readers from the seismological and engineering communities, that the questions raised above are scientifically sound. To this end, we will show that these phenomena may be important from both scientific and engineering viewpoints, at least under some specific conditions.

We first present a brief review of the few observations available that indicate that SCI effects are real. Second, we consider the effects due to a single building, summarizing several numerical results that may be found in greater detail in other papers. We will show that these numerical results are in good agreement with instrumental data obtained during an ad hoc experiment. Based on this agreement, we then use our computing codes to evaluate the response of a group of buildings, representing a city (in a simplified way). The numerical simulations allow us to evaluate the effects of different soil and building characteristics and to determine under which conditions such SCI effects may be significant. Finally, we will conclude with some considerations on the kinematic energy in soils and buildings, respectively, which confirm that SCI effects should not be overlooked.

5.2. Experimental evidence

5.2.1. IN SITU OBSERVATIONS

As stated by Wirgin and Bard (1996), the first observation is now more than 30 years old and was reported by Jennings (1970). When forcing the Millikan library building on the Caltech campus into vibration with roof actuators, harmonic, stationary records corresponding to the building period were obtained on distant seismographs (up to distances of a few kilometres). The same experiment has been repeated recently (H. Kanamori and T. Heaton, personal communication), and confirmed the emission of surface waves propagating outward from the building base.

The second one was associated with the re-entry into the atmosphere of the Columbia space shuttle on its way back to Edwards Air Force base in California (Kanamori et al., 1991). Two broad-band stations in Pasadena and USC (downtown Los-Angeles) recorded a distinct pulse, with a period of 2-3 seconds, which arrived 12 s before the shock wave at Pasadena, and 3s after it at USC. Kanamori et al. (1991) clearly identified this specific arrival as due to "a seismic P wave excited by the motion of high-rise buildings in downtown Los Angeles, which were hit by the shock wave". The same authors add the following explanation: "the proximity of the natural period of the high-rise buildings to that of the Los Angeles basin enabled efficient energy transfer from shock wave to seismic wave".

The most recent observations occurred during the terrorist attacks against the World Trade Centre; the two plane impacts were recorded in several seismological stations in New-York state, at distances of several tens of kilometres (Kim et al., 2001).

In these three observations, the excitations to the buildings were artificial. They both show that there are cases where the energy of the vibrating building may be efficiently transmitted back into the soil as outward propagating waves. Our point in this chapter is to argue that the same kind of phenomena may occur when the vibration of the building is caused by earthquake loading. In this case, however, direct observation is much more difficult, as ground motion in the vicinity of the buildings is a superposition of the incident wave field and that diffracted by the building. Only very dense seismograph arrays could allow separation of the different contributions to ground motion.

Another interesting set of observations comes from the Ullevi stadium in Gothenburg (Sweden), which underwent unexpected forced vibrations, as reported in Erlingsson and Bodare (1996) and Erlingsson (1999). This stadium is built on a soft clay layer with variable thickness. During a rock concert held in the stadium, the audience began to jump according to the beat (with a frequency around 2 Hz). The waves emitted in the stadium by these jumps were trapped in the soil layer, reverberated up and down and propagated outward as surface waves. These surface waves in turn excited the tribune foundations and were then amplified by the tribune's own vibration modes leading to steady vibrations in the tribunes strongly felt by the spectators. A thorough numerical study showed that the large amplitude of these induced vibrations was due to the concomitance of several factors: the softness of the clay, its geometry with lateral thickness variations which made the wave trapping more efficient, and the coincidence between the frequency of the beat (around 2 Hz) and the frequency of the soil. Erlingsson and Bodare (1996) and Erlingsson (1999) estimated the jumping load to be

approximately 3 kPa, and computed a resulting displacement at the base of the tribune base, about 100 m away, of around 2 mm. This value corresponds to an acceleration of about 0.3 m/s². We may use these values to extrapolate to what may happen during an earthquake. As a very first approximation, the shear stress τ acting on the soil-structure interface may be taken as the ratio between the base shear force F and the foundation surface S :

$$\tau = F / S \quad (5.1)$$

Denoting α the "seismic coefficient", g the acceleration of gravity, ρ the equivalent mass density of the building, V the building volume, and h its height, we will have :

$$F = \alpha g \cdot \rho V = \alpha g \cdot \rho S h \quad (5.2)$$

Hence

$$\tau = F / S = \alpha \rho h g \quad (5.3)$$

Similar equations may be derived for the rocking moment, and thus for the vertical forces acting on each side of the foundation. In the case of a zone of moderate seismicity, with $a = 0.2$, a standard 7-story building with $r = 250 \text{ kg/m}^3$ and $h = 20 \text{ m}$ will be subjected to a base shear of:

$$\tau = 10 \text{ kPa, (i.e., 3 times the Ullevi stadium load)} \quad (5.4)$$

If the resonant frequency of the building is similar to that of the soil (around 2 Hz), we may thus expect that the soil-structure interaction phenomena will generate diffracted waves causing accelerations of the order of 1 m/s² ($3 \times 0.3 \text{ m/s}^2$), i.e., half of the input acceleration, within a distance of about 100 m around the building.

These values are only a rough estimate of the order of magnitude, and may be wrong by a factor of 2 to 3 depending on the actual building/soil system. However, they suggest that the perturbations in the building neighbourhood generated by the vibration of the building are not negligible.

An additional, indirect evidence comes from analysis of strong motion records obtained in instrumented buildings. As reported in various papers (Bard, 1988; Afra et al., 1990; Farsi, 1996; Paolucci, 1993; Meli et al., 1998; Cardenas et al., 1999), very often buildings founded on soft soils exhibit noticeable rocking motion due to soil-structure interaction. This has been observed even in structures built on pile foundations. By noticeable we mean that the rocking motion represents more than 10% of the pure flexural motion. In some particular cases, this proportion reaches 100% (see Bard et al., 1992). These observed rocking motions demonstrate the existence of large rocking moments acting on the soil at the foundation level, and it is well known that transient forces applied at the surface of a layered soil generate outward propagating surface waves.

In summary, although no clear observations have been yet made of the modifications of "free-field" ground motion by the presence of nearby structures during earthquakes, the observations we have discussed demonstrate that SSI effects can be quite large, and generate outward propagating waves in the ground. In particular, the reported series of

unexpected observations legitimates the design of specific experiments to obtain well controlled results.

5.2.2. CENTRIFUGE MODELLING

5.2.2.1. *Reduced scale modelling in the centrifuge*

Centrifuge modelling is a powerful experimental mean in soil dynamics, which combines reduced scale and representativity of full-scale phenomena, under well controlled conditions.

As mechanical properties of soils are strongly related to the stress state, working on reduced scale physical models meets a difficulty: the induced stresses are only very weak, and the soil response is completely different from its full scale response. The artificial gravity created within a centrifuge enables us to overcome this problem: the density of the model soil is kept constant and, as the length scale factor is $1/N$, an N times increase of the gravity will restore the stress field.

Reducing the scale makes parametric studies possible and, specifically in the earthquake domain, on-demand experiments are conceivable. For these reasons, studies utilizing a centrifuge in earthquake engineering and soil dynamics have met with great success since the beginning of the 1980's. They are generally well documented in the "Centrifuge" conferences (Corté, 1988; Ko and McLean, 1991; Leung et al., 1994; Kiimura et al., 1998; Phillips et al., 2002). Of course, attention must be paid to scale and boundary effects as only a limited volume of soils can be included in the test.

5.2.2.2. *Evidence for significant SSI from simple centrifuge experiments*

Our first objective was to check whether the motion of one building could be affected by the presence of another building. We thus designed an experiment with one "active" building, forced into vibration by an impulse shock (with a "ball cannon"), and a second, passive, identical building located at some distance. The motion was recorded at the top of each building, and the dependence of each building response upon the separating distance was investigated.

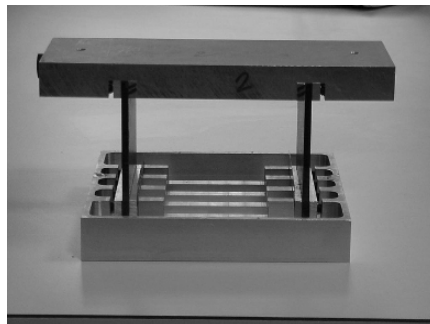


Fig. 5.1. Building model for centrifuge testing

The design of the model buildings was intended to reproduce a seven storey building with a foundation of 15 m x 15 m, following studies by Guéguen (2000), Guéguen et al. (2002) in Mexico City. The chosen reduction scale was $1/N = 1/100$. Parameters for which it seemed mandatory to respect scale factors were the stress state under the

foundation (i.e., the ratio of the total mass to the foundation surface, scaling factor equal to 1), the momentum computed at the bottom of the foundation (scaling factor equal to $1/N^2$) and the first modal frequency (scaling factor equal to N). In order to simplify the analysis, the design (Figure 5.1) intended to reproduce a Single Degree of freedom (SDOF) system: a system with two blades carrying the mass of the superstructure and embedded in a foundation allowed to limit the vibrations to one single direction. The frequency factor was not perfectly respected due to mechanical assembly (Table 5.1). The soil model, $1.20 \times 0.80 \times 0.36 \text{ m}^3$ in size, was made of Fontainebleau fine dry sand with a homogeneous specific gravity of 16.3 kN/m^3 obtained through a raining process. Additional details may be found in Chazelas et al. (2003).

Table 5.1. Respective characteristics of the reference and the model buildings

	Full Scale	Model Scale
Superstructure mass	945 103 kg	1,013 kg
Foundation mass	567 103 kg	0,549 kg
Foundation surface	15 x 15 m	15 x 15 cm
Momentum /foundation	$1,88 \cdot 10^5 \text{ kg.m}^2$	$1,8 \cdot 10^{-5} \text{ kg.m}^2$
First modal frequency	4,76 Hz	275 Hz on the sand 300 Hz embedded

The "active" building (the one shocked B1) was first embedded in the sand, in the middle of the soil model. The "passive" building B2 was then simply laid on the sand, successively at different distances and in different positions, along the radial and transverse directions.

Figures 5.2, 5.3, and 5.4 display the motions recorded at building top for three different configurations. In the absence of any interaction, the response of the active building should remain the same, while the "passive" one should not move. Clearly, this is not the case: the passive building does move, and the active one exhibits beating, which is more and more pronounced as the second building is closer. Both buildings talk to each other through the soil, and the beating comes from the similar values of their resonance frequencies. These observations are consistent with the full scale experimental observations of Kitada et al. (1999), reporting variations in the resonance frequencies of a building depending on the existence or not of neighbouring buildings.

Two other significant results can be derived from these simple centrifuge experiments.

- First, this structure to structure through soil interaction is efficient only when the frequencies of the structures are close enough: as the models were weakly damped (1%, due to their mechanical constitution), a separation of 0.3 Hz of their resonance frequencies (full scale) was enough to cancel the interaction. Larger damping values (which is often the case for real structures, see Dunand et al., 2002, 2003; Farsi, 1996) will enlarge this separation limit.
- Secondly, the efficiency of this phenomenon has a limited range: under the present, specific, experimental conditions (dry sand, building frequency, $f^B=275 \text{ Hz}$), it is noticeable (on the active building) only when the distance between buildings is less

than 25 - 30 m. This value should however be considered as only indicative: it depends on the damping properties of the soil and it may be different also for taller or smaller, or groups of buildings.

5.3. Modelling simple interaction

Both the "unexpected" and "on purpose" experimental observations have thus shown the possible contamination of ground motion by surface buildings and the fact that buildings may influence each other through the soil. Modelling these effects may be approached along two directions, exactly in the same way seismologists approached the crustal scattering:

- "single" interaction might be modelled by considering each building as if it was alone, and simply adding the contributions from each building, and neglecting feedback effects,
- "multiple" interaction, which includes feedback effects, i.e. dialog between buildings through the soil.

The first approach is valid if there is only a weak interaction, the second one should be applied in case of strong interaction. This section will briefly recall some already published results about the first approach.

5.3.1. MODEL AND CALIBRATION : THE VOLVI EXPERIMENT

This approach consists in computing the wave field emitted from a building when shaken by an incoming signal. Such computations may be separated into two main steps: a) estimating the forces deriving from soil-structure at the foundation level and b) computing the waves radiated back in the ground with a numerical scheme solving the elastodynamics equation. The developed algorithm (Guéguen et al., 2000, 2002) uses impedance functions to achieve step a), and the discrete wave number technique (Bouchon, 1981) for step b), in the modified version proposed by Hisada (1994, 1995).

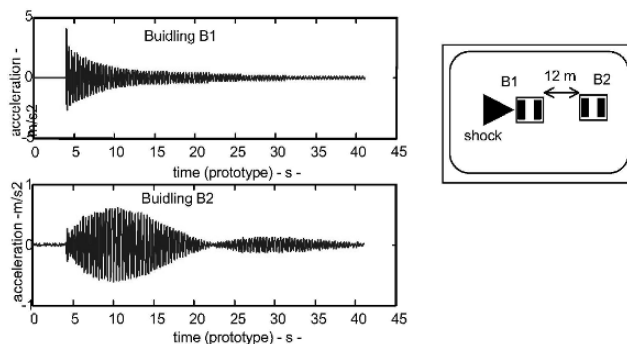


Fig. 5.2. Centrifuge tests of SSSI. Interaction between B1 and B2 with longitudinal transmission. Horizontal acceleration on top of the two 12 m distant building. (Test S4-M1210604-prototype scale)

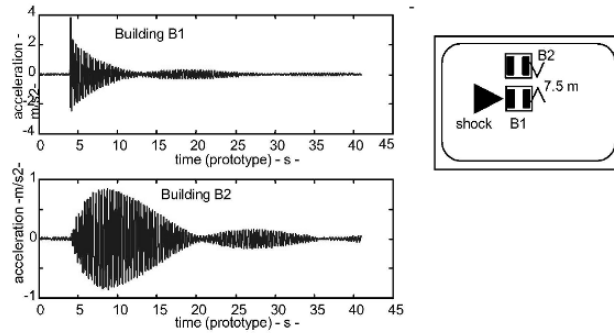


Fig. 5.3. Centrifuge tests of SSSI. Interaction between B1 and B2 with transverse transmission. Horizontal acceleration on top of the two buildings separated by 7.5 m. (Test S4-M1210202 – prototype scale)

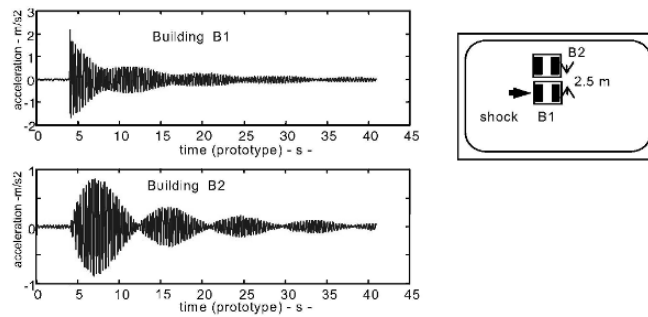


Fig. 5.4. Centrifuge test of ISSS. Interaction B1-B2. Transversal transmission Rocking axis// Distance 2.5 m. Horizontal acceleration on top of buildings. (Test S4-M121040-prototype scale)

This approach was validated through an experimental study performed at the Volvi test site (Greece), as reported in Guéguen et al., 2000. In addition to detailed investigations on site conditions and site response, this test site hosted the construction at the valley centre of a reduced scale (1/3), 5-story RC structure (Manos et al., 1995).

A series of pull-out tests (POT) was performed on this structure, consisting in shaking it by the sudden release of a pre-stressed steel cable, anchored to the building top and to the ground. The ground motion resulting from the free oscillations of the structure was recorded by a series of sensors at increasing distances from the structure. These records were then compared with the computations derived from the two-step model described in Guéguen et al. (2000, 2002).

The main results of this comparison are summarized in Figure 5.5, displaying the vertical and radial components of motion for a pull-out excitation in the longitudinal ("L") direction, and the transverse motion for a pull-out excitation in the transverse ("T") direction.

The records clearly exhibit a monochromatic signal similar to the free response of a damped oscillator. The corresponding frequency and damping do not depend on the distance, and are thus directly linked to the free-oscillation characteristics of the building (4.761 Hz in the T direction, and 4.944 Hz in the L direction). As expected, the amplitude is decaying with increasing distance from the building base, keeping however non-negligible values: at a distance twice the size of the building base, it still amounts to about 25% of the base motion, while at a distance five times larger, this ratio amounts to about 5%, corresponding to an overall decay shaping as $1/\sqrt{R}$. The fairly good resemblance between computations and observations provides a validation of the simple model: this model was therefore used for an investigation of the effects of SSI in cities with a large number of buildings.

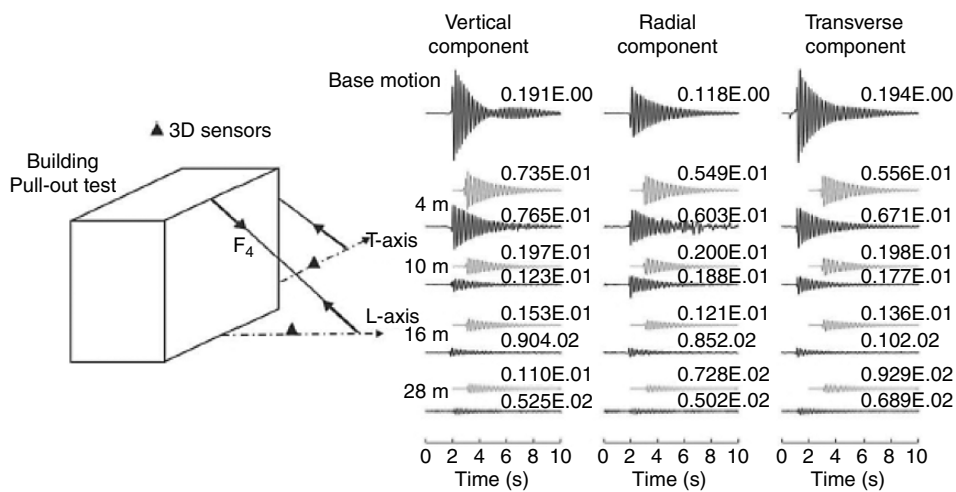


Fig. 5.5. Results of pull-out tests on the 1/3 scale model building in Volvi (after Guéguen et al., 2000). Left: schematic representation of the POT with axis orientation.

Right: Comparison of the computed ground motion (grey lines) with the actual recordings (thick black lines) obtained at increasing distances from the building along the L axis (from 0 to 28 m). The two left columns display the vertical and radial motion for a POT along the L direction, the right column displays the transverse motion for a POT along the T direction

5.3.2. APPLICATION TO MEXICO-CITY

This simple model has thus been applied to evaluate the effects of SSI on the "free-field" motion within a city, composed of many buildings. In this simplified approach, the total wave field radiated back into the soil from the buildings is simply considered to be the superposition of the effects of each individual building: they are supposed not to interact with each other.

While such computations were performed for three different cities (Mexico City, Grenoble and Nice, both in France), we will briefly discuss here only the results obtained for the "Colonia Roma" area of Mexico City. Additional details may be found in Guéguen (2000) Guéguen et al. (2002) and Bonnefoy-Claudet (2001).

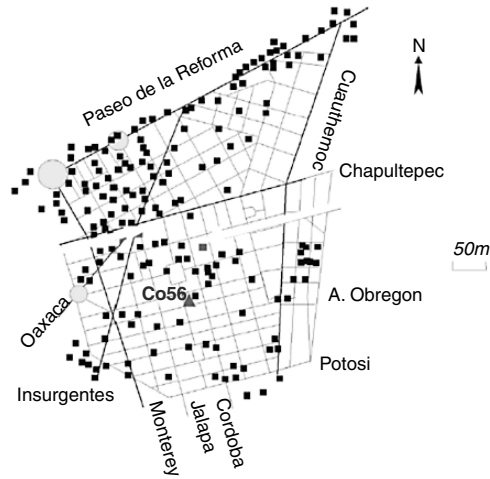


Fig. 5.6. Location of buildings having 7 storeys and more in the Colonia Roma in Mexico City; the ground motion is computed at site "Co56", where an accelerometer is located

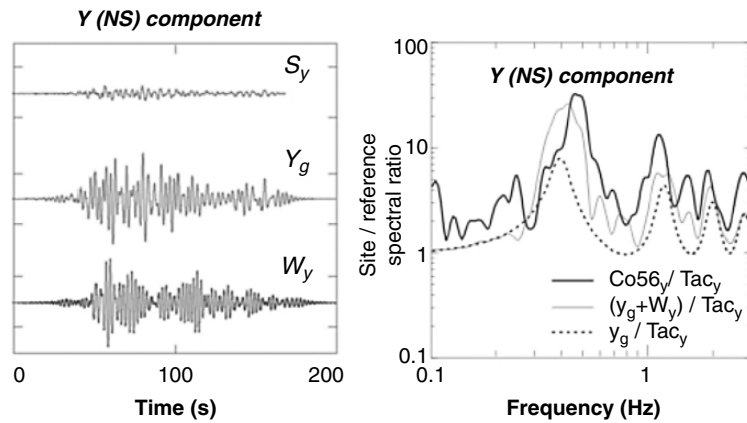


Fig. 5.7. Example effects of single interaction for Mexico City: the ground motion due to the waves radiated from each of the 180 buildings (W_y) is compared with the free-field motion (Y_g) at site Co56. The input rock motion S_y is displayed on top left. The comparison is performed in the time domain (left) and in the frequency domain (right), with a comparison of the site to reference rock spectral ratios (with: $Y_g + W_y$ and without - Y_g) buildings) with the actual observed amplification at Co56

As well known, Mexico City is characterized by the presence by a very soft clay layer ($V_s \approx 60$ m/s) underlain by much stiffer sediments ($V_s \approx 600$ m/s). In the Colonia Roma area, its thickness is around 30-40 m, leading to large amplification with a fundamental frequency around 0.5 Hz. Within the modelled area having a size of about 500 by 500 m², only buildings having 7 storeys and more were considered (180 in total) (Figure 5.6).

The time domain results displayed in Figure 5.7 for a site located approximately in the centre of the area clearly show that the ground motion induced by the presence of buildings is comparable with the free-field motion in terms of amplitude and duration, while its frequency content is essentially peaked at the site's fundamental frequency (0.5 Hz). In the frequency domain (Figure 5.7, right), this approach shows that the effects of SSI help in filling the gap between theoretical 1D transfer functions and actual observed amplifications (site/reference spectral ratios).

Moreover, a parametric study keeping the same geographical location for the 180 buildings, but changing their size and height (i.e., their resonance frequency), very clearly shows that the maximum effects occur when the frequencies of buildings coincide with soil frequency: would all the 180 buildings be identical and have a resonance frequency of 0.5 Hz, then this approach predicts that the energy associated with the radiated wave field (in terms of Arias intensity) would reach 20 times the free-field energy ! In that case however the validity of the "single interaction" approach is questionable, and one must consider multiple interaction models since the centrifuge tests showed that each building in the city may be influenced by its neighbours.

Similar results were obtained for the simulations performed on the city of Grenoble and Nice (Guéguen, 2000; Bonnefoy-Claudet, 2001), although with significantly lower amplitude (energy perturbations around 10 %) of the free-field energy.

5.4. Multiple interaction

Accounting for multiple interaction requires more advanced numerical models (such as finite elements or boundary integral methods), and much more computational time, especially when one wants to consider fully 3D cities. The first results were therefore obtained only recently, either for 2D models (Wirgin and Bard, 1996; Kham et al., 2003; Tsogka and Wirgin, 2003; Kham, 2004; Semblat et al., 2004), or for 3D models (Clouteau and Aubry, 2001; Mezher, 2004; Bielak, 2004, personal communication). We will limit ourselves in this section to the presentation of a few typical results in the 2D case, and refer to recent results in the 3D case, that all show the same trends and changes with respect to a) the free-field case and b) the single interaction approach.

5.4.1. 2D CASE

We consider here several model cities consisting of a large number of buildings laid over a 2D valley, and compute their response to vertically incident plane SH waves with the boundary elements method. Both buildings and soils are supposed to be invariant and infinite along the third axis. We first focus on a simple "canonical" model with a very simple geological structure, and investigate the sensitivity of the response to some parameters (soil/building frequency ratio, building density), and then consider a more realistic configuration (derived from the city of Nice).

5.4.1.1. 2D site-city canonical model

The geological structure (upper left Figure 5.8) consists in a 2.4 km wide alluvial valley with a trapezoidal shape lying over a semi-infinite bedrock. The sediment thickness H is constant over the main part of the valley (2 km), and vanishes over a 200 m distance on

each edge with a constant slope. The mechanical properties of both sediments and bedrock (upper right of Figure 5.8) correspond to a large impedance contrast (8.6), and standard damping (2% in the sediments and 0.5 % in the bedrock). Since the sediment thickness is always taken very small compared to the width (ratios smaller than 0.04), the "free-field" valley response is essentially one dimensional (vertical reverberations) with however some 2D perturbations due to late arrivals.

Two city configurations are then considered above the valley. The first one (top left), or "periodic city", consists in N identical buildings regularly distributed in the central part of the valley, over a total width of 500 m. Varying N is equivalent to modifying the "urban density". The second one (middle part), less regular, consists in a set of irregularly spaced, different buildings, still located in the central part of the valley. The exact geometrical configuration of this non-periodic city is displayed in the middle of Figure 5.8. However, for sake of simplicity only two different types of buildings are considered (B1S and B2S), characterized by their respective natural frequencies (1 Hz and 2 Hz) and size (Table 5.2).

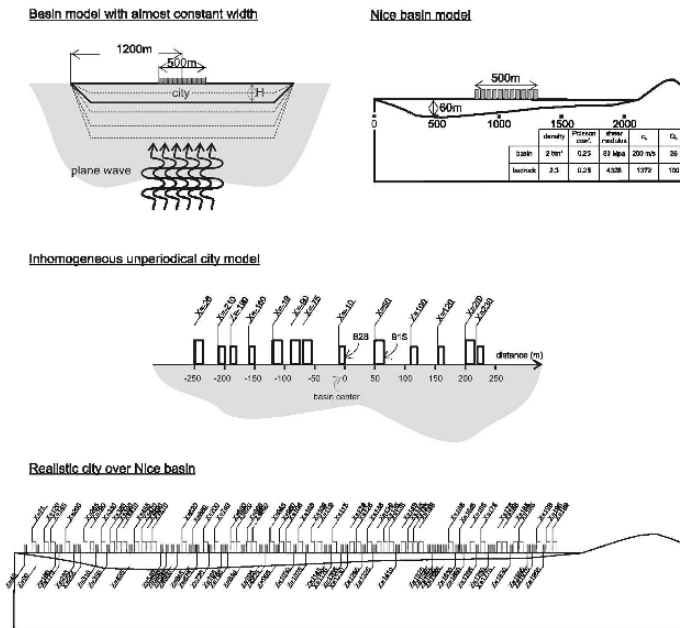


Fig. 5.8. Valley and city models considered for the 2D site-city interaction analysis: top left cross section for the canonical model, top right cross-section for the Nice case; middle: building layout for the non-periodic canonical model; bottom: building layout for the Nice case

Table 5.2. Mechanical properties of the buildings considered in the city models

Building type	Height	Base width	Density	Q_s / ξ_s	f^B
B1S	40 m	15 m	250 kg/m ³	10 / 5%	1 Hz
B2S	30 m	10 m	250 kg/m ³	10 / 5%	2 Hz

In the numerical model, buildings are approximated by homogeneous, continuous elastic elements, characterized by equivalent, homogeneous mechanical properties. These properties are given in Table 5.2 for the two building canonical types B1S and B2S. The boundary conditions considered for the soil-building interface are straightforward: continuity of displacement and stress vector.

The computations were performed for various configurations in order to estimate the sensitivity of the site-city interaction phenomena to several important parameters:

- The "urban density" $\theta = N \cdot B / L$, where N is the number of buildings, L the width of the urbanized area, and B the building width. For the periodic city case, we considered four different values for N (10, 16, 25, 33), corresponding to urban density values of 0.2, 0.32, 0.5 and 0.66, respectively. For the "non-periodic" city with B1S and B2S buildings, $\theta = 0.32$.
- The thickness H controls the 1D resonance frequency of the valley f_0^S through the formula $f_0^S \approx C_S / 4H$ (where C_S is the shear wave velocity). We considered five different thickness values ($H = 12.5, 25, 33, 50, 75$ m), corresponding respectively to fundamental frequencies of (4, 2, 1.5, 1.0 and 0.67 Hz). Therefore, for the periodic city case involving B2S buildings, the corresponding site to building frequency ratio f_0^S / f^B is equal to 2, 1, 0.67, 0.5 and 0.33.

5.4.1.2. Typical results

Figure 5.9 displays the modifications in the ground motion response within the city for various valley thicknesses, for the periodic city case with maximum density (33 buildings). Transfer functions (left) are computed for each surface site at mid-distance from the buildings: as there are variations from site to site, there are shown here only the average response within the city (thick solid line) and the average plus-minus one standard deviation (thin solid lines) to quantify the variability. Their comparison with the free-field average transfer functions (dotted line) shows clearly that the largest modifications occur for $H=25$ m, i.e., when the valley frequency coincides with building frequency (2 Hz); moreover, one may also notice that whatever the valley thickness the maximum differences occur around this frequency, in particular for $H=75$ m (the building frequency then coincides with the first higher resonance frequency of the site). The same observations can be made on time domain results (right), displaying only the perturbations introduced by the buildings (i.e., $u^P = u - u^{FF}$) submitted to an incident Ricker with central frequency $f^R = 2$ Hz and unit amplitude. Once again, the maximum effects clearly appear for $H = 25, 33$ and 75 m, i.e., when the free-field response exhibits a resonance (fundamental or first harmonic) close to 2 Hz. Most interesting is the fact that the overall effect of buildings is to slightly reduce the amplification level at this frequency. In addition, the rather small dispersion of the solutions indicates the response remains quite similar within the whole city. We can thus infer that the building array induces a "group effect": the added mass acts as a "cap" that slightly decreases the frequency of the whole system and reduces its motion. These results, shown here only for one type of incident waves, were shown in Kham (2004) to be very general: site-city effect occurs only when site and building frequencies coincide, while it is negligible when they don't.

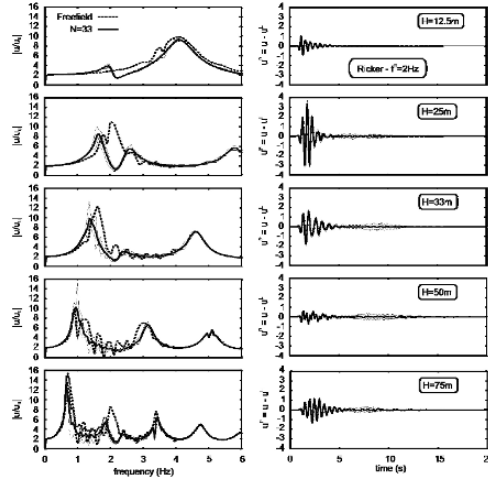


Fig. 5.9. On the left- Surface transfer functions (average value plus and minus one standard deviation) inside the homogeneous and periodical city (with B2S) for $N = 33$ and different thickness values (H). Solutions are compared to the free-field (dotted line). On the right- Corresponding free surface perturbation $u^P = u - u^{FF}$ for a Ricker central frequency $f^R = 2\text{Hz}$

Considering now the free-field perturbation u^P outside the city (Figure 5.10), one can clearly observe a surface wave propagating outward from the city. As its amplitude is strengthened when the number of buildings (urban density) increases, we can conclude this wave is generated by the "city": soil-structure interaction occurring for all the buildings results in the emission of a coherent wave propagating away from the city. This interpretation is also supported by the observation that the amplitude of this wave is maximum when site and building frequencies coincide (see later Figure 5.11), and is consistent with observations in the Volvi test site.

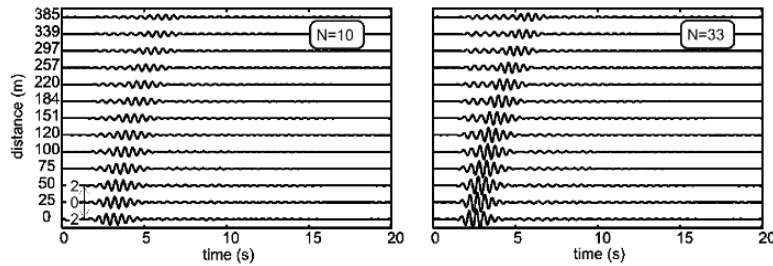


Fig. 5.10. Free surface perturbation outside the city for $H = 25\text{ m}$, a Ricker central frequency $f^R = 2\text{ Hz}$ and $N = 10$ and 33 . The distance origin is settled at 500 m from the city centre (i.e., 250 m from the nearest building). The amplitude scale between each trace is 2

In order to summarize the main features of the site-city interaction, we have considered the signal “energy” $E(x) = \int_0^T \dot{u}(x,t)^2 dt$, where \dot{u} is the ground velocity and T the

signal duration. It was then averaged for surface points within the city (at mid-distance between neighbouring buildings) and also outside the city (sites shown in Figure 5.10), and normalized by the corresponding free-field value E^{FF} . This was done for all the periodic city configurations (various thicknesses and urban densities) impinged by a 2 Hz Ricker wavelet, and the non-periodic city as well (various thicknesses only). Figure 5.11 summarizes the results by displaying the variations of surface energy with valley thickness for different urban densities, both inside (left) and outside (right) the city. These results call for several comments:

- Within a periodic city, effects of site city interaction are beneficial: the average ground motion is reduced (these results are also valid when considering the building roof motion).
- This reduction is increasing with increasing urban density and is maximum when building and soil frequencies coincide (here, $H = 25$ and 75 m). In optimal conditions (largest density, $H=25$ m), the reduction reaches 50%.
- The "density" effect can however be significant even when frequencies do not coincide (for example, we have similarly $E/E^{FF} = 67\%$ for $N = 10$ at $H = 25$ m and $N = 33$ at $H = 50$ m).
- These reduction effects unfortunately drop significantly when the building regularity is broken: the reduction for non-periodic cities does not exceed 15% This may be explained both by the low effective density of 2 Hz buildings ($NB2S = 7$) and the weakness of the group effect due to irregular layout.

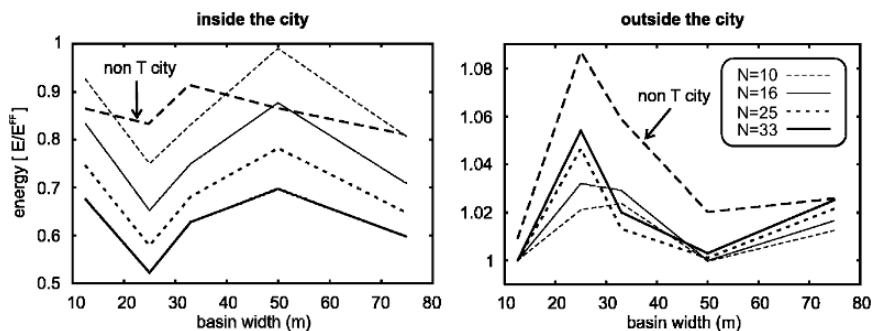


Fig. 5.11. Variations of the average normalized signal energy inside (left) and outside (right) the periodic city with B2S buildings with the valley thickness and urban density, for an incident Ricker wavelet with central frequency $f^R = 2$ Hz. Also included is the comparison with the case of the non periodic ("non-T") city

In contrast, outside the city the signal energy is slightly increased. This increase is due to the signal lengthening related with the city diffracted waves, and thus follows the same dependence on density and thickness already observed within the city – except for the fact that a non-periodic city leads to larger effects. It never exceeds, however, 10%. This increase may no longer be systematically observed in case of longer incident signals (destructive as well as constructive interferences may occur between the free-field response and the radiated waves).

5.4.1.3. From canonical to real cities: an example from Nice

We now consider the more realistic geological structure corresponding to an east-west cross-section within the city of Nice (Figure 5.8). The free-field response (i.e., without buildings) exhibits a fundamental resonance around 1 Hz in the deepest part of the middle-west ($H = 60$ m), with large amplification due partly to 2D effects (Semblat et al., 2000; Kham, 2004). The shallower western and eastern edges exhibit an efficient surface wave diffraction power for frequencies exceeding the corresponding fundamental resonance around 2 Hz.

In Figure 5.12, we compare the normalized signal energy distribution along the basin for the four city models: the periodic cities with either B1S ($f_0^B=1\text{Hz}$) or B2S ($f_0^B=2\text{Hz}$) buildings over a total lateral extent of 500 m, the non-periodic city over the same extent and the realistic city spanning the whole valley. Two Ricker frequencies $f^R = 1\text{Hz}$ and 2Hz are considered. The main features are the following:

- Almost all cases give rise to a reduction of ground motion energy inside the city, due either to group (frequency coincidence) or inertial (urban density) effect. For example, the energy reduction for the periodic B1S city under an incident 2 Hz Ricker wavelet is probably due to the inertial effect.
- The only exceptions correspond to the B2S periodic city and the easternmost part of the "realistic" city, both under an incident 1 Hz Ricker wavelet. This may be interpreted as due to the shift towards lower frequency induced by the presence of buildings, which therefore increases the ground motion response since input energy is larger at lower frequency.
- Some energy increase often appears at the city borders. These peaks may reach 50%: smaller structures built on the immediate outskirts of dense downtown areas may be exposed to increased ground motion.

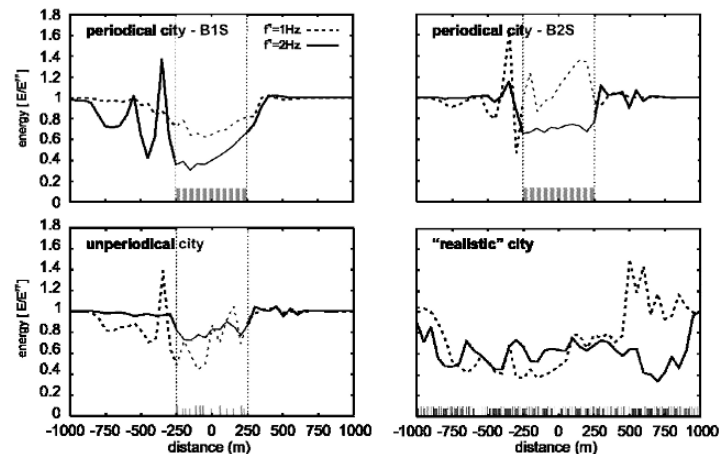


Fig. 5.12. Variations of signal energy (normalized by the free-field energy) for the Nice cross-section, for different city configurations and under two Ricker wavelets: $f^R = 1\text{Hz}$ (dotted line) and 2Hz (solid line). Four city configurations are considered: periodic cities with B1S (top left) and B2S (top right) buildings, the non-periodic city (bottom left) and a realistic city spanning the whole valley (bottom right)

Other computations (not shown here) for the "realistic" city case show that, despite a general trend to energy reduction, there may exist locally some significant increase (together with significant decrease at some other location): the occurrence and location of local maxima depend on many factors, like the city configuration, the dynamic properties of the buildings and the site, and the frequency range of the input signal.

5.4.1.4. Conclusions

This 2D analysis allows inferring that, contrary to what was obtained with "single interaction" models, a dense urbanization should have generally a global beneficial effect on the seismic risk. This apparent inconsistency between multiple and single interaction models may be explained by the fact there is a very strong interaction, and that single interaction models are not valid, at least in case of a large urban density. The ground motion reduction has two major origins: the group effect due to dynamic resonance of the buildings connected to one another through the soil, and the inertial effect due to the accumulated mass of the buildings. Nonetheless, the effects are much less pronounced in the (usual) case of heterogeneous, non-periodic building distributions, which in addition often give rise to local increase in ground motion energy, especially at the borders of homogeneous building blocks.

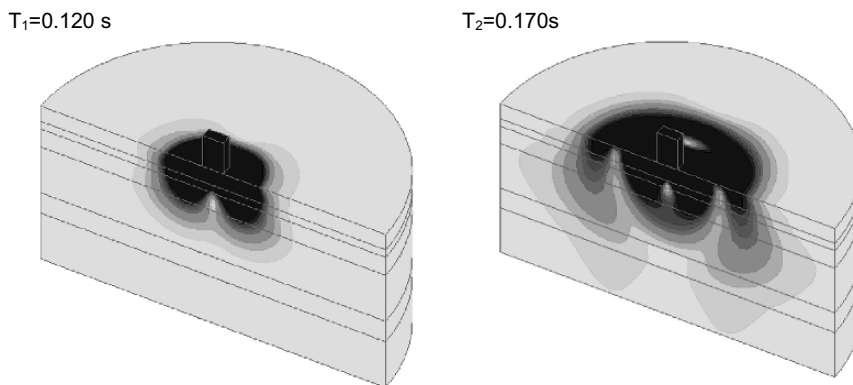


Fig. 5.13. Modelling SSI effects in 3D with finite element methods (CESAR-LCPC): snapshots of the displacement field generated by the free vibration of a model building on a horizontally layered soil (this case corresponds to the pull-out tests in Volvi, see section 5.3)

5.4.2. HINT ON 3D RESULTS

The next step is then to consider 3D multiple interaction. This certainly requires more sophisticated and powerful numerical models, and very large computation time. It has, however, several interests linked to the physics of the phenomenon:

- As already mentioned and clearly shown in Figure 5.13, the origin of site-city interaction is the radiation of waves from the building foundations and their trapping as surface waves in the surface layers. In 2D models, such surface waves do not have any geometrical expansion, while in 3D they decrease basically as $R^{-1/2}$: this may decrease the importance of the site-city interaction observed in 2D models.

- This phenomenon also induces a strong directivity in the radiated wave field, depending on the building motion. This directivity is not accounted for in 2D models

5.4.2.1. *Modelling 3D site-city interaction*

SCI configurations can be much more diverse in the 3D case than in the 2D case, and the definition of models thus requires careful attention. The site may be horizontally stratified, but may as well have a fully 3D geomechanical structure. The "city" may be anything between a fully periodic city with identical buildings, and a completely irregular layout of different buildings. The model variability, however, is often limited by the actual capabilities of the numerical techniques. Reliable modelling of SCI should properly represent both the 3D seismic wave field in the soil, and the structural dynamic behaviour, which suggests combining different numerical schemes adapted to these various requirements (e.g.: the BEM for the first aspect and the FEM for the latter). Comprehensive studies should then address successively / simultaneously the following issues:

- 3D dynamic response of the buildings (modelling by shells, beams, masses...).
- 3D building arrangement in the city model.
- 3D radiation of the seismic wave field.
- 3D polarization of the incident/scattered fields and associated wave conversion processes (directivity, longitudinal vs transverse motion...).
- 3D geological structure of the site and related amplification phenomena.

Another very interesting approach, followed by Ishizawa et al. (2003), is to consider the whole system as a quasi-random medium, for which the leading phenomenon follows the diffusion theory: the resulting average effects, for city configurations described by statistical properties, are in very good agreement with more traditional, deterministic approaches.

5.4.2.2. *Current results on 3D site-city interaction*

Several numerical approaches have been combined to analyse 3D site-city multiple interaction: homogenisation theory, boundary integral equations, sub-structuration, finite element techniques. They are able to cope with realistic models involving fully 3D geometries, deep or shallow foundations, and complex city layouts, but they generally considered only horizontally stratified sites (Clouteau and Aubry, 2001; Mezher and Clouteau, 2003; Ishizawa et al., 2003; Mezher, 2004; Lombaert et al., 2004).

The main results obtained up to now may be summarized as follows:

- For the considered cases (Mexico City, Nice), 3D site-city interaction does modify the motion at ground surface: it affects the location of resonance peaks and their amplitude as well (with either decrease or increase, depending on the frequency and on the location).
- It also leads to a duration lengthening and a significant decrease of the spatial coherency of ground motion, except at the system resonance frequencies where "group effects" result in a coherent motion.

- The comparison with results derived from simple interaction models (for instance those considered in section 5.3.2) shows the latter generally overestimate the final additional amplification due to site-city effect, especially around the fundamental frequency of the system.
- The 3D numerical results show that the effects are not systematic: for Mexico City, the average effect is an amplitude decrease, while it is the opposite for the city of Nice. However, whatever the average trend, the added variability induces some local maxima exceeding by at least 50% the amplitude due to site effects alone.

All these results, though obviously still sparse and partial, do confirm the possible importance of such effects, which should not be overlooked. It is not possible however to perform full 3D computations for any site-city configuration: the following section is thus aimed at proposing a simple criterion to detect whether a city may be prone to such effects or not.

5.5. A simple energetic model

5.5.1. AN INDEX FOR SITE-CITY INTERACTION

The above results may sound bizarre for many seismologists or structural engineers, especially as one generally imagines that the energy required to force a building into vibration is small compared with the total energy carried by seismic waves. For this reason, we consider this point in more detail (though with very rough approximations), for a collection of N buildings built on a soft soil layer. We estimate successively the total kinematic energy of the soil layer, and the total kinematic energy of the buildings. We propose that the interaction may occur when the two energies are comparable, which leads us to propose an index based on the ratio between soil and building kinematic energies.

5.5.1.1. Soil layer

Let us consider a soft soil layer, characterized by its specific mass ρ_s , its S-wave velocity v_s (or β_s), and its thickness h_s . When impinged upon by seismic waves, the whole soil volume will vibrate, with some characteristic frequencies linked to soil rigidity.

At a given time, its kinematic energy E_s over an urban area having a total surface S can be written as follows:

$$E_s = 0.5 S \int \rho_s \cdot v^2(z) dz \quad (5.9)$$

where $v(z)$ is the ground velocity at depth z . We implicitly consider in the following that the impedance contrast with the underlying bedrock is large enough (i.e., beyond 4 to 5), to induce an efficient band-pass filtering of surface ground motion around the fundamental resonance frequency f_s of the soil layer. Thus, the ground velocity may be written as:

$$v(z) \approx v_{\max} \cos(\pi z/2h) \quad (5.10)$$

where v_{\max} is the peak ground velocity at surface. Considering again the band-pass filtering around f_s , the peak velocity may also be related with the peak ground acceleration through the relation :

$$v_{\max} = K \cdot a_{\max} / (2\pi f_s) = 2 K \cdot a_{\max} \cdot h \cdot / (\pi \beta_s) \quad (5.11)$$

where K is a coefficient comparable to 1 ($K = 1$ for a purely monochromatic wave).

The kinematic energy of the soil layer may thus be roughly approximated as:

$$E_s \approx S \cdot \rho_s \cdot h \cdot v_{\max}^2 / 4 \approx S \cdot (\rho_s \cdot h^3 \cdot K^2 a_{\max}^2) / (\pi^2 \beta_s^2) \quad (5.12)$$

5.5.1.2. Buildings

Let us now consider that, over the same area [surface S], exists a total number N of buildings, with various sizes (height h_i , foundation surface σ_i). The resulting kinematic energy for all the buildings together can be written as:

$$E_b = \sum_i (1/2 m_i V_i^2) \approx \sum_i [\rho_b \sigma_i h_i S_v^2(f_i) / 2] \quad (5.13)$$

The velocity V_i to be considered here is the peak velocity, i.e., the amplitude of the velocity response spectrum at the building frequency f_i , $S_v(f_i)$. This value may be related to the acceleration (pseudo-)spectrum as $S_v \approx S_a / 2\pi f_i$. Further, this peak velocity may be approximated by considering that, when the building frequency is larger than the soil frequency (the usual case), we are in the "plateau" region of the acceleration spectrum and may relate it simply to the peak ground acceleration $S_a(f_i) \approx R \cdot a_{\max}$, with R being close to 2.5.

$$E_b \approx \sum_i [\rho_b \sigma_i h_i S_a^2(f_i) / 8 \pi^2 f_i^2] \approx R^2 a_{\max}^2 / 8 \pi^2 \sum_i [\rho_b \sigma_i h_i / f_i^2] \quad (5.14)$$

Each of these buildings has its own vibratory characteristics, but we may, as a very first approximation, consider that their fundamental frequencies f_i are simply related to their size, in the form:

$$f_i \approx C / h_i^\gamma \quad (5.15)$$

Such a form is indeed often suggested in earthquake regulations. The C coefficient, which depends on the structural type (concrete or steel frames, shear walls, etc.), is indeed related to the equivalent S -wave velocity of the building β_b . We will consider here, for simplicity, $\gamma = 1$ (in UBC97, a value of 0.85 is recommended). This value of 1 is consistent with the well-known rule of thumb $T_b = N/10$, where N is the number of storeys, and with empirical formulae as well (Farsi and Bard, 2003; Dunand et al., 2003). Thus:

$$C \approx \beta_b / 4 \quad (5.16)$$

We will consider here an equivalent velocity β_b of 400 m/s for shear wall buildings, and of 120 m/s for frame buildings (which implies $f=30/h$, identical to the rule of thumb when one assumes a story height of 3 m). We also consider an equivalent specific mass ρ_b of 250 kg/m³.

The total kinematic energy of the buildings has thus the following expression:

$$E_b \approx (R^2 \cdot a_{\max}^2 \cdot \rho_b) / (8 \pi^2 C^2) \cdot \sum_i [\sigma_i h_i^3] \quad (5.17)$$

$$E_b \approx (2 R^2 \cdot a_{\max}^2 \cdot \rho_b) / (\pi^2 \beta_b^2) \cdot \Sigma_i [\sigma_i h_i^3] \quad (5.18)$$

5.5.1.3. Ratio : site-city interaction index

The ratio between the total kinematic energy of buildings and that of the soil layer may then be written in a simple (approximate) form:

$$E_b / E_s \approx (2R^2 \cdot a_{\max}^2 \cdot \rho_b) / (\pi^2 \beta_b^2) \cdot \Sigma_i [\sigma_i h_i^3] / [S \cdot (\rho_s \cdot h^3 \cdot K^2 \cdot a_{\max}^2) / (\pi^2 \beta_s^2)] \quad (5.19)$$

$$E_b / E_s \approx 2 \rho_b / \rho_s \cdot R^2 / K^2 \cdot \beta_s^2 / \beta_b^2 \cdot \Sigma_i [\sigma_i / S \cdot h_i^3 / h^3] \quad (5.20)$$

Or

$$E_b / E_s \approx 2 \rho_b / \rho_s \cdot R^2 / K^2 \cdot \Sigma_i [\sigma_i / S \cdot h_i / h \cdot f_s^2 / f_i^2] \quad (5.21)$$

The first term of the right hand side of this approximate equation has rather constant values, since the density ratio ρ_b / ρ_s very generally ranges between 0.1 and 0.20, R around 2.5 and K around 1. This kinematic energy ratio then transforms into:

$$E_b / E_s \approx 2 \beta_s^2 / \beta_b^2 \cdot \Sigma_i [\sigma_i / S \cdot h_i^3 / h^3] \approx 2 \Sigma_i [\sigma_i / S \cdot h_i / h \cdot f_s^2 / f_i^2] \quad (5.22)$$

For a set of identical buildings, this formula simplifies into :

$$E_b / E_s \approx 2 \rho_b / \rho_s \cdot R^2 / K^2 \cdot \beta_s^2 / \beta_b^2 \cdot S_b / S \cdot h_b^3 / h^3 \approx 2 S_b / S \cdot h_b / h \cdot f_s^2 / f_b^2 \quad (5.23)$$

The ratio, which we call "SCI index", is thus controlled by a few simple parameters:

- The contrast between S wave velocity in the soil and in the building, β_s / β_b : the larger this contrast the larger the energy ratio. One must keep in mind, however, that when the soil velocity is too high, the impedance contrast with the underlying bedrock is too small to allow diffracted waves to be trapped, and therefore our simple formulae are not valid: SSI has small importance.
- The urbanization density, or proportion of the free-surface occupied by the buildings $\Sigma_i \sigma_i / S = S_b / S$.
- The ratio between building height and soil thickness h_i / h : high-rise buildings will increase the ratio and favour the interaction.
- The ratio between soil and building fundamental frequencies f_s / f_b : cities with low soil frequencies and comparatively higher building frequencies will have only a small amount of energy going from soil into buildings, and therefore will undergo only weak interaction.

Another approach based on the physics of soil-structure interaction, approached through the cone model (Boutin and Roussillon, 2003), leads to another representative parameter:

$$\sigma_o \approx 2 \pi S_b / S \cdot \rho_b / \rho_s \cdot 30 / \beta_s \quad (5.23)$$

5.5.2. EXAMPLE VALUES AND DISCUSSION

The relevancy of this parameter has been first checked through a sensitivity study for the Mexico City case, as reported in Guéguen et al., 2002, and illustrated in Figure

5.14, showing the correlation between this SCI index and the energy ratio of the radiated wave field to the free-field one, considered as more quantitative and reliable estimates of these site-city interaction effects. Although these checks have been performed with a single interaction model, the fact that 2D and 3D multiple interaction models confirm the reality of the interaction phenomena (though with different, generally reduced amplification effects) leaves us rather confident that this simple index is a useful tool for a first screening on the possible existence of such effects.

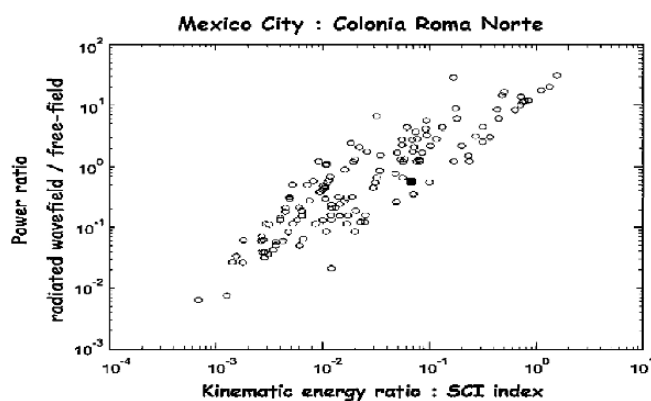


Fig. 5.14. Correlation between the proposed SCI index and the normalized energy of the ground motion radiated from the case of Colonia Roma Norte in Mexico City. The geometrical layout displayed in Figure 5.6 was kept, but each location was assigned different buildings to allow a sensitivity study: each point corresponds to one particular set of buildings (see Guéguen et al., 2002)

To provide a realistic range of values for this building / soil energy ratio, we have listed in Table 5.3 the values obtained for different configurations corresponding successively to 3 different cities. In Mexico City, the β_s / β_b value is around 2/3 (the soil is very soft but the buildings are frame buildings, and are rather flexible), the urbanization density reaches high values, and includes numerous buildings exceeding 10 storeys. The subsoil in Grenoble exhibits significant contrasts at two different scales: a very thick, but rather stiff deposit leads to a low fundamental frequency (0.25 Hz), but thin soft materials at the surface induce additional effects at higher frequencies (around 2-3 Hz, see Lebrun et al., 2001 and Cornou et al., 2003). Urbanization density is smaller in Grenoble compared to that in Mexico, especially as far as high-rise buildings are concerned. Finally, the city of Nice offers an intermediate situation, with a high density of 5 to 8 story buildings (in downtown Nice), and with a soil fundamental frequency ranging between 1 and 5 Hz, depending on the local thickness of the soil deposits (Semblat et al., 2000).

The largest energy ratio values listed in Table 5.3 correspond to the Mexico City case. If there exists some places of downtown Mexico City occupied exclusively by 10 to 15 story building (leading to an "occupied" surface ratio of 0.5, case M5), the soil and building energies would be comparable, allowing very efficient coupling between the soil and the structures. It is not clear to us whether such a situation exists at present in Mexico City. There do exist, however, areas built exclusively with 5 to 10 story

buildings, and with an "occupied" surface ratio around 0.4 to 0.5. For these areas (case M3), the energy ratio value is around 10%, and it is therefore scientifically legitimate to anticipate significant interaction effects at the "site-city" scale.

Table 5.3. SCI Index for various site-city configurations

Case	Site	H (m)	β_s (m/s)	S_b/S	β_b (m/s)	h_b (m)	f_s/f_b	E_b/E_s
M1	Mexico	40	80	0.2	120	5	0.08	4.10⁻⁴
M2				0.4		10	0.17	0.007
M3				0.5		20	0.33	0.07
M4				0.5		30	0.50	0.23
M5				0.5		50	0.83	1.09
G1	Grenoble	700	700	0.50	400	20	0.05	1.10⁻⁴
G2						40	0.10	6.10⁻⁴
G3		25	250	0.50		20	0.50	0.20
N1	Nice	40	200	0.20	400	5	0.06	2.10⁻⁴
N2				0.40		10	0.125	0.003
N3				0.50		20	0.25	0.034
N4				0.50		30	0.375	0.12
N5		20		0.50		20	0.50	0.28
N6		10		0.20		5	0.25	0.014
N7		10		0.40		10	0.50	0.22

On the opposite, for very thick soils, low constructions, and/or sparse urbanization (cases M1, M2, G1, G2, N1, N2), the ratio is negligible, and the interaction phenomenon may be completely discarded. There exist, however, a few intermediate cases, where the phenomenon may be significant despite the absence of high-rise buildings. This would be the case of a site where the soil is thin enough to have frequencies comparable to building frequencies, as it may be the case in some areas of downtown Nice, or even some areas in Grenoble where thin softer materials overlay the thick, stiffer post-glacial deposits. From Table 5.3 (cases N6 and N7), we may even expect significant to large coupling even with 2 to 3 story buildings or houses built on thin soils. For instance, one may think of some parts of the "damage belt" area of Kobe, very densely occupied by 2-3 story wooden houses with heavy tile roofs (leading to fundamental frequencies around 2-3 Hz), and lying on thin soils with similar frequencies.

5.6. Concluding comments

From this compilation of observations, specific experiments, and numerical computations, we feel comfortable to draw some definite conclusions about effects of building motion on ground motion.

Concerning their origin and existence conditions first, our results indicate that:

- The idea itself is not stupid: the Volvi experiment did show that the ground motion is significantly contaminated in the immediate vicinity of a building, the centrifuge

tests reveal that buildings do talk to each other through the soil, all numerical models support the existence of strong interaction in case of favourable conditions, i.e. for dense urban areas where site and building frequencies coincide.

- The physical origin is multi-fold. On one hand, the basis remains the radiation of waves emitted from the foundations of the vibrating buildings, and their trapping as surface waves inside the surface soft layers. On the other hand, similar buildings close to one another interact with each other through the soil, which gives rise to "group" effects. Finally, in case of large urban density and/or large size buildings, the inertial effect associated with the added mass produces some (slight) frequency shifts.
- As the first two processes in the previous paragraph are particularly efficient when soil and building frequencies coincide, the "optimal conditions" for a significant SCI are the simultaneous presence of a thin soft layer and a dense urbanization with homogeneous buildings having similar frequencies. The proposed "SCI index" provides a simple way to detect areas where such effects may be significant.

Next, concerning the effects of SCI, although there is still a need for additional 3D computations, a few results seem robust enough to be listed:

- In case of strong (i.e., multiple) interaction, the effects seem globally beneficial: the average ground motion "energy" within cities is decreased, especially for homogeneous building sets. In that latter case, the building motion is also significantly reduced. More heterogeneous urbanized areas will give rise to quantitatively smaller SCI effects, which may however span a broader frequency range. Additional amplifications, however, can not be completely ruled out.
- That "good news" of a globally beneficial effect should nevertheless be balanced by the fact SCI effects significantly increase the ground motion variability and decrease its spatial coherency. Some significant "over-amplifications" (at least up to 50%) may occur locally, at locations which however are almost impossible to predict since they depend a lot on the incident wave field (frequency and phase characteristics).
- There is however one observation on the spatial distribution of SCI effects that seems consistent over all the computations: the areas located at the border of dense, homogeneous urban centres are exposed to increased ground motion due to outward propagating waves (the phenomenon is very similar to the "basin-edge" effect observed for instance in Kobe)

These results seem also consistent enough to issue some warning about the potential consequences of such effects:

- From the seismological viewpoint, it draws attention to the need to be cautious when interpreting seismological records obtained within cities: in addition to the classical source, path and site terms, a fourth "urban" term may significantly contaminate the record and induce misinterpretations for the three other terms (especially the "site effect" term). This issue is particularly important when dense arrays are deployed within cities for investigations on the seismic wave field.

- A symmetric lesson can be drawn for the interpretation of damage observations: SCI may offer a partial explanation to the sometimes (often indeed) erratic pattern of damage distribution in cities, which may not be due only to variability in vulnerability or site conditions. The engineering consequence would then be to consider a new safety margin to envelop these possible quasi random effects.
- From the seismic risk viewpoint, the main lesson is that seismic hazard in urban areas may undergo anthropic modifications. This might lead to many unpredictable developments, for instance in urban planning (trying to design an "optimal land-use" to reduce the ground motion), time dependent hazard estimates (hazard may vary depending on newly built and/or deleted structures), insurance and law issues (imagine the nightmare where urban earthquakes would be followed by series of cases with lawyers claiming the damage in a given building is the responsibility of the owner of the next building, or of the city planners...).

However, before entering these developments, the next necessary step is to get unquestionable experimental proof of the occurrence of these effects in real cities under real earthquakes. This is an uneasy but challenging task, calling for innovative instrumental strategies and signal processing techniques.

Acknowledgements

Part of this work was achieved with a grant from the French Ministry of Education (project "Urban seismic hazard and Site city interaction", programme "ACI CATastrophes NATurelles"). We also thank Francisco J. Chavez-Garcia for his comments and corrections to an earlier, unpublished version of this text.

CHAPTER 6 VULNERABILITY ASSESSMENT OF DWELLING BUILDINGS

A. H. Barbat¹, S. Lagomarsino² and L. G. Pujades¹

1. *Universitat Politècnica de Catalunya, Barcelona, Spain*

2. *University of Genoa, Genoa, Italy*

6.1. Introduction

Risk is defined as the potential economic, social and environmental consequences of hazardous events that may occur in a specified area unit and period of time. Its estimation requires a multidisciplinary approach that takes into account not only the expected physical damage understood as the damage suffered by structures, the number and type of casualties or the economic losses, but also social, organizational and institutional factors. At urban level, for example, vulnerability should be also related to the social fragility and the lack of resilience of the exposed community, that is, to its capacity to absorb the impact and control its implications. Nevertheless, a holistic approach to estimate risk aiming to guide the decision making at urban level should start with the evaluation of physical damage scenarios as an essential tool, because they are the result of the convolution between hazard and physical vulnerability for buildings and infrastructure (Cardona, 2001; Barbat, 2003). Accordingly, the evaluation of physical vulnerability and risk of buildings is the main purpose of this chapter. Some definitions related to these concepts are introduced here below.

Risk, $Rie|_T$, can be defined as the probability of loss in an exposed element e as a consequence of the occurrence of an event with intensity larger than or equal to i during an exposition period T .

Hazard, $Hi|_T$, can be understood as the probability of occurrence of an event with an intensity greater than or equal to i during an exposition period T .

Vulnerability, Ve , is the intrinsic predisposition of the exposed element e to be affected or of being susceptible to suffer a loss as a result of the occurrence of an event with intensity i .

Starting from these definitions, risk is a function f of the convolution between hazard Hi and vulnerability Ve during an exposition period T

$$Rie|_T = f(Hi \otimes Ve)|_T \quad (6.1)$$

where the symbol \otimes stays for convolution (Cardona and Barbat, 2000).

The major part of losses due to earthquakes has its origin in the deficient seismic behaviour of structures. In spite of the advances of research in earthquake engineering in general and particularly on seismic design codes, catastrophic losses have occurred recently in many countries in the world, including countries in which earthquake engineering studies are priority tasks. It is clear that new developments in earthquake resistant design can only be applied to new projects, which represent a small part of the existing structures in a seismic area. Therefore, the only possibility of reducing earthquake losses is improvement of the seismic behaviour of existing structures. The aim of risk studies is to predict the expected damage in structures due to a specified

earthquake. A seismic risk analysis addressed to earthquake emergency management and protection strategies planning, requires territorial scale evaluation. Once the expected damage is predicted, it is possible to find solutions to diminish it, which rebound in the cost of the structures; this cost can be compared with the expected losses, in order to decide if structural retrofit or structural reinforcement are feasible. In spite of the importance of this type of studies, standard methodologies to estimate the vulnerability of structures are not available.

6.2. Methodologies for vulnerability assessment

Dolce et al., (1994) classified methodologies for the evaluation of structural vulnerability in four groups: (a) direct, which assesses in a simple way the damage caused in a structure by a given earthquake; (b) indirect, which determines first a vulnerability index of the structure and then assesses the relationship between damage and seismic intensity; (c) conventional, which is essentially a heuristic method, introducing a vulnerability index independent of the damage prediction; (d) hybrid, which combines elements of the previous methods with expert judgments. The selection of one of these methods depends on the objectives of the study, the type of the results required and on the available information. On the other hand, fragility functions, damage probability matrices and vulnerability functions obtained from observed structural damages during past earthquakes in a seismic area were the preferred tools in seismic risk studies performed in the past (Kappos et al., 1995; Benedetti and Petrini, 1984; Barbat et al., 1996).

The damage probability matrices and vulnerability functions are defined in the following way: 1) Damage Probability Matrices (DPM) express in a discrete form the conditional probability $P[D = j|i]$ to obtain a damage level j , due to an earthquake of severity i (Whitman 1974); and 2) Vulnerability Functions are relations expressing the vulnerability in a continuous form, as functions of certain parameters that describe the size of the earthquake (Benedetti and Petrini 1984). The vulnerability assessment is performed in terms of qualitative parameters: buildings are classified in vulnerability classes, and a DPM is assigned to each class or, alternatively, scores are attributed to the buildings considering their typological, structural, geometric and constructive characteristics; a simple model is then defined as a function of the evaluated scores relating the seismic input to the expected damage (Benedetti and Petrini, 1984; FEMA, 1998).

A complete observed damage data base would be desirable for applying such approaches; however, this is only possible in certain high seismicity areas where post-earthquake survey studies have been properly performed. Where the information is limited, damage matrices and vulnerability functions can be established using the available data and local expert opinion (Anagnos et al., 1995). Finally, in countries without any available damage data base, the information obtained in other similar areas is applied in a direct (Chavez and García-Rubio, 1995) or modified form, using expert judgment (Bustamante et al., 1995). Some authors have used hybrid methodologies to assess the vulnerability of buildings (Chavez and García-Rubio, 1995), developing fragility curves and damage probability matrices in order to estimate the feasibility of seismic rehabilitation of existing reinforced concrete (RC) buildings.

As the available data are often incomplete and do not concern all the building typologies and all the intensities that would be necessary to be represented in a model, probabilistic processing of the observed data is supported or completely replaced by other approaches such as structural analysis methods (Milutinovic and Trendafiloski, 2003), expert judgement (ATC-13, 1985), neural network systems (Dong et al., 1988) or fuzzy set theory (Sanchez-Silva and Garcia, 2001). To complete the undesirable lack of earthquake damage information in an area, simulation procedures can be also applied. The probabilistic analysis of computer generated structural responses obtained by using complex or simplified models and nonlinear analysis procedures of representative buildings can provide fragility curves, damage probability matrices and vulnerability functions relating seismic intensity or peak ground acceleration with damage (Nocevski and Petrovski, 1994; Kappos et al., 1995; Singhal and Kiremidjian, 1996). In these studies, the damage estimated for a generic structure pertaining to a given typology is considered as representative for the whole range of structures belonging to the mentioned structural typology.

In the vulnerability index method, the study is extended to a large number of classes of buildings within each of the considered typologies; these classes are defined through parameters which cover most of the structural characteristics, aiming to discriminate among different seismic behaviours of buildings with the same structural typology located in a specified seismic area (Benedetti and Petrini, 1984). This method, based on a great amount of damage survey data corresponding to several seismic zones of Italy, identifies the most important eleven parameters controlling the damage in buildings caused by earthquakes and qualifies them individually by means of qualification coefficients K_i affected by weights W_i which try to emphasize their relative importance. The method makes an overall qualification of the buildings by means of a vulnerability index I_v . Thus, the global vulnerability index of each building is evaluated by means of the formula

$$I_v = \sum_{i=1}^{11} K_i \times W_i \quad (6.2)$$

Using vulnerability functions, it is possible to relate I_v with an overall damage index D of the buildings, whose values, expressed as a percentage, also range between 0 and 100. The eleven mentioned parameters are: structural system organization, structural system quality, conventional strength, retaining walls and foundation, floor system, configuration in plant, configuration in elevation, maximum distance between walls, roof type, non-structural elements and preservation state.

An economic damage index corresponding to the physical risk of buildings could be defined as the relation between the damage repair cost and reposition cost. Both in the case of unreinforced masonry buildings and reinforced concrete buildings it is not reasonable to consider the overall structural damage index equal to the economic damage index, due to the presence of non- structural elements (architectural elements, equipment, installations, etc.) which usually contribute to the major part of the economic losses (Gunturi, 1993).

A damage index can be obtained for each structural component of a reinforced concrete building. Then it is possible to evaluate an economic damage index for each floor $D_{ec,k}$ by means of the equation

$$D_{ec,k} = \frac{\sum D_{ec,i} \times w_i}{\sum w_i} \quad (6.3)$$

where $D_{ec,i}$ is the structural damage index for each element i of floor k and w_i is the reposition cost of this element. The economic damage index of the entire structure can be then obtained as the average of all the structural floor indices. The economic floor damage index for architectural elements and equipment can be also evaluated starting from the maximum drifts and accelerations of floors obtained from a nonlinear analysis of the structures. Finally, the global economic damage index of the building can be obtained as a weighted average of the economic structural and non-structural economic damage indices.

In the United States, and nowadays also in Europe, the most recent trends in the field of vulnerability evaluation for risk analysis operate with simplified mechanical models, essentially based on the Capacity Spectrum Method (Freeman, 1998b; NIBS, 1997, 1999 and 2002). This method permits evaluating the expected seismic performance of structures by comparing, in spectral coordinates (Sd, Sa), their seismic capacity with the seismic demand, described by Acceleration-Displacement Response Spectra (ADRS) adequately reduced in order to take into account the inelastic behaviour (Fajfar, 2000). For purposes of territorial vulnerability assessment, capacity spectrum procedures do not necessarily use capacity curves obtained by pushover analyses, but they ascribe bilinear capacity curves defined by yielding (D_y , A_y) and ultimate (D_u , A_u) capacity points to each building typology; these curves vary depending on geometrical and technological parameters, characteristic of the buildings (number of floors, code level, material strength, drift capacity, etc.). Such an approach provides reliable results if applied to a built-up area characterized by a typological building homogeneity and by consolidated seismic design codes. This is not the case in the European Union where seismic codes are very different and where various typologies of masonry buildings can be distinguished in the territory. In this case, the employment of capacity based methods needs, yet, a robust experimental validation, at least on the traditional masonry constructions; for this reason, statistical methods based on damage observations are required.

A method derived in a theoretically rigorous way, starting from EMS-98 macroseismic scale (Grünthal, 1998) definitions overcomes the distinction between typological and rating methods and allows carrying out a vulnerability analysis with a single approach, graded to different levels according to the quantity and quality of the available data and the size of the territory. The method, which is applicable to all the European regions, has been verified on the basis of data observed after earthquakes occurred in different countries. The vulnerability index method in its version mentioned before and the capacity spectrum method are described in detail in the following sections of this chapter.

6.3. Vulnerability index method based on the EMS-98 macroseismic scale

6.3.1. EMS-98 BASED VULNERABILITY CURVES

6.3.1.1. *Vulnerability model implicitly contained in the EMS-98 scale*

The aim of a macroseismic scale is to measure the earthquake severity starting from the observation of the damage suffered by buildings and therefore it represents, for forecast purposes, a vulnerability model able to supply, for a given intensity, the probable damage distribution. In this sense, the EMS-98 scale, which will probably be used in the future at European level, contains a clear and detailed definition of the different building typologies and a precise description of the degrees of damage and of the damage distribution related to each degree of intensity. It makes reference to vulnerability classes, which are a way to group together buildings characterized by a similar seismic behaviour; six classes (from A to F) of decreasing vulnerability are introduced and, for each of them, the intensity, that can be estimated from a certain damage pattern, is supplied in terms of damage matrices. The damage matrix defined in the EMS-98 scale, which considers 5 damage grades and also the absence of damage, gives the probability that buildings belonging to a certain vulnerability class suffer a certain damage level for a given seismic intensity (see the example given in Table 6.1).

These damage matrices can be used for vulnerability assessments, but the model that they provide is vague and incomplete. The definition for the damage quantification in Table 6.1 is, indeed, provided in a vague way through the quantitative terms “Few”, “Many”, “Most” as the aim is a post-earthquake survey and a precise determination of quantities is not envisaged. Moreover, the distribution of damage is incomplete as the macroseismic scale only considers the most common and easily observable situations (for example, no information is provided for damage grade 3, 4 and 5 for I = VI and vulnerability class B in Table 6.1).

Table 6.1. Damage model provided by the EMS-98 scale for classes of vulnerability B (Milutinovic and Trendafiloski, 2003; Giovinazzi and Lagomarsino, 2004)

Class B					
Damage level	1	2	3	4	5
Intensity					
V	Few				
VI	Many	Few			
VII		Many	Few		
VIII			Many	Few	
IX				Many	Few
X					Many
XI					Most
XII					

6.3.1.2. *The incompleteness problem*

In order to solve the incompleteness problem, the damage distributions of earthquakes occurred in the past has been considered; the idea is to complete the EMS-98 model

introducing a proper discrete probability distribution of the damage grade. The binomial distribution could be a possibility as it has been successfully used for the statistical analysis of data collected after the 1980 Irpinia earthquake (Italy) (Braga et al., 1983); but the simplicity of this distribution, which depends on only one parameter, does not allow defining the scatter of the damage grades around the mean value.

Sandi and Floricel (1995) observed that the dispersion of the binomial distribution is too high, when you consider a detailed building classification; this may lead to overestimating the number of buildings suffering serious damages, in the case of rather low values of the mean damage grade. The distribution that better suits the specific requirements is the beta distribution (also employed in ATC-13, 1985):

$$PDF : p_{\beta}(x) = \frac{\Gamma(t)}{\Gamma(r)\Gamma(t-r)} \frac{(x-a)^{r-1} (b-x)^{t-r-1}}{(b-a)^{t-1}} \quad a \leq x < b \quad (6.4)$$

$$\mu_x = a + \frac{r}{t} (b-a) \quad (6.5)$$

where a , b , t and r are the parameters of the distribution; μ_x is the mean value of the continuous variable x , which ranges between a and b and $\Gamma(r)$ is the gamma function.

In order to use the beta distribution, it is necessary to make reference to the damage grade D , which is a discrete variable (5 damage grades plus the absence of damage); for this purpose, it is advisable to assign value 0 to the parameter a and value 6 to the parameter b . Starting from this assumption, it is possible to calculate the probability associated with damage grade k ($k=0, 1, 2, 3, 4, 5$) as follows:

$$p_k = P_{\beta}(k+1) - P_{\beta}(k) \quad (6.6)$$

Following from this assumption, the mean damage grade, defined as the mean value of the discrete distribution:

$$\mu_D = \sum_{k=0}^5 p_k \cdot k \quad (6.7)$$

The mean value μ_x (6.5) can be correlated through the following third degree polynomial:

$$\mu_x = 0.042\mu_D^3 - 0.315\mu_D^2 + 1.725\mu_D \quad (6.8)$$

Thus, by using (6.5) and (6.8), it is possible to correlate the two parameters of the beta distribution with the mean damage grade

$$r = t(0.007\mu_D^3 - 0.0525\mu_D^2 + 0.2875\mu_D) \quad (6.9)$$

The parameter t affects the scatter of the distribution; if $t=8$ is used, the beta distribution looks very similar to the binomial distribution.

6.3.1.3. *The vagueness problem*

Once the problem of incompleteness is solved by using the discrete beta distribution, it is necessary to tackle the problem of the vagueness of the qualitative definitions (few, many, most) in order to derive numerical DPM for EMS-98 vulnerability classes. As translation of the linguistic terms into a precise probability value is arbitrary, they can be better modelled as bounded probability ranges. Fuzzy sets theory (often proposed for seismic risk assessment methods) has offered an interesting solution to the problem, leading to the estimation of upper and lower bounds of the expected damage (Bernardini, 1999). According to fuzzy sets theory, the qualitative definitions can be interpreted through membership functions χ (Dubois and Parade, 1980). A membership function defines the belonging of single values of a certain parameter to a specific set; the value of χ is 1 when the degree of belonging is plausible (that is to say almost sure), while a membership between 0 and 1 indicates that the value of the parameter is rare but possible; if χ is 0, the parameter does not belong to the set.

Figure 6.1 shows the range of percentage of damaged buildings corresponding to the quantitative terms given by the EMS-98. It contends that while there are some definite ranges (few, less than 10%; many, 20% to 50%; most, more than 60%), there are situations of different terms overlapping (between 10% and 20% can be defined as both few and many; 50% and 60%, both many or most). These qualitative definitions are represented through the membership functions χ in Figure 6.1.

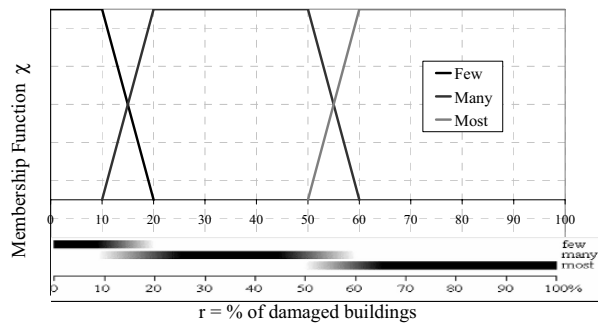


Fig. 6.1. Percentage ranges and membership functions χ of the quantitative terms “Few”, “Many”, “Most”

6.3.1.4. *EMS-98 damage probability matrices*

Using fuzzy sets theory and starting from EMS-98 definitions (e.g. Table 6.1), it is possible to build a DPM through the discrete beta distribution. Recalling that to each value of parameter μ_D having definitely assumed $a=0$, $b=6$ and for a fixed value of t , corresponds a fixed damage grade distribution, researchers have looked for μ_D values able to represent the terms “Few”, “Many”, “Most” in a plausible and then in a possible way, according to the membership functions associated to the quantitative definitions. In order to make the operation easier, a value $t=8$ may be used, but it has been verified that for different values of t , the differences observed are negligible. From the probabilistic

distributions corresponding to the computed μ_D values, the percentages of damage have been attributed to the different damage grades. As an example, it is possible to consider the vulnerability class B and the macroseismic intensity VI. Table 6.2 shows for the vulnerability class B, the upper and lower bounds of the mean damage grade related to plausibility and possibility. The corresponding distributions of the damage grades are also shown; the dark and light grey cells correspond to the control definitions and the value that determines the bound is shown as a bold character (Giovinazzi and Lagomarsino, 2004).

Table 6.2. Damage distributions and mean damage values related to the upper and lower bounds of plausibility and possibility ranges for vulnerability class B

Class B						
Damage level	1	2	3	4	5	
Intensity VI	Many	Few				μ_D
B ⁺ Upper plausible	32.0	10	1.9	0.2	0.0	0.68
B ⁻ Lower plausible	20	4.3	0.6	0.0	0.0	0.43
B ⁺⁺ Upper possible	40.6	20	5.5	0.7	0.0	1.81
B ⁻ Lower possible	10	1.6	0.2	0.0	0.0	0.25

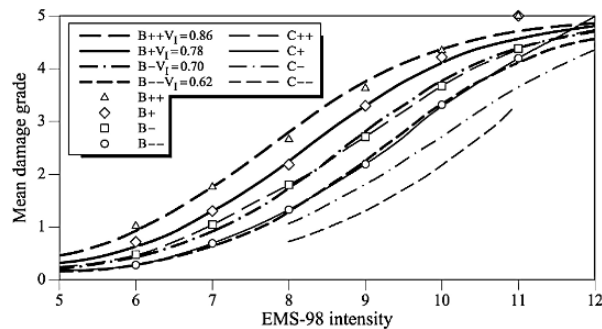


Fig. 6.2. Class B and C plausibility and possibility curves and their interpolation

Repeating this procedure for each vulnerability class and for the different intensity degrees, it is possible to obtain, point by point, the plausible and possible bounds of the mean damage. Connecting these points, draft curves are drawn, which define the plausibility and possibility areas for each vulnerability class, as a function of the macroseismic intensity (see Figure 6.2).

6.3.1.5. Vulnerability index and vulnerability curves

Observing the curves of Figure 6.2, it stands out that there is a plausible area for each vulnerability class and intermediate possible areas for contiguous classes. In other words, the area between B⁺ and B⁻ is distinctive for class B, while there is a contiguous area in which the best buildings of class B and the worst of class C coexist (the B⁻ curve coincides with the C⁺⁺ one; the B⁻⁻ curve coincides with the C⁺ one). Another important observation is that curves in Figure 6.2 are, more or less, parallel because the damage produced to buildings of a given vulnerability class by an earthquake of certain intensity, is the same as that caused by an earthquake with the next intensity degree to

buildings of the subsequent vulnerability class. On the basis of these considerations, a conventional Vulnerability Index V_I is introduced within the frame of the fuzzy set theory, indicating that a building pertains to a vulnerability class. The numerical values of the vulnerability index are arbitrary as they are only scores which quantify, in a conventional way, the seismic behaviour of a building (they are a measure of the weakness of a building to resist earthquakes). For the sake of simplicity, a 0 to 1 range has been chosen, allowing all possible behaviours to be covered. The values close to 1 correspond to the most vulnerable buildings and the values close to 0 to high-code designed structures. Thus, the membership of a building to a specific vulnerability class can be defined by means of this vulnerability index (see Figure 6.3); in compliance with the fuzzy set theory they have a plausible range ($\chi = 1$) and linear possible ranges, representative of the transition between two adjacent classes.

According to the fuzzy definition of the vulnerability index, Table 6.3 shows the most probable value for each vulnerability class V_I^{c*} , the bounds V_I^{c-} V_I^{c+} of the uncertainty range and the upper and the lower bound of the possible values $V_{I_{max}}^c$ and $V_{I_{min}}^c$. It must be noticed, according to Figure 6.3, that the partition of the fuzzy field is not restricted to the minimum value of -0.02 and to the maximum value of 1.02 ; actually it is not possible to keep out of the evaluation buildings weaker than those of class A or better designed than those of class F.

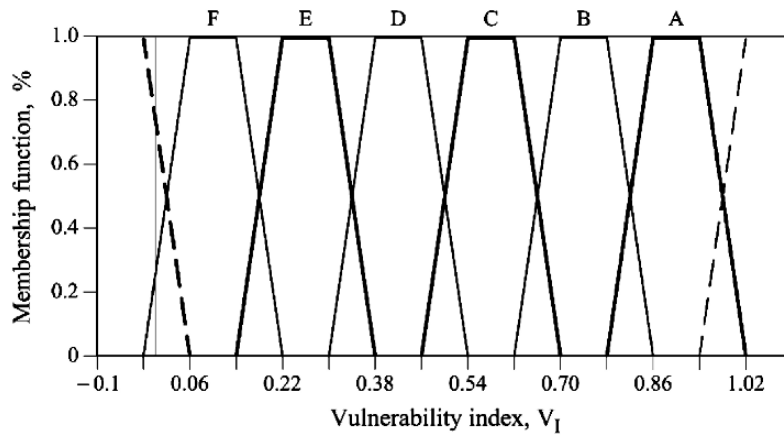


Fig. 6.3. Vulnerability index membership functions for the EMS-98 vulnerability classes

For the operational implementation of the methodology, it is particularly useful to define an analytical expression, capable of describing the curves in Figure 6.2; therefore, the mean damage grade μ_D is expressed by means of the following function depending on the macroseismic intensity I and the vulnerability index V_I :

$$\mu_D = 2.5 \left[1 + \tanh \left(\frac{I + 6.25 \cdot V_I - 13.1}{2.3} \right) \right] \quad (6.10)$$

Table 6.3. Vulnerability index values for the different vulnerability classes

	$V_{I \min}^c$	V_I^{c-}	V_I^{c*}	V_I^{c+}	$V_{I \max}^c$		$V_{I \min}^c$	V_I^{c-}	V_I^{c*}	V_I^{c+}	$V_{I \max}^c$
A	1.02	0.94	0.9	0.86	0.78	D	0.54	0.46	0.42	0.38	0.3
B	0.86	0.78	0.74	0.7	0.62	E	0.38	0.3	0.26	0.22	0.14
C	0.7	0.62	0.58	0.54	0.46	F	0.22	0.14	0.1	0.06	-1.02

6.3.2. EVALUATION OF THE VULNERABILITY INDEX

The EMS-98 macroseismic scale contains a table with a typological classification of buildings representative for the European countries and vulnerability table (Table 6.4), which distinguishes the buildings as functions of the structural material: masonry, reinforced concrete, steel and timber. Different buildings having the same structural typology are characterized by a prevailing seismic vulnerability class; nevertheless, it is possible to find buildings with a better or worse seismic behaviour within the same vulnerability class, depending on their design, constructive or structural characteristics. Therefore, the EMS-98 scale subdivides the seismic behaviour of the buildings in six vulnerability classes for which damage probability matrices and vulnerability curves have been evaluated.

The idea highlighted by the EMS-98 scale, according to which the seismic behaviour of a building not only depends on the behaviour of its structural system but also on other factors, has suggested the following definition of the vulnerability index:

$$\overline{V}_I = V_I^* + \Delta V_R + \Delta V_m \quad (6.11)$$

where ΔV_R and ΔV_m are, respectively, a factor of regional type and of behaviour type.

6.3.2.1. Typological vulnerability index

EMS-98 table describes the possibility of a given building typology belonging to a vulnerability class through linguistic terms, as it can be seen in Table 6.4: “Most probable class”, “Possible class”, “Unlikely class”. Even in this case, the fuzzy set theory can provide a useful contribution for the linguistic term interpretation. The belonging of each typology to the vulnerability classes is represented in a fuzzy way, by discriminating the most likely class ($\chi = 1$), the possible class ($\chi = 0.6$) and the unlikely class ($\chi = 0.2$) of Table 6.4. It is possible to define the membership function of each building type as a linear combination of the vulnerability class membership functions, each one considered with its own degree of belonging. As an example, the membership function for massive stone masonry buildings (M4) is shown in Figure 6.4 and it is defined as:

$$\chi_{M4}(V_I) = \chi_C(V_I) + 0.6 \cdot \chi_B(V_I) + 0.2 \cdot \chi_D(V_I) \quad (6.12)$$

where χ_C , χ_B and χ_D are defined in Figure 6.3 (see also Table 6.4.).

From the membership function of each typology, five representative values of V_I have been defined (see Figure 6.4) through a defuzzification process (Ross, 1995): the most probable value of the typological vulnerability index V_I^* for a specific building type is calculated as the centroid of the membership function. V_I^- and V_I^+ , evaluated by a 0.5-cut of the membership function, are the bounds of the uncertainty range of V_I^* for that

building type. V_{Imin} and V_{Imax} correspond to the upper and lower bounds of the possible values of \bar{V}_I , that is the final vulnerability index value, for the specific building type. Whatever is the estimated amount of the behaviour modifiers and the regional factor, the final vulnerability index has to comply with this possibility range.

Table 6.4. Vulnerability classes of different building typologies (Building Typology Matrix, BTM)

Typologies		Building type	Vulnerability Classes					
			A	B	C	D	E	F
Masonry	M1	Rubble stone	■					
	M2	Adobe (earth bricks)	■	■				
	M3	Simple stone	■	■				
	M4	Massive stone	■	■	■	■		
	M5	Unreinforced M (old bricks)	■	■	■	■		
	M6	Unreinforced M with r.c. floors	■	■	■	■		
	M7	Reinforced or confined masonry			■	■	■	
Reinforced Concrete	RC1	Frame in r.c. (without ERD)	■	■	■	■		
	RC2	Frame in r.c. (moderate ERD)			■	■	■	
	RC3	Frame in r.c. (high ERD)			■	■	■	■
	RC4	Shear walls (without ERD)		■	■	■	■	
	RC5	Shear walls (moderate ERD)		■	■	■	■	
	RC6	Shear walls (high ERD)		■	■	■	■	■
Steel	S	Steel structures			■	■	■	■
Timber	W	Timber structures			■	■	■	■
Situations:		■	■	■	■	■	■	■
		Most probable class	Possible class			Unlikely class		

ERD – “Earthquake Resistance Design”

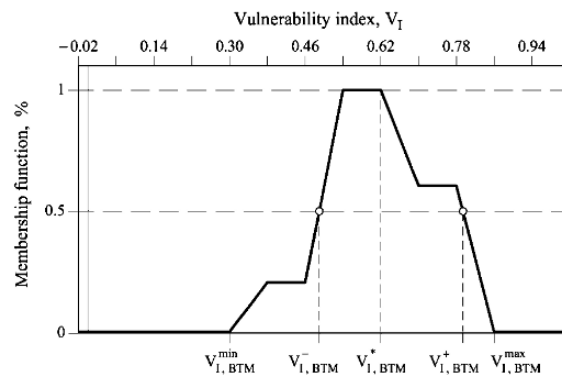


Fig. 6.4. Vulnerability Index membership functions for M4 massive stone typology and V_I values

$$\max(\bar{V}_I; V_{Imin}) \leq \bar{V}_I \leq \min(\bar{V}_I; V_{Imax}) \tag{6.13}$$

These values are represented in Figure 6.4 for the massive stone masonry typology and in Table 6.5 for all the EMS-98 buildings typologies.

Table 6.5. Vulnerability index values for the EMS-98 building typologies

Typologies		Building type	Vulnerability classes				
			V_{Imin}	V_I^-	V_I^*	V_I^+	V_{Imax}
Masonry	M1	Rubble stone	0.62	0.81	0.873	0.98	1.02
	M2	Adobe (earth bricks)	0.62	0.687	0.84	0.98	1.02
	M3	Simple stone	0.46	0.65	0.74	0.83	1.02
	M4	Massive stone	0.3	0.49	0.616	0.793	0.86
	M5	Unreinforced M (old bricks)	0.46	0.65	0.74	0.83	1.02
	M6	Unreinforced M with r.c. floors	0.3	0.49	0.616	0.79	0.86
	M7	Reinforced or confined masonry	0.14	0.33	0.451	0.633	0.7
Reinforced Concrete	RC1	Frame in r.c. (without ERD)	0.3	0.49	0.644	0.8	1.02
	RC2	Frame in r.c. (moderate ERD)	0.14	0.33	0.484	0.64	0.86
	RC3	Frame in r.c. (high ERD)	-0.02	0.17	0.324	0.48	0.7
	RC4	Shear walls (without ERD)	0.3	0.367	0.544	0.67	0.86
	RC5	Shear walls (moderate ERD)	0.14	0.21	0.384	0.51	0.7
	RC6	Shear walls (high ERD)	-0.02	0.047	0.224	0.35	0.54
Steel	S	Steel structures	-0.02	0.17	0.324	0.48	0.7
Timber	W	Timber structures	0.14	0.207	0.447	0.64	0.86

ERD – “Earthquake Resistance Design”

6.3.2.2. The behaviour modifier factor

The typological vulnerability index V_I^* calculated for each building typology has to be increased or decreased according to the vulnerability recognized for a certain building. The overall score that modifies the characteristic vulnerability index V_I^* can be evaluated, for a single building, simply summing all the modifier scores.

$$\Delta V_m = \sum V_m \quad (6.14)$$

These modifiers are related to the state of preservation of the buildings, the structural system, the height of the building within each building typology, irregularities in plan, elevation and of stiffness, retrofitting interventions, soil morphology and foundation, as well as aggregate building position and elevation (Milutinovic and Trendafiloski, 2003).

If a group of buildings, belonging to a certain typology, is considered, the modifier factor ΔV_m , is evaluated as:

$$\Delta V_m = \sum_k r_k \cdot V_{m,k} \quad (6.15)$$

where r_k is the ratio of building affected by the behaviour modifier k characterized by a $V_{m,k}$ score. Making reference to single buildings, the behaviour modifier factor ΔV_m is simply the sum of the scores $V_{m,k}$ for the recognized behaviour modifiers. The identification of the behaviour modifiers can be made empirically, based on the observation of typical damage pattern and taking also into account the suggestions made in several inspection forms (ATC-21, 1988; Benedetti and Petrini, 1984; UNDP/UNIDO, 1985) and by previous proposals (Coburn and Spence, 2002). The modifying scores V_m can be also assigned using expert judgment followed by a partial calibration by comparison with other vulnerability evaluations; but a better calibration is desirable on the basis of damage and vulnerability data collected after earthquakes.

Giovinazzi and Lagomarsino (2004) propose behaviour modifier factors and the corresponding scores for masonry and reinforced concrete buildings.

6.3.2.3. *The regional vulnerability factor*

The range bounded by V_1^- , V_1^+ is quite large in order to be representative for the huge variety of the constructive techniques used all around the different countries. The regional vulnerability factor takes into account the characteristics of the buildings belonging to a certain typology at regional level: a major or minor vulnerability could be indeed recognized due to some traditional constructive techniques used in the region.

According to this regional vulnerability factor the V_1^* typological vulnerability index is modified on the basis of an expert judgment or on the basis of the historical data available. The first case is achieved when precise technological, structural and constructive information is available, attesting an effective better or worse average behaviour with regard to the one proposed in Table 6.5. The second one occurs when observed damages data are available; the average curve ($\bar{V}_1 = V_1^*$ in Equation 6.11) can be shifted in order to obtain a better approximation for the same data.

6.3.2.4. *Uncertainty range in the vulnerability assessment*

The uncertainties affecting a seismic risk analysis are both epistemic and random. The epistemic ones refer in this case to uncertainties associated with the classification of the exposed building stock into a vulnerability class or into a building typology and by the uncertainties associated with the assignment of a characteristic behaviour to the vulnerability class or building typology (Spence et al., 2003). Considering both kinds of uncertainties allows obtaining the most probable vulnerability index as well as its plausibility and possibility ranges for each vulnerability class (Table 6.3) and for each building typology (Table 6.5).

It must be noticed that the uncertainty affecting building typologies is higher than the one affecting vulnerability classes because the building typology behaviour has been deduced from the one observed from vulnerability classes and, furthermore, because with few data it is more difficult to classify a building into a typology rather than into a vulnerability class. But the knowledge of information additional to the typological one, limits the uncertainties of the building behaviour; it is therefore advisable not only to modify the most probable value V_1^* (according to Equation 6.11), but also to reduce the range of its uncertainty ($V_1^- \rightarrow V_1^+$). This goal is achieved by modifying the membership function through a filter function f , centred in the new most probable value \bar{V}_1 , depending on the parameter ΔV_1 , representing the width of the filter function (Giovinazzi and Lagomarsino, 2004).

6.3.2.5. *Example*

The city of Barcelona, Spain, is located in an area of low to moderate seismic hazard, but its buildings show a high vulnerability and, consequently, a significant probability of being damaged even in the case of a not excessively severe earthquake. The total number of dwellings of Barcelona is about 700,000, with an average of 2.2 inhabitants in each, and about 63,000 buildings. The majority of Barcelona's most representative unreinforced masonry buildings, with an average age of 60 years, were designed only

considering vertical static loads, without any seismic design criteria, greatly influencing the overall seismic vulnerability of the city. Additionally, some of its particular features, typical for the constructive techniques of the city at that time, have been identified as potential damage sources. The slabs of these unreinforced masonry buildings are made of wood, steel or reinforced concrete, according to the building period, and have ceramic ceiling vaults in all the cases. Due to the higher height of the first floor, almost all of these buildings have soft first floors. In many cases, cast iron columns were used instead of masonry walls at the base and ground floors, reducing thus even more their stiffness. The majority of the reinforced concrete buildings of Barcelona have waffle slabs, a structural member not adequate for seismic areas. Many of the buildings in Barcelona are part of aggregates.

Traditionally, the vulnerability index method identifies the existing building typologies within the studied area and defines their vulnerability class (Table 6.4). For each vulnerability class, the relationship between intensity and damage may be defined by using Damage Probability Matrices. The specific buildings of Barcelona are classified in different groups characterized by a similar seismic behaviour. All the buildings belonging to each typology are cast within the most probable class.

Table 6.6. Vulnerability index for typologies and periods of construction of Barcelona, according to the seismic design level

Periods	Period of construction	Spanish Code	Obligation in Barcelona	Lateral bracing in constructive practice	Seismic Design level	Buildings (%)	Vulnerability Index (V_i)		
							M31 M32 M33	M34	RC32
I	<1950	----	----	Absent	Pre-code	50.69	0.938	--	--
II	1950-1962	----	----	Deficient	Pre-code	17.30	0.875	--	--
III	1963-1968	Recommendation MV-101 (1962)	No specified	Deficient	Pre-code	10.91	0.813	0.750	0.750
IV	1969-1974	Seismic code P.G.S.-I (1968)	Yes	Acceptable	Low-code	9.80	0.750	0.625	0.625
V	1975-1994	Seismic code P.D.S. (1974)	Yes	Acceptable	Low-code	11.07	0.688	0.563	0.500
VI	1995 until now	Seismic code NCSE-94 (1995)	No	Acceptable	Low-code	0.23	0.688	0.563	0.500

Vulnerability indices are assigned to the most representative building typologies of Barcelona, representing scores that quantify their seismic behaviour. A first refinement of this average initial vulnerability index is performed by taking into account the age of the building. The building stock is grouped in 6 age categories by considering reasonable time periods as functions of the existence of seismic codes in Spain and its level, as well as other specific construction features (see Table 6.6) (Lantada et al., 2004).

Figure 6.5 shows vulnerability maps for both the unreinforced masonry and reinforced concrete buildings of Barcelona.

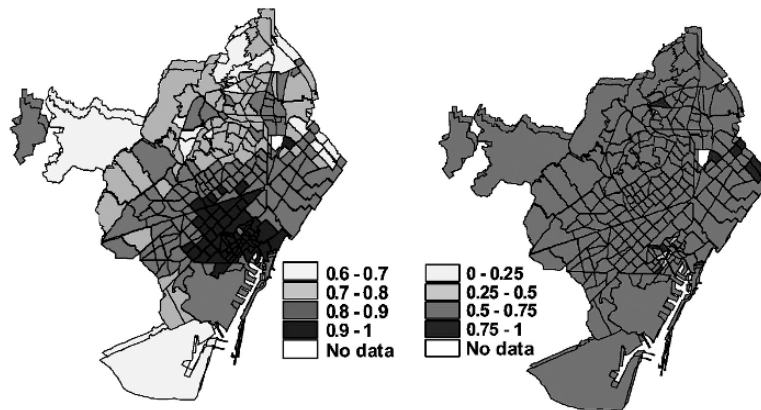


Fig. 6.5. Vulnerability indices maps for unreinforced masonry buildings (left) and reinforced concrete buildings (right)

The global vulnerability index of each building is now evaluated by applying behaviour modifiers (eq. 6.14), which are different for isolated and aggregate buildings. For isolated buildings, the following 4 modifiers were considered: number of floors, irregularity in height, length of the façade and state of preservation. For building in aggregates the effects due to the different heights of adjacent buildings and the effects due to the position of the building in the aggregate (i.e. corner, header, or intermediate) have been taken into account.

6.4. Capacity spectrum method

The capacity spectrum method uses the capacity and demand spectra to obtain the performance point of the structure which corresponds to its maximum spectral displacement, and uses fragility curves to obtain the damage probability for the expected seismic input. Capacity curves are force-displacement diagrams of the structure which correspond to the first mode maximum response of buildings and governing the structural damage; they mainly depend on the structural design and construction practice. The performance of a building is directly influenced by the level and frequency content of the seismic action which controls the peak building response levels. The seismic input is modelled by means of the demand spectrum, which is the inelastic structural response spectrum. This demand spectrum can be obtained by using a nonlinear structural analysis or, in a simplified way, starting from the 5% damped building-site specific elastic response spectrum modified to account for the inelastic structural behaviour. Both the capacity and demand spectra are represented in the spectral acceleration (Sa)-Spectral displacement (Sd) domain.

Fragility curves define the probability that the expected damage d exceeds a given damage state d_s , as a function of a parameter quantifying the severity of the seismic action. Thus, fragility curves are completely defined by plotting $P(d \geq d_s)$ in ordinate and the spectral displacement Sd in abscissa. If it is assumed that fragility curves follow a lognormal probability distribution, they can be completely defined by only two

parameters which, in this case, are the mean spectral displacement \overline{Sd}_{ds} and the corresponding standard deviation β_{ds} .

Fragility curves can be obtained in a simplified way starting from the bilinear representation of capacity curves (see Figure 6.6 and Table 6.7). Crossing demand and capacity spectra, the performance point is established and thus the expected spectral displacement which, together with the corresponding fragility curves, allows obtaining probability matrices for the damage scenario corresponding to earthquakes defined by their demand spectra. Therefore, all the fragility and damage analyses are based in a straightforward manner on capacity and demand spectra and fragility curves.

The method for analyzing the seismic damage considers 5 damage states: none, slight, moderate, extensive and complete. For a given damage state, a fragility curve is well described by the following lognormal probability density function:

$$P[ds / Sd] = \Phi \left[\frac{1}{\beta_{ds}} \ln \left(\frac{Sd}{\overline{Sd}_{ds}} \right) \right] \quad (6.16)$$

where \overline{Sd}_{ds} is the threshold spectral displacement at which the probability of the damage state ds is 50%, β_{ds} is the standard deviation of the natural logarithm of this spectral displacement, Φ is the standard normal cumulative distribution function and Sd is the spectral displacement. Figure 6.6 and Table 6.7 show how the \overline{Sd}_{ds} thresholds are obtained from the capacity spectra. Concerning β_{ds} , it is well known that the expected seismic damage in buildings follows a binomial probability distribution. Therefore, it is assumed that at the \overline{Sd}_{ds} threshold, the probability of this damage state is 50% and then the probabilities of the remaining damage states are estimated.

Starting from the spectral displacement corresponding to the performance point, damage probability matrices can be obtained by using the corresponding fragility curves. A weighted average damage index, DS_m , can be calculated by using the following equation:

$$DS_m = \sum_{i=0}^4 DS_i P[DS_i] \quad (6.17)$$

where DS_i takes the values 0, 1, 2, 3 and 4 for the damage states i considered in the analysis and $P[DS_i]$ are the corresponding probabilities.

Table 6.7. Damage state thresholds defined in agreement with the capacity spectrum

$\overline{Sd}_1 = 0.7D_y$	Slight
$\overline{Sd}_2 = D_y$	Moderate
$\overline{Sd}_3 = D_y + 0.25(D_u - D_y)$	Extensive
$\overline{Sd}_4 = D_u$	Complete

It can be considered that DS_m is close to the most likely damage state of the structure. According to Equation 6.17, a value $DS_m=1.3$, for example, indicates that the most probable damage state of a building ranges between *slight* and *moderate*, being more probable the *slight* damage state. This average damage index permits plotting seismic damage scenarios by using a single parameter. Of course, alternative maps may plot the spatial distribution of the probability of occurrence of a specific damage state, that is $P[DS_j]$.

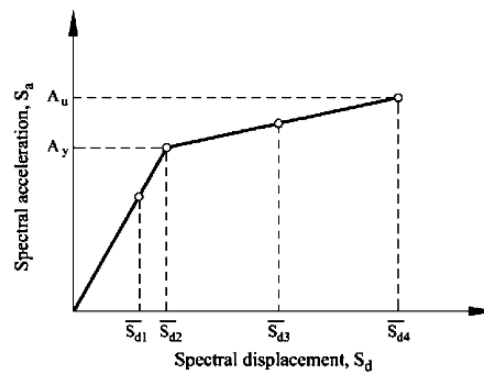


Fig. 6.6. Damage state thresholds from capacity spectrum

6.4.1. EXAMPLE

For illustration of the method we use the same example of Barcelona which has a moderate seismicity and weak tectonic motions; its seismic hazard has been recently re-evaluated defining the action in terms of elastic response acceleration spectra both from a deterministic and a probabilistic approach (Irizarry et al., 2003). Two earthquake scenarios have been developed and used to perform the simulations of seismic risk scenarios, one deterministic, based on a historical earthquake that occurred quite far from the city and whose intensity at the basement and outcrop has been estimated, and the other probabilistic, corresponding to a 475 years return period. The result of both simulations can be seen in Figure 6.7 in acceleration-displacement format (ADRS). The same figure shows a seismic risk scenario in macroseismic intensities, used to develop seismic risk scenarios according to the vulnerability index method.

Detailed structural plans have been used to model representative buildings for low-rise (two stories, 5.2 m high) mid-rise (five stories, 15.8 m high) and high-rise (eight stories, 24.0 m high) reinforced concrete buildings. Capacity curves were obtained by performing non-linear static analyses using RUAUMOKO-2D program (Carr, 2000). In a similar way, based on detailed structural plans, two stories (low-rise), four stories (mid-rise) and six stories (high-rise) buildings of the Eixample district of Barcelona have been modelled. TreMuri program (Galasco et al., 2002) was used to perform the dynamic analyses of the buildings. Pushover analyses allowed obtaining the capacity curves for each building class. Table 6.8 shows the yield and ultimate capacity points defining the bilinear capacity spectra for reinforced concrete and masonry buildings. It

can be seen how the capacity decreases with the height of the building both for masonry and for RC buildings.

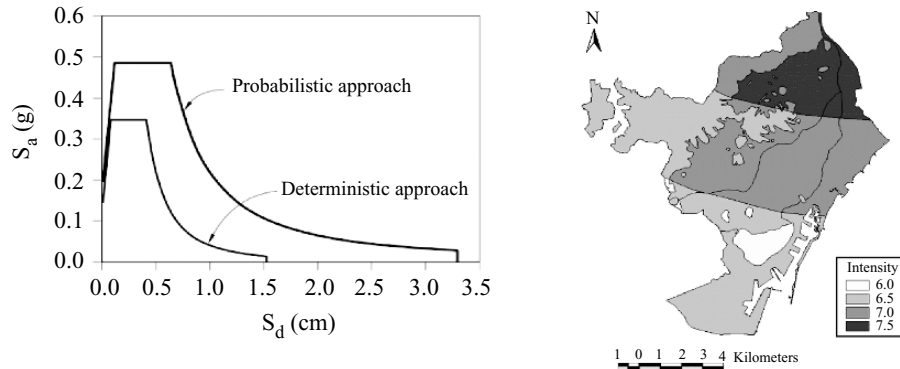


Fig. 6.7. Response spectra for deterministic and probabilistic hazard scenarios (left) and deterministic seismic hazard scenario including local soil effects in intensity (right) (Irizarry et al., 2003)

Table 6.9 shows the expected probabilities of all the damage states when a particular damage state probability is fixed to 50% and a binomial or equivalent beta probability distribution is assumed. In this table, the damage states are represented by numbers from 1 to 4 for damage states *slight* to *complete*, respectively. The probabilities in this table are cumulative and correspond to the points shown in Figure 6.8. Parameter DS_m controls the assumed probability distribution. Finally, the function expressed by Equation 6.16 is fitted to the obtained points by means of a least square criterion.

Table 6.8. Yield and ultimate capacity for reinforced concrete (RC) and masonry (M) buildings

Building class	Yield capacity		Ultimate capacity	
	Dy (cm)	Ay (g)	Du (cm)	Au (g)
Low-rise, RC	0.70	0.129	5.240	0.138
Mid-rise, RC	1.418	0.083	5.107	0.117
High-rise, RC	1.894	0.059	4.675	0.079
Low-rise, M	0.27	0.651	1.36	0.558
Mid-rise, M	0.63	0.133	2.91	0.117
High-rise, M	0.68	0.105	2.61	0.079

Table 6.9. Probabilities of the expected damage states when fixing a 50% probability for each damage state: 1-slight, 2-moderate, 3-extensive and 4-complete

Condition	DS_m	P_β (1)	P_β (2)	P_β (3)	P_β (4)
P_β (1)=0.5	0.911	0.500	0.119	0.012	0.00
P_β (2)=0.5	1.919	0.896	0.500	0.135	0.008
P_β (3)=0.5	3.081	0.992	0.866	0.500	0.104
P_β (4)=0.5	4.089	1.000	0.988	0.881	0.500

Figure 6.8 shows an example of such a fit. Points in this figure correspond to the damage state probabilities and lines are the fitted fragility curves. This figure corresponds to the mid-rise reinforced concrete building class. Table 6.10 shows the corresponding parameters, namely \overline{Sd}_i and β_i , where $i=1, \dots, 4$ defines the fragility curves corresponding to reinforced concrete (RC) and unreinforced masonry (M) building classes. The demand spectra, together with the capacity spectra have been used to obtain the performance point which defines the maximum expected spectral displacement related to a specific demand. Entering in the fragility curves with the spectral displacement of the performance point, the structural damage probabilities are established and seismic risk scenarios can be then obtained.

Table 6.10. Parameters characterizing the fragility curves, for reinforced concrete buildings (RC) and unreinforced masonry buildings (M)

Building class	Damage states thresholds							
	\overline{Sd}_1 (cm)	β_1	\overline{Sd}_2 (cm)	β_2	\overline{Sd}_3 (cm)	β_3	\overline{Sd}_4 (cm)	β_4
Low-rise, RC	0.49	0.28	0.70	0.37	1.84	0.82	5.24	0.83
Mid-rise, RC	0.99	0.28	1.42	0.36	2.34	0.50	5.11	0.61
High-rise, RC	1.33	0.28	1.89	0.29	2.59	0.34	4.68	0.45
Low-rise, M	0.19	0.28	0.27	0.37	0.54	0.54	1.36	0.72
Mid-rise, M	0.44	0.40	0.63	0.50	1.20	0.75	2.91	0.70
High-rise, M	0.46	0.30	0.68	0.65	1.68	0.65	2.61	0.65

The response spectra for the deterministic and probabilistic hazard scenarios (Figure 6.7), together with the capacity curves described in Table 6.8, allowed obtaining the performance point and, using the corresponding fragility curves of Table 6.9 and the damage probability matrices of Table 6.10.

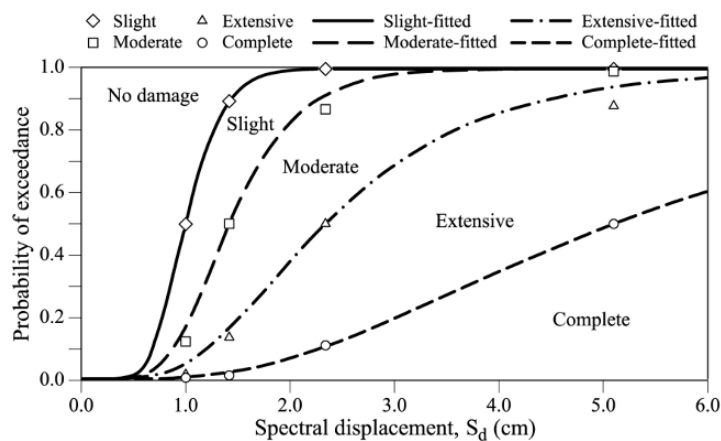


Fig. 6.8. Fragility curves for mid-rise reinforced concrete buildings

6.5. Final remarks

Both the vulnerability index and capacity spectrum methods provide excellent results, showing an excellent correlation with the main features of the built-up environment of Barcelona. It is clear in both cases that a city located in a low to moderate hazard region has paid no attention to the seismic performance of their buildings, and therefore, a high seismic vulnerability and a considerable risk are expected.

Another interesting feature of the described methodologies is their ability to draw the main characteristics of the built-up environment of the city, underlying the radial pattern of the damage. Downtown, where population density is higher and economy is more active, we find the highest vulnerability. The methods described here may be easily adapted to outline risk evaluations for other cities. Probably most of the vulnerability indices adopted for Barcelona may be slightly modified and directly used for obtaining risk scenarios for other cities of Spain and, in particular, for those situated in the Mediterranean region.

Acknowledgements

This work has been partially sponsored by the Spanish Ministry of Science and Technology and with FEDER funds (projects: REN 2001-2418-C04-01 and REN2002-03365/RIES) and by the European Commission (RISK-UE Project: “An advanced approach to earthquake risk scenarios with applications to different European towns”, contract EVK4-CT-2000-00014).

PART II: VULNERABILITY ASSESSMENT

CHAPTER 7 VULNERABILITY ASSESSMENT OF HISTORICAL BUILDINGS

S. Lagomarsino
University of Genoa, Genoa, Italy

7.1. Introduction

Going through the different ages of architecture history, it can be concluded that earthquakes always have, for many reasons, represented the main cause of damage and losses to the cultural heritage.

All ancient masonry buildings, including the biggest and most important monuments, have been constructed following the *rule of thumb*, learning from the experience of previous similar structures. Earthquake is a rare action and the builders experience was different from area to area and from time to time. In areas of high seismicity, where significant earthquakes occur quite often, buildings are characterized by constructive details and reinforcements specifically adopted to protect from seismic actions. In areas of moderate seismicity, these solutions may be found only in the buildings constructed immediately after a big earthquake, together with traditional repair techniques (tie rods, buttresses, scarp walls, foil arches between facing buildings); however, the awareness of the importance of these details disappears after two or three generations.

In the past, masonry buildings were constructed by refining the proportions of structural elements by a deep perception of the structural behaviour; this trial and error process took into consideration only static actions, mainly the dead loads. Notions such as dynamic amplification, damping, soil-structure interaction are not simple to be managed without a theoretical approach. For all these reasons, masonry buildings were proportioned to bear vertical loads and the static horizontal thrusts of arches and vaults. Considering the low tensile strength of masonry, both mortar joints placing and size and shape of structural elements were optimised. The seismic horizontal actions change significantly the thrust lines and usually produce widespread cracks and local collapses.

The vulnerability of historical buildings is thus related to the quality of masonry, the architectural shape and the dimensions and the presence of aseismic reinforcements.

Minor buildings in historical centres are usually very vulnerable due to the low quality of masonry material, the poor state of maintenance and the successive transformations (obstructions, raising up of buildings, partial demolitions).

Monumental buildings are equally vulnerable, even if for different reasons. Indeed, they are usually made by good quality materials, but their dimensions are significant: wide halls, thin long span vaults, slender towering or projecting parts, slender walls with large openings. Considering monuments, the importance and uniqueness of these structures may lead to dealing with the problem of seismic vulnerability through a detailed seismic analysis on each single building. However, even for the cultural heritage, seismic vulnerability is a problem that must be faced at territorial scale, due to the large number and the high density of monuments that are present in seismic prone areas. The aims of a vulnerability analysis of the monumental buildings in a big town or in a region are to be aware of the impact of an earthquake on the cultural heritage in the

area, list the monuments by seismic vulnerability, plan preventive interventions for risk mitigation and manage the emergency after a big earthquake.

After recent Italian seismic events, the damage assessment to monumental buildings showed the high seismic vulnerability of this kind of structures and the relevance of this topic in a risk analysis both from the economic and the cultural point of view. In particular, churches turned out to be numerous and very vulnerable, compared to palaces or other ancient structures. In the case of low intensity earthquakes (Reggio Emilia, 1995; Piedmont, 2000 and 2003), churches have been the only types of structures that systematically suffered some damage. In the case of Umbria and The Marches earthquake (1997), besides the Assisi Basilica, more than 2000 churches suffered significant damage (Lagomarsino, 1998).

Even in the case of urban seismic risk scenarios, the number of monuments in a town is so large that a detailed evaluation on each single building is not possible. As an example, the RISK-UE Project, *An advanced approach to earthquake risk scenarios* (Mouroux et al., 2004), that aimed to develop seismic risk scenarios in some European towns, the monuments considered in the vulnerability assessment were: 67 in Barcelona (ESP), 194 in Catania (ITA), 151 in Nice (FRA) and 218 in Thessaloniki (GRE). According to the Ministry of Fine Arts, the list of monuments is huge, especially in the big cities: 3400 in Barcelona (ESP); 5000 in Bucharest (ROM); 700 in Sofia (BUL).

Well known methodologies for seismic risk scenarios of monumental buildings are not available, although some studies have been developed in the past, especially in Italy, on the observed vulnerability of a wide number of buildings (Doglioni et al., 1994; Lagomarsino and Podestà, 2004a; Lagomarsino and Podestà, 2004c). A vulnerability method has also been established for churches, through the statistical analysis of surveyed damage data (Lagomarsino and Podestà, 2004b). This chapter proposes a holistic approach to the seismic vulnerability assessment of monuments, which is able to profit from all the available information, both regarding the building vulnerability and the seismic hazard.

The seismic hazard map, in the town or in a larger area, may be defined by two different parameters:

- *Macroseismic intensity*: it is a hybrid measure of the seismic input, as it indirectly depends on the building vulnerability (even if the modern macroseismic scales try to overcome this restraint). The macroseismic intensity is useful when the hazard is derived by historical seismicity, both considering deterministic or probabilistic scenarios. Basically, intensity is a discrete variable, if you consider its definition in the macroseismic survey, but in a risk analysis it should be used as a continuous variable, if the vulnerability models are able to manage it properly.
- *Peak ground acceleration (PGA) and spectral values*: this is a mechanical representation of the seismic input, related to the structural response of an equivalent single degree of freedom system. PGA is a continuous variable, the spatial variability may be represented better than through the macroseismic intensity and, moreover, site effects may be taken into account, both as an amplification of the PGA and changing the spectral shape.

The vulnerability of a monumental building is its intrinsic predisposition to be affected and suffer damage as a result of the occurrence of an event of a given severity. It is represented by a model able to assess the physical damage (in probabilistic terms) as a function of the intensity or the PGA/spectrum.

In the case of a macroseismic scenario, a vulnerability curve correlates the intensity to a histogram of damage grades, D_k ($k=0,1,2,3,4,5$), expressed by the mean damage grade μ_D (a continuous parameter, $0 < \mu_D < 5$), and a proper discrete probabilistic distribution. This *macroseismic approach* is based on the observed vulnerability, as these curves have been obtained, for classes of buildings, through damage assessment data, collected after earthquakes of different intensities. The vulnerability curve is defined by two parameters, the vulnerability index V and a toughness coefficient β , which should be evaluated from the information about the building.

In the case of a PGA scenario, the vulnerability model is the capacity spectrum method, in which the capacity curve represents the non-linear behaviour of the building to seismic horizontal actions, through an equivalent single degree of freedom system (Freeman, 1998; Fajfar, 2000). On the capacity curve, some damage thresholds d_k ($k=1,2,3,4$) may be identified. Once the performance point is obtained, through the intersection of the capacity curve with a properly reduced spectrum, the probability of occurrence of each damage state is obtained by means of fragility curves. This method constitutes a *mechanical approach*, as a capacity curve may be obtained through more or less detailed mechanical models, but a validation with observed vulnerability data is necessary, due to the complexity of modelling historical masonry structures.

Both vulnerability models depend on the characteristics of the building (typology, materials, dimensions and shape, constructive details) and their assessment can be more or less accurate according to the level of knowledge of the exposed elements. Thus, a three levels approach is proposed (Level 0, 1 and 2), in relation to the accuracy and the meaningfulness of the collected data, both for the macroseismic and the mechanical approach. This allows using for the risk analysis on the cultural heritage in a given region, without distinction, the most suitable method depending on the characteristics of the hazard scenario; moreover, the same model may be applied to all the monuments, allowing a unique comparable damage scenario, but the evaluation results are more or less accurate in relation to the level adopted (usually level 1 or 2 for the most important buildings and level 0 for the others).

Level 0. The lowest level of information is the inventory of monuments, without any specific data except the typology (church, monastery, palace, villa, tower, etc). Even in this case a very rough evaluation can be made with the macroseismic or the mechanical approaches. In the first case a vulnerability index is assigned to each typology (some values are proposed in 7.3, based on observed vulnerability and expert judgement); if a mechanical approach has to be used, a capacity curve may be defined, in order to get comparable results with the two approaches. The vulnerability assessment at this level may be useful for an overall knowledge of the seismic risk of the cultural heritage in a big town or in a region, in order to plan preventive interventions for the risk mitigation, establishing priorities and allocating funding (Bianchi and Accardo, 1998).

Level 1. In this case some data are available, in particular the one connected to the structural seismic behaviour: regularity (in plan and elevation), quality of materials,

dimensions (number of floors, slenderness of elements), state of maintenance, transformations and interventions. Usually a quick field survey may provide this kind of information, when it is not contained in the available databases. In the macroseismic approach, to each one of these parameters a score is awarded, which modifies the vulnerability index assigned to the typology. In this way, each monument is characterized by its own vulnerability index, and the vulnerability assessment is more accurate and allows making a list of vulnerabilities for the monuments of the same type. The capacity curves may be derived as for level 0, not using a mechanical model but directly from the vulnerability index and taking into consideration some structural parameter (e.g.: dimensions and period of vibration).

Level 2. Going deep in the damage observation, recurrent damage and collapse mechanisms have been observed, which usually don't involve the whole structure but only single architectonic parts, named macroelements, which are characterised by a mostly autonomous structural behaviour in comparison with that of the rest of the building; for example, in the case of churches, façade, nave, triumphal arch, dome, apse, bell tower are the most important macroelements (Doglioni et al., 1994). At this level, the vulnerability assessment methodology analyses the seismic behaviour in terms of local mechanisms, but it is also possible to define a global vulnerability of the structure by a proper combination of the contributions of different macroelements. Due to the wide experience with churches, in this chapter reference is made to this typology but the method may be extended also to other types of monumental structures. The macroseismic approach is again based on a vulnerability index that is obtained in this case through scores related to a detailed survey in the macroelements of the church, to be performed by means of a proper form (Lagomarsino et al., 2004a). The diagnostic survey of the possible damage and collapse mechanisms in each single part of the church, allows us to take into account the source of vulnerability information and the effective constructive details of each macroelement. The mechanical approach may consider simplified mechanical models, representative of the most probable local collapse mechanisms. As local mechanisms are considered, only a sub-structure has to be modelled (macroelement); the application of the safe and unsafe theorems of limit analysis, applied to masonry structures (Heyman, 1966; Heyman, 1982), may be very useful to this aim. The masonry structure is considered to be made of rigid blocks, due to the low tensile strength and the relevant compressive strength and stiffness. With this approach, only few geometrical parameters and technological details are needed, which can be obtained during a field survey. An incremental non-linear limit analysis may be performed, in order to evaluate the displacement capacity of the masonry structure, by an approximate approach that makes use of the capacity spectrum method (Lagomarsino et al., 2004b).

Finally, it is worth noticing that all the above mentioned methods are far from the close examination that is needed in the design of seismic improvement interventions on monumental structures (Level 3). The high complexity that is necessary for an exhaustive study is outside the scope of a vulnerability analysis, because it is impossible to be implemented for a territorial analysis.

7.2. The observed vulnerability in historical buildings

Damage assessment represents a remarkable source of information of the seismic emergency, as an earthquake represents a test of the actual vulnerability of structures. This activity, usually coordinated by the Civil Protection Department and made using proper survey forms, in order to get systematic and objective data, may be useful to: 1) verify if the structure is fit to use in the emergency (green, yellow or red tag); 2) decide for provisional interventions (propping, hopping), in order to prevent further damage due to after shocks; 3) evaluate economic losses, to be charged to insurance companies or for funding from the State; 4) make a preliminary diagnosis of the building performance, in order to design the proper repairing and strengthening interventions.

Besides the above mentioned uses for the single building and the emergency management, the damage assessment gives a lot of data useful for statistical analyses aimed to develop observational vulnerability models, related to homogeneous typologies, which can also consider the influence of some details and the effectiveness or the deficiencies of the most used strengthening interventions.

7.2.1. DAMAGE AND VULNERABILITY ASSESSMENT OF CHURCHES

During the last twenty years, the damage to churches caused by various earthquakes in Italy has been systematically assessed and interpreted from the structural point of view. The seismic response of churches showed recurrent behaviours, according to damage and collapse mechanisms of the different architectural parts, called macroelements, which behave almost independently. Typical examples of macroelement are the façade, the nave, the triumphal arch, the dome, the apse and the bell tower.

In particular, the damage to the churches after the Umbria and Marche earthquake, in 1997, has been assessed by a proper form, which considers eighteen indicators, each one representative of a possible collapse mechanism in a macroelement:

- façade: 1) façade overturning; 2) overturning of the gable; 3) in plane mechanisms;
- nave and transept: 4) transversal vibration of nave or of the transept; 5) longitudinal vibration of the central nave; 6) vaults of the central nave; 7) vaults of the lateral naves and of the transept;
- triumphal arch: 8) kinematics of triumphal arches;
- dome and “tiburio”: 9) collapse of the dome and the “tiburio”;
- apse: 10) overturning of the apse; 11) vaults of the apse and of the presbytery;
- other mechanisms: 12) overturning of walls (transept façade, chapels); 13) shear failure of the walls; 14) hammering and damage in the roof covering; 15) interaction with adjacent structures;
- bell tower: 16) global collapse of the bell tower; 17) mechanisms in the bell cell;
- bell gable, spires and projections: 18) overturning of standing out elements.

For each mechanism, the survey form asks for the suffered damage level (explained by proper sketches - Figure 7.1), and some constructive characteristics and reinforcements of the macroelements, relevant to judging the seismic vulnerability (Lagomarsino, 1998). This is a diagnostic approach, as it is not aimed to measure the length and the size of cracks, but to recognize the mechanisms started up by the earthquake and their

severity and dangerousness with respect to the local collapse. A damage index and a vulnerability index may be defined by the data in the form.

2. DAMAGE AT THE TOP OF THE FACADE	<input type="checkbox"/>
CRACKS IN THE TOP PART OF THE FACADE	<input type="checkbox"/> <input type="checkbox"/> <input type="checkbox"/>
<input type="checkbox"/> Facade weakened by wide openings <input type="checkbox"/> Lack of a connection with the roof covering	

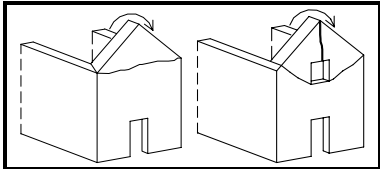


Fig. 7.1. Abstract of the damage assessment church form: survey of the damage in a macroelement in terms of collapse mechanisms and vulnerability indicators

More than 2000 churches were assessed in Umbria and Marche, characterized by different typologies (from basilicas to small rural churches) and struck by different levels of macroseismic intensity I (from V to VIII of the MCS scale, according to the survey of INGV, the Italian National Institute of Geophysics and Volcanology).

The statistical analysis of the data produced a Damage Probability Matrix (DPM) for the churches, that is a matrix in which for four different values of the macroseismic intensity, the probability histogram of the damage levels is listed. The five damage levels are defined according to the modern macroseismic scales, in particular the EMS98, *European Macroseismic Scale* (Grünthal 1998): 0) no damage; 1) slight damage; 2) moderate damage; 3) heavy damage; 4) very heavy damage; 5) destruction. For each intensity, the mean damage grade μ_D may be defined, by the probability P_k of each damage grade D_k :

$$\mu_D = \sum_{k=1}^5 kP_k \quad (7.1)$$

The damage histograms (Figure 7.2) are well fitted by the binomial distribution, which is defined only by one parameter, just the mean damage grade μ_D :

$$P_k = \frac{5!}{k!(5-k)!} (0.2\mu_D)^k (1-0.2\mu_D)^{5-k} \quad (7.2)$$

Figure 7.2 shows the gradual increase of the damage with the intensity; this trend appears very regular if you consider the mean damage grade μ_D . Many churches have been surveyed with this approach after earthquakes in other regions of Italy; the statistical analyses corroborated the correlation obtained in Umbria and Marche.

The DPM considers all the churches as a homogeneous typology, characterizing on average its vulnerability. However, the survey form allows taking into account the specific vulnerability of each church, evaluated through a vulnerability index. Dividing the sample of the churches, in areas that suffered the same seismic intensity, into smaller samples characterized by ranges of the vulnerability index V , a more refined correlation may be set up (Lagomarsino and Podestà, 2004b), which also considers this intrinsic parameter of the church: Figure 7.2 shows the gradual increase of the damage with the intensity; this trend appears very regular if you consider the mean damage grade μ_D . Many churches have been surveyed with this approach after earthquakes in

other regions of Italy; the statistical analyses corroborated the correlation obtained in Umbria and Marche.

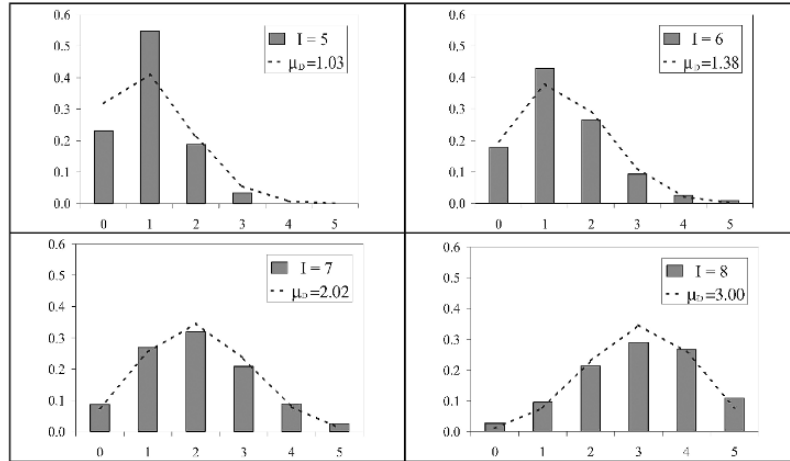


Fig.7.2. Damage probability histograms for the churches

The DPM considers all the churches as a homogeneous typology, characterizing on average its vulnerability. However, the survey form allows taking into account the specific vulnerability of each church, evaluated through a vulnerability index. Dividing the sample of the churches, in areas that suffered the same seismic intensity, into smaller samples characterized by ranges of the vulnerability index V, a more refined correlation may be set up (Lagomarsino and Podestà, 2004b), which also considers this intrinsic parameter of the church:

$$\mu_D = 2.5 \left[1 + \tanh \left(\frac{I + 6.25V - 13.1}{3} \right) \right] \quad (7.3)$$

where V assumes values between 0.67 and 1.22 (for the more vulnerable churches).

7.2.2. VULNERABILITY CURVES OF PALACES AND CHURCHES

The vulnerability curve (7.3) represents a model to evaluate the probability damage distribution of a church, for which the vulnerability index V has been evaluated by a proper survey, as a function of the hazard, in terms of the macroseismic intensity I. A similar model has been derived for current buildings (Giovinazzi and Lagomarsino, 2004), on the basis of the European Macroseismic Scale, using fuzzy set theory, and after a validation through damage observation data.

The method is based on the assignment to any building, or to a group of buildings, of a vulnerability index V, which is obtained as the sum of the typological vulnerability index V_0 , related to the EMS98 building classification, and the vulnerability scores, assigned to some relevant parameters of the construction (state of maintenance, material quality, structural regularity, etc.). The mean damage grade is given by:

$$\mu_D = 2.5 \left[1 + \tanh \left(\frac{I + 6.25V - 13.1}{2.3} \right) \right] \quad (7.4)$$

The vulnerability index V usually varies from 0 (for structures with a high level of earthquake resistance design) to 1 (for the very vulnerable poor masonry buildings).

Among the different typologies there is the one of massive stone buildings. Monumental palaces may be, on average, associated to this typology, because their construction is typically characterized by good quality materials and craftsmanship. For massive stone buildings $V_0=0.62$, and the vulnerability index may vary, according to the vulnerability scores, from 0.3 to 0.86 (a plausible range is $0.49 < V < 0.79$).

It is worth noting that the vulnerability curves of churches (7.3) and palaces (7.4) are similar, with the exception of denominator, which controls the rate of increase of the damage with the intensity. It is defined as the ductility index, Q . The vulnerability curves of the churches and of the monumental palaces are compared in Figure 7.3. Due to higher values, on average, of the vulnerability index, churches turn out to be more vulnerable for the lower intensities; actually, in the case of minor earthquakes in Italy, the churches always exhibited a higher damage among the built environment. The higher ductility of the churches ($Q=3$ for churches, $Q=2.3$ for palaces) determines that for higher intensities, the seismic response tends to be similar to the one of palaces.

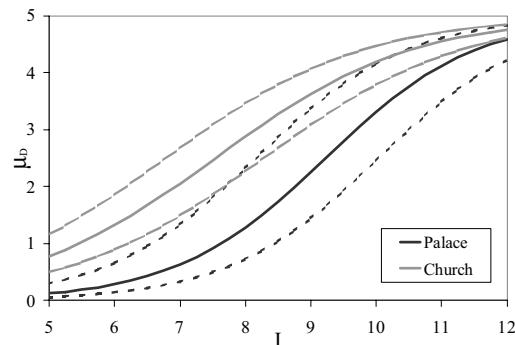


Fig. 7.3. Vulnerability curves of palaces and churches (mean value, plausible range)

7.3. The vulnerability assessment methodology

Also in the case of historical buildings, a vulnerability model suitable for application at the territorial scale has to be referred to a typological classification. Considering the wide variety of the artefacts that constitute the cultural heritage in the world, according to geographic location, architectural styles and ages of construction, this classification is not a straightforward task. However, for the sake of a simplified structural evaluation of the seismic vulnerability on a wide population of monuments, a typological classification is usually possible, gathering into groups the structures which are similar with reference to the architecture and the seismic behaviour.

An example of typological classification, which may be considered as a reference for monuments in European countries, is the following: palace, church, monastery/convent, mosque, tower, obelisk, theatre, castle, triumphal arch, arch bridge.

Considering the two vulnerability approaches described in the introduction of this chapter (macroseismic and mechanical), in the following paragraphs the basis of the methods are stated, both for level 0 and level 1 grades of detail in the analysis.

7.3.1. BASIS OF THE MACROSEISMIC APPROACH (LEVEL 0)

The damage assessment after earthquakes and the definition of the macroseismic scale (EMS98) allow us to state the observational vulnerability model, through a correlation between the intensity I of the earthquake and the mean damage grade μ_D , which represents the mean value of the probability histogram of the damage grades D_k ($k=0,1,2,3,4,5$), typical of easily observable levels of damage, in terms of cracks and deformations. The vulnerability curves are:

$$\mu_D = 2.5 \left[1 + \tanh \left(\frac{I + 6.25V - 13.1}{Q} \right) \right] \tag{7.5}$$

The model is defined by two parameters, the vulnerability index V and the ductility index Q . The vulnerability index V ranges from 0 to 1, in the case of the six building types defined in EMS98; for masonry building, V is greater than 0.4. In the case of churches, V can assume values between 0.67 and 1.22. A decrease of V equal to 0.16 means that you need an increase of one degree in the intensity of the earthquake, in order to produce the same damage grade. The ductility index Q determines the rate of increase in the damage with intensity. If $Q=2.3$ (as for buildings), one intensity degree corresponds to one damage grade; greater values of Q are typical of ductile structures.

Reference values for the other monumental types may be deduced from them, according to expert judgment and taking advantage of some observed data on each typology. The values in Table 7.1 may be used for a Level 0 vulnerability assessment, having at disposal only the list of monuments in the city or in the region.

Table 7.1. Parameters for the macroseismic and the mechanical models

Model parameters	Macroseismic		Mechanical		
	V_0	Q	T (s)	a_y (g)	μ
Palace	0.62	2.3	0.35	0.35	4.8
Church	0.89	3.0	0.40	0.09	7.5
Monastery/Convent	0.74	2.3	0.40	0.23	4.3
Mosque	0.81	2.6	0.35	0.15	6.1
Tower	0.78	2.0	0.70	0.13	3.4
Obelisk	0.74	3.0	1.00	0.06	7.5
Theatre	0.70	2.3	0.45	0.23	4.3
Castle	0.54	2.0	0.25	0.56	4.8
Triumphal arch	0.58	2.6	0.60	0.23	5.5
Arch bridge	0.46	2.3	0.30	0.63	5.4

Once the hazard scenario is known, damage level can be evaluated immediately for each structure (damage scenarios) and obtain a list of the monuments by their risk can be obtained. The mean damage grade μ_D , given by (7.5), represents a synthetic meaningful

parameter for the damage scenario; Figure 7.4 shows the mean vulnerability curves for the different monumental typologies. If a probabilistic evaluation is needed, the probability P_k ($k=0,1,2,3,4,5$) joined to each damage grade is given by the binomial distribution (7.2); these values may be useful for more detailed scenarios, aimed at showing, for example, the probability of collapse of each building (P_5) or the probability that the building is unfit for use in the emergency ($P_3+P_4+P_5$). The fragility curves are then:

$$P[D_k|\mu_D] = \sum_{i=k}^5 P_i = \sum_{i=k}^5 \frac{5!}{i!(5-i)!} (0.2\mu_D)^i (1-0.2\mu_D)^{5-i} \quad (7.6)$$

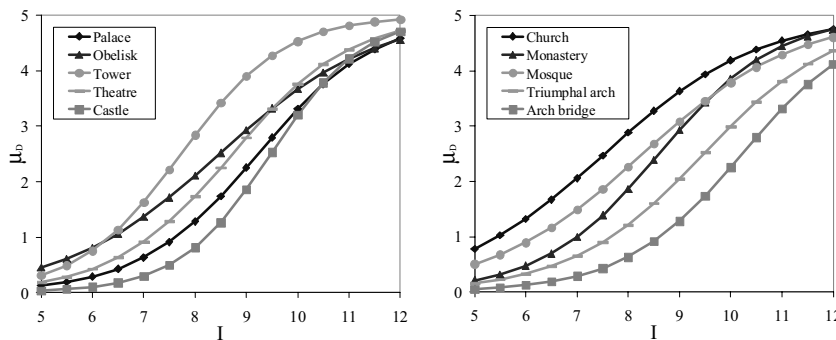


Fig. 7.4. Mean vulnerability curves for the different types of monumental buildings

7.3.1.1. The macroseismic vulnerability assessment (Level 1)

It is evident that a vulnerability index assigned to a monument simply by a typological classification represents an average value, which doesn't take into account the distinctiveness of the single building and doesn't allow us to single out the most vulnerable structures among buildings of the same type. To refine the vulnerability assessment a quick survey is at least necessary, with the purpose of collecting by proper survey forms some relevant parameters, such as: state of maintenance, quality of materials, structural regularity (in plan and in elevation), size and slenderness of relevant structural elements, interaction with adjacent structures, presence of retrofitting interventions, site morphology.

Vulnerability scores V_k may be awarded to each one of the above mentioned parameters and the vulnerability index of each monument may be refined, modifying the typological value:

$$V = V_0 + \sum V_k \quad (7.7)$$

where the summation is extended to all the available modifiers. The vulnerability scores may assume different values for different typologies; moreover, some relevant information may be distinctive only of one typology (e.g.: the presence of a raising façade in churches).

The choice of the specific vulnerability parameters has been made empirically, on the basis of the observation of the typical damage. This approach is similar to many well-

known vulnerability procedures, proposed in different countries for ordinary buildings (Benedetti and Petrini, 1984; ATC-21, 1988). The values of the modifying scores have been tuned, for churches and palaces, by statistical analysis of data that come out from damage assessment (§ 7.2.1). Some reference values are proposed in Table 7.2.

Table 7.2. Reference values for vulnerability scores V_k of the main parameters

Parameter	V_k
state of maintenance	very bad (0.08) – bad (0.04) – medium (0) – good (-0.04)
quality of materials	bad (0.04) – medium (0) – good (-0.04)
planimetric regularity	irregular (0.04) – regular (0) – symmetrical (-0.04)
regularity in elevation	irregular (0.02) – regular (-0.02)
interactions (aggregate)	corner position (0.04) – isolated (0) – included (-0.04)
retrofitting interventions	effective interventions (-0.08)
site morphology	ridge (0.08) – slope (0.04) – flat (0)

7.3.2. STATEMENT OF THE MECHANICAL APPROACH (LEVELS 0 AND 1)

The use of a mechanical approach for the vulnerability assessment has been proposed, in particular for current buildings, by HAZUS (NIBS, 1997, 1999 and 2002), which considers the capacity spectrum method. This method permits evaluating the expected seismic performance of a structure, assumed as an equivalent non-linear Single Degree of Freedom system, by intersecting, in spectral coordinates (S_d , S_a), its seismic capacity curve with the seismic demand, described by the Acceleration-Displacement Response Spectra (ADRS), adequately reduced in order to take into account the inelastic behaviour.

7.3.2.1. Application of the capacity spectrum method for the vulnerability assessment

The capacity curve of a structure should be obtained by a pushover analysis, but in the case of a territorial vulnerability assessment, at levels 0 or 1 of available data, a bilinear capacity curve must be defined by the typology taking into account some qualitative information. In the case of monuments, the characteristics of masonry structures suggest neglecting the possibility of a global hardening behaviour; thus, the capacity curve is defined by three parameters: the fundamental period (T), the yielding spectral acceleration (a_y) and the ductility (μ).

Instead of using overdamped spectra, for which we need to know the equivalent damping as a function of the displacement and to evaluate the performance point by an iterative procedure (Freeman 1998), in the case of bilinear capacity curves it is preferable to adopt the inelastic spectra approach (Fajfar, 2000), which can be applied in a very simple way and is reliable for structures characterized by high hysteretic dissipation.

A mechanical approach is used when the hazard scenario gives the elastic response spectrum (at 5% damping) $S_{ac}(T)$, usually by discrete values for fixed periods or by the peak ground acceleration a_g and a predefined spectral shape (related to the local soil conditions). In both cases a characteristic period T_C may be defined, which separates the periods of almost constant spectral acceleration ($T < T_C$) by the almost constant spectral velocity range ($T > T_C$). The performance point, which is the spectral displacement demand (target displacement), is obtained by:

$$S_{d*} = \begin{cases} [1 + (q - 1)T_C / T]d_y & T < T_C \text{ and } q > 1 \\ qd_y & T_C \leq T < T_D \text{ or } q \leq 1 \\ S_{ac}(T_D)T_D^2 / 4\pi^2 & T \geq T_D \end{cases} \quad (7.8)$$

where: T is the period of the structure; $d_y = a_y T^2 / (4\pi^2)$ is the yielding displacement of the structure, $q = S_{ac}(T) / a_y$ is the ratio between the demand to an elastic system and the strength of the non-linear structure; T_D is the period that defines the constant spectral displacement range.

The capacity curve represents the progress of the structural response to horizontal seismic actions, from the initial undamaged elastic behaviour, through the formation and the development of cracks, to the loss of stability, near to collapse. Four damage states, which are usually related to performance levels of the structure, may be defined according to Table 7.3, where the mean values $S_{d,k}$ ($k=1,2,3,4$) of the displacement thresholds are indicated. It is worth noting that the bilinear behaviour is an approximation of the actual curved response, usually made considering an equivalent period (of the cracked structure) and with an equivalent energy dissipation; in particular, the slight damage occurs before yielding, while moderate damage, corresponding to the achievement of the maximum strength, is attained for a spectral displacement greater than d_y .

Table 7.3. Mean values of the damage state thresholds $S_{d,k}$

D_k	damage state	performance level	$S_{d,k}$
1	Slight	fully operational	$0.7d_y$
2	Moderate	Operational	$1.5d_y$
3	Heavy	life safe	$0.5(1+\mu)d_y$
4	Complete	near collapse	μd_y

Figures 7.5 show the capacity curves of two different structures (rigid and flexible), with the damage state thresholds and the target displacement, obtained by (7.8) in the case of two different demand spectra.

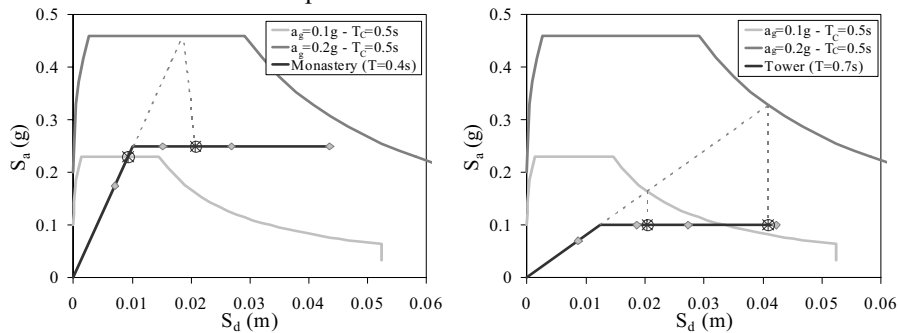


Figure 7.5. Capacity curves, damage state thresholds and evaluation of the target displacement for rigid ($T < T_C$) and flexible structures ($T > T_C$), for two demand spectra

As for the macroseismic approach, the output of the vulnerability assessment is the probability distribution of the expected damage state. The fragility curves give the probability that the damage is equal to or higher than a certain state D_k , as a function of

the target displacement S_{d^*} (performance point, obtained by eqn 7.8); a lognormal cumulative probability function may be used:

$$P[D_k|S_{d^*}] = \Phi \left[\frac{1}{\beta_k} \ln \left(\frac{S_{d^*}}{S_{d,k}} \right) \right] \quad (7.9)$$

where Φ is the normal cumulative distribution function and β_k is the normalized standard deviation of the natural logarithm of the displacement threshold $S_{d,k}$. The probability histogram of the damage state is then given by:

$$P_4 = P[D_4|S_{d^*}] \quad P_k = P[D_k|S_{d^*}] - P_{k+1} \quad (k=1,2,3) \quad P_0 = 1 - P_1 \quad (7.10)$$

Comparing the damage state in Table 7.3 with the damage grades of the macroseismic approach (see § 7.2.1), a direct correspondence of the first four levels can be observed, while the fifth damage grade (destruction) cannot be defined by a mechanical approach, as the softening behaviour should be included in the capacity curve.

As the distribution of the macroseismic method has been validated by observed vulnerability data, the binomial distribution may be used to take out from the probability P_4 , the part that corresponds to the building collapse (P_5). It results that a reliable estimation is given by:

$$P_5 = 0.09 \operatorname{senh}(0.6 \mu_{DS}) P_4 \quad \text{where } \mu_{DS} = \sum_{k=1}^4 k P_k \quad (7.11)$$

Moreover, the use of binomial distribution allows us to define a reliable estimation of the coefficient β_k , which results are dependent on the ductility μ of the capacity curve, while the same value can be assumed for all the damage state:

$$\beta_k = 0.4 \ln \mu \quad (k=1,2,3,4) \quad (7.12)$$

Fragility curves are shown in Figure 7.6a, with reference to the more flexible structure in Figure 7.5 (tower). Figure 7.6b shows the histograms of damage state probability, for the two different values of the peak ground acceleration; light grey represents the share of P_4 that is assumed as destruction (D_5), according to (7.11).

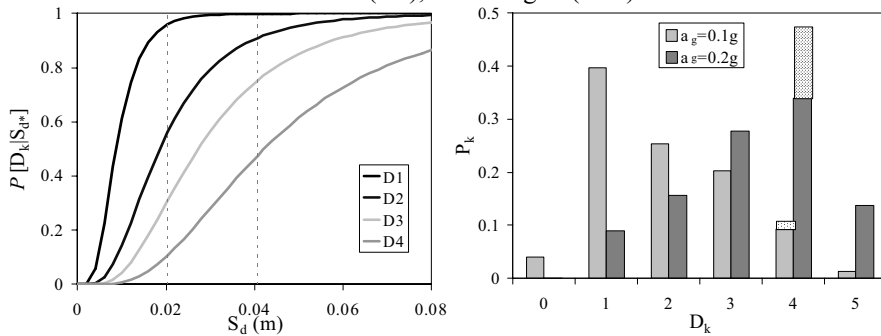


Figure 7.6. Evaluation of damage states probability for the two structures of Figure 7.5: a) fragility curves; b) damage histograms

If the hazard scenario is defined only by the peak ground acceleration a_g , fixing the spectral shapes for one or a limited number of soil conditions, the fragility curves (7.9) may be expressed directly as a function of a_g :

$$P[D_k|a_g] = \Phi \left[\frac{1}{\beta_k} \ln \left(\frac{a_g}{a_{g,k}} \right) \right] \quad (7.13)$$

where $a_{g,k}$ is the ground acceleration that produces the damage state D_k ($k=1,2,3,4$), which is obtained, for each structural typology, by substituting the value $S_{d,k}$ of Table 7.3 in eq. (7.8).

7.3.2.2. Definition of capacity curves for monumental buildings

If the vulnerability assessment is performed with information at level 0 or 1, it is impossible to evaluate capacity curves even by a simplified structural analysis, because the data are too poor. However, it is possible to deduce capacity curves for the monumental typologies in the classification of Table 7.1, to be used for a very rough vulnerability assessment. This can be made by establishing an equivalence of the results that are obtained by the macroseismic and the mechanical approach.

To this aim, first of all it is necessary to set a correlation between intensity I and peak ground acceleration a_g . These parameters are completely different, the second being a physical parameter of the motion, variable from point to point due to local soil conditions, and the former a subjective measure, average in a wide area, that implicitly includes the vulnerability itself (even if the EMS98 scale tries to overcome this limitation). Different correlations have been proposed in the literature and they are extremely scattered, but most of the analytical relations may be expressed in this form:

$$a_g = c_1 c_2^{(I-5)} \quad I = 5 + \frac{1}{\ln c_2} (\ln a_g - \ln c_1) \quad (7.14)$$

Moreover, the spectral shape has been assumed to have a constant value equal to $s a_g$, for $T < T_C$, followed by a constant velocity phase ($S_a(T) = 2.5 a_g T_C / T$); s and T_C are free parameters that define the demand spectrum.

One of the three parameters of the mechanical method (T , a_y , μ) have to be assumed on the base of the typology, as the macroseismic method is defined only by two parameters (V , Q); the period T has been chosen, the easiest one to be estimated by expert judgement and the one that has the lowest influence on the evaluation of the displacement demand. By requiring that the two approaches give the same results for damage levels 1 and 4, we have the necessary relations for deriving the parameters of the mechanical method:

$$\begin{aligned} T < T_C & \begin{cases} a_y = 1.43 s c_1 c_2^{(8.1-6.25V-0.95Q)} \\ \mu = 1 - \frac{T_C}{T} + 0.7 \frac{T_C}{T} c_2^{1.35Q} \end{cases} \\ T \geq T_C & \begin{cases} a_y = 1.43 s c_1 c_2^{(8.1-6.25V-0.95Q)} \frac{T_C}{T} \\ \mu = 0.7 c_2^{1.35Q} \end{cases} \end{aligned} \quad (7.15)$$

As it is evident, having fixed the period T , the yielding spectral acceleration a_y mainly depends on the vulnerability index V , while the ductility μ is correlated only with the ductility index Q , which influences the rate of damage increasing with the intensity. Comparing the results of the two methods with reference to damage levels 2 and 3, it comes out, on average, to be a very good agreement; this confirms that the values of $S_{d,k}$ adopted in Table 7.3 are reliable, due to the validation with the observational approach.

In Table 7.1 values are proposed for the monumental types; the corresponding capacity curves are shown in Figure 7.7. The values of parameters a_y and μ have been obtained by adopting for the spectral shape: $s=2.5$, $T_C=0.4$ s, and for the correlation $I-a_g$: $c_1=0.03g$, $c_2=1.8$. Both yielding accelerations and ductilities seem to be realistic, even if derived analytically; this represents a cross-validation of the macroseismic method and of the vulnerability and ductility indexes assumed.

The mechanical method here proposed may be applied also if the vulnerability assessment is made at level 1. In this case, the available information allows us to refine the typological vulnerability index, by means of the vulnerability scores (eq. 7.7, Table 7.2). For each single monument, a proper fundamental period may be assumed, considering the size and other characteristics of the structure, and a capacity curve may be defined by (7.15), using a $I-a_g$ correlation (7.14) calibrated in the study area.

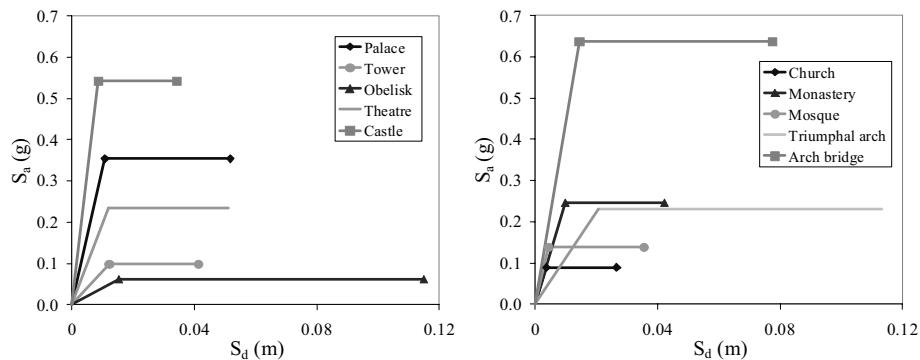


Fig. 7.7. Capacity curves for monumental buildings

7.4. Macroseismic vulnerability assessment of churches (Level 2)

The limitation of level 1 methodology is that vulnerability is considered in a global way. On the contrary, the damage observation has highlighted how, according to the architectonic complexity of monumental buildings (geometry, constructive phases, transformations, etc.) and to the poor tensile strength of the masonry, the damage and collapse often takes place locally. Thus, a proper approach should be the evaluation of the vulnerability in each macroelement, an architectonic element of the building characterized by a substantially independent seismic response. A comprehensive vulnerability index, representative of the overall behaviour of the monument, may be defined as a weighted average of the characteristics in each macroelement.

As a result of the wide experience in assessing damage and vulnerability to churches after the earthquakes in Italy (see § 7.2.1), a level 2 macroseismic vulnerability method has been stated (Lagomarsino et al., 2004a), which considers 28 damage mechanisms, able to represent the seismic behaviour of churches of different architectonic styles and configurations (one or three naves, with or without transept, etc.).

The vulnerability of each macroelement is the result of two complementary shares: 1) the vulnerability indicators (poor masonry, slenderness of elements, presence of thrusting elements, etc.), weakness of the macroelement with reference to a specific collapse mechanism; 2) the specific aseismic reinforcements (tie rods, buttresses, etc.), constructive details that reduce the vulnerability.

The use of this methodology in different regions in Italy and also in some other countries has proved its wide applicability and effectiveness. The vulnerability index which is obtained is fully compatible with the one defined in § 7.3.1; thus, for the vulnerability assessment of churches in a wide region, it is possible to assess the vulnerability of the most important churches with the level 2 vulnerability form, and evaluate the others with a quick survey (level 1) or only with available data (level 0).

7.5. A mechanical model for capacity spectrum method on monuments (Level 2)

The mechanical approach at level 0 and 1 is based on capacity curves directly derived from the macroseismic vulnerability index, in order to have a methodology applicable with a hazard scenario in terms of peak ground acceleration and spectral values. If information is detailed (level 2), the capacity curve should be defined by a simplified mechanical model, for the sake of a more reliable and consistent approach.

However, only in the case of some monumental typologies (tower, obelisk, etc.) is the definition of a capacity curve describing the global behaviour of the monument conceptually correct. Usually, as shown in the previous paragraph, the damage and collapse mechanisms are related to parts of the building (macroelements) and the capacity curve should represent this local behaviour. Thus, the first step of a vulnerability assessment with a mechanical approach is to single out the weakest macroelement and the corresponding collapse mechanism.

In order to define the capacity curve, a pushover analysis by the non-linear finite element method (f.e.m.) should be done. However, modelling a complex historical structure is not a straightforward task (lack of homogeneity in the materials, uncertainty in the connection between elements, etc.) and reliable constitutive non-linear models for masonry are not widespread (Lourenço et al., 1997; Calderini and Lagomarsino, 2004).

An alternative approach for a pushover analysis on a historical masonry structure (Lagomarsino et al., 2004b) is the use of the kinematic theorem of limit analysis (Heyman, 1966), based on the a priori selection of the collapse mechanism, that is the transformation of the structure in a kinematic mechanism, by positioning a sufficient number of hinges or sliding planes. Each resulting block is subjected to dead loads and to horizontal seismic action, proportional to the dead loads through a coefficient α . Under the hypothesis of non-tensile strength of masonry, unlimited compressive

strength and rigid blocks, the seismic coefficient α_0 that induces the loss of equilibrium is obtained by the principle of virtual works:

$$\alpha_0 \left(\sum_{i=1}^n W_i \delta_{x,i} + \sum_{j=n+1}^{n+m} W_j \delta_{x,j} \right) - \sum_{i=1}^n W_i \delta_{y,i} + \sum_{h=1}^o F_h \delta_h = L_{fi} \quad (7.16)$$

where:

n is the number of carried weights W_i , applied in their centres of gravity to the blocks;

m is the number of weights W_j , which are not born by the macroelement but that induce a horizontal seismic action, as not effectively connected to other building elements;

o is the number of external actions F_h , such as the thrusts of roof, arches and vaults;

$\delta_{x,i}$ and $\delta_{x,j}$ are the virtual horizontal displacements of the points where the weights W_i and W_j are applied (positive if coherent with the mechanism development);

$\delta_{y,i}$ is the virtual vertical displacement of the point where the weight W_i is applied (positive if upward);

δ_h is the virtual displacement of the point where F_h is applied, in this direction;

L_{fi} is the virtual work of possible internal actions (friction sliding, interlocking, etc.).

The virtual displacements are obtained by applying to the kinematic mechanism an infinitesimal deformation; for example, if an infinitesimal rotation θ_k is applied to the block k , the rotations of the other blocks are obtained by the kinematic mechanism, only considering geometry, and the same is for the displacements of each relevant point.

A pushover analysis is an analysis of the seismic performance of the structure, not only by the evaluation of coefficient α till maximum strength is reached but also by increasing the displacements till collapse. In this case, as an earthquake is a dynamic action, the static loss of equilibrium doesn't correspond to the collapse, and the kinematic mechanism is able to sustain some horizontal action also after its activation. To this end, an incremental kinematic analysis may be performed, by applying (7.16) to different configurations, obtained incremental displacement d_k of a properly chosen control point k . As finite displacements are considered, the seismic coefficient α usually decreases gradually because of the reduction of the stabilizing contribution of the dead loads; an exception is in the case of presence of forces F_h that increase their value with the progression of the kinematic mechanism (tie rods). The incremental analysis must be performed till the zeroing of the coefficient α , that occurs for a displacement $d_{k,0}$; if the different actions may be considered as constant during the progression of the kinematic mechanism, the pushover curve is well approximated by a straight line:

$$\alpha = \alpha_0 (1 - d_k / d_{k,0}) \quad (7.17)$$

As an example, the typical collapse mechanism of a triumphal arch in a church is shown in Figure 7.8a. The progress of the coefficient α with the displacement of the upper block (Figure 7.8b) usually points out a linear descending branch; if a steel tie rod is present, the coefficient α_0 that induces the activation of the kinematic mechanism increases (due to the initial pull in the tie rod) and the curve is characterized by a further

increase (due to the increasing of the pull) and by the failure of the tie rod (with the return to the behaviour of the arch without the tie rod).

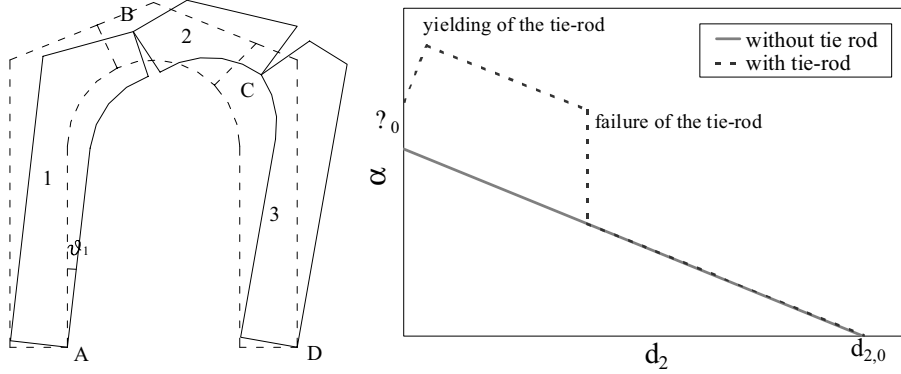


Fig. 7.8. Mechanical model for the triumphal arch in the churches: a) three blocks kinematic mechanism; b) typical pushover curves, with and without a steel tie rod

The application of the capacity spectrum method requires the transformation to an equivalent single degree of freedom system; to this aim, a well-known procedure uses a vector of nodal displacements (usually the fundamental modal shape), normalized to the value 1 in the control point (the one used for the pushover curve). In this case, the vector of the virtual horizontal displacements δ_x , used in (7.16), may be used, as it represents the mode of failure. The transformation factor is:

$$\Gamma = \delta_{x,k} \frac{\sum_{i=1}^{n+m} W_i \delta_{x,i}}{\sum_{i=1}^{n+m} W_i \delta_{x,i}^2} \quad (7.18)$$

where $\delta_{x,k}$ is the virtual displacement of the control point k (due to normalization). The spectral displacement of SDOF system is then:

$$S_d = \frac{d_k}{\Gamma} = \frac{d_k}{\delta_{x,k}} \frac{\sum_{i=1}^{n+m} W_i \delta_{x,i}^2}{\sum_{i=1}^{n+m} W_i \delta_{x,i}} \quad (7.19)$$

while the spectral acceleration is:

$$S_a = \frac{\alpha g \delta_{x,k} \sum_{i=1}^{n+m} W_i}{\Gamma \sum_{i=1}^{n+m} W_i \delta_{x,i}} = \frac{\alpha g \sum_{i=1}^{n+m} W_i \sum_{i=1}^{n+m} W_i \delta_{x,i}^2}{\left(\sum_{i=1}^{n+m} W_i \delta_{x,i} \right)^2} = \frac{\alpha g}{e_m} \quad (7.20)$$

where g is the gravity acceleration and e_m is the fraction of the mass that participates in the kinematic mechanism.

The capacity curve obtained, by transforming the seismic coefficient α and the control displacement d_k of the pushover curve (7.17) by (7.19) and (7.20), disregards the deformability of the macroelement that is involved in the collapse mechanism, as it is considered made by rigid blocks. Hence, an estimate of the vibration period T , associated to the mechanism in the phase preceding its activation, must be done. To this aim, the f.e.m. is very useful, even with linear elastic models (proper values of the modulus of elasticity should be used, in order to take into account the stiffness degradation due to micro-cracking). Non-linear finite element models may be useful also to verify and suggest the correct choice of the kinematic mechanism, as the proposed approach is reliable if the most vulnerable mechanism is selected; on the contrary, as already stated, it is very difficult to manage non-linear f.e.m. for a pushover analysis, particularly in a vulnerability analysis at territorial scale. When no specific evaluation of the period T is possible (for instance in the case of a local mechanism with a multiple connection to the rest of the building), a reference value $T=0.1s$ may be assumed.

Thus, the capacity may be assumed as a bilinear curve:

$$\begin{aligned} S_a &= \frac{4\pi^2}{T^2} S_d & S_d \leq d_y \\ S_a &= \frac{\alpha_0 g}{e_m} \left(1 - \frac{\Gamma}{d_{k,0}} S_d \right) & S_d > d_y \end{aligned} \quad (7.21)$$

where d_y is the yielding spectral displacement, given by:

$$d_y = \left(\frac{\Gamma}{d_{k,0}} + \frac{4\pi^2 e_m}{T^2 \alpha_0 g} \right)^{-1} \quad (7.22)$$

In order to implement a mechanical approach at territorial scale, it is necessary to define the collapse spectral displacement. Even if the dynamic equilibrium is theoretically possible all along the softening branch of the capacity curve, the displacement demand increases tremendously when the capacity comes down to a certain rate of the initial one. According to the results of many non-linear dynamic analyses, performed by different authors (Doherty et al., 2002; Restrepo-Vélez and Magenes, 2004) collapse is assumed at 40% of the spectral displacement $d_{k,0}/\Gamma$ that corresponds to the zeroing of the spectral acceleration capacity. In the case of bilinear capacity curve (7.21), the ductility is expressed by:

$$\mu = 0.4 \left(1 + \frac{4\pi^2 e_m d_{k,0}}{T^2 \alpha_0 g \Gamma} \right) \quad (7.23)$$

Thus, the damage state thresholds $S_{d,k}$ ($k=1,2,3,4$) may be defined analogously to what has been done in § 7.3.2.1 for level 0 and 1 approaches (Table 7.3), except for the moderate damage ($D_k=2$). The evaluation of the fundamental period T is, indeed, rather uncertain and the ductility resulting from (7.23) is usually very high, as these local

collapse mechanisms are related to the loss of equilibrium (overturning) rather than to the failure of masonry. Thus, it is better to define $S_{d,k} = \max(1.5d_y, 0.15\mu d_y)$.

As these local collapse mechanisms are related to the loss of equilibrium (overturning) rather than to the failure of masonry, the ductility resulting from (7.23) is usually very high. However, it is worth noting that the use of equilibrium limit analysis for the evaluation of the capacity curve may lead to unreliable results, if the validity of the hypotheses is not properly checked. The a-priori selection of the kinematic mechanism is the first critical aspect, as only plausible mechanisms should be considered; to this end, the seismic damage observation may give valuable advice. Regarding the assumption of no masonry tensile strength, it should be noted that this represents the actual behaviour in the mortar joint planes, while on a generic masonry plane a certain tensile strength should be assumed due to the interlocking among stone or brick elements; the singling out of the mechanism, by separation of the macroelement into parts, should consider planes where the tensile strength is really negligible (for instance, in the case of a façade overturning, if the interlocking between the façade and the lateral walls is good, a wedge of the latter ones should be considered in the mechanism, which contributes to stability). Contrary to this problem, which produces results on the safe side, the limited compressive strength determines lower values both of the seismic coefficient α_0 and of the zeroing control displacement $d_{k,0}$; in order to take into account this problem, the hinges that connect each couple of blocks may be placed in a rear position with respect to the border, considering a stress block behaviour; the shift of the hinge should be related to the quality of masonry and the level of initial stress on that plane.

The evaluation of the performance point (target displacement) cannot be made with the approach adopted in section 7.3.2, which considers an inelastic demand spectrum, because the cyclic behaviour of the kinematic mechanism is non-linear elastic, with no significant hysteretic dissipation. Thus, the target displacement may be obtained by the elastic demand spectrum (5% damping), considering a properly defined equivalent secant stiffness. A statistical analysis on the results of non-linear dynamic analyses with different earthquakes shows that at collapse, when the displacement demand is close to μd_y , the equivalent period may be defined on the capacity curve considering the point in which $S_d = 0.5\mu d_y$; it is evident that in the linear range, the elastic period T has to be used. The equivalent period T^* , useful for the evaluation of the target displacement S_{d^*} , is defined by a linear interpolation between the two above mentioned situations, and the target displacement may be obtained by an iterative procedure:

$$S_{d^*} = S_{de}(T^*) = \frac{T^{*2}}{4\pi^2} S_{ae}(T^*) \quad (7.24)$$

$$T^* = 2\pi \sqrt{\frac{\kappa S_{d^*}}{S_a(\kappa S_{d^*})}} \quad (7.25)$$

where: S_{de} is the elastic displacement demand spectrum, S_a is the capacity curve (7.21) and the coefficient κ is given by:

$$\kappa = \frac{\mu - 0.5(S_{d^*} / d_y + 1)}{\mu - 1} \quad (7.26)$$

Once the target displacement S_{d^*} is obtained, the lognormal fragility curves (7.9) give the probability that the damage is equal to or higher than a certain state D_k .

Figure 7.9 shows the entire procedure for the definition of the capacity curve and the evaluation of the target displacement (performance point). Figure 7.9a depicts the transformed pushover curve, the linear elastic branch, the damage state thresholds and two different demand spectra. Figure 7.9b highlights the performance point evaluation.

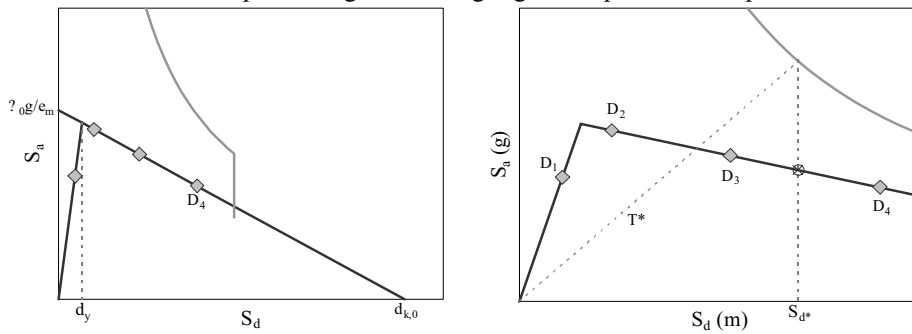


Fig. 7.9. Capacity curve and target displacement evaluation

As regards the demand spectrum, it is worth noting that usually local mechanisms in the macroelements interact with the rest of the building and in many cases they are located at a certain level, quite far from the soil foundation (for instance, the gable overturning in the church façade or the collapse of the belfry in the tower). Only in the case of macroelements which are founded on the soil and behave independently, the site response spectrum can be used. In the other cases, the demand spectrum is defined starting from the seismic coefficient proposed in Eurocode 8 (EC8, 2003) for non-structural elements, as it considers that, at the base of the macroelement, the dynamic excitation is amplified according to the dynamic properties of the whole building and the position with respect to the base:

$$S_{ac}(T^*) = a_g \left[\frac{3(1+z/H)}{1+(1-T^*/T_1)^2} - 0.5 \right] \quad (7.27)$$

where: z is the height of the macroelement above the soil foundation (usually it is referred to the base of the macroelement or to its barycentre, when it is connected to the building in different points); H is the building height; T_1 is the fundamental vibration period of the building in the direction of the kinematic mechanism.

This spectrum is not valid for the high periods, because it has been proposed for the elastic verification of non-structural elements, which usually are quite stiff; on the contrary, the use with the capacity spectrum method requires reliable values also for the high periods. Thus, for $T^* > 1.5T_1$, the spectrum is extended with the constant velocity trend ($S_{ac}(T^*) \propto 1/T^*$). Moreover, in the case of flexible buildings with respect to the characteristic period of the soil ($T_1 > T_C$), this spectrum overestimates the demand, as it doesn't consider the reduction of the seismic amplification in the building; to this end, a

correction factor $\zeta(T^*)$ is applied to (7.27), which reduces the spectrum consistently (for $T^*=T_1$ the reduction is T_C/T_1):

$$\zeta(T^*) = \begin{cases} 1 & T_1 \leq T_C \\ \left[1 + \left(\frac{T_1}{T_C} - 1 \right) \frac{T^*}{T_1} \right]^{-1} & T_1 > T_C \end{cases} \quad (7.28)$$

In Figure 7.10a the demand spectrum for two macroelements at different heights is compared with a typical site spectrum ($T_1=0.3s$, $T_C=0.5s$): if the macroelement is close to the foundation ($z/H=0.2$), the demand spectrum is similar to the site dependent spectrum, filtered by the building fundamental period, while, if the macroelement is on top of the building, the amplification is huge. In Figure 7.10b the demand spectra for a macroelement at medium height ($z/H=0.4$) are compared, in the case of different buildings ($T_1=0.15/0.3/0.6$ s). If the building fundamental period is not known, a value $T_1=0.8T_C$ may be assumed.

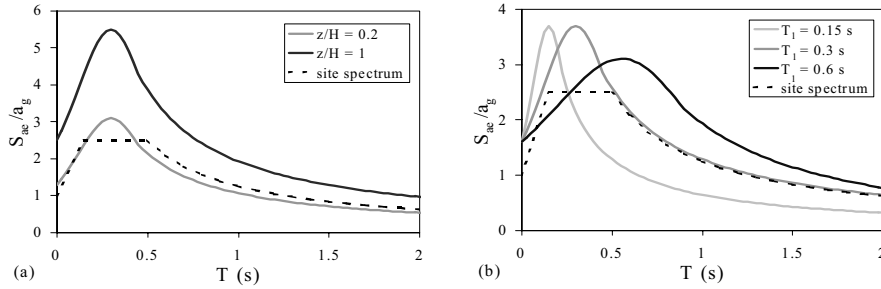


Fig. 7.10. Acceleration demand spectra for macroelements: a) influence of the height ($T_1=0.3s$); b) influence of the fundamental building period ($z/H=0.4$)

The target displacement S_d^* may be obtained by the iterative procedure (7.24-25-26), by the following displacement demand spectrum:

$$\begin{aligned} S_{de}(T^*) &= \frac{a_g \zeta(T^*) T^{*2}}{4\pi^2} \left[\frac{3(1+z/H)}{1+(1-T^*/T_1)^2} - 0.5 \right] & T^* < 1.5T_1 \\ S_{de}(T^*) &= \frac{1.5a_g \zeta(T^*) T_1 T^*}{4\pi^2} \left(1.9 + 2.4 \frac{z}{H} \right) & 1.5T_1 < T^* < T_D \\ S_{de}(T^*) &= \frac{1.5a_g \zeta(T_D) T_1 T_D}{4\pi^2} \left(1.9 + 2.4 \frac{z}{H} \right) & T^* > T_D \end{aligned} \quad (7.29)$$

7.5.1. EXAMPLES AND APPLICATIONS

The level 2 mechanical approach has been widely applied in the RISK-UE Project, *An advanced approach to earthquake risk scenarios* (Mouroux et al., 2004).

The vulnerability of the churches in Catania (ITA) has been assessed with reference to the overturning of the façade and the collapse mechanism of the triumphal arch (Lagomarsino et al., 2004b).

A very interesting example of application of the limit analysis to monumental buildings is the vulnerability assessment of Santa Maria del Mar church in Barcelona, Spain (Irizarry et al., 2004). The seismic transversal response of the nave was analysed by extracting a macroelement corresponding to a central bay (Figure 7.11) and performing both finite element analyses (modal and pushover) and the seismic limit analysis.

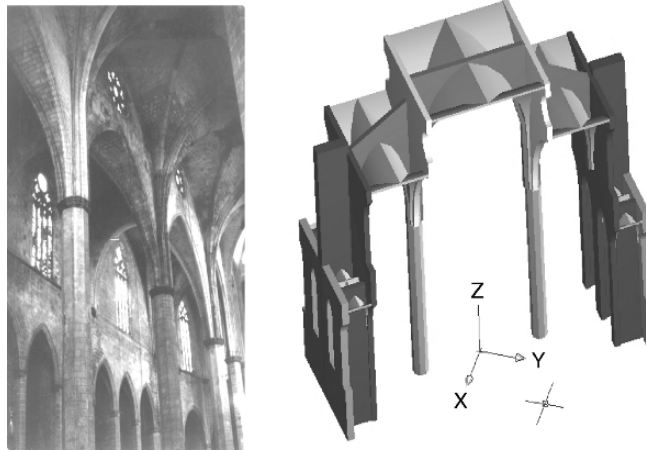


Fig. 7.11. An internal view of the nave of Santa Maria del Mar church and the macroelement extracted for the analysis of the seismic transversal response

The fundamental period obtained by the modal analysis is $T_1=0.8s$; the pushover analysis allows to single out the collapse mechanism, by the position of the cracked areas (Figure 7.12), obtained by a proper non-linear constitutive model for masonry (Calderini and Lagomarsino, 2004). The kinematic mechanism is made by ten rigid blocks and seven hinges; the weight and the centroid of each block are obtained by a CAD 3D geometrical model; Figure 7.12 shows the collapse mechanism, for a finite value of the incremental displacement.

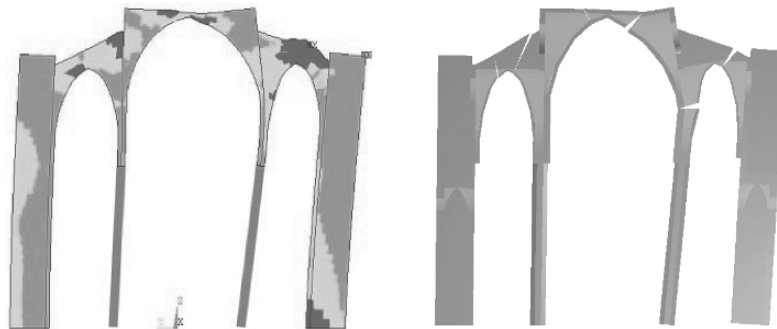


Fig. 7.12. Cracked zones (in red) obtained by a finite element pushover analysis and collapse mechanism analysed by the equilibrium limit approach

The capacity curve is shown in Figure 7.13, together with the damage state thresholds. A probabilistic hazard analysis of Barcelona has provided, for the proper site

conditions, the demand spectrum ($a_g=0.15$ g, $T_C=0.4$ s); the target displacement, obtained with the procedure (7.24) and (7.25), is lower than $S_{d,2}$, thus the probability of suffering a moderate damage is less than 50%.

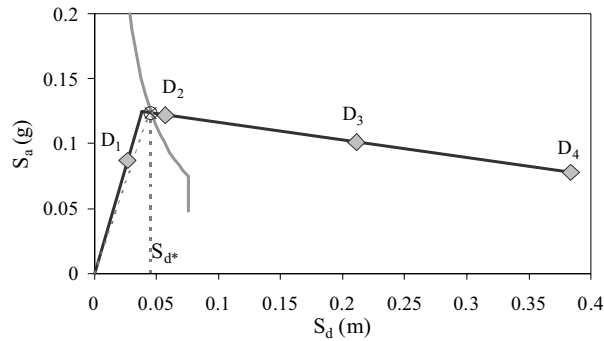


Fig. 7.13. Capacity curve of the transversal response of the nave, with the damage state thresholds, and evaluation of the target displacement

7.6. Final remarks

The vulnerability of the cultural heritage may be assessed also at territorial scale, with the aim of planning preventive mitigation strategies. Both observational and mechanical based methods have been stated, which have to be used respectively with intensity and PGA hazard scenarios. The methods are more or less detailed, depending on the level thoroughness of the available information.

The level 0 methodologies may be applied using poor data, even with a simple list of monuments, and provides a general estimation of the vulnerability of the monumental heritage, on the base of the typology, in a wide seismic area or in a big city.

The level 1 methodologies require a quick survey for the appraisal of vulnerability parameters in each structure; it results in a differentiation among monuments of the same typology, which is useful for preventive mitigation strategies and emergency planning.

The level 2 methodologies consist of a deep analysis of the single monument, by the survey of the most vulnerable macroelements. Besides the typical use in a seismic risk analysis, as for level 1 methods, these results may influence the effectiveness of different retrofitting interventions, applied systematically for the risk mitigation.

CHAPTER 8
EXPERIMENTAL TECHNIQUES FOR ASSESSMENT OF DYNAMIC
BEHAVIOUR OF BUILDINGS

M. Navarro¹ and C. S. Oliveira²

1. *University of Almeria, Almeria, Spain*

2. *Instituto Superior Técnico, Lisbon, Portugal*

8.1. Introduction

It is well known that site effects have remarkable influence on damage distribution during an earthquake that unconsolidated soil and sediment deposits were responsible for important modifications in ground motion amplitude in a range of periods, and how building damage increases when the fundamental vibration period of the building is the same as the predominant period of the soil motion.

Examples of damage from resonant situations is illustrated, among many others, in the cases of Caracas (1967), Mexico City (1985), Leninakan (1988), Loma Prieta (1989), Izmit (1999), Colima (Mexico) (2003) and Al Hoceima (Morocco) (2004), and in Europe the cases of Adra (1993), Umbria-Marchè (1997), Azores (1998) and Mula (1999). Therefore, the determination of seismic hazard oriented to seismic risk management in urban areas forces us to know the resonance range between the dynamic behaviour of soil and the one of buildings. This data is of great importance for early evaluations of seismic damages, quantification of the seismic risk and for planning of scenarios of seismic damages in urban areas.

In the analysis of the dynamic behaviour of buildings, the natural period of vibration and the damping coefficient are essential parameters, since the response of the buildings to a seismic shake is dominated mainly by these parameters. To measure them different exciting sources have been used: induced vibration, record of earthquakes or explosions and ambient vibration or microtremors. The technique of induced vibration (e.g. Jeary, 1986) is, in general, applicable to singular structures and its application to a great number of buildings supposes a very high cost. To obtain records of earthquakes and/or explosions it is necessary to maintain a permanent instrumentation in the building, which supposes a high cost and a low yield in areas with a moderate seismicity. The application of the microtremor measurements has been proved as a quick, efficient and economic method (e.g.: Kobayashi et al., 1986, 1987, 1996; Midorikawa, 1990; Oliveira, 1997; Navarro et al., 2002; Dunand et al., 2002; Brownjohn, 2003; Satake et al., 2003; Navarro and Oliveira, 2004) and it is based on the principle that the microtremor is the input to the structure of the building and it is amplified at different periods depending on the dynamic response of the building.

This Chapter shows that there is a simple method to determine the natural period and damping of buildings for low amplitude input motions, and that these determinations are very much dependent on construction types for different regions around the world. It also refers to some of the alterations that occur for larger inputs.

In the context of the book, this Chapter bridges in a simplified way the knowledge on predominant periods of (i) the seismic action, (ii) the soil layers (site effects) and (iii)

the building structure, emphasizing the importance of the proximity of those values on the seismic performance of the building. It has great advantages due to the simple technicality required and to the accuracy of obtained results, and can complement the complex analytical modelling of soil and structural systems, calibrating mechanical parameter values. However, the method proposed considers soil-structure uncoupling and cannot follow with accuracy the non-linearity of both soil and structure. These two issues are important and can only be accurately analysed on an individual basis.

8.2. Brief characterisation of dynamic properties of buildings

The response of a structure to the seismic shake depends on its dynamic characteristics (fundamental period, damping coefficient and modal shape). On the other hand, the determination of earthquake effects on structures needs a dynamic study that includes many factors (structural system, material of the structural system, mass distribution, geometry, non-structural elements, type of foundation, aging, amplitude of vibration, etc.). Generally, this process is long and complex in many cases.

With the objective of studying the dynamic behaviour of a real building, the structure is often schematized as discrete systems of masses interconnected by resisting elements and connected to the soil. The movement possibilities that have the masses are the degrees of freedom of the system.

The discrete system described by a single variable with one degree of freedom (SDOF) is the simplest case and it allows evaluation of the dynamic behaviour of complex structures with results that are worthy of attention. Nevertheless, a more precise study of the dynamic behaviour of a building will require that we look at a structure such as a system with a continuous distribution of mass and a finite number (multi) of degrees of freedom (MDOF).

The wave field propagating through the medium is applied to the foundation of the building which will be vibrating responding to this excitation. The vibration is transmitted back and forward between the medium and the building causing a diffracted wave field. Chapter 5 describes this phenomenon in detail. In an urban environment where several buildings may release a considerable quantity of energy, some constructive interference may take place and influence both the soil and the building behaviour. A radius of influence with approximately 2 wavelengths in the neighbourhood of each building should be considered as the contaminated field.

8.2.1. LINEAR BEHAVIOUR

The most general case of a damped SDOF system is a structure of mass m subjected to forced harmonic loading with amplitude F_0 and excitation frequency ω^* .

The differential equation of motion under linear behaviour is given by:

$$\ddot{x} + 2\xi\omega \dot{x} + \omega^2 x(t) = \frac{F_0}{m} \sin \omega^* t \quad (8.1)$$

where ζ is the damping ratio and ω is the circular natural frequency of the SDOF system.

The general solution of Eq. (8.1) is the sum of the homogeneous solution of damped free-vibration response (assuming that the structure is less than critically damped, as is the case for all practical structures) and a particular solution which can be assumed as a combination of a sine and a cosine wave with circular frequencies equal to the excitation frequency ω^* :

$$x(t) = e^{-\zeta\omega t} (A \sin \omega_D t + B \cos \omega_D t) + C \sin \omega^* t + D \cos \omega^* t \quad (8.2)$$

where

$$\omega_D = \omega \sqrt{1 - \zeta^2} \quad (8.3)$$

is the damped natural frequency.

The constants A and B could be evaluated for any given initial conditions and the constants C and D are of the form:

$$C = \frac{F_0}{k} \frac{1 - \beta^2}{(1 - \beta^2)^2 + (2\xi\beta)^2} \quad (8.4)$$

$$D = \frac{F_0}{k} \frac{-2\xi\beta}{(1 - \beta^2)^2 + (2\xi\beta)^2} \quad (8.5)$$

Where β represents the frequency ratio:

$$\beta = \frac{\omega^*}{\omega} \quad (8.6)$$

Assuming that the homogeneous part of the general solution will be damped out sooner or later, we can only express this general solution in terms of the resultant amplitude E and the phase lag δ :

$$x(t) = E \sin(\omega^* t - \delta) \quad (8.7)$$

with

$$E = \frac{F_0}{k} \left[(1 - \beta^2)^2 + (2\xi\beta)^2 \right]^{-1/2} \quad (8.8)$$

$$\delta = \tan^{-1} \left(\frac{2\xi\beta}{1 - \beta^2} \right) \quad (8.9)$$

The ratio of the resultant response amplitude to the static displacement which would be produced by the force F_0 will be called the dynamic magnification factor D , Figure 8.1:

$$D = \frac{E}{F_0/k} = \left[(1 - \beta^2)^2 + (2\xi\beta)^2 \right]^{-1/2} \quad (8.10)$$

When the frequency of the applied load equals the undamped natural vibration frequency ($\beta = 1$), is called resonance effect and the dynamic magnification factor is inversely proportional to the damping ratio:

$$D(\beta=1) = \frac{1}{2\xi} \quad (8.11)$$

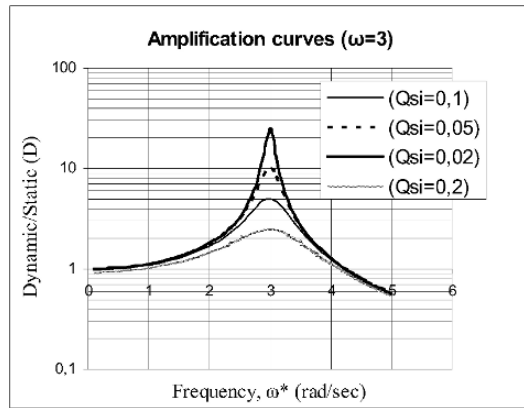


Fig. 8.1. Variation of dynamic magnification factor (D) with damping and frequency

8.2.2. INFLUENCE OF AMPLITUDE ON MOTION - NON-LINEAR BEHAVIOUR

Increasing the amplitude of motion will change the dynamic properties of building structures due to the occurrence of non-linear effects originated in the resisting properties of the elements. Friction between adjacent elements and cracking of important elements are the first causes of non-linear behaviour. The simplest case can be summarized in Figure 8.2 for the SDOF, where in a force-displacement diagram ($F-\Delta$), departure from linearity is present when a certain limit ($F-\Delta$) is exceeded. In the continuation of the experiment with changes of the direction of application of forces, hysteretic loops are formed with a tendency to aggravate the non-linearity with the increased number of cycles.

The consequences of the non-linear behaviour in a SDOF are the elongation of the natural period of vibration with a decrease of stiffness (given by the slope ($F-\Delta$)) and the increase of damping ratio (given by the area of the hysteresis loop). These effects are

more pronounced as the amplitude of motion (here translated into forces-displacements) increases.

The non-linear effects are very much dependent on structural type and material, and become much more complex in MDOF systems.

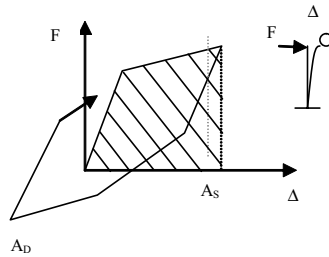


Fig. 8.2. Schematic non-linear representation (force-displacement) for a SDOF

8.3. Dynamic testing

8.3.1. EQUIPMENT - VELOCITY VERSUS ACCELERATION TRANSDUCER

Equipment for measuring *in-situ* the motion of buildings is constituted by sensors, commonly transducers of velocity or acceleration. There is a great variety of possibilities in the market, under extremely rapid technological developments, and the readers interested in this topic are recommended to look into references of the speciality for recent novelties. Several key points should be envisaged in conjunction with equipment such as data treatment.

8.3.2. SOURCES OF EXCITATION

Several sources of excitation can be used for inducing vibration in a building, some of natural origin such as earthquakes and winds, other provoked by traffic and other human activity – so called cultural noise or microtremors – and, finally, the forced vibration as the one provoked by dynamic shakers, “man-induced” vibrations, explosions in the immediate neighbourhood, free vibration originated from the rupture of pulling cables, and other types of human activity. These sources are of different quality in respect to amplitude of motion, frequency content and location of application within the structure.

8.3.2.1 Forced vibration

Forced vibration testing in buildings is not usually made due to its cost, preparation period, and because the results obtained have not differed essentially from microtremor for the case of no damage inflicted to the structure. In fact, the forced vibration may be of great value to other types of structures such as large dams for which large forces are needed to excite those structures, but the few examples made with buildings show a remarkable coincidence of results with microtremor, both in frequency estimation as well as for damping. Of course mechanical shakers using a controlled harmonic force applied can be used to trace transfer functions and consequently derive the dynamic properties of the building. In some cases, if forces are significant, the influence of

amplitude is also captured. The classical shaker works as rotating masses, thus forces are proportional to the square of the rotating velocity and very small for low frequencies. In these cases other techniques have been implemented. Among them one should mention the “man-induced” vibration produced by a few persons pulling a wall at the top floors of a building in phase with the movement of the building. Very good results are obtained with this old technique for damping evaluation.

8.3.2.2 Earthquake records

Records obtained in a building during earthquakes are of most importance because they can depict a great deal of information on how the building has performed. We can classify these records into two main categories: weak and strong motion as the amplitude of incoming wave is capable of inducing significant nonlinear effects or not. For a modern reinforced concrete (R.C.) building built in a moderate seismic environment, this threshold might be 100 mg. On the other hand, for an old masonry building the value might not be above 30 mg. Figure 8.3 presents a weak motion record made in a 14 storey building described in section 8.5, and the corresponding Fourier spectrum.

Recent monitoring of buildings, some with online recording (Celebi et al., 2004), will inform on the alterations suffered by the building through its life, in particular, during earthquakes. But, so far, the data on earthquake recordings are essentially from buildings which recorded the California, Mexico and Japanese earthquakes, with one station on top and another at ground floor. There are a few other cases some of which will be reported in here.

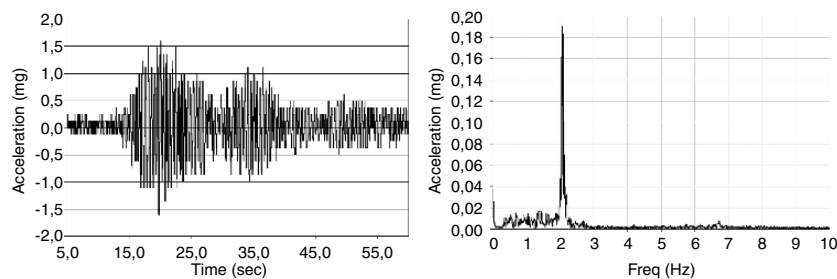


Fig. 8.3. Weak motion recorded (radial component) in the building referred to in section 8.5, during an $M=5.2$ earthquake 500 km away: time history (left); Fourier spectrum (right)

8.3.2.3 Microtremor measurement

The microtremors are vibrations on the order of several micrometers, caused by natural phenomena (atmospheric front, geothermal reactions, marine waves, etc.) and/or artificial sources (traffic vehicles, heavy machinery, human activities, etc.). The range of vibration period is between 0.1 sec and 10 sec. The vibrations that have period smaller than 1 sec are usually called microtremors and those with a larger period range are called microseisms. Kanai (1957) originally introduced a theoretical interpretation and practical engineering applications of microtremors. An application includes the natural period and damping characteristics of a structure. Generally, a building is excited by ambient (wind conditions), microtremor and artificial sources, and the amplitude of vibration is from 1 to 10 micrometers approximately (Figure 8.4).

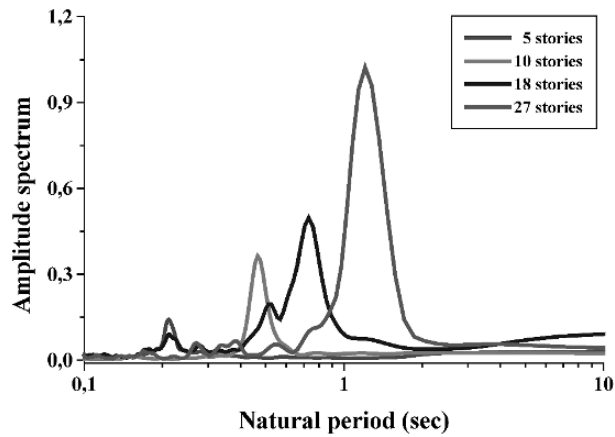


Fig. 8.4. Examples of amplitude Fourier spectra from microtremor records on top of buildings with different numbers of storeys in Lisbon city (Portugal): 5 storeys; 10 storeys; 15 storeys and 27 storeys

8.4. Techniques for identification of natural periods and evaluation of damping ratio

8.4.1. NATURAL PERIOD

The determination of the natural period of a building can be obtained by experimental methods with observation of the dynamic *in-situ* behaviour of the structure or using analytical modelling of its entire structure, including all elements contributing either to the mass or stiffness of the system as well as the foundation. Experimental methods constitute a large variety of techniques essentially by measuring the vibration of the structure by means of highly sensitive dynamic transducers, which can capture the main trends of the way the structure is vibrating. Within this Chapter we want to emphasize that one can extract easily and at a small cost the longest period of vibration, the so-called natural period or its inverse, the natural frequency.

As we are in the presence of a building which is a complex system with so many elements (beams, columns, slabs, shear walls, infilled walls, stairways, piles, caves, etc.) one might question the accuracy of such measurement and what is the minimum amount of information one needs to obtain reliable results.

The best technique for both the determination of period and associated damping is to identify the vibration mode shapes which can only be achieved if two or more transducers with common timing can record the motion at different locations in the building. However, for determining only the fundamental period, a single instrument located at the top of the building can in most cases accurately determine that period. The method is based on the fact that motion of a building is the result of multiple sources of ambient or other types of noise which act over the structure, in its façade as

the case of wind, through the foundations as the case of traffic noise, or internal noise as the case of elevators, moving shafts, workmanship, etc. With the sole exception of the presence of a strong harmonic source in the neighbourhood of the instrument, all other sources of noise contain energy with a wide spectrum and the building acts as a filter enhancing its dynamic properties.

Experience has shown that the best location to obtain the fundamental period in each orthogonal direction is to place the transducer at the top floor, where the highest noise level is expected and the recording should be taken for a long period of time. The Fourier amplitude spectrum will then show a pronounced peak, centred at the fundamental period/frequency of the building. This peak is more pronounced for the case of longer periods, that is, for tall buildings (Figure 8.4). In the case of smaller buildings the peaks might be more difficult to identify. There are other cases for which caution should be taken to exclude spurious peaks which can be observed due to interaction of the study building with adjacent ones, or due to complex configurations of the building for which the two orthogonal modes and the torsion mode might stand close to each other.

8.4.2. DAMPING RATIO

The damping ratio is not an intrinsic parameter of the building, thus its determination constitutes an extremely complicated problem, as much from a theoretical point of view as empirically, because many factors take part (structure and soil characteristic and soil-structure interaction). The time variation of these factors due to, for example, frictions in the connections, dissipation of heat, plastic deformations of the soil, etc., modifies the damping ratio of the structure, so damping values should be considered only as information of general character.

In order to estimate the damping ratio of a singular building structure, several methods using induced vibration techniques have been applied based on free-vibration response (*Free-vibration Decay method*), frequency-response curve (Half-Power method) or damping-energy loss curve (Energy Loss per cycle method). Recently, the application of microtremor measurements has been proved to be a quick, efficient and economic method to analyze the dynamic behaviour of existing R.C. buildings in the small amplitude region. The Random Decrement Technique (Randomdec) has been applied to determine the damping ratio of R.C. buildings. This method, has been shown to be applicable to determine the damping of dynamic systems subject to unknown random excitation, such as microtremor vibration.

A brief survey of the methods for evaluating the damping for one mode of vibration from experimental measurements follows.

8.4.2.1. Free-vibration Decay

This method is based on the decay of free vibration. The damping ratio (ξ) can be determined from the ratio of two displacement amplitudes measured at an interval of m cycles by:

$$\beta_{peak} = \sqrt{1 - 2\xi^2} \quad (8.12)$$

where x_n is the amplitude of vibration at any time and x_{n+m} is the amplitude m cycles after. For low damping ratio (less than 2 percent), Eq (8-12) can be approximated by:

$$\xi = \frac{\ln\left(\frac{x_n}{x_{n+m}}\right)}{2\pi m} \quad (8.13)$$

8.4.2.2. Half-power bandwidth

From the shape of the frequency-response wave, the damping ratio is determined from the frequencies for which the power input is half the input at resonance and it is given by:

$$\xi \cong \frac{1}{2}(\beta_2 - \beta_1) = \frac{f_2 - f_1}{f_1 + f_2} \quad (8.14)$$

where f_1 and f_2 are the frequencies corresponding at $1/\sqrt{2}$ times the resonant-response value.

8.4.2.3. Energy Loss per cycle

If it is possible to control the phase between the input force and the resulting displacements, the damping ratio can be obtained on the ratio of damping-energy loss per cycle A_D to the strain energy stored at maximum displacement A_S by (see Figure 8.2):

$$\xi = \frac{A_D}{4\pi\beta A_S} \quad (8.15)$$

8.4.2.4. Random decrement

The Random decrement technique was first developed by Cole (1968) as a structural monitoring technique for space craft and it has been proved as an effective crack detection method. This method has been shown to be applicable to determine the damping of dynamic systems subject to unknown random excitation, such as microtremor, and it has been applied to detect damages in structures (Yang and Caldwell, 1976; Yang and Dagalakis, 1980) and to determine damping ratio of soil (Yang et al., 1982) and R.C. buildings (e.g. Lin, 1981; Navarro et al., 2002; Dunand et al., 2002). Analysis requires only the measured output of the dynamic response of a structure, and not the random excitation input. After analysis we obtain the damped free vibration response of the structure.

The solution of Eq. (8.1) depends on its initial conditions (displacement and velocity) and forcing loading. The Randomdec analysis permits one to obtain the response due to

initial displacement (Randomdec signature), representative of free vibration decay curve of the system from the ensemble averaging N segments of the length τ of the response of a linear system.

The randomdec signature $\delta(t)$ is expressed as (Yang and Dagalakis, 1980):

$$\delta(t) = \frac{1}{N} \sum_{i=1}^N x_i(t_i + \tau) \quad (8.16)$$

where $x_i(t_i)$ is the threshold value and the initial slope is alternately positive and negative.

This technique has been compared with the spectral damping estimation approach using the half-power bandwidth method (Kareem and Gurley, 1996) and results are of the same order of magnitude if frequency of the mode under analysis is well constrained. An illustration of the method is presented in Figure 8.5 for two different building heights.

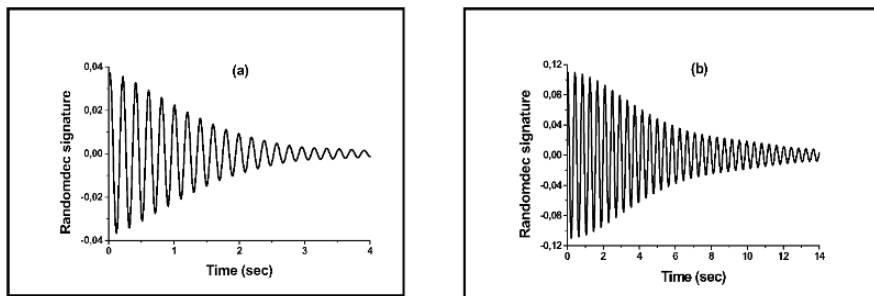


Fig. 8.5. Examples of random decrement signatures for several R.C. buildings with different story number in Lisbon city (Portugal), excited from microtremors. (a) with 4 storeys ($\xi = 2.9\%$); (b) with 11 storeys ($\xi = 1.5\%$)

8.5. Comparison of methods. Calibration with analytical techniques

The dynamic characteristics of a prototype isolated reinforced concrete building were evaluated through the development of a structural analytical model of a building, which was also subjected to weak motion records, ambient noise and microtremors. This single example illustrates the potentialities of the experimental techniques versus the analytical modelling of a building. Even though the results suggest a good confidence on the experimental methods, more examples are needed for a more robust calibration.

8.5.1. CHARACTERISTICS OF A PROTOTYPE ISOLATED BUILDING

The structure under analysis is a typical reinforced concrete building constructed in Lisbon in the 1970's, prior to the present Portuguese seismic code (RSA, 1985). It is an isolated 14 storey building, founded on a thick gravel soil, the first two floors with

storage rooms and the others with four housing units per storey (Figure 8.6 a). The plan is almost square with $21 \times 21 \text{ m}^2$, (Figure 8.6 b) with columns spanning 4 to 6 m and beams connecting them forming a quite regular grid (Figure 8.6 b). The larger columns are about 1.40×0.40 at the first floor and reducing their dimensions to the upper floors. Slabs are 17 cm thick, cast in-situ concrete. The central part of the building, which gives access to each apartment, is an open space with $6 \times 6 \text{ m}^2$ where a full stair and two elevators are located (Figure 8.6 b). The room space is divided by the current tradition partitions of hollow clay brick walls, 15 cm thick in the interior plant and 30 cm in the outer façades.

8.5.2. SIMULATION OF RESPONSE

A 3-D model structure was made for this building using the most modern commercial technologies to simulate the linear dynamic behaviour (SAP2000®, 2000). Columns and beams were considered as R.C. frame elements with geometrical characteristics taken from the design and mechanical properties from statistical studies and slabs were considered as rigid diaphragms. Infilling brick walls were simulated as diagonal struts with geometrical and mechanical properties taken from analytical and laboratorial testing (Baptista and Oliveira, 2003).

The masses were estimated from material weights and existing live loads (Figure 8.6). The model was assembled and run for two hypotheses, one assuming that the infilling walls were not participating in the stiffness of the wall structure, and the second, corresponding to the “real” structure placing the infilling walls at their locations. Frequencies and corresponding modes were computed for those two situations and results are presented in Table 8.1 together with the experimental values obtained by *in-situ* measurements. As it can be observed, the results are quite similar when comparing the experimental values with the second model with infilling brick walls.

Table 8.1. Comparison of frequencies measured and computed with an analytical model (units: Hz)

Modes	<i>in-situ</i> measure	Analytical model	
		Without infilling	With infilling walls
1 st - Direction X	2.15	0.72	2.11
1 st - Direction Y	2.15	0.81	2.14
1 st - Torsion	2.61	0.86	2.98
2 nd - Direction X	7.03	1.94	6.36
2 nd - Direction Y	7.03	2.23	6.61
3 rd - Direction X, Y	13.6	3.53	11.4

8.5.3. MICROTREMORS

The microtremor measurements were performed at the center of plan on the roof floor of the building, using a data acquisition system composed by a three component short period seismometer with natural period of 1 sec, amplifier and notebook computer with A/D converter. The system was used to record the horizontal and vertical components of microtremor. The first channel was adjusted to the longitudinal direction, the second one to the transverse direction and the third to the vertical direction, respectively. A

time history 300 sec long of microtremor signal was recorded, sampled at a rate of 100 samples per sec (Figure 8.7 a). Fast Fourier Transformation was applied to a record in order to compute Fourier spectrum, smoothening with a Parzen's window of 0.3 Hz width (Figure 8.7 b). The longitudinal and transversal components show 0.47 sec natural periods.

The random decrement signature for each horizontal component was obtained applying the random decrement technique and the damping ratio has been calculated using the free vibration decay method. The damping ratio value for longitudinal component is 0.85% and 1.19% for the transverse component, respectively.

8.5.4. EARTHQUAKE RECORDS

Many observations have been recently made with earthquake records obtained at different locations in buildings which were subjected to earthquake loading. This information is of most value as it can serve to validate other techniques for the dynamic characterization in building properties, as well as to determine the influence of amplitude of motion on these properties.

We have recorded in three cases (Figures 8.3, 8.8 a and b) with weak motion exhibiting spectral amplitudes 5 to 10 times the values recorded during microtremor testing. In these circumstances, the frequencies of lower modes are similar.

8.5.5. COMPARISON OF METHODS

The technique of *in-situ* measurement at the top floor, for obtaining the first natural frequency of a building in each orthogonal horizontal direction, as well as the corresponding damping ratio, as described in the above sections, can be considered an efficient and cost-effective tool. Efficient because it only requires a single instrument and presenting the best values for high level noise. Some caution might be exercised for identification of modes, especially for the cases of low rise buildings, for complex buildings or in cases of interaction either with adjacent buildings or with soil layers. The last topic is analysed in detail in Chapter 5 under the soil point of view, for which case microzonation may lead to a soil spurious frequency (frequency attributed to the building).

The classic HVRS (spectral ratio for horizontal to vertical components), which can lead to very good results in identification of predominant soil frequencies, does not add much value to the identification of frequencies in buildings, contrarily to the cases of microzoning. This technique (Mucciarelli et al., 2004), which is not supported on any theoretical building behaviour, presents the same results as the simple analysis of peaks in the Fourier spectra. As already said before, further research in this area with various examples with different types of buildings is needed for setting more sound conclusions.

8.5.5.1. Influence of infilling walls

The influence of infilling "brick walls" inside R.C. structures is another issue of great importance at several levels: First of all, these "non-structural" elements are part of a large majority of buildings in southern Europe and Latin-American countries. Secondly, these elements are usually built against the structural frames and no engineering design office considers their stiffness, which is of particular relevance especially in the in-plane

direction. And, in the third place, the dynamic behaviour of the buildings is greatly influenced by the interaction between the infilling walls and the frame, dictating in several instances the entire behaviour of the building for large input motions.

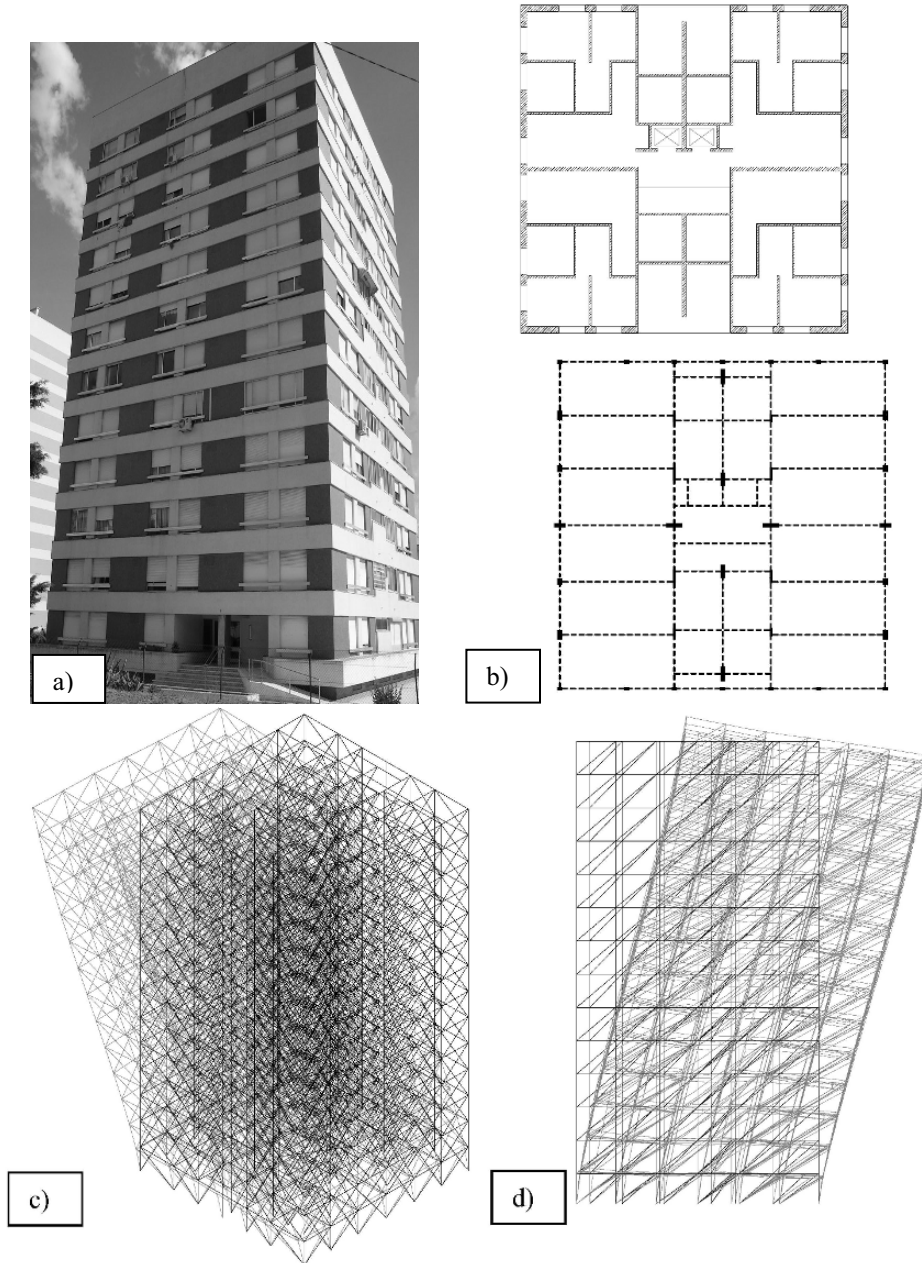


Fig. 8.6. Building for comparison of experimental techniques vs analytical modelling: a) photo; b) plant view with infill brick walls and structural elements; c) and d) deformed shape of fundamental mode (deformation scale highly exaggerated)

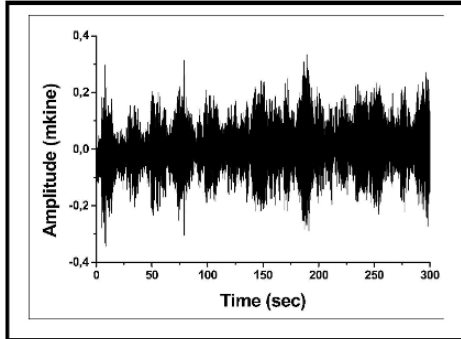


Fig. 8.7 a. Microtremor record at the center of plan on the roof floor of the building

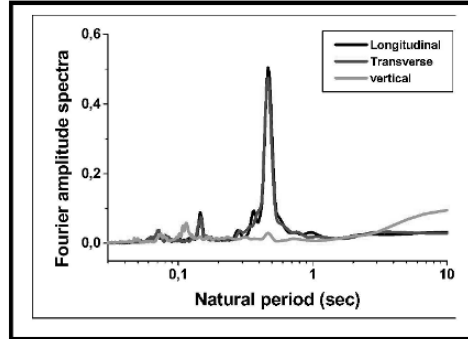


Fig. 8.7 b. Three components Fourier spectrum

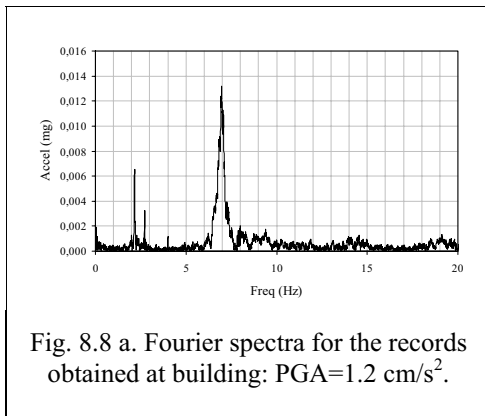


Fig. 8.8 a. Fourier spectra for the records obtained at building: $PGA=1.2 \text{ cm/s}^2$.

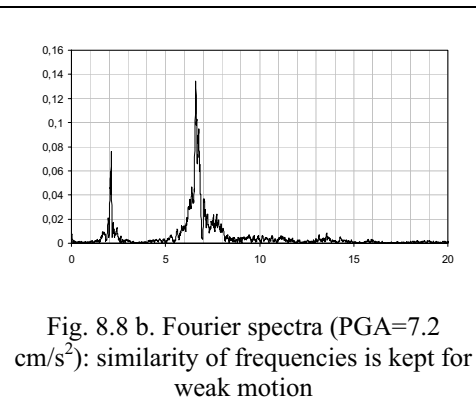


Fig. 8.8 b. Fourier spectra ($PGA=7.2 \text{ cm/s}^2$): similarity of frequencies is kept for weak motion

Noise measurements made in several buildings with different percent of infilling walls (Figure 8.9 a) revealed that the frequencies obtained are much higher (up to about five times, Figure 8.9 b) than what would be predicted by the analytical model which does not takes the infillings into consideration.

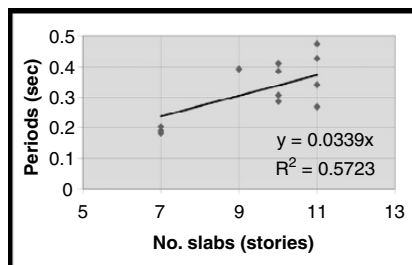


Fig. 8.9.a. R.C. Buildings under analysis

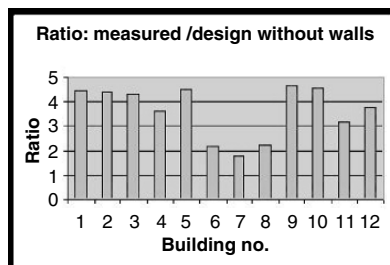


Fig. 8.9.b. Ratio of frequencies for the cases with and without infilling walls

Baptista et al. 2003 have shown that it is possible, using a detailed analytical model which considers the infilling walls as diagonal struts to arrive to a model leading to frequency values differing not more than 5% from the *in-situ* values.

It is recognized that the influence of the infilling walls in the percent of increase of the frequencies relatively to the values not considering these walls depends essentially on the “quantity” of infilling walls as a percent of the total horizontal area and also on the amount of shear walls present in the building. The increase is larger the higher the presence of infilling walls and lower the presence of shear walls. By using only the noise technique, see Tables 8.2 to 8.4, the frequency suffers an increase of about 180% for the case of no shear walls, 150% for the case of a few shear walls and 120% when a large portion of shear walls are present.

Table 8.2. R.C. buildings with 8/9 storeys above the ground and variable % of shear walls: frequencies of first mode (Hz)

% of “shear walls” (SW)	Type of mode	Without walls	With walls	Increase
9 storeys No “SW”	Transversal	0.88	1.73	1.96
	Longitudinal	1.27	2.15	1.69
8 storeys Some “SW”	Transversal	1.27	1.68	1.32
	Longitudinal	1.17	2.05	1.75
	Torsion	1.18	2.64	
9 storeys Large % of “SW”	Transversal	2.15	2.64	1.25
	Longitudinal	1.76	1.86	1.07

The same conclusion was obtained by Kobayashi et al. (1996) for the case of a 7 storey R.C. building tested under construction when infill walls were not present and after the completion of the building. In this case, the microtremor information gave a shifting in period from 0.56 to 0.35 sec, which means an increase in frequency of 50%.

8.6. Correlation of natural frequencies and damping with geometry of buildings

8.6.1. GENERALITIES

The formulas used for predicting fundamental period (T) as a function of geometry of buildings are usually proportional to the power of height (H) or number of storeys (N),

$$T = \alpha H^\beta \tag{8.17}$$

This expression is sometimes corrected by using the depth (B) in plan or the percent of area of walls in relation to total in-plan area. (α and β are constants to fit data)

$$T = \alpha H^\beta f(B) \tag{8.18}$$

β is under 1, but in many cases very close to 1, specially for the cases of a large number of shear walls. General dispersion of data leads to global variance $R^2 = 0.6$ to 0.7 .

For some structural types closed-form solutions can be derived, as the case of “pure shear walls” (Ellis, 1980), taken as a cantilever,

$$T_1 = \alpha_1 H \sqrt{1 + \beta_1 \frac{H^2}{L.t}} \quad (8.19)$$

where H is the height, L the length and t the thickness of the wall. α_1 and β_1 are constants related to material properties.

The presence of wall partitions increases the frequency in a way proportional to the square root of an equivalent cross section area of these partitions.

Damping ratios present more scatter than natural periods because they are influenced not only by the amplitude of motion but also by the foundation type, soil-structural interaction, density of internal partitions, etc. (Satake et al., 2003, Carydis and Monzatakis, 1986). For small amplitude, before clear non-linear behaviour takes place, damping has essentially two plateaus (Jeary, 1997), one for very small amplitudes and corresponds to “large imperfections” existing in all connecting surfaces, and the other when “small imperfections” are mobilized at larger amplitudes. In between, damping shows an increased linear trend.

The so-called Rayleigh damping, commonly used to treat damping in structural dynamics

$$C = \alpha M + \frac{\beta}{K} \quad (8.20)$$

where M and K are the mass and stiffness matrices, respectively, and α and β are values to be adjusted, leads for any mode k to a situation of the type (Lagomarsino, 1993)

$$\xi_k = \alpha' T_k + \frac{\beta'}{T_k} \quad (8.21)$$

where now T_k is the period of k -mode and ξ_k is the corresponding damping ratio. Lagomarsino (1993) has shown that the second term is more important for structures with periods less than 1 sec, whereas for larger periods the contribution of the first term becomes more and more important as T increases.

As it will be seen next, in the context of this book, preference is given, whenever possible, to simple formulas of the type eq. (8.20) with $\beta=1$ and eq. (8.21) with $\alpha'=0$.

8.6.2. VALUES FOR DIFFERENT REGIONS AND STRUCTURAL TYPES (LOW AMPLITUDE MOTIONS)

The natural period and damping predictors of various types of buildings in different regions were analysed based on several collected full-scale data. In common they have a reinforced concrete (R.C.) structural system with infilling wall panels. A few cases of steel frames (S.F.) are also presented. Each set of data is formed by a number of buildings, ranging from 20 to a couple of hundred, with a quite uniform distribution of storeys.

The example of Lisbon buildings illustrates the type of data for fitting to eqs. (8.17) and (8.21) in their simplified form.

The dynamic characteristics of existing R.C. buildings in Lisbon (Portugal) excited by microtremors were analyzed using full-scale experimental measurements on 261 buildings (Oliveira, 2004). The average relationship obtained was $T = 0.045 N$. This result is similar to the one obtained with another set of 37 R.C. buildings, with a number of storeys between 4 and 29 (Navarro and Oliveira, 2004) (Figure 8.10 a). The average value of damping ratios, estimated by using the Random Decrement Technique was $2.6 \pm 1.7\%$ and the product between damping ratio and natural period exhibits large scatter, with an estimated average value as $\xi T = 1.1 \pm 0.6\%$ (Figure 8.10 b).

All results are summarized in Table 8.3 and Figure 8.11. Significant marginal notes from some of these data are as follows:

- ⇒ Kobayashi et al. (1987) conclude that the buildings with natural period from 0.5 sec to 2.0 sec and 5% damping ratio, suffered most severe damage during September 19, 1985 Michoacan, Mexico earthquake.
- ⇒ Lagomarsino (1993) preferred to use a damping predictor described by Rayleigh type damping for R.C. buildings expressed by $\xi = 0.0072T + 0.007/T$.
- ⇒ Kobayashi et al. (1996) proposed an empirical relationship $T = 0.046 N$ for torsional motion. The damping ratio distributed from 2% to more than 10%, depending on soil condition on the site and the average ξT value is around 2%. These results show good agreement with the relationship obtained in several cities in southern Spain.
- ⇒ Satake et al. (2003) describe the damping ratio characteristics of steel-framed buildings, R.C. buildings and steel-frame reinforced concrete (SRC) buildings, based on analyses of full-scale data on 205 buildings (137 steel-frame, 25 R.C. buildings and 45 SRC buildings tested with different vibration methods. The relation between natural period and building height H for RC/SR.C. buildings is $T = 0.015 H$ and for steel-framed buildings $T = 0.020 H$.

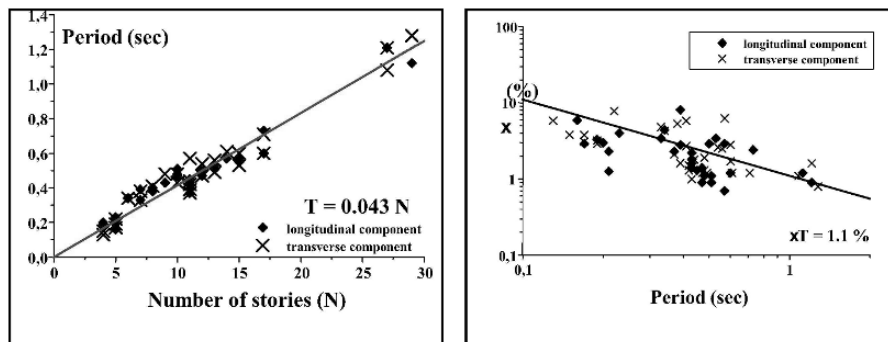


Fig. 8.10. a). Relation between the natural period of vibration (T) and the number of storeys N for R.C. buildings

Figure 8.10 b) Relation between damping ratio (ξ) and natural period (T) for horizontal movement

⇒ In Grenoble (France), Dunand et al. (2002) obtain the relation between frequency and damping as $\xi = 0.7 * f^{1.4}$.

Overall information (Figure 8.11) shows similar trends on the relationship between natural period and number of storeys for the RC buildings analysed with the exception of Mexico City which shows much larger periods for the same number of storeys.

8.6.3. AMPLITUDE DEPENDENCE OF NATURAL PERIODS

The seismic behaviour of a building under different input motions depends, in the first place, on both the amplitude of motion and on the proximity of resonance (period of input of motion equal to the period of the building). In the second place it depends on the capacity and integrity of the structural system to support that input. Damping for small amplitudes is also small though important for amplification.

Table 8.3. Summary of results on periods and damping for different regions

Authors	City (Country)	No. buildings	T(N)	T(H)	$\xi(T)$
Kobayashi et al. (1987)	Mexico City (Mexico)	20 RC	T = 0,105 N		$\xi T = 4,0\%$
Midorikawa (1990)	Santiago de Chile (Chile)	107 RC	T = 0,049 N		$\xi T = 0,8\%$
Midorikawa (1990)	Villa del Mar (Chile)	21 RC	T = 0,049 N		$\xi T = 1,2\%$
Lagomarsino (1993)		182 RC+SF			$\xi = 0,0073 + 0,007 T^{-1}$
Kobayashi et al. (1996)	Granada (Spain)	21 RC	T = 0.051 N		$\xi T = 2,0\%$
Enomoto et al. (1999)	Almeria (Spain)	-	T = 0.05 N		$\xi T = 0,8\%$
Espinoza (1999)	Barcelona (Spain)	25 RC	T = 0.089N + 0.032		
Enomoto et al. (2000)	Caracas (Venezuela)	57 RC	T = 0,06 N		
Sanchez et al. (2002)	Adra (Spain)	-	T = 0.049 N		
Navarro et al. (2002)	Granada (Spain)	89 RC	T = 0.049 N		$\xi T = 2,1\%$
Messele and Tadese (2002)	Addis Ababa (Ethiopia)	-	T = 0,057 N	T = 0,018 H	
Satake et al. (2003)	(Japan)	205 RC+SF		T = 0,015 H	$\xi T = 1,4\%$
Dunand et al. (2002)	Grenoble (France)	26 RC		T = 0,015 H	$\xi = 0,7 * T^{-0,25}$
Oliveira (2004)	Lisbon (Portugal)	261 RC	T = 0,043 N		
Navarro and Oliveira (2004)	Lisbon (Portugal)	37 RC	T = 0,045 N		$\xi T = 1,1\%$

All methods bringing out the possibility to evaluate resonance (periods and damping ratios of buildings) are important tools for anticipating their seismic behaviour. With the increase of amplitude of input motion there is a tendency to increase the period of the

content of input motion as well as an increase of the natural period of the building. This phenomenon in the building depends on the amount of damage that might be inflicted. Both tendencies, either for the predominant period of input and of the building, are in the same direction; an initial tuning between them causing resonance might disappear, depending on the rates of change of period in both cases. But also the opposite may appear, e.g. an initial linear de-tuning might turn into tuning at a later stage.

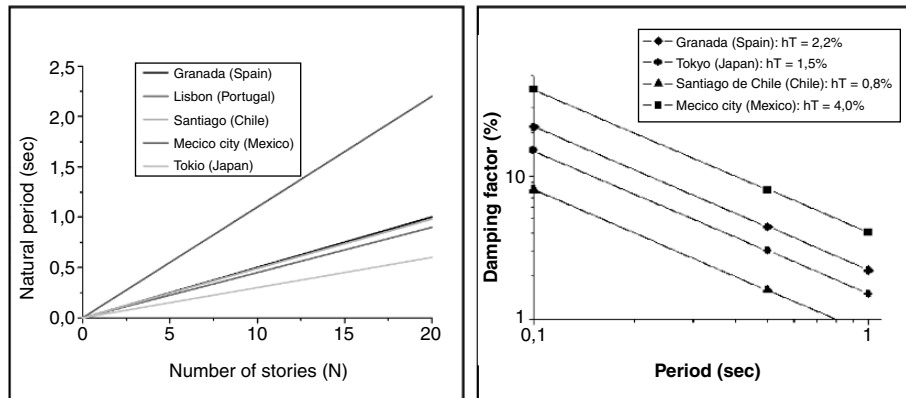


Fig. 8.11. Comparison of relationships for different regions (Cities around the world): left) period vs. number of storeys; right) damping ratio vs period

Recent monitoring of buildings, which already recorded a few earthquake inputs, are important elements to quantify the effect of nonlinearity and evaluate the reliability of the methods that exclusively use linear techniques. They are also essential keys to eventually allow corrections of the linear methods accounting for the non-linear effects.

Let’s give a few examples already available in the literature.

The Imperial County Service Building was subjected to a large event in 1979. The 6 storey R.C. structure was monitored with several acceleration transducers which recorded the event with a free-field $PGA=220 \text{ cm/s}^2$. The building was severely damaged in the ground floor columns due to poor design and construction, and was demolished. Several modes were identified and their values estimated along the course of the event (Table 8.4). For this type of amplitude the increase of period was around 45-50% in all three modes, but after the event the damaged building recovered to a period 128% of initial.

Table 8.4. Imperial County Service Building, Imperial County Earthquake, 1979, $PGA=220 \text{ cm/s}^2$. Increase in period for the first modes

Type of mode	1 st mode	2 nd mode	3 rd mode
E-W	45%	50%	50%
N-S	40%	45%	
Torsion	60%	50%	

These are the minimum values attained during the course of the event. After the event the frequencies went up again to values of 78% of the initial ones, denoting a “self healing” process. Trifunac et al. (2001) after the Northridge earthquake of 1994

observed at the damaged Holiday Inn subjected to a $PGA=270 \text{ cm/s}^2$ that an increase in period of 54% for the first mode took place during the event, with a similar recovery to a value of 78% of initial. They claim that the “self healing” was caused by settlement and compactation of soil with time due to aftershocks.

Naeim (1997) report refers to a set of 17 buildings fully instrumented with strong motion accelerometers and that suffered various types of damage. All of them are described in detail, allowing the determination of correlations between damage and change of frequency from the initial linear state.

In places with large seismicity as the cases of California and Japan, and when many buildings are instrumented with strong motion networks, it is possible to constitute databases with period estimation from moderate to large amplitude motion. This is the case of the study by Chopra and Goel (2000) which make use of a large number of buildings (R.C. frames, R.C. shear walls and Steel frames) subjected to PGA's which in a few cases exceeded 0.15 g. Periods in all cases for all kinds of modern buildings are essentially 2.5 times the values obtained elsewhere. The reason for such a difference is due, not to amplitude of motion, but to the geometric characteristics of USA structures, the non-existence of “infilling brick walls” and the considerable lower vertical loads commonly practiced there.

Chopra and Goel (2000), concerned with the use of experimental measured frequencies to incorporate the concepts of acceleration-displacement-response spectrum in code input ground motion applications, propose two different formulas for frequencies, one for using with the acceleration spectrum and the other for the displacement spectrum, keeping certain conservatism in both determinations. They play with uncertainties in data measurements, using upper or lower estimates (average $\pm 1\sigma$) to cover this conservatism.

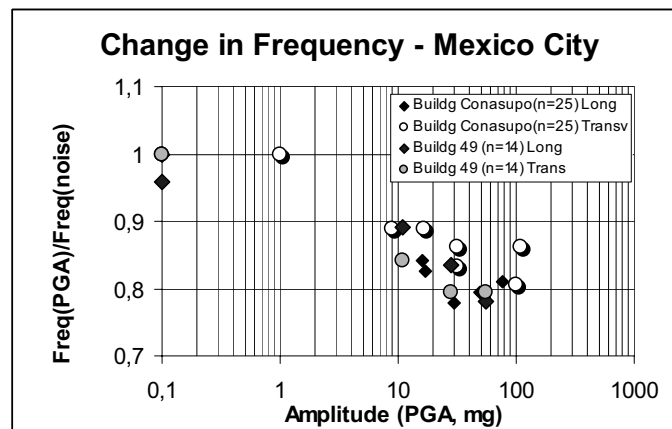


Fig. 8.12. Decrease in frequency of fundamental mode as a function of amplitude measured at roof level of two buildings in Mexico City

With the event of real time monitoring of large important buildings as a measure to control the structural behaviour of a building under its life-time, it is an important time to better assess that behaviour for different dynamic loadings both in amplitude, spectra

and duration. It will be possible in a continuous way to understand the evolution of frequencies and detect the presence of nonlinearities due to damage suffered in any element (Celebi et al., 2004).

Muria Vila and González Alcorta (1995) studied a group of 60 buildings in Mexico City with different structural and soil foundation types and number of storeys up to 20 and they observe a clear decrease of frequency with increasing PGA (Figure 8.12). They also concluded that there are various aspects which control the frequency for microtremors, being the type of structural system, the presence of “infilling walls” and the soil (stiff or soft) the most important ones (Table 8.5).

Table 8.5. Values of α for the formula $T=\alpha N$ for Mexico (Muria Vila and González Alcorta (1995)

Structural type	Stiff soil (15 buildgs)	Soft soil (45 buildgs)
R.C. Frame	0.100	0.126
R.C. Frame+walls	0.063	0.102
Masonry	0.040	0.073

They claim that noise measurements produce the same results (as far as frequency of first modes and mode shapes) as forced vibration by means of eccentric mass vibrators, pullout tests or impulse actions, in spite of the fact that amplitude of induced vibration might attain one order of magnitude above noise. They only differ for the case of very stiff structures on very soft material, for which the soil behaviour controls the overall response (see explanation at section 8.6.5). In this case forced vibration tests can excite the building emphasizing its dynamic properties. The decrease of frequency in the building for larger amplitude motions (above the $PGA > 10 \text{ cm/s}^2$) depends on a number of items difficult to express in a simple formula. The non-linearity in the overall behaviour starts with small adjustments of structural and non-structural elements, change of modulus of elasticity of main structural elements and behaviour of soil. It also depends on the type of structure and on the engineering design level.

Trifunac et al. (2001) studying a 7-story damaged building in Van Nuys, California, have found great changes in frequency from 1.1 and 1.4 Hz (respectively for the longitudinal and transversal directions) from microtremors after damage to 0.4 and 0.5 Hz during the damaging motions with large PGA. The approximate factor of 3 of increase in the period is partially attributed by the authors to non-linear behaviour of soils, and a “self healing” process within the structure.

In case the soil is playing an important role, “self healing” (Trifunac et al. 2001), with the partial recovery of frequency after the earthquake, may take place. This may be due to settlement of soil with time and compactation due to aftershock activity. In the case of the building above referred to during the Northridge earthquake, an increase in period of 54% took place during the event ($PGA \approx 270 \text{ cm/s}^2$) with a final healing to 22% of original.

Dunkerley’s method may be a good approach for including the soil influence in case of shear wall structures (Goel and Chopra, 1998). These authors propose upper and lower limits in the equations, to be used in conjunction with the design acceleration and displacement, respectively.

In a recent work with the objective of code applications, Crowley and Pinho (2004) established period-height equations for R.C. buildings without infillings admitting some non-linear behaviour of the structures. They use the simple eq (8.17) and got large variations of α as function of type of method for computation. These values are almost one order of magnitude above the measured ones for the case of low amplitude motion and contrast with the most conservative numbers in the case of moderately intense motions, even for the cases of long period structures which depend very much on the displacement spectrum.

8.6.4. AMPLITUDE DEPENDENCE OF DAMPING RATIOS

Jeary (1986) proposed a damping predictor to assess frequency and amplitude dependency as

$$\xi = 0.01f + 10 \sqrt{D}/2 + \frac{x}{H} \quad (8.22)$$

where x is the vibration amplitude at the top of a building; h and f (Hz) are the damping ratio and the frequency in the fundamental mode; and D (m) is building dimension.

The full-scale data base for the small amplitude region in Japan (Satake et al., 2003) proposes for R.C. buildings a relation:

$$\xi = 0.014f + 470 \left(\frac{x}{H} \right) - 0.0018 . \quad (8.23)$$

The damping ratios predictor by expression (2) show good agreement with damping ratios selected from the Japanese damping database.

For steel-framed buildings the proposak by (Satake et al., 2003) is:

$$\xi = 0.013f + 400 \left(\frac{x}{H} \right) + 0.0029 . \quad (8.24)$$

Soil-structure interaction for large amplitude levels may cause an erroneous assessment of damping when this is obtained from low amplitude motions, due to the fact that small volumes of soil are mobilized in this case.

8.7. Relation between building damage and soil predominant frequencies

There are several examples clearly showing a dependence of damage observed in buildings and the proximity of natural frequencies of buildings and predominant frequencies of soil layers. In order to evaluate the relationship between the predominant period of soil and damage distribution in masonry houses and reinforced concrete buildings in Mula town (Murcia, Spain) after the 1999 Mula earthquake, microtremor measurements were recorded near to damaged buildings. In general, the most important

damage in masonry houses with 1–3 storeys have been produced in soils with an average predominant period about 0.17 ± 0.03 s. The reinforced concrete buildings with 4 and 5 storeys, located in soils with an average predominant period about 0.27 ± 0.04 s, show the most serious damages (Navarro et al., 2000). If we consider the natural period of building estimated in several cities in southeast part of Spain (Kobayashi et al. 1996; Enomoto et al., 1999; Caselles et al., 1999; Sánchez et al., 2002; Navarro et al., 2004), the distribution and grade of damage in Mula town could be due to nearness between natural period buildings and predominant period values of soil.

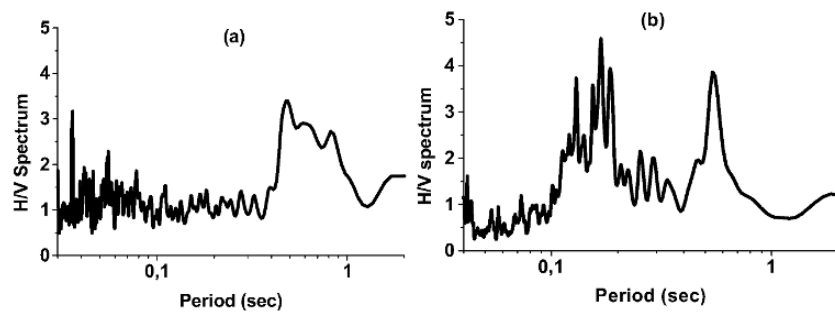


Fig. 8.13 Examples of H/V Spectrum characteristics at several sites in Villa de Alvarez, Colima, Mexico: (a) in non- damaged zone; (b) in heavy damaged zone

The case of Colima (Mexico), shows for the $M_L=7.6$ earthquake of January 21, 2003 with epicentre 200 km away, that buildings with 2/3 storeys suffered severe damage along two main streets. Apart from these locations, damage to the same type of construction did not occur. Typical frequencies for these buildings are in the range 5 to 8 Hz. Microtremor measurements made in the damaged streets for identification of predominant soil frequencies using the H/V revealed two peaks, one around 0.8 Hz and the other in the range 5-7 Hz, Figure 8.13. The same procedure applied in zones away from the damaged area shows that only the low frequency peak (0.8 Hz) is present (Enomoto et al., 2004). The reason for the existence of two peaks is not yet completely explained due to lack of geological investigation and seismic prospection, but one may advance the hypothesis of a thick soft layer covered by a thin hard material. The thick layer is responsible for the lower frequencies and the hard cover for the presence of higher frequencies. This geological situation is very common in volcanic environments such as in Colima.

This phenomenon of resonance which is taking place in the damaged area due to the proximity of predominant frequency of soil and of buildings is explained in Figure 8.14. We have plotted the response of a single degree of freedom (SDOF) representing the building, on top of another (SDOF) representing the soil strata, under the excitation of a harmonic input applied at the soil column base. For this simplified exercise no coupling between soil-structure exists, and we assume that both soil and building are represented by one single mode. The concept can be extended to the multi-mode situation if adequate multiple interactions are included.

Figure 8.14 introduces also the influence of the predominance frequency of the input motion taken as abscissa. Generally, even though the stochastic character of the input is always present in ground motion, large magnitude events tend to show energy content

towards the lower frequencies. Depending on the relative position of p_{soil} and p_{building} and the frequency of input the response of the building is amplified or de-amplified.

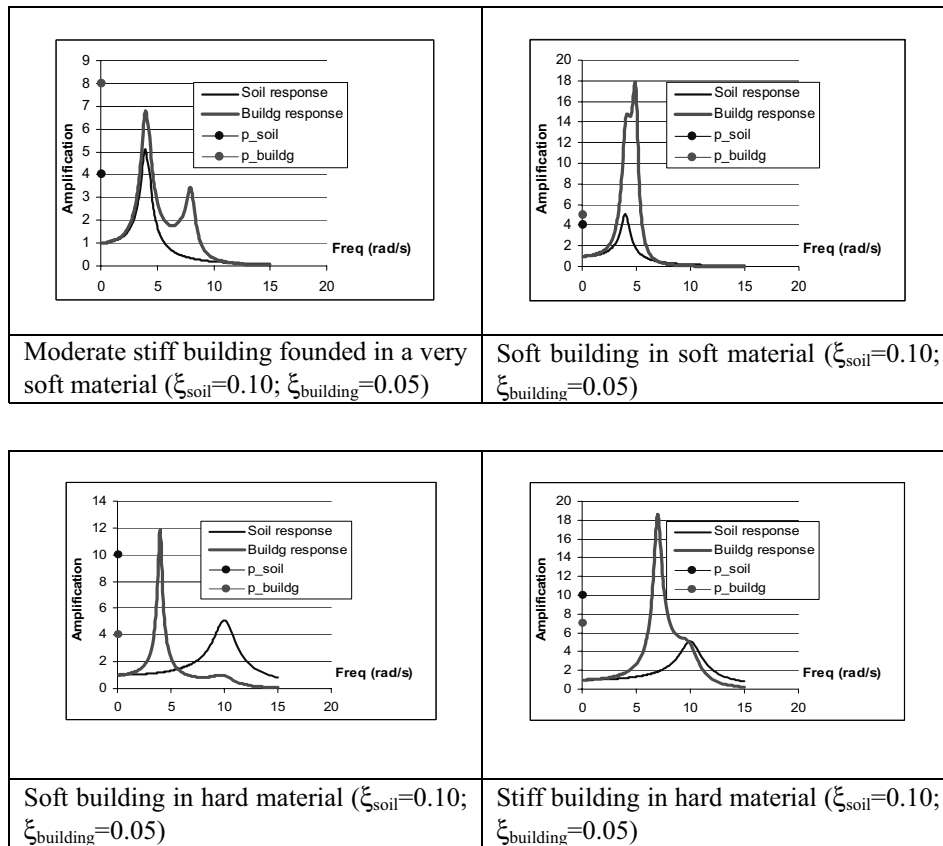


Fig. 8.14. Model of (SDOF) representing a building on top of a (SDOF) representing the soil predominant frequency, subjected to a harmonic input motion

The consideration of non-linear aspects of both the soil and of the building due to the large amplitude of input motion can introduce several modifications to the illustration of Figure 8.14. In fact, depending on the characteristics of soil and the structural system, non-linear effects can be more pronounced in soil, building or in both. In all cases damping increases, but the final situation is a combination of factors and depends very much on the predominant input motion frequency, as well.

8.8. Final Considerations

The simple method presented is a fine tool for an expedited characterization of in-situ lower frequencies of buildings. It presents great advantages in terms of effectiveness, precision and cost. In some cases it may require qualified expertise; moreover, for complex buildings, it might be impossible to obtain those frequencies with confidence.

Besides informing on the lower frequencies of a given building and from this point allow some indication on the possible resonant effects, the knowledge of the frequencies is of great importance to calibrate analytical models (check the value of elasticity modulus, check the influence of “infilling walls” and of other always forgotten characteristics such as stairways, depth of columns and beams, border conditions, etc.)

The creation of a data-base with frequency and damping information on a large amount of different buildings, where elements dealing with the geometry, in plan and height, type of structure and foundation, soil characteristics, presence of “infilling walls”, etc., is of great potential to provide a better knowledge of building performances. The greater the number of entries the higher the confidence in the results. Dispersion is still very large and difficult to reduce significantly. It depends very much on the type of building and on the type of soil underneath and foundation. Only with a detailed selection of buildings, may this dispersion be reduced.

The influence of “infilling walls” is clearly depicted from any in-situ measurement for the low amplitude noise levels. The influence of amplitude is also a remarkable property of all these systems.

The equation type $T=\alpha N$ is still the most common and simple way to express the variation of period for the different building types and regional situations, and has been adopted in many countries in Europe and Latin-America to represent their buildings, through clear differences in construction types, materials and existing loads.

Acknowledgements

The authors want to acknowledge Dr. Adrião Baptista from University of Beira Interior, Covilhã, Portugal, for the modelling of the building structure presented in part 8.5. We are also grateful to Dr. Takahisa Enomoto from University of Kanagawa for the information contributed. This work has been partially supported by the Spanish Ministry of Science and Technology and with FEDER, project REN2003-08159-C02-01.

PART II: VULNERABILITY ASSESSMENT

CHAPTER 9 VULNERABILITY AND RISK ASSESSMENT OF LIFELINES

K. Pitilakis¹, M. Alexoudi¹, S. Argyroudis¹, O. Monge² and C. Martin²

1. Aristotle University of Thessaloniki, Thessaloniki, Greece

2. GEOTER International, Marseille, France

9.1. Introduction

Like veins, nerves, and all other internal organs of the human body, lifelines are vital for the community life. In a certain degree the development and the growth of a society is reflected in the quality and the efficiency of its lifeline system.

The word *lifelines* refer to the complex set of components and systems that are essential to sustain the life and the growth of a community. Without them the high standard of living enjoyed today would vanish (Buckle and Cooper, 1995). Modern societies are totally dependent on a complex network of infrastructures, which supply energy, fresh water, provide transportation and communication services, manage urban waste disposals. Infrastructure systems together comprise the fabric by which society and its built environment is threaded together. They are the basic installations and facilities on which the continuance and growth of a community depended.

The risk assessment of lifelines, infrastructures and essential facilities follows the general scheme described in previous chapters (see for example chapter 6, section 6.1):

$$[\text{Seismic risk}] = [\text{seismic hazard}] \times [\text{vulnerability}] \times [\text{elements at risk}]$$

The complexity of elements at risk in the case of lifeline systems, their variability from one place and one country to another, and till recently, the lack of well validated damage and loss data from strong earthquakes, make the vulnerability assessment of each particular component and of the network as a whole, a very difficult problem. Adding to that the spatial extend of lifelines, the synergies between different systems and the uncertainties in seismic hazard estimates, it is obvious that the risk assessment of lifelines is indeed an extremely complex and challenging issue. This is probably the reason why seismic risk assessment of lifelines has been of limited use for the management of emergencies and natural disasters. At best, they have been regarded as a passive activity to help insurance companies set premiums for coverage of infrastructural damages.

The situation has been changed the last decade. Important strong earthquakes provided valuable data, while the public awareness and the reported huge direct and indirect losses associated to lifeline damages drew the attention of the scientific community and the governmental authorities. Moreover, the development of the Geographical Information System (GIS) technology offered an excellent platform for the implementation of efficient and innovative techniques. Several procedures were proposed for lifeline risk assessment in urban environment, aiming to minimize losses, enhance the reliability of the systems or to improve mitigation policies. Risk assessment is also the process used to determine risk management priorities by evaluating and comparing the level of risk to specific standards; either defined by a code, or a set of target risk levels and criteria. The estimation of losses, both material and immaterial, is

the ultimate target of the risk assessment. Then the risk management should define pre-seismic (retrofitting and strengthening actions), co-seismic and post-seismic strategies and policies. Figure 9.1 describes the different steps of the methodology proposed for the vulnerability assessment and the risk management of lifelines.

Inventory, classification and typology definition are the necessary steps to describe the elements exposed to seismic risk and to quantify their importance in normal, crisis (i.e. earthquake) and recovery period. Vulnerability is the expected response of an element (building, bridge, pipeline, roadway, oil tank, etc), or a network of specific elements (i.e. sewage or gas system) to a specific earthquake event, defined in the seismic hazard analysis. The estimation of site specific seismic ground motion for different earthquake scenarios is the basis of the seismic hazard analysis.

Many uncertainties are associated to the estimation of all parameters describing typology, seismic hazard, vulnerability-fragility curves, damage states or losses. Epistemic uncertainties are also involved regarding the scientific background and the tools and methods used for the various analyses. Considering also the complexity of lifeline systems and all types of possible uncertainties it may be concluded that vulnerability and risk assessment is really a very complicated task. Many combined efforts are needed to reach the ultimate goal and the present work is a contribution to this long way.

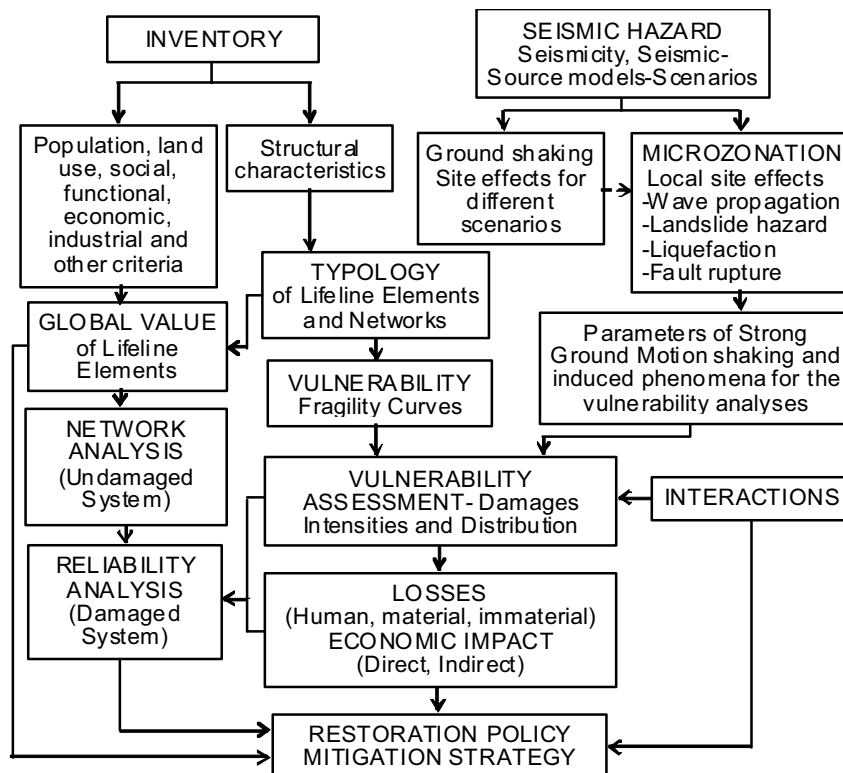


Fig. 9.1. Flowchart of the methodology

9.2. Social and economic consequences of lifeline damages

The operation of lifeline systems during and after a destructive earthquake is of vital importance for society as they contribute to the rescue operations, the emergency and recovery actions. Lifeline damages are classified as following:

- Direct economic losses that include repair and replacement costs of structural and non- structural elements.
- Indirect economic losses related to loss of utility and infrastructure services, induced business and production interruption, relocation expenses, rental income etc.
- Casualty losses.
- Internal instability of certain society actions.
- Environmental pollution due to oil or waste disposals leakages and other collateral damages.
- Collateral effects as a result of the interactions between systems.

Recent experience from major earthquakes such as Loma Prieta (1989), Northridge (1994), Kobe (1995), Kocaeli (1999) and Ji-Ji (1999) proved that lifeline elements are quite vulnerable, and the mid and long -term effects, mainly in terms of financial losses, may be very important. A typical example of long term effects is the port of Kobe, one of the largest container cargo ports in the world, which suffered major damage as a result of the 1995 Hyogoken-Nanbu earthquake. A year after almost all port infrastructures had been reconstructed, but it is remarkable that in 1998, 3 years after the disaster, cargo traffic remained at roughly half of pre-disaster levels (Chang, 2000).

Bridges are the most vulnerable components of roadway systems. Their damage is greatly disruptive due to the lack of redundancy, the lengthy repair time or the rerouting difficulties. The disruption to the highway network can strongly affect the emergency efforts immediately after the earthquake or the rebuild and other business activities in the following period. For the Loma Pieta earthquake (1989) the repair cost for bridges was about \$280 million; in Northridge earthquake (1994) the repair cost was \$190 million, while the total cost of the transportation system was \$1.8 billion (Basoz and Kiremidjian, 1998). The repair cost for the Hansin Expressway after the Kobe (1995) earthquake was \$4.6 billion (Shinozuka, 1995), while the total cost was actually much higher if the \$3.4 million of daily income from tolls and the losses from business interruption and traffic delays is taken into account.

Severe damage to individual facilities of electric power and communications systems didn't affect significantly the performance of the entire system due to the highly redundant character and reliability of these systems. Moreover as a large earthquake has not occurred recently in a major metropolitan area, the performance of the modern technologies (e.g. optical fiber, digital switches) of the above networks is not well known (Schiff and Tang, 1995). However loss of power or communication can severely impact the emergency response, especially when the disruptions concern critical facilities, such as hospitals, command centres, police stations, etc. Loss of power may have severe indirect effects due to the synergies between the lifelines and the dependence of all networks on the power supply system. As an example, the disruption of the electric power during the Loma Prieta earthquake, caused pollution to San Francisco and Monterey Bay areas due to the malfunction of the pumping stations that

boosted waste-disposals to the waste-water treatment facility (EERI, 1990). In Loma Prieta earthquake (1989), the 350 breaks/linkages occurred in the water distribution network, greatly affected the fire-fighting capacity in the area of San Francisco, Oakland and Berkeley (EERI, 1990). In Kobe, 1995 the water system was severely damaged; more than 1600 repairs in the primary network and 72.000 repairs in customer's connections (NIST, 1996) were reported. A large area was burned down due to the disruption and the inefficiency of the fire-fighting network. Similar problems occurred during the Northridge earthquake in Los Angeles. The direct and indirect cost related to the gas system in Ji-Ji (1999), Loma Prieta (1989) and Kobe (1995) earthquakes, was \$24,7 million (Chen et al., 2000), \$32 millions (Phillips and Virostek, 1990) and \$2,3 billions (Shinozuka, 1995) respectively.

Besides direct and indirect economic losses and of course human losses, the immaterial losses as well should not be disregarded; cultural, commercial, reduction in radiance and long term economic effects, due to potential decline of some habitation or production sectors of the city or commercial and industrial zones in favour of other parts of the same city or regions or even countries.

9.3. Advancement in risk management of lifelines

The risk analysis studies of lifelines can be grouped according to FEMA (1994), into five categories:

1. General studies for vulnerability of components and systems.
2. Scenario study without serviceability analysis.
3. Scenario study with serviceability analysis.
4. Prioritisation and mitigation studies.
5. Other studies that include interactions of lifelines.

Typical examples of the first category are ATC-13, (1985) and ATC-25 (1991), methodologies for estimating direct and indirect economic losses and functionality of lifelines. The level of details provided is suitable for scenario type analysis and they can offer a broad understanding of losses and earthquake impact. RADIUS methodology (RADIUS, 1999), a result of a European research project, can also be classified in the first category making extended use of GIS technology. HAZUS (NIBS, 1997, 1999 and 2002) is an advanced powerful methodology that can be classified into the second and partially the fourth category. HAZUS provides detailed maps (in G.I.S format) suitable for risk management purposes and it is proposing specific tools to evaluate both direct and indirect damages as well as the consequences to society. Recently a new general methodology, similar to HAZUS has been developed in Europe, RISK-UE project (Mouroux et al., 2004), which is taking into account the distinctive features of European structures and makes use of state-of-the-art European and international know-how in many important parts of the methodology like seismic hazard, inventory, classification, fragility curves etc. The present work reflects the basis of this methodology with respect to lifelines.

Among the first loss estimation studies were the works of Ballantyne et al. (1990a, b), Ballantyne and Heubach (1991) and Wang et al. (1991) for the water systems of Portland, Everett and Seattle. O'Rourke (1989) developed an early GIS-based methodology to assess the seismic risk of water systems that takes into account

uncertainties in earthquake hazards, material and soil properties as well as water demand. The method has been applied to study the serviceability of the auxiliary water supply in San Francisco. Another GIS based risk model for water system using a Monte Carlo simulation, has been developed by Sato and Shinozuka (1991) and Okumura and Shinozuka (1991). It has been applied to evaluate the reliability of the Memphis water system.

Werner et al. (2000) developed a modular methodology for the seismic risk assessment of a highway network, including models for transportation network analysis, hazard estimation, seismic performance of highway components and evaluation of the economic impact. Both direct losses, in terms of repair cost ratio and functional losses in terms of repair procedures and traffic states are estimated. Indirect economic losses are also evaluated based on the traffic time delays due to damages of the system.

Methods referring to the fourth category are considering pre-seismic, co-seismic or post-seismic policies. A characteristic example of such study is a work referring to the seismic performance and the upgrading needs of a gas utility system (Clark et al., 1991). Similar work was performed by Matsuda et al. (1991) for the performance of electric high voltage transmission systems.

Studies including synergies among lifelines are aiming to account for interactions that may influence the seismic performance and the restoration process of each particular system. (Hoshiya and Ohno, 1985, Nojima and Kameda, 1991, Scawthorn, 1992, Eidingen, 1993, Shinozuka et al., 1993 and Shinozuka and Tanaka, 1996).

Risk analysis studies have been also performed using fuzzy techniques to account for various uncertainties and to assist the decision making procedure (Katayama et al., 1991) and expert system analysis to diagnose pipeline network response (Takada et al., 1991).

Finally, important progress is expected in the risk management of lifelines by applying real-time damage estimation data under GIS platforms. The few efforts made so far (i.e. Eguchi et al., 1997, Shimizu and Yamazaki, 1998), have proved that these systems are probably the most powerful and efficient way to mitigate seismic risk reducing the uncertainties involved in all other methodologies. In the future each large city exposed to seismic risk will dispose a real time warning system. Emergency services, predictions of damages intensity and spatial distribution for future events, loss estimations for each material and immaterial element at risk and mitigation strategies, all will be based on accurate data, and thus they will be much more reliable. Much effort is needed to reach this goal but the global benefit is extremely important.

9.4. Basic features of lifelines

Lifelines and essential facilities are singular, in the sense that every system has its own distinctive characteristics, and being a complex network of elements is characterized by the following basic features:

- Spatial distribution usually exceeding the urban area which is served by it.
- Lifelines are composed by “lines” and “nodes” of different typology in each system. A line may be a pipeline section or a sector of road, and a node may be a

reservoir, a central telecommunication building or a sewage station. It may be also possible to consider material or immaterial links with numerous critical equipments or components.

- Each lifeline system has its own intrinsic characteristics, namely network structure (treelike, with loops or mixed), directly related to their functionality.
- Interactions and synergies amongst different lifelines.

Lifeline and infrastructures may be separated in two major categories:

- Transportation systems comprising roadways, railways, airport and port facilities.
- Utility systems including potable water, waste-water, natural gas, electric power and communication.

Essential buildings are critical facilities, like governmental buildings, hospitals, police stations, fire stations, schools, gymnasiums, stadiums and open areas, which are also considered as part of urban lifeline systems. They provide essential services to the community, especially during the crisis period and should be remain functional during and after an earthquake. Regarding lifeline vulnerability assessment they should simply be taken into consideration for the synergies involved from their existence and function.

In most cases lifeline systems are also characterized by an inherent poor knowledge of their geometrical and mechanical characteristics and the limited documentation of past earthquake damages observations. Adding to these difficulties the increased market competition and management inadequacies, the availability of data in GIS format is considered as the most serious and expensive problem to be solved.

Another distinctive feature of lifelines is their specific exposure to earthquakes. Due to their wide extent, lifeline systems are crossing different geological and geotechnical conditions; so the expected seismic ground motion is not uniform and there is higher probability of exposure to permanent ground displacement induced by fault offset, liquefaction phenomena and landslides.

9.5. Overview of seismic risk assessment methodology for lifelines

9.5.1. INVENTORY

Inventory is an essential step to identify, characterize and classify all types of lifeline elements according to their specific typology and their distinctive geometric, structural and functional features. Attributes such as location, geometry, morphological details (i.e. for bridges), material properties, age and seismic design level are considered to be mandatory in the inventory database of the lifeline elements.

There are several inventory databases for many lifeline systems of varying resolution and relevance. Some of these were explicitly developed to support regional loss estimation studies and some others in the generic sense. Many data are currently available but contrary to the building inventory which is rather well developed, standardized inventory databases oriented to seismic risk analysis of lifelines do not exist on an international/ national or regional level. The first attempt for lifeline inventory is presented in ATC-13 (1985); the effort continued in ATC-25 (1991). Jones and Chang (1993) proposed indirect methods for large-scale estimate of the built

environment, which includes some improvements in the lifelines inventory database. For bridges the Federal Highway Administration USA established a rather general electronic database, called National Bridge Inventory (NBI), not specifically developed for the evaluation of seismic performance. Jernigan et al. (1996) developed a comprehensive database for fragility estimation of bridges in Shelby County, Tennessee, while Mander and Basoz (1999) developed a simplified methodology using information from the NBI inventory. In Europe a few individual efforts are recently reported mainly based on European or national funded research projects.

GIS offers the perfect platform to implement any inventory inquires. However, several difficulties arise in the collection and archiving of the data, related to the aging of networks (unknown location, material etc), digitisation process, competition between the lifeline companies, security issues or unwillingness of lifeline owners to provide data.

A typical inventory for bridges is given in Table 9.1 (Werner et al., 2000, after Jernigan et al., 1996), while Table 9.2 synthesizes and enhances the proposed inventory for water system from the American Lifeline Alliance (ALA, 2002) and HAZUS (NIBS, 1999).

Table 9.1. Inventory for bridges in Shelby County, Tennessee (Werner et al., 2000, after Jernigan et al., 1996)

<ul style="list-style-type: none"> - Relevant information from NBI database - Bridge ID number, route, location, feature crossed by bridge, maximum span length, total length, roadway width, bridge width, average daily traffic, year built, skew angle, superstructure types (main span and approach span), number of main spans, number of approach spans. - Abutment attributes - Bridge ID number, abutment type (material, type, and fixity), abutment bearing and expansion type, seat width, foundation type, whether seismic retrofit was implemented. - Bent File No. 1 - Bridge ID number, bent type and material, superstructure to substructure connectivity, bent bearing and expansion type, seat width, number of columns per bent, maximum column height, minimum column height. - Bent File No. 2 - Bridge ID number, column fixity (to bent cap and to pile cap or footing), column shape, vertical reinforcement, transverse reinforcement, foundation type.

Table 9.2. Inventory for water system (ALA, 2002, NIBS, 1999)

Detailed inventory for water pipelines
<p><i>General information</i></p> <p>Geographic location (coordinates), Location of pressure reduction valves (coordinates), Exact location of connections (coordinates), Location of manhole (central, smaller), Location of isolation valves, of SCADA, In case of failure: Isolation of pipe segments (area coverage, number of customers).</p>

<p><i>Geometrical and construction detail</i></p> <p>Length (m), Type (fragile, ductile), Diameter (mm), Thickness (mm), Elevated or buried, Material, Strain: σ_y, σ_f (Mpa), Connection type (compression coupling, bell & spigot, heat fusion, arc or oxyacetylene gas weld), Rotation tolerance, Depth (m), Type of coating, Type of lining, Type of protection material (if any), Operational characteristics (free-flow, with pressure), Operation pressure (atm), Directivity of flow, Year of construction, Corrosion (yes, no, possible, unknown), Description of construction technique, History of failures/ repairs (not only from earthquakes but also from operation use), Method of repair.</p>
<p><i>Urban & economic characteristics</i></p> <p>Type of customers served (important, common), Connection with essential/ critical facilities (e.g. hospitals, clinics etc), Alternative routing, Time of emptying pipe segment, Economic cost of construction, Cost of reconstruction if damaged by an earthquake.</p>
<p>Basic features of water pipelines</p>
<p>Geographic location, Diameter, Thickness, Material, Connection type, Operational characteristics, Distances between connections, Type of customers served, Connection with essential/ critical facilities, Description of construction technique, Alternative routing, Location of manhole, Location of valves, isolation valves etc, Location of SCADA, Economic cost of construction.</p>

9.5.2. TYPOLOGY

Besides the great inherent uncertainties the key assumption in the vulnerability assessment of lifeline systems is that structures having similar structural characteristics, being in similar geotechnical conditions, are expected to perform in the same way for a given seismic loading (source and path effects are excluded). Within this context, the damage is directly related to structural properties of lifeline elements. Typology is thus a fundamental descriptor of a system, derived from the inventory of each element at risk. Geometry, material properties, morphological features, age, seismic design level, anchorage of the equipment, soil conditions, foundation details etc are among typical typology descriptors/parameters. The availability of data may certainly influence the choice of the classification descriptors and thus the typology.

Table 9.3. Typology of tanks (ALA, 2001a, b)

Unanchored redwood tank ($5 \cdot 10^4$ - $5 \cdot 10^5$ gallons)
Unanchored post-tensioned circular concrete tank ($>1 \cdot 10^6$ gallons)
Unanchored steel tank with integral shell roof ($1 \cdot 10^5$ - $2 \cdot 10^6$ gallons)
Unanchored steel tank with wood roof ($1 \cdot 10^5$ - $2 \cdot 10^6$ gallons)
Anchored steel tank with integral steel roof ($1 \cdot 10^5$ - $2 \cdot 10^6$ gallons)
Unanchored steel tank with integral steel roof ($>2 \cdot 10^6$ gallons)
Anchored steel tank with wood roof ($>2 \cdot 10^6$ gallons)
Anchored reinforced (or pre-stressed) concrete tank ($5 \cdot 10^4$ - $1 \cdot 10^6$ gallons)
Elevated steel tank with no seismic design
Elevated steel tank with nominal seismic design
Roof over open cut reservoir

Table 9.4. Bridge Sub-categories (Basoz and Kiremidjian, 1998)

Bridge Sub-Category	Abutment Type	Column Bent Type	Span Continuity
Single Span Bridges			
C1S1	Monolithic	Not applicable	Not applicable
C1S2	Non-monolithic	Not applicable	Not applicable
C1S3	Partial integrity	Not applicable	Not applicable
Multiple Span Bridges			
C1M1	Monolithic	Multiple	Continuous
C1M2	Monolithic	Multiple	Discontinuous
C1M3	Monolithic	Single	Continuous
C1M4	Monolithic	Single	Discontinuous
C1M5	Monolithic	Pier Wall	Continuous
C1M6	Monolithic	Pier Wall	Discontinuous
C1M7	Non-monolithic	Multiple	Continuous
C1M8	Non-monolithic	Multiple	Discontinuous
C1M9	Non-monolithic	Single	Continuous
C1M10	Non-monolithic	Single	Discontinuous
C1M11	Non-monolithic	Pier Wall	Continuous
C1M12	Non-monolithic	Pier Wall	Discontinuous
C1M13	Partial Integrity	Multiple	Continuous
C1M14	Partial Integrity	Multiple	Discontinuous
C1M15	Partial Integrity	Single	Continuous
C1M16	Partial Integrity	Single	Discontinuous
C1M17	Partial Integrity	Pier Wall	Continuous
C1M18	Partial Integrity	Pier Wall	Discontinuous

HAZUS (NIBS, 1997, 1999 and 2002), based on previous ATC-13 (1985) and ATC-25 (1991) propositions, defined an adequate to USA practice typology, for the components of the utility systems (water, waste-water, gas, telecommunication and electric power system) and for infrastructures (roads, railway, port, and airport). ALA (2001a, b) provided a more detailed typology for water system components. Several researchers developed different typological patterns for individual lifeline components; in general it may be concluded that there is no unanimous agreement on the typology content. As an example, ATC-13 (1985) identified three categories for tanks according to the type of foundation (underground, on-ground, elevated), while HAZUS distinguishes tanks according to material, type of foundation and anchorage. Recently, ALA (2001a,b) recognized 11 different types of tanks according to their size, material, seismic code, type of roof, type of foundation and anchorage (Table 9.3).

For bridges HAZUS (NIBS, 1999) asserts 28 classes, while Basoz and Kiremidjian (1998) proposed for R/C bridges a classification scheme with 21 categories (Table 9.4).

9.5.3. GLOBAL VALUE OF LIFELINE SYSTEMS

A conventional seismic risk analysis is limited to the evaluation of the direct impact (usually in economic terms), of isolated components, based on the seismic hazard and the physical vulnerability of the elements. An advanced seismic risk study of a lifeline system should include the functional and social vulnerability, taking into account the functional relations between the different elements, urban activities (production, consumption, exchanges) and relations of the network with its surrounding urban or

rural environment. In that way each lifeline network will be analysed as an integrated part of the seismic risk scenario and as a part of the urban system, with human, material and immaterial elements. In addition, the main issues of the lifeline system will be identified through ranking of the value of the exposed elements, based on various factors that describe the importance and role of each element in the urban system.

An approach having these characteristics is based on the assessment of the “global value” of all elements at risk composing the lifeline systems in order to define the lifeline value distribution, prioritise pre-earthquake retrofitting actions and quantify the overall importance of different complex and coupled lifeline systems. The global value of each element at risk, will depend not only on its direct specific value or content (physical and human), but also upon its indirect/immaterial value that is represented by the usefulness and relative role in the whole urban system at a specific time. The indirect value may be very different according to the situation and the time circumstances; thus it is evaluated according to three main periods: normal, crisis and restoration. The global value and the main issues of each element is defined with criteria such as operational attributes, land use, population influences, human losses, economic and social weight under normal, crisis and recovery circumstances, identity/radiance, environmental impact and other. To achieve this, appropriate qualitative or quantitative indicators are defined according to the considered period, which are evaluated with value scales that refer to relevant measuring units. Such indicators and measuring units have been proposed for each lifeline system in RISK-UE (Mouroux et al., 2004) methodology. In general the main steps are as follows:

1. Definition of the appropriate criteria for the estimation of the global value for each element at risk for normal, crisis and recovery period.
2. Collection of all necessary data required for the evaluation of the global value and GIS organization.
3. Definition of value scale (0-1) for the calculation of the relative value for each criterion and for each element. Assessment of the global value for each period.
4. Definition of the main, important and secondary issues in each period.

A typical example of the selected indicators for gas pipes is given in Table 9.5. The method has been applied for the gas (Figure 9.2) and other utility and transportation systems in Thessaloniki. Risk management priorities in terms of post seismic restoration strategies, pre-seismic retrofitting decisions and co-seismic rescue actions are influenced by this description of global value.

Table 9.5. Indicators and value scale for gas pipes (Alexoudi, 2004)

INDICATOR	MEASURING UNIT	RELATIVE VALUE	PERIOD		
			N	C	R
Function (Supply- Diameter)	≥200mm	1.00			
	200mm>x≥150mm	0.75	+	+	+
	150mm>x≥100mm	0.50			
	<100mm	0.25			
Emergency (Existence of SCADA)	Yes	1.00	-	+	-
	No	0.00			
Radiance	Subtransmission pipes	1.00			
	Transmission pipes	0.50	+	-	+
	Distribution pipes	0.25			

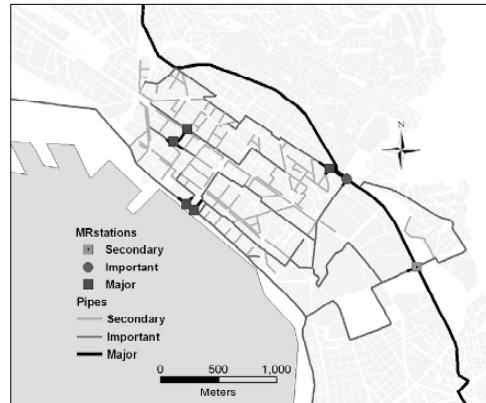


Fig. 9.2. Main issues of Thessaloniki's gas system in crisis period

9.5.4. INTERACTIONS

Interaction means synergies in mutual or reciprocal actions or influence. High dependence among different lifeline systems and also with essential facilities is a very important aspect within an advanced seismic risk management study. Thus, interactions between systems may be very important and exceed direct consequences. Rigorously, an iterative approach could be necessary to develop series of consequences.

To describe and quantify interactions, it is essential to know the typology and functioning of systems involved, the nature of the reciprocal influence, when the specific synergy is evolved (normal, co-seismic or restoration/recovery period) and the importance of the link (slight / strong).

Kameda (2000) considered four types of interactions between lifelines systems:

- Physical damage propagation (e.g. blockage of roads due to debris of collapsed buildings, failure of pipeline located on a bridge due to damage of the latter).
- Functional damage propagation (e.g. breakdown of lifeline components due to loss of electric power).
- Recovery interruption (e.g. disruption due to repair of buried pipelines of different networks).
- Back-up functions of substitute systems (e.g. overloading of railways due to failure of roadway system).

A representative case of interactions among different lifeline systems during the restoration period is reported after the 1995 Kobe earthquake by Hada and Meguro (2000). They outlined the problems in the restoration activities of the water and gas networks in the Kobe area due to traffic congestion, street blockades, damaged buildings and water that flowed into gas pipelines; they also analysed their effects based on real data. It is clear that an efficient rescue policy and an optimum recovery strategy require the evaluation of the interactions between different lifeline systems. Unfortunately, until now little improvement has been reported to this issue.

9.5.5. SEISMIC HAZARD

Seismic hazard in case of vulnerability analysis and risk assessment of lifelines must be specified according to the precise needs for the particular lifeline components, networks as well as the models used to describe vulnerability and fragility curves or relationships (see §9.5.6.). Moreover due to the large extent of lifeline systems, it should describe the spatial variability of ground motion considering the local soil conditions. Consequently intensity descriptors i.e. in MSK scale are not adequate. In particular it has been proved that for pipelines peak ground velocity is better correlated to the observed damages and thus the vulnerability assessments should be based on ground velocity estimates. For bridges the best descriptor is a response spectral value at a specific period (i.e. $T=1.0\text{sec}$). For other lifeline components it may be peak ground acceleration (i.e. buildings, tanks, waterfront structures) or even the permanent ground deformations (i.e. embankments, roadways, railways). So, it is absolutely necessary to perform site specific seismic hazard analyses. In case of urban sites these studies are commonly referred as microzoning studies (Mouroux et al., 2004). For no-urban lifelines (i.e. an oil or gas pipeline crossing large remote areas) it may be a site specific study along the axis of the pipeline. In any case specific geotechnical-surface geology information is required and adequate studies should be performed to estimate the necessary ground shaking or deformation parameters.

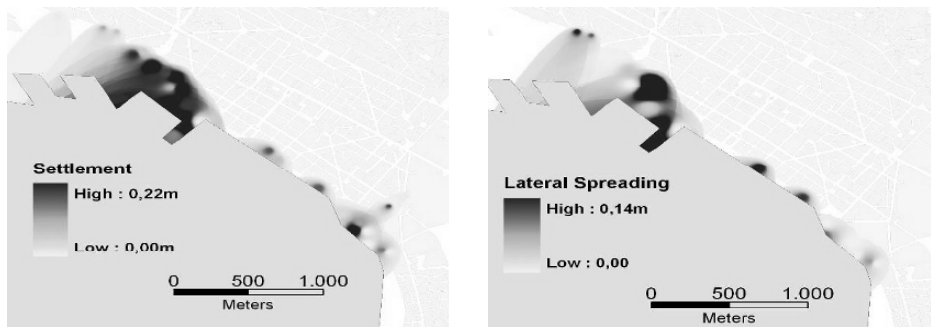


Fig. 9.3. Estimated settlement (m) and lateral spreading due to liquefaction in the coastal zone of Thessaloniki city

Another important issue is related to the level of the expected seismic event. For normal constructions all seismic codes prescribe a 475 years mean return period. This is not always enough for lifelines which in many cases are considered as structures of high importance. Additionally a lower intensity seismic event may also have some damages to certain components. So in case of lifelines seismic hazard assessment must be performed in terms of scenarios with different mean return periods (i.e. 100, 475, 950 years).

Uncertainties related to all these studies are of major concern. It is suggested that all seismic parameters must be estimated with a mean value \pm a standard deviation, while specific models are deemed to be developed to account for these uncertainties in the vulnerability assessment of lifeline systems. A typical example of site specific microzonation study is given in Figures 9.3 to 9.6. Maps for peak horizontal ground

acceleration (PHGA) values (at $T=0.0s$ and $1.0s$), peak horizontal ground velocity (PHGV), liquefaction risk and associated settlements and horizontal lateral spreading displacements are calculated for Thessaloniki-Greece using a 475 years seismic scenario (Mouroux et al., 2004 and Anastasiadis et al., 2002). Similar maps must be available for other mean return periods as well.

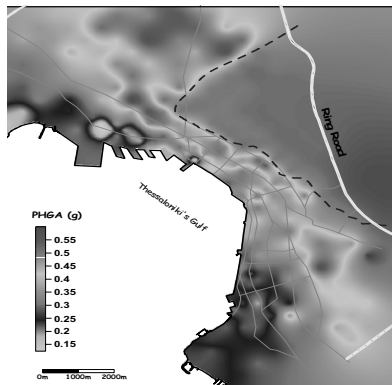


Fig. 9.4. Distribution of mean peak horizontal acceleration for Thessaloniki

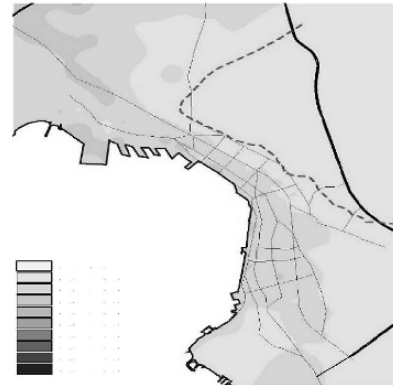


Fig. 9.5. Distribution of mean peak acceleration (g) for Thessaloniki at $T=1.0s$

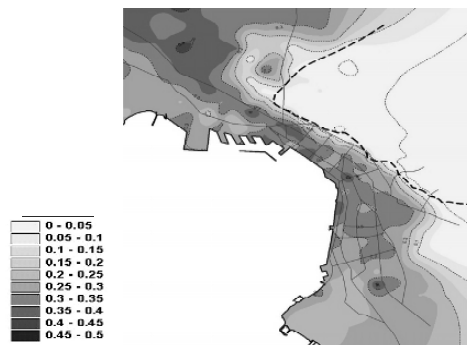


Fig. 9.6. Distribution of mean PGV (m/s) values in the city of Thessaloniki

9.5.6. VULNERABILITY

A fundamental requirement for assessing the seismic performance of a system is the ability to quantify the potential for component damage as a function of the level of seismic hazard intensity. In general, the vulnerability expresses the behaviour of an element at risk subjected to a phenomenon with variable intensity. It is given in terms of a vulnerability relationship, referring to a general deterministic, statistical or probabilistic relationship relating the component's damage state, functionality, economic losses etc, to an appropriate measure of the intensity of the earthquake hazard. The relationship between the probability of the component damage and the level of seismic hazard is normally referred to as a fragility relationship or fragility curve.

There are different methods to construct vulnerability or fragility curves and to quantify damages according to the shaking intensity. In the following we attempt a short description of the different approaches and methods giving representative examples of fragility-vulnerability curves or relationships for various components of different utility and transportation lifelines

9.5.6.1. *Damage states*

The most common way to define earthquake consequences in lifeline components is a classification in terms of the following damage states:

No damage - Slight / minor - Moderate - Extensive - Complete.

This qualitative approach requires an agreement about the meaning and the content of each damage state and in general the definition of damage states is rather subjective. Alternative ways of expressing losses are also suggested like:

- Functionality (binary decision: Yes or No).
- Possibility of damage (usually between 0 and 1 or 100%).
- Repairs/km (especially for pipes).
- Serviceability.
- Nominal use, Reduced use or Not usable.
- Usable without repairs, after repairs or not repairable.
- Damage factor or replacement cost (usually between 0 and 1 or 100%).

An example of damage state definition for urban roads is given in Table 9.6.

Table 9.6. Possible consequences of earthquake on urban roads (Monge et al., 2003)

Serviceability	Damage state	Direct damages	Indirect damages
Fully closed due to temporary repairs for few days to few weeks. Partially closed to traffic due to permanent repairs for few weeks to few months.	Extensive	Major settlement or offset of the ground (>60 cm).	Considerable debris of collapsed structures.
Fully closed due to temporary repairs for few days. Partially closed to traffic due to permanent repairs for few weeks.	Moderate	Moderate settlement or offset of the ground (30 to 60cm).	Moderate amount of debris of collapsed structures.
Open to traffic. Reduced speed during repairs.	Minor	Slight settlement (<30cm) or offset of the ground.	Minor amount of debris of collapsed structures.
Open to traffic. Reduced speed during repairs.	Minor	Slight settlement (<30cm) or offset of the ground.	Minor amount of debris of collapsed structures.
Fully open.	None	/	No damage/ Clean road.

9.5.6.2. *Vulnerability index*

Approaches using the vulnerability index intend to assess vulnerability of lifeline components without complex calculations, based on the definition of an index resulting in most cases from an analytical expression that combines the main factors affecting the seismic behaviour of the element at risk. A rating system is used to assign a score in each attribute of the selected factors. The scaling values are defined based on expert judgment and the experience of past earthquakes, while the expression usually includes weighting factors in order to account for the relative contribution of each attribute to the total vulnerability of the component. Typical examples are the methods developed by ATC-6-2 (1983), Kawashima and Unjoh (1990) or Kim (1993) for bridges. The main factors affecting the vulnerability rating of bridges in those approaches are the year of design, the type and geometry/morphology of superstructure, the pier and abutment

detailing, the seat length, and the skewness. Similar methodologies are also proposed for utility networks (Muhlbauer, 1996).

As an example, the model that was proposed by Kim (1993) calculates the expected level of bridge damage according to the following expression:

$$y_i = \sum_{i=1}^N \beta_i \cdot X_i + C \tag{9.1}$$

where y_i is the degree of damage, X_i are the factors affecting the vulnerability, β_i and C are constants. The corresponding rank of vulnerability is shown in table 9.7, while the 12 factors affecting the vulnerability are presented in table 9.8 together with beta and C values. According to this model, a simply supported multi span bridge designed in 1981, without internal hinges, having a skewness of about 200, pinned multicolumn bent, pile bent foundation, ductile concrete material, differences in column heights more than 1.25 times and satisfactory seat length, is estimated to have a damage index equal to 2.64 and thus a high degree of vulnerability, when the expected PGA at the bridge site is 0.35g, the soil profile is soft to medium-stiff clay and the liquefaction severity index (LSI) is near to 10.

Table 9.7. Ranking of seismic vulnerability of bridges Kim (1993)

Damage Index	Rank of Vulnerability
$y_i < 1.5$	C: Low
$1.5 \leq y_i < 2.5$	B: Moderate
$2.5 \leq y_i$	A: High

The model is based on the statistical analysis (i.e. multiple regression technique) of data from damaged bridges during past earthquakes around the world. The dominant factors affecting the vulnerability of bridges are the intensity of peak ground acceleration, the effect of liquefaction, the design specifications and the seat length of the bridge.

Table 9.8. Factors affecting vulnerability of bridges, Kim (1993)

VARIABLES	
X_1 =Intensity of Peak Ground Acceleration	X_7 =Type of Foundation
X_2 =Design Specifications	X_8 =Material of substructure
X_3 =Type of Superstructure	X_9 =Irregularity in Geometry or in Stiffness
X_4 =Shape of Superstructure	X_{10} =Site Condition
X_5 =Internal Hinge	X_{11} =Effect of Liquefaction
X_6 =Type of Pier	X_{12} =Seat length

9.5.6.3. Expert judgment based models

In many cases, and especially in the early 1980's, the lack of rigorous damage data necessitated the use of expert opinion for the evaluation of the seismic behaviour of lifeline components with different typology. ATC-13 (1985) produced damage probability matrices (DPM) and fragility curves based on questionnaires, by which the experts were queried on the probability of a lifeline component being in a certain damage state for a given Modified-Mercalli Intensity (MMI) value. These expert evaluations are always useful but for reasons described previously and with the increased number of data after the recent strong earthquakes, they are less used.

9.5.6.4. Empirical models

The development of empirical fragility curves is based on statistical analysis of damage data from previous earthquakes. The fragility curves are usually provided as medians and dispersions of lognormal distribution. Several uncertainties are involved in such analysis related to:

- The inconsistency or heterogeneity of damage data.
- The lack of ground motion records where damages are observed.
- The reliability and incompleteness of the inventory of the damaged network.
- The inconsistency and subjectivity of damage descriptions among different engineers.
- The statistical analysis method that is used in the correlation study.

However, real reported and validated damage data and the derived methods are extremely valuable, even to check the reliability of other more accurate methods.

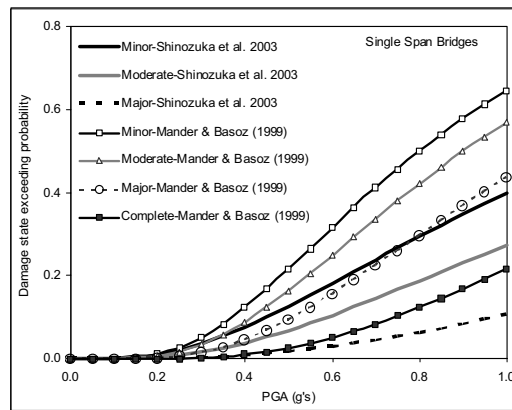


Fig. 9.7. Comparison between empirical and analytical fragility curves for single span R/C bridges

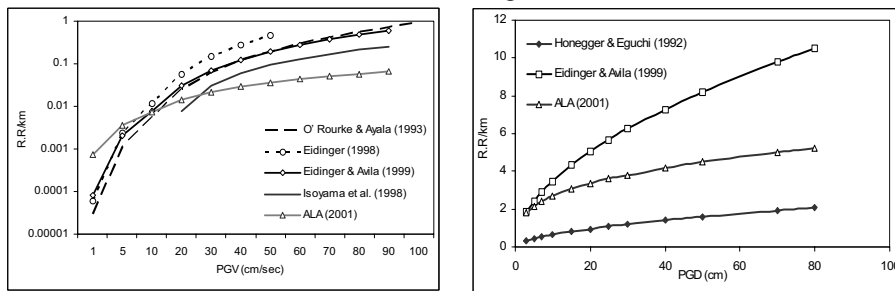


Fig. 9.8. Comparison between different empirical vulnerability relations for ductile pipes due to PGV (left) and PGD (right)

For bridges Basoz and Kiremidjian (1998) analysed bridge damage data from the 1989 Loma Prieta and 1994 Northridge earthquakes and developed ground motion - damage and ground motion - repair cost ratio relationships; empirical fragility curves were also developed using regression analysis. Likewise, empirical fragility curves were generated for bridges from actual data for the 1995 Kobe earthquake by Yamazaki et al.

(1999), while Shinozuka et al. (2003) provided fragility curves for bridges utilizing damage data obtained from the 1994 Northridge and the 1995 Kobe earthquakes. A typical example is given in Figure 9.7 for single span R/C bridges, where a comparison is made between empirically (Shinozuka et al., 2003) and analytically (Mander and Basoz, 1999) derived fragility curves. It is clear that the analytical curves which have been included in HAZUS methodology as well, overestimate the damage state probability for this type of bridges. Nevertheless, this is not the rule and it should be noticed that the empirical curves represent also the characteristics of specific earthquakes and construction practice.

Table 9.9. Fragility relationships for pipelines

Ground shaking	Ground failure
O'Rourke and Ayala (1993): $K*(10^{-4} * PGV^{2.25})$, K: type (fragile, ductile)	Honegger and Eguchi (1992): $K*(7.821 * PGD^{0.56})$ K: type (fragile, ductile)
Eidinger (1998): $1,2*10^{-3} * PGV^{0.7677}$ asbestos-cement $6*10^{-4} * PGV^{1.5542}$ cast-iron $6*10^{-5} * PGV^{2.2949}$ ductile iron	Eidinger and Avila (1999): $K_2*23.674*(PGD)^{0.53}$ K ₂ : material, connection type
Eidinger and Avila (1999): $K_1*1.512*(PGV)^{1.98}$ K ₁ : material, connection type, soil, diameter	ALA (2001a, b): $K_2*11.223*PGD^{0.319}$ K ₂ : material, connection type
Isoyama et al. (1998): $C_p * C_d * 3.11 * 10^{-3} * (PGV-5)^{1.3}$ C _p & C _d : material, diameter	
ALA (2001a, b): $K_1 * 0.241 * PGV$ K ₁ : material, connection type, soil, diameter	

For water and gas pipelines O'Rourke and Ayala (1993), Eidinger (1998), Eidinger and Avila (1999), Isoyama et al. (1998) and ALA (2001a, b) developed damage relations in terms of Repair Ratio/km, using estimated and recorded values of peak ground velocity (PGV) and data from USA, Mexico and Japan (Figure 9.8). Furthermore, Honegger and Eguchi (1992), Eidinger and Avila (1999) and ALA (2001a, b) produced relationships that correlate permanent ground displacement (PGD) with pipeline failures (Figure 9.8). The comparison among different empirical relations is not always good due to many reasons, such as the assumptions made by different researchers, the type of correlation analyses, the method of estimating the PGV and PGD in each site, the accuracy of damage data or the reliability of the pipeline inventory. A major conclusion derived from this remark is that fragility relations should be specifically defined for every country and city with respect to the design-construction practice, the seismotectonic background and the local soil conditions. The later two parameters modify considerably the ground velocity for large earthquakes and consequently the fragility relations expressed in terms of ground velocities. Recent validations with the Lefkas, Greece (2003) earthquake (Alexoudi, 2004) proved that O'Rourke and Ayala (1993) and Honegger and Eguchi (1992) relations are better correlated to the observed damages both for ground shaking and permanent deformations.

Figure 9.9 and tables 9.10 and 9.11 illustrate the distribution of the expected damages to the gas system in the central part of Thessaloniki city. The application is based on the fragility relationship provided by O'Rourke and Ayala (1993), while the input seismic hazard scenario is based on the microzonation study of the city (10% exceedance in 50 years) in terms of peak ground velocity.

Table 9.10. Damage Rating for Thessaloniki gas system

Damage state	
No	27%
Low	70%
Low-Moderate	3%
Average Repair Rate	
Leaks/km	0.04
Breaks/km	0.01

Table 9.11. Pipeline Vulnerability Risk

Vulnerability Class	Repair Rate (R.R)
High	$1.4 < R.R$
Moderate-High	$0.7 < R.R \leq 1.4$
Moderate	$0.1 < R.R \leq 0.7$
Low-Moderate	$0.01 < R.R \leq 0.1$
Low	$0.001 < R.R \leq 0.01$
No-damage	$0 \leq R.R \leq 0.001$

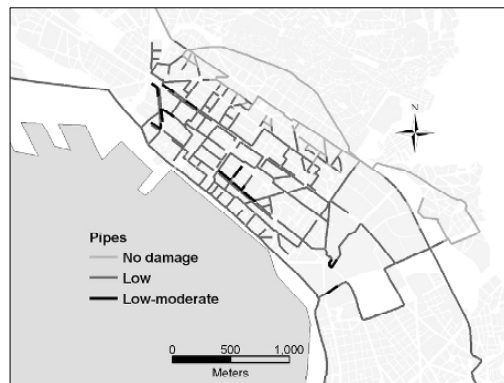


Fig. 9.9. Vulnerability assessment of Thessaloniki's gas system

HAZUS (NIBS, 1999) developed fragility curves for bored and cut and cover tunnels according to an expert opinion approach. ALA (2002) produced empirical fragility curves for bored and cut and cover tunnels with poor-to-average and good construction, based on regression analysis of a worldwide damage database. The curves are based on PGA values which have been back-calculated at the tunnel location using attenuation models, while the uncertainties in the ground motion and in the tunnel performance are also considered. Recently, fragility curves for metro tunnels in alluvial deposits, when subjected to transversal seismic loading were developed based on a numerical approach (Argyroudis et al., 2005). The comparison with HAZUS and ALA (2001a) curves demonstrates a good accuracy to the latest when the quality of the tunnel's lining is not perfect, however it is not always realistic to compare the empirical and analytical fragility curves as they are constructed using two different methods and input data (Figure 9.10).

An advanced method for the assessment of component fragilities based on empirical data and expert judgment using Bayesian statistical technique, to deal more rigorously

with uncertainties, is developed by Kiureghian (2002), to assess the fragility of electric power substations.

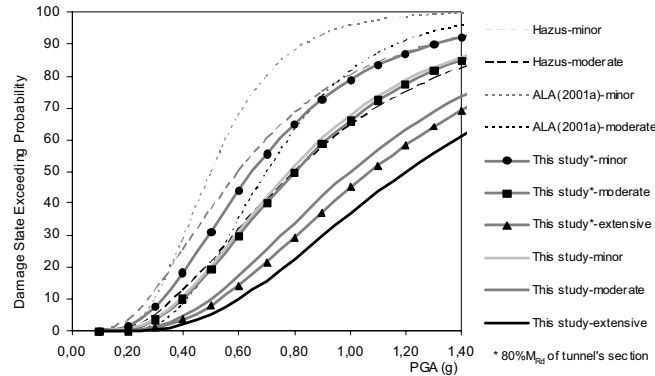


Fig. 9.10. Comparison between HAZUS, ALA, 2001a and numerically derived fragility curves for drilled tunnels

9.5.6.5. Analytical models

Fragility curves can also be constructed analytically. The models could be simple or more complicated according to the type of analysis, the characteristics and the simulation method of the component. As an example Karim and Yamazaki (2001) developed fragility curves for bridge piers as a function of PGA and PGV, modelling the pier as a single degree of freedom system and performing sectional, static push over and non-linear dynamic analyses. The latest is performed using strong motion records from Japan and USA, while the produced analytical curves are compared with empirical ones derived from actual damage data from the 1995 Hyogoken-Nanbu earthquake. The comparison demonstrates that the analytical fragility curves of the pier designed according to the 1964 Japanese seismic code fits better, as it should be expected, to the empirical ones than the curves of the piers designed according to the 1998 code (Figure 9.11). Moreover, the level of damage probability is different for the same pier when the analysis is made using input from different earthquakes, (Figure 9.12), indicating thus, the importance and sensitivity of the input motion characteristics.

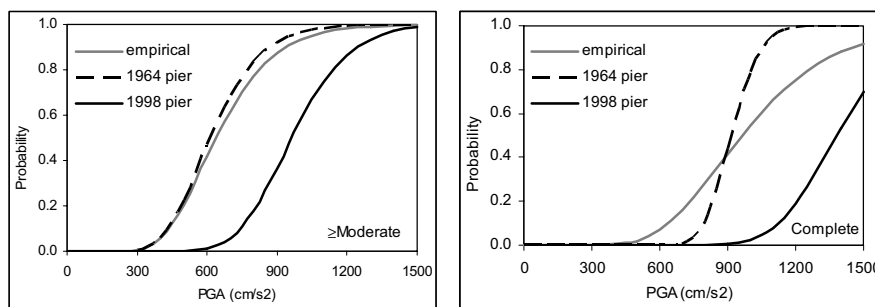


Fig. 9.11. Comparison between the analytical fragility curves for the 1964 and 1998 piers and the empirical for Kobe earthquake (Karim and Yamazaki, 2001)

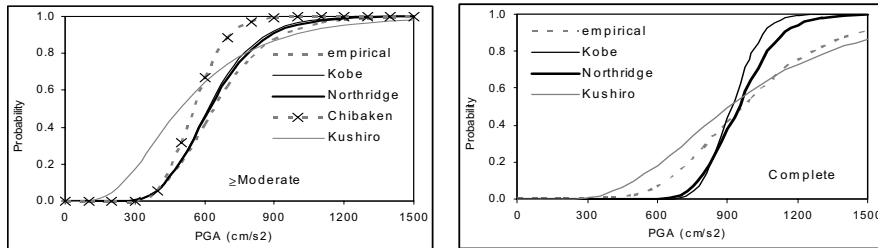


Fig. 9.12. Comparison between the analytical fragility curves for the 1964 pier produced for inputs of different earthquake events (Karim and Yamazaki, 2001)

9.5.7. PERFORMANCE CRITERIA AND ANALYSIS

There are co-seismic and post seismic criteria describing the performance of any lifeline systems. Co-seismic criteria quantify the component's structural behaviour according to certain predefined standards and the network global performance in terms of serviceability, system reliability, connectivity indices etc. Structural performance is evaluated using fragility curves; in case of complex components more complicated methods are used like event tree or fault tree and reliability assessment of individual subcomponents (Scawthorn, 1996, NIST, 1997). Different system performance criteria are assigned to different lifeline systems for different periods (crisis or recovery). Water and power supply networks are very important and should remain at a high operational level even for strong seismic events. On the other hand all transportation sectors are not equally important during the crisis period, while some parts of them (port, airport, main road arteries etc) are crucial both in crisis and recovery period.

Post seismic performance is practically related to the social performance and restoration process. People, society and economy can stand lifeline disruptions for some period immediately following the earthquake but not for long periods. It is the main responsibility of the government, local community authorities and lifeline operators to define the performance criteria making a good compromise between actual demands and the living-economic standards of the society.

Generally the seismic reliability analysis of large-scale lifeline networks is given in terms of density of damage (%), connectivity or serviceability analysis. The definition of serviceability and connectivity varies according to the system and the period studied. In a normal period, connectivity for a given origin-destination pair, is usually defined as the accessibility to the destination point from the respective original point. In crisis and recovery period, connectivity is defined as the accessibility between open-spaces, critical or essential facilities and origin sites. Serviceability can be expressed by a certain demand in a specific node or by reduced flow. A rigorous serviceability analysis seeks many items of information to count on. Generally it can be evaluated assuming either the remaining capacity of the considered path (or paths) connected with selected nodes, or the residual capacity between specific nodes. Especially for water systems, serviceability analysis involves a relatively large number of hydraulic analyses of the system in various damage states.

A serviceability analysis of the Memphis Water delivery system was performed by Okumura and Shinozuka (1991) using Monte Carlo simulation technique. Reliability analysis of the system under various seismic conditions was defined either in terms of connectivity or by the total amount of available flow. Sato and Toki (1991) proposed a method to assess the seismic reliability of large-scale gas networks using polynomial complexity to enumerate paths and a simple connectivity measure that accounts for the probability that gas can reach all terminals or selected terminal nodes. Probabilistic reliability analysis was performed by Odeh et al. (1995) for fire protection of the water system of San Francisco. Simulation base procedure included demand, hazard, and damage estimation as well as hydraulic analysis, to model the system for various possible operating conditions, like large fires following an earthquake.

Shortest path algorithm or other algorithms are available for the identification of critical bridge sets for a given highway transportation network. Using maximum flow minimum cut theory Basoz and Kiremidjian (1993) identified critical bridge sets. Chang and Nojima (1997) developed a model in order to measure the performance of highway systems using data from Northridge and Kobe. The model is used to estimate the reduction in economic losses associated with alternative repair strategies and pre-earthquake mitigation measures. Shinozuka et al. (2003) proposed a simplified approach in order to perform a seismic risk assessment of highway networks, introducing a link damage index as a function of the bridge damage state.

System reliability analyses were also performed in Europe. Vanzi (1996) developed a model for the seismic reliability analysis of electric power transmission systems in central and southern Italy and later, he also proposed a structural upgrading strategy for the electric power system in Italy (Vanzi, 2000).

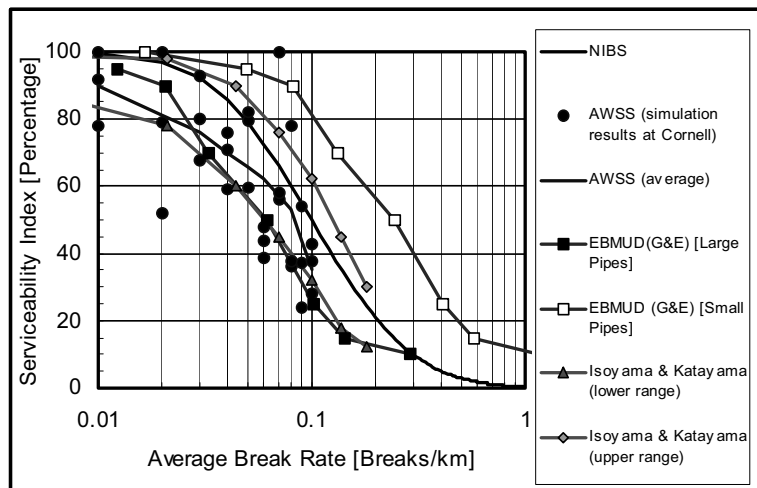


Fig. 9.13. Damage index versus average break rate for post-earthquake system performance evaluation (NIBS, 1999)

The performance analysis is finally a vulnerability analysis of the system for a given seismic scenario and at the same time a general control and evaluation of operational level and the serviceability of the system. An estimation of water system functionality

(i.e. the percentage of customers served immediately after the event) can be determined from a hydraulic model of the damaged system. A rough estimation can be based using a serviceability index for the entire system, through the identification of RR/km. Different researchers, institutes (NIBS) or consultants (G&E) performed detailed hydraulic analyses for specific networks and provided system performance relations (Figure 9.13). Some of the analyses utilize real data from East Bay Municipality Utility District (EBMUD) and Auxiliary Water System of San Francisco (AWSSA). Such relations should be used with caution due to several uncertainties like system specifications, definition of average leaks and breaks, and type of analysis. For large cities a detailed hydraulic analysis is always the best way to assess more accurately system performance.

The vulnerability analysis of Thessaloniki's water system is performed using ALA (2001a, b) relation for both wave propagation and permanent ground deformation (Figure 9.14). For the 475 years seismic scenario and the resulting PGV, and PGD values (see Figures 9.3, 9.6), it is expected to have 72 breaks and 69 leaks. Assuming 80% leaks and 20% breaks in case of wave propagation and 20% leaks and 80% breaks for permanent ground displacements, the average break ratio, for a total length of 1352km, is calculated equal to 0.053. A rough estimation of the water system serviceability applying Figure's 9.13 relations is given in Table 9.12.

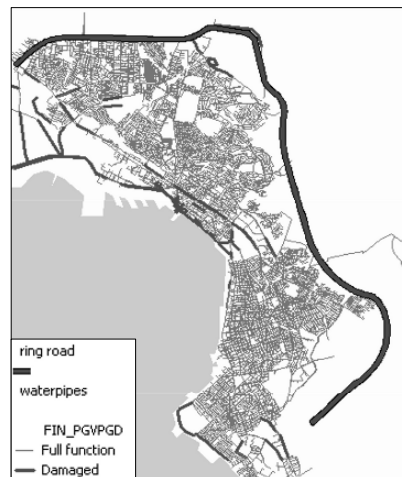


Fig. 9.14. Vulnerability analysis of water system in Thessaloniki

Table 9.12. Serviceability of water system in Thessaloniki

Serviceability Index (%)	
Isoyama and Katayama (upper limit)	85
Isoyama and Katayama (lower limit)	55
AWSS (average)	65
NIBS	80

9.6. Losses, Mitigation

9.6.1. LOSSES ESTIMATION

The losses from a destructive earthquake are distinguished as direct and indirect. Indirect losses are generally more important, as after the event a chain of induced losses are generated. For example, a damaged roadway network can cause losses not only due

to the structural damages of the individual components, but mainly because the potential inability of transportation facility, which is affecting seriously all production, economic and social sectors. The estimation of direct losses is usually based on the repair or replacement cost of the damaged elements according to the vulnerability assessment and the definition of damage states (see §9.5.6). The estimation of indirect losses is a more complicated issue where time is an important factor due to the restoration process. In any case the result of loss estimation is a valuable tool for decision-makers in order to develop appropriate seismic risk mitigation strategies.

Recently, researchers from economic science, engineering, hazard and risk management sections, developed models for the evaluation of lifeline losses from earthquakes and other natural hazards. Rose (2002) reviews and categorizes the natural hazard economic loss estimation methodologies into the following:

- Empirical procedures that are based on primary or secondary data having been collected after the seismic event. These data can be statistically analysed or adapted and applied for other scenarios.
- Deterministic simulation analyses such as the input-output (I-O) and the computable general equilibrium (CGE) models that are well known for economic impact analysis.
- Stochastic simulation analyses that are based on techniques such as Monte Carlo in order to overcome the lack of data and the associated uncertainties.
- Combination of the above procedures.

Typical examples of empirical procedures are those of Ichii (2003) who proposed risk curves for quaywalls in terms of the annual expectation of loss and Basoz and Kiremidjian (1998) who developed fragility curves for bridges in terms of repair cost ratio based on data from 1989, Loma Prieta and 1994, Northridge earthquakes. Audigier et al. (2000) developed a model that estimates the expected losses due to downtime of a port's facilities.

Representative examples of other procedures are the following: Okuyama et al. (1999), used a multiregional commodity flow model and an input-output system to estimate the impacts of transportation system disruption in New Madrid region. Moore et al. (1999) integrated seismic, transportation network and input-output models in order to study the economic impact of transportation and industrial earthquake induced losses to the Los Angeles metropolitan area. Rose and Liao (2004) applied the computable general equilibrium analysis, in a case study of the economic impact of a disruption to the Portland Metropolitan Water System due to a seismic scenario. Chang et al. (1999) simulated the economic losses using the Monte-Carlo technique, in order to construct an economic fragility curve that reflects potential loss from earthquake induced loss of lifeline system serviceability. Shinozuka et al. (1998) developed a case study for the metropolitan Memphis area and analysed the socioeconomic and regional impacts due to the disruption of the electric power system.

9.6.2. MITIGATION

The decision for mitigation of lifelines against seismic hazard is a quite complex issue as different institutions such as government, local authorities, lifeline companies or the insurance industry are involved. Moreover the decision by itself is very difficult because

it should be made based on the results of the seismic risk assessment of lifelines which includes various uncertainties owing to seismic hazard (§9.5.5), vulnerability (§9.5.6), performance (§9.5.7) and loss estimation (§9.6.1) procedures. The loss results can be used in order to prioritise the pre-earthquake mitigation measures such as the retrofitting or redundancy of the elements with greater risk. Moreover, the loss results are considered to be the guide for an effective restoration policy.

9.6.2.1. Prioritisation

The pre-earthquake mitigation plans must be based on appropriate prioritisation criteria that combine engineering techniques, economic analysis tools and decision-making or political aspects. Pre-earthquake mitigation actions include upgrading of structural performance of lifeline components (bridges, pipelines etc), improvement of the network performance, organization of redundant systems, implementation of advanced technologies during earthquake emergency (early warning systems, real time damage estimation etc).

Alesch et al. (2002) summarize financial decision criteria for natural disasters that have been applied for lifelines, such as the traditional cost-benefit analysis or more advanced procedures, such as the mean variance criterion or the stochastic dominance criteria. The cost-benefit analysis is the most commonly used method that compares the investment cost for mitigation and the benefits that will be gained from the investment. As an example Maffei (1995) developed a prioritisation formula for bridges using cost benefit criteria. Grossi et al. (2002) provide a framework for cost benefit analysis for lifeline mitigation.

Several other approaches were used for prioritisation based on the definition of seismic risk index. This index is evaluated with a mathematical model, which incorporates the main factors of seismic risk, namely the seismicity of the site, the structural variability and the importance of the component, while the attributes of the prioritisation criteria are usually ranked through a scoring system. The priority index is computed by multiplying the seismicity, vulnerability and importance factors. Buckle (1991) and Basoz and Kiremidjian (1995) review such methods that have been developed for retrofit prioritisation of bridges in US.

Table 9.13. Risk analysis matrix showing gas pipeline seismic retrofit priorities (Alexoudi et al., 2004)

Urban Risk/ Seismic hazard	Issues		
	Main	Important	Secondary
High	1st priority	1st priority	2nd priority
Moderate- High	1st priority	2nd priority	3rd priority
Moderate	2nd priority	3rd priority	4th priority
Low-Moderate	4th priority	4th priority	5th priority
Low	5th priority	5th priority	5th priority
No-damage	-	-	-

Another method for prioritisation of pipelines was presented by Wang et al. (1995) that takes into account the importance, the rehabilitation time of each pipeline and the damage probability evaluation. Three factors are assumed for the calculation of the importance, namely the pipeline usage (connection with essential facilities), the system factor (primary network is more important than branches) and the population served.

Based on a multicriteria analysis, an evaluation model for the strategic importance of bridges and tunnels in Lisbon was developed (Vieira et al., 2000). The main goal is to develop a prioritisation method for the formulation and implementation of policies to prevent and repair seismic damages in bridges and tunnels.

The method applying the “global value” approach defined in §9.5.3, uses the classification of lifeline system components into main, important and secondary issues according to their global value (see for example Table 9.5). The vulnerability assessment attributes different damage states to the elements at risk (i.e. Figure 9.9, §9.5.6). Combining “global value” evaluation and vulnerability assessment and using an “expert opinion” it is possible to estimate priorities to account for the economic and social losses for a specific utility system and a given seismic scenario. Table 9.13 and Figure 9.15 summarize the application of the proposed methodology for gas pipelines of Thessaloniki (Alexoudi et al., 2004).

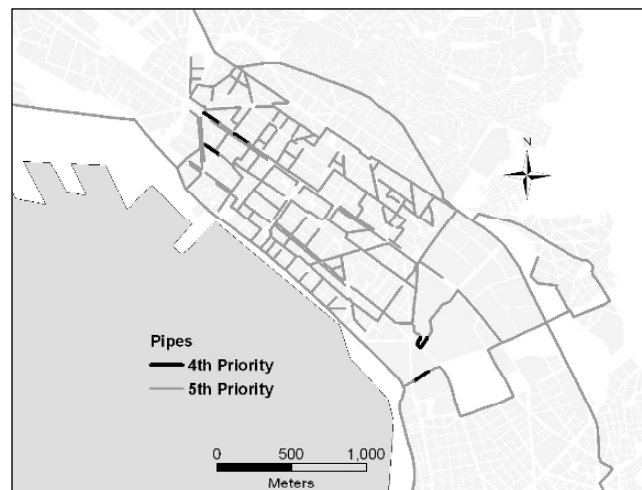


Fig. 9.15. Replacements priorities of gas system of Thessaloniki

9.6.2.2. Restoration

The restoration process starts immediately after the earthquake disaster and continues until the community return to its initial stage. It can be described in terms of days needed to re-organize society, services, activities and functions. The restoration process is expressed by restoration curves, which define the fraction of initial capacity of the lifeline (restored or remaining) as a function of elapsed time since the earthquake. For any system, restoration depends on individual component and network performance as well as the interactions with other lifelines. However, the estimation of the required time for recovery is a complicated task and varies significantly between different

countries or cities, as it depends on numerous factors. In general, restoration process is mainly based on the following parameters:

- Available techniques, local experience and expertise.
- Regulations and regional politics.
- Available man-power, material and equipment.
- Knowledge of the system.
- Economic funds.
- Interactions of individual components and networks.
- Accessibility of the damaged components.

It is obvious that restoration curves for lifelines may differ considerably from one country or city to another. In ATC-13 (1985), several restoration curves are presented for the United States based on opinions of experts. They are defined by continuous (normal distributions described by means and standard deviations) or discrete functions of time. Figure 9.16 shows an example of restoration curves for bridges from NIBS (1999). However the actual restoration time of each component may be very different, as a result of the parameters that influence the restoration process. Moreover, the recovery of the whole system is an even more complicated issue as it depends on the restoration of all individual components. Kameda (2000) compared the restoration curves for water systems from different earthquakes (Figure 9.17). It was observed that the restoration period after the 1995 Hanshin-Awaji earthquake was much longer mainly because of the cascade effects and interactions that were observed among different systems. In general, the functional restoration for the damaged networks in Kobe needed much longer times, (five to ten times more), than those experienced in other major earthquakes. The final recovery period in Kobe was 82 days for water supply, 85 days for natural gas supply, 7 days for power supply, 20 months for highway bridges, and 6 months for major lines of railways.

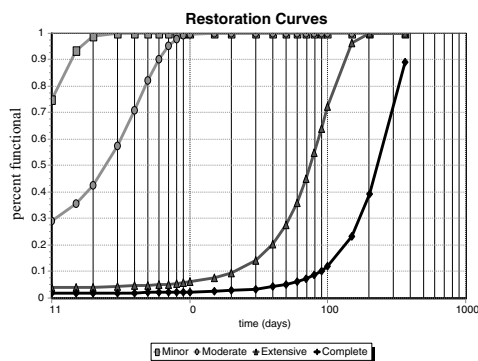


Fig. 9.16. Restoration curves of bridges (NIBS,1999)

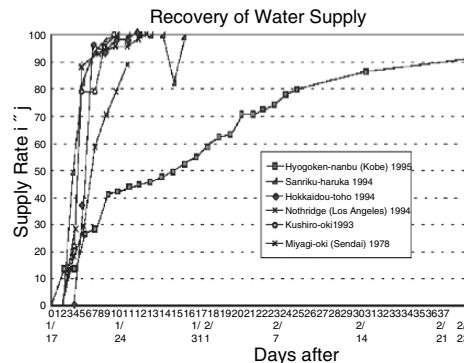


Fig. 9.17. Restoration of water supply systems in recent urban earthquakes

In conclusion restoration curves for any component and each lifeline system must be defined by local actors, using basically expert evaluation. The reduction of the time delays is actually a political decision of great importance, where local authorities, government and lifeline actors have a major role. It is also important to notice that any

pre-earthquake action (upgrading, retrofitting of the most vulnerable elements and sectors), have a very beneficial impact on the definition of the specific restoration curves. So finally the whole process is a cost benefit evaluation process.

9.7. Earthquake risk reduction policy

A rigorous disaster management process includes mitigation, preparedness, response and recovery actions in three periods: normal, crisis and recovery. A breakdown between the different processes and periods can help to evaluate the contribution of each phase to the overall safety management. A reliability earthquake risk reduction policy needs a multidisciplinary team of engineers and social scientists and economists to estimate the likely emergency response resource needs and socioeconomic impacts of large earthquakes in urban areas. The expected economical consequences (direct, indirect) of an earthquake should be balanced with the level of tolerable risk.

Decisions on the appropriate level of investment when dealing with natural hazard depend drastically on the way that each society defines the acceptable risk. Strictly speaking, no level of risk is “acceptable”, but risk can be considered tolerable when there are commensurate benefits. Safety doesn’t require all risk to be eliminated but an appropriate balance among cost, risk and benefits should be accomplished. Earthquake risk reduction policy should also take into account the organization of the community, the human and material resources and certainly the available funds.

The identification of “main”, “important” and “secondary” elements at risk in the “normal” period provides a prioritisation according to the importance of the activities, the social and economic values and the daily demand for serviceability. A disaster management plan can enhance the pre-earthquake activities for retrofitting important and critical components in the urban environment and prepare an efficient organization of public services and local authorities for the “crisis” period. For the “recovery” period an efficient management plan must minimize the restoration time, the efforts and the cost.

Earthquake hazard has in general low probability but high social and economic impact. The aim of a risk management strategy, especially for lifelines, is to maintain community safety and also to reduce physical damage and social and economic disruption. All decisions are based on the selection of the acceptable risk for the estimated seismic scenario. The selection of the “worst” scenario for all elements at risk is very expensive and no community can afford it. Several scenarios, including the most commonly used of 475 years mean return period, are most appropriate and adequate to society needs.

Concluding, the organization of mitigation policies for lifelines is a political and economic decision and surely not a decision that is based on emotion or public feeling, which however, should be seriously considered. The selection of the acceptable risk and the appropriate seismic scenario or scenarios should combine the level of detail of the seismic hazard (microzonation study), the will of central and local actors, the available funds, the financial capability of the community and the country without neglecting the epistemic and physical uncertainties involved in every path of any earthquake risk reduction policy.

CHAPTER 10
DAMAGE SCENARIOS AND DAMAGE EVALUATION

M. Erdik and Y. Fahjan
Boğaziçi University, Istanbul, Turkey

10.1. Introduction

In recent decades, earthquake disaster risks in cities have increased mainly due to a high rate of urbanization, faulty land-use planning and construction, inadequate infrastructure and services, and environmental degradation. Thus for urban centres under possible exposure to large earthquakes it is imperative that certain preparedness and emergency procedures be contrived in the event of and prior to an earthquake, which in turn requires quantification of the effects of the earthquake on the physical and social environment. The main element of such quantification is the building losses, which is directly related to casualties, planning of emergency response, first aid and emergency shelter needs. Rational earthquake building and infrastructure loss assessments provide the necessary input for contingency planning and retrofit prioritisation of urban physical elements (Khater et al., 2003).

A compilation of worldwide investigations on urban earthquake risk is presented in Erdik (1994). In Japan, Oyo Corporation has produced an earthquake damage scenario development methodology (Komaru et al., 1995) that has found application in several cities (e.g., Kawasaki City, Saitama Prefecture, Kanagawa Prefecture, Quito, Tehran) as well as in the IDNDR RADIUS (<http://geohaz.org/radius/>) Project (see Chapter 23). EPEDAT (The Early Post-earthquake Damage Assessment Tool) (Eguchi et al., 1997) is a GIS-based system capable of modelling building and lifeline damage and estimating casualties in near real-time given the source parameters of an earthquake. HAZUS (<http://www.fema.gov/hazus/>) is a standardized earthquake loss estimation methodology intended for national application in the U.S. (Whitman and Lagorio, 1999). HAZUS provides quantitative estimates of losses in terms of direct costs for repair and replacement of damaged buildings and lifeline system components; direct costs associated with loss of function; and casualties and people displaced from residences. To generate this information, the methodology includes: classification systems for assembling information on the building stock, highway lifelines, demographic and economic data; methods for evaluating damage and calculating various losses (see Chapter 23). A number of cities worldwide (Addis Ababa, Antofagasta, Bandung, Guayaquil, Izmir, Tashkent, Skopje, Tijuana and Zigong) were engaged in risk modeling in the UN-IDNDR program RADIUS (<http://geohaz.org/radius/>). Several earthquake loss scenario assessment studies at various levels of sophistication have also been carried out in Europe (ENSERVES, 2000); Basel (Faeh et al., 2001); Barcelona (Barbat et al., 1996); Catania (Faccioli et al., 1997); Quito (Fernandez et al., 1994); Istanbul (Erdik et al., 2003b, 2004a, JICA, 2003); Izmir (Erdik et al., 2000) and; Bucharest (Wenzel et al., 1998).

An earthquake risk assessment study has been developed for Catania, a mid-sized city in Italy, project (<http://www.stru.polimi.it/catania/>, also *Journal of Seismology*, Vol. 3, No.3, 1999). The study involves a comprehensive assessment of the earthquake hazard

and seismic microzonation. The inventory of elements exposed to risk included ordinary buildings, old churches, and bridges and viaducts. The vulnerability assessments included both traditional and displacement limit state approaches.

A EC- funded research project, RISK-UE (<http://www.chez.com/riskue /scope.htm>) has developed a general and modular methodology for creating earthquake-risk scenarios that concentrates on the distinctive features of European towns, including both current and historical buildings. It is based on seismic-hazard assessment, a systematic inventory and typology of the elements at risk and an analysis of their relative value and vulnerability. The participant cities included Barcelona, Bitola, Bucharest, Catania, Nice, Sofia and Thessaloniki (see Chapter 23). Also, within the EU-funded Safety Assessment for earthquake Risk Reduction Project (SAFERR - <http://www.saferr.net/index.htm>), several European research groups have undertaken investigations of characterization of seismic hazard and risk assessment systems to provide tools for application of risk assessment.

This chapter will provide a comprehensive evaluation of urban earthquake damage scenarios and damage evaluation. The chapter will cover the methodologies and sample applications of physical damage and socio-economic loss assessments under exposure to scenario earthquakes. After this introduction, the chapter encompasses the sections on earthquake hazard, elements at risk, earthquake vulnerabilities and earthquake risk scenario results. Each section presents the state-of-the-technology with references to important approaches and actual applications. The balance of coverage in the sections is adjusted with respect to the scope and coverage of other chapters in the book. For sake of completeness almost all the example illustrations were taken from the comprehensive Istanbul earthquake risk assessment study conducted by the Department of Earthquake Engineering of Bogazici University (Erdik et al., 2003b and 2004a).

10.2. Earthquake hazard

Earthquake hazard assessments, conducted in connection with risk analysis in urban centres, can be performed using probabilistic or deterministic approaches. To obtain the probable losses in a given urban subdivision or geo-cell, a probabilistic approach would be appropriate. However, since all the probabilistic losses at a given geo-cell cannot take place simultaneously, the sum of these individual losses will overestimate the total loss in the urban area. Furthermore for assessment of lifeline damages, where a spatial system-based approach is needed, the probabilistic approaches may also be inadequate. As such urban earthquake loss assessments have been traditionally linked to a (or set of) scenario earthquake in a deterministic manner. The scenario earthquake can be assessed through disaggregation of the probabilistic hazard to find the source that contributes most to the overall hazard (Thenhaus and Campbell, 2003; Somerville and Moriwaki, 2003; Faccioli and Pessina, 2003).

Attenuation models provide for the change of ground motion severity with source mechanism, distance and local geology. All empirical attenuation relationships are based on or calibrated against strong motion databases (Campbell, 2003b). Currently reliable empirical models exist in terms of peak ground acceleration, velocity and displacement (PGA, PGV and PGD) and, pseudo spectral velocity (PSV), at specific

frequencies and damping ratios, for given earthquake magnitude, distance, fault mechanism and local geology (e.g. Boore et al., 1993; Campbell and Bozorghnia, 1994; Gregor, 1995; Fukushima and Tanaka, 1990; Ambraseys and Bommer, 1995; Campbell, 2003a). The availability of intensity-based vulnerability information has dictated the use of site-specific intensity attenuation relationships. These relationships are based on macroseismic data obtained from past earthquakes and yield MM, MSK or JMA intensities for given earthquake magnitude, distance and, possibly, for site conditions and fault mechanism.

The general methodology of probabilistic seismic hazard using a homogeneous Poisson model is well established in literature (Cornell, 1968). The Conditional Probability (Renewal) Model essentially relies on the characteristic earthquake hypothesis which is based on the premise that the slip is dominated by earthquakes that rupture the entire segment with a characteristic displacement (Thenhaus and Campbell, 2003; Erdik et al, 2003a and 2004b). Deterministic seismic hazard assessment is conducted to determine the spatial distribution of the earthquake ground motion that would result from a given (scenario) earthquake. The geological and seismological information forms the basis to predict the appropriate scenario earthquake, which is usually given in broad terms, involving rupture length, location and magnitude (see Chapter 2 and 3).

For quantification of the site effects in the urban earthquake hazard assessment or in earthquake microzonation maps, there exist analytical and empirical approaches (see Chapter 4). In hazard assessments based on empirical intensity attenuations, the modification of the ground motion has been traditionally expressed by some ad-hoc judgmental rules or, preferably, in terms of intensity changes empirically correlated with the ground conditions (e.g. Medvedev, 1962; Evernden and Thomson, 1985 and Kagami et al., 1988). Most of the earthquake loss scenario developments in the United States have utilized such empirical correlations (e.g. Topozada et al., 1988, 1993 and 1994). In another approach (e.g. Oyo, 1988), the PGA distributions on competent ground have been computed on the basis of attenuation relationships and then modified on the basis of analytical techniques applied to representative soil profiles. The modified PGA values have then converted to intensity values. The use of the "Average Horizontal Spectral Amplification" factors originally proposed in NEHRP (FEMA, 1997b) recommendations provides practical means for incorporation of the average spectral ratio between the horizontal ground motions at a site with respect to a nearby rock site.

For proper assessment of the seismic risk in urban centres the potential of the earthquake induced ground failure hazard, such as liquefaction, land sliding and surface fault rupture, need to be determined. Techniques to evaluate the liquefaction potential are well established and generally involve the preparation of two types of maps: one showing the liquefaction susceptibility and the other expressing the opportunity for critical levels of shaking. The susceptibility and opportunity maps are merged to depict the areal liquefaction potential (Youd et al., 1979). In most of the earthquake loss scenario applications the liquefaction susceptibility has been identified on the basis of geotechnic/geomorphic criteria (Youd et al., 1979, Youd et al., 1978, Youd, 1991). Techniques for the site-specific assessment of landslide susceptibility based on engineering parameters are developed (EERI, 1986, ISSMFE, 1986). In earthquake loss

scenario developments, however, the most commonly used indicators of susceptibility have been based on geomorphic criteria (Wilson and Keefer, 1985).

10.2.1. EXAMPLES: EARTHQUAKE HAZARD IN ISTANBUL

To provide examples for urban earthquake hazard assessment carried out in connection with earthquake risk assessments, illustrations from earthquake scenario loss assessment for Istanbul will be provided (Erdik et al., 2003b and 2004a). In Istanbul the earthquake hazard has been assessed using deterministic (scenario earthquake) and probabilistic means. For the seismic hazard in terms of MSK intensities, the region specific intensity attenuation relationships developed on the basis of Anatolian earthquakes Erdik et al. (1985) have been considered. Figure 10.1 depicts the distribution of site-specific MSK intensity distribution that would result from $M_w=7.5$ earthquake on the Main Marmara Fault. The limited strong motion data in Turkey and ambiguities in the station site descriptions does not allow for the development of a reliable region and site specific development of ground motion attenuation relationships. Owing to the geological and geo-tectonic similarity of Anatolia, California and also on the basis of favorable predictive comparisons (e.g., Ozbey, 2001), we have decided to utilize the Boore et al. (1997) and Sadigh et al. (1997) attenuation relationships, currently being used for the assessment of earthquake hazard for the Western U.S. (Leyendecker et al., 2000). To reduce the epistemic uncertainty, we used the average ground motion parameter obtained from each of these attenuation relationships. The spectral accelerations for the periods $T=0.2s$ and $T=1s$, calculated for NEHRP B/C boundary site class, are modified using the site coefficients presented in the 1997 NEHRP Provisions. The site-dependent spectral accelerations, provided in Figure 10.2 and Figure 10.3, will be used in the construction of the so-called “Uniform Hazard Response Spectrum” (FEMA, 1997b) to model the earthquake demand for spectral displacement-based vulnerability assessments (Erdik et al., 2004a). In Figure 10.4 the liquefaction susceptibility map prepared for Istanbul is provided.

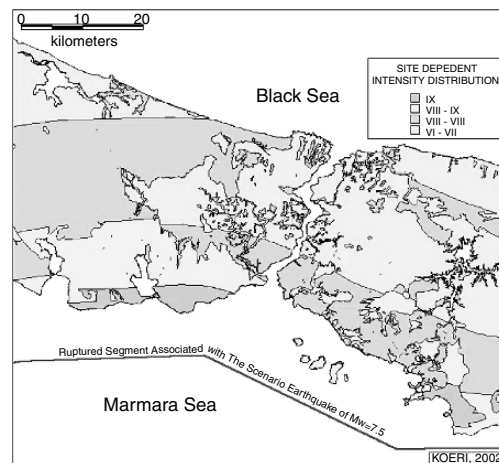


Fig. 10.1. Site dependent deterministic intensity (EMS'98) distribution in Istanbul that would result from the scenario earthquake

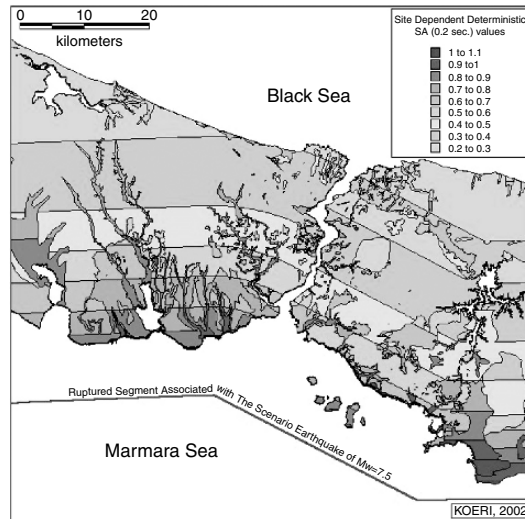


Fig. 10.2. Site dependent spectral acceleration ($T=0.2s$, in g) distribution in Istanbul that would result from the scenario earthquake

10.3. Elements at risk

In urban areas the population, structures, utilities, systems, and socio-economic activities constitute the "Elements at Risk". Buildings and lifeline systems are generally termed "Built Environment". The physical losses to elements at risk that would result from a specified earthquake scenario necessitate an extensive and comprehensive collection of their inventories. Preparation of urban earthquake damage/loss scenarios involve compilation of information on: Demographic structure for different times of the day; Building stock and its characterization; Lifeline and infrastructure (major roads, railroads, bridges, overpasses, public transportation, power distribution, water, sewage, telephone, and natural gas distribution systems) including their nodal points (stations, pumps, switchyards, storage systems, transmission towers, treatment plants, airports, marine ports etc.); Major and critical facilities (dams, power plants, major chemical and fuel storage tanks) in the form of GIS databases.

Unfortunately the general incompleteness, if not unavailability, of this information create a serious bottleneck for the urban earthquake loss assessments. The building classification systems used in inventories (and eventually in vulnerability matrices) are country-, even region-, specific and cannot have uniform applicability in all major urban centres. The inter-regional difference in building architecture and construction practices necessitate region-specific building classifications for the development of inventories and vulnerability information. For urban centres where building inventories are unavailable or unreliable practical surveying methods, such as: aerial imagery and rapid visual screening (sidewalk survey), needs to be developed. Both day- and night-time population distribution need to be assessed and should be taken into account separately in the earthquake loss scenario studies. Determination of the night population is easier

than the day population since most census data relate essentially to night-time population.

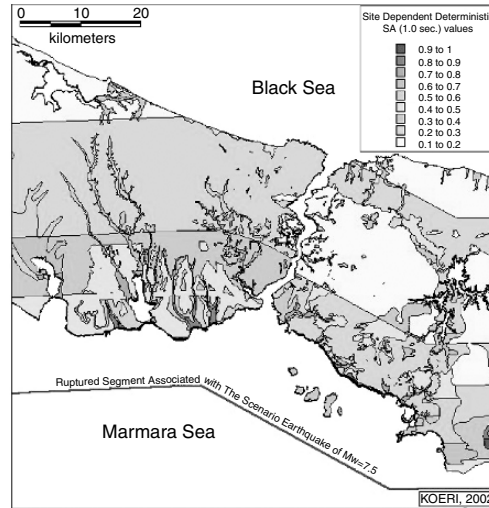


Fig. 10.3. Site dependent spectral acceleration ($T=1.0s$, in g) distribution in Istanbul that would result from the scenario earthquake

The information on the lifelines and major facilities are easier to obtain and the related design and construction practices may have more international conformity. The lifelines should be inventoried in sufficient detail for conducting vulnerability assessments and impact of disruption. The inventory classification scheme for transportation systems include highways, railways, light rail, bus, port and harbours, ferries and airports. Lifeline utility systems include potable water, waste water, oil, natural gas, and electric power and communication systems. Pipeline systems can be further divided with respect to their location (surface or buried) and type (brittle or ductile). An electric power system consists of substations, distribution circuits, generation plants and transmission towers (see Chapter 9).

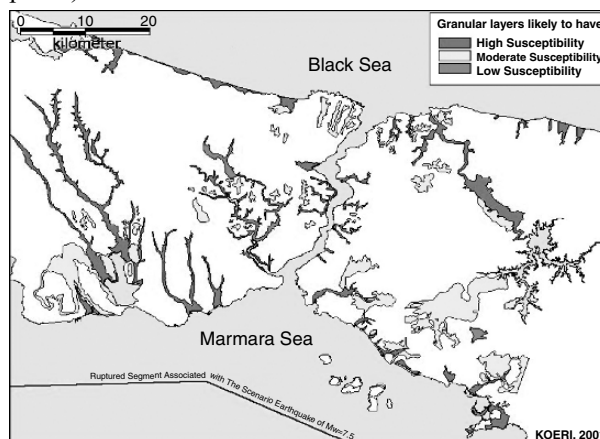


Fig. 10.4. Liquefaction susceptibility map for Istanbul

10.3.1. STANDARDIZING AND CLASSIFYING BUILDING DATA

In HAZUS (NIBS, 1997, 1999 and 2002) the general building inventory includes residential, commercial, industrial, agricultural, religious, government, and educational buildings. A building inventory classification system is utilized to group buildings with similar damage/loss characteristics into a set of pre-defined building classes commensurate with the relevant vulnerability relationship classes. For general building stock the following parameters affect the damage and loss characteristics: Structural (system, height, and building practices), Nonstructural elements and Occupancy (residential, commercial, and governmental). Building structure types include: Wood-Light Frame, Wood-Commercial and Industrial, Steel Moment Frame, Steel Braced Frame, Steel Light Frame, Steel Frame with Cast-in-Place Concrete Shear Walls, Steel Frame with Unreinforced Masonry Infill Walls, Concrete Moment Frame, Concrete Shear Walls, Concrete Frame with Unreinforced Masonry Infill Walls, Precast Concrete Tilt-Up Walls, Precast Concrete Frames with Concrete Shear Walls, Reinforced Masonry Bearing Walls with Wood or Metal Deck Diaphragms, Reinforced Masonry Bearing Walls with Precast Concrete Diaphragms and Mobile Homes. The Building Occupancy Classes encompass: Residential, Commercial, Industrial, Agriculture, Religion/Non/Profit, Government and Education Buildings that are essential to remain functional after an earthquake, such as hospitals, police stations, fire stations and schools, which are generally treated on a building-specific basis.

For earthquake loss estimation purposes, the building inventory in Istanbul was divided into three main groups based on the construction type, number of stories and construction date (Erdik et al., 2004a). Each group was further subdivided to yield the following classification:

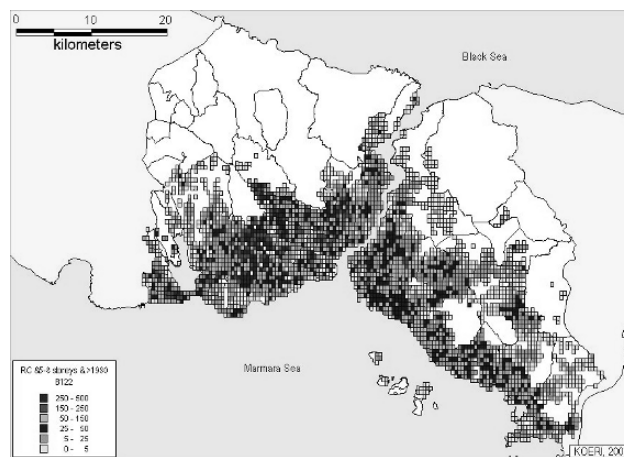


Fig. 10.5. Distribution of (numbers per cell) mid-rise reinforced concrete buildings (post-1980) in Istanbul

- Construction Type: Reinforced concrete frame, Masonry, Reinforced concrete shears wall and Precast.
- Number of Stories (including basement): Low-rise (1-4 stories), Mid-rise (5-8 stories) and High-rise (9 and more stories).

- Date of Construction: Pre-1979 and Post-1980.

Using the above classification, a query matrix with a dimension of $4 \times 3 \times 3 = 24$ was constituted for the assessment of building inventory needed for earthquake risk assessment in Istanbul (Erdik et al., 2003b and 2004a). The data provided from the queries were matched with building inventory in terms of footprints based on aerial photos and then transferred to 8131 cells ($0.005^\circ \times 0.005^\circ$). This type of uniform gridding provides a better resolution than the irregularly sized sub-districts. Spot checks for the inventory have been conducted using video imagery obtained from helicopter flights. To provide an example the distribution of post-1980 mid-rise reinforced concrete buildings are illustrated in Figure 10.5. Using the same geo-cells the night-time population in Istanbul is provided in Figure 10.6. (Erdik et al., 2004a).

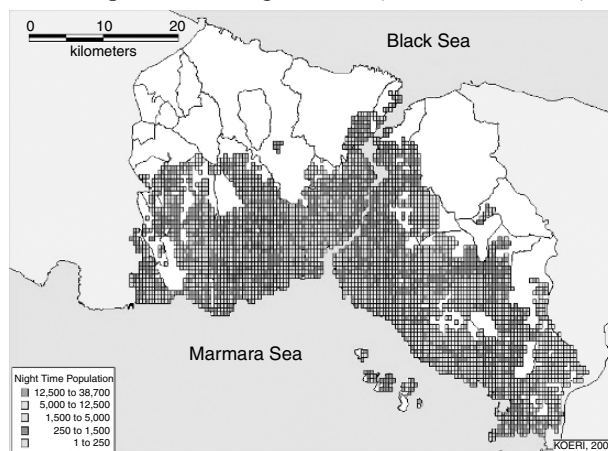


Fig. 10.6. Distribution of (numbers per cell) night-time population in Istanbul

10.4. Earthquake vulnerabilities

Vulnerability is defined as the degree of loss to a given element at risk, or a set of such elements, resulting from the occurrence of a hazard (see Chapters 6 and 7). Vulnerability functions (or Fragility curves) of an element at risk represent the probability that its response to earthquake excitation exceeds its various performance limit states based on physical and socio-economic considerations. The vulnerabilities of lives, structures, systems, and the socioeconomic structure are the main factors influencing the earthquake risk and losses in urban areas. Vulnerability analysis involves the elements at risk (physical, social and economic) and the type of associated risk (such as damage to structures and systems and human casualties). Vulnerability assessments are usually based on past earthquake damages (observed vulnerability and, to a lesser degree, on analytical investigations (predicted vulnerability)). Primary physical vulnerabilities are associated with buildings, infrastructure and lifelines. These vulnerabilities are agent- and site-specific. Furthermore they also depend on design, construction and maintenance particularities. Secondary physical vulnerabilities are associated with consequential damages and losses. Socio-economic vulnerabilities include casualties, social disruption and traumas and economic impacts (Porter, 2003).

10.4.1. PRIMARY PHYSICAL VULNERABILITIES

Earthquake vulnerability is a measure of the damage a building is likely to experience given that it is subjected to ground shaking of specified intensity. The dynamic response of a structure to ground shaking is a very complex behaviour that is dependent on a number of inter-related parameters that are often very difficult, if not impossible, to precisely predict. These include: the exact character of the ground shaking that the building will experience; the extent to which the structure will be excited by and respond to the ground shaking; the strength of the materials in the structure; the quality of construction and condition of individual structural elements; the interaction of the structural and non-structural elements of the building; the weight of furnishings and contents present in the building at the time of the earthquake; and other factors. Most of these factors can be estimated, but never precisely known. As a result, it is typically necessary to define vulnerability functions for buildings within levels of confidence.

Almost all of the earthquake loss scenario developments have used building vulnerability matrices that relate descriptive damage classes to earthquake motion intensities. Coburn and Spence (1992) provide observed vulnerability functions (percent of buildings damaged) for common building types. ATC-13 (1985) provides loss estimates for 78 different building and facility classes for California. To overcome the data limitations, the damage probability matrices and time estimates for restoration of damaged facilities were obtained by aggregating the expert opinions. Intensity-based vulnerability matrices also exist for different parts of the world, and for indigenous building typologies. In these vulnerability functions the distinction between damage and loss is not explicit, since only very limited data exist on the cost of repairs. There is only limited experience with the earthquake performance of flexible structures such as moment resisting open frame structures and the base isolated buildings. These structures are responsive to ground displacements, for which we currently do not have much information. Future vulnerability of buildings, especially steel structures, which might have developed undetected weaknesses in past earthquakes, remains an issue that needs to be addressed.

In addition to buildings, many other engineered urban structures; infrastructures, lifelines and services are vulnerable to the effects of earthquakes. Direct damage to lifeline facilities exacerbates damage to socio-economic fabric by interrupting business. These secondary losses may exceed the direct loss. The earthquake vulnerability of lifelines is critical in the control of induced losses and socio-economic losses. Observations acquired from past urban earthquakes (EERI, 1986), supplemented by the worldwide experience have been used as a guide to assess their physical vulnerabilities. A compilation of lifeline vulnerability functions and estimates of time required to restore damaged facilities are provided in ATC-25 (1991). The vulnerability functions are based on the review of existing models and the expert opinion in ATC-13 (1985) supplemented by an expert technical advisory group (see Chapter 9).

10.4.2. SECONDARY PHYSICAL VULNERABILITIES

Only limited vulnerability models exist for secondary damages for secondary hazards, such as: post-earthquake fire, hazardous material release, explosions and water inundation. Recent developments in fire following earthquake models include three

stages: ignition, spread and suppression, and provide first-order estimates of total losses as functions of intensity, wind, building density and fire engine number. There is no practical method for modelling hazardous material release and/or explosions. Tsunamis, seiches and dam failures may immediately precede an earthquake in many urban centres and contribute significantly to the losses. High resolution mapping of areas susceptible to inundation necessitates accurate prediction of water run-up heights and water velocities affected by the interaction of onshore structures and topography.

10.4.3. SOCIO-ECONOMIC VULNERABILITIES

In addition to the physical vulnerabilities, the socio-economic vulnerability of the urban system also needs to be assessed in terms of casualties, social disruption and economic loss for a comprehensive earthquake damage and loss scenario. Casualties in earthquakes arise mostly from structural collapses and from collateral hazards. Lethality per collapsed building for a given class of buildings can be estimated by the combination of factors representing the population per building, occupancy at the time of the earthquake, occupants trapped by collapse, mortality at collapse and mortality post-collapse. Most current urban seismic loss studies have considered only the direct physical losses. However, it is generally known that loss due to collateral hazards and the indirect economic losses constitute a major portion of the total earthquake loss in an urban system. Indirect economic losses arise from discontinued service of damaged facilities and include: Production and/or sales lost by firms in damaged buildings; Production and/or sales lost by firms unable to retrieve supplies from other damaged facilities; Production and/or sales lost by firms due to damaged lifelines; Losses arising from tax revenues and increased unemployment compensations. Partial quantification of these indirect economic losses can be found in ATC-25 (1991). More than detailed economic models, practical rules need to be incorporated in the loss assessments for the evaluation of complex economic impacts.

10.4.4. INTENSITY-BASED BUILDING VULNERABILITIES

Certain classes of constructed facilities tend to share common characteristics and to experience similar types of damage in earthquakes. The 1998 European Macroseismic Scale (Grünthal, 1998), an updated version of the MSK-81 scale (MSK-81, 1981), differentiates the structural vulnerabilities into six classes (A to F). Reinforced Concrete buildings with low levels of earthquake resistant design are assigned an average vulnerability class of C.

The damage to reinforced concrete buildings are classified as:

- D1: Negligible to slight Structural Damage (SD), Slight Non-Structural Damage (N-SD));
- D2: Moderate damage (Slight SD, Moderate N-SD);
- D3: Substantial to heavy damage (Moderate SD, Heavy N-SD);
- D4: Very heavy damage (Heavy SD, very heavy N-SD) and
- D5: Destruction.

The ratio of the cost of repair of the damage to the cost of reconstruction, expressed as the Repair-Cost Ratio, corresponding to the damage grades D1 through D5 can be approximately given as 0.05, 0.20, 0.50, 0.80 and 1.0. Damage levels encompassing

damages D3, D4 and D5 (i.e. $D \geq D3$) is an important descriptor of the earthquake damage since D3 represents an approximate borderline between repair and replacement of the building stock exposed to an earthquake. A series of standard vulnerability functions that uses intensity to define the seismic demand can be developed for these classes of buildings have been developed (e.g. ATC-13, 1985; Spence et al., 1992; Pomonis et al., 1992; Orsini, 1999; Yamazaki and Murao, 2000; Miyakoshi et al., 1997). The Parameter-less Scale of Intensity (PSI), used in Spence et al. (1992) and Orsini (1999), was proposed as a continuous alternative to the traditional discrete intensity scales. The intensity-based vulnerability curves for the general building types in Turkey have been developed on the basis of available empirical data, compilations from post earthquake damage reports and engineering interpretations (Erdik et al, 2004a). To provide an example, the vulnerability curve for the mid-rise (4-8 stories) reinforced concrete frame type buildings are provided in Figure 10.7. The horizontal axis indicates the range (uncertainty) of MSK intensities and the vertical scale indicates the percentage loss for the five different damage grades, D1 through D5. This vulnerability relationship compares favourably with those presented in Coburn and Spence (1992). Considering the damage level relations between low, medium and high rise R/C frame structures, the vulnerability curves for low-rise (1 – 4 stories) and high-rise ($9 \geq$ stories) R/C frame type buildings are obtained by left shifting of the intensity scale in the horizontal axis of the vulnerability curves of the medium rise R/C frame buildings by half a intensity unit.

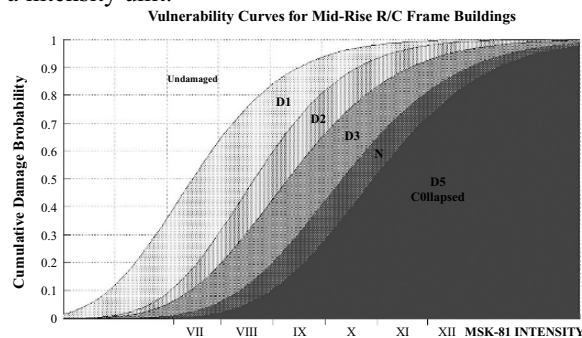


Fig. 10.7. Intensity based vulnerability curves for mid-rise reinforced concrete frame type buildings in Turkey

10.4.5. SPECTRAL DISPLACEMENT-BASED VULNERABILITIES

The analytical estimation of structural damage has been recently standardized in HAZUS (NIBS, 1997, 1999 and 2002), where the vulnerability relationships (also called fragility curves) are described in terms of spectral displacements, which in turn are calculated from the estimated mean inelastic drift capacities of buildings for various damage states. The HAZUS methodology is essentially based on four fundamental ingredients: fragility curve, capacity spectrum, demand spectrum (seismic demand) and the design point. In HAZUS buildings are assumed to be either undamaged or severely damaged due to ground failure. Given the earthquake demand in terms of permanent ground deformation (PGD), the probability of being in the Extensive/Complete damage state is estimated using fragility curves of a form similar to those used to estimate shaking damage. There are several approaches to defining the values of the critical

parameters to be used in spectral-displacement based vulnerability estimation in urban settings other than USA. One is to adjust the parameters proposed for US buildings (given in HAZUS) using expert judgment, based on a knowledge of both local and US design and construction practices; a second is to develop alternative values for these parameters (i.e. Griffith and Pinto, 2000; Aydinoglu, 2000a; Faccioli et al., 1999). The fragility curves represent the probability-based relation between the expected response and the performance limits in terms of the cumulative density function of the probability of exceedance of specific damage limit states for a given peak value of a seismic demand. The analytical expression of each fragility curve is based on the assumption that earthquake damage distribution can be represented by the cumulative standard lognormal distribution function, Φ , (NIBS, 1997, 1999 and 2002, Kircher et al., 1997):

$$P [D \geq ds | S_{di}] = \Phi [(1 / \beta_{ds}) \ln (S_{di} / S_{d,ds})] \quad (10.1)$$

where D refers to the damage, S_{di} is the inelastic spectral displacement demand, $S_{d,ds}$ is the median spectral displacement threshold of the damage state (ds) and β_{ds} is the standard deviation of the natural logarithm of the $S_{d,ds}$. Median spectral displacement corresponding to each damage state ($S_{d,ds}$) are estimated in terms of story drift ratios specified for each building type. The standard deviation β_{ds} is empirically estimated to cover the uncertainties associated with the definition of the damage level concerned, the building load capacity and the earthquake ground motion specified. Once median story drift ratios are estimated for each building and for each damage state, the $S_{d,ds}$ for the fundamental vibration mode, is expressed as,

$$S_{d,ds} = \alpha_2 D_{ds} H \quad (10.2)$$

where D_{ds} refers to median storey drift ratio estimated for the damage state concerned, H represents the total building height and α_2 is the modal parameter defined as

$$\alpha_2 = 1 / (\Phi_{t,1} * L_1) \quad (10.3)$$

where $\Phi_{t,1}$ represents the first mode shape amplitude at the building top and L_1 denotes the “participation factor” of the same mode. Values of these parameters appropriate for the Turkish building stock have been derived for building types in Istanbul (Erdik et al, 2004a). To provide an example H , α_2 , median story drift ratios and spectral displacements are given in Table 10.1 for mid-rise reinforced concrete buildings (pre-1979 and post -1980) for different damage levels.

Spectral displacement-based fragility curves developed in accordance with the above-given data are plotted in Figure 10.8 for mid-rise reinforced concrete frame buildings constructed after 1980. Starting from the top, the curves in each figure represent slight, moderate, extensive and complete damage states

Table 10.1. Spectral displacement-based fragility curve data for mid-rise reinforced concrete buildings in Istanbul

Mid-rise R/C Buildings	H m	α_2	Damage Level											
			Slight (s)			Moderate (m)			Extensive (e)			Complete (c)		
			D_s %	$S_{d,s}$ [cm]	β_s	D_m %	$S_{d,m}$ [cm]	β_m	D_e %	$S_{d,e}$ [cm]	β_e	D_c %	$S_{d,c}$ [cm]	β_c
Pre-1979	15	0.75	.35	3.9	.7	.8	9.0	.74	1.6	18.0	.9	3.0	33.8	1.
Post-1980	15	0.75	.40	4.5	.7	1.	11.3	.70	2.0	22.5	.7	4.0	45.0	.9

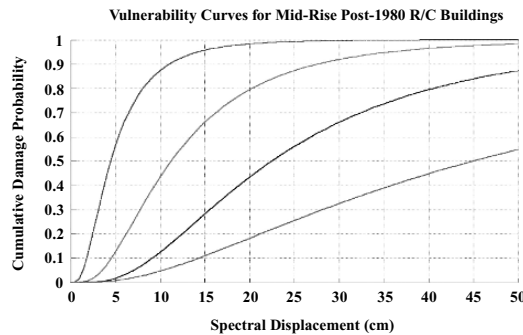


Fig. 10.8. Spectral displacement based vulnerability curves for mid-rise, post-1980 reinforced concrete frame type buildings in Istanbul

10.4.6. CAPACITY AND DEMAND SPECTRUM

The spectral displacement demand for given building type under a specified earthquake motion is based on the intersection of the seismic demand spectrum with the capacity spectrum for the building class considered (NIBS 1997, 1999 and 2002; ATC-40, 1996; Kircher et al., 1997). In this method, inelastic structural capacity of the structure is represented by the so-called “capacity spectrum” (capacity curve) plotted in terms of spectral acceleration versus spectral displacement. Capacity spectrum can be approximated from a “pushover” analysis in which monotonically increasing lateral loads are applied to the structure and the characteristic deformations (usually top displacement) are plotted against the lateral load. The lateral load and the top displacement coordinates are converted respectively to spectral acceleration and spectral displacement (S_a , S_d) for comparison with demand spectrum. As an example a capacity spectrum is shown in Figure 10.9. As it can be seen the capacity spectrum is controlled by the points of design, yield and ultimate capacities. These capacities can be correlated with the damage limit states.

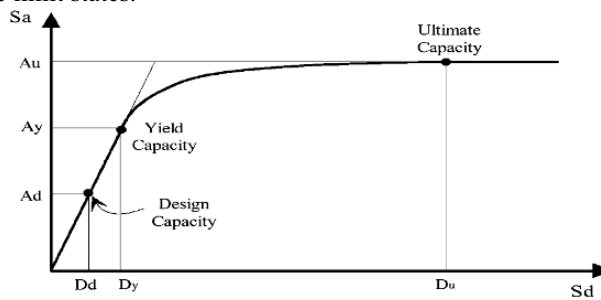


Fig. 10.9. Typical structural capacity spectrum

The capacity curve of a given structure type can be approximated through its “yield spectral acceleration, S_{ay} , defined as:

$$S_{ay} = \frac{V_y}{M_{x1}} \tag{10.4}$$

Where V_y is the base shear capacity at yield and M_{x1} is the participating modal mass in the first mode of vibration, defined as:

$$M_{x1} = \frac{W}{g} \alpha_1 \quad (10.5)$$

Where W is the total seismic weight of the structure, g is acceleration of gravity and α_1 is the participating mass ratio. The normalized base shear capacity at yield can be estimated as

$$\frac{V_y}{W} = C_s \gamma \lambda \quad (10.6)$$

where C_s is the code-based (or estimated) design lateral strength factor and, γ and λ are the estimated “over-strength factors”.

In HAZUS (NIBS, 1997, 1999 and 2002) the demand spectrum is obtained by reducing the elastic acceleration spectrum with reduction factors (κ). In FEMA (2000) the inelastic spectral displacement demand, $S_{di}(T, R_y)$, is given as:

$$S_{di}(T, R_y) = C_1 C_2 S_{de}(T)$$

where C_1 is the spectral displacement amplification factor given by:

$$C_1 = [1 + (R_y - 1) T_s/T] / R_y \quad (T < T_s) \quad (10.7)$$

$$C_1 = 1 \quad (T \geq T_s) \quad (10.8)$$

C_2 is the spectral displacement modifier and $S_{de}(T)$ is the elastic spectral displacement given by:

$$S_{de}(T) = \left(\frac{T}{2\pi} \right)^2 S_{ae}(T) \quad (10.9)$$

where R_y represents the strength reduction factor, T is the natural period of the structure and T_s refers to the transition period from the constant acceleration region to the constant velocity region of the code-based elastic acceleration spectrum. The strength reduction factor R_y is defined as

$$R_y = \frac{S_{ae}(T)}{S_{ay}} \quad (10.10)$$

where $S_{ae}(T)$ represents the elastic spectral acceleration and S_{ay} is the yield spectral acceleration. To provide an example the relevant parameters defining the spectral displacement demand for mid-rise reinforced concrete buildings (pre-1979 and post-1980) in Istanbul are provided in Table 10.2.

Table 10.2. Demand and Capacity parameters for mid-rise reinforced concrete buildings in Istanbul

T [s]	α_1	γ	λ	C_s		S_{ay} [cm/s ²]		C_2	
				Pre-1979	Post-1980	Pre-1979	Post-1980	Pre-1979	Post-1980
0.75	0.80	1.15	2.00	0.06	0.08	169	225	1.1	1.0

10.4.7. CASUALTY VULNERABILITIES

The number and severity of casualties are strongly related with the extent of both structural and non-structural building damage. In smaller earthquakes non-structural damages govern the number and type of casualties, whereas in stronger shakings casualties are highly affected by structural damages, especially by the number of partially or totally collapsed structures. One of the major inputs necessary for earthquake casualty estimation is a correlation between the number and severity of injuries and the damage level of the structures. This however, is not easily attainable due to the limited quality and lack of information in earthquake casualty data. Several studies that establish casualty rates with respect to various building types and damage levels are available in the literature (e.g. Coburn and Spence, 1992; NIBS 1997, 1999 and 2002; Seligson and Shoaf, 2003).

The earthquake casualties for total deaths can be expressed by the following general equation (Coburn and Spence, 1992):

$$K = K_s + K' + K_2 \quad (10.11)$$

where K_s is the fatalities due to structural damage, K' is fatalities due to non-structural damage and K_2 arises from follow-on hazards, such as fire, landslide etc. The above equation can also be used to express all levels of injury severity, such that:

$$K_i = K_{si} + K'_i + K_2 \quad (10.12)$$

K_i is the i^{th} level of severity, ranging from Severity-1 (light injuries) to Severity-4 (death). In HAZUS (NIBS, 1997, 1999 and 2002) methodology a direct relationship is established between structural damage and casualties.

Casualty for any given structure type, building damage level and injury severity level can be calculated by the multiplication of: Population per Building, Number of Damaged Buildings and the Casualty Rate. Casualty rates for different building types are established in HAZUS for urban settings in USA. For other urban settings appropriate casualty rates need to be developed using empirical earthquake damage and casualty data. The casualty rates for reinforced concrete structures in Turkey are given in Table 10.3.

Table 10.3. Casualty rates for Reinforced Concrete Structures for Istanbul

Injury Severity	Casualty Rates for R/C structures (%)			
	Low Damage	Medium Damage	Heavy Damage	Very Heavy Damage
Severity 1	0.05	0.2	1	10-50
Severity 2	0.005	0.02	0.5	8-15
Severity 3	0	0	0.01	4-10
Severity 4	0	0	0.01	4-10

The percentages given in the tables above should be multiplied by the number of people in the building at the time of earthquake. Two different values are given in the column "Very Heavy Damage". The smaller values are related with partial collapse of the building, whereas the larger values are given for total collapse (the pancake type of collapse).

JICA (2003) has conducted a study to find the most appropriate indicators for the death toll and the building damage. For the death toll parameter, the number of deaths and death ratio are used. For the building damage parameter, the number of heavily damaged buildings, the heavily damaged building ratio, the number of heavily damaged housing units, the number of moderately to heavily damaged buildings, the ratio of moderately to heavily damaged buildings, and the number of moderately to heavily damaged housing units are used. The best correlation exists between the number of deaths and the number of heavily damaged housing units. Figure 10.10 shows the empirical relationship between the number of deaths and the number of heavily damaged housing units in Turkey.

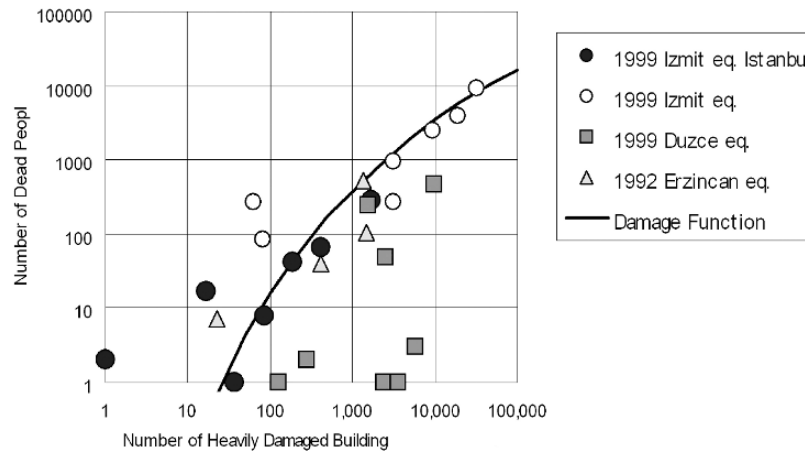


Fig. 10.10. Empirical relationship between the number of deaths and the number of heavily damaged buildings in Turkey (After JICA, 2003)

This relationship fits to and enhances the similar relationship for world-wide data provided by Coburn and Spence (1992).

10.4.8. LIFELINE VULNERABILITIES

Lifeline is an earthquake engineering term denoting those systems necessary for human life and urban function, without which large urban regions cannot exist. Lifelines basically convey food, water, fuel, energy, information, and other materials necessary for human existence from the production areas to the consuming urban areas. Prolonged disruption of lifelines such as the water supply or electric power for a city or urbanized region would inevitably lead to major economic losses, badly affected public health and eventually population migration. Earthquakes are probably the most likely natural disaster that would lead to major lifeline disruption (Eguchi et al., 1997). Observations acquired from past urban earthquakes, supplemented by the worldwide experience can be used as a guide to assess their physical vulnerabilities. An extensive compilation of lifeline vulnerability functions and estimates of time required to restore damaged facilities are provided in ATC-25 (1991). Direct physical damage to lifelines aims to assess the extent and distribution of existing lifelines in a metropolitan area, their associated seismic risk, identification of the most critical lifelines, and the development of a prioritized series of steps for reduction of lifeline seismic vulnerability, based on

overall benefit. Physical damage vulnerabilities lifelines will be summarized on the basis of ATC-25 (1991), ATC-13 (1985) and HAZUS (NIBS, 1997, 1999 and 2002) methodologies.

Transportation systems (Roads)

Roads are generally affected by ground failure and faulting (Peak Ground Displacement, PGD). Motorway (Road) damages consist of the surfacing damages and collapse of the neighbouring slopes or retaining walls. Also collapse of the underpasses or buildings block the traffic even if the motorway is not damaged. According to ATC-25 (1991), the ratio of damage of motorways during an earthquake are given as %0 for MMI VI, %1 for MMI VII, %2 for MMI VIII, %4 for MMI IX and %8 for MMI X. In JICA (2003) study the roads were classified into 4 types: evacuation or escape roads, emergency transportation roads, roads to be urgently developed for emergency and other roads. The traffic (such as volume, direction) and road characteristics (such as land use, building collapse risk and existence of bridges) were treated as attributes in loss assessment with appropriate weighting factors.

Bridges and Viaducts

Bridge damages can create an extensive malfunction even though each failure is limited to a particular point in the line of a road system. Bridges can be classified in terms of the level of seismic design, geometry, structural type and span continuity. In HAZUS (NIBS, 1997, 1999 and 2002) the fragility curves for bridges are modelled as log-normally distributed functions that give the probability of reaching or exceeding different damage states for a given level of ground motion (PGA or SA) or ground failure (PGD). A methodology proposed by Kubo and Katayama in Japan has been shown to be effective in “girder fall-off” evaluations for bridges (JICA, 2003). The methodology is based on the qualitative and quantitative physical information on the bridge (girder type, bearing type, seat widths, abutments and foundations), soil conditions, liquefaction susceptibility and the scenario earthquake (Intensity, PGA and PGV). Each physical attribute is given a score and a weighting factor. Total grade points for each bridge are then linked to its expected earthquake performance. Although the damage to bridges (nodal points) in the transportation system can be evaluated by the fragility curves, the assessment of the functionality of the whole transportation system requires a network system analysis.

Power Transmission System

Substations are the most vulnerable elements in the electrical power delivery system. Major substations contain switches, porcelain insulators, circuit breakers, transformers, and control equipment. Damage generally occurs in improperly anchored electrical equipment (Schiff, 2003). For non-upgraded electrical transmission substations, ATC-25 (1991) assigns 16, 26, 42 and 70 per cent damage values, for earthquake intensities of MMI VII, VIII, IX and X respectively. The corresponding percentages for the distribution substations are 8, 13, 25 and 52 percent. In general, transmission towers and overhead cables have performed well in past earthquakes. High voltage transmission lines are assumed to suffer no damage based on the past earthquake experiences. Underground cables are prone to damage due to ground failure and at connections to buildings. In the 1995 Kobe Earthquake, no electricity poles were damaged in areas of seismic intensity (MMI) less than 8, while 0.55% of poles and 0.3% of underground

cables were damaged in areas of seismic intensity (MMI) 9 and over. The damage function (in terms of damage percent) to overhead power cables as provided in ATC-13 (1985) and HAZUS are shown in Figure 10.11. Also plotted on this figure are damages experienced in 1995 Kobe, 1992 Erzincan and 1999 Kocaeli (in provinces of Yalova, Sakarya, Kocaeli, Bolu and Istanbul) earthquakes (After JICA, 2003).

Natural Gas Transmission System

A natural gas system consists of compressor stations and buried/elevated pipelines. In general, transmission lines in the natural-gas system are located underground except where they emerge for connection to the compressors or pumping stations. All of these components are vulnerable to damage during earthquakes. In addition to economic losses, failure of natural gas systems can also cause fires. The behavior of the pipelines is related with the damage of the soil they are buried or supported. According to ATC-25 (1991), for intensity MMI VIII about 0.5-1 pipe breaks per one kilometer of pipe should be expected depending upon the soil and pipe conditions. The following expression is provided by Disaster Prevention Council of the Tokyo Metropolitan Area (1997) for the assessment of gas pipeline damage ratio, $R_m(PGV)$ in points/km, earthquakes.

$$R_m(PGV) = R(PGV) \times C_p \times C_g \times C_l \quad (10.13)$$

$$R(PGV) = 3.11 \times 10^{-3} \times (PGV-15)^{1.3} \quad (10.14)$$

where PGV is the Peak Ground Velocity (cm/s), C_p is the pipeline material coefficient (0.01 for concrete and 0.0 for polyethylene), C_g is the ground condition coefficient that varies between 1.5 (soft soils) to 0.4 (rock) and C_l is the liquefaction coefficient that varies between 2.0 (susceptible) to 1.0 (non-susceptible). In Japan, polyethylene pipes are treated as suffering no damage. Similarly, no damage was reported to polyethylene gas distribution pipelines in 1999 Kocaeli earthquake in Turkey (O'Rourke et al., 2000).

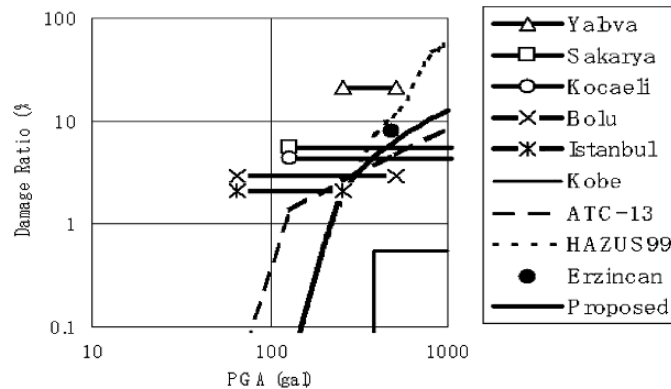


Fig. 10.11. Relation between damage ratio of overhead power cables and the PGA

Water and Wastewater Transmission System

In general, various types of transmission aqueducts can be used for transporting water depending on topography, head availability and environmental and economic

considerations. Pipelines are most susceptible to damage from surface faulting and soil failures such as differential settlement, liquefaction or landslide (O'Rourke, 2003; Ballantyne, 2003). For water supply lines, ATC-25 (1991) assigns the damage rates of 0.5, 1, 4 and 12 breaks/km, respectively for earthquake intensities (MMI) of VII, VIII, IX and X. These damage rates should be doubled for sanitary sewer mains. For pipelines HAZUS (NIBS, 1997, 1999 and 2002) provides empirical relations that give the expected repair rates due to ground motion (Peak Ground Acceleration, PGV) or ground failure (PGD) is provided. The PGV (cm/s) algorithm is based on the empirical data presented in a work done by O'Rourke and Ayala (1993).

$$\text{Repair Rate [Repairs/km]} = 0.0001 \times (\text{PGV})^{(2.25)} \quad (10.15)$$

This relationship essentially applies for brittle pipelines. For ductile pipelines, the above relation is multiplied by 0.3.

Japan Waterworks Association (1998) provides the following damage ratio, $R_m(\text{PGV})$ in points/km, for water pipelines exposed to earthquake.

$$R_m(\text{PGV}) = R(\text{PGV}) \times C_p \times C_d \times C_g \times C_l \quad (10.16)$$

$$R(\text{PGV}) = 3.11 \times 10^{-3} \times (\text{PGV}-15)^{1.3} \quad (10.17)$$

where, PGV is the Peak Ground Velocity (cm/s), C_p is the pipeline material coefficient (1.0 for concrete and cast Iron, 0.3 for ductile steel and 0.1 for polyethylene), C_d is the pipeline diameter coefficient that varies between 1.6 for diameters less than 190mm and 0.5 for diameters greater than 500mm. C_g is the ground condition coefficient that varies between 1.5 (soft soils) to 0.4 (rock) and C_l is the liquefaction coefficient that varies between 2.0 (susceptible) to 1.0 (non-susceptible). The damage function of HAZUS estimates a much higher damage ratio than the other damage functions, including that of the Japan Waterworks Association. Toprak (1998) pointed out that the HAZUS relationships is based on the damages due to the 1985 Michoacan, Mexico Earthquake, which has an extremely long duration; therefore, associated with a higher damage ratio.

Fire Following Earthquake and Hazardous Material Release

Fire following earthquakes is a common occurrence, and can cause significant additional damage. Losses become significant if the fires spread in an uncontrolled manner. Many factors affect the severity of such spreads. Among them are the number of fires started initially, which in their turn depend on the type of heating and cooking equipment in use and fuel storage and distribution methods, the density of combustible material available, and the rate of spread which will also depend on the weather and climatic conditions and the ability of the fire fighting services in suppressing fires. The effectiveness of the fire fighting activities depend on the capability of the services, the availability of water, accessibility of the fires, and the extent of involvement of the fire fighting services in activities such as search and rescue (Coburn and Spence 1992). Models have been developed for low and mid-rise buildings in Japan, based on their experience on wooden frame structures (Scawthorn, 2003). The methodology used in HAZUS is also based on statistical analyses of data from US earthquakes.

In Japanese practice (JICA, 2003) the potential of fire outbreaks result from facilities where flammable liquids or gas materials are handled, such as: LPG Storage Tanks, Factory of Paint/ Polish Products, Warehouse of Chemical Products, LPG Filling

Stations and, Fuel Filling Stations. The leaking liquids or gases will ignite to fire with different probabilities (LPG Storage, LPG Filling Station - 57.9%; Factory of Paint/ Polish Products, Warehouse of Chemical Products - 3.66% and; Fuel Filling Station - 2.55%). If there are many closely spaced wooden buildings in the area fire can easily spread. Japanese Ministry of Construction (1982) findings reveals that fire will never spread if the wooden building coverage area is under 30% in the given urban region. There exists a small possibility of a great fire occurrence and spread if the urban setting encompasses predominantly reinforced concrete and masonry buildings. However, fires can occur after an earthquake and, due to blockage of the roads by debris, fire fighting cannot be conducted in an efficient manner. However, earthquake scenario studies should also pay a particular attention to the hazardous materials, i.e. to chemicals, reagents or substances that, if released from their containers in an uncontrolled manner, would cause health or physical hazards. The experience shows that human casualties occur only if the release leads to an explosion. The release of hazardous materials other than explosives may cause physical damages, environmental contamination or temporary health problems in humans and it can also lead to fires (Sevaduray, 2003 and Scawthorn, 2003).

10.5. Urban earthquake risk results

10.5.1. METHODOLOGIES AND SOFTWARE

In the context of damage scenarios risk can be defined as the losses to the elements at risk that can result from the occurrence of scenario earthquake(s). Damage scenarios are the vehicles to portray these risks. Following is a brief review of current developments in earthquake damage and loss scenarios:

In Japan, Oyo Corporation has produced an earthquake damage scenario development methodology (Komaru et al., 1995) that has found application on several cities (e.g. Kawasaki City, Saitama Prefecture, Kanagawa Prefecture, Quito-Equator and Tehran-Iran) as well as in the IDNDR RADIUS Project. The methodology encompasses: Identification of disaster prevention problems in the objective area; Postulation of the kinds of earthquakes that may affect the area; mapping the distribution of their seismic intensities and assessing the probable effects of their seismic motion; Estimation of damage to structures, lifeline facilities; Estimation of fires, casualties and time to restoration of normal conditions. The Seismic Intensity Distribution estimation constitutes a basic part of the earthquake damage scenario. Several earthquakes are generally hypothesized for the scenario including the historical earthquakes. The geological conditions in the region are divided into representative soil profiles, and the amplification characteristics of seismic motion were calculated for each profile. The basement motions are obtained by using a semi-empirical method that considers the fault model. Seismic intensity values are converted from calculated surface motion.

Under the general title of "Planning Scenario", California Department of Conservation-Division of Mines and Geology has prepared earthquake damage scenarios for several areas in California (Toppozada et al., 1988, 1993 and 1994). The seismic shaking intensity maps were developed on the basis of an Evernden et al. (1981) type model where various geologic units are assigned intensity adjustment factors relative to the

bedrock. Assessment of the building damage was limited to public high schools and hospitals. Damage, loss of service to highways, airports, marine facilities, railroads, electric power (plants and facilities), natural gas (storage, transmission and distribution pipelines), water supply (source, transmission, treatment, distribution), dams and reservoirs, waste water (collection, treatment, discharge), telephone systems have been assessed and the restoration periods have been estimated by treating these elements as parts of a network as well as on nodal point basis.

With the advent of GIS technologies in late 1990's several earthquake loss assessment software have been developed for urban earthquake loss scenario applications.

HAZUS, a standardized nationally applicable earthquake loss estimation methodology implemented through PC-based geographic information system software (Whitman and Lagorio, 1999). HAZUS is being developed under the Multi-hazard Loss Estimation Program sponsored by the Federal Emergency Management Agency (FEMA) through a cooperative agreement with the National Institute of Building Sciences (NIBS). The latest version of HAZUS provides quantitative estimates of losses in terms of direct costs for repair and replacement of damaged buildings and lifeline system components; direct costs associated with loss of function (e.g., loss of business revenue); casualties; people displaced from residences; quantity of debris; regional economic impacts; functionality losses in terms of loss-of-function and restoration times for buildings, critical facilities such as hospitals, and components of transportation and rudimentary analysis of loss-of-system-function for utility lifeline systems. To generate this information, the methodology includes: classification systems for assembling information on the building stock, the components of highway and utility lifelines, and demographic and economic data; methods for evaluating damage and calculating various losses; and databases containing information useable for calculations and as default (built-in) data. EPEDAT (The Early Post-earthquake Damage Assessment Tool) Developed by EQE International (Eguchi, et al., 1997) is a GIS-based system capable of modelling building and life line damage and estimating casualties in near real-time given the source parameters of an earthquake. In reality, EPEDAT and HAZUS employ similar methodologies and provide similar outputs. However, they differ in that HAZUS is nationally applicable while EPEDAT is customized with detailed building inventories for five southern California counties. Emergency Preparedness Canada (EPC), in cooperation with several public- and private sector partners, has developed the Natural Hazards Electronic Map and Assessment Tools Information System (NHEMATIS) (http://www.nobility.com/apps/emerg/index_fr.htm). NHEMATIS is a software tool for the collection, representation, and analysis of natural hazard information. Combined with population and infrastructure data, enables people to perform diverse risk and vulnerability analyses through integration of an expert system rule base, geographic information system, relational database, and quantitative models. The system will integrate information on all natural hazard types, capture location-specific information, provide multi-layer analysis, and permit hazard-impact assessment modelling on selected areas of interest and hazard types.

KOERILoss is software developed by the Earthquake Engineering Department of Bogazici University, Kandilli Observatory and Earthquake Research Institute (KOERI). The software applies a loss estimation methodology (Probabilistic vs Deterministic) developed by KOERI to perform analyses for estimating potential losses from

earthquakes. KOERILoss Version 1.0 in its current form is capable to perform building damage estimation analysis using both intensity and spectral displacement based methodology. It is also able to estimate the direct economic losses and casualties related to building damages. KOERILoss is a user-friendly software that operates through Geo-cells systems. Geo-cells (Grids) facilitate the manipulation of data on building stock, population and, earthquake hazards. The software is developed using the MapBasic language and runs efficiently under MapInfo software. Therefore, the software is fully integrated with MapInfo and capable to utilize the powerful features in displaying, querying, manipulating and mapping inventory databases. KOERILoss provides a great flexibility in displaying the outputs. Tables of building damages, social and economic losses can be easily mapped and displayed on the screen, printed or pasted into electronic documents. A code to evaluate seismic scenarios has been developed by the Italian National Seismic Service (SSN) (Di Pasquale and Orsini, 1997). In this tool, intensity is used for loss estimate. The seismic demand over the urban region (municipality) is assigned an average intensity. The inventory of elements exposed to risk includes buildings (dwellings), hospitals, main roads, dams and the industries, but no vulnerability data are available on those elements. Vulnerability relationships exist for buildings. Another code exists to evaluate losses for fault-controlled (i.e. linear source) earthquake scenarios (Galli et al., 2002). A new tool for probabilistic assessment and real time updating of post-earthquake losses (called ESPAS) is developed.

10.5.2. EXAMPLE URBAN EARTHQUAKE LOSS ASSESSMENTS FROM ISTANBUL

The results from the earthquake risk assessment in Istanbul conducted by the Department of Earthquake Engineering of Bogazici University (Erdik et. al, 2003b and 2004a) will be used to provide illustrative examples of urban earthquake loss assessment. Under exposure to the scenario earthquake ($M_w=7.5$ on the Main Marmara Fault) the expected number of buildings damaged beyond repair (i.e. EMS'98 damage grade $> D3$), calculated both by the intensity-based and the spectral displacement-based approaches, are provided in Figure 10.12 and Figure 10.13. Results indicate that, on the basis of two independent approaches, a total of about 35,000 to 40,000 buildings (about 5% of the total building stock) are estimated to be damaged beyond repair (complete damage). Furthermore about 70,000 buildings will receive extensive damage and about 200,000 buildings will be moderately damaged. Both of these damage groups are repairable. The similarity of both results (intensity-based and spectral displacement-based approaches) indicates confidence in the loss assessments.

The total monetary losses due to building damages caused by the scenario earthquake are estimated to be in the range of about USD 11 billion (Figure 10.14). The expected scenario earthquake casualties in Istanbul were estimated using both the intensity-based and the spectral displacement-based approaches. The results for night time population obtained for severity level 4 (death) from the spectral displacement-based approach is given in Figure 10.15. In Figure 10.16 the most risky cells in terms of search and rescue efforts are indicated. In these cells the estimated number of heavily damaged buildings is above 30, deaths are above 100 and the accessibility due to road closure is very poor. To provide an example for the assessment of urban lifeline losses the distribution of

“High Risk” bridges and viaducts in Istanbul overlaid with the peak ground velocity map resulting from the scenario earthquake is provided in Figure 10.17. For the earthquake performance assessment of bridges and viaducts the ATC-6-2 (1983) method is used.

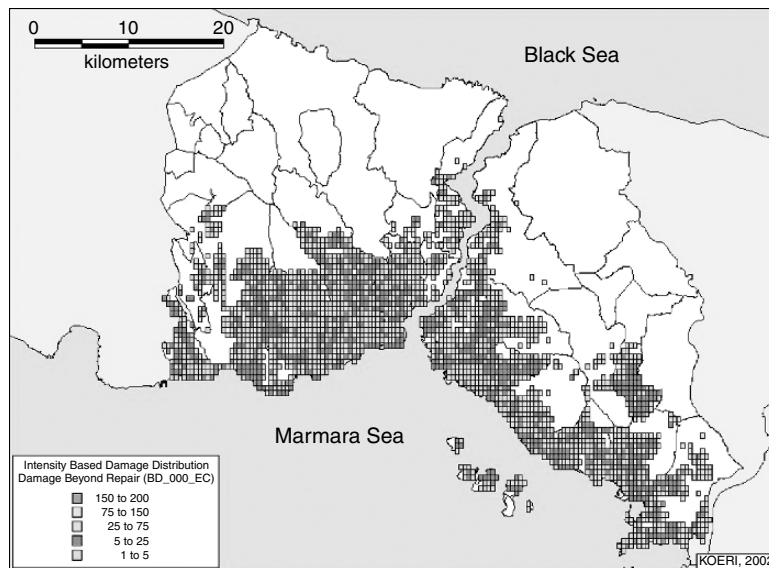


Fig. 10.12. Distribution of all buildings damage beyond repair under exposure to scenario earthquake (intensity-based loss assessment approach)

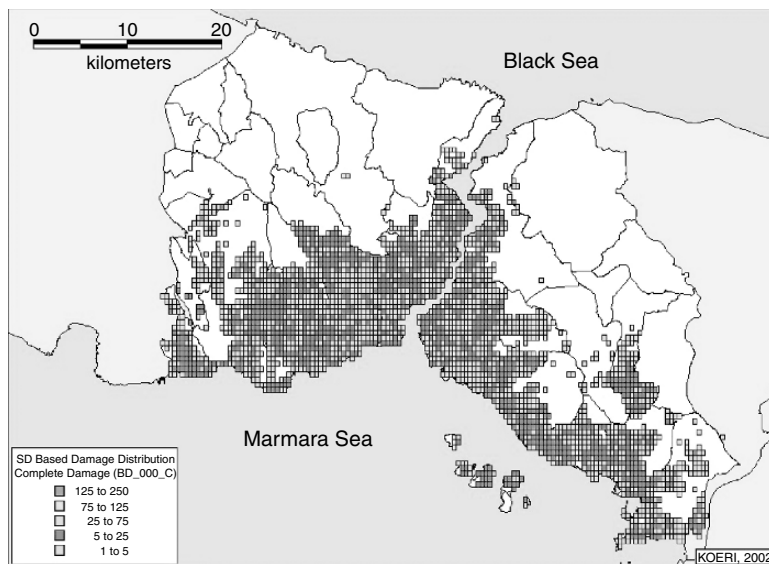


Fig. 10.13. Distribution of all buildings damage beyond repair under exposure to scenario earthquake (spectral displacement – based loss assessment approach)

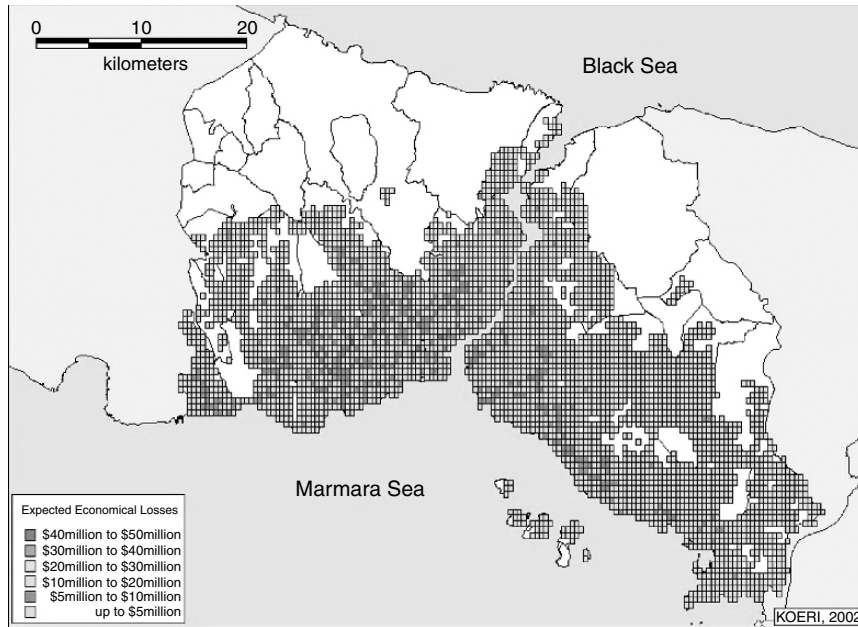


Fig. 10.14. Distribution of monetary loss due to building damage under exposure to scenario earthquake (spectral displacement – based loss assessment approach)

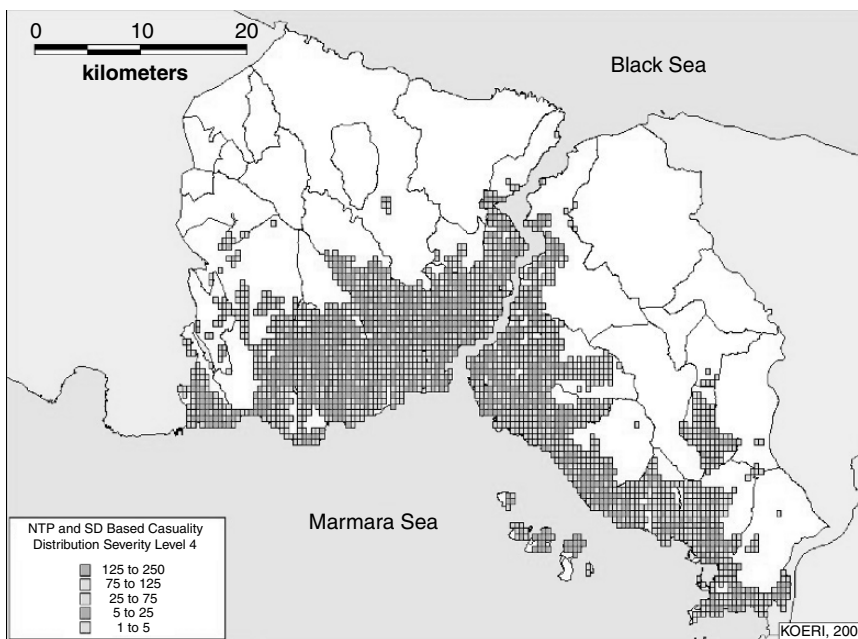


Fig. 10.15. Distribution of casualties (severity level -4) under exposure to scenario earthquake (spectral displacement – based loss assessment approach)

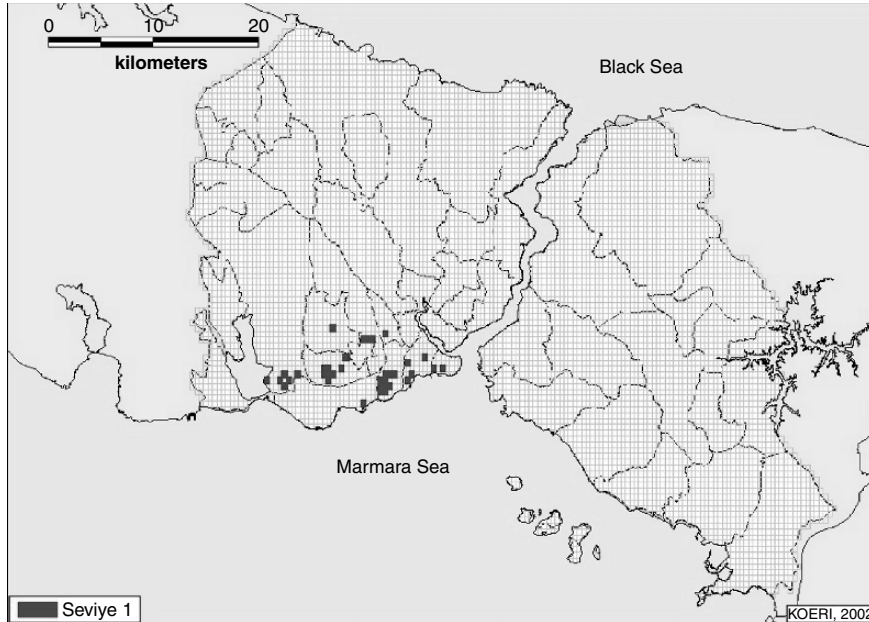


Fig. 10.16. Most risky cells in Istanbul in terms of search and rescue efforts under exposure to scenario earthquake. In these cells the estimated number of heavily damaged buildings is above 30, deaths are above 100 and the accessibility due to road closure is very poor

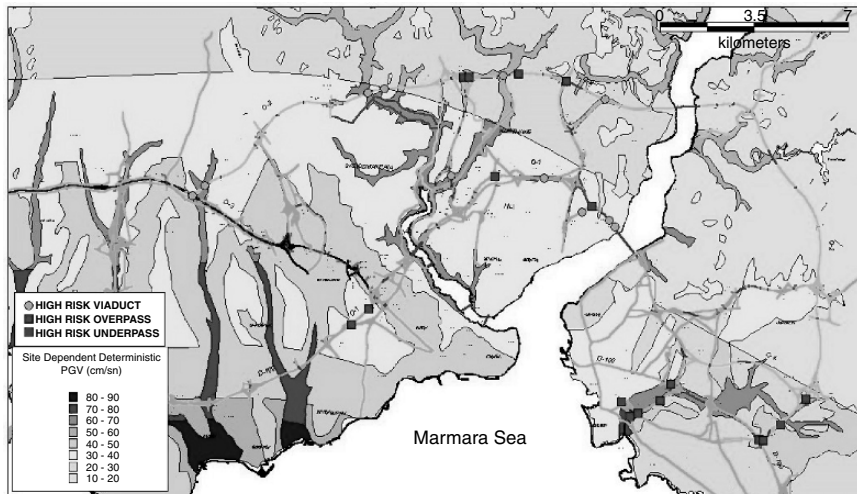


Fig. 10.17. Distribution of the “high risk” bridges and viaducts based on the ATC-6-2 (1983) method, overlaid with the peak ground velocity map resulting from the scenario earthquake

CHAPTER 11
URBAN SYSTEM EXPOSURE TO NATURAL DISASTERS: AN INTEGRATED APPROACH

P. Masure and C. Lutoff

Bureau de Recherches Géologiques et Minières, Chambéry, France

11.1. Introduction

Risk is a probability of damage during a given period of time. It includes the potential effects of correlative impacts (socio-economic impacts on employment, production, etc.) or induced effects (hazardous industries impacts, dams collapses, fires and explosions, etc.) and the human or social dimension through the analysis of "vulnerability factors" (demographic, social organizational, political, educational and cultural aspects).

During the 1980s, some authors proposed the suppression of the variable "exposure" given it is implicit in the notion of "vulnerability" and recommended the convolution of the two factors hazard and vulnerability in the expression of risk. This proposal induced some shifts in the risk assessment process. The importance of the Exposure analysis (including a value assessment) of the threatened geographic systems has been reduced to their elements at risk analysis. Now, a geographic system threatened in only a part of its territory have a global vulnerability and resistance which can't be limited to the vulnerability analyses of its physical elements at risk.

Urban-risk analyses for instance, must consider all exposed elements, be they human, material (buildings, infrastructure, lifelines, architectural patrimony, natural resources, etc.), or immaterial (culture, social fabric, heritage, image), but also the functional relations between the elements, urban activities (production, consumption, exchanges), municipal government, the relations of the city with its surrounding environment, etc. Finally, they should evaluate the chain reactions that can be caused by a weak link in the system or its limitation by multi-barriers resistance. A vulnerability diagnosis must cover the urban system as a whole, i.e. the constituting elements either taken individually or in homogeneous groups, but also the system as such, with its structure, its components, its internal functioning, and its relations with the outside environment (Masure, 1996).

It is necessary to introduce the concept of "factors of vulnerability" (Masure, 1999): accumulative process of permanent fragilities, deficiencies and limitations that pay a role in the existence of higher levels of vulnerability. The "factors of resilience", on the contrary, should put emphasis on good practices such as preparedness, social cohesion, environmental planning, rehabilitation and protection processes, responsibility, education, training, etc.

In fact, the global vulnerability of a city should be defined through three complementary analyses:

- The fragility of the physical elements at risk.
- The systemic vulnerability of the city considered as a global system.
- The factors of vulnerability and resilience of the community.

Even if a holistic approach can avoid this difficulty, we are promoting since 1996 (Masure, 1996), in the GEMITIS method, a three factors approach of risk: "Hazard", "Exposure" and "Vulnerability", with a convolution of the last two terms. The factor "Exposure" defines the system at risk (its components, elements, functions, activities, etc.) and its value (social, economic, functional, etc.).

According to this concept, it is important to analyse the existing information on physical, socioeconomic and human dimensions in order to define the elements at risk in the considered geographic unit, and to characterize the main issues and critical facilities to be protected.

According to the GEMITIS method implemented for urban agglomerations, the clear analysis of the systemic exposure of cities is a basic argument for the integration of risk reduction policies in land-use, spatial and development planning (Masure, 1999).

11.2. Characterisation of the Urban System

A city or an urban agglomeration can be considered as a system (Masure and Lutoff, 2003). To understand how this system works, we analyse the city in two main approaches (Figure 11.1). In the first approach, we define urban components and the system's functioning, its representative indicators, their characteristics as urban resources, and their vulnerability. In the second, complementary, approach we analyse the elements at risk and their distribution in the urban components. A multidisciplinary team of urban planners or geographers, architects, civil engineers, and sociologists implements both approaches.

In practice, the analyses of urban-system components and of their constituting elements take place in an interactive or integrated manner. Even though it might seem useful to present them separately in a conceptual and pedagogical framework, as earlier applications mostly concerned the exposed elements, we strongly recommend that the multidisciplinary team not carry out the corresponding studies separately.

11.2.1. THE CITY AS AN OPEN SYSTEM: URBAN COMPONENTS AND ELEMENTS INTERDEPENDENCY

An urban system can be studied from several viewpoints. It is a place where heterogeneous groups of humans congregate; a place of living; a place of economic, cultural and administrative activities; a place of power and decision-making. It also assures a certain number of services and occupies a specific place within a given geographical and decision-making environment. It is the place where different systems converge, assuming specific shapes, and marking the urban identity and image through radiating its influence.

Urban development and functioning also depend on numerous internal relations between the urban components. The damage caused by an earthquake to the same elements at risk in two different cities will not create the same disruptions and consequences for the whole system. The corresponding impact will depend on internal and external relationships, and possible functional substitutions of damaged elements. This means that risk analysis not only must consider the vulnerability of elements at risk, but should also assess the failure and resistance chains due to interdependency of

the main functions, activities, decision-making, and human behaviour in an urban system.

In conclusion, a city can be defined as an open working system, being the place of numerous social, economic, political, and physical exchanges. The urban system is not only dependent on inner flows, but also on its external environment and relationship at regional and national (or international) levels.

In Figure 11.1 the urban system is composed by 7 components. We now propose to define more precisely each one of them.

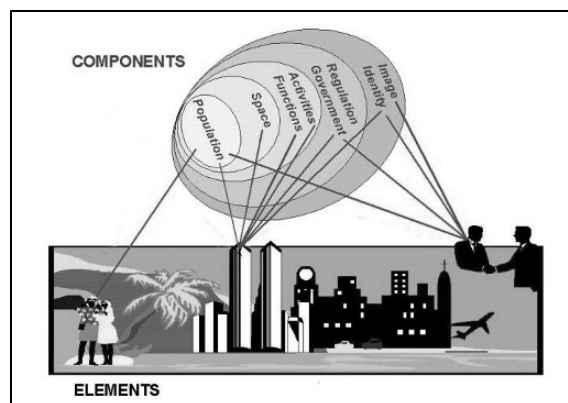


Fig. 11.1. Urban system characterisation. Relations between elements at risk and components

11.2.2. CHARACTERISING THE URBAN COMPONENTS: A GLOBAL APPROACH TO THE CITY

The global analysis of a city aims at identifying the remarkable characteristics that form the basis of an urban identity and are the mainsprings of the city (Lutoff, 2000). Underlain by risk-management preoccupations, this sub-approach should help in defining the characteristic entities of each component. Even though most of these entities can be considered as constant, regardless of the city, others vary from city to city. Table 11.1 lists the various components and entities that we used for interpretation of Nice data.

As part of a systemic approach, a city is characterized by seven components that refer to its human content, its physical space, its operation, its activities, its government, its identity, and its outside influence.

These seven components are defined with regard to the aim of risk analysis:

1. Population: inhabitants (age, social level, etc.), workers, tourists, transients, demographic distribution, demographic growth, etc. The inhabitants are the city's heart and a part of the city's vulnerability.
2. Urban space: natural environment (air, water, soil, sub-soil, biotope), built-up environment (buildings, infrastructure, lifelines, etc.), and policy environment

(spatial organization, land-use, urban fabric and natural features, natural resources). It is the physical support of the city, and the first hurt by an earthquake.

3. Urban functional activities and services bear on the main urban services: housing, supply, sanitation, transportation, communication, social and emergency functions, presenting different levels of adaptation to seismic threat.
4. Urban activities: economic (production, consumption, exchanges), administrative, and cultural activities that are variably vulnerable to earthquakes.
5. Urban government and actors: institutional, socio-economic, and political organizations, urban actors, urban policy (choices of growth and development), decision-making processes with special emphasis on emergency management.
6. Identity and culture: social cohesion, local culture and history (with special emphasis on the culture and memory of risks), symbolic images and representations, etc.
7. External radiance: symbolic features, external image and representations, regional position, etc.

Table 11.1. Some basic elements at risk in Nice

Component	Entities / Indicators
Population	- Number of residents - Number of workers - Number of visitors/day
Space	- Natural - Built-up (buildings, infrastructure)
Functions	- Housing - Shelters - Supply (energy, water, etc.) - Transportation - Telecommunication - Emergency resources - Maintenance
Activities	- Business-Trade - Administration - Culture-Leisure
Government	- Decision power - Emergency managers
Identity	- Identity-Culture
Radiance	- External relationship - Image

Finally, the analysis should consider the city's growth, its evolution through space and time, and the necessary adaptations in terms of spatial organization of the environment and of collective organization. This aspect is of particular importance in the search for solutions that will reduce urban vulnerability.

11.2.3. AN ANALYTIC APPROACH OF THE URBAN ELEMENTS AT RISK

In an analytical approach, an urban system can be characterized by three –material, human, and immaterial– groups of elements that are potentially exposed to natural risks.

11.2.3.1. *Material (or physical) elements*

By material elements are meant:

- Buildings: Housing; Economic activity units (industry, commerce, services); Administrative activity units (governmental, municipal, social, judicial, financial); Cultural and sports activity units; Urban-function units (health, safety, education).
- Main infrastructures and roads: Transportation terminals (airport, port, terrestrial, etc.); Civil engineering infrastructures; Highways, roads, streets, bridges, etc.
- Lifelines and reservoirs: Energy systems (electricity, gas, oil, etc.); Drinking-water system; Sewage system; Waste-disposal system; Telecommunications system; Radio system; etc.
- Patrimony: Natural resources (woods, waters, etc.); Historical buildings; Other physical symbols.
- Areas or geographic units identified as being homogeneous according to the urban frame.

11.2.3.2. *Human elements*

By human elements are meant:

- City users: Citizens, visitors (tourists, etc.), workers, etc.
- Urban actors: Institutional and socio-economic managers; Political and economic actors; Decision-makers (economic, associations, etc.); Public-service representatives; Health and crisis-management specialists, etc.
- Outstanding personalities: Key political figures (mayor, governor, etc.); Captains of industry; Well-known artists; etc. Such persons can play determinant roles in city life, either directly such as the mayor, or indirectly such as captains of industry.

11.2.3.3. *Immaterial elements*

Immaterial elements correspond to certain symbols or representations of the city, related to inhabitants, its image, its culture, or to its social fabric or history. One place will be considered as particularly young and dynamic, whereas another will be known for its calm and good life. Such immaterial and subjective –though quite real– elements share in a city’s development and its position in relation to the outside world. Just like the other elements, they are vulnerable to a major disaster such as an earthquake.

- Identity: culture, history, social cohesion, preparedness.
- Radiance of the system: projected image, external relationship.

To evaluate the consequences of an earthquake, the proposed method aims at identifying the main issues (essential elements) for the functioning and development of an urban system. This refers to the elements of “significant value”, in terms of social or utility value for city operations. This ranking is necessary for fine-tuning the vulnerability analyses, by subjecting the main issues to in-depth analysis and limiting the secondary issues to a rapid evaluation.

Nice will serve as an example to explain the method. In this city the elements at risk are defined as presented in Table 11.2.

The aim of the Urban System Exposure approach is to evaluate the role of these elements at risk in the urban system’s functioning. To do it, it is necessary to use some adapted tools.

Table 11.2. Some basic elements at risk in Nice

Material elements	Human elements	Immaterial elements
Surface area: 72 km ²	350,000 inhabitants	Tourist capital of the French Riviera
20,000 blocks with 40 to 60,000 buildings	3 millions tourists/year	Artistic centre with an International Painting School
200,000 housing units		The “Sophia Antipolis” high-technology centre of international standard
16,000 firms		

11.2.4. URBAN DATA COLLECTION AND ORGANISATION INTO THE GIS

The data obtained through the analysis of the urban system has to be organized in a GIS for optimum implementation of the subsequent steps:

- Value analysis of the elements at risk.
- Assessment of element interdependency and vulnerability factors.
- Vulnerability analysis.
- Implementation of earthquake scenarios.

Figure 11.2 illustrates the process; hereafter, we explain the data characteristics and organization for easy integration within the next phases of risk analysis.

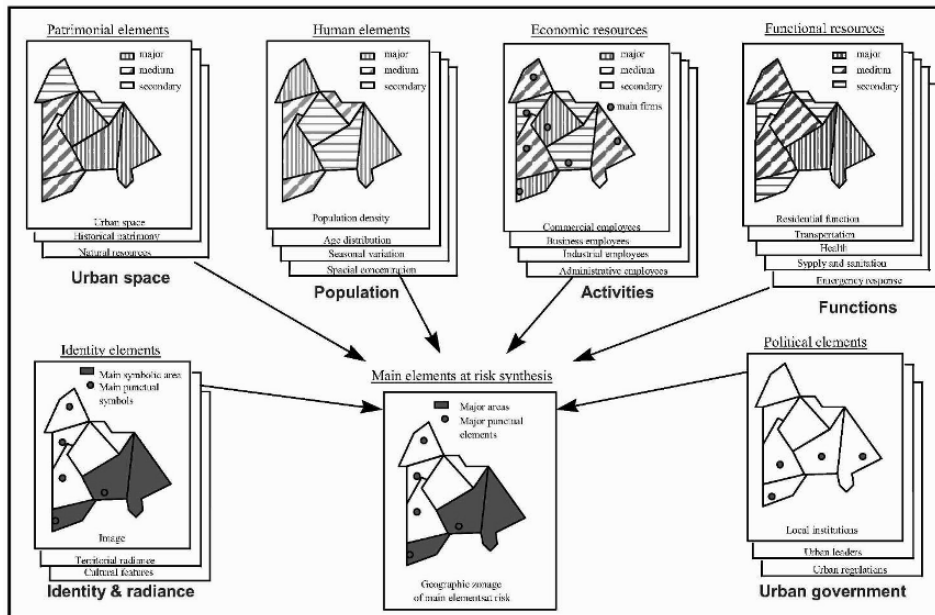


Fig. 11.2. Schematic urban data organisation through GIS

11.2.4.1. Elements' formats

The elements at risk must be represented as geo-referenced units. The question is how to represent and evaluate all the elements that make up a city, apart from the question of whether they really have to be represented individually.

A first answer to these questions involves appropriate geographic formats of urban elements. We can distinguish three main formats that can be directly included in the GIS:

- Point elements: buildings, lifelines nodes, etc.
- Linear elements: lifeline networks, roads, etc.
- Polygonal elements (areas).

The last format needs to be precise. It is not necessarily pertinent to show all elements individually; some can be identified through statistically representative samples of geographic units. This concerns population concentration, housing (construction types), activities, natural or cultural resources, etc. The corresponding statistical analysis has suitable forms that can be chosen by specialized teams.

The definition of geographic units (or homogeneous units of urban fabric) is a very useful support for data integration (Figure 11.3). There are two main approaches or techniques to be used for their identification:

- Geographic or urban-planning expertise (environment, history, etc.) for defining landscape units.
- Satellite-image or air-photo analysis for defining morphologic units.

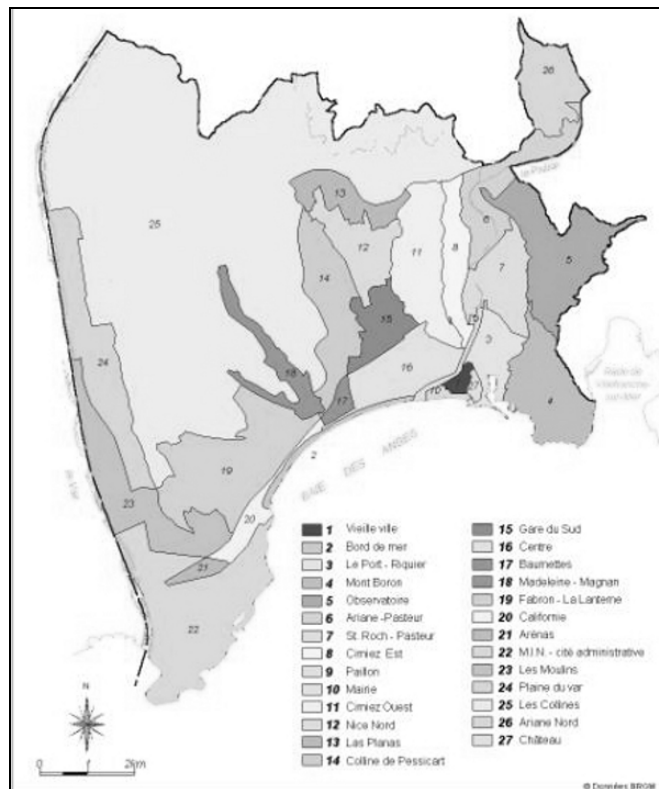


Fig. 11.3. Homogeneous units of urban fabric in Nice

The characterisation of urban units emphasizes:

- Topography and natural environment.
- Roads, streets, and the main organisation and features of the infrastructure fabric.
- Construction types.
- Types of activities.

11.2.4.2. *The GIS organisation*

The data are integrated in several layers of a GIS database. The GIS structure depends on the available data formats and will be different for each city.

To facilitate the treatment of such data, we recommend to group all point data in a single layer with a coding that allows keeping the information on the nature of such points:

- Civil engineering works, roads, railways.
- Transformers, gas-distribution sources, etc.
- Reservoirs, water-treatment or waste-incineration plants, drinking-water wells, etc.
- Telephone switchboards
- Hospitals, clinics, first-aid centres, etc.
- Decision-making centres.
- Symbolic elements.
- Main administrative units and buildings receiving public.
- Education centres, cultural centres, etc.
- Main companies and industrial sites.

Each layer must contain:

- Identification of the element: ID / Name / Type code.
- Type of collected data: e.g., number of inhabitants for the population, number of jobs and financial turnover for an industrial installation.
- Data needed for analysing the value of elements, or resulting from this analysis (e.g., global value of each element by period), which will be explained in the next chapter.

The final structure of the layers is guided by the steps taken for analysing the value of elements as explained in the next chapter.

Table 11.3 gives the GEMITIS Nice GIS structure as an example: it contains 19 main layers of which 11 are polygonal, 7 linear, and 1 isolated. Sanitation, gas, electricity, drinking-water networks, railways, roads, and harbour quays were available in linear numeric format. Some the files of geo-referenced elements were collected from public establishments and firms. This directly provided 7 data layers in linear format and we had to integrate isolated data points in only one specific layer. The municipality further provided some information integrated on the district scale (especially census data).

The other layers were created through our fieldwork. Some types of data, in particular patrimonial and economic ones, were not collected building per building, but rather for specific geographical units. From the above it is clear that the GIS structure must be adapted to the geographic format of available data and to the precision level of the data collected.

Table 11.3. GIS structure for GEMITIS Nice

Layer identifier	Geographic form	Data references
ARTISAN	Zonal	Human, economic, functional
FONCTIO	Zonal	Human, economic
FORETS	Zonal	Natural resources
SYSHYDRM	Zonal	Natural resources, functional
PROFLIB	Zonal	Human, economic
RESIDENT	Zonal	Human, functional
SCTCOM	Zonal	Human, economic, functional
SCTSERV	Zonal	Human, economic, functional
TOURISTE	Zonal	Human, functional
ZHABITAT	Zonal	Financial, functional
ZIMAGE	Zonal	Financial, symbolic
ASSAINISS	Linear	Financial, functional
GDF	Linear	Financial, functional
LEDF	Linear	Financial, functional
PORTS	Linear	Financial, functional
POTAB	Linear	Financial, functional
VOIEFER	Linear	Financial, functional
VOIRIE	Linear	Financial, functional
POINTS	Point	Human, specific physical elements (critical facilities, etc.), financial, economic, functional, decisional, symbolic

11.3. Valuation and classification of elements at risk

Once the data have been collected and the GIS organization of the elements at risk has been completed, the method proposes to estimate their values through different indicators (qualitative or quantitative values).

11.3.1. REFERENCE VALUES, MEASURE UNITS, AND INDICATORS

Each of the elements at risk is part of one or more components of the urban system (Figure 11.1) ; for each of these, it is characterised by its "importance" or relative value.

We have defined eight reference values related to the urban components:

- Financial: money value (market prices).
- Human: number of persons within it.
- Environmental or patrimonial: natural resources and urban patrimony it represents.
- Economic: number of jobs involved and turnover (or financial weight) of all activities within it.
- Functional: user value for urban functions (or collective usefulness).
- Strategic: emergency-response usefulness.
- Decisional: decision-power influence and capability.
- Symbolic: representation and image value, radiance.

These eight reference values are expressed by several indicators corresponding to relevant measuring units. For each indicator and depending on available data, the element's value is expressed in quantitative or qualitative units.

As an example, assessment of the symbolic weight or value of an element is not so easy; we propose to express this indicator through a qualitative scale such as:

- Major symbol: known throughout the city.

- Medium symbol: only known by inhabitants and regular visitors.
- Secondary symbol: known in a neighbourhood, but not outside.

For Nice, each GIS layer has been informed as shown in Table 11.4.

Some quantitative data can be difficult to classify, such as tourist flow in Nice. The city receives each year about 3 million tourists, most of them in summer. We know that, in global terms, the city has around 100,000 tourists every summer day, but we have little information about their geographical location at any time. This meant that we had to rely on local knowledge for identifying the most visited areas and to assign a percentage of tourists for each corresponding geographic unit.

Table 11.4. Indicators selected for the different layers

	Resident	Worker	Visitor	Building	Resource	Business	Administr	Culture_leisure	Housing	Supply	Emergency	Transport	Communication	Maintenance	Decision	Identity	Radiance
Artisan			x			x									x		
Assainis				x						x							x
Fonctio		x															
Forets					x												
GDF				x						x							x
Ledf				x						x							x
Pionts	x	x	x	x	x	x	x	x	x	x	x	x	x	x	x	x	x
Ports				x								x					x
Potab				x						x	x						x
Proflib		x				x											x
Resident	x																
Sctcom		x	x			x				x							x
Sctserv		x				x											x
Sishydrm					x					x	x						x
Touriste			x						x								
Voiefer				x								x					x
Voirie				x								x					x
Zhabita				x					x								
Zimage																x	x

So, every element at risk is evaluated through one or more indicators depending on its nature. However the objective of the method is to give a numerical expression of the global value of these elements for the urban system as a whole.

This global value of an element at risk depends not only upon its financial value or its physical and human content, but also upon its usefulness in the urban system at a given time. This indirect value varies for each situation. For instance, the usefulness of a school is great in normal times, but reduced for crisis management.

We propose an evaluation of the global value of elements at risk in three main periods (Figure 11.4): the normal period (or development period of a city), crisis period due to an earthquake (days to weeks) and recovery and reconstruction period after the disaster (months to years).

We propose now to explain how we transform the evaluation based on 8 indicators in a global value corresponding to one specific period.

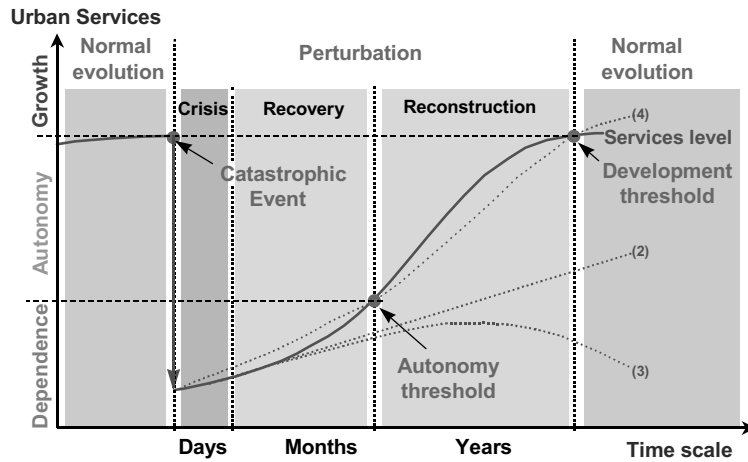


Fig. 11.4. Referenced period for evaluation

11.3.2. VALUE ASSESSMENT OF THE ELEMENTS AT RISK

In the beginning of the evaluation, one particular element is affected by one or more values, depending on the indicators selected as pertinent. Figure 11.5 gives an example of evaluation for a commercial zone.

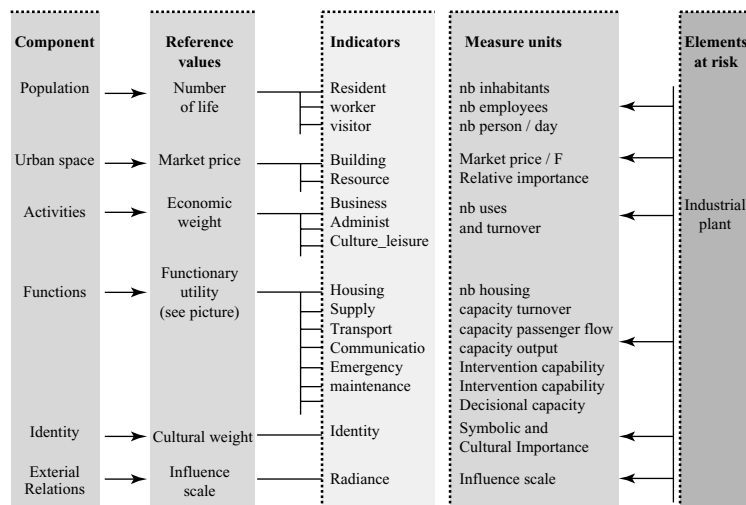


Fig. 11.5. Evaluation process

We can see here, that the global value synthesises the importance for urban functioning of a particular element. To calculate this global value, the different values affected to the element (quantitative or qualitative one) must be transcribed onto a common relative value scale, using for instance only 4 levels represented by numbers from 0 to 1 (0 ; 0.3 ; 0.5 ; 1). An element considered as essential in the urban economy for instance is

represented in economic evaluation by the highest value (= 1). However, an element that has no economic significance is given the smallest value (= 0).

For indicators that are connected with qualitative measuring units, the attribution of relative values consists in a numerical transcription of these values. This transcription can take place directly during data input. The symbolic value of an element will thus be expressed as:

- 1 = Major symbol: known throughout the city.
- 0.5 = Medium symbol: only known by inhabitants and regular visitors.
- 0.3 = Secondary symbol: known in a neighbourhood.
- 0 = no symbolic representation.

However, the attribution of relative values of quantitative origin should be based on statistical analysis. The different elements related to a same indicator, and thus evaluated with the same measuring unit, are assembled in a statistical distribution (Figure 11.6).

This is the subject of descriptive analysis, i.e. decreasing ranking of the cumulated relative values of the various data layers, in order to visualise the discontinuities within the distribution; these discontinuities are then adopted as the class thresholds for determining the relative values.

The definition of the threshold for quantitative classes could be based on different methods. In Nice's study, we choose to analyse the discontinuities in the statistic series, based on distribution diagrams. Figure 11.7 identifies the discontinuities selected as representative thresholds for building price valuation.

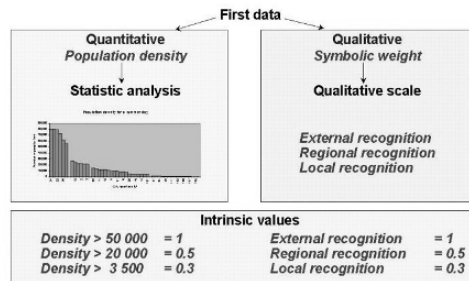


Fig. 11.6. From first data to relative values

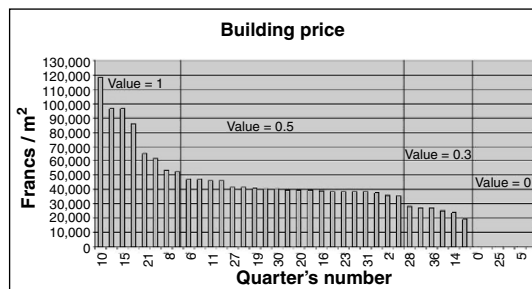


Fig. 11.7. Threshold definition for building price valuation

It is evident that the proposed method comprises a part of subjectivity in the determination of thresholds limits. Other methods of statistical discrimination can be envisaged in order to reduce it.

At the end of the value analysis, each element at risk has thus been given one or several relative values (between 0 and 1), depending on its nature and the indicators selected for its evaluation.

According to the situation of the considered city (normal, crisis, or recovery period), the relevant indicators are selected as expressed in Table 11.5.

Table 11.5. Reference values and indicators per period

Components	Reference values	Indicators	Periods		
			Normal	Crisis	Recovery
Population	Human : <i>Nb of lives</i>	Nb residents Nb workers Nb visitors/day	✓ ✓ ✓	✓ ✓ ✓	✓
Urban Space	Financial : <i>Market price / Patrimony</i>	Buildings-Infrastr. Natural resources	✓ ✓		
Functions	Functional : <i>Social utility</i>	Housing Shelters Supply Transportation Telecommunication Emergency resour. Maintenance	✓ ✓ ✓ ✓ ✓ ✓ ✓	✓ ✓ ✓ ✓ ✓ ✓	✓ ✓ ✓ ✓ ✓ ✓
Activities	Economic weight (<i>nb of firms, employs, turn over</i>)	Business-Trade Administration Culture-Leisure	✓ ✓ ✓		✓ ✓ ✓
Government	Decision capability	Decision power Emergency managers	✓ ✓	✓ ✓	✓
Identity	Symbolic : <i>Cultural weight, Image</i>	Identity-Culture External relations Image	✓ ✓ ✓	✓	✓ ✓ ✓

Adding the different values selected for each period gives the global value of the element.

Table 11.6 gives a detailed evaluation for the commercial zone in Nice for the normal period taken as an example.

We can propose a generalisation of this global value estimation:

$$\text{Global value} = \sum (\text{Relative values selected for each period}) \quad (11.1)$$

At the end of the valuation, each element considered in the analysis, is characterised by one or several relative values and three global values: one for the development period, one for the crisis period, and the last for the recovery period. So, this valuation method allows a comparison between two elements in terms of importance for the city, even if they are not evaluated through the same indicators.

Table 11.6. Commercial area valuation

Indicators	Measures		Values		
			Normal	Crisis	Recovery
Workers	Employees	50 000 persons/km ²	1	1	1
Building			0,5		
Business	Employees	50 000 persons/km ²	1,0		1,0
	Turnover	1,4 billions €/km ²			
Supply	Food supply	ad hoc - Local	0,5	0,5	0,5
Radiance	Influence area	Regional	0,5		0,5
<i>Global values</i>			<i>3,5</i>	<i>1,5</i>	<i>3,0</i>

11.3.3. CLASSIFYING ELEMENTS AT RISK AND IDENTIFYING THE “CRITICAL ISSUES” OF THE URBAN SYSTEM

According to the form of the objects at risk (point, linear, or area), their classification may define significant objects (points or lines) and significant or critical zones.

Calculating the global value of individual or grouped elements at risk enables their classification into three issue levels of the urban system:

- Main issues, essential for the city and whose loss would be a major handicap (they are also called vital issues, strategic issues, or essential issues).
- Important issues, but whose loss does not jeopardize the basic functioning of the city.
- Secondary issues, whose loss can be considered as less fundamental for the city.

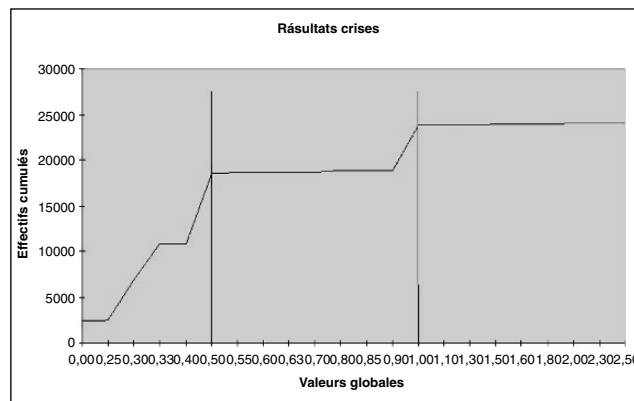


Fig. 11.8. Crisis global values distribution diagram

This classification implies a threshold definition specific to each city to determine the limits of each class. The global values assigned to the elements, constitute the statistical reference distribution in the same manner as for determining the class thresholds of the indicator values. As before, the identification of the discontinuities forming the class thresholds is based on a descriptive analysis of this distribution. As an example, Figure 11.8 gives the process used to define class thresholds for the crisis period in Nice.

This makes it possible to define a list of the main, important, and secondary issues for each period of urban functioning. The main issues identified for Nice are presented in Figure 11.9.

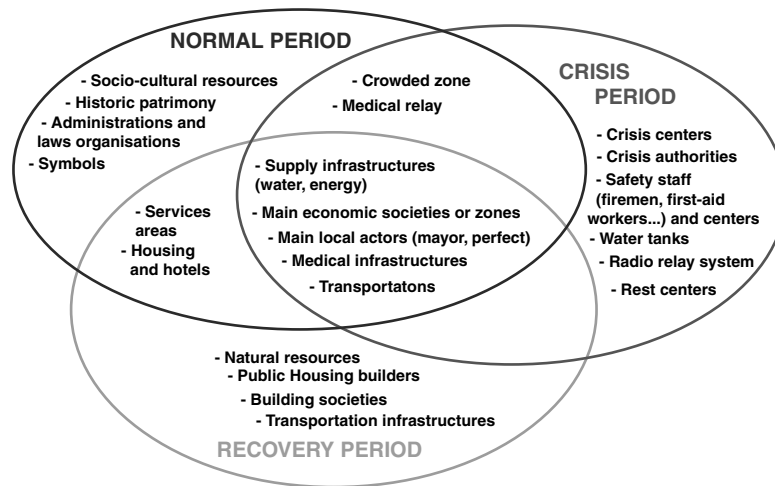


Fig. 11.9. Critical elements at risk in Nice's urban system

Shown as a map, this synthesis presents the main, important, and secondary risks for each category of elements. The synthesis maps thus show for each period both the main point and linear issues, and the main geographic-area issues.

This urban system representation gives an image of the areas concentrating the most important elements for urban functioning depending on the period. It has to be validated by local actors with an intimate knowledge of the city. Crossing these synthesis maps with seismic-zonation or vulnerability maps provides a spatial representation of the sensitive points or areas in the urban space. This GIS function gives additional information elements for completing the earthquake-risk scenarios. Beforehand the interdependence between the elements should be studied, identifying those that might have a particular sensitivity for the overall functioning of the city, such as weak points or failure in element chains.

One of our aims in Nice's case was to validate some hypothesis of sensitive points or areas in an urban system. That's why we have developed the value analysis as a quantitative approach of element at risk classification. It has been proven here that some supposed major elements are really sensitive for urban system functioning.

Based on these results, it is possible now to simplify the analysis. The different classes of elements (given on Figure 11.9) provide the list of elements which have to be considered to make the Urban System Exposure Assessment. This list, mixed with the homogeneous units map, can be taken as a base of the evaluation concerning another city, with a complement of analysis through some experts' interviews.

11.4. Analysis of vulnerability factors and element interdependency

Urban development and functioning depends on numerous internal relations between its elements and components, through sector-related sub-systems. Damage to certain elements can cause breakdown in the operating chain of such sub-systems or of the urban system as a whole. Other elements may then assure a substitution function, for which reason it is necessary to analyse all possible dysfunctions and defence responses of the city, i.e. to identify the critical elements or configurations that might cause breakdown chain reactions, or, conversely, that might strengthen the system because of their substitution role in the city's functioning.

The double – global and analytical – approach of an urban system enables tackling of the work in a coherent manner. We already saw that the corresponding analyses permit defining the socio-functional (or resistance) vulnerability factors of the urban system. This analysis must be completed by a detailed examination of the role of such elements in the city's functioning and of their interdependent relation (chain reactions, resistance, substitutions). This identifies the weak points of the urban system and its defences. Identification of the main issues of the city (significant objects and zones) will thus be completed by that of the sensitive elements or configurations for urban functioning. This step is necessary to ensure that we do not ignore some important objects. It is a major aspect of the global vulnerability assessment of the city which needs the physical fragility analysis of the elements at risk and the characterisation of weak points and resistance of the system as a whole (Figure 11.10).

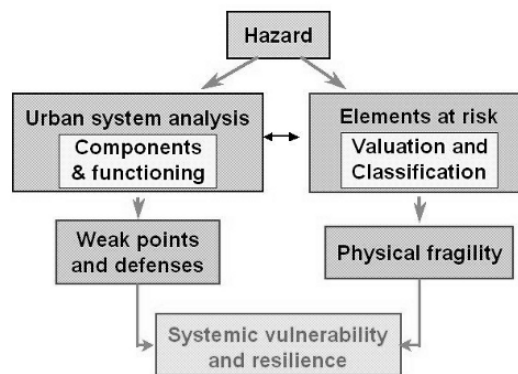


Fig. 11.10. Bases of the global vulnerability assessment

11.4.1. ANALYSING DYSFUNCTION AND DEFENCES OF THE URBAN SYSTEM

It is necessary to assess the failure and resistance chains caused by the interdependency of the main functions, activities, decision-making, and human behaviour in the urban system. This task has to be realised with and by the lifelines operators (electricity, sanitation, water distribution companies), through interviews or specialised approaches.

The ranking of significant objects and zones leads to a systematic analysis of potential dysfunction in case of a breakdown in one or more elements at risk. Copied exactly

from the procedures for breakdown analysis in the industrial world (fault-tree or events-tree analysis), the grid proposed here permits to take an inventory of:

- The different types of dysfunction that might affect a given element of the system.
- The causes of such dysfunction.
- Their duration.
- Existing security systems.
- Potential consequences for other elements or for the system as a whole.

Table 11.7 shows an example of this type of analysis for the health function.

Table 11.7. Analytical grid for dysfunction of the health function

Elements	Possible dysfunction	Initial causes	Duration of the dysfunction	Back-up security systems	Probable consequences
HOSPITALS	Decreased emergency room capacity	Damage to the buildings	Time needed for repairing the damage	Transfer to other hospitals or clinics	Slowdown in medical care. Increase in human loss of life
		Electricity- and water-supply breakdowns	Time needed for repairing networks and damages apparatus	Internal systems: water tanks, generator sets, etc.	Impossibility to provide medical care. Increased loss of life.
		Staff physically affected	Several hours Time needed to replace missing staff for duration of the crisis (or less)	Recalling absent staff, or calling in outside personnel Replacement staff, calling in help from other nearby or distant hospital centres	Slowdown in medical care. Increased loss of life. Slowdown in medical care. Risk of aggravating human traumatisms during transfer to other hospitals
		Inflow of slightly wounded persons	Duration of the crisis (several hours to days)	Direct slightly wounded persons to clinics and medical district centres	Slowdown in medical care. Increased loss of life
CLINICS, MEDICAL DISTRICT CENTRES	Decreased capacity for handling slightly wounded patients	Damage to the buildings	Time needed for repairing the damage	Transfer to other clinics or nearby or distant medical centres	Slowdown in the recovery time for the populations. Congestion in the secondary medical services
		Staff physically affected	Time needed to replace missing staff for duration of the crisis (or less) Several hours to days	Other clinics or nearby medical centres Recalling absent staff, calling in help from NGOs	Slowdown in aid to slightly wounded patients and persons requiring psychological help Recovery difficulties for part of the population
				Physical damage to access means	Time needed for creating access to the stricken parts of the city
MOBILE MEDICAL INTERVENTION SYSTEMS, RED CROSS, ETC.	Field intervention difficulties for first-aid teams				

By extrapolating this example, the grid can be applied to the main issues during a crisis period. This highlights any possible dysfunction in emergency management after an earthquake. Where the analysis applies to issues during a normal period, medium to long-term dysfunctions appear as direct consequences of the event.

This method identifies the “weak points” and “resistant points” of the urban system, leading to improved defence systems. It is one of the elements for analysing the global vulnerability of the system. By extending this analysis, crisis managers and urban developers receive highly useful information (Figure 11.11). Decision-makers need this sort of information to understand the global risk concerning their city and to improve preventive effectiveness.

11.4.2. IDENTIFICATION OF SENSITIVE ELEMENTS OR CONFIGURATIONS

Global analysis of the urban system gives information on urban vulnerability factors. This approach can be complemented by feedback from crisis experience (e.g. Northridge, Kobe, Izmit), and potential vulnerability factors can be determined for each urban component:

- Urban space and environment: urban density; fire propagation factors (accessibility, street width), etc.

- Population: spatial concentration and socio-cultural characteristics (age, risk understanding, etc.).
- Main activities and employment: nature of the activities and size of the structures; external dependence.
- Urban functions and services: external dependence, concentration; substitution capability.
- Urban government and actors: the knowledge, perception, and consciousness of potential risk and its consequences.
- City identity and external image: risk culture awareness; mass-media sensitivity.

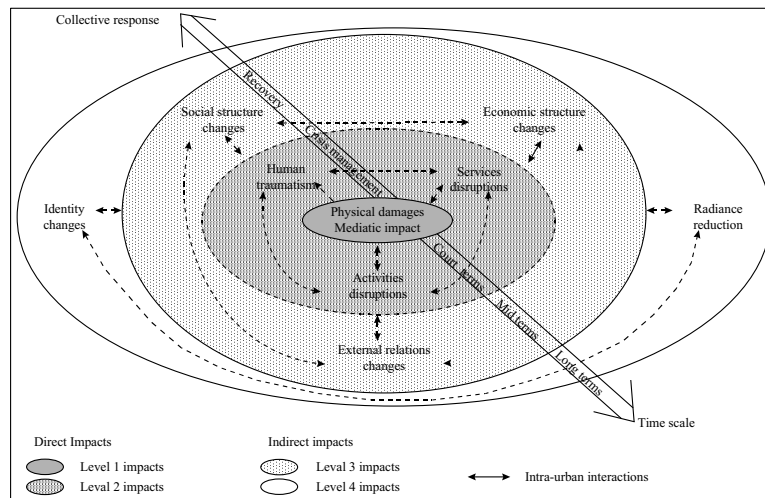


Fig. 11.11. Urban disruptions faced to an earthquake

Certain sensitive sites require a specific analysis because of their potential risk-generating nature. Examples are the transport of dangerous substances by road or rail, tinder-dry forests, the presence of industrial complexes (especially with environmentally sensitive installations), tank farms, gas-bottle depots, energy networks (pipelines, high-tension lines, etc.), harbour installations, airports, train stations, and public buildings and especially those that receive large numbers of persons such as sports stadiums. In the same manner, all elements that could serve to mitigate such hazards, or which would serve as substitutions in case of breakdown of other elements, must be analysed in terms of sensitive issues or objects for the urban system.

This analysis completes the assessment of main issues. It focuses on the main urban resources for development and functioning, but also identifies and localises sensitive objects. Combining the maps of main issues and of hazard zonation, this urban analysis opens the way to scenario development, including an evaluation of potential disruptions and mid or long term perturbations due to physical damage.

11.5. Validation phase with the local actors

The main issues defined with the proposed method have to be validated and, if necessary, adapted through a critical approach with local actors. This can be the mayor

or a member of the municipal council, directors of technical services, economic leaders, persons in charge of civil defence and of public services, university professors (urban planners or geographers), and representatives of local associations. The preliminary results obtained through the Urban System Exposure method are compared with the experience and ideas of the primary interested parties, which should also facilitate acceptance of the project by the latter.

It is suggested first to organize some meetings for presenting the compilation maps and lists of main issues (classes and categories of elements at risk), thus obtaining a first collective reaction from the interested parties. As a second step, they are given two *questionnaires*, one on the question of 'main issues', and the other touching upon the subject of functional vulnerability of the urban system, which should help them to clarify their answers.

Questionnaire on main issues

The aim of this questionnaire was the clarification of the main results of the USE method. The collected data helped in refining the evaluation of main issues and in proposing the most suitable solutions in terms of risk prevention.

Two sets of questions were proposed. The first concerned specifically the main points, networks, and highways identified as 'main issues'. The second concerned the maps for ranking of homogeneous geographic units (significant zones) for normal and crisis periods.

Questionnaire on vulnerability

This questionnaire concerned:

- *The population: access conditions to the different neighbourhoods in case of damage to buildings, to the areas where tourists concentrate, and in terms of commuting to and from work.*
- *The physical medium: land ownership, the location of Dangerous Materials Transports, and the specifics of the climate.*
- *Economic activities: level of competition, and dependency relations.*
- *Functional activities: security, first aid, health, urban functions, public transport, and communications.*
- *The decision-making process in crisis periods.*

Some remarks

The services had problems with making absolute judgments, preferring to reason from the premise of an earthquake scenario. The validation step thus had to be preceded by the rough outline of a crisis scenario. The request of ranking the issues showed that many persons confused the terms 'issue' and 'vulnerability'.

It was thus not always possible to obtain a strict validation of our ranking of issues from the questionnaires. They did, however, provide highly valuable information for drawing up the scenarios, clarifying vulnerability factors and potential dysfunction situations.

Finally, some of the answers on the questionnaires were divergent, in particular concerning the issues directly touching professional or personal preoccupations of the interrogated persons, which modulated their evaluation. The validation phase thus forced them to realize certain realities that had hitherto been repressed.

The meetings with local actors and decision-makers should emphasise:

- Development issues.
- Vital and strategic issues.
- Autonomy issues.
- Cultural issues.

Involving the local actors should ensure that not a single element that locally is considered important will be left out of the analysis. It also helps in verifying the reality of the thresholds retained for the indicators and, if necessary, in their redefinition.

The individual remarks and answers are then analysed and integrated, before comparing them to the earlier obtained results. In case of convergence of opinion the first results can be confirmed, but in case of doubt the initial results will either have to be revised, or they may require further contact and data.

As an example, we present hereafter some clarification on the *modus operandi* used in the GEMITIS Nice application.

In conclusion, this validation phase turned out to be not only necessary, but it also contributed very useful additional data that, in some cases, went beyond the initially set objectives.

11.6. Conclusion

Evaluating the exposure of an urban system with the GEMITIS method permits:

- To rank the physical vulnerability analyses for a city, in addition to making a complete assessment of vulnerability and reliance.
- To develop a complete earthquake scenario generation and impact assessment.

11.6.1. A COMPLETE VULNERABILITY ASSESSMENT

The Urban System Exposure analysis identifies the main, important and secondary issues of the urban system and can be used to guide the physical vulnerability analyses of an urban system:

- Main issues: a deterministic vulnerability analyses is required for the main issues of the urban system (only for point and linear elements that are considered essential or critical for the system).
- Important issues (significant zones and important point or linear elements): they need a statistical approach, based on the vulnerability analysis of representative samples.
- Secondary issues: the vulnerability of secondary elements can be based on a global (or analogical) assessment.

However, vulnerability studies of an urban environment should not limit themselves to understanding its physical fragility. A more in-depth understanding of the vulnerability factors, of the dependency relations between elements, and of the chain reactions (weak points and defences of the urban system) as developed in GEMITIS, also permits

estimating the global vulnerability of the urban system and on the importance of the city to its inhabitants.

11.6.2. A TOOL FOR EARTHQUAKE SCENARIO GENERATION AND IMPACT ASSESSMENT

Seismic-risk analyses are based on the development of predictive scenarios based on one or more seismic reference events. The first step of the risk analysis consists in evaluating the immediate direct impact provoked by the earthquake; all existing methods permit the completion of this phase.

The second step measures the disturbance caused by the immediate impact of the earthquake on system operations (chain reactions, substitutions, resistance) and by the resulting crisis (fires, explosions, panic, etc.). This makes it necessary to evaluate the deferred direct impact (physical damage, human loss), and the short-, medium-, and long-term indirect effects (economic and functional impacts). Most existing methods cannot handle this second approach, but the GEMITIS method was designed for it.

The evaluation of direct impacts allows proposing protection measures (reinforcement of buildings, information about safety instructions, etc.). However, this first stage gives little information for improving preventive effectiveness. Neither does it give any information on the indirect consequences of an earthquake. Nevertheless, decision makers need this sort of information to understand the global risk concerning their city. Their decisions depend on the risk representation provided by the scenario.

11.6.3. A GUIDE FOR PREVENTIVE PLANNING AND RISK REDUCTION PRIORITIES

The good practice aims to establish a risk-reduction and environmental-protection policy integrated into the urban planning and development schemes at national, regional and local levels, promoting an appropriate legislative and standards framework. The four steps of the risk management plan are:

1. Risk assessment (individual perceptions, social representation, objective estimations).
 - Physical, environmental, social, economic and cultural vulnerability.
 - Classifying of development problems and deficiencies.
 - Prioritisation of political, economic, social and environmental actions to achieve balanced development.
2. Risk reduction (prevention, mitigation, protection).
3. Disaster management (response, relief, recovery).
4. Risk transference: insurance, financial protection (solidarity, mutualisation, share).

The risk of natural disasters in urban areas can be reduced on the basis of resilience initiatives, which include:

- Reduction of the vulnerability of structures.
- Reduction of the exposure (elements at risk).

- Adapted or appropriate land-use and improvement of urban settlements.
- Business continuity.

The effectiveness of public expenditures to be utilized for such activities should be compared with the cost of repair after the disaster. Urban settlements can be improved by changing their functional characteristics through land-use planning and increasing the redundancy of the infrastructure, such as building an additional bridge at a strategic crossing for instance.

So, the main preventive initiatives in territorial planning, construction and infrastructures can be organized as follows:

1. Preventive planning at national, regional and urban levels: land-use control, urban fabric and main infrastructures, etc.
2. Prevention in construction: strengthening of vital and strategic buildings, new constructions control, etc.
3. Sector related measures to reduce the sectorial vulnerability (lifelines, transportation, communication, services, architectural heritage, business continuity, etc.).

A close collaboration and continuity (relationship and linking) between central and local administrations is needed for ensuring necessary incentives to transfer foreign investment and development aid as well as national incomes to threatened territories, for reducing the population's concentration, for co-producing sector plans, encouraging tourism, services, trade, industry, as well as for a global crisis management preparedness (Masure, 2000).

CHAPTER 12
RESPONSE OF HOSPITAL SYSTEMS

L. G. Pujades¹, A. Roca², C. S. Oliveira³ and S. Safina¹

1. Universitat Politècnica de Catalunya, Barcelona, Spain

2. Institut Cartogràfic de Catalunya, Barcelona, Spain

3. Instituto Superior Técnico, Lisbon, Portugal

12.1. Introduction

Hospitals are in the first level category of essential buildings due to their critical role after an earthquake. Moreover, the hospital system of a given region or country has to be considered as a whole for risk assessment and for planning relevant improvements in their vulnerability, due to the multiple interactions among the different elements of the system. The performance of each one of the elements (general hospitals, hospitals of reference and other specialised centres as well as field hospitals) has to be assessed and the organic dependence between hospital, transportation and communication systems has to be taken into account. The evaluation of the adequacy of the hospital's and the system's response to the seismic hazard of a given area, as well as the convenience and efficiency of an eventual reinforcement of the hospital system by means of, for example, field hospitals, should be based on the seismic hazard of the area, the population density and hospital distribution as well as on the efficiency of the transportation system. This chapter describes an overview of this topic and, in particular, an account of the various available approaches to analyse the seismic performance of a given health system. The general strategy for the assessment of vulnerability and for the generation of damage scenarios is based on a systemic approach and focus on the analysis of the capacity-demand relationship. In fact, the evaluation of the seismic performance of a hospital should be based on the adjustment between its individual capacity and the demand of their facilities that is caused by the reasonably expected earthquakes in the area. But this demand also strongly depends on the seismic response of the whole hospitals' network, in terms of its overall capacity for treating injured people. In turn, the seismic performance of a local or regional health care system mainly depends on the treatment capacity of their individual hospitals as well as on the management of the casualties' queue produced by the seismic disaster. Most of this study is based on two previous works. Fawcett and Oliveira (2000) developed a regional simulation model addressed to care of injured people after an earthquake disaster. Safina (2003) investigated the seismic performance of essential buildings and analysed a regional health system, in some detail. The seismic evaluations are based on numerical simulation of seismic scenarios. The iteration of adequate scenarios allows evaluating the seismic adequacy of the system, through the study of potential losses, and characterizing the seismic response of each hospital, through risk analyses.

12.2. The seismic behaviour of hospitals

Essential buildings play a fundamental role in society's reaction to an emergency. This is particularly true for earthquake produced emergencies because of their function in restoring normal development to the activity of the society. Failure of essential

buildings complicates the management of the emergency and increases the dimensions of the catastrophe. This happened in San Francisco in 1906, when the dimensions of the seismic disaster were severely increased because of a great fire, collapsing of the Fire Station, the death of the firemen's captain and the malfunctioning of the water system. Safina (2003) made a compilation of important cases in which the degradation of hospitals caused bad management of an earthquake emergency. Let us focus on two significant cases. During the 6.8 magnitude earthquake of San Francisco, which occurred on February 9th 1971, several hospitals suffered significant damage so they could not function or take care of those affected by the earthquake. Most of the casualties arrived at two collapsed hospitals complicating thus the job of the medical staff. Among the damaged hospitals were the Olive View Hospital, a new facility that had just opened its doors three months before the earthquake and which collapsed; the Indian Hill Medical Center, which was not operating again till a week after the earthquake; the Holy Cross Hospital which had to be demolished (Rutenberg, 1994); the Veterans Administration Hospital, where one of the wings collapsed causing the death of 49 patients (Rutenberg et al., 1982). Likewise, the Sylmar Hospital, recently built (Stahlin, 1997), collapsed while the Hospital Santa Cruz endured severe damage. Many accesses were blocked due to land or rock sliding. From then on, the earthquake design criteria of the city were modified so that nowadays they are considered among the strictest in the world and must be used for the design of all new hospitals in California. The new Veterans Administration Palo Alto Medical Center was projected and built following these new design criteria. Another example of the health system failure was the M6.5 earthquake occurred in December 23, 1972 in Managua. This earthquake, not only severely damaged many essential business and government buildings, but also the Hospital General was highly affected, causing its evacuation in order to demolish it, as all the first floor columns failed (OPS, 1992). The Social Security hospital and the so-called "*Reformatorio*" also endured significant damage, as well as the Military Hospital, although the latter was affected in a lesser way. The collapse of the second floor of the two-story building of the fire station made the facilities useless and avoided the extinction of the fires that extended freely. The damage caused by this earthquake required a special attention from the hospital, fire and emergency systems. The capacity of these essential centers was drastically diminished by the earthquake.

12.3. Response of the hospital network to an emergency: general aspects

Thus, immediately after an earthquake, hospital networks endure an exceptional demand. The response of the system depends on its ability to absorb this demand in a period of time, which normally will last for a few days after the earthquake (De Bruyler et al., 1985; Tanaka et al., 1998). Most of the studies of the effect of earthquakes on the hospital system concentrated on the analysis of vulnerability of individual hospitals (for instance, Nuti and Monti, 1994; Monti et al., 1996, Nuti and Vanzi, 1998). Fawcett and Oliveira (2000) model, step by step, the evolution in time of health care and establish three main factors in the model:

1. Casualties: number and place
2. Hospital system: capacity and location
3. Transportation and pathways in systems

The first factor refers to the quantity and geographic distribution of the demand, the second refers to quantity and regional distribution of the capacity, while the third refers to other systems that may contribute, in a positive or negative way, to the celerity at taking care of the casualties. The quantification of each of these aspects is not simple and depends on many factors. Many studies tried to model the relationship between the demand caused by these disasters and the capacity of the health system by means of indexes. De Boer et al. (1989) introduced a Medical Severity Index (MSI) that depends on the number and severity of the casualties (demand), as well as on three factors that characterise the capacity of the hospital system: ability to rescue, ability to transport and ability to treat. Another index introduced by De Boer (1997) refers only to the severity of the disaster, not taking into account the response of the health system, namely Disaster Severity Scale (DSS). This index is based on a seven-variable score system that produces values between 1 and 13. The present study also suggests some hospital response indexes and hospital system response indexes, based on the relationship between demand and capacity. Although the indexes here proposed are simplified, they can be easily extended to calculate the indexes suggested in other works.

12.3.1. DEMAND: THE CASUALTIES

The most critical factor in an earthquake disaster is the number of deceased and injured. De Boer et al. (1989) classify casualties in four groups: 1) Deceased in the earthquake or before entering the hospital; 2) casualties whose life is highly at risk and require immediate care; 3) other casualties which require hospitalization and 4) slightly injured that do not require hospitalization. The emergency management cannot treat those that die almost instantly, but its role is critical regarding life saving, not only of those that may succumb in the first minutes or hours, but also of those that may die if they are not appropriately treated. Earthquake situations indicate that most of the deaths occur rapidly and immediately, while there are few later deaths. Thus, a crucial aspect to diminish casualties depends on immediate treatment, previous even to their admission in a hospital. This medical care should be administered before the first, let's say, 6 hours. In recent earthquakes in California, it was estimated that only 10% of the casualties needed health care, as most of the injuries were extremely slight: cuts, bruises and sprains (Shoaf et al., 1998). In a recent review of the earthquakes that occurred in other places, the rate of slight injuries is of 70-90% (Alexander, 1996). The number of casualties needing hospitalization depends mainly on the damage suffered by the buildings where they were when the earthquake happened. Thus, it depends on the population distribution, the vulnerability of the buildings and the moment at which the earthquake took place. Likewise the estimation is affected by uncertainties and its modelling is based on simplified laws focusing on statistics regarding the number and distribution of casualties caused by past earthquakes (see, for instance, Alexander, 1996; Coburn and Spence, 1992, 2002; Smardjjeva and Badal, 2002). In this study the ATC-13 (1985) is used because of its simplicity when calculating slight and severe injuries and deaths. Nevertheless, the model can easily include other proposals or specific laws synthesizing several alternatives, such as for instance the ATC-13 methodology adjusted to that of Coburn and Spence (2002) in order to take into account the exact time at which the earthquake occurs.

12.3.2. HOSPITALS: POTENTIAL AND EFFECTIVE CAPACITY

The geographic distribution of population and hospitals directly affects the characteristics of an earthquake emergency and its management. The number of casualties depends on the population density in the areas damaged by the earthquake. The number of casualties assigned to each hospital can be determined by considering aspects such as nearness and attractiveness, by pre-assigning geographic areas and hospitals or by taking into account both types of criteria.

The characterization of a hospital's performance during an emergency is not a trouble-free task and it may be a difficult undertaking. Two of the main factors could be: 1) the potential capacity to treat casualties and 2) the physical and functional vulnerability that decreases its effective capacity. The former factor refers to the number of casualties that a hospital is able to admit and treat per time unit. In the case of casualties needing surgery, this ability depends on the number of surgeons, anaesthetists and nurses available, as well as the schedule of the operating rooms and material stocks. In fact, there is no standard way to determine the capacity of treating injured people under emergency conditions from data related to the normal operating of a hospital. De Boer (1995), for example, claims that the capacity of medical attention in a medical emergency does not depend on the number of beds of a hospital. Fawcett and Oliveira (2000) suggest estimating this capacity and multiplying the number of surgical cases treated per day in normal conditions by a factor. This factor depends on the category and conditions of the hospital and, by considering their seismic performance after the earthquake of Azores of 1980 they estimated factors of up to 12 for the best hospitals (Oliveira et al., 1996). In addition to the injured people requiring surgical treatment the affluence of other wounded people needing other types of treatment must be considered. In any case it is advisable that medical staff and experts in emergency management. It may be also convenient to include a temporary variation of the capacity of the hospital based on a time of reaction and on the maintenance of the attention level. Fawcett and Oliveira (2000) estimate that the minimum time required for the activation of the emergency services is about two hours and that the maximum performance is reached in 24 hours. In any case a realistic model should consider that, not only the number of casualties, but also the effectiveness of a hospital depends strongly on the hour at which the earthquake occurs and if it is during a working day or a holiday. The effective capacity of a hospital depends on its capacity and its functioning degradation, which in turn depends on the damage caused by the earthquake to the buildings that contain the hospital and to the infrastructures that its normal operation requires. The analysis of the physical damage requires knowing the vulnerability classes, damage states and damage probability matrices. Fawcett and Oliveira (2000) solve the problem in a simplified way by establishing three types of vulnerability: high, medium and low; three damage levels that they call: total failure, short-term failure and time-delayed failure. Total failure occurs when the hospital undergoes such a damage degree that prevents the care of casualties and must be evacuated. Short-term failure takes place when the hospital undergoes damage and cannot offer immediate care but recuperates its normal functioning before the emergency ends. Finally, time-delayed failure occurs when the hospital loses its effectiveness during the emergency, due to fatigue or exhaustion of the resources available. Likewise, they define a simplified matrix assigning the probability that a hospital of vulnerability type V undergoes a damage degree D , due to an

earthquake of intensity I . Thus, the model estimates the effective capacity of each hospital as the number of casualties it is able to treat. Time-delayed failure only occurs 24 hours after the beginning of the emergency and those hospitals undergoing time-delayed failure, as well as short-term failure, recover in 24 hours.

Safina (2003) determines specific vulnerability types for each hospital, focusing on EMS-98 scale proposals, and develops fragility curves and damage probability matrices which are specific for each hospital. The degrees or states of damage are also the proposed ones in the EMS-98 scale. The functional degradation is considered starting from the fragility curve corresponding to the moderate damage state (Nuti and Vanzi, 1999). In order to simplify the model, the number of beds is used as an indicator of the initial capacity of the hospital, taking into account that it is a value that can be easily adapted to the effective number of casualties the hospital is able to treat, as described above.

12.3.3. TRANSPORTATION, HOSPITAL ACCESS AND COMMUNICATION SYSTEM

The temporary evolution of the management of the emergency is based on the rescue rate of trapped casualties and on its medical attention, which eventually could consist of a first aid in the place of rescue or in field hospitals and their subsequent transportation towards the destination hospital. Travelling times usually are modelled by means of the distance from the centre of the casualty town to the assigned hospital. This distance is measured on the road network map and, in order to estimate travel times, an average speed is assigned to each road of the transportation system based on its category and characteristics. Furthermore, the model, based on the severity of the earthquake, can incorporate the deterioration of highway sections to modify the route anticipated by choosing alternative ways. The ratio between distance and speed allows estimating the time needed for the transport of injured people to the hospital.

12.3.4. TIME DISCRETIZATION, RESCUE AND MORTALITY

The model can consider the time of rescue of the victims and mortality considering discrete time intervals. Safina (2003) adopts a simplified model for the time evolution of the crisis. Fawcett and Oliveira (2000) consider 2-hour time intervals. A significant amount of casualties remain trapped between the debris and destroyed buildings. Several past cases show that between 85 and 95% of the casualties who are rescued alive, that rescue occurs between the first 24 and 48 hours. Fawcett and Oliveira (2000) assume that 40% of the casualties are not trapped and 60% need to be rescued, and the rate at which casualties are rescued at each area is greater where the amount of casualties is lower as there is less trouble and more rescue resources. The number of casualties at each area is simulated by means of a decreasing exponential function that depends on two parameters: the initial number of rescued casualties and their decrease, which is adjusted so that in the areas where there is a greater average of casualties, the last casualties are rescued within three days. In those areas with low casualty percentages, the simulation takes into account that the last rescue takes place in 24 hours. The problem is equivalent to knowing a geometric progression whose sum is equal to the number of victims. The first term and the ratio are then determined so that

the last rescued casualty takes place after the considered time. Equations (12.1) describe the model for the number of rescued casualties.

$$\begin{aligned} A_k &= A_1 r^{k-1} \quad k=1 \cdots N_T \\ N_{\text{casualties}} &= \frac{A_1 [r^{N_T} - 1]}{r - 1} \end{aligned} \quad (12.1)$$

A_k is the number of casualties rescued within a period k . $N_{\text{casualties}}$ is the total number of casualties trapped and N_T is the number of time intervals considered. Given A_1 and the time interval needed to rescue all casualties, then r would be equal to:

$$r = \left[\frac{1}{A_1} \right]^{\frac{1}{N_T - 1}} \quad (12.2)$$

Equation (12.2) is obtained assuming that in equations (12.1) $k=N_T$ and $A_{N_T}=1$. Iterating over A_1 we obtain the parameters A_1 and r , which correspond to the total number of casualties $N_{\text{casualties}}$.

Figure 12.1 shows a case in which the total number of victims is 14000, of which we assumed that 60% (8.400) are trapped. It is assumed that the last victim is rescued after 60 hours (2 days and a half), producing $A_1=1928$, and $r=0.771$. The geometric progression of Equation (12.1) is equivalent to the following exponential function:

$$A_k = A_1 \exp[-\lambda(k-1)\Delta t] \quad k=1 \cdots N_T, \quad \Delta t = 2 \text{ hours} \quad (12.3)$$

with $r=\exp(-\lambda\Delta t)$ and $\lambda \approx 0.13$.

Another significant aspect is death rate. Within the first 4 to 6 hours of a seismic crisis, a high death rate is detected among those casualties severely injured. According to Coupland (1994) this death rate ranges from 20 to 25%. From these first hours to a week, the death rate remains almost constant, averaging 1% per day, for those casualties receiving treatment at a hospital, and 3% per day, for those casualties that do not receive any treatment. The death rate in those casualties not treated, can be diminished to 2% per day if those casualties are treated before reaching the hospital. This death pattern can be easily represented by a decreasing exponential equation modelling death rate in approximately the first 8 hours, establishing constant rates for the different casualty types in the following days. For each time interval, the number of deaths is then obtained by multiplying the number of casualties for each category by its corresponding death rate. The number of casualties corresponding to each category in the following period of time is calculated subtracting subsequent deaths. Figure 12.1 shows the number of deaths corresponding to each period. Death rates during the first 2, 4, 6 and 8 hours respectively are considered to be 30%, 15%, 10% and 5% for those casualties not admitted in the hospital. For latter periods of time a constant death rate of 2% is considered. The death rate of admitted casualties was not taken into account. Figure 12.1 also shows the number of rescues for each period and the time evolution of the emergency management, estimating that the hospital system admits some 2000 casualties per day. The medical resolution of this seismic crisis characterized by 14000 casualties, 8400 of whom were trapped, requires 5 days and a half. The great number of deaths, 7168, is basically due to the high death rate among the population not treated during the first 8 hours and to the low medical attention rate. Thus, if we apply the

corresponding rescue and death rates, during the first 2 hours, only 167 casualties from 5600 are treated, 1928 are rescued and 2258 die while waiting for treatment, which leaves a waiting queue of 5103 casualties. In the following 2 hours again only 167 casualties enter the hospitals while 1487 casualties more are rescued, 1083 perished, leaving a waiting list of 5341 casualties. In any case, the fine-tuning of the rates for trapped casualties, treated casualties and deceased in those cases admitted in the hospital, and the rates for those cases not admitted gives a great flexibility to the model, which allows representing a wide variety of cases. We also observe that a rapid intervention at the first hours of the seismic crisis would decrease the number of deaths.

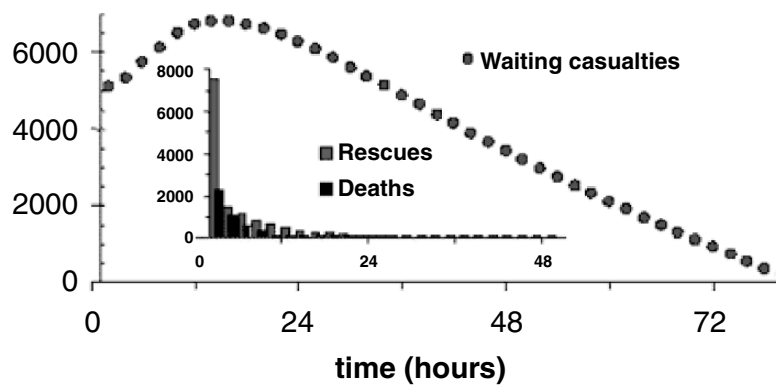


Fig. 12.1. Simulation of the temporary evolution of the number of casualties of a seismic crisis causing 14000 severely injured people. The number of rescues, deaths and casualties waiting to enter a hospital, at 2-hour intervals are shown (modified after Fawcett and Oliveira, 2000)

12.3.5. MANAGING CASUALTIES QUEUES

The model should also define the assignment of casualties to each hospital. For a seismic scenario, the simulation includes the area affected and nearby areas whose medical resources could be required to manage the emergency. This management depends on the capacity of the hospital and on the distance to the area affected by the earthquake. Equations (12.4) and (12.5) slightly modify the proposal made by Fawcett and Oliveira (2000) to assign casualties, not treated yet, to the different hospitals at each time interval.

Three cases, corresponding to different capacities, distances and reluctances are shown (see also Table 12.1)

$$c'_{ij} = A_j \times \exp[-\mu t_{ij}] \tag{12.4}$$

$$c_{ij} = C_i \times \frac{c'_{ij}}{\sum_{j=1}^{N_{hosp}} c'_{ij}} \tag{12.5}$$

Table 12.1. Simulations of the distribution of 1000 casualties of zone i , in 8 hospitals characterised by their capacity, distance and reluctance. Cases analysed: 1) No reluctance nor dependency on distance, 2) no reluctance but dependence on distance, and 3) reluctance and distance dependency

Hospital	Municipality zone i , and $C_i=1000$					
	r_j Hospital's capacity	t_{ij} (hours)	$\rho=1, \mu=0.0$	$\rho=1, \mu=0.05$	$\mu=0.05$	
			C_{ij}	C_{ij}	C_{ij}	ρ
1	0	0.5	0	0	0	1.5
2	50	1	41	44	50	1.5
3	150	1	122	131	150	1.5
4	150	1.5	122	127	146	1.5
5	155	1.5	126	132	151	1.5
6	220	2	178	182	209	1.5
7	160	3.5	130	123	94	1
8	348	4	282	261	200	1
TOTAL	1233		1000	1000	1000	

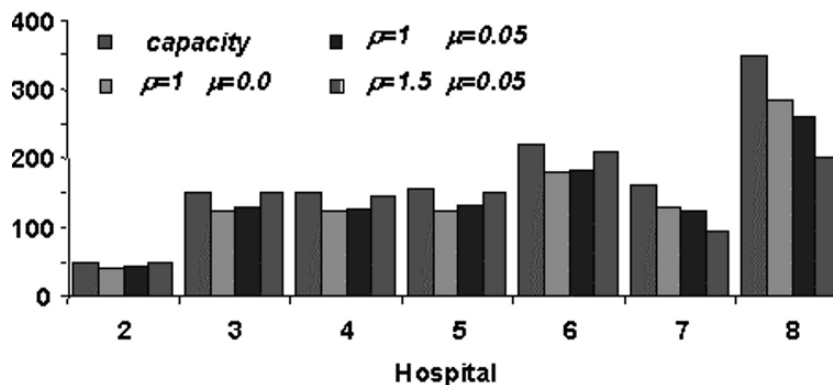


Fig. 12.2. Simulations to assign 1000 casualties from the zone i , to eight hospitals

c_{ij} is the number of victims that travel from zone i to hospital j . C_i is the number of casualties that still have not been treated in zone i . A_j is an attractiveness coefficient of hospital j so that $A_j=r_j$ for $i \neq j$, that is for those hospitals outside zone i and $A_j=\rho r_j$ for $i=j$. r_j equals the number of resources of hospital j , which should be evaluated by means of the number of casualties that hospital j is able to admit per time unit. ρ is a parameter that allows considering the reluctance of casualties to travel to those hospitals outside their area. μ allows calibrating the effect of distance, t_{ij} is the time it takes to reach hospital j from area i . Equation (12.5) is a normalization condition that guarantees that the sum of casualties of zone i assigned to hospitals j coincide with the total number of casualties of zone i , that is:

$$C_i = \sum_{j=1}^{N_{\text{hosp}}} c_{ij} \quad i=1 \dots N_{\text{zones}} \quad (12.6)$$

In order to illustrate a practical case of this way of assignment, a zone i is considered, where 1000 casualties must be distributed between 8 hospitals. Table 12.1 summarises the cases considered.

The first column contains the r_j factors for each hospital, the second column stands for the time it takes to go from zone i to hospital j , the third column shows the distribution of casualties among the hospitals when the influence of distance ρ and reluctance μ factors is not considered, the fourth column shows the case with dependency on distance while the last column incorporates moreover the reluctance factor of all those hospitals in which the time it takes to reach them is less than or equal to 2 hours. Parameters ρ and μ seem to allow optimising the distribution of casualties regarding the capacity of hospitals and their distance from the zone. Figure 12.2 shows the results in Table 12.1. Both in Table 12.1 and Figure 12.2, hospitals are ordered by increasing distance.

There are other ways to assign casualties to hospitals (De la Barra, 1985; Fawcett and Oliveira, 2000). Safina (2003) uses a simplified procedure: the basic unit or information cell is the zone and each hospital has a series of zones assigned to it. Thus the casualties of each zone are directed to a reference hospital.

12.4. Simplified model: seismic analysis of a regional system

Safina (2003) develops a simplified model in order to characterise the seismic performance of individual hospitals and the whole health care system in areas with low to moderate seismic hazard. The model is based on simulating and monitoring the time evolution of the emergency for selected earthquake scenarios. The simulation allows characterising the seismic response and performance of each hospital as well as the whole regional health care system. This simplified model and the most significant results of its application are described below.

12.4.1. HOSPITAL RESPONSE

The behaviour of a hospital i at the time t of an earthquake produced emergency is described by the following response factor $FRHi$:

$$FRHi(t) = \left(1 + \frac{NHi(t)}{NCDi}\right) \left(1 + Fli \frac{NCPi}{NCTi}\right) - 1 \quad (12.7)$$

$NHi(t)$ is the total number of casualties which have been moved to hospital i till time t , $NCDi$ is the number of beds available ($t=0$), $NCPi$ is the number of beds lost, $NCTi$ is the total number of beds in the hospital, Fli is a factor allowing consideration of the hospital i 's relevance or attractiveness. This Fl factor is equivalent to coefficient A_j in equation (12.4) and, in this case, for each hospital j , this is defined as $Fl = F_1 \times F_2$. F_1 refers to the hospital relevance, which in this application included three levels: F_1 has a value of 1 for basic general hospitals (G), 1.3 for reference hospitals (R) and 1.5 for specialized or high-tech hospitals (S). Out of 64 analyzed hospitals, 33 gave an F_1 value

of 1, 23 scored 1.3 and the rest, 8, scored 1.5. The mean value for F_1 is 1.17 ± 0.19 . F_2 is a relevance factor for beds and in this case it is obtained by dividing the number of inhabitants of each hospital area by the total number of beds of that area, normalized in such a way to be the unit for the lowest value obtained. The maximum value for F_2 is 2.67 and its mean value is 1.47 ± 0.33 . Sixteen hospitals have $F_2=1$. When there is no physical degradation of the hospital ($NCPi=0$) and the number of casualties taken to the hospital is greater than the number of beds available, the response factor in Equation (12.7) is greater than 1. A response factor equal to 1 indicates the exhaustion of the hospital's capacity, which is thus ruled out in order to take care of the emergency. Null response factor corresponds to those hospitals that, having available beds, do not take part in the emergency ($NHi=0$). When there is no functional degradation ($NCPi=0$) the response factor takes values between 0 and 1 and it can be written as:

$$FRHi = \frac{IO_f - IO_0}{1 - IO_0} \quad (12.8)$$

where IO_0 and IO_f are, respectively, the initial ($t=0$) and final ($t=T_{max}$) occupation indexes, the occupation index being the ratio between the number of beds occupied and the total number of beds. When, even if there are beds available, the hospital has suffered some damage, an adjustment factor should be taken into account. Thus, a hospital with a 10% loss in functional capacity and a relevance factor of, for instance, 2 will adjust response factor to a 1.2 value. A hospital with 46 available beds and 30 casualties just admitted has a non-degraded response factor of 0.65. Nevertheless if the hospital endures damage of 10% of its capacity, it has a relevance factor of 1, 4 and 10, respectively, it shows response factor values equal to 0.85, 1.31 and 7.15, considering that they have the same number of available beds. This relevance factor F_1 , is a key factor to estimate the response of hospitals and should always be carefully calibrated mainly because it is not delimited and its evaluation could be highly subjective. For typical response factor values in this case study, it is estimated that those values inferior to 10 correspond to hospitals showing an acceptable seismic performance, while greater values indicate an insufficient response. Those values surpassing 100 show a critical condition calling for a detailed checking of the hospital.

12.4.2. RESPONSE OF THE SYSTEM

In order to evaluate the global response of the system, a global response factor is defined by means of the following integral between the beginning ($t=0$) and the end (T_{max}) of the earthquake crisis:

$$FR = \int_{t=0}^{t=T_{max}} NH(t) R(t) dt \quad (12.9)$$

where $NH(t)$ is the number of casualties not yet admitted at time t . $R(t)$ is a risk function that considers the increase of the risk of casualties after a critical time, T_{crit} . After that time the risk of death of casualties travelling to the hospital and not treated yet is augmented and can be defined as follows:

$$R(t) = \begin{cases} 1 & \text{if } t \leq T_{crit} \\ 1 + \alpha(t - T_{crit})^n & \text{if } t > T_{crit} \end{cases} \quad (12.10)$$

where α and n are numerical factors that should be adjusted according to the medical recommendations for typical injuries suffered by casualties during earthquakes. The following values have been assumed in our case study: $T_{crit}=60 \text{ min}$, $\alpha=0.0003$ and $n=2$. Figure 12.3 (Safina et al., 2002) shows the procedure to obtain the system response factor.

This index, as defined here (see Equation (12.9) and Figure 12.3), strongly depends on the particular earthquake scenario. In effect, the response factor increases with the number of casualties produced by the earthquake, NHI , and with the time needed to provide treatment to all injured people, T_{max} . But it also depends on the time evolution of the treatment of casualties, because it is the area below the function defining this time evolution, which represents the management of the emergency. A rapid reaction to the treatment of casualties will reduce the response factor of the system. This factor also increases when the critical time, T_{crit} , of causing additional risk to casualties is surpassed, as curve $R(t)$ starts to contribute to the integral of Equation (12.9). Because of the dependency of the response factor on the number of casualties at the beginning of the emergency $NHI (t=0)$ it is useful to define also a normalized response factor:

$$FRN = \frac{FR}{NHI} \quad (12.11)$$

where NHI is the number of initial casualties.

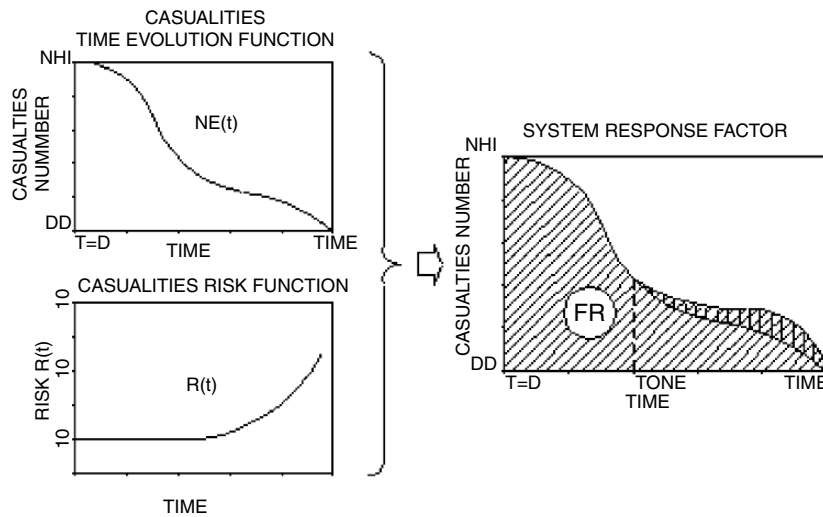


Fig. 12.3. Scheme of the procedure to obtain the response factor of the system. The figure shows the time evolution function for the number of casualties not yet treated $NH(t)$, the risk factor of casualties $R(t)$ and the curve whose integral causes the response factor (FR) as defined by equations (12-9) and (12-10)

For different health care systems managing the same earthquake scenario, system response factor and normalized system response factor are equivalent. Nevertheless, when analyzing the response of a system to different earthquake scenarios, the normalized system response factor better characterizes the response of the hospitals to the earthquake disaster. In effect, two scenarios leading to the same system response factor means that the most severe one will produce the lowest standardized system response factor and, thus, the lower is the standardized system response factor, the greater is the system capacity to solve earthquake crisis. Therefore we conclude that although the system-scenario trade-off cannot be completely avoided, the normalized system response factor is more adequate to characterize the earthquake response of the health system when facing different earthquake cases as it describes, in an appropriate way, the capacity of the regional health system to handle a seismic disaster. The greater the normalized system response factors worse the ability to manage the emergency.

12.4.3. THE DEMAND: THE EARTHQUAKE SCENARIO (T=0)

The characterization of the behaviour of a health care system in the face of an emergency is based on the analysis of earthquake scenarios. Nevertheless, the response to the system mainly depends on the scenario, that is, to the distribution in time and in space of the demand caused by the earthquake. In urban areas, for instance, in spite of the high hospital density, a moderate earthquake scenario could collapse the system due to the population density. In rural areas, the health system could suffer because of the distance to the hospitals or poor transportation systems. Modelling the time evolution of the medical attention to an earthquake disaster must be based on the initial demand, distribution in time and space of the casualties; the initial capacity, distribution in time and space of the treatment units; and the evolution of casualties' treatment during the emergency and till it is finally solved. Therefore we need to know about the seismic action, buildings vulnerability, expected damage and casualties at each municipality or geographical unit considered. Different approaches to estimate all these components are discussed in Chapters 2, 3, 4, 6, 10, 21, 22 and 23. These components allow the definition of the earthquake scenarios that constitutes the initial demand of the system and it is the departure point to estimate the size of the disaster and, of course, for analyzing the temporary evolution of the emergency management, which will allow characterizing the seismic response and performance of the hospital system and of each particular hospital.

12.4.4. CAPACITY: THE DEGRADATION OF THE SYSTEM

Facing this treatment demand corresponds to the hospital network, which eventually would be degraded by the earthquake. As important as the physical damage suffered by hospitals are their functionality losses. There are different methodologies to evaluate the functional fragility of hospitals. We follow here the work by Monti and Nuti (1996), which allows estimating functional failure probability starting from physical damage states. Each hospital is modelled as a system. In fact, hospitals are complex systems, with several installations whose facilities and services are frequently located in different pavilions or buildings, which, in its turn, may belong to different vulnerability classes. These buildings usually contain a great number of elements, such as mechanical, electrical and high-tech equipment, which are highly sensitive to ground shaking and

that are much more fragile than the buildings where they are installed. Really the hospitals functionality strongly depends on the seismic performance of these kinds of non-structural elements. On the other hand, many hospitals, in order to adapt to advances in medicine or reorient their functions and facilities, have been severely modified with significant improvements that, quite often, also affected their essential resistant structures. This is the case of many hospitals, which are housed inside old buildings but their function in the local and regional health system is still significant. Therefore, the fragility analysis and functional degradation of the hospitals is a subtle issue and a detailed study must be carried out, establishing a specific damage probability matrix for each hospital.

12.4.4.1. Hospital Vulnerability and fragility

In order to assess the vulnerability of each hospital of the health system, the first step is to collect as much information as possible including specific characteristics of each hospital, and specially, other aspects such as the regularity of the building, its actual condition and the precautionary measures established in case of an emergency. One simplified way (González et al., 2000; González et al., 2001; Safina, 2003) to carry out vulnerability assessment is to describe the typology of the hospital in terms of probability of pertaining to vulnerability classes A, B, C, D, E and F of the EMS-98 scale (Grünthal, 1998).

The estimation of the damage that a hospital is expected to undergo is based on obtaining specific DPM matrices corresponding to their particular features. These specific DPM are obtained starting from the DPM established for the A, B, C and D buildings' classes. In fact, given a new particular structural typology, T_s , defined as a combination of vulnerability classes, the probability that a damage grade occurs, $P[GD=d|T_s, I]$, can be obtained by applying the total probability theorem (Benjamin and Cornell, 1970), according to which:

$$P[GD = d|T_s, I] = \sum_T \sum_I P[GD = d|T, I] P[T] P[I] \quad (12.12)$$

where $P[GD = d|T, I]$ is the conditioned probability that a damage grade $GD=d$ be observed, in a T -type building when an I intensity earthquake takes place. $P[T]$ is the probability that the building belong to a vulnerability class T , and $P[I]$ is the probability of occurrence for an earthquake of intensity I . Assuming $P[I]=1$ for a given intensity and $P[I]=0$ for all other intensities, Equation (12.12) allows obtaining DPM for the new typology by means of the following equation:

$$P_{d, T_s, I} = P[GD = d|T_s, I] = \sum_T P[GD = d|T, I] P[T] \quad (12.13)$$

Alternatively, when an intensity with a given occurrence probability, or with a specific return period, is considered, the damage probabilities defined by Equation (12.12) will correspond to the same occurrence probabilities or return periods.

Fragility curves constitute another common way to define the damage expected in a building class. Given a damage state d_j , the corresponding fragility curve is defined by the probability that the expected damage be equal or greater than the damage defined by the considered damage state. In case of the null or no-damage state ($j=0$) it is clear that

the fragility curve is the unit, because this is the probability that any building undergoes no-damage or damage when put under any seismic intensity. For other damage states d_j , the corresponding fragility curves define the probabilities that the building undergoes a damage grade $D \geq d_j$, where $j=1, \dots, 5$ numbers the corresponding damage states d_j . These functions can be easily calculated from DPM by means of the following expression:

$$P[GD = D \geq d_j | I] = 1 - \sum_{i=0}^{j-1} P[GD = d_i | I] \tag{12.14}$$

Figure 12.4 shows an example of fragility curves for a given hospital.

On the other hand, once the fragility curves are known, the damage probability matrices can be also trivially calculated:

$$P[GD = d_i | I] = P[GD = D \geq d_i | I] - P[GD = D \geq d_{i+1} | I] \quad i = 0, \dots, 5 \tag{12.15}$$

12.4.4.2. Functional degradation

The functional degradation of a hospital is quantified by means of a functionality index, *HFI* that reaches values ranging from 0 (without degradation) to 1 (functional collapse). *HFI* scores 0 when the probability that it reaches or surpasses a moderate damage state (D2) is lower than 20%, and it is equal to 1 when the probability surpasses 60% (Nuti and Vanzi, 1999).

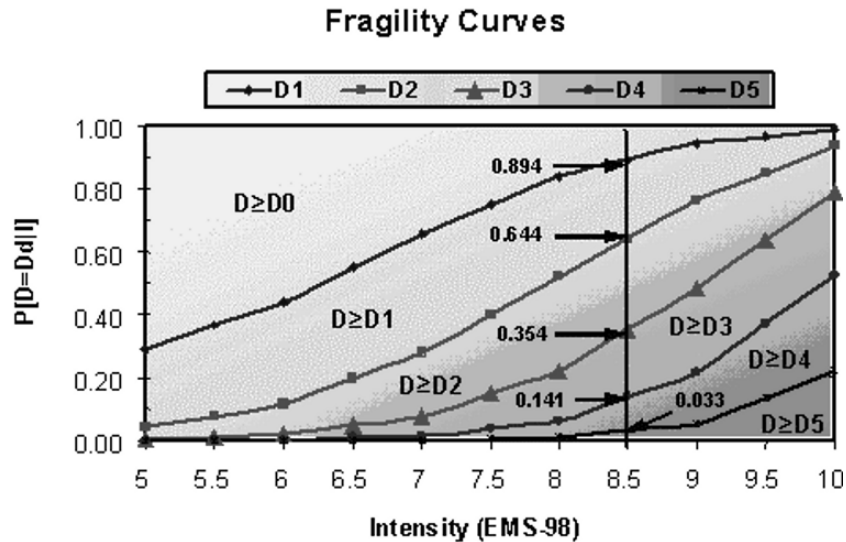


Fig. 12.4. Example of fragility curves for a hospital

Over the fragility curve of this damage grade (GD2), the seismic intensities corresponding to occurrence probabilities 0.2 and 0.6 are determined. These two intensities are called I_{min} and I_{max} being characteristic of each hospital and determining the points at which the functionality index is equivalent to 0 and 1 respectively. For intermediate intensities a lineal variation for *HFI* is assumed. Figure 12.5 shows, on the left, the procedure used to obtain these minimum and maximum intensities (I_{min} and I_{max}) from

the fragility curve corresponding to the moderate damage state. On the right of that same figure there is the function defining the functional degradation index of the hospital (*HFI*). In this example I_{min} ranges between V-VI and VII intensities with a mean value of 6.1 ± 0.36 , while I_{max} varies from VII-VIII to IX intensities and has a mean value of 7.98 ± 0.39 . For each intensity, the hospital's loss in functional capacity is obtained multiplying the hospital nominal functional capacity by the *HFI* index value corresponding to the analyzed seismic activity.

12.4.5. TIME EVOLUTION OF THE SYSTEM

The celerity and efficiency of the treatment of casualties will depend on the spatial distribution of casualties and hospitals, the residual capacity of the centers, availability to transport the casualties and the coordination when distributing the casualties among the hospitals that, in their turn, is determined by the efficiency of the communication and coordination protocols. In prior sections we have considered the demand and capacity evaluation. In this section we analyze the time evolution of the emergency management.

12.4.5.1. Target hospital and transfer time

Each municipality has a reference hospital assigned where casualties must be transferred in case of earthquake. This hospital is decided regarding the hospital category, proximity and quality of the roads available between the municipality and the hospital. The *transfer time* is the time required to transfer casualties from the municipality's urban center to the target hospital.

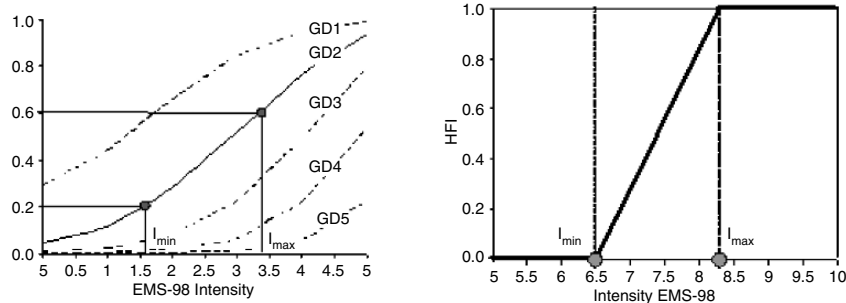


Fig. 12.5. Procedure to obtain I_{min} and I_{max} from the fragility curve corresponding to the moderate damage state, GD2 (left) and variation function of the hospital functionality index *HFI* (right)

12.4.5.2. Emergency management

The emergency starts with an earthquake, which can be modeled by means of the seismic intensity that is expected to arise at each municipality. This seismic action determines the casualties' treatment demand defined by the number of severely injured people in each municipality. This demand should be faced by the hospital network capacity, which probably will be degraded by the earthquake. The dynamic evolution of

the response of the system is modelled so that the casualties are taken to the municipalities' nearest hospitals.

At the beginning, it is assumed that no information is broadcasted to the emergency managers about the real situation of the hospitals where they intend to transfer the casualties, thus ignoring the residual capacity of the target hospital. The key parameter of the emergency time evolution is the transfer time. In our case study this time depends on the effective distance between the center of the municipality and the target hospital, the kind of road and its condition. The hospitals placed inside the affected area will admit casualties till their capacity is saturated. From then on, casualties are transferred to another hospital. In this second casualties' transferring it is assumed that detailed information about the new target hospital is available, so that now casualties are transferred directly to the nearest health center having capacity for treating casualties. Again the effective distance and the type and state of the roads are used to estimate traveling speeds and transportation times. At this moment we implicitly also are assuming that the communication system is in good condition and has not been damaged at all by the earthquake. Otherwise the criterion for selecting the new target hospital should be again only the proximity.

Figure 12.6 sketches the dynamic evolution of the emergency. Casualties of municipality M1 are transferred to the corresponding reference hospital H1. H1 hospital has suffered functional collapse and must transfer its patients together with assigned casualties to hospital H2, which, in its turn, is receiving casualties from municipality M2. Once H2 saturates, it must transfer the casualties not yet treated to the nearest available hospital H4, possibly located outside the epicentral area. On the other hand, hospital H3, which has not endured functional degradation, admits casualties from municipalities M3a and M3b until its saturation requires transferring the excess of casualties to hospital H4, which is placed outside the epicentral area, inside the so-called peripheral area.

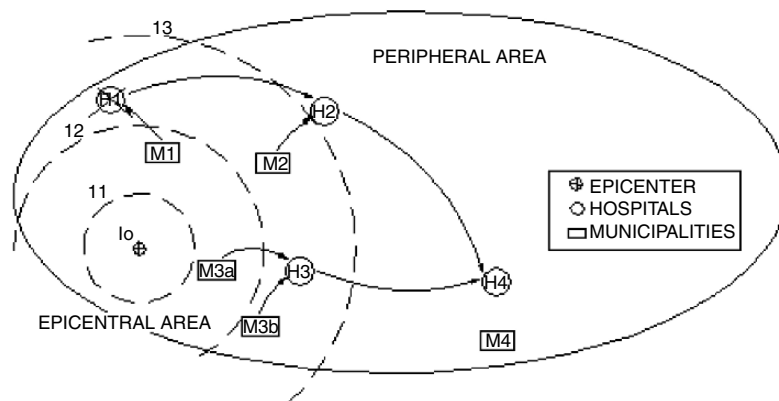


Fig. 12.6. Sketch showing the time evolution of the casualties' transferring to the hospitals for their treatment during an earthquake emergency. (See explanation in the text)

The emergency ends when all the casualties are admitted in a hospital. We call T_{max} the time elapsed between the earthquake break out and the end of the emergency.

12.5. Case study

Catalonia has approximately 6 million inhabitants, more than half of them living in the Barcelona area and the coast. Figure 12.7 (right) shows the distribution of population in the 964 municipalities of Catalonia. Population data were obtained from the census data for the 1998 year. The hospital network is structured in basic health units managed by the Catalan Health Services (Servei Català de la Salut -SCS). Each unit is responsible for between 20000 to 25000 inhabitants of the nearby geographical area (SCS, 1996a, 1996b). The hospital network here analyzed consists of 64 hospitals having 16172 beds. The mean occupation index is 82%, thus leaving 2915 beds for emergency situations.

Figure 12.7 (left) shows the distribution of hospitals. Hospitals are represented with a circle whose radius is proportional to its capacity. The city of Barcelona has been enlarged.



Fig. 12.7. Hospital network of Catalonia. The size of the circle is proportional to the capacity of the hospital. A detail of the city of Barcelona is also presented. On the right, the number of inhabitants for each municipality in Catalonia

12.5.1. HAZARD

Catalonia is a region with low to moderate seismic hazard where few severe historical earthquakes occurred in the past. Estimated intensities for a return period of 475 years range from VI to VII degrees in the EMS-98 scale. The greater historical earthquake occurred in Camprodon (Ripollés), in February 2, 1428, with a maximum intensity of IX. The seismic hazard map for the region can be seen in Chapter 22 (Figures 22.1 and 22.8)

12.5.2. FEASIBLE SEISMIC PERFORMANCE

Fragility curves of each hospital can be used to give a first idea of the adequacy of a health system. Four performance levels are considered. *Undamaged*: the hospital does not undergo damage (C1); *Operative*: the hospital undergoes damages but its functionality does not collapse (C2); *Non-operative*: the hospital, although it is still habitable, completely loses its functionality (C3); *non-habitable* (C4). Each of these performance levels are defined on the basis of the damage expected in the hospital. Thus, a seismic scenario is needed. If we consider the scenario defined by seismic intensities with an occurrence probability of 10% in 50 years, a reasonable estimation of the adequacy between the seismic hazard of the region and the vulnerability level of its hospital network can be stated. Figure 12.8 shows the distribution of hospitals indicating its feasible performance level. Table 12.2 shows the correspondence between these performance states and the damage levels undergone by the hospital.

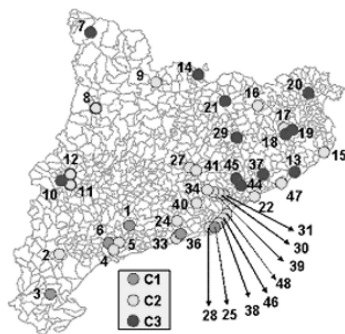


Fig. 12.8. Hospitals' feasible seismic performances in Catalonia

Table 12.2. Classification of the performance levels of the hospitals based on four damage grades.

	Level	Description	Criteria	N.	%
○	C1	Undamaged	$P(\text{GD}2) < 10\%$	5	8
◐	C2	Operative	$10\% \leq P(\text{GD}2) \leq 40\%$ $P(\text{GD}3) < 10\%$	41	64
◑	C3	Non operative	$P(\text{GD}2) > 40\%$ $10\% \leq P(\text{GD}3) \leq 40\%$ $P(\text{GD}4) < 10\%$	18	28
●	C4	Non habitable	$P(\text{GD}3) > 40\%$ $P(\text{GD}4) > 10\%$	—	—

That same Table 12.2 contains the number and percentages of hospitals of the hospital network in Catalonia included in each behaviour level. Safina (2003) also analyzes the specific case of Barcelona, whose hospitals are included in Table 12.2, but not in Figure 12.8.

12.5.3. TARGET HOSPITAL AND TRANSPORTATION TIME

In this application the official roadmap that also gives traffic densities has been used (ICC, 2001) and the following classification was established: 1) local and regional roads, 2) national roads and main roads; and 3) highways. We assigned 60, 90 and 120 km/h mean speeds respectively to type 1, 2, 3 and 4 paths. Furthermore, a target hospital to which to transfer its casualties is also assigned to each city and town. Figure 12.9 shows the transfer times' map computed. It is shown that the road network penalizes the central and northwestern regions of Catalonia, where the longer transfer times are required. Transfer times range from 5 minutes, in municipalities near well-communicated hospitals, to an hour, for those underprivileged cases.

12.5.4. SEISMIC RESPONSE OF THE HOSPITALS AND OF THE HOSPITAL SYSTEM: PRELIMINARY ANALYSIS

Once the model is defined, it can be used to analyze the seismic behaviour of the hospitals as well as the seismic performance of the whole hospital network. Depending on the aim of the analysis, historical or simulated earthquakes may be used.

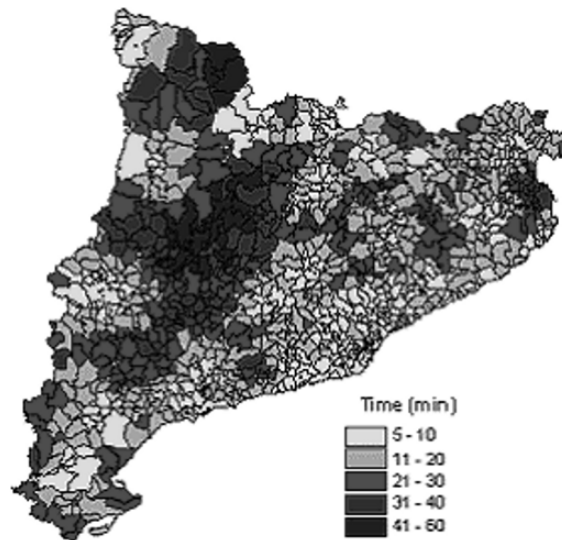


Fig. 12.9. Transfer time for each municipality in Catalonia

Scenarios for some historical events have been produced. The repetition today of the largest earthquake of the region known in historical times which occurred in Camprodon, in the Pyrenees (North region) in 1428, with epicentral intensity IX would cause more than 10000 casualties and a degradation of the treatment capacity of the health care greater than 100%. A not so large event, as that occurred in Vielha (NW extreme of Catalonia) in 1923 with intensity VIII would produce 929 casualties and a capacity degradation of about 2%. Two hospitals were disabled and 3 underwent degradation of their capacity. The resolution of this emergency would involve 57 hospitals, 9 would saturate their capacity and the total time of the emergency would be 3 hours and 40 minutes. The system response factor and the normalized response factor would be respectively 10670 and 11.5. The repetition of another event of epicentral intensity VII as that occurred in 1927 at Sant Celoni (about 30 km NE from the city of Barcelona) would cause about 916 casualties and a capacity degradation of about 7%. Three hospitals would be disabled and one would have to be evacuated. The management of the emergency would involve 30 hospitals, two of which underwent a partial degradation of its initial capacity, 11 hospitals would become saturated and the total time taken to solve the emergency is estimated as 45 minutes. The response factor and the normalized response factor were respectively 3491 and 4. Differences between the distances to the hospitals and between the characteristics of the road network resulted in the responses of the systems to two earthquakes that produced a similar number of casualties being quite different. The hospital density in the macroseismic

area and the road network efficiency allows solving the Sant Celoni emergency in a faster and more acceptable way than the Vielha case. Nevertheless, the high population density and vulnerability of the buildings to a seism of intensity VII produced damages comparable to those observed in the VIII intensity Vielha.

Given a region, ATC-40 (1996) defines typical earthquakes, corresponding to occurrence probabilities of 50, 10 and 5% in a period of 50 years. These earthquakes correspond to those having approximate return periods of 75, 500 and 1000 years respectively and are called *service earthquake*, *design earthquake* and *maximum earthquake*. The Vision-2000 Committee (SEAOC, 1995) called these typical earthquakes *occasional*, *infrequent* and *very exceptional* earthquakes. These three typical events are used in both referred documents to establish the seismic performance that should be expected for conventional and essential buildings. Thus, for instance, for essential buildings the Vision-2000 Committee recommends buildings to remain completely functioning in case of an *occasional* earthquake and operational in case of an *infrequent earthquake* but the building should guarantee life security in case of a *very exceptional* earthquake. *Occasional*, *exceptional* and *very exceptional* earthquakes for the Central Pyrenees area, where the 1923 Vielha seism took place, have intensities of VIII-IX, VII-VIII and VI-VII respectively. Such earthquake scenarios have been simulated and the main results concerning the hospitals performance are summarized in the following. Figure 12.10 shows the appointed hospitals. In red is indicated the sole hospital that was involved in the occasional earthquake case, in yellow are the other hospitals involved in the case of the *infrequent* event, while in green there are the other hospitals in Catalonia. All the hospitals belonging to the hospital network were requested by the emergency situation produced by the *very exceptional* earthquake. Note that Figure 12.10 does not include 22 hospitals from the municipality of Barcelona that also intervened in the crisis.

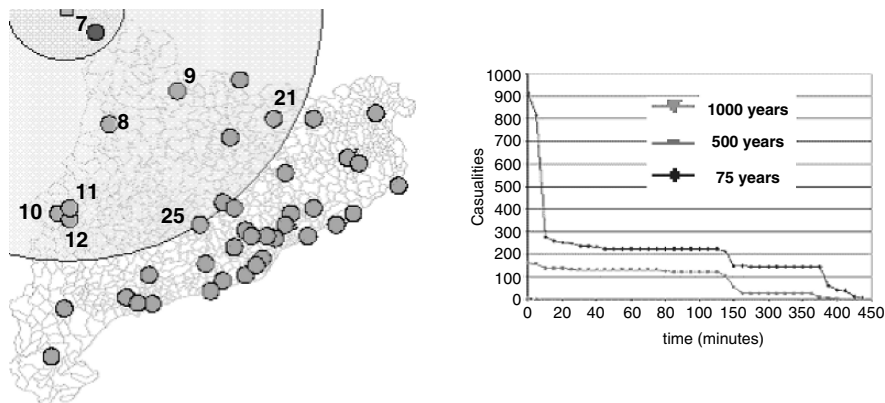


Fig. 12.10. Hospitals requested by the seismic crises corresponding respectively to the simulations of earthquakes with return periods of 75, 500 and 1000 years (see comments in the text). The right side Figure shows the time evolution of untreated casualties for *occasional*, *infrequent* and *very exceptional* earthquakes corresponding to the same seismo-genetic area

The right side of Figure 12.10 shows the number of casualties waiting for treatment and allows analyzing the time evolution of the emergency. The *occasional* earthquake rarely produces casualties (4), which are treated in 5 minutes, the system's response factor is 4 and the normalized response factor equals 1. Nevertheless, in spite of the fact that the *infrequent* earthquake causes 159 casualties and the *very exceptional* one, 916, the time of the emergency resolution is quite similar (3 hours for the rare seism and 3 hours and 15 minutes for the *very exceptional* earthquake), indicating a better efficiency of the system, which is able to manage a greater crisis in a similar time. This fact is clearly revealed by the system response factors. In the case of the *infrequent* seism, response factor is 4400 and in the case of the *very exceptional* seism, 13587. Normalized response factors score 28 for *infrequent* earthquake and 15 for *the very exceptional* seismic event. The 500-year return period event disables the hospital number 7 and saturates hospitals numbers 8, 10, 11 and 12. The rest of the casualties had to be treated in hospitals 9, 21 and 25, which admit respectively 2, 1 and 24 severely injured people. Hospital 10 was the last one to saturate, 2 hours and 5 minutes after the beginning of the crisis.

This time (Figure 12.10, right side) coincides with the sudden reduction in the number of untreated casualties. The transfer to the farthest hospitals from the epicenter, particularly in the case of the 24 casualties taken to hospital 25, lengthens the treatment time of this simulated earthquake emergency. The seism with a 1000-year return period needs the support of the whole health system in Catalonia. This disables hospitals 7 and 9 and saturates hospitals 8, 10, 11 and 12, as well as 25 and 27. Despite this, all these hospitals admitted only 226 of the 916 casualties. The rest had to be treated by farther hospitals delaying thus the resolution of the emergency. The communication among the saturated hospitals and those available makes the solution of the emergency, caused by a seism of intensity VIII-IX, not to last more than that caused by an earthquake of intensity VII-VIII.

Regarding the response of the hospitals, let us consider the behaviour of hospitals numbers 7, 10, 21 and 25. Table 12.3 shows the main characteristics of the capacity, significance and physical and functional fragility of the hospitals. *G* stands for General Hospital; *R*, for Reference Hospital. *F1* takes into account the category of the hospital; *F2* takes into account the relative importance of the hospital regarding the assigned population.

Table 12.4 summarizes the capacity of the hospitals analyzed and shows the characteristics of the demand and the individual response of each hospital for the *infrequent* earthquake case. The response factor of the hospital is an excellent indicator of the hospital's seismic behaviour. Values of response factors close to 1 indicate that the demand quite reaches the residual capacity of the hospital, that is, the hospital saturates although it treats all the casualties admitted. Null values of response factor indicate that the hospital does not participate in the management of the crisis, the lower the response factor, the lower the hospital participation. Values surpassing 1 indicate that the demand is greater than the residual capacity. Values higher than this factor indicate a significant physical degradation and a demand surpassing the residual capacity. Therefore, high values of hospital response factor indicate hospitals close to the place of the catastrophe and poorly dimensioned to face it.

Table 12.3. Main characteristics of hospitals numbers 7, 10, 21 and 25

		HOSPITAL NUMBER			
		7	10	21	25
Initial capacity parameters	Category	G	G	G	R
	Capacity (available beds)	31	132	64	273
	Occupation index (%)	62	58	82	70
	F1	1	1	1	1.3
	F2	1.48	1.48	1.55	1.6
	Relevance factor (F1·F2)	1.48	1.48	1.55	2.08
Physical fragility parameters	Percentage class A	0.05	0.250	0.050	0.200
	Percentage class B	0.250	0.450	0.150	0.750
	Percentage class C	0.450	0.250	0.700	0.050
	Percentage class D	0.250	0.050	0.100	0.000
Functional fragility Parameters	I_{min}	6.5	6	6.5	5.5
	I_{max}	8.5	7.5	8.5	7.5

Table 12.4. Capacity, degradation and response factor of hospitals numbers 7, 10, 21 and 25. The scenario is that corresponding to a 500-year return period simulated to the seismo-genetic region of the Central Pyrenees area

		HOSPITAL NUMBER			
		7	10	21	25
Capacity	Hospital Capacity	31	132	64	273
	Occupied beds	19	76	52	191
infrequent earthquake $T_r=500$ years Int=VII-VIII 159 casualties $T_{max}=3$ hours FR=4400 FRN=28	Functional degradation	100%	0%	0%	0%
	Initial available beds	0	56	12	82
	Admitted casualties	129	59	1	24
	Treated casualties	0	56	1	24
	Saturation time	0	2 h 5 min.	–	–
	Response factor	28.14	1.05	0.08	0.29

12.5.5. GLOBAL CHARACTERIZATION OF THE SYSTEM AND THE HOSPITALS

In order to characterize the global system performance as well as its adequacy for the seismic hazard of the region a study of likely losses and a risk analysis has been carried out.

12.5.5.1. Potential losses

The study of potential losses has been achieved by analyzing the effects that the occurrence of all the earthquakes having the same probability rate, would have on the

hospitals and on the hospitals system. To do this, we built a grid covering the region and the seismo-genetic areas having influence over the region. For each grid node we simulated the earthquake scenario produced by the seismic event which has the epicenter at this node and the considered return period. Then we assign to this node the typical parameters concerning the emergency management and the health system response.

An adequate interpolation allows mapping the representative values of the seismic emergency and the response of the system. Return periods of 75, 500 and 1000 years were analyzed. For a return period of 75 years not much damage occurs and the capacity of the system fully surpasses the scarce demand (Safina, 2003). Nevertheless, the return periods of 500 (Figure 12.11) and 1000 years produce a significant number of victims in the great urban areas mainly due to the high population density and to the high vulnerability of its buildings. Figure 12.11 highlights the nuclei of the province capitals (Barcelona, Tarragona and Girona), the coastal areas and the Ebro river delta. The case of the 1000-years return period adds the nucleus of the city of Lleida in the western central zone of Catalonia.

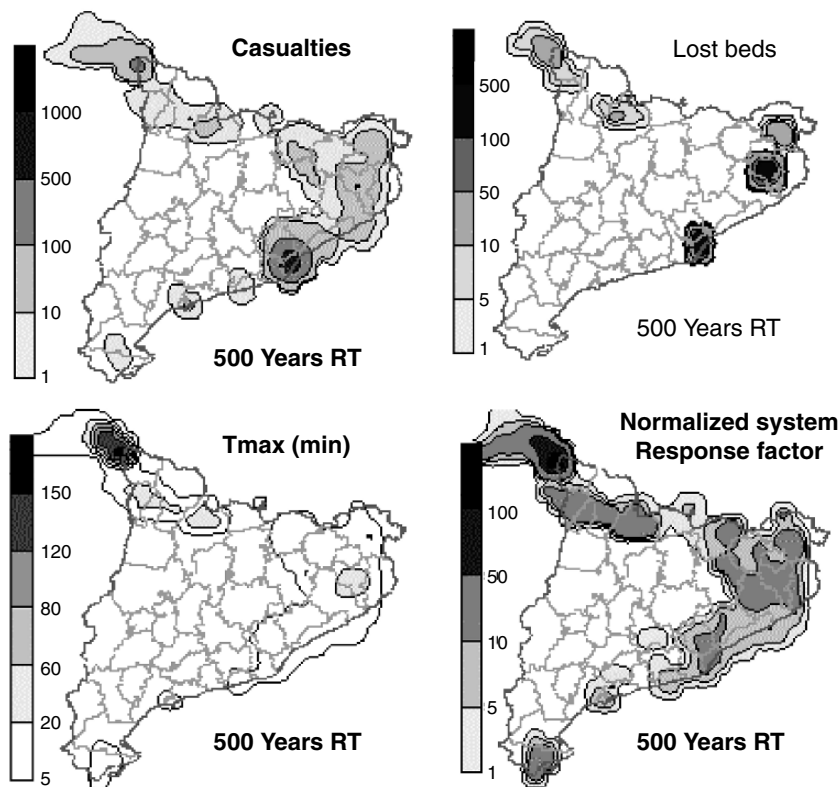


Fig. 12.11. Several results of the study of potential losses for typical scenarios having a 500 years return period (slightly modified from Safina, 2003). (See explanation in the text)

The northern and northwestern areas of the region suffer because of the relatively high seismic hazard and the deficiencies of the hospitals and road networks. Outside these regions, the likely demand is well satisfied by the capacity of the existing health care system

12.5.5.2. Risk analysis

The study of potential losses allowed analyzing the adequacy of the hospitals' system to the seismic characteristics of the country indicating that its capacity is not well-dimensioned in the areas with high population density and in high seismic hazard areas. The risk analysis allows evaluating the adequacy of each hospital. Risk analyses are based on yearly probabilities. A risk analysis is understood as the procedure that allows estimating the annual probability that a parameter or a quantity be equal or greater than a typical value. In this case and for each hospital, the parameter chosen is the hospital response factor FRH . The risk analysis will determine the response factors having a 0.21% yearly probability to be equalled or exceeded. This 0.21% typical yearly probability corresponds to a 475 years return period. The estimation of the hospital response factor probabilities will be based on the probabilities of occurrence of earthquakes capable of generating an emergency to be faced by the hospital with a given response factor. Therefore the risk analysis requires knowing the complete regional seismic hazard model, including seismo-genetic zones and earthquake occurrence probabilities as well as distance-intensity attenuation laws. We will use the hazard model proposed by Secanell et al. (2004). Each seismo-genetic zone is modelled by means of a double truncated Gutenberg-Richter law that characterizes the probability that a given seismic intensity will be equalled or exceeded.

Safina (2003) develops the mathematical formulation of the method as well as the details of its application to Catalonia. This application required the simulation of 60940 seismic scenarios. For each emergency scenario we estimate the response factor of all the hospitals in the system. Finally, for a given hospital, the annual frequency of participation in a seismic emergency with a determined response factor will be equal to the sum of the annual frequencies of occurrence of earthquakes causing the emergency. That is, for each hospital H , the annual frequency of occurrence of a hospital response factor value FRH_v is expressed by:

$$N_{FRH_v} = \sum_k \sum_h \sum_I n_{hk}(I) \quad (12.16)$$

For each hospital, $n_{hk}(I)$ is the number of earthquakes of intensity I , occurred in the cell h belonging to the seismo-genetic zone k , that causes the hospital response factor FRH_v . Then the mean annual probability of a hospital response factor FRH_u is defined by:

$$P_H(FRH \geq FRH_v, \text{ in one year}) = 1 - \exp(-N_{FRH_v}) \quad (12.17)$$

We define three categories for the expected seismic behaviour of a hospital: *Acceptable*, *Critical* and *Intermediate*.

These three categories correspond to hospitals whose response factors (FRH), with a 475 years return period, are respectively equal to or smaller than 10, greater than or equal to 100, or take values between 10 and 100.

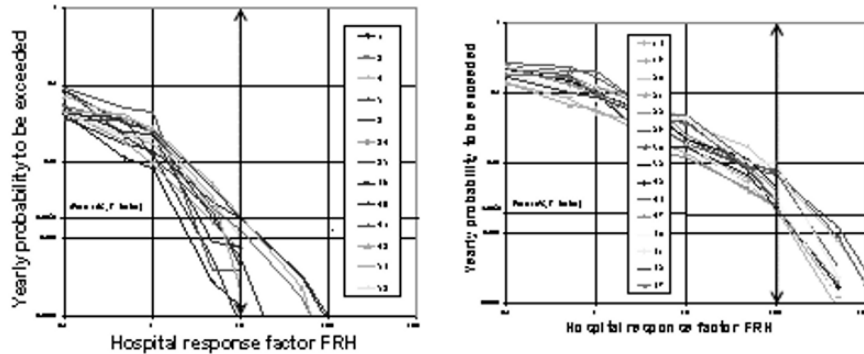


Fig. 12.12. Examples of risk curves defining the probability that the hospital response factor equals or surpasses a given value. Curves corresponding to hospitals showing *acceptable* (left) and *critical* (right) behaviour

Figure 12.12 shows two examples of typical risk curves corresponding to those hospitals with an *acceptable* and *critical* behaviour. That is, respectively those hospitals whose response factor *FRH* are smaller than or equal to 10 and those ones with response factors equal to or greater than 100 for a 475 years return period or having a yearly occurrence probability of 0.0021.

Figure 12.13 shows the estimated seismic behaviour of the hospitals. The computer program developed requires inputting all the information needed for the computation of the capacity and demand of the hospitals and of the whole health care system but it also allows us to get other specific outputs regarding the seismic performance of each hospital. For instance, in the case of Hospital number 7 (Figure 12.10) displaying an *Intermediate* behaviour (Figure 12.13), the yearly probability that an earthquake happens, saturating its capacity, is 2% while the probability of occurrence of an earthquake not saturating the hospital is 5%.

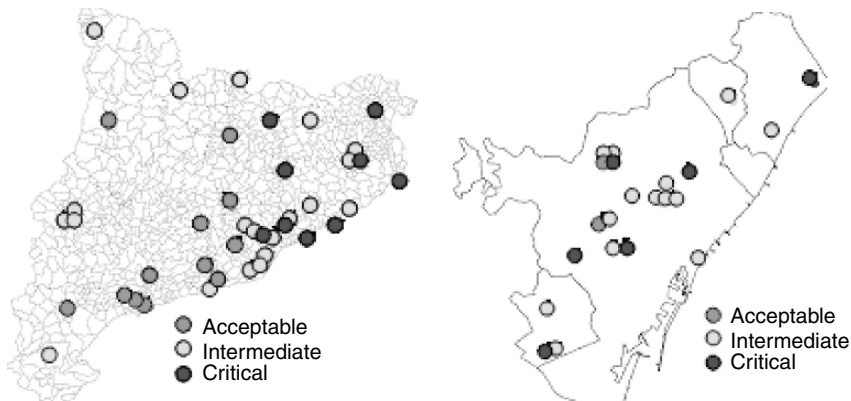


Fig. 12.13. Classification of the 64 hospitals in Catalonia concerning its seismic performance. On the right side, detail of the 22 hospitals in the city of Barcelona (see explanation in the text)

On the other hand, the yearly probabilities for the occurrence of an earthquake degrading by 100%, more than 66% and more than 33% the hospital capacity, are respectively 0.2%, 0.4% and 1%.

The results that can be obtained with the approaches presented herein need to be considered in the preparation of future policies for earthquake risk mitigation. The methodology has been applied to a specific region with moderate seismicity but it can be used for other regions with higher seismicity. The method accepts different ways to compute the various components of the problem according to the quality and detail of the existing information and the objective of the risk analysis.

Acknowledgments

Miss Mar Obrador helped in the English version of this chapter. This work has been partially funded by the Spanish Ministry of Science and Technology and with FEDER funds (project: REN 2001-2418-C04-01).

CHAPTER 13
BUILDING AGAINST EARTHQUAKES

F. Mañá¹, L. Bozzo² and J. Irizarry³

1. *Institut de Tecnologia de la Construcció de Catalunya, Barcelona, Spain*

2. *Estructuras y Proyectos, S.L., Barcelona, Spain*

3. *Institut Cartogràfic de Catalunya, Barcelona, Spain*

13.1. Introduction

In the complex process of designing a building the designer goes through two complementary stages, unfortunately not too much coordinated. In the first stage, the procedure tends to use methods still anchored in absolute empiricism, where the designer makes use of his intuitions and of his own experiences to try to fit the architectonic forms to a great number of requirements (obvious, among them, resistance to the maximum attributed acceleration). In the second stage, totally rational in its exposition and development, in which theories, norms, codes and legislations are applied, the assumptions made in the first stage are verified and coordinated. This chapter tries to deal with the tools needed in both stages. In the first part, data of qualitative type are provided with the intention of discussing the most intuitive part of the process. In the following, seismic engineering norms and a little history is presented, together with actual design trends.

13.2. Architectural design

Many experts and more than a few regulatory standards erroneously interpret earthquake-proof building design as synonymous with the earthquake-proof structural calculation of buildings. Some standards define vibration periods and construction layouts, for example, only in terms of the structure and its component elements. This approach, which needs a thorough revision, does not help building designers to acquire the insight needed to meet the true aim of any building in an earthquake zone, namely, to reduce personal injuries and property damage in the event of an earthquake of the greatest foreseeable magnitude.

While the objective remains to strengthen the structure of conventionally designed buildings somewhat, no real effort is being made to develop an architecture that must address a very specific issue: resistance to dynamic effects. It is important to have in mind that most insight on the part of buildings designers has been generated on the basis of the behaviour of architectural forms built of stone under the force of gravity, and a huge effort is required to change that insight, which is the fundamental element in decisions on architecture today.

Although structural failure leads to an unusable building, it is important to remember (in connection with what is known as “damage limitation”) that the high cost of other aspects of construction can lead to the building being financially unviable even where structural collapse does not occur (the cost of the structure represents no more than around 10% to 15% of the total cost of a building). This leads to two relatively crucial considerations:

- a) Earthquake protection must take into account the building as a whole, and constitute a special approach to building design: glass falling to a sidewalk or the collapse of the ceiling in a large hall can cause more victims than a partial failure of the structure, for example.
- b) Failure of the façade can make a building financially ruinous owing to the high cost of replacement. Therefore, a certain criticism of the ways in which damages are appraised would be in order, since that appraisal is normally based only on structural damage.

As consequence, before, or while, complex procedures for damage appraisal are implemented based on the effects of earthquakes on structures, a sizeable task relating to quality in the assessment of the risks involved in living in (or near) a building that is not equipped to withstand earthquakes should be carried out.

13.2.1. PRINCIPLE OF ORDER

Order in both composition and structure is a classical architectural requirement. The work must be comprehensible at first glance. The observer must find sufficient known and ordered points of reference to ensure that the created space causes sensations of satisfaction rather than sensations of disquiet and/or disorientation (even though in painting there are styles that aim simply to create sensations, regardless of their nature, even if they are disagreeable).

This classic architectural tendency is also based on the need for the construction to be structured so that it can be rationalised, and to ensure that the behaviour of the structural elements is relatively true to the assumptions made in their calculation (those assumptions being more restrictive where the available calculation methods are more rudimentary).

Thanks to the apparent availability of calculation methods that can be used to simulate the stress states of any form under any action, certain contemporary lines of architecture being developed are making structural disorder a fundamental part of their composition.

In the past, buildings were attractive when erection of the structure was completed, and less so when they were furnished with an outer skin showing their most representative architectonic elements. Just the opposite is true nowadays; the structures of buildings show a considerable degree of disharmony, and they are disordered and difficult to comprehend, but in the end, when all that confusion is covered by a skin (in some cases made of titanium plates), that solves its aspect and in many cases satisfies everyone.

The disparity between calculation methods, euphemistically known today as numerical modelling, and reality is often substantial. This is the case, for example, when partitions limit the structure's freedom of deformation, and calculation models lose their usefulness if they do not make allowance for those limitations on the models themselves, which is not normally the case.

The disparity between the results of the calculations and reality can be so substantial that we have come to accept that most methods have been validated on the basis that, having been used repeatedly, they are found not to cause problems beyond a level that is acceptable by those involved (including the users!), and little more. As structural

disorder grows, the results differ more and more from what is predictable by available theories and it becomes increasingly necessary to introduce new hypotheses (or new extrapolations), if we wish to use the same calculation tools. Risk increases, since there is presumably a greater difference between the models and actual behaviour.

The problem is aggravated when dynamic forces come into play, giving rise to local stresses in excess of the elastic limitations of the materials. Immediately prior to collapse, the redistribution of stresses and the appearance of “other” forms of equilibrium in the structural elements, among other factors, give rise to serious doubts as to the validity of the methods used to determine the values of the forces in extreme situations.

Practically, the only way in which we can monitor the validity of models is through the recovery of the structural order mentioned earlier, so as not to add, in view of the largely unrepresentative nature of the calculation procedures, the uncertainty that can result from the use of an inappropriate geometry.

However, we often forget that structures must also be optimised with respect to the stresses to which they will be subjected. This is an engineering principle that will become increasingly important, since it fosters resolution of the principles of environmental protection (such as energy savings and reduction of the use of raw materials) that we must take into account, regardless of the issues that are being dealt with.

All gratuitous formalisms that involve excessive use of materials and therefore excessive weight for buildings have, in addition to the aforementioned environmental effects, a considerable impact on seismic loads. These loads are created by the forces of inertia that arise in the course of an earthquake and these forces are a function of the masses that are placed in motion.

In the case of structures that are meant to be earthquake resistant, all these aspects of optimisation of forms must be carefully considered, since, in addition, they lead to other important considerations:

- a) A distribution of masses that tends to accumulate them in the upper part of the building will give rise to deflection forces on the ensemble that are greater than they would be if the centre of gravity was relatively low.
- b) A non-homogeneous and disordered distribution of the more rigid elements of the storey (e.g. dedicated screens for resistance to horizontal loads) will give rise to parasitic torsion forces (on the vertical axis) that will substantially increase the shear forces on columns and piers.
- c) The more rigid elements of the storey, particularly where they are few in number, will become the focus of a heavy concentration of deflection stresses that could cause them to fracture.
- d) Where the dimensions of buildings exceed the wavelength of the oscillation of the surface of the ground (in soft soils), differential deformations can occur in foundations. This effect would be added to the inertial forces caused by the earthquake, giving rise to a complex stress state (deflection-traction-shear) that

would lead to extensive fissuring precisely at the moment when the full strength reserve of the building is required.

These considerations are illustrated with an example shown in Figure 13.1.

13.2.2. PRINCIPLE OF INCLUSIVENESS

As mentioned in the Introduction, when planning buildings efforts at prevention in connection with the effects of earthquakes on the buildings must go beyond structural calculation and design. This is a requirement that affects all the elements involved and the complete process from start to finish. In fact, the first step must consist of an analysis of the risks that might exist where the building is to be located.

Ideally, regional planning should be based on a risk map drafted by experts who are familiar with the area, taking into account that an earthquake could impinge upon certain latent risks and activate them (such as the liquefaction or instability of slopes).

The best way of starting off a building project in an earthquake zone is to carry out regional planning that takes into account the area's seismic characteristics, since at that time a building code can be established that tends to make buildings take on the appropriate forms (e.g. with characteristic frequencies that are as different as possible from those of the underlying ground, to avoid amplification caused by resonance). It is also important, at the time of planning, to take into account the presence of wells and troughs filled in with soft soils, since they normally cause a local amplification of the accelerations.



Fig. 13.1. This building successfully withstood the great Managua earthquake, thanks to its suitable distribution of masses, although someone had the idea of placing a large water tank on the roof, supported on a floor of columns that collapsed, and after the earthquake it was observed that the water tank had come to rest directly on top of the lower structure

Once such areas have been identified, they can be eliminated from eligibility for construction use or local values for accelerations can be established that are on the side of safety.

In addition, and focusing more on the building itself, it is important to take into account all aspects relating to access and mobility. It is worthwhile recalling the hospital in Mexico City that, although it withstood the effects of a severe earthquake, was rendered totally inoperative after the incident, since the roof of the ambulance zone collapsed and destroyed all the vehicles.

It is also necessary to consider the elements comprising all meeting places and particularly the emergency exits, since a heavy element situated high up (such as a ceiling or equipment) and inadequately attached to the structure can cause a large number of victims. The same can occur with a poorly-placed staircase or inappropriate flooring. Nevertheless, these aspects are normally the object of careful consideration, since emergency exits are dealt with in a variety of safety hazard prevention regulations (fires, for example).

The elements comprising façades deserve separate consideration, particularly those made of glass. The deformation of frames normally causes their breakage, with a shower of broken glass falling onto sidewalks at the precise moment when alarmed users, not knowing where to go, remain next to the doorways of their buildings. It is important for entryways to buildings in earthquake zones to be protected by canopies that are strong enough to withstand reasonably heavy impacts. It is also important to disregard technology for panes of glass attached simply by means of structural silicone on the market today (an earthquake-proof building bears no resemblance to an automobile). A building can remain standing for centuries, while adhesives have a limited lifetime. These considerations are illustrated by Figure 13.2.



Fig. 13.2. A building that has lost its façade in an earthquake (located in Mexico City), in addition to the effects it may have on frightened pedestrians, can suffer financial damage comparable to the failure of the whole building

The elements supporting the façades must be attached to the general structure using strong, ductile connectors and not just propped against the edges of ceilings as is normally the case, and heavy elements projecting outwards from façades should also be avoided.

The cladding of many buildings needs to be considered, as it is in a state of precarious equilibrium, either because the anchors have aged or because the adhesives and/or mortars, due to fatigue under thermal stress, no longer perform their function.

As a rule, these issues are not addressed by the laws and regulations governing the design of buildings in connection with seismic factors, given the structural bias of the content of those laws and regulations. It would be of most importance that codes can provide detailed guidelines on these issues.

13.2.3. PRINCIPLE OF SHEAR STRENGTH

A building that is exposed to a horizontal action (whether oscillating or otherwise) is subjected to deflection loads, i.e. to a combination of deflection and shear forces. In theory, the increase experienced in comparison with normal forces is relatively small, since the inertia of the ensemble is usually enormous, but the shear forces, which depend only on the size of the section involved, can easily reach the breaking point.

Shear forces are not discriminating and affect the partitions just as much as the structure. In any event, the shear forces are distributed according to the rigidity of each element in respect of the rest, and it is here that the potential for unexpected events arises:

- a) The elements of greatest rigidity are the partitions and, in addition, they tend to be the least able to resist this type of force, even though, once they have been fissured by the deflection-shear force, they can maintain additional rigidity thanks to their ability to function as struts in compression, where their ends are confined (a circumstance that is usually taken as an advantage in the ultimate resistance analysis due to an earthquake).
- b) The shortest elements of the storey (partitions or columns) are the ones that receive the greatest part of the load and are the first to collapse. This is known as the “short column effect”. Construction in earthquake zones requires great care to be taken with architectural approaches that use mezzanines and with buildings abutting on each other without joints and with floor slabs on different levels from each other.
- c) To the forces already mentioned, a substantial increase in shear forces can be added when the shear force created does not act on one of the main axes of the storey (the axes passing through the centre of gravity of the masses), since that circumstance gives rise to torque along the vertical axis that can only be balanced by an increase in the shear forces on the elements that are capable of withstanding that increase.

The model for failure of a building made up of a linear structure (e.g. concrete) and rigid partitions (e.g. ceramics) would be as follows: In the first place, the partitions would undergo stress, since they are the elements of the ensemble that are most rigid to deflection and resist the free deformation of the structural frames. The partitions would break quickly, due to their lack of strength to withstand traction, mainly in the form of sloping cracks. Since the force is of a back-and-forth nature, these cracks often intersect and appear in the form of an X. Once the rigidity of the partitions is lost due to breakage, the structure, where very sizeable nodal forces arise, becomes subject to the load. It is important to bear in mind that at this point the ensemble has lost a great deal of its rigidity. While previously the forces had been amplified as a result of resonance,

when the partitions are no longer effective the natural period has changed considerably and it must be assumed that the dynamic forces fall to much lower values.

In other words, after an earthquake a building can have a deplorable appearance, with severe damage to all its partitions, while its structure remains almost intact. In financial terms, even though the building remains standing, it is most often considered a total write-off and needs to be replaced (an approach that is contrary to some of established principles with respect to the “extent of damage”).

In any event, if the aim is to attempt to avoid the collapse of the system in the last stages of equilibrium, the structural nodes must be designed in such a way as to retard the formation of mechanisms in the presence of such actions. Structures that are subjected to loads by severe earthquakes often show structural nodes that have been severely damaged by X-shaped fractures, where the stirrups have split and allowed the crushed mass of concrete that had formed the core of the pillars to run out.

When the number of plastic hinges formed allows the creation of mechanisms (either locally or overall), the system can collapse, either all at once, or by falling in a chain reaction, owing to a local failure that destabilises the rest.

One good practice is to make stirrups denser near structural nodes, increase reinforcement against shear, increase the length of overlap of reinforcement and avoid having sections work in service beyond their elastic range, so that in the event of an earthquake they have a reserve of strength to withstand deflection-shear forces.

13.2.4. PRINCIPLE OF MONOLITHISM

By keeping with normal construction methods, conventional construction, attains, almost automatically, a very high degree of continuity. Proper construction (taking into account the principles of bonding) involves the mobilisation of frictional forces (depending upon weights) between different elements that are sufficient to ensure resistance to moderate actions in a horizontal direction.

The same is true in the case of buildings made of amorphous concrete. Where no serious errors are committed, continuity is attained simply through pouring the concrete and overlapping the reinforcing steel bars.

On this structural base (an effectively continuous one, even if it is made up of small elements), the roofs are installed with their strength to withstand traction (required to balance deflection) and, as required by regulations, the connection between roofs and walls or frames is made by means of reinforced concrete bonds that provide the ensemble with a certain degree of ductility. In other words, a conventional building that conforms to current construction criteria (regulated to a greater or lesser extent) shows a degree of monolithism that allows it, where necessary, to bring a variety of resources into play in order to withstand certain overloads of a dynamic nature. Only the degradation of building methods (often the result of the pursuit of greater returns, changes of materials, architectural speculation or structural modifications caused by change of use) will lead such buildings to undergo situations of risk in the event of moderate seismic activity.

In conventional construction, the façades are tied to perpendicular walls, since they are made of the same materials and are normally built at the same time, in keeping with the aforementioned principle of bonding.

These circumstances can be compromised where unconventional construction methods are used in pursuit of a more rational approach to building. In this connection, prefabricated construction methods will be specifically discussed.

Where, in place of conventional continuous finishes, systems are organized into structure (linear) and partition (surface), there is the risk that there will not be sufficient bonds between the façade and the structure to ensure that the façade remains stable in the event of an earthquake. Furthermore, it is being increasingly demonstrated (almost too frequently) that between a structure with relatively deformable edges (slabs resting directly on columns), and rigid partitions supported by those edges, certain types of incompatibilities arise that tend to result in breakage of the more rigid element (the partition) and, in a variety of cases, tend to eject it from its position. This tendency, added to a dynamic effect directed outward, can cause disastrous results.

Blachère established the principle that prefabricated construction should not be any less safe than conventional construction. He was aware that the basic objective of prefabricated buildings is to replace construction with assemblage. Any assemblage procedure is made easier by reducing the number of bonds between the component parts (and by reducing the amount of cement used in establishing those bonds). It is clear, then, that the slightest oversight, where such a prefabricated system (even if it is made up of very high quality components) is not properly attached to the rest of the building, will make the system unsafe, justifying the principle established by Blachère. By extension, this tendency to disintegration can be also found in all procedures for components that are made at the construction site: structures of pre-cast concrete components, bolted metal structures, prefabricated decorative panels, etc.



Fig. 13.3. The failure of the building occurred at the structural nodes. The plastic bearings were formed in unsuitable places, namely where the columns met the beams, when it would have been better that they form where the beams met the columns

These observations are not meant as a criticism of prefabricated systems, but rather as a reminder that the industrialised systems developed in areas prone to earthquakes must pay special attention to the use of procedures that ensure monolithism where this initial

discontinuity exists. It is sufficient to think back to how the gas explosions that occurred in the 1960s and 1970s gave rise to crises in several highly-developed prefabrication systems, due to their sensitivity to chain reaction collapse, in the event of failure of any of their components (Roland Point disaster). An illustration of these ideas is shown in Figure 13.3. The Spitak earthquake (Armenia) in 1988 also showed the weakness of pre-fabricated systems due to lack of proper detailing at connections.

13.2.5. PRINCIPLE OF STRUCTURAL DESIGN WITH A LOW LEVEL OF STRESS

At present, thanks to the powerful numerical methods available to us, it is usual to optimise structural design by adopting models of behaviour that allow (without going so far as to constitute mechanisms) the yielding of the various sections of the structure where the greatest deflection loads occur. These sections, where the yielding of the reinforcement is allowed for relatively low load states, are normally concentrated in the structural nodes, at the joints between columns and lintels. This approach is not the most appropriate for providing the structure with the ability to sufficiently withstand incidental actions of great magnitude. A horizontal load (which is the most frequent type in earthquakes) gives rise to bi-triangular moment diagrams that attain their maximum values precisely at the nodes.

Although the vertical component of forces created by earthquakes is normally ignored, it is important to bear in mind that there are elements, usually caused by inadequate architectural design or improper adaptation of an existing building to other uses, that can fail under a relatively small increase of the load produced by an oscillating force. These are the elements that undergo heavy deflection loads from the building components resting on them. More specifically: façades of penthouses, which, since they are set back, rest on the underlying slab; the props of columns on girders to accommodate other functional systems; trimmed joists or large cantilevers, etc. particularly in cases where the shear or torsion forces are predominant.

13.2.6. PRINCIPLE OF FREE DEFORMATION

The models of buildings normally taken as an object for the development of regulations are usually isolated buildings. In these circumstances of free deformation, buildings show certain behaviours in response to the dynamic loads that provide the starting point for the theories that have been taught to most experts as methods for verifying safety. This fact has led to most buildings being studied as individual buildings when, in reality, a substantial proportion, standing within built-up areas, have proximity relations with other buildings.

In order for a building to function as an isolated building in an urban complex, joints between it and the adjoining buildings must be provided. These joints should be large enough to allow freedom of deformation as imposed by the corresponding dynamic effects. The necessary size of the joint (depending on the height of the building, acceleration, type of vibration, etc.) is normally on the decimetric scale, although this circumstance is not usually considered in regional or municipal planning, nor in the regulations governing the thickness of heat-seal. Furthermore, there are no building systems on the market that provide a solution for this problem, since it would require a device that could act as a breakaway strip in the event of an earthquake, establishing

weak links between the parts that would, in everyday use, provide a continuous surface for walking, for example.

On the basis of current data, all joints between buildings should be considered to be free deformation joints and all joints separating a complex floor plan into simpler parts should be of sizes on the decimetric scale of free deformation joints in order to ensure a better seismic response. The same should also be true of all heat-seal. However, this problem has not been solved, and, from the standpoint of building it has not even been considered. Could it be that in earthquake zones buildings should not be longer than the compulsory 30–40 metres in order to avoid thermal overloads? Could it be that the joints between different buildings should maintain a distance for free deformation? If so (and this is in fact the case), it is time to inform all officials in charge of planning our cities and all those who draft municipal by-laws so that they can act in accordance with these principles, since it is known that Mediterranean cities are made of buildings that normally abut on one another, in a system sharing a common partition wall.

Depending on the era in which they were built, city centres are composed of coexisting buildings, constructed using very different technologies. Depending on the regulations applied at a given time and the different construction methods used, the limit between two reference buildings can be very different.

In Catalonia, the law governing shared walls was regulated under the *Ordinacions de Santacilia*, an antic text dating from the reign of James II (combining Roman law and Frankish customs). From the date of the *Ordinacions* onwards, buildings were constructed in the following manner: the first builder would make the foundation and the wall that would later be shared by both buildings, and when the neighbour decided to build, they would pay the first builder for half the cost of the common foundation and wall already in place.



Fig. 13.4. Where the joints between buildings are not sufficiently large to allow them to deform freely, it is highly likely that, in the event of an earthquake, they will collide

13.2.7. PRINCIPLE OF LIGHTNESS

The methods normally used to predict the effects of an earthquake of a given magnitude on a building are based on deduction of the accelerations acting on the various masses that will be put in motion, and, on the basis of those accelerations (a) and masses (m), deduction of the forces (F) that will be released, taking into account the simple formula:

$$F=m \times a \quad (13.1)$$

In fact, the forces calculated are inertial forces that are directly proportional to the masses put in motion and therefore these forces are linked directly to the amount of the materials used and to the construction systems that are created on the basis of the type of materials.

Taking this approach into account, it is obvious, from a purely seismic standpoint, that buildings should be as light as possible. In this respect, there are different building cultures in areas highly prone to seismic activity that are based on wood and paper (traditional Japanese architecture), while other cultures that are equally exposed to seismic activity, possibly owing to scarcity of resources, still construct their buildings of earth and stone (Middle East), with disastrous effects in the event of earthquakes (as we are frequently reminded by events in the Middle East, Central America and North Africa).

In spite of this and driven by a variety of different requirements (some of them relating to fireproofing, strength, soundproofing or durability), modern construction methods have adopted the accumulation of materials, i.e. massiveness, as a means of addressing those requirements. Thus, buildings in the actual economic sphere are increasingly heavy and therefore less able to withstand, economically, the forces that are unleashed when an earthquake occurs.

For some time now, the rationalisation of masonry and formwork has been leading in the direction of construction methods based on flat slabs resting directly on columns, which involve serious problems of lack of ductility in the finished building, as already mentioned, and also imply a failure to optimise sections in relation to forces. The excess use of materials that this approach requires also causes environmental problems, such as overuse of raw materials and excess consumption of energy.

Irreconcilable differences appear to exist between the need to make buildings as light as possible (earthquakes and environmental protection) and the need to satisfy other requirements (durability, fireproofing, soundproofing, etc.). A great deal of regulatory pressure and imagination will have to be brought to bear in order to resolve this incompatibility.

Looking more closely at various aspects of the mentioned issues, the problem that exists about the insufficient durability found in the concrete used in buildings some years ago is now being resolved through regulations that require the use of more cement, improved impermeability of the concrete, greater protection of reinforcing steel bars (thicker and heavier coverings), less fissuring (i.e. less stress on the reinforcing steel bars) and therefore more steel. The manufacturers of construction materials are assured a substantial market share, particularly when considering that this excess weight implies larger and stronger sections to withstand earthquakes, in other words, increased weight.

Most architects design buildings on the basis of relics of classicism. In many cases, the proportions, the basic aspect of the design, still correspond to the proportions found in stone buildings from centuries ago. In the era of plastics and metals, this may seem surprising, but it could be related to an unusual fact that is not normally considered: 54% of the weight of the materials used in modern buildings corresponds to crushed stone (the aggregate used to make different components).

A recent study evaluated the weight of the materials used for an average building in Catalonia taken as a reference. It is believed that the sample is representative of a large spectrum of European construction, since, according to recent figures, 40% of the new buildings under construction in the European Union are located in Spain. Whether owing to the frequency of construction of basements involving the use of heavy retaining walls, or to the fact that foundations are increasingly complex (because they extend into land filled areas), or owing to the fact, mentioned above, that structures are increasingly heavy, the average weight of buildings, based on the available figures, is nearly 2.5 ton/m². It is worth noting that just fifty years ago conventional buildings were not even half as heavy.

Building must be one of the few areas of design where the reduction of weight, while maintaining the same or equivalent features, is not one of the main objectives.

In the review of what is the buildings weight, it is worthwhile to take into consideration the opinions of users. In respect of their personal requirements, users tend to prefer conventional stone buildings. There are a number of reasons for this attitude, but the most important ones have to do with apparent durability, ease of maintenance, or a simple reaction against the prefabrication methods used in the past (associated in Spain with times of economic difficulties). In short, the market tends to foster the construction of "heavy buildings".

Summing up, it can be concluded that modern buildings require greater strength to hold themselves up than to withstand the loads involved in their use. While this, in itself, constitutes an anomaly in our highly evolved world, it is even more anomalous considering that such excess mass, when placed in movement, will possibly result in the failure of the building.

13.2.8. PRINCIPLE OF NON-RESONANCE

At least since the Athens Charter, one of the factors taken into account in urban planning is the characteristics of the region. Aspects relating to environment conditions (based on orientation, humidity, prevailing winds), and aspects relating to risks (flooding, slope stability, etc.) among others, are normally considered to be basic requisites (both in connection with the layout of streets and subdivision into parcels), but seldom is heard, in this field of design, that regional organisation is carried out on the basis of seismic risk taking into account the characteristics of the soil.

It is known that the frequency (and its inverse, the period) of the impacts reaching buildings is determined by the particular characteristics of the underlying soil. This is one parameter that should, in all cases, be known when suitability for building is regulated in a region.

On the basis of this knowledge, urban planners should be capable of defining preliminary plans for buildings and recommending certain architectural forms whose characteristic period is as distant as possible from the period of the soil, to ensure that the accelerations that might impinge on the components of the building will not be made unbearable due to resonance (see Chapters 3, 5 and 8 for details).

An earthquake that affected an extensive area of Mexico caused heavy damage to tall buildings in Mexico City and to low buildings in Acapulco. At the same time, low buildings in the capital and tall buildings in the tourist resort showed hardly any damage at all. This was due to very different dynamic characteristics of the soil in the two cities. While an important part of Mexico City is built in extremely soft soil, the soil under Acapulco is rocky, and the types of buildings that were affected by the earthquake were those that most closely resembled the rigidity of the underlying geological formations.

It is clear that urban planning has a leading role to play in regional organization, by adapting buildings (basically, their slimness) to the deformability of the soil supporting their foundations. This would give rise to substantial savings in buildings in earthquake zones, which would permit not only improved cost control, but would also have considerable impact on the sustainability of actions, since they would apply the desirable and rarely used principle of optimisation.

13.2.9 PRINCIPLE OF DUCTILITY

This principle is based on the fact that buildings should be able to dissipate the kinetic energy generated during an earthquake by means of deformation rather than through cracking.

In order to satisfy this basic requirement for the survival of the building, the architectural forms (partitions, structures and installations) must use materials with a substantial relaxation component in their stress/deformation diagrams and the components made from these materials must maintain a high degree of continuity with other components, allowing them to redistribute the overloads that they are incapable of withstanding.

In short, at the critical moment there must be the possibility for other forms of equilibrium to arise, more or less spontaneously, above and beyond the forms of equilibrium found in normal service (to a greater or lesser extent foreseen by the architect/engineer), before the ensemble is transformed into a mechanism.

In theory, the ductility of reinforced concrete structures (the most commonly used) depends on:

- The characteristic ductility of the steel (it is recommended to have an extensive yielding component before the breakage deformation is reached. There could be nothing worse than the fragile steels that were placed on the market in Germany several years ago).
- The amount of reinforcing steel correctly placed and correctly anchored. It is important to keep in mind that the dimensions provided only in respect of gravitational forces are normally calculated with selective sections in respect of the sign of the moments. It would be worthwhile, in areas with a medium-to-high

earthquake risk, for sections of reinforced concrete to be made with symmetrical reinforcement (already done in countries with frequent earthquakes, such as Mexico).

- Overlaps between reinforcing steel bars ensuring transmission of dynamic forces. Regulations normally call for overlaps longer than would be strictly necessary to withstand static actions, e.g. increments on the order of 10 diameters.
- Adaptation of sections to forces. Slabs resting directly on columns or flat beams are normally components with low ductility, while beams on edge normally form structural ensembles where plastic bearings can be formed on the beams near the structural nodes (the place recommended by all regulations).
- The resistance of elements to shear force. In the case of slabs resting directly on columns, the concrete's own ability to resist shear forces should not be taken into account. That would lead to a form totally lacking in ductility.
- The quality of design and execution, particularly the latter. The most representative image of a building just demolished by blasting is the number of construction defects that are brought to light. In such circumstances, it can be observed that all the preferential breaking points were cold joints (between concrete pours that were not correctly bonded), errors in anchoring, errors in distribution of stirrups, or improper reinforcement (a surprising number of cantilevers are reinforced backwards!).

Planning and building with the goal of ensuring ductile responses requires, under most regulations, consideration of seismic forces with values that are significantly lower than would be the case otherwise. Therefore, even if strictly out of consideration of economic factors, it is worthwhile to work with structural approaches that can satisfy this requirement. An illustration of this principle is shown on Figure 13.5.



Fig. 13.5. Due to a lack of ductility, structures with slabs as ceilings normally provide unsatisfactory responses

13.3. Code design and construction details

Many of the architectural design principles exposed in the previous section are taken in consideration within the seismic provision and guidelines applied in countries with a high level of seismic code, but the application of some of them depend on the seismic conscience of the building designer. The seismic provisions and guidelines applied in a region depend mostly on the seismicity level affecting it. The most advanced seismic code provisions come from regions like Japan and USA where strong earthquakes hit frequently causing high losses. In such regions, the seismic conscience is very high due to the losses past earthquakes have caused. In consequence, regions like these develop high level seismic codes enforcing their application not only to the new buildings but also to the existing buildings to ensure their seismic performance is acceptable.

The situation is very different for regions with a moderate to low seismicity like several European countries. Their seismicity is characterized by important historical earthquakes that occurred centuries ago. Today, cities are more vulnerable than at that epoch, so the damages caused by earthquakes similar to the historical ones can be quite larger than those suffered in the past. Unfortunately, the seismic conscience of the region is almost nonexistent; as a result its seismic design provisions can be classified as a low code level. Regions like this should not wait for the occurrence of a disastrous earthquake to enhance their building's seismic performance by applying a higher level code and evaluating the seismic performance of the existing building stock.

In Europe there has been a great effort launching the Eurocodes (EC), which define all the normative in the building construction industry, including the seismic provisions (EC-8, 2004). These provisions, supported on the most modern knowledge and adapted to the specific regional constrains imposed, for example, by the seismological conditions, will be in the near future the basis for national codes for the European Union.

Seismic design codes have the purpose of providing guidelines for the reduction of both property and life losses due to seismic events. These building design codes define standards for the seismic resistant design and construction of new buildings and for the retrofit of the existing ones. This set of guidelines is developed based on sound theoretical and physical modelling and on the observed damages caused by important earthquakes. These observed damages serve as an evaluation of the provisions and methods used for design by pointing out deficiencies both during the design and construction process. These lessons given by past earthquakes help to promote advances in the development of design methods, the knowledge of materials performance and the enhancement of construction practices. So, through an interactive process each new earthquake that severely affects a region acts as an inspector that shows how effective are the applied seismic provisions and shows the issues that require more attention.

Basically, a seismic code contains specifications for the seismic hazard, soil and possible near fault affects that should be used to design buildings in the considered region, defines the base shear load that should resist the building, makes recommendations about the structural detailing and sets displacements limitations. The first design provisions defined the required base shear as a mere percentage of the structures weight and no distinction was made based on any other characteristic of the building. With a better understanding of the interaction between the natural seismic

hazard and the building's behaviour, base shear is now defined using several factors relating to both the seismic hazard and the buildings characteristics. As the development of seismic provisions advanced, more conservative criteria have been adopted for buildings that are essential for the public health and safety, and ductility requirements have become stricter.

Seismic design of buildings at the beginning of the nineteenth century was limited in various countries to apply a lateral force roughly equivalent to 10% of the vertical one. This simple static equivalent method is still used but certainly with many improvements derived from the dynamic analysis suitable from modern computers and past experience with damage observed in previous earthquakes. In general codes allow the use of either code equivalent static loads for simple structures or dynamic analysis for more complex systems. Dynamic analysis may be mode superposition for linear systems (or structures that may be represented by such simplification) or step by step using earthquake time histories for more complex systems.

The equivalent lateral loads are different according to the country but in general they have the following form:

$$V = \text{function}(Z, I, C, R, W) \quad (13.2)$$

where V is the base shear; Z is a zone or local seismicity factor; I is an importance factor; C is a dynamic factor that depends on the structural period and local soil conditions; R is a reduction factor taking into account ductility and redundancy, and W is the reactive weight of the whole building. The Z , I and W factors can be defined more clearly than the other two factors which may vary significantly according to local country regulations.

Besides forces, most codes establish limitations in lateral displacements and structural systems. For example, Peruvian 1998 code establish a maximum inter-story drift for reinforced concrete buildings of only 0,007 for displacements calculated without taking into account any reduction in seismic forced, i.e. $R = 1$. Reticular slabs are prohibited in various high seismicity areas unless a significant amount of stirrups are added in order to improve their punching shear strength.

Vertical distribution of static equivalent horizontal forces also varies according to local regulations. Combinations of uniform, triangular and/or added local force on top of the building are, in general, distributions assumed in codes. For complex buildings with local discontinuities dynamic analysis is required based on spectra for local soil conditions. For example, CUBE tower, shown in Figure 13.6, is an example of a complex building that requires a dynamic analysis. The building, in Guadalajara, Mexico, is located in a high seismicity area. Certainly a building of this magnitude has to be calculated using modern precise methods but it is as important to provide conceptual design as presented in the introduction. In this case the load transfer mechanism is quite simple since there are three macro-columns corresponding to the services nucleus which carry the full load. Supported on these curve macro-columns there are steel-wall-beams that carry the unidirectional post-tensioning 40 cm slabs that provide a flat office area. The post-tensioning allows spanning up to 22 m without columns and with just 40 cm thickness reducing considerably the self weight (seismic forced are directly proportional to weight). For example, a typical 16 m span post-

tensioned unidirectional slab of the building weighs only 450 kg/m^2 . Moreover, the steel-wall-beams provide a redundancy mechanism. In case that any diagonal in the building is suppressed, the remaining elements provide alternative mechanisms to support the vertical and lateral loads. Finally, shear walls limit lateral deflections due to their large stiffness limiting damage to non-structural elements.

Modern codes, namely the 1997 US Uniform Building Code (UBC-97, 1997) and the EC-8 (2004), specify a base shear that depends on the seismic hazard level of the site, possible site effects from the site's geology, possible near fault effects, and the use, weight, fundamental period and lateral force resisting system of the building. In areas of high seismicity, sufficient ductile detailing to accommodate the inelastic demand (Bachman and Bonneville, 2000) had been mandatory. To achieve this goal codes impose story drift limitations and a maximum inelastic response displacement. They also require the evaluation of the deformation compatibility considering P- Δ effects.

Conventional seismic design of buildings, based on ductility and structural redundancy and developed in the 1970's, allows reduction in seismic design forces between 1 and 10 (R factor in the UBC-97 (1997)), compared to linear elastic forces. The reduction depends on the material and structural system selected for transferring the lateral loads. This approach allows for smaller sections and provides safe systems as long as fiber, sectional and global ductility is provided. An important aspect to note is that the analysis is based on a linear elastic response reducing directly the forces without taking into account the non-linear nature of the problem. This gross simplification allows a simple approach using the wide-spread mode superposition dynamic analysis method applicable to many practical situations. However, this approach has various drawbacks such as that the global ductility demand may require a large local ductility and, consequently, local failures do occur. Besides, large reduction in forces implies structural damage (non-structural damage is controlled limiting inter-story drift) which may be costly to repair after a major earthquake. Finally, minimum steel reinforcement, necessary to provide sectional ductility, is applied to all the elements in the lateral load system, resulting in expensive structures.



Fig. 13.6. CUBE tower in high seismicity area showing strong discontinuities and long cantilevers (The structural design was done by L. Bozzo)

Figure 13.7 shows the reduction in seismic forces that may be achieved providing ductility for a particular earthquake ground motion representative of stiff local soil conditions.

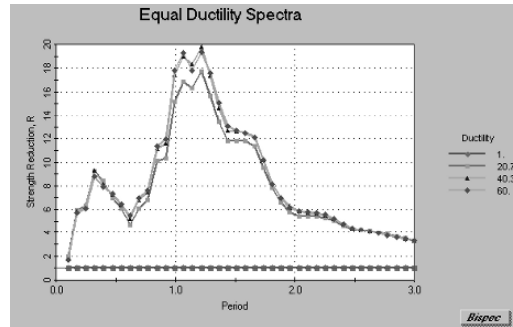


Fig. 13.7. Reduction in seismic forces providing local ductility (Loma Prieta earthquake, $\xi=5\%$)

The ductility levels considered in the figure are $\mu = 1; 20, 7; 40, 3$ and 60. The R factor represents the relation between linear and non-linear forces for various levels of ductility (the first curve for ductility 1 is a straight line corresponding to $R = 1$ since, clearly, there is no reduction). This figure shows significant reductions for the whole period range considered, particularly for $T > 0.5$ s with maximum values of $R = 20$. Certainly, there are other factors such as lateral flexibility and damage to non-structural elements that may limit this reduction but it is clear the advantages of providing ductility for seismic design.

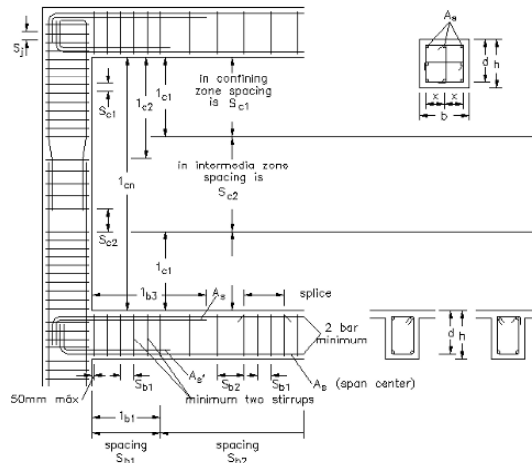


Fig. 13.8. Ductile frames according to UBC-97 (1997)

The practical way to provide ductility for frames is illustrated as an example in Figure 13.8. This drawing represents the UBC requirements for ductile structures and it can be considered a general way to provide this structural response. Stirrups are added at the ends of the columns/beams in order to restrain longitudinal reinforcement from buckling once the concrete cover is spalled during a strong earthquake. In these zones, plastic hinges would be formed during a strong movement and the stirrups allowed developing

a ductile sectional response. Splices should be done at the centre of the column (minimum moment zone) and stirrups should be added. Figure 13.9 shows the construction practice in Mexico where steel reinforcement for columns is placed up to 12m high in order to reduce splices. In the photo a construction worker is on top of the longitudinal reinforcement.



Fig. 13.9. Column construction practice in Mexico to reduce reinforced splicing

13.4. Actual trends for seismic design

An alternative to improve current design practice based on ductility and redundancy is the development of structural systems that localize the non-linear structural response. Examples of these systems in reinforced concrete structures are coupled shear walls or, in steel, the eccentric braces (Bozzo and Barbat, 1999). In the first one the link between the walls acts as a “seismic fuse” that controls the response during earthquakes. Similarly, in the second one the horizontal “link” between the diagonal elements provides a ductile response based on the stable hysteretic steel response under shear stresses. Both alternatives have two important drawbacks since interaction with surrounding elements may affect the ideal response of the “seismic fuse” or “link” and they are difficult to repair since they are an integral part of the overall structure.

On the other hand, alternatives for seismic design have been developed in the 1980's using the so-called base isolation (Naeim and Kelly, 1999) and energy dissipaters. Base isolation is an established technique for small to medium size buildings that allow significant reduction in seismic forces by either shifting the fundamental natural period of the building or introducing a low-friction-interface that limits the force transmitted to the upper structure. There are hundreds of buildings constructed with this technique, which, however, have some important drawbacks. Among them, the non-linear response

of the upper structure may be conditioned by the base-isolation connection (Ordoñez et al., 2003); the cost is increased; a flexible (usually about 30 cm) gap must be provided around the building and for all the service lines; the effectiveness is reduced as the number of stories (or natural period) is increased.

On the other hand energy dissipaters are a different alternative suitable for medium to high rise buildings that do not require special construction techniques or analysis. There are various systems such as the “Adding Damping And Stiffness (ADAS)” (Scholl, R, 1993) or the honeycomb (Kobori et al., 1992). There are also many examples of structures equipped with these systems.



Fig. 13.10. BOZZO-GERB energy dissipater

Shown in Figure 13.10, the BOZZO-GERB dissipater is an innovative shear link type dissipater. This proposed dissipater is based on the aforementioned eccentric braces since the overall shape is a well stiffened wide-flange section. However, the system is not based on standard shapes or specially welded ones. Instead, the device is milled from a plane standard shape. This fabrication process proposed by Cahis et al. (2000) allows very thin dissipative areas without welding. In the other hand, as in eccentric braces, dissipation of energy is uniform in the whole section, and it is very stable provided web buckling is avoided. Another important feature of this dissipater is that it presents a double mode work. Initially the energy is dissipated mainly in the web by uniform shear stresses in a “shear mode”. After the web degrades, the stiffeners continue dissipating energy in a “flexural mode”. The deflected shape changes significantly among those modes from a linear one to a curved one. The importance of this feature is that it provides a robust system that continues dissipating energy even after the web is degraded. Even though the design of the connection counts only with the first working mode, the second one provides an additional safety factor.

Figure 13.11 shows typical hysteretic experimental curves for a device performed at ISMES (Italy) in 2002. The Figure 13.11, part (a) includes the slippage in the connection while the curve in part (b) does not include any slippage. This indicates that the first curve is obtained using displacement transducers above the holes and the second curve within the holes and, consequently, does not include the slipping of the bolts. The experimental yielding force was about 150 kN and the yielding displacement about 0.5-1 mm. The total cumulative dissipated energy before any degrading of the devices was 77.528 kN.mm and 53.851 kN.mm for the first and second curves, respectively. For the second case the total dissipated energy after degradation of the device, i.e. including the flexure mode, was 97.210 kN.mm. This indicates that a

significant additional energy may be attained by the flexural mode as well as by the slipping of the connection. However, slippage is not considered a good response characteristic since it is difficult to predict, and so the tolerance is reduced as much as possible, just to accommodate for installing the devices.

The basic concept behind the proposed dissipater is to provide a general plastic-hinge available in different yielding forces and displacements. Therefore, it is not intended to have a unique system or specific geometry but a set of alternatives from which the designer can choose. All the connections should, however, have similar response characteristics and behaviour.

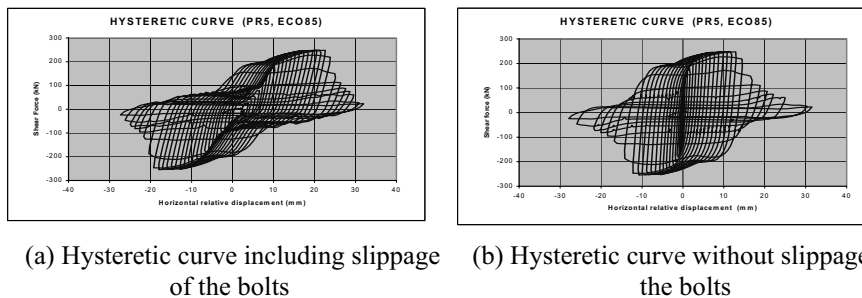


Fig. 13.11. Typical experimental hysteretic curve for devices

Recently many seismic design codes had been setting requirements relating to the performance of the buildings. This performance-based design sets an acceptable performance for a building that depends on the building's function and the level of seismic hazard considered. The acceptable performance is usually defined as an allowed damage condition, always avoiding achieving the collapse of the structure. Therefore, the challenge for designers is to ensure that cumulative damage is to remain within acceptable bounds so that people within and around buildings are able to escape from damaged buildings even after a major earthquake (King and Shelton, 2004). The use of the so-called "push-over analysis" (Fajfar, 2000) is a feature already included in commercial software to allow the designer a first non-linear analysis of buildings.

Several publications such as ATC-40 (1996) and the Vision 2000 (SEAOC, 1995) have introduced the definitions of the performance levels. The performance level required for a building is described by the physical damage within the building, the threat to the life safety of its occupants due to the damage, and the post serviceability of the building (ATC-40, 1996; SEAOC, 1995). The performance level definitions proposed by Vision 2000 are shown in Table 13.1.

Figure 13.12, from Rodgers and Mahin (1999), shows the building performance requirements as a function of the intended occupancy and use of the building. As can be seen, under a given level of hazard or earthquake probability, the damage considered acceptable decreases as the importance of the building's use and occupancy increases. For buildings designed using the performance based concepts, moderate or worse damage levels are considered to be an unacceptable performance when affected by a frequent level of hazard, while for rare hazard levels even collapse is considered an acceptable performance level. This performance based design philosophy is being recommended as a useful tool to evaluate the seismic performance of existing buildings

in order to verify if they comply with new performance requirements (Comartin et al. (2000)).

Table 13.1. Definition of the performance level from Vision 2000

Performance Level	Condition
Fully Operational	Continuous to give service. Negligible structural and non-structural damage.
Operational	Most operations and functions can be resumed immediately. Structure is safe for occupancy. Essential operations are protected, non-essential operations are disrupted. Repair is required to restore some non-essential services. Damage is light.
Life Safety	Damage is moderate, but the structure remains stable. Selected buildings systems, features, or contents may be protected from damage. Life safety is generally protected. The building may be evacuated following the earthquake. Repairs are possible, but may be economically impractical.
Near Collapse	Damage is severe in structural elements, but structural collapse is prevented. Non-structural elements may fall. Repair is generally not possible.
Collapse	Partial or total loss of structural integrity. Partial or total collapse. Repair is not possible.

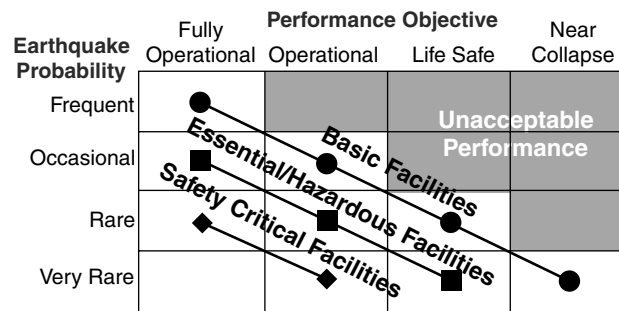


Fig. 13.12. Building performance requirements from Vision 2000

13.5. Final Remarks

Having a set of seismic design provisions and guidelines appropriate for a given region is an important step for reducing its seismic risk. This chapter has exposed both architectural design principle and design provisions that are considered to be the most important aspects for having earthquake resistant buildings. It must be mentioned that as important as having an appropriate design code, this seismic code has to be enforced in order to be as effective as it can be. Laws should be implemented requiring adequate supervision through the design and construction stages in order to ensure projects truly conform to the seismic design codes. Such concept has been implemented in Turkey after the 1999 earthquakes Kocaeli and Düzce with the establishment of the new role of building supervision specialist (Spence, 2004) in order to certify that new buildings do follow the seismic design provisions.

CHAPTER 14
INDUSTRIAL FACILITIES

B. Mohammadioun¹ and L. Serva²

1. *Robin's Wood Consulting, Whaleyville, Maryland, USA*

2. *Agencia Nazionale per la Protezione dell'Ambiente, Roma, Italy*

14.1. Introduction

The first phase in the environmental hazard analysis of industrial facilities is sitting. This entails selecting a suitable location, taking into account, amongst other aspects, an appropriate assessment of hazard parameters in order both to protect the facility appropriately against them and to minimize the plant's impact on the environment. This process becomes increasingly important and sophisticated as the complexity of the facility being designed increases, and accordingly the risk associated in case it fails. The sitting process includes an analysis of the geological stability of the site under static and dynamic conditions and the definition of the design loads related to natural phenomena, such as earthquakes, whatever their origin (tectonic, volcanic, or man-induced).

The second phase consists in the facility's design. This must take into account the parameters defined during the first phase (seismic design parameters, for instance) in order to guarantee proper behaviour of the installation (often designated as "critical"-nuclear power plants, dams, chemical plants) in the event of natural hazards and also, more importantly yet, to prevent the release into the environment of any hazardous materials they may contain. Concerning this phase, we will be dealing exclusively with facilities which, should they fail, are liable to occasion disastrous effects to man and to the environment: these are nuclear installations (Nuclear Power Plants (NPP), nuclear waste reprocessing plants, and repository sites of whatever nature) and facilities containing hazardous substances as defined under the Seveso2 Directive.

14.2. Seismic hazard-some recent developments in engineering seismology

A major earthquake counts among the greatest and most dangerous of natural hazards. The engineering seismology and earthquake engineering fields strive to integrate knowledge gained in the earth sciences and engineering fields so as to reduce loss of life, to protect the environment, and to mitigate economic impact. To achieve seismically resistant design, the level of hazard expected on a given site must be known; this evaluation calls on results from geological, seismological, and geotechnical investigations. The hazard level is represented by response spectra for various levels of damping or by the ground motion acceleration versus time (time history). The crucial parameter in this evaluation is magnitude, that is, the size of the source.

The physical parameter best characterizing the process at the source is the seismic moment, defined by:

$$M_0 = \mu \times A \times D \quad (\text{dyne-cm}) \quad (14.1)$$

where A is the rupture surface, D, the average slip on the fault, and μ , the rigidity on the fault plane. The energy transformed into seismic waves is $E = (\Delta\sigma/2\mu) M_0$, in which

not only the seismic moment M_0 , but also the stress drop $\Delta\sigma$ (the difference between the initial level of stress and that remaining once the fault has ruptured) are involved.

Hanks and Kanamori (1979), taking into account the hypothesis of a constant stress drop of approximately 30 bars, introduced the parameter of “moment magnitude” having the form:

$$M = 2/3 \log M_0 - 10.7 \quad (14.2)$$

Clearly the concept of moment magnitude constitutes a valuable contribution (despite the debatable 30-bar hypothesis) in the attempt to achieve a uniform measurement of the size of an earthquake at its source, variously expressed in seismology by m_b , M_S , M_L , etc., determined from the amplitudes of short- or long-period seismic waves and which are liable to saturate at higher levels of motion.

As to geologists, they frequently have recourse to empirical statistical relations associating the magnitude M (of whatever type) with the rupture length L along the fault plane, thereby integrating both geological and seismological data:

$$M = a \log L + b \quad (14.3)$$

where a and b are correlation coefficients. The most frequently used version of this was established by Wells and Coppersmith (1994) using worldwide data.

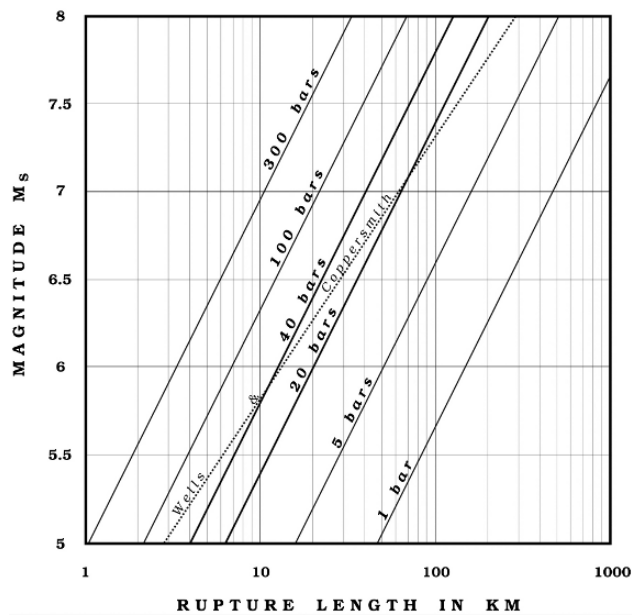


Fig. 14.1. Scaling law for various levels of stress drop (in bars), showing the relationship between surface-wave magnitude and rupture length (solid lines); one of the correlations from Wells and Coppersmith (1994) linking moment magnitude M to rupture length (dashed line) (from Mohammadioun and Serva, 2001)

However, the seismic energy emitted by a source depends not only on M_0 , but also on the stress drop $\Delta\sigma$. The following relation was established (Mohammadioun and Serva, 2001) supposing a simple circular fault model:

$$M_S = 2 \log L + 1.33 \log \Delta\sigma + 1.66 \quad (14.4)$$

Thus, we note on Figure 14.1 that, for a given magnitude, the higher the stress drop is the shorter the rupture length.

Recent observations indicate that stress drop does not depend on rupture length (as presupposed in the “L model”, cf. Scholz, 2003), but rather upon the fault width (w), as $\Delta\sigma = Kw^n$. Accordingly, in Equation 14.4, $\Delta\sigma$ could actually be replaced by Kw^n , and the scaling relationship between seismic moment or form of magnitude could be written:

$$M = f(L^2, w^n) \quad (14.5)$$

In practice, to evaluate the maximum magnitude on a fault, Equation (14.4) could be used once a plausible value of rupture length and of stress drop varying with the fault width and the slip type were chosen (stress drop being largest for the reverse fault mechanism, smallest for normal faults, and between the two for strike-slip ones).

Although a majority of attenuation relations have been established using moment magnitude, future research will increasingly be inclined to use seismic moment instead of magnitude, thereby integrating the concept of stress drop into the resulting models. A problem does remain, however, as to how to determine seismic moment for historical earthquakes in the absence of recordings. Perhaps the estimated fault geometry (length L and width w) could somehow be used to overcome this difficulty.

14.3. Design earthquakes in IAEA Safety Guides

The International Atomic Energy Agency (IAEA) has issued standards of safety for the protection of health and life in the development of nuclear energy for peaceful purposes. The main objective of the safety guides dealing with seismic risk is to provide recommendations on how to determine the ground motion hazards for a plant at a particular site, the potential for surface faulting, which could condition the feasibility of construction of a plant (NS-G-3.3), and design procedures (NS-G-1.6).

14.3.1. DESIGN EARTHQUAKES AND ASSOCIATED TOPICS FOR NPP SITING ACCORDING TO THE IAEA NS-G-3.3 GUIDE

In selecting a site, particular attention should be paid to two categories of earthquake-related features:

- Class A features liable to have a direct influence on the acceptability of the site;
- Class B features liable to influence the severity of the design basis earthquakes substantially.

14.3.1.1. *Class A features*

Class A features are active/capable faults at the site and/or a potential for the occurrence of other unforeseeable geological hazards such as large landslides, liquefaction phenomena and karst collapses. If engineering solutions are not available or, if available, the cost of applying them is such that the project is no longer economically viable, another site should be recommended. This is usually the case when a site is near one or more capable faults. A fault is considered capable if it shows evidence of past movement (significant deformation and/or dislocation) of a recurring nature within a period such that it is reasonable to infer that further movement can occur at or near the surface. In highly active areas, where both earthquakes and geological observations consistently reveal short earthquake recurrence intervals, periods of the order of tens of thousands of years may be appropriate for the assessment of capable faults. In less active areas, it is likely that much longer periods may be required (usually on the order of ten to the sixth, depending on the age of the present tectonic regime of these areas).

When faulting is known or suspected, investigations should include detailed geological-geomorphological mapping, topographical analyses, geophysical (including geodesy, if necessary) surveys, trenching, boreholes, determining ages of faulted sediments or rocks, local seismological investigations and any other appropriate techniques, to ascertain when the last movement occurred.

14.3.1.2. *Class B features*

Class B features define the parameters of the ground motion of the design-basis earthquakes. To accomplish this, a specific and complete database must be compiled in order to construct a seismotectonic model from which the potential earthquakes affecting the site (of tectonic and/or volcanic and/or man induced origin), can be derived. These earthquakes are then used to define the ground motions used as a basis for the design of the facility. It is thus essential to obtain an integrated geological and seismological database. The elements of this database should be studied in greatest detail in the region close to the site, where it needs to be more complete. In this connection, four scales of investigation are appropriate: regional, near regional, the vicinity of the site, and the immediate area of the site. The main purpose of the regional studies is to provide knowledge of the tectonic framework of the region and its general geodynamic setting and to identify and characterize those seismogenic features that may influence seismic hazard at the site. The main purpose of near regional investigations is to characterize the more important seismogenic structures for assessing seismic hazards. Investigation of the site vicinity, as already mentioned, is expected to define in greater detail the neotectonic history of faults, with the special purpose of resolving the possibility of surface faulting at the site (fault capability) and identifying sources of potential instability (Class 1 features). On-site investigations should prioritise defining the geotechnical properties of the foundation materials and determining their stability and response under dynamic earthquake loading.

14.3.1.3. *Determination of the design-basis ground motions*

At least two levels of design-basis ground motion, SL-1 and SL-2, are evaluated for each plant. The SL-2 level corresponds directly to ultimate safety requirements. This level of extreme ground motion will normally have a very low probability of being exceeded during the service life of the plant and represents the maximum level of ground motion to be used for design purposes. Its evaluation will be based on the seismotectonic model

and a detailed knowledge of the geology and engineering parameters of the strata beneath the site area. The SL-1 level corresponds to less severe, but more probable, earthquake load conditions, with safety implications that differ from those of SL-2. In some IAEA member states, licensing authorities require only one level, SL-2, which corresponds to a probability of being exceeded 10^{-4} per year. In other member states, SL-1 corresponds to a level with a probability of 10^{-2} per year of being exceeded. The assessment of appropriate ground motion levels for SL-2 and SL-1 may entail analyses based on deterministic and/or probabilistic considerations.

Deterministic techniques. As applied to the evaluation of SL-2, deterministic techniques involve:

- 1) Deriving the seismogenic structures from the seismotectonic model that was obtained by integrating the four scales of geological and seismological data.
- 2) Identifying the maximum earthquake potential associated with each seismogenic structure.
- 3) Performing the evaluation as follows:

For each seismogenic structure the maximum potential earthquake should be assumed to occur at the point on the structure closest to the site area, taking into account the physical dimensions of the source. When the site lies within the boundaries of a seismogenic structure, the maximum potential earthquake shall be assumed to occur under the site. In this case, special care should be taken to demonstrate that the seismogenic structure is not capable.

An appropriate attenuation relation should be used to determine the ground motion level which each of these earthquakes would generate at the site, taking into consideration the local site conditions.

Probabilistic techniques. The probabilistic technique entails the following steps:

- 1) Refining the seismotectonic model in terms of source type (e.g. volume, area, linear, point sources), geometry and depth.
- 2) For each source, identifying the following parameters (including their related uncertainties):
 - magnitude-frequency or intensity-frequency (recurrence) relationships,
 - maximum (or cut-off) magnitude or maximum intensity,
 - attenuation relationships.
- 3) Choosing appropriate stochastic models (e.g., Poisson, Markov, cluster, renewal).
- 4) Evaluating the best-estimate hazard curve, with appropriate confidence intervals, illustrating the dispersion.
- 5) Using those levels of ground motion for design purposes at which probabilities of being exceeded meet the safety standards set by the member state.

The characteristics of the design-basis ground motions for SL-1 and SL-2 level earthquakes is expressed in terms of response spectra for a range of damping values and compatible time histories. Several methods can be used to generate the design response spectra: standard response spectrum anchored to a PGA value corresponding to SL-1 or SL-2 levels; site-specific response spectrum; or uniform confidence response spectrum. In selecting the damping values to be used for the design response spectra for SL-1 and SL-2, it is important to bear in mind both the damping values associated with structures for which the response spectra will be used and the level of strain/stresses that will be induced in these structures. Time histories corresponding to both SL-1 and SL-2 are developed for use in applications such as studies of non-linear behaviour of structures, soil-structure interaction, and equipment response. These time histories should reflect all the prescribed ground motion design parameters including duration and several levels of damping.

The number of time histories to be used in the detailed analyses and the procedure called on to generate these time histories depend on the type of analysis performed. Earthquake ground motion duration is determined mainly by the length and velocity of the fault rupture. Duration can also be correlated with magnitude. It is very important that a consistent definition of duration be used throughout the evaluation. If no specific information is available on the peak ground acceleration (PGA) of vertical ground motion in the site vicinity, it may be reasonable to assume a prescribed ratio between peak acceleration in the vertical and horizontal directions (e.g. 2/3). Empirical evidence has shown that this ratio typically varies from 1/2 to 1 and may be largest in the near field, depending on the source and site characteristics as well as other factors.

14.3.2. REPOSITORY SITES FOR NUCLEAR WASTE DISPOSAL

One of the crucial issues in nuclear safety is how to dispose of high-level nuclear waste permanently and safely. The solution preferred by experts is to bury the waste in deep geological repositories. A variety of geological media are considered. Important amongst the criteria taken into consideration in the siting of such facilities is geological stability: any potential modification on the site must remain compatible with safety imperatives, of particular concern being the presence of one or more active faults on the site, and of seismic activity in general. The characteristics of a maximum physically plausible earthquake shall be investigated on the basis of the tectonic context of the site considered. Further, it will be necessary to assess the degree of disturbance to the hydro-geological system foreseeable at the site (the effect of an earthquake on ground water circulation between the repository and discharge zones (see Escalier des Orres et al., 1992).

Three safety guides dealing with the subject have been issued by IAEA to date:

- Predisposal management of low- and intermediate-level radioactive waste, Safety Guide WS-G-2.5. The objective of this guide is to provide regulatory bodies and operators that generate and manage radioactive waste with recommendations on how to meet the principles and requirements established for the predisposal management of low- and intermediate-level waste;

- Predisposal management of high-level radioactive waste, Safety Guide WS-G-2.6. This safety guide, as in the preceding one, provides guidance for the predisposal management of high-level waste;
- Safety assessment for near-surface disposal of radioactive waste, Safety Guide WS-G-1.1. This safety guide addresses the subject of safety assessment for the near-surface disposal of radioactive waste.

14.4. Earthquake-resistant design

The risk assessment and earthquake resistant design of a facility involves two main phases:

- 1) An assessment of the seismic hazard level on the site prior to construction.
- 2) Earthquake resistant design.

Building codes are the most frequently used earthquake resistant design tool for conventional structures (USB in the United States, for example), to which simple, static calculations generally apply. For critical structures, on the other hand, the failure of which, or of part of which, is liable to trigger environmental disasters, more sophisticated methods are called on to compute or verify their design. Safety margins intended to compensate for the uncertainties encountered at various stages of the analysis are often built into these methods.

14.4.1. IAEA SAFETY GUIDES FOR THE SEISMIC DESIGN OF NUCLEAR POWER PLANTS

Regarding nuclear power plants (NPP's), IAEA Safety Guide NS-G-1.6, entitled, Seismic Design and Qualification for Nuclear Power Plants, has recently replaced the earlier Guide 50-SG-S2. The objective of the guide is to provide recommendations on a generally accepted manner for designing a nuclear power plant such that an earthquake motion at the site corresponding to the SL-2 level will not jeopardize the plant's safety. It also affords guidance on a consistent application of methods and procedures for analysis, testing, and qualifications of structures and equipment to ensure they meet the safety requirements.

The guide makes recommendations on general safety concepts, namely on categorizing the structures, systems, and components of a nuclear power plant in terms of their impact on safety in the event of a design-basis earthquake. Guidelines are also provided concerning the design of different categories to guarantee an appropriate safety margin.

Following is a summary of the topics addressed in the guide:

- Seismic design, comprising: selection of an appropriate plant layout; geotechnical parameters; civil engineering structures; earth structures; piping and equipment; selection of appropriate standards; and periodic safety review.
- Seismic qualification and verification (see Figure 14.2, below), comprising: testing; actual earthquake experience; and indirect methods.

- Seismic instrumentation, comprising: seismic monitoring and automatic scram systems; data processing; and post-earthquake actions.

The establishment and implementation of a quality assurance program is mandatory to cover items, services, and processes that affect the safety of the plant

14.4.2. IAEA SAFETY GUIDES FOR WASTE DISPOSAL AND REPOSITORY SITES

To address the radioactive waste disposal issue, IAEA has published documents for surface and subsurface storage sites, and notably a position paper drafted by international experts entitled, *The Long-Term Storage of Radioactive Waste: Safety and Sustainability*. This document reflects expert opinion concerning the multiple aspects of safety, and notably geological hazards in the case of both surface storage and underground repository sites. The respective advantages and disadvantages of these two modes of storage are examined in considerable detail. Additional information is available on the IAEA website: www.pubiaea.org-MTC.

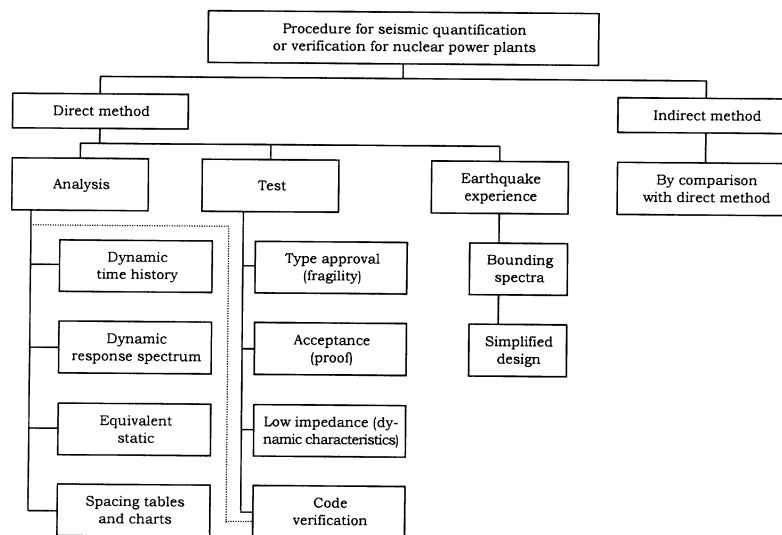


Fig. 14.2. Summary of seismic qualification or verification methods (from IAEA Safety Guide NS)

14.5. Approach for exclusion criteria and minimum seismic design for NPP's, followed by a description of practice in some countries

Table 14.1, below, summarizes exclusion criteria and minimum seismic design for NPP's of some nations prominent in the nuclear industry. On the strength of experience gained during many IAEA missions to more than forty countries on four continents, we can make the following comments on this table. Exclusion criteria depend mainly on the

availability of suitable sites in a country, the sensitivity of the technical and scientific community to the earthquake risk phenomenon, and design restrictions against seismic loads for nuclear power plants. For example, the exclusion criterion of intensity IX or above (MSK) in the former USSR (in other words, in practice, nuclear power plants were not designed for a seismic input exceeding 0.2 g) is obviously linked to the wide availability of sites and to the design restrictions of VVER type reactors for coping with high seismic loads.

Table 14.1. Minimum requirements and exclusion criteria for NPP's siting and design (data from Serva, 1993)

Code	Exclusion criteria	Minimum requirements
IAEA	Presence of capable faults at the site.	Minimum SL-2=0.1 g anchored to a site-specific response spectrum.
Italy	Area of historically observed intensity equal to X MCS (MMI or MSK) or greater. Presence of capable faults at the site.	Minimum SSE=0.18 g anchored to a wide-band standard response spectrum.
Former USSR	Sites having a potential for intensity IX MSK or greater. In other words, NPP's cannot be designed for more than 0.2 g. Presence of tectonically active faults at the site (capable faults).	Bearing capacity of the foundation soil > 0.2 kg/cm ² .
USA	None	Minimum SSE = 0.1 g anchored to a wide-band response spectrum.
Japan	Sites having capable faults or close to faults having a Quaternary slip-rate higher than 1 mm/y.	Foundation must be on sediments not younger than Tertiary. S2 shall withstand a near-field earthquake (minimum distance 10 km) of M=6.5.
Germany	Presence of a capable fault at the site.	Minimum peak ground acceleration = 0.05 g.
France	None	SMS=0.1 g.
U. K.	None	none

The minimum ground motion selected as the basis for design at the site may be based on a near-field or far-field earthquakes (or both). In the case of near-field earthquakes, this is considered the maximum value of the random (floating or background) event, which in Japan can be as high as M=6.5. In Japanese practice, however, it is assumed that this earthquake is not associated with surface faulting if un-faulted terrains not younger than Tertiary are present at the site. All standards indicate that an earthquake that lies within the seismotectonic province of the site and cannot be related to any known structural feature should be placed, conservatively, at a certain depth, under or very close to the site. Although such an assumption has no physical basis, it is useful in terms of cost-benefit analyses when this earthquake is in the intensity range of VII–VIII MSK ($M=5\pm 0.5$). The same assumption is not appropriate when the value reaches IX MSK ($M=6\pm 0.5$) because such earthquakes should always be associated with structures detectable by state-of-the-art methods of geology and geophysics. In conclusion, more effort should be devoted in this latter case to attempting to identify the seismogenic source associated with the event in question.

Where a potential for surface faulting exists, (examples in Figures 14.3 and 14.4, from Akkar and Gulkan, 2002), a majority of standards more or less explicitly recommend the exclusion of the sites.

Surface faulting, including subordinate rupture (Figure 14.5), depends on the subsurface (structural and rheological) characteristics of the site, on the magnitude (M) and on the depth of the earthquake source. For example, as mentioned earlier, the practice in Japan has been to assume that a $M=6.5$ earthquake, in their seismotectonic environment, cannot produce surface faulting in Tertiary bedrock that has not already been faulted. This assumption, however, does not hold true for other parts of the world, especially in strike-slip or dip-slip tectonic stress regimes. Figure 14.5 (Serva et al., 2000) represents a viewpoint for the Apennines. It shows that in this area earthquakes with a magnitude in the range of 6 may have a potential for producing surface faulting (Cello et al., 1998; Michetti et al., 2000; Vittori et al., 2000). The two models show the formation of “intermountain” basins within the mountain range. These were generated by earthquakes mainly during Quaternary times. Model A represents basins like Colfiorito (Michetti et al., 2000) and Norcia, while model B represents basins like Mugello, Rieti (Brunamonte et al., 1995) and Fucino (Michetti et al., 1996). Similar models should be established, at an appropriate scale, for all the different seismogenic regions of the world.



Fig. 14.3. The 1999 Sea of Marmara earthquake. Effects of surface faulting (see the arrows) on the viaduct, near Düzce, part of TEM (Trans-European Motorway).
Courtesy of Prof. Polat Gulkan



Fig. 14.4. The Sea of Marmara earthquake. Effects of surface faulting on a 2-meter diameter water main. Courtesy of Prof. Polat Gulkan

To define the design-basis earthquake, the approach recommended by existing guides may be either deterministic or probabilistic. Both methodologies require a more or less accurate seismotectonic model of the site region on which the investigations focus. The input motion is considered to be the free-field value. The engineering treatment of this input (convolution, de-convolution) will differ from one expert to another.

The procedure outlined in the first version of the USA-NRC (1978) Guide recommends that the region investigated extend over a radius of at least 200 miles around the site. This value could be reasonable for intraplate areas, but it may be excessive in areas near plate margins, where most significant seismogenic structures lie within a radius of 100 km from the site. It is important to note that the guidelines proposed by experts require a significant amount of judgment in defining the seismotectonic model and assessing the maximum potential earthquake related to the seismogenic structure or, in the case of

diffuse seismicity, to the province. Although the quality of the investigation is influenced by the skill of the expert, it depends even more heavily on the reliability of the database. Every possible effort should accordingly be made to ensure the accuracy and completeness of the database, especially for the more significant data, i.e., data revealing the type, rate and style of the ongoing earth movements and seismicity.

14.6. A proposed approach for other critical facilities

14.6.1. MITIGATION OF MAJOR RISKS: THE SEVESO DIRECTIVE

The wave of public feeling that followed upon the accidental release of dioxin in 1976 in the town of Seveso, Italy, prompted the European states to adopt a common policy concerning the mitigation of major industrial risks. Issued on June 24, 1982, the so-called Seveso Directive requires both states and industry to identify the risks associated with certain hazardous industrial activities and to take appropriate measures to cope with them. This directive has since undergone a number of revisions, and its scope has progressively been widened. The most recent regulatory text, 96/82/CE, also known as Seveso2, replaced the Seveso Directive as of February 3, 1999 (see Tables 14.2 and 14.3). This newer directive places more emphasis on the notion of major accident prevention, making it mandatory for the operator to implement a system of risk management and a safety-related organization commensurate with the risks inherent to the concerned installations.

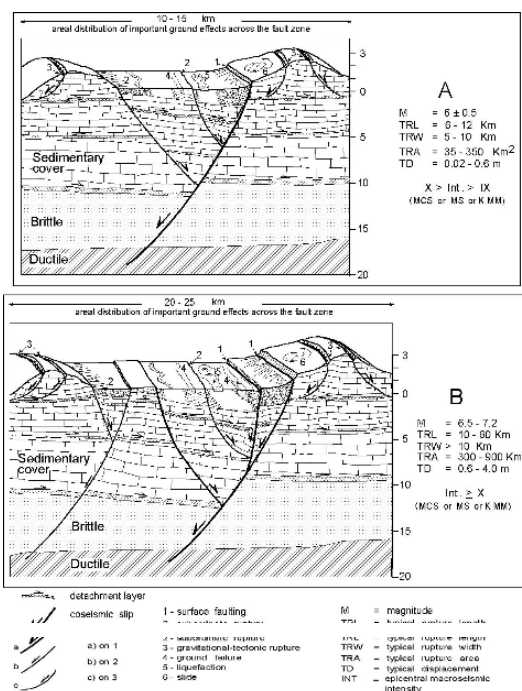


Fig. 14.5. Earthquake magnitude and coseismic surface effects in the Apennine Range (from Serva et al., 2000)

14.6.2. SEISMIC RISK MITIGATION

The nuclear approach has been described and commented on because it seems to be the most appropriate one to use in the earthquake resistant design of the industrial plants we are dealing with. This is because this approach provides the specialist with an overall view of the problem, compelling him to make a decision as to what level of information is sufficient for making a reliable assessment of the plant he is dealing with, taking into account both its location (hazard level at the site) and the cost. In other words, the detail required in the database (quality, quantity and type of geological, geophysical, seismological and engineering data) must be compatible with the level of risk/environmental impact of the plant analysed. However, one requirement that should remain the same is the Quality Assurance of the whole process in terms of data and how they are processed.

Clearly, none of these plants present the same level of risk as an NPP; however, an industrial area containing different types of plants, including some working with highly toxic substances (Table 14.2), should be dealt with almost as stringently as an NPP. With respect to some aspects, even a single plant manipulating highly toxic materials that is located in a densely populated urban area, or a sizeable dam, should be treated in a similar way.

Table 14.2. Most hazardous industrial plants

For man	Large V LPG storage plants
	Large-scale storage of chlorine
	Phosgene storage facilities and process users
For the environment	Large diesel oil or fuel oil tank farms

More generally it can be said that the methodology should be similar to NPP's if a system of plants is concerned where an accident is liable to cause significant risks to man and/or the natural environment in terms of areal extent and level of contamination. A similar concept is also expressed in Gürpınar (1997). In such a case, as for nuclear installations, the design earthquake chosen should be SL-2—the maximum potential earthquake, i.e. the ten-thousand-year return-period event, and SL-1 may not be necessary. How this earthquake should be coped with from an engineering standpoint can differ significantly from the nuclear case, and this theme is not taken up here. Class A features should be analysed as exhaustively as for nuclear facilities.

This is admittedly a high-cost approach, but the benefit is commensurately high should such an event occur during the plant's service life. In any case, the owners of these plants could resort to a weighted synergy (in terms of cost/risk reduction benefit) to solve the problem, and public institutions, at national and local scales, should assist the owners of such plants, providing not only guidance, but also data and expertise.

Meanwhile, the details are of minor concern if one is dealing with hazardous plants (Table 14.2), or ones handling materials listed in Table 14.3, concerned by the Seveso2 Directive but not located in a large industrial area, with dangerous (but not radioactive) waste repositories, and more generally with plants presenting minor risk but requiring an emergency plan. In this case it could be adequate to use a 500-to-100-year return-period earthquake as the design-basis event, in lieu of SL-2. An approach of this type is reported on in Barone et al. (1998). The geological and seismological database required

for an oil pipeline, a strategic communication centre, a sludge plant or a municipal waste landfill (because of its long service life) may be less demanding yet. It is important, however, to point out that, here too, the data derived from the rich historical seismicity catalogues (Italy and France, for example) might not afford a solution to all problems. In particular, the geological stability of the site under static and dynamic loads should always be established, and the existing catalogues are still incomplete for a number of areas of Italy, as evidenced by the ongoing paleo-seismological investigations (see, for example, Michetti et al., 2000; Michetti et al., 1997).

Table 14.3. Dangerous substances according to the Seveso2 Directive

Dangerous substances	Qualifying quantity (tons) for the application of the law	
	Articles 6 and 7	Article 9
Ammonium nitrate	350	2500
Ammonium nitrate	1250	5000
Arsenic pentoxide, arsenic (V) acid and/or salts	1	2
Arsenic trioxide, arsenious (III) acid and/or salts	–	0,1
Bromine	20	100
Chlorine	10	25
Nickel compounds in inhalable powder form (nickel monoxide, nickel dioxide, nickel sulphide, trinickel disulphide, dinickel trioxide)	–	1
Ethyleneimine	10	20
Fluorine	10	20
Formaldehyde (concentration (90 %)	5	50
Hydrogen	5	50
Hydrogen chloride (liquefied gas)	25	250
Lead alkyls	5	50
Liquefied extremely flammable gases (including LPG) and natural gas	50	200
Acetylene	5	50
Ethylene oxide	5	50
Propylene oxide	5	50
Methanol	500	5000
4, 4-Methylenebis (2-chloraniline) and/or salts, in powder form	-	0,01
Methylisocyanate	-	0,15
Oxygen	200	2000
Toluene diisocyanate	10	100
Carbonyl dichloride (phosgene)	0,3	0,75
Arsenic trihydride (arsine)	0,2	1
Phosphorus trihydride (phosphine)	0,2	1
Sulphur dichloride	1	1
Sulphur trioxide	15	75
Polychlorodibenzofurans and polychlorodibenzodioxins (including TCDD), calculated in TCDD equivalent	-	0,001
The following carcinogens:	0,001	0,001
4-Aminobiphenyl and/or its salts, Benzidine and/or salts, Bis(chloromethyl) ether, Chloromethyl methyl ether, Dimethylcarbamoyl chloride, Dimethylnitrosamine, Hexamethylphosphoric triamide, 2-Naphtylamine and/or salts, and 1,3 Propanesultone 4-nitrodiphenyl		
Automotive petrol and other petroleum spirits	5000	50000

It is important to point out here that other non-industrial structures like bridges, communication facilities, and galleries, can also play a significant role in risk reduction, especially in emergency phases. It is actually common knowledge that these structures,

in a young geological context such as Italy, can be cut by active (capable) faults (Azzaro et al., 1998 and Figures 14.3 and 14.4). This explains why these structures could justifiably also be assimilated with the third category of industrial plants. Regarding these long structures, it should be emphasized that the limitations of the acritical application of the Gutenberg-Richter earthquake frequency distribution ($\log N = a + bM$) as described in Mochan et al. (1997) and the considerable importance of having a realistic definition of the differential motion of bridges and lifelines, insofar as it enables wave passage, loss of coherency, and site effects to be taken into account, makes deterministic seismo-synthesis (e.g. Panza et al., 2001) particularly suitable for the purpose.

On the other hand, the quantity and quality of data could be much higher than that required for NPP's; this is the case for high-level radioactive waste sites. In such instances, site stability, in particular, needs to be demonstrated for periods of tens or even hundreds of thousands of years.

Lastly, it is important to point out that the sitting procedure can also be implemented *a posteriori*, even if the plant already exists, in which case it allows engineering solutions to be properly defined in order to increase the facility's safety. This effort, for many Eastern European plants in the nuclear sector, either has been completed successfully or is underway without entailing prohibitive economic costs.

CHAPTER 15
EARLY WARNING AND RAPID DAMAGE ASSESSMENT

M. Erdik and Y. Fahjan
Boğaziçi University, Istanbul, Turkey

15.1. Background and introduction

Technological advances in seismic instrumentation and telecommunication permit the implementation of real-time rapid response and early warning systems. During large earthquakes, such systems are capable of providing from a few seconds to a few tens of seconds of warning before the arrival of strong ground shaking and enable quick reports about the damage estimates to determine where emergency response is most needed. An earthquake early warning and rapid response system can provide the critical information needed to minimize loss of lives and property, and to direct rescue operations. (Kanamori et al., 1997; Teng et al., 1997; Allen and Kanamori, 2003; Lee and Espinosa-Aranda, 2003).

The basic idea of an earthquake early warning system was proposed more than one hundred years ago by Cooper (1868) for San Francisco, California. A modern approach of an earthquake early warning system for a seismic computerized alert network was proposed by Heaton (1985). In Japan, a method of earthquake early warning was employed by its bullet train operation, Nakamura (1989). The rapid response systems implemented in California (USGS, Caltech and CDMG TriNet ShakeMaps - <http://www.trinet.org/shake/>, Caltech-USGS Broadcast of Earthquakes (CUBE) System <http://www.gps.caltech.edu/~bryant/cube.html>, UC Berkeley Seismological Laboratory and USGS Menlo Park (REDI) www.seismo.berkeley.edu/seismo/redi), Taiwan (Earthquake Rapid Reporting System of Taiwan Central Weather Bureau, CWB <http://www.earth.sinica.edu.tw/cdr/IASPEI/data/cwb/rapid.html>) and Japan (Real-time Earthquake Assessment Disaster System in Yokohama –READY -<http://www.city.yokohama.jp/me/bousai/eq/index.html>) are current examples. Earthquake early warning in urban and industrial areas allows for clean emergency shutdown of systems susceptible to damage such as power stations, transportation, computer centres and telephone systems. Currently such systems are either implemented or in construction or planning stage in Mexico, Romania, California, Japan, Taiwan, Turkey and Greece. Early warning systems, currently in operation in Bucharest (<http://www.infp.ro/publications/ews.htm>) and Mexico (<http://www.gfz-potsdam.de/ewc98/abstract/espinosa.html>), have the capability of issuing an earthquake early warning in advance, by relying on significant distances between the source and the populated urban regions.

15.1.1. BASIC COMPONENTS OF EARLY WARNING AND RAPID RESPONSE SYSTEM

The first priority in earthquake protection is to save lives, and the basic components of a seismic alarm system are:

- (1) Monitoring system composed of various sensors.
- (2) Communication link that transmits data from the sensors to computers.

(3) Data processing facilities that converts data to information.

(4) System that issues and communicates the rapid response information and early warning.

The earthquake early warning consists of seismic stations as close as possible to the potential source zone which transmit continuous on-line data to provide near-real time warning for emerging potentially disastrous earthquakes. For rapid response system, the seismic stations are located in critical buildings and distributed uniformly in an urban area. After triggered by an earthquake, ground motions recorded by an array of seismic stations and/or locally processed real-time data (peak ground acceleration, peak ground velocity, spectrum intensity, response spectra, Fourier spectra, etc.) are transmitted to a central data processing. These parameters will be automatically used to generate shake maps and damage distributions and make them available for the end users.

15.2. Early warning

An earthquake early warning system requires seismic stations (strong motion instruments, which can provide real-time seismic data or strong ground motion parameters (spectrum intensities, peak ground accelerations, peak ground velocities) close to the source of earthquakes and continuous communication between the seismic stations and a central processing station.

The early warning systems utilize the fact that seismic waves propagate slower than electromagnetic waves that are used for communications of the warning. The maximum pre-warning times in areas with well-defined fault zones can be as high as 60 to 80 seconds (Mexico City). In other areas, where the fault zones are close or the active faults are not known, the warning time may be less than 5 seconds.

An Early Warning System (EWS) forewarns an urban area of the forthcoming strong shaking, normally with a few seconds to a few tens of seconds of early warning time before the arrival of the destructive S-wave part of the strong ground motion. However, even a small time window can provide opportunities to automatically trigger measures such as shutdown computers; remote electrical power; shutdown high precision facilities; shutdown airport operations; shutdown manufacturing facilities; shutdown high energy facilities; shutdown gas distribution; alert hospital operating rooms; open fire station doors; start emergency generators; stop elevators in a safe position; shutoff oil pipelines; issue audio alarms; shutdown refineries; shutdown nuclear power plants; shutoff water pipelines; maintain safe-state in nuclear facilities (Goltz, 2002 and Harben, 1991).

Every EWS consists of four components:

- (1) a monitoring system composed of various sensors,
- (2) a real-time communication link that transmits data from the sensors to a computer,
- (3) a processing facility that converts data to information, and
- (4) a system that issues and communicates the warning.

For earthquake early warning systems, the output of the system can be an estimate of magnitude and location of the event but equally well a projection of the expected acceleration or intensity at specific sites.

15.2.1. RAPID ASSESSMENT OF EARTHQUAKE MAGNITUDE AND LOCATION

The main parameters of an earthquake (epicentre, time of origin, magnitude, focal mechanism, and amplitude of ground shaking) may take about one minute from the time an earthquake has been detected for reliability estimates (Wu et al., 1998). The rapid location can be achieved in the ten seconds time window immediately following the first P-arrival. The rapid determination of the earthquake magnitude would be more difficult because the shear wave trains may not be recorded completely within this time window, and, more importantly, since a damaging event is large, a moment magnitude or its equivalent must be developed for damage potential assessment (Wu et al., 1998). In literature, many researchers (e.g., Nakamura, 1988; Grecksch and Kumpel, 1997; Tsai and Wu, 1997; Allen and Kanamori, 2003) have tried to estimate magnitude from the initial portion of accelerograms, but large uncertainties are a major problem.

15.2.2. DIRECT (ENGINEERING) EARLY WARNING: PGA AND CAV THRESHOLD

For earthquake early warning and alarm systems there is usually insufficient time to compute the hypocentre, focal parameters and the magnitude of an earthquake, as this time is needed for the more complex alarm decision- making process. The benefits of an early warning system increase with increasing pre-warning time.

Considering the complexity of fault rupture and the short fault distances involved, a simple and robust early warning algorithm, based on the exceedance of specified threshold time domain amplitude levels needs to be implemented. The band-pass filtered peak ground accelerations (PGA) and the cumulative absolute velocity (CAV-time integral of the absolute acceleration) can be compared with specified threshold levels. To declare the first early warning alarm, a simple algorithm can be implemented. When any acceleration or CAV (on any channel) in a given station exceeds specific threshold values it is considered a vote. Whenever we have 2 or 3 (selectable) station votes within selectable time interval, after the first vote, the first alarm is declared (Erdik et al., 2003b).

More complex algorithms based on artificial neural networks (ANN) can be used (Boese et al., 2003). ANN approach considers the problem of earthquake early-warning as a pattern recognition task. The seismic patterns can be defined by the shape and frequency content of the parts of accelerograms that are available at each time step. ANN can extract the engineering parameters PGA, CAV from these patterns, and map them to any location in the surrounded area.

15.3. Rapid post-earthquake damage assessment

The Rapid Response has the objective of providing:

- Reliable information for accurate, effective characterization of the shaking and damage by other rapid post-earthquake maps (Shake, Damage and Casualty maps) for rapid response.
- Recorded motion for post-earthquake performance analysis of structures.
- Empirical basis for long-term improvements in seismic microzonation, seismic provisions of building codes and construction guidelines; and to improve the understanding of earthquake generation at the source and seismic wave propagation.

Current earthquake rapid response system methodologies have different approaches to measure and estimate the ground shaking of earthquake area, in order to estimate the intensity and damage maps. The first approach uses the seismic source parameters (hypocentre, magnitude, intensity) in order to compute the ground shaking and potential damage.

The second approach uses the direct engineering parameters such as peak ground acceleration (PGA), peak ground velocity (PGV), spectra displacements (SD) maps to compute the potential damage. For an earthquake rapid response system a large number of seismic stations (strong motion instruments) is needed, which are distributed uniformly over an urban area. The stations may not need a continuous communication with a central station. After triggering by earthquake, the stations will send electronic messages (SMS, E-mail, etc.) to the central station a few seconds after the end of an earthquake. The messages sent may contain information about the peak ground acceleration and the spectrum intensity, which will be the basis for the automatic preparation of damage maps.

Both systems transmit this critical information electronically to emergency response agencies and other cognizant governmental agencies. These agencies can then take actions (some of which are pre-programmed) immediately after an earthquake.

15.3.1. SHAKE MAPS

ShakeMap is a representation of ground shaking produced by an earthquake. The information it presents is different from the earthquake magnitude and epicentre that are released after an earthquake because ShakeMap focuses on the ground shaking produced by the earthquake, rather than the parameters describing the earthquake source. So, while an earthquake has one magnitude and one epicentre, it produces a range of ground shaking levels at sites throughout the region depending on distance from the earthquake, the rock and soil conditions at sites, and variations in the propagation of seismic waves from the earthquake due to complexities in the structure of the Earth's crust (<http://quake.wr.usgs.gov/recent/shaking.html>).

15.3.2. PEAK ACCELERATION MAPS

Peak horizontal acceleration at each station is contoured in units of %g. The peak values of the vertical components are not used in the construction of the maps because the regression relationships used to fill in data gaps between stations are based on horizontal peak amplitudes. The contour interval varies greatly and is based on the maximum recorded value over the network for each event.

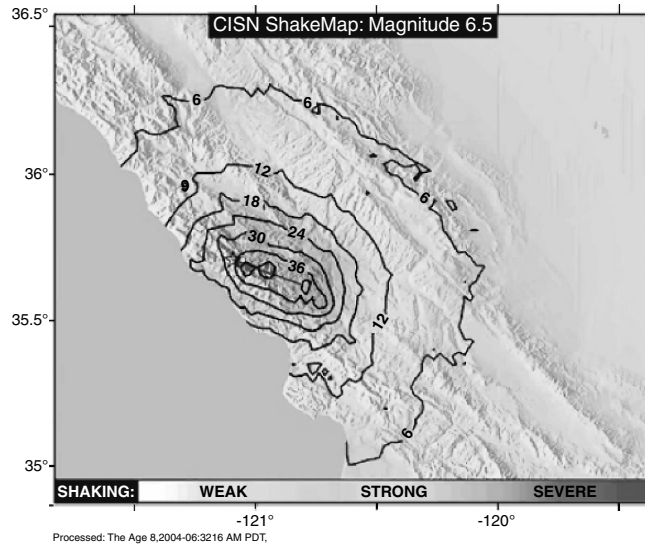


Fig. 15.1. Peak Acceleration Shake Map for San Simeon of Dec 22, 2003 earthquake;
<http://quake.wr.usgs.gov>

For moderate to large events, the pattern of peak ground acceleration is typically quite complicated, with extreme variability over distances of a few km. This is attributed to the small scale geological differences near the sites that can significantly change the high-frequency acceleration amplitude and waveform character. Although distance to the causative fault clearly dominates the pattern, there are often exceptions, due to local amplification. Although, this makes interpolation of ground motions at one site to a nearby neighbour risky, the peak acceleration pattern usually reflects what is felt from low levels of shaking up to moderate levels of damage. An example of the peak ground acceleration map for San Simeon of Dec 22, 2003 earthquake is given in Figure 15.1.

15.3.3. PEAK VELOCITY MAPS

Peak velocity values are contoured for the maximum horizontal velocity (in cm/sec) at each station. As with the acceleration maps, the vertical component amplitudes are disregarded for consistency with the regression relationships used to estimate values in gaps in the station distribution. Typically, for moderate to large events, the pattern of peak ground velocity reflects the pattern of the earthquake faulting geometry, with largest amplitudes in the near-source region, and in the direction of rupture (directivity). Differences between rock and soil sites are apparent, but the overall pattern is normally simpler than the peak acceleration pattern. Severe damage and damage to flexible structures is best related to ground velocity.

15.3.4. SPECTRAL RESPONSE MAPS

Following earthquakes larger than magnitude 5.5, spectral response maps are made. Response spectra portray the response of a damped, single-degree-of-freedom oscillator to the recorded ground motions. This data representation is useful for engineers

determining how a structure will react to ground motions. The response is calculated for a range of periods. Within that range, the Uniform Building Code (UBC) refers to particular reference periods that help define the shape of the "design spectra" that reflects the building code.

ShakeMap spectral response maps are made for the response at three UBC reference periods: 0.3, 1.0, and 3.0 seconds. For each station, the value used is the peak horizontal value of 5% critically damped pseudo-acceleration.

15.4. Earthquake early warning and rapid response systems

15.4.1. URGENT EARTHQUAKE DETECTION AND ALARM SYSTEMS (UrEDAS) IN JAPAN

In the mid 1950's Japanese National Railways started the installation of simple alarm seismometers along their railway lines. Later, with the operation of the "bullet" trains, the alarm system was improved by the installation of seismometers at every 20 km along the lines. The stations issue a warning whenever a preset level of horizontal ground acceleration (40 gal) is exceeded (Nakamura, 1989). Trains in the vicinity to the respective alarm station are automatically slowed down or stopped in order to avoid derailments. The contemporary real-time earthquake disaster prevention, earthquake detection and alarm systems (UrEDAS) used for railways in Japan consist of 30 strong motion instruments. The main feature of the system is utilizing the information from P-wave data. Systems for different railways have been in operation since 1983 (Nakamura, 1989). UrEDAS detects initial P-wave motions, estimates epicentre azimuth and magnitude, calculates epicentral distance and local depth within about 3 seconds.

15.4.2. SEISMIC ALERT SYSTEM OF MEXICO CITY

The high probability for an earthquake greater than magnitude 7.0 to occur on the Guerrero Gap, between Acapulco and Zihuatanejo ports would be a potential risk for Mexico City. Most of the large earthquakes, which are likely to cause damage in Mexico City have their source in the subduction zone of the Pacific coast at a distance of about 320 km (Espinosa-Aranda et al., 1995). The Seismic Alert System (SAS) is a public earthquake early warning system developed with the sponsorship of the Mexico City government authorities. The SAS is operating since August 1991. The seismic alert system for Mexico City consists of four parts: the seismic detection system, a dual telecommunications system, a central control system and a radio warning system for users. The seismic detector system consists of 12 digital strong motion field stations located along a 300 km stretch of the Guerrero coast, arranged 25 kilometres apart. Each detector continually processes local seismic activity which occurs within a 100 km radial coverage area around the station. The stations estimate a forecast for the local ongoing seismic activity and send it by radio links to the central recording station, in Mexico City. The dual telecommunications system consists of a VHF central radio relay station, located near Acapulco, and three UHF radio relay stations located between the Guerrero coast and Mexico City. Two seconds are required for information sent by one of the field stations on the Guerrero coast to reach Mexico City; this data is sent

digitally coded. The Central Control System continually receives information on the operational status of the field stations and communication relay stations, as well as the actual detection of an earthquake in progress. Information received from the stations is processed automatically to determine magnitude and is used in the decision to issue a public alert.

The system is capable of generating warning signals about 60 s average in advantage to the "S" waves first arrivals in Mexico City, when it detects strong earthquakes occurring 280 km faraway, in the "Guerrero Gap". The SAS was programmed to issue a general alert signal when the earthquake magnitude forecasting estimation is strong ($M > 6$), and to issue a restricted one if this evaluation is moderated ($5 < M < 6$). The SAS earthquake warning signal disseminates via local AM/FM commercial radio stations allowing the operation of the audio alerting mechanisms to residents of Mexico City, public schools, government agencies with emergency response functions, key utilities, public transit agencies and some industries. Public and private entities are equipped with specially designed radio receivers to obtain the SAS alert. Triggering prevention procedures, designed in each public school within the earthquake hazard reduction program applied by the Secretariat of Public Education in the valley of Mexico, since September, 1985 (Espinosa-Aranda et al., 1995).

Up to June 2000, after nine years of continuous operation, the SAS has successfully detected more than 755 earthquakes with magnitude from M4 to M7.3 (Espinosa-Aranda et al., 2003). Until now the greatest seismic event detected by the SAS was the September 14, 1995, M7.3 "Copala" earthquake. In a live test that checked the whole system, the SAS was activated and a general warning signal was issued in Mexico City, 72 sec. prior to the arrival of strong ground motion effects (<http://www.cires.org.mx>).

15.4.3. ISTANBUL EARTHQUAKE RAPID RESPONSE AND THE EARLY WARNING SYSTEM

Istanbul faces a significant earthquake hazard and risk as illustrated by the recently developed earthquake risk scenario for Istanbul (Erdik et al., 2003a). To assist in the reduction of losses in a disastrous earthquake in Istanbul a dense strong motion network is established (Erdik et al., 2003b).

One hundred strong motion accelerometers have been placed in populated areas of Istanbul, within an area of approximately 50×30 km, to constitute a network that will enable rapid shake map and damage assessment after a damaging earthquake (Figure 15.2). After triggered by an earthquake, each station will process the streaming strong motion to yield the spectral accelerations at specific periods and will send these parameters in the form of SMS messages to the main data centre through available GSM network services. A shake map and damage distribution will be automatically generated. The shake and damage maps will be available on the Internet and will also be pushed to several end users. For earthquake early warning information ten strong motion stations were located as close as possible to the Marmara Fault (Figure 15.3). The continuous on-line data from these stations will be used to provide near-real time warning for emerging potentially disastrous earthquakes.

The remaining 40 strong motion recorder units will be placed on critical engineering structures in addition to the already instrumented structures in Istanbul

<http://www.koeri.boun.edu.tr/depremmuh/stromotion.htm>). All together, this network and its functions, is called Istanbul Earthquake Rapid Response and Early Warning System (IERREWS). The system is designed and operated by Bogazici University with the logistical support of the Governorate of Istanbul, First Army Headquarters and Istanbul Metropolitan Municipality.

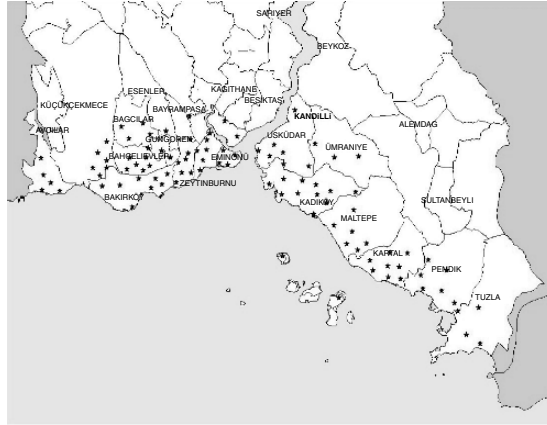


Fig. 15.2. Istanbul Rapid Response Stations

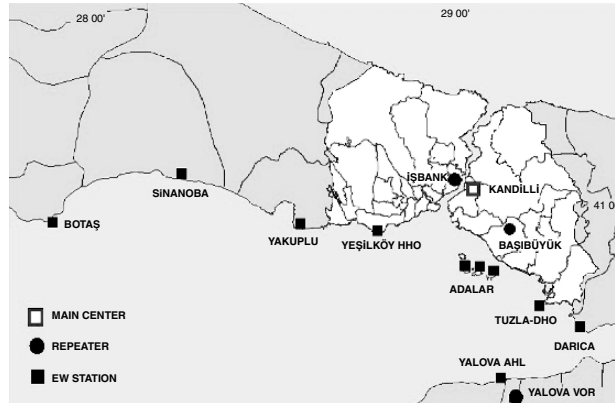


Fig. 15.3. Istanbul Early Warning Stations

15.4.3.1. Istanbul Rapid Response System

The Rapid Response System satisfies the COSMOS (The Consortium of Organizations for Strong-Motion Observation Systems) Urban Strong-Motion Reference Station Guidelines (www.cosmos-eq.org) for the location of instruments, instrument specifications and housing specifications. The relative instrument spacing is about 2-3 km which corresponds to about 3 wavelengths in firm ground conditions and more than 10 wavelengths for soft soils for horizontally propagating 1s shear waves. Strong-motion instruments are generally located at grade level in small and medium-sized buildings. As such the recorded ground motion corresponds to free-field conditions on the site geology. Certain stations have borehole data. New borehole surveys for other stations are being planned. For communication of data from the rapid response stations

to the data processing centre and for instrument monitoring a reliable and redundant GSM communication system (backed up by dedicated landlines and a microwave system) is used, on the basis of a protocol agreement with the AVEA GSM Service provider. In normal times the rapid response stations are interrogated (for health monitoring and instrument monitoring) on a regular basis. After triggered by an earthquake, each station will process the streaming three-channel strong motion data to yield the spectral accelerations at specific periods, 12Hz filtered peak ground acceleration and peak ground velocity and will send these parameters in the form of SMS messages at every 20s directly to the main data centre through the GSM communication system. The main data processing centre is located at the Department of Earthquake Engineering - Kandilli Observatory and Earthquake Research Institute of Bogazici University (KOERI-BU). A secondary centre located at the Seismological Laboratory of the same Institute serves as a redundant secondary centre that can function in case of failure in the main centre. Shaking, damage and casualty distribution maps will be automatically generated at the data centres after the earthquake and communicated to the end users within 5 minutes. Full-recorded waveforms at each station can be retrieved using GSM and GPRS modems subsequent to an earthquake.

For the generation of Rapid Response information two methodologies based on spectral displacements and instrumental intensities are used. These methodologies are coded into specific computer programs similar to HAZUS (<http://www.fema.gov/hazus/>). Both of the methodologies essentially rely on the building inventory database, fragility curves and the methodology developments in the Istanbul Earthquake Risk Assessment Study conducted by the Department of Earthquake Engineering of Bogazici University (Erdik et al., 2003a). For the computation of input ground motion parameters, spectral displacements obtained from the SMS messages sent from stations are interpolated to determine the spectral displacement values at the centre of each geo-cell using two-dimensional splines. The earthquake demand at the centre of each geo-cell is computed using these spectral displacements. The instrumental intensity at the centre of each geo-cell is computed as a function of short-period spectral acceleration. Using the response spectra and the instrumental intensities the building damage and the casualties are computed separately by using the spectral-displacement based and intensity based fragility curves. The computations are conducted at the centres of a $0.01^\circ \times 0.01^\circ$ grid system comprised of geo-cells (1120 m \times 830 m) size. The building inventories (in 24 groups) for each geo-cell together with their spectral displacement and intensity based fragility curves are incorporated in the software. The casualties are estimated on the basis of the number of collapsed buildings and degree of damage. An example of a building damage map that results from a randomly simulated strong motion data is provided in Figure 15.4. For transmission of the Rapid Response information to the concerned agencies (Istanbul Governorate, Istanbul Municipality and First Army Headquarters) digital radio modem and GPRS communication systems are used. The data will also be made available on the Internet.

15.4.3.2. *Istanbul Early Warning System*

In the Early Warning part of the IERREWS, ten strong motion stations were located as close as possible to the Great Marmara Fault in “on-line” mode. Continuous telemetry of data between these stations and the main data centre is realized with a digital spread spectrum radio modem system involving repeater stations selected in the region.

Considering the complexity of fault rupture and the short fault distances involved, a direct (engineering) early warning algorithm based on the exceedance of specified threshold time domain amplitude levels is implemented. The early warning information (consisting of three alarm levels) will be communicated to the appropriate servo shut-down systems of the recipient facilities, which will automatically decide proper action based on the alarm level. Depending on the location of the earthquake (initiation of fault rupture) and the recipient facility the alarm time can be as high as about 8 s. So far, the system has been exposed to only small magnitude earthquakes. An example data set from a small magnitude earthquake is illustrated in Figure 15.5.

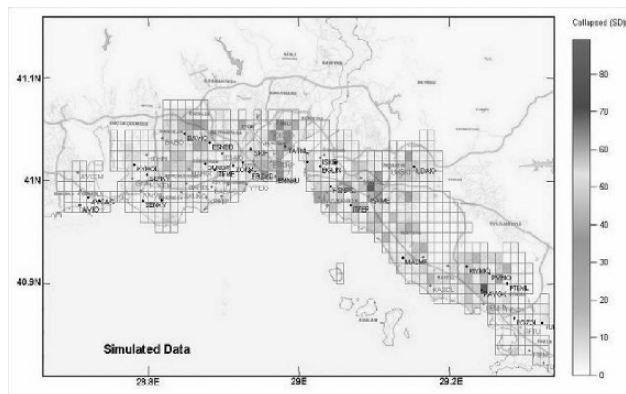


Fig. 15.4. Example of building damage map that results from a randomly simulated strong motion data

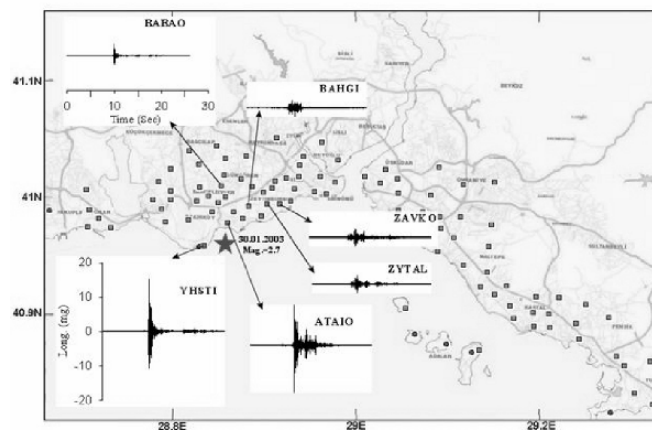


Fig. 15.5. Recorded strong motion data by rapid response stations for small event at Marmara sea

15.4.4. EARTHQUAKE RAPID REPORTING AND EARLY WARNING SYSTEMS IN TAIWAN

Taiwan, with an area of 36,000 km² is situated at the junction of the Ryukyu Island Arc and the Philippine Island Arc. As the Philippine Sea Plate subducts northward under the

Eurasia plate along the Ryukyu trench, and the Eurasia plate subducts eastward under the Pacific plate off the southern tip of Taiwan, the entire Taiwan island is under a NW-SE compression with a measured slip rate as large as 7 cm/ year. The high seismicity is located along the east coast and its offshore, while Taiwan population centres are developed over the western plains where occasional large events constitute a large part of the earthquake damage history (Shin and Teng, 2001).

Earthquake Rapid Reporting and Early Warning Systems in Taiwan uses a real-time strong-motion accelerograph network that currently consists of 82 telemetered strong-motion stations distributed across Taiwan, an area of 100 km x 300 km and monitored by Taiwan Central Weather Bureau (CWB). Each station has 3-component force-balanced accelerometers with signals digitized at 50 samples per sec per channel at 16-bit resolution. The full recording dynamic range is $\pm 2g$, and a sensitivity sufficient to record $M > 4.0$ events at distance of 100 km or more. Currently, the rapid reporting system can offer information about one minute after an earthquake occurrence. Information includes earthquake location, its magnitude and shaking maps of Taiwan area. Rapid damage assessment is under development. By applying the sub-network method approach, the early warning part of the system achieves earthquake reporting time about 20 sec. It will offer effective earthquake early warning for metropolitan areas located more than one hundred km from the epicentre (Tsai and Wu, 1997; Teng et al., 1997; Wu et al., 1998; Wu et al., 1999; Shin and Teng, 2001; Wu and Teng, 2002).

15.4.4.1. Rapid Reporting System (RRS)

Digital signals (of 3-channel strong-motion and 3-channel weak-motion) are continuously telemetered to the headquarters of the CWB in Taipei via 4,800 baud leased telephone lines. The incoming digital data streams are parallel processed by a group of computers (Figure 15.6). Whenever the pre-specified trigger criteria are met, the digital waveforms are stored in the memory and are automatically analysed by a series of programs (Wu et al., 1998). The results were immediately disseminated to governmental emergency response agencies electronically in many ways such as internet, FAX, pager, telephone on demand and mobile phone short message. Results include earthquake location, local magnitude, and intensities in the Taiwan area. Generally, the RRS of the CWB can offer information about one minute after an earthquake occurrence. The information gives an average error of 10 km in hypocentral location and an uncertainty of 0.3 units in local magnitude. Except basic information, more detailed information such as moment magnitude determination, ground motion calculation, and potential damage assessment can be analysed by the RRS within a few minutes.

15.4.4.2. Early Warning System (EWS)

The approach of the EWS was motivated by the experience of the 15 November, 1986 Hualien, Taiwan, earthquake of M_L 6.8 (or M_w 7.8). Although the epicentre of that earthquake was located near Hualien, the most severe damage occurred in the Taipei metropolitan area, about 120 km away. According to the travel times of past earthquakes in Taiwan, the shear waves travelling over this distance take more than 30 sec (Figure 15.7). If a seismic monitoring system can reliably inform the location and magnitude within 30 sec of a large earthquake that could threaten an area, then several or more seconds of advanced warning will be available for pre-earthquake response (Lee, 1995; Lee et al., 1996).

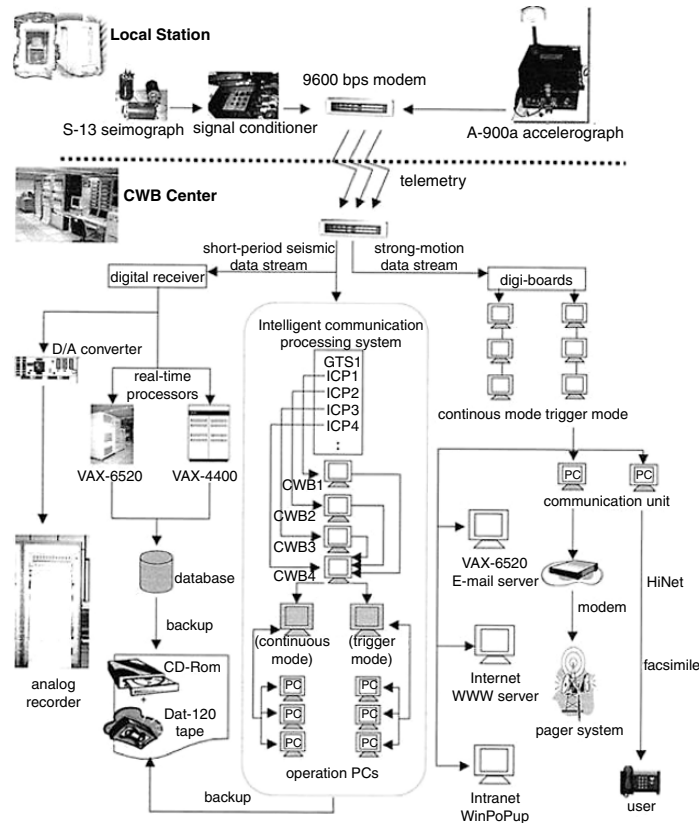


Fig. 15.6. A Block Diagram of Taiwan Rapid Report System (Tsai and Lee, 2004)

Currently, the RRS of the CWB can routinely broadcast the location and magnitude of a strong earthquake as well as the distribution of intensity about 60 sec after the origin time of the earthquake. However, the 60 sec time lapse is still too long to be practical for earthquake early warning. Because of the elongated shape of Taiwan (about 350 km from north to south) and because most of the historical damaging events occurred in the middle and eastern offshore parts of the island, an effective warning time must be made less than 30 sec for it to be effective. For shortening the reporting of the RRS to achieve early warning function, many studies including rapid magnitude determination, sub-network, and virtual sub-network approaches were developed by the CWB in recent years (Lee, 1995; Lee and Espinosa-Aranda., 1996; Wu et al., 1998, 1999; Wu and Teng, 2002).

15.4.5. EARLY WARNING SYSTEM FOR BUCHAREST

The Romanian capital Bucharest faces a significant earthquake hazard with a 50% chance for an event in excess of 7.6 moment magnitude every 50 years. Within the last 60 years Romania experienced 4 strong Vrancea earthquakes: Nov. 10, 1940 ($M_w = 7.7$, 160 km deep); March 4, 1977 ($M_w = 7.5$, 100 km deep); Aug. 30, 1986 ($M_w = 7.2$, 140

km deep); May 30, 1990 ($M_w = 6.9$, 80 km deep), (Wenzel et al., 1999; Wenzel et al., 2001).

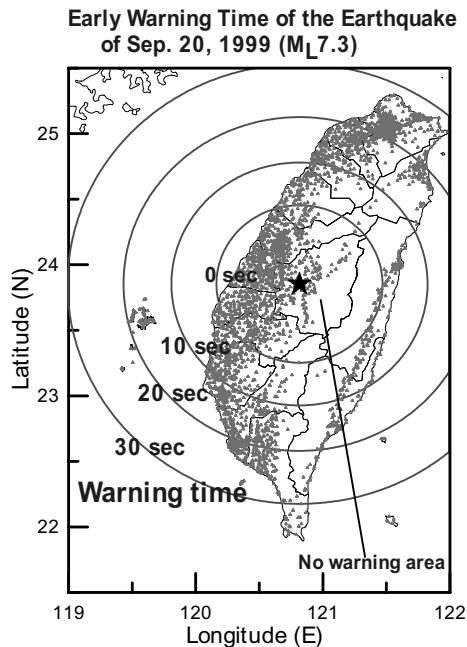


Fig. 15.7 Early Warning Time for Taiwan Early Warning System (Tsai and Lee, 2004)

The 1977 event had catastrophic character with 35 high-rise buildings collapsed and 1500 casualties, the majority of them in Bucharest. An Early Warning System (EWS) based on the travel time differences between the primary P-wave and the destructive S-wave allows a warning time of about 25 s. Peculiarities of the Romanian intermediate depth seismicity such as the stationary epicentres and the stability of radiation patterns, and a line-of-sight connection between the epicentral area and the capital allow design of a simple and robust EWS. Simplicity and robustness of the system are sought in order to reduce the risk of false alarms, which is crucial for making the system cost-beneficial.

Early Warning System (EWS) for the capital city of Bucharest is designed and operated by a group of civil engineers and seismologists from the National Institute of Earth Physics (NIEP) in Romania and Karlsruhe University in Germany. The group studied the seismological boundary conditions of EWS for the Romanian capital of Bucharest. The earthquakes threatening the capital are intermediate deep events with magnitudes close to $M_w = 8.0$ at an almost fixed epicentral distance of about 150 km. The travel time difference between the destructive S-wave arriving in Bucharest and the epicentral P-wave is always greater than 25 s, which represents the maximum possible warning time.

Moreover source mechanisms are extremely stable for larger and smaller events so that a projection of the level of ground motion to be expected in Bucharest can be based on the amplitude of the epicentral P-wave rather than on cumbersome determination of magnitude and depth. This feature allows the design of a simple, robust and fast EWS.

Within 25 s, a system with the largest warning time after the seismic alarm system for Bucharest City could be established (Wenzel et al., 1999).

It is expected however that after an initial phase of testing, governmental institutions and the commercial sector will supply warning receiver systems once the EWS is fully operational. These systems could include either pager messages that display an alert message or at an advanced stage pager-driven switches to stop technical operations automatically. The value of the EWS for the latter option can only be judged on the basis of an application specific costs-benefit analysis, but simple considerations suggest that it will be cost-efficient.

15.4.6. RAPID RESPONSE AND DISASTER MANAGEMENT SYSTEM IN YOKOHAMA, JAPAN

The city of Yokohama is the second largest city in Japan with a population of 3.5 millions. Just after the 1995 Kobe earthquake, the city began to develop the dense strong-motion array for disaster management under the strong initiative of the mayor. Within 433 km square of the city, accelerographs at 150 free field stations have been installed for ground shaking monitoring. Spacing between stations is about 2 km. A high precision digital accelerograph is used to record weak to very strong ground motion. Ground acceleration up to 2000 cm/s^2 is registered on an IC memory card with 18 bits A/D resolution at 200 sampling rate. In addition to the accelerographs at ground surface, borehole accelerometers are installed at 9 stations for liquefaction hazard assessment. These stations are connected to three observation centres, the disaster preparedness office of the city hall, the fire department office of the city and Yokohama City University, by the high-speed and higher-priority telephone line. At 18 stations, the backup communication system by satellite is available. The dense strong motion array and its components are shown in Figure 15.8. The full operation of the monitoring system started on May, 1997 (Midorikawa, 2004).

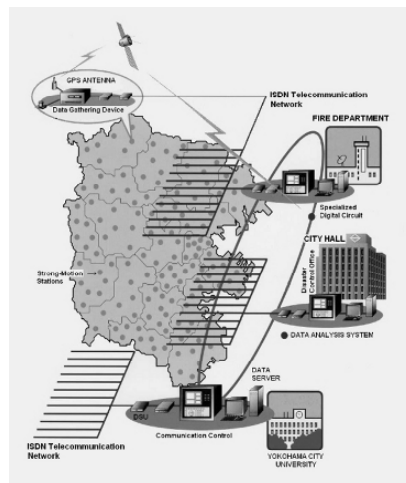


Fig. 15.8. Dense Strong Motion Array in Yokohama
(<http://www.city.yokohama.jp/me/bousai/eq/index.html>)

15.4.6.1. Seismic Intensity Map

When the accelerograph is triggered by an earthquake, the station computes ground-motion parameters such as the instrumental seismic intensity, peak amplitudes, predominant frequency, total power, duration and response spectral amplitudes. These parameters are automatically reported to the centres. On receiving more than 10 reports in a prescribed time interval, the centres activate alert systems. The seismic intensity data is conveyed to the city officials by the pager, and the intensity map of the city is drawn within a few minutes after the earthquake. The map is immediately open to the public through the Internet (www.city.yokohama.jp/me/bousai/eq/index.html) and local cable TV (Figure 15.9). The map is utilized as the earliest information for disaster management. The seismic intensity data at 36 stations are also reported to the Japan Meteorological Agency. The data are put together with those from the other sources and are transmitted by nationwide broadcasts.

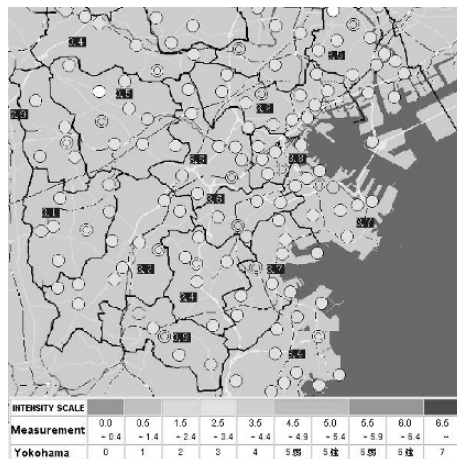


Fig. 15.9. Yokohama Seismic Intensity Map of 20 September, 2003 Earthquake

15.4.6.2. Damage Estimation Map

In order to grasp a scale of the disaster and its spatial distribution immediately after the event, the ground motion data from the stations are used for the real-time seismic hazard and risk assessment. The assessed items are ground motion, liquefaction and building damage. The various GIS (Geographic Information System) data which have been built by the different departments of the city are gathered and compiled for the assessment. The operation of the assessment system started on June, 1998. In the mapping of ground motion hazard, the city is divided into 170,000 elements with the mesh size of 50×50 meters. The fine mesh system is adopted because of strong spatial variation of the geologic conditions in the city. More than 15,000 borehole data in the city are compiled. The soil profile sections are drawn from the borehole data and the geomorphological information, and the soil condition of the city is classified into 268 types. The data from borings or measurements of S-wave velocity are used to build up the generalized underground model for each soil type. The amplification factor of the corresponding soil type is assigned to each element. To eliminate the site effects from the observed ground motion, the bedrock motion spectrum at each station is estimated by dividing the

observed response spectrum by the computed amplification factor. The ground motion spectrum at each element of the fine mesh system is computed by multiplying the bedrock motion spectrum at the neighbouring station by the amplification factor at the element. Thus, the very detailed ground shaking map is constructed by using the observed ground motion records and the underground model. Although there are many commercial buildings in the city, the majority of the buildings in the city are wooden houses. Generally, they are more vulnerable to strong shaking than non-wooden buildings such as reinforced concrete buildings. Accordingly, the assessment of the seismic risk of wooden houses is included in the system. The GIS database of about 450,000 wooden houses is built up by the data matching of the fixed asset tax inventory and the digital base map. The dynamic vibration characteristics of each house are assigned according to the types of structure, use, roof and the construction age. The response of the house is computed by using the response spectrum of ground motion, to determine the degree of the damage. The distribution of the wooden-house damage is mapped within twenty minutes after the event. The damage map is displayed with other information such as locations of hospitals, refuges and major roads for emergency transportation. Thus, the hazard and risk maps are created within twenty minutes after the earthquake, almost in real-time, so that the maps can be used for selecting strategy of emergency response activities (Midorikawa, 2004).

15.4.6.3. *Liquefaction hazard Assessment*

A dynamic load induced in a soil element during an earthquake is computed not by the record at surface, but by the record of the borehole accelerometer at bedrock. The liquefaction resistance of soil is calculated by the method adopted in the specifications for highway bridges. The liquefaction potential for each element of the fine mesh system is evaluated by comparison of the liquefaction resistance with the dynamic load. The shaking and liquefaction maps are drawn within ten minutes after the event.

15.4.6.4. *Damage Status Map*

The damage information gathering system is constructed to overlay the actual damage information that is gradually obtained after the event on the estimated damage map. The city has an agreement with about 500 civil construction firms. When the seismic intensity larger than in the Japanese scale (approximately 7 in the M.M. scale) is observed, they will immediately survey the damage to road structures on the major 93 roads, and report the damage to the 18 civil construction branch offices of the city. The damage information reported to the 18 branch offices is transmitted to the city hall in the form of the GIS data by the intranet GIS system. The damage GIS data such as the damage of the road and restriction of the traffic are overlaid on the estimated damage map in order to update the damage information. The operation of the gathering system started on April, 1999. The city conducts earthquake drills twice a year; one is on the day of the Kanto earthquake (September 1) and another is the day of the Kobe earthquake (January 17). At the drill, the simulated results from the real-time system for a scenario earthquake are used to make the drill more practical and realistic.

PART IV: MANAGING EARTHQUAKE RISK

CHAPTER 16 TECHNICAL EMERGENCY MANAGEMENT

A. Goretti and G. Di Pasquale
Civil Protection Department - USSN, Rome, Italy

16.1. Introduction

Just after an earthquake thousands and thousands of buildings can be damaged and further shocks can occur. Of main interest is then the safety of the buildings against further shocks. As citizens are not usually able to evaluate the residual building strength and as the number of buildings to be inspected is very huge, safety inspections are usually managed by proper institutions. Inspectors have to balance the safety of the citizen, since once the building is judged safe people will keep living there, against the need to reduce the peoples' discomfort. Often associated to the safety assessment is the evaluation of the short term countermeasures able to guarantee private and public safety, as propping, supports, barriers, protected crossings, etc. Concerning the time schedule of the activities within the emergency cycle before, during and after the earthquake, safety evaluation and short term countermeasures are managed during the earthquake (see Chapter 17). Although all the above items have an undoubted importance, it is only recently that, in most of the seismic prone countries in the World, post-earthquake safety and damage assessment is being approached in a comprehensive way.

In Japan, experiences date back to 1978 after the Miyagiken-oki earthquake. On that occasion the importance of having a proper methodology for post-earthquake inspections appeared. A research program was then started in 1981, leading in 1985 to the publication of the "Guidelines for Post-earthquake Inspection and Restoring Techniques". The methodology was tested after the 1983 Nihonkai-chubu earthquake and after the 1985 Mexico City earthquake. The methodology was revised in 1989 and published by the Japanese Association for Building Disaster Prevention. The actual version has been revised in September 2001.

In Italy technical activities after destructive earthquakes, like 1908 Messina-Reggio and 1915 Avezzano earthquake, were mainly devoted to short term countermeasures, temporary shelters and damage assessment to support the reconstruction funding. Also the damage survey performed after 1976 Friuli earthquake ($M_s=6.5$) was aimed to the quantification of the economic loss. After 1980 Irpinia earthquake ($M_s=6.9$) the need of procedures for usability evaluation was evident, the homeless being of the order of hundreds of thousands. However after the event no successful effort was made to establish a proper methodology and procedures and forms varied from earthquake to earthquake. A few academic proposals were published (Gavarini, 1985), mostly based on a previous OES (1978) study. A research program aimed at introducing a first level usability and damage inspection form started in 1995, but, when 1997 Umbria-Marche earthquake struck, the form was in a preliminary version. Nevertheless it was used in Marche Region (40,000 inspected buildings). The form was then revised and tested after Pollino 1998 earthquake, when 18,000 buildings were inspected. The final version, with

its manual, was published in 2000 and recently used after Molise 2002 earthquake, when 23,000 buildings were inspected.

Greek experiences on building usability date back to 1978 on the occasion of Thessaloniki earthquake, when about 43,000 buildings were inspected. Forms and procedures were updated in the following years and validated in the 1986 Kalamata destructive earthquake when more than 13,000 buildings were inspected. The form used in the survey included data related to damage to all building components and to building usability. That form was reputed too complicated to be used in emergency and hence all the methodology has been revised. The present one was published in 1996 and used the first time after Konitsa earthquake (1,500 inspected buildings) and more recently after 1999 Athens earthquake when more than 65,000 buildings were inspected.

Also in California usability assessment dates back to 1978 (OES, 1978), when a 3 pages form was established. It contained the damage grade to several building components together with an overall measure of damage. Forms and procedures have been continuously updated as earthquakes occurred. The actual methodology originates in 1989 just before Loma Prieta earthquake (ATC-20, 1989). On the basis of the lesson learnt after the earthquake, the procedure has been revised in 1995 (ATC-20-2, 1995).

From the above overview it appears that a) methodologies are relatively recent and date back to almost the same period, the end of the 1970s and b) forms and methodologies have been often revised, due to lessons learnt after each destructive earthquake.

In the remainder of the chapter, definitions, methodologies and procedures of safety inspection, damage assessment and short term seismic countermeasures will be discussed, comparing the state of practice in seismic prone countries. Such activities are usually called technical emergency activities, where the term technical is to indicate the engineering competence and the term emergency is to distinguish them from the same activities performed in peace-time.

16.2. Immediate occupancy and damage survey

The post-earthquake building survey can consist of safety evaluation or damage assessment. Depending on the aim of the survey, both items can be performed. From a conceptual point of view damage and usability are strictly correlated and, hence, any usability classification implies damage classification. However, damage assessment can take more time than the safety evaluation. This is the reason why in many countries, as in Japan and Turkey, damage assessment is performed after safety evaluation.

Post-earthquake usability assessment is commonly aimed to evaluate the possible short term use of the damaged buildings (BRI, 2002; ATC-20, 1989; ATC-20-2, 1995; Baggio et al., 2000; Goretti, 2001; Dandoulaki et al., 1998). Inspectors individuate buildings that can be safely used in case of aftershocks, together with the emergency countermeasures to be taken in order to reduce the citizen's risk and, if necessary, to preserve the building. Safety inspections are directed towards reducing human discomfort, promoting the return to the pre-event social situation and limiting the number of temporary shelters, guaranteeing, at the same time, the safety of the citizens. Although the purpose is rather clear, seismic codes do not usually address the topic.

Recently it was reported (Gavarini, 1999) that "... *technical activities requiring the same skills as safety inspections are for a long time now included in codes and, hence, technicians know what is to be done in the building design in terms of drawings, calculations, qualifications, responsibilities. The same framework for safety inspections is often lacking, especially in terms of codes and responsibilities...*". This is the reason why no clear and unambiguous definition of usability can be found in the literature. Sometimes the usable building is defined as the one that is not unsafe (Japan), sometimes as the one with minor or null damage (Turkey). In other cases (California) the term usable is not used, and possibly safe buildings are classified as inspected. It is then deemed useful to include here the Italian usability definition (Baggio et al., 2000):

"Post-earthquake usability evaluation is a quick and temporarily limited assessment, based on expert judgement, on visual screening and on data easily collected, aimed to detect if, during the actual seismic crisis, buildings damaged by earthquake can be used, being reasonably safeguarded the human life".

Further damage is then accepted during aftershocks, but, in order for the building to be usable, life must remain reasonably safe. This definition does not include functionality of plant, although the Italian form considers damage to plant. In other forms, as in the Japanese one, damage to plant is not included. The concerns regarding this concept centre on those structures where the utilities have been damaged and turned off. There is no sanitation, electricity, or gas. This means the structure does not comply with the minimum requirements of other Codes (i.e. Health and Safety Code in California).

Damage assessment definition is not so controversial. Differences among countries are found on the damage classification (definition of intensity and extension of the damage, overall measure of damage or damage to single component, failure modes, etc.). Once the damage is classified, surveyors have to select the appropriate damage level in the inspected building.

Differently from the safety inspections, a damage survey can be performed for many reasons (BRI, 2002; Baggio et al., 2000). In Japan the aim of the damage assessment is to evaluate the long term use of the buildings. The result of the evaluation is a suggestion to the owner of the building concerning the repair, the retrofit or the demolition of the building. In Italy something similar happened in the past, but today the main purpose of the damage survey is to support the usability classification and, at the same time, to estimate the overall amount of direct economic loss, in order to establish the need for the reconstruction. The decision on long term use of the building is postponed to an engineering evaluation in the reconstruction process. In Greece damage survey is not performed, because financial contributions are established on the basis of the usability classification. In Turkey the damage classification is performed to assign financial contribution to each building.

Strictly related to the aim of the damage survey is the way in which it is performed. In Italy not very detailed information is required and the data collection can be performed together with the usability survey. The advantage is to speed up the overall survey and hence the reconstruction process, as it is demonstrated (Kaas et al., 1987) that the time for the reconstruction process is very strictly related to the time for the emergency phase. The main drawback of this joint survey is to slow down the completion of the usability survey, although many of the data to be collected in the damage survey need to

be taken into account in the usability survey. The slow-down is compensated by the fact that, in Italy, the usability and damage survey is performed in 2 steps, with a limited percentage of buildings requiring the second inspection (about 5%). In Greece and California, the usability assessment is still performed in 2 steps, unlike the engineering evaluation in California, but the number of buildings requiring the second inspection is very high. Main features of the usability and damage assessment in some countries all over the world are summarised in Table 16.1 (BRI, 2002; ATC-20, 1989; ATC-20-2, 1995; Baggio et al., 2000; Goretti, 2001; Dandoulaki et al., 1998).

Table 16.1. Purpose of usability and damage survey in several countries

	Usability survey	Steps	Damage survey	Survey
Italy	Short term use of the building	2	Establish overall amount of direct economic loss	Joint
Greece	Short term use of the building	2	Not performed	
Turkey	Short term use of the building	1	Establish financial contribution for each building	Distinct
California	Short term use of the building	3	Not performed	
Japan	Short term use of the building	1	Suggestion for long term use of buildings	Distinct

It is worthwhile to mention other important deliverables related to the damage survey. They are: a) macroseismic intensity assessment (Di Pasquale and Galli, 2001), b) vulnerability assessment (Braga et al., 1982), c) building classification (Zuccaro et al., 2000) and d) site effects evaluation (Goretti and Dolce, 2002).

The same technical activities (damage assessment and safety evaluation) can also be performed in normal times. In this case the number of buildings to be inspected is lower, as there is less urgency of inspection. This is the reason why in normal times standards methodologies of seismic engineering can be used and results can be accurate enough. In post-earthquake emergency the need to reduce immediately the citizen's risk press the inspectors to a quick evaluation. Hence the required data have to be easily collected, calculations are not feasible and accuracy is not reached. The time validity of the safety evaluation is limited to the emergency period and ends when a new shock occurs. The differences between damage and usability assessment in normal times and in emergencies are of main importance in order to understand the limits of the assessment and the inspectors' responsibility.

This is particularly relevant in case of usability assessment, but it applies also to damage collection if a huge number of buildings is involved. The main features of the post-earthquake usability and damage evaluation, together with their consequences, are reported in Table 16.2. All the items interact with each other. For instance buildings may have to be re-inspected after a large aftershock, increasing the number of inspections to be performed and requiring more inspectors.

The quantitative dimension of safety inspections and damage evaluation depends on the magnitude of the event and on building density and vulnerability. When comparing different earthquakes it should be kept in mind that it is very difficult to collect homogeneous data concerning usability and damage assessment. This is due to the fact that procedures and forms are very different in each country and, also within each country, procedures and forms have been frequently revised. Sometimes data are reported in terms of dwellings, sometimes in terms of buildings. The usability and the

damage classification are also different, making the comparison sometimes questionable. In spite of the above mentioned drawbacks, some data concerning recent world-wide earthquakes are reported in Table 16.3, where I_0 is the epicentral intensity.

Table 16.2. Features of usability and damage assessment

Features	Consequences for usability assessment	Consequences for damage assessment
The seismic crisis is not ended	A new shock can occur. It must be taken into account in the usability evaluation. The assessment is valid until a new shock occurs. Reduced safety level should be accepted.	Cumulative damage is often observed, while ground motion is recorded for each shock. A cumulative macroseismic felt intensity is usually assigned.
The number of inspections is very huge	Many inspectors are required, the inspection management should be effective and computerised. Procedures and forms should be prepared, and inspectors trained, possibly before the event, but if needed also during the emergency.	
Inspections should be completed as soon as possible in order to reduce the risk for inhabitants, usability assessment, and to speed up the reconstruction, damage assessment.	The available time for each inspection is very limited. It is not possible to make a detailed dimensional or mechanical survey and perform numerical analysis. Usability assessment must be based on visual inspection, expert judgement and interviews with local technicians to gather information on the local constructive practice.	The available time for the damage assessment is very limited. Collected data can only be I level data, mainly the observed physical damage, the building type and rough dimensional data.

Table 16.3. Inspected and unusable buildings in recent seismic events

Event	Year	I_0 (MCS)	Inspections	Unusable buildings	Homeless
Friuli (ITA)	1976	X	>70,000 (§)	43,000 (°)	190,000
Irpinia (ITA)	1980	X	250,000	160,000 (°)	300,000
LomaPrieta (USA)	1989	XI	25,000	1450 (^^)	10,000
Northridge (USA)	1994	XI	66,000	5,700	40,000
Kobe (JAP)	1995	XI	46,000	144,000 (**)	240,000
Marche (ITA)	1997	IX-X	100,000	27,000	30,000
Pollino (ITA)	1998	VI-VII	18,000	4,100	N.A.
Kocaeli & Bolu (Turkey)	1999	XI	330,000	100,000 (**)	500,000
Athens (GR)	1999	XI	65,000	32,000	70,000
Molise (ITA)	2002	VIII-IX	23,000	6,000	12,000

(§) Damage assessment, (*) Damaged or collapsed buildings, (°) Estimated from 480,000 damaged or collapsed dwellings, (^^) only in San Francisco (**) Heavy damaged or collapsed buildings, (+) Exhaustive damage assessment of 38,000 buildings in 41 Municipalities; about 250,000 inspections of the damaged buildings in all the Municipalities.

Note that after the Kobe earthquake about 144,000 buildings collapsed or were heavily damaged and only 46,000 buildings were inspected for damage assessment. Hence the damage assessment has been performed on a (pre-) selected set of damaged buildings. In Table 16.3 one can see that, after destructive earthquakes, the number of buildings to be inspected can easily be in the range of 100,000, and could grow even more if a big city would be involved. Consequently, procedures should be adequately predisposed.

Usability classification usually distinguishes safe and unsafe buildings, with a third category in between. In Tables 16.4 to 16.7 main differences in classification are reported.

Table 16.4. Italian building classification for post-earthquake usability

USABLE	Building can be used without measures. Small damage can be present, but negligible risk for human life.
USABLE WITH COUNTERMEASURES	Building has been damaged, but can be used when short term countermeasures are provided
PARTIALLY USABLE	Only a part of the building can be safely used
TEMPORARY UNUSABLE	Building to be re-inspected in more detail. Unusable until the new inspection.
UNUSABLE FOR EXTERNAL RISK	Building can be used in relation to its damage level, however it can not be used due high risk caused by external factors (heavy damaged adjacent or facing buildings, possible rock falls, etc.)
UNUSABLE	Building can not be used due to high structural, non structural or geotechnical risk for human life. Not necessarily imminent risk of total collapse.

Table 16.5. Japanese building classification for post-earthquake usability

INSPECTED	Building can be used without countermeasures. Small damage can be present, but negligible risk for human life. Buildings that are neither CAUTION nor DANGER
LIMITED ENTRY	Building has been damaged. The risk of collapse or falling objects is not so high, but building behaviour is not predictable. Restricted use.
UNSAFE	High risk of collapse or falling objects. It is suggested to do not use the building. Compulsory if public safety is involved.

Table 16.6. California building classification for post-earthquake usability

INSPECTED	No apparent hazard found; repairs may be required; lateral load capacity has not been significantly decreased; vertical load capacity has not been significantly decreased; lawful occupancy is permitted.
RESTRICTED USE	The building has been damaged but may or may not be habitable; there may be a falling hazard present in part of the structure; there may be damage to the lateral force and/or vertical load resisting systems, however, they are still able to resist loads; occupancy is permitted in accordance with noted restrictions.
UNSAFE	Extreme hazard and risk of collapse or imminent danger of collapse from an aftershock or significant decrease in lateral and/or vertical load capacity. The building is unsafe for occupancy or entry except by authorities.

Table 16.7. Greek building classification for post-earthquake usability

USABLE	Building with no visible damage and or whose original seismic capacity has not been significantly decreased
TEMPORARILY USABLE	Buildings whose seismic capacity has been decreased and/or they pose a danger condition due to damage to non-structural elements.
UNUSABLE	Imminent danger of sudden collapse. Entry is absolutely prohibited.

It can be seen that the Italian classification places emphasis on restrictions in building use (partially usable, temporary unusable, external risk). It is aimed to increase as much as possible the number of buildings that can be used with short term countermeasures. It should be noted, however, the difficulty to include all the possible restrictions in the usability classification (i.e. a building can be partially usable after emergency countermeasures, a condition not initially included in the Italian classification).

16.3. Basis of methodology

Usability and damage can be assessed for dwellings or buildings. However from the structural point of view, it is necessary to inspect the whole building, as damage can be highly localised and, at the same time, detrimental to the whole building safety.

In all the procedures where inspections are requested by the dwelling's owners or users, there is a difference between the object of the request, the dwelling, and the object of the inspection, the building. It can then happen frequently to have erroneous repeated requests on the same building. Inspection of buildings requires also defining and selecting the building. This is particularly difficult in countries, such as Italy, where most of the villages show historical areas where buildings have been aggregated during the centuries, often sharing the same walls. This problem is not so important in countries such as Japan, where buildings are recent and can be considered as isolated buildings.

The process of usability assessment is highlighted in Figure 16.1. In $T=T_0$ a shock occurred and possibly damaged a building. An inspection is then requested and inspectors should judge about the future behaviour of the damaged building when stricken by another shock in $T=T_1$. Sources of uncertainty are the intensity of the next shock and the behaviour of the damaged building. They motivate the difficulty of a reliable quantitative assessment.

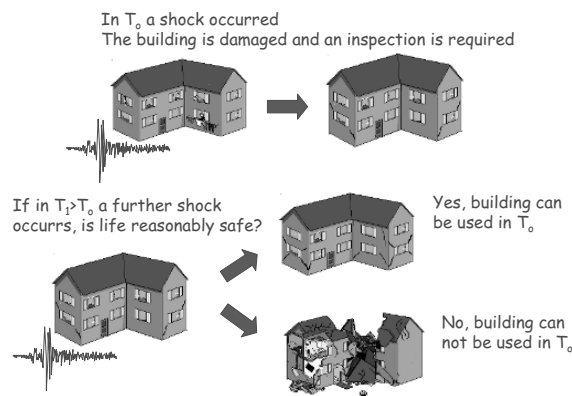


Fig. 16.1. Safety inspection process

The time evolution of the seismic sequence in relation to the safety inspection process is reported in Figure 16.2.

From a methodological point of view, usability evaluation should be based on the three following items:

- The reference earthquake, to which the building should withstand.
- The damage suffered by the building.
- The building vulnerability.

All the available methodologies consider the building damage as the main item to decide on building safety. Few of them address the reference earthquake and the

building vulnerability, but, at least conceptually, they should be included in the methodology.

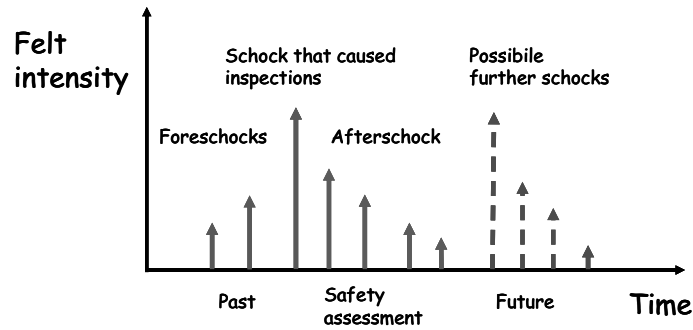


Fig. 16.2. Seismic sequence and safety inspection

From the safety inspection process it appears that the same damaged building can be safe or unsafe depending on the intensity of the possible further shock that is supposed to occur. It is also important to point out that, at least implicitly, everyone has in his mind a given reference earthquake when judging about the post-earthquake building safety, just as in the design of a new aseismic building. For a homogeneous action the reference earthquake, being the external action which buildings should withstand, should be the same for all the inspectors in the same location and it should be clearly stated before the inspections. It can be different from location to location, depending on the probability of occurrence of a further shock of a given intensity. In this the moving of the epicentre during the seismic sequence should be considered and, hence, some non-epicentral areas can become epicentral areas in a successive shock. In principle the following logical tree should be used to evaluate the reference earthquake.

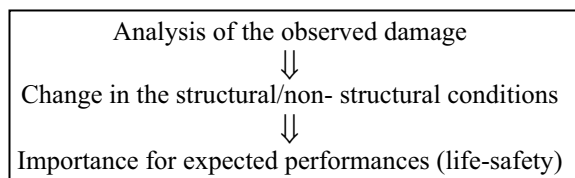
Table 16.8. Logical tree for the selection of the reference earthquake

Information	Seismic crisis	Areas	Reference earthquake
No		All	Maximum felt intensity at site during the sequence
Yes	Ended	All	-----
	In progress	Epicentral area	Maximum felt intensity at site during the sequence
		Non epicentral Area	Future non epicentral area
		Possible future epicentral area	Intensity (MCS) 1 or 2 degree greater than the felt one

If it is for sure that the seismic sequence is ended, short term safety assessment can be performed in relation only to gravity loads. In practice this never happens. Generally, due to the inability to predict the evolution of the seismic activity, the reference earthquake is hardly ever stated before the inspections and is selected, in a given location, as the maximum felt intensity during the sequence in the same location. So ATC-20 reports that the building, in order to be judged safe, should withstand an earthquake at least of the same intensity. The same appears in Baggio et al. (2000) and in Goretti (2001).

The damage is the main item to be considered in usability assessment. The analysis should be extended to: structural elements, non- structural elements, soil and foundation and external elements. Structural damage is associated to structural elements as columns and walls. It can lead to the building partial or total collapse. Non -structural damage is associated to non- structural components as partitions, infill walls, signs, banners, plants. Damage to non- structural components does not involve necessarily the collapse of the whole building, but, in case of heavy damage, life safety cannot be assured, due to local partial collapses. Damage to soil can be due to landslide, liquefaction, lateral spreading, etc. They can produce settlement and tilting of the building as a rigid body, as well as cracks in the foundation. Damage to external elements can increase the life risk if objects can fall on the building under inspection. Typical is the case of adjacent bell towers, tall buildings or even rocks.

The general methodology for damage analysis is reported in the following scheme



Risk assessment in relation to life-safety requires the analysis of the observed damage under the building material, constructional type and possible failure modes. The same crack width can be more or less dangerous if occurred in a masonry building or in a RC building. A 3 mm crack width can be serious in a RC column but can be negligible in a masonry wall. At the same time the failure mode can give more or less relevance to the crack pattern. Vertical cracks at the corner of masonry walls indicate a possible dangerous overturning of the wall, while the same crack type but at the edge of a refill of an existing opening, not connected to the wall, is not so dangerous. The damage analysis is made explicit in two following examples, specific to masonry buildings shown in Figures 16.3 and 16.4.



Observed damage	Separation cracks between walls and walls and floor
Change in structural conditions	Walls are no more connected each other
Consequences on building performance	Possible out of plane overturning and fall of the floor

Fig. 16.3. Masonry building. Structural damage

Damage grade is often established according to the classification included in macroseismic scales as MSK76 (Medvedev, 1977) or EMS98 (Grüntal, 1998). As the damage is classified taking into account the building material, the structural system and the failure mode, they should be determined in the building under inspection. This can

be accomplished through visual inspection. However, when plaster or wallpaper hide the features of the building components, inspectors have to resort to interviews with the owner, tenants or with local technicians. As the damage can not be immediately visible, it is also important to know where to look for the physical damage. Inspectors can take advantage of the fact that failure modes are characterised by specific cracks patterns.



Observed damage	Fallen tiles
Change in structural conditions	Tiles are not anchored to the roof
Consequences on building performance	Possible further fall of tiles

Fig. 16.4. Masonry Building. Non- structural damage

The third item in post-earthquake safety assessment is vulnerability. In principle, vulnerability should be taken into account only when the intensity of the reference earthquake is one or two degrees higher than the maximum felt intensity during the sequence and at the same time the building is not seriously damaged. In this case the absence of damage is not evidence of good seismic performance because the shock has been of small intensity. Hence to extrapolate the building seismic behaviour to higher intensities, one has to resort to vulnerability indicators. Referring to the specific literature for a complete treatment of building vulnerability (GNDT, 1993), here we just recall a (non- exhaustive) list of major vulnerability indicators.

In case of masonry buildings, main vulnerability factors are: bad quality materials (HCT, round stones, pebbles, etc.) or irregular layout; lack of connections between the two withes of the same wall, in the so- called “a sacco” walls; lack of vertical connection among walls at the same level; lack of horizontal connection among walls and floors; heavy and thrusting floors or roofs; excessive distance between parallel walls; excessive, irregular or near corner openings; excessive leaning; poor maintenance. Other contributing factors include modifications made over time, such as buttresses and ties (which improve performance) and additional stories (which tend to compromise performance); the characteristics, quality, and condition of the mortar; the thickness of the bearing and non-bearing walls; the method and configuration of the attachment of the floors and roof to the walls; the presence of chimneys inside the walls.

In case of RC buildings, main vulnerability factors are: poor concrete resistance; irregularity in plan or height (soft story); weak columns and strong beams; short columns due to shear walls or partial infill walls; frames in only one direction; age of

construction in relation to seismic code and seismic zonation; infill walls not inserted in the structural frame; poor maintenance; lack of detailing.

According to the presented methodology, in case of significant structural, non-structural or geotechnical deficiencies, not worsened by the earthquake, as pre-existent cracks or settlements, the buildings should be judged safe if the reference earthquake is equal or less than the maximum felt intensity in the sequence, unsafe if it is significantly greater. Hence, as the reference earthquake is usually assumed as the maximum felt intensity, building vulnerability should not be considered in safety assessment. In practice, however, at least in the Italian experience, the percentage of buildings judged unsafe by inspectors increases as the building vulnerability increases, given the same suffered damage (see following statistics).

After observation of damage to building and soil, the safety evaluation is made with a synthesis of all the information acquired, interpreting damage and, if necessary, vulnerability, in relation to the possible further shocks to be felt by the building. The safety is evaluated associating the life-safety risk to the observed physical damage. Hence inspectors have to deal with structural risk, non-structural risk, geotechnical risk and external risk.

If the risk is judged low for each of the above items, the buildings will be safe; if it is high at least for one item the buildings will be judged unsafe. Restrictions in the building use can be imposed when the risk is highly localised in an area of the building and the possible partial collapse of that area does not involve risk in other areas. When the risk is high, but can be lowered with emergency countermeasures, the use of the building can be accepted only with the execution of the proper countermeasures. When buildings and soils are undamaged and hence the structural, non-structural and geotechnical risk can be considered low, but the external risk is high due, for instance, to the possible collapse of a bell tower, the building should be judged unsafe. When the situation is not clear and/or inspectors are not enough experts to decide on building safety, inspection should be repeated by an expert team. However inspectors should be informed that this case should be avoided as much as possible in order to not increase the number of inspections to be done. In the Figures 16.5 to 16.7 examples are reported for unusable, restricted use buildings and usable buildings. The relationship between damage and usability classification is not strictly imposed in any methodology. It will be examined in the following.

16.3.1. BUILDING SAFETY EVALUATION IN ITALY

In the Italian methodology, damage to structural components and to infill walls is recorded by inspectors in an appropriate section of the safety form, reported in Figure 16.8. The values D0,...,D5 represent the damage grade, while damage extension is classified in percentage as less than 1/3, between 1/3 and 2/3, greater than 2/3. It is possible to select more than one damage grade (except in case of null damage) but the sum of relative extensions should be limited to 1.



Fig. 16.5. An example of unusable building



Fig. 16.6. An example of restricted use building



Fig. 16.7. An example of usable building

Level Extension	DAMAGE									D0 Null
	D4-D5 Very heavy or collapse			D2-D3 Medium or heavy			D1 Slight			
	2/3 ^	1/3 - 2/3	< 1/3	2/3 ^	1/3 - 2/3	< 1/3	2/3 ^	1/3 - 2/3	< 1/3	
	A	B	C	D	E	F	G	H	I	
Component										L
1	Vertical structures	<input type="checkbox"/>	<input type="checkbox"/>	<input type="checkbox"/>	<input type="checkbox"/>	<input type="checkbox"/>	<input type="checkbox"/>	<input type="checkbox"/>	<input type="checkbox"/>	<input type="checkbox"/>
2	Horizontal structures	<input type="checkbox"/>	<input type="checkbox"/>	<input type="checkbox"/>	<input type="checkbox"/>	<input type="checkbox"/>	<input type="checkbox"/>	<input type="checkbox"/>	<input type="checkbox"/>	<input type="checkbox"/>
3	Stairs	<input type="checkbox"/>	<input type="checkbox"/>	<input type="checkbox"/>	<input type="checkbox"/>	<input type="checkbox"/>	<input type="checkbox"/>	<input type="checkbox"/>	<input type="checkbox"/>	<input type="checkbox"/>
4	Roof	<input type="checkbox"/>	<input type="checkbox"/>	<input type="checkbox"/>	<input type="checkbox"/>	<input type="checkbox"/>	<input type="checkbox"/>	<input type="checkbox"/>	<input type="checkbox"/>	<input type="checkbox"/>
5	URM Infill walls	<input type="checkbox"/>	<input type="checkbox"/>	<input type="checkbox"/>	<input type="checkbox"/>	<input type="checkbox"/>	<input type="checkbox"/>	<input type="checkbox"/>	<input type="checkbox"/>	<input type="checkbox"/>
6	Pre-existing damage	<input type="checkbox"/>	<input type="checkbox"/>	<input type="checkbox"/>	<input type="checkbox"/>	<input type="checkbox"/>	<input type="checkbox"/>	<input type="checkbox"/>	<input type="checkbox"/>	<input type="checkbox"/>

Fig. 16.8. Damage classification in building components

The damage classification, in terms of grade and extension to building components, is explained in a field manual (Baggio et al., 2000), depending on building material and failure modes. For RC buildings the damage classification is summarised in Table 16.9

Table 16.9. Damage classification in RC buildings

Damage	Description
D1	Cracks up to 1.0 mm in beams and up to 0.5 mm in columns or walls, if not related to concrete crushing. Diagonal crack in external walls up to 1 mm (up to 2 mm if at the frame interface)
D2-D3	Cracks up to 4-5 mm in beams and up to 2-3 mm in columns. Imperceptible leaning. Incipient buckling of reinforcing bars and concrete cover spalling. Diagonal cracks in external walls up to few mm.
D4-D5	Collapse or inclination more than 1%. Cracks width is more than 5 mm in beams and more than 3 mm in columns. Buckling of reinforcing bars.

The suggested relationship between damage and usability is reported in Table 16.10. It is considered appropriate for every building type, as damage classification already reflects the influence of building type and failure modes.

Table 16.10. Relationship between damage and usability classification

Damage to structural components	Classification
D0, D1	Usable
D2	Usable, but also partially usable or unusable depending on damage extension
D3 or greater	Unusable
Life risk due to damage to non structural components	Classification
Low	Usable
High but can be reduced with countermeasures	Usable with short term countermeasures
High	Partially usable, unusable

16.3.2. BUILDING SAFETY EVALUATION IN JAPAN

During the inspection the following items should be analysed (BRI, 2002):

- Structural risk, including: adjacent buildings or surrounding ground failure; overall settlement; overall inclination; structural damage.
- Non- structural risk, including: object falling; object overturning.

Each item is classified as A, B or C, depending on damage and/or risk. In the following only RC buildings will be addressed. Overall inclination and overall settlement is considered as a rigid body motion due to soil or foundation damage. Structural damage is evaluated on the external vertical bearing structures (columns or walls for RC buildings) at the most damaged floor. Although usability assessment is a rough evaluation, the Japanese methodology is rather quantitative. Adjacent buildings or surroundings ground failure is classified A, B or C if not present, uncertain or present. Overall settlement is classified A, B or C, if less than 20 cm, between 20 and 100 cm, greater than 100 cm. Overall inclination is classified A, B or C if less than 1 degree, between 1 and 2 degrees or greater than 2 degrees. Structural damage is classified A, B or C, if the damage level V (or IV), defined in Table 16.11, in the most seriously damaged story, involves less than 1% (or 10%) of the columns (or wall's length), between 1 and 10% (10-20%), more than 10% (20%). Damage level III should be also analysed and if there is at least one column or wall in damage grade III the building is classified as B. If no serious damage to a column, but some to beams and/or beam-column joints is found above or below the column, one must consider it as damage to the column.

The non- structural risk is directly classified as A, B, or C on the following items: frame and glass of the window, exterior finishing material, signboard and fitting, exterior escape stair, depending on damage grade.

The building usability classification depends on the number of B and C results among all the items. It is reported in Table 16.12.

Table 16.11. Damage classification in RC columns

Damage	Description
I	Cracks invisible from a remote distance. Crack width is less than 0.2 mm.
II	Visible clear cracks on concrete surface. Crack width is about 0.2 – 1.0 mm.
III	Spalling of concrete cover. Considerably wide cracks Crack width is about 1-2 mm.
IV	Remarkable crush of concrete with exposed bars. Crack width is more than 2 mm.
V	Rebars bent, core concrete crush, visible vertical deformation of column or shear wall, visible settlement and/or inclination of floors.

Table 16.12. Relationship between damage and usability classification

At least 1 C on structural or non structural risk or at least 2 B on structural risk	Unsafe
1 B and no C on structural risk or at least 1 B on non structural risk	Limited entry
All A on structural and non structural risk	Inspected

Damage assessment is performed in a second step. It provides information about the residual strength of the building. When damage in columns or walls is classified as 0, I, II, III, IV and V, the residual strength is evaluated as 1.00, 0.95, 0.60, 0.30, 0.00 and 0.00 times the original strength. In case of columns with flexural behaviour the residual strength is 1.00, 0.95, 0.75, 0.50, 0.10 and 0.00 times the original one. The sum of the residual strength in columns and walls in the most damaged storey gives the residual strength of the building. The relationship between damage classification and seismic response, according to the Japanese standards, is highlighted in Figure 16.9.

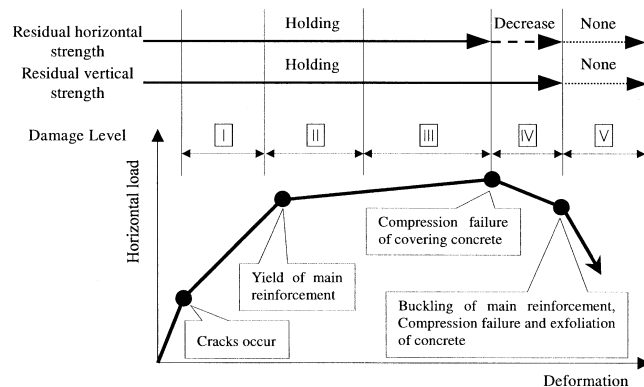


Fig. 16.9. Damage classification and seismic response (BRI, 2002) in case of member with plastic deformation capability

16.3.3. BUILDING RAPID EVALUATION IN CALIFORNIA

In ATC-20-2 (1995) it is suggested to inspectors to check the following 6 items:

- Collapse, partial collapse, or building off foundation.
- Building or story leaning.
- Racking damage to walls, other structural damage.
- Chimney, parapet, or other falling hazard.
- Ground slope movement or cracking.
- Other (specify).

Each one of these items is to be classified in relation to 3 conditions: Minor/none, Moderate or Severe. The usability classification should be based on the evaluation and team judgement. Severe conditions endangering the overall building are grounds for an UNSAFE classification. Localised Severe and overall Moderate conditions may allow a RESTRICTED USE classification. According to ATC-20 (1989), ATC-20-2 (1995) and SAP (2003), the most important unsafe conditions are summarised in Table 16.13.

Table 16.13. Unsafe conditions according to ATC-20 (1989) and SAP (2003)

System		Damage or risk
Vertical System	Load	Columns noticeably out of plumb, Buckled or failed columns, Framing separation from walls or other vertical support, Bearing wall, pilaster, or corbel cracking that jeopardizes vertical support, Other failure of vertical load-carrying element.
Lateral System	Force	Buckled, torn, or displaced diaphragm, Broken, leaning, or seriously degraded moment frames, Severely cracked shear walls, Broken or buckled frame bracing, Broken or seriously damaged diaphragms or horizontal bracing, Other failure of lateral load-carrying element or connection.
Degradation of Structural System	of	Cracking, spalling, or local crushing of concrete or masonry
Falling Hazard		Falling hazard present
Slope Foundation Distress	or	Base of building pulled apart or differentially settled, fractured foundations, walls, floors or roof, Building in zone of faulting, Suspected major slope movement, Building in danger of being impacted by sliding or falling landslide debris from upslope
Other Hazards		Spill of unknown or suspected dangerous material, Other hazards (e.g. downed power line).

16.3.4. BUILDING SAFETY EVALUATION IN GREECE

EPPO in 1997 (Dandoulaki et al., 1998) published a short booklet with instruction and basic information. In the booklet the classification reported in Table 16.14 was proposed. Due to the fact that the distinction between usable and temporarily unusable buildings is based on a very low damage threshold, a high percentage of temporarily unusable buildings is expected. This is confirmed by results of 1999 Athens earthquake safety assessment, where 55,9% of the inspected buildings were usable, 41,2% temporarily unusable and 2,9% unusable.

Table 16.14. Usability and damage relationship in Greece

Usability Classification	Indicative damage description
Usable	Fine cracks to the walls and ceiling mortar. Hairline cracks in horizontal RC structural members
Temporarily Unusable	Large patches of mortar falling off walls and ceilings. Light damage to the roof. Large cracks or failure of chimneys, gable walls, etc. Diagonal or other large cracks to bearing walls. Diagonal cracks or failure of the material in bearing walls. Cracks in structural RC members (beams, columns, shear walls), but to an extent that does not constitute a danger of collapse. Heavy damage or collapse of the roof. Slight distortion of structural elements.
Unusable	Heavy damage and distortion of structural elements. Large number of crushed structural elements and connections. Considerable dislocation of a storey and of the whole building. Bearing walls suffer dislocation or the material is crashed. Total or partial collapse.

16.4. Time and space evolution

Evolution of safety inspections depends on the number of buildings to be inspected, on availability of evaluators and on the time required for each inspection. The former variable depends on the magnitude of the event and on building density. The latter variable depends on building volume (number of stories and floor area), on building constructional type (more time is required when building components are not easily identified), on damage grade (more time is required for intermediate damage grades) and on building location (more time is required in rural areas).

Few standards include the time required to complete inspections. Japanese procedures require completing the safety inspections in a few days (3 days), but in practice the assessment usually takes one or two weeks. Generally speaking in countries where safety inspections are performed before and separately from damage assessment, as in Japan or Turkey, the time to complete safety inspections is lower than in countries, as in Italy, where safety and damage inspections are performed jointly. However, the time required to complete both safety and damage assessment is almost the same. For instance, after 1995 Kobe earthquake, emergency view assessment and reconnaissance report took 3 days, quick inspections and safety assessment 2 weeks and damage inspections 2 more weeks. The time required to complete safety inspections is significantly lower than in Italy. However the time required to complete both safety and damage inspections, was more than one month, similar to the time required after 1997 Umbria-Marche or 2002 Molise earthquake. In the comparison one should also take into account, for the Italian cases, the need of repeated inspections due to repeated shocks.

In Figure 16.10 the number of daily inspections and the cumulative values are reported as occurred in 2002 Molise earthquake ($I_0=IX$ MCS). The daily distribution shows that the mode of daily inspections occurred at the end of the second week. The maximum number of daily inspection is about 900 that corresponds to about 5% of the final inspections. This value is within the range of other Italian moderate earthquakes: 9% in Umbria Region after 1997 Umbria-Marche earthquake and 3.5% after 1998 Pollino earthquake. After one month, approximately 70% of the final number of buildings were inspected. The distribution decreases with a long tail, due to inspections in rural areas, emigrant building owners who could not come back at the time of the earthquake, and validation of the collected data that required some repeated inspections. Note also that a periodic component can be added to the above-mentioned time evolution. Figure 16.10 shows a decrease in inspections during the weekend due to the decrease in the team members involved. In Figure 16.11 the average number of daily inspections per team is reported. Apart from the early days, the team productivity has been higher during the first week. The thicker line represents the mean number of daily inspections per team up to a certain time after the event. It is a decreasing function of time ranging from 8.6 inspections/day at the beginning of the survey to 6.5 at the end of the survey. This again reflects the great difficulty in performing the very last inspections. The above values are somewhat higher than the team productivity after 2002 Etna earthquake that was about 5.5 inspections per day per team.

The mean team productivity can be used to evaluate the needed resources, in terms of evaluators, once the total number of buildings to be inspected and the total time required to complete the inspections is known. The former one can be estimated from a seismic scenario, the latter can be obtained from local authorities, civil protection or decision makers.

Buildings located in epicentral areas are usually inspected before the ones located in non-epicentral areas. This is due to the higher damage level and hence to the higher risk of partial or total collapse. It can happen, however, that building inspections proceed almost everywhere in the affected area. In the former case the inspections spread from the epicentre towards the non-epicentral areas, in the latter the completion of the inspections occurs at the same time in almost all the affected area. In both cases there is a spatial-temporal interaction during the inspections. In some countries, as in Italy, the area to be inspected is not established in advance, while in other countries, as in Japan, buildings to be inspected are selected in advance. The latter procedure is reputed more effective in terms of inspection planning, but it requires an initial not negligible effort.

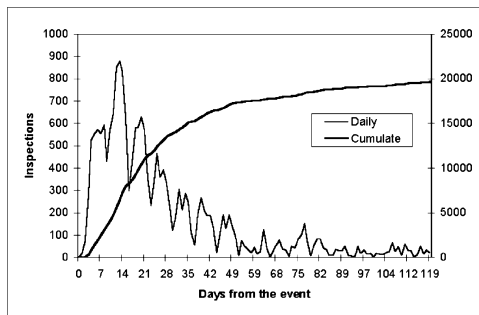


Fig. 16.10. Evolution of the inspections in 2002 Molise earthquake (only Molise Region) (Goretti and Di Pasquale, 2004)

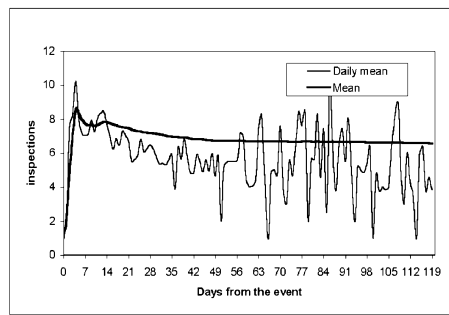


Fig. 16.11. Mean number of inspection in 2002 Molise earthquake (only Molise Region). (Goretti and Di Pasquale, 2004)

In 2002 Molise earthquake, 8500 inspector working days were required. For data computerization, 9 data entry computers and 19 people were employed daily, from November 6, 2002 to January 15, 2003. Adding the people involved in management, a total of approximately 10,000 working days is reached which corresponds to about 1 working day for every 2.3 inspected buildings.

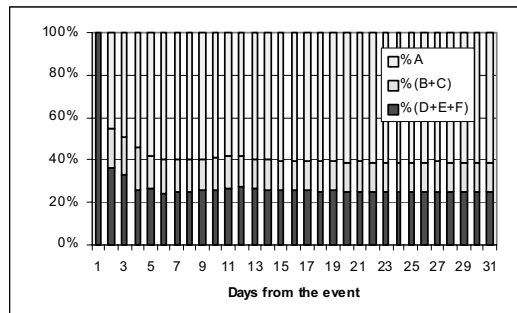


Fig. 16.12. Evolution of building immediate occupancy (2002 Molise earthquake)

The time evolution of the immediate occupancy is reported in Figure 16.12 for the whole data set of Molise buildings. Note that, after one week, the resulting percentages almost coincide with the final ones. On the first day few technicians were available. They inspected the most hazardous cases, judging them all unusable. The final

percentages (Red=Unusable To be re-inspected+Unusable for only external risk=25%; Yellow=Usable after interventions+Partially usable=15%; Green=Usable= 60%) are very similar to the ones observed after the Etna earthquake.

16.5. Procedures and forms

Due to the number of buildings to be inspected and to the number of technicians involved, the inspection management is as important as the technical judgement. It includes receiving requests from citizens, building identification, team composition, sending teams to buildings to be inspected, data collection, management of short term countermeasures, computerisation and validation of data-bases, printing of reports.

In every country local authorities are in charge of the safety assessment, according to the fact that, during the response to disaster situations, the lowest ranking level of government is always in charge. In case of destructive earthquakes, when local resources are no more sufficient, a high level management is activated, up to the State level. International intervention is not common in safety assessment, due to differences in building types, forms, language and concepts. Usually both local and global intervention is managed according to some standardized emergency management system.

In Italy, post-earthquake building inspections are performed on citizen demand, addressed to the Mayor of the Municipality. Once the different requests concerning the same building, in case of multi-owner buildings, have been grouped, requests are redirected to one of the Centres for inspection management (COM), usually located in the epicentral area. Evaluators inspect buildings, filling out appropriate forms that are delivered each day to the management Centre, where they are computerised. On this basis, the list of inspected buildings and buildings to be inspected is updated. A copy of the form is delivered also to the Municipality. By suggestion from inspectors, the Mayor of the Municipality promulgates *evacuation decrees or limited use decrees*. Countermeasures suggested by the inspectors, when inserted in the Mayoral decree, are compulsory. Usually Fire Brigades are in charge of countermeasures when public safety is involved. No posting system is adopted. In the reconstruction process, as financial contributions for the building strengthening depend on damage level, damage is assessed again, and in more detail, by professionals. Inspections on demand and the lack of a posting system are the main reasons for erroneous repeated inspections on the same building, which overload the inspection management. The inspection is generally performed outside and inside the building and it takes 20-30 minutes. The form is the same for usability and damage assessment, because the evaluation is performed at the same time. The form has 3 pages, the 4th page deals with instructions.

In Japan inspections are performed only on multi-owner buildings and, generally, only from outside. Buildings to be inspected are selected after a rapid post-earthquake building screening. Due to citizen's privacy rules, the results of usability inspections are to be considered, usually, just a suggestion. A posting system, reflecting the building usability classification, is adopted. The buildings inspected to assess usability are then inspected to assess damage. In Kobe, damage assessment has been performed sending to each inspector a map of the city containing the buildings to be inspected. The

inspectors, after completing the damage collection, deliver to the Building Research Institute the one page form, already computerised. After the damage classification, the repair, upgrade or demolishing of the damaged buildings is suggested to the owner. The suggestion, unless public safety is involved, is not compulsory for the building owners. The Japanese form for usability assessment differs from the damage evaluation form, as the evaluations are performed at different times. Each form consists of one page. Japanese standard (BRI, 2002) includes different forms for RC, steel and wooden buildings.

In California safety assessment is performed on demand, usually addressed by telephone. A quick safety assessment, called Rapid Evaluation, is at first performed, spending approximately 10 to 20 minutes per building. If access to the interior is available, and the building is safe enough, it is entered for a quick walk-through. When requested by evaluators and at discretion of Building Department, a second, detailed inspection is performed. Detailed Evaluations can take from one to four hours. Due to the huge number of buildings to be inspected, especially in highly densely populated areas, it is not always possible to proceed with the detailed evaluation. An Engineering Evaluation, where buildings are inspected using all available data to ascertain the damage, its cause, and how to repair it, is sometimes performed by architects and engineers contracted by the building owner. A 1 page form is used for the quick inspection and a 2 pages form for the detailed evaluation. The posting system is reported in Figure 16.13. As only authorized representatives of a jurisdiction can post official placards, the jurisdiction deputizes responding resources as Deputy Building Inspectors. Otherwise, jurisdiction has to send one of their inspectors who will post the official placard.

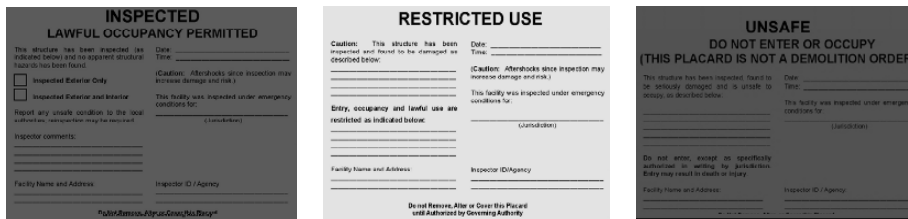


Fig. 16.13. Posting system in California (USA)

In Greece, usability assessment is performed on all the buildings located in urban centres in epicentral areas, while it is performed on citizen demand outside the urban centres or in non- epicentral areas. A posting system, similar to the Californian one, was used in the past. However, as placards were easily detached, now a green, yellow and red spray paint is used. Buildings classified as temporarily unusable and unusable are to be inspected again in more detail. The one page usability form is the same both for quick and detailed evaluation. The form is filled out in two copies, one handed to the owner of the building and the other delivered to the Engineering Department that coordinates the inspections.

In Turkey, inspections are performed by engineers employed by the Ministry of Public Works. Requests are recorded for inspection with the ombudsman teams. Placards were not used, but teams scrawl painted marks on the side of the building. For each building,

collected data are recorded on a single line of a 1 page form. School buildings usually have guards guarding them.

Information is usually recorded in appropriate forms. A complete review of forms used all over the world is beyond the scope of this chapter. An overview of forms used in the past in Italy for data collection is reported in Goretti and Di Pasquale (2002). Main differences in procedures and forms among Italy, Greece, Japan and Italy are summarised in Table 16.15 (Goretti, 2001; Goretti, 2002).

Besides procedures and forms, tools are necessary to speed up the procedures and to give immediate information on the earthquake impact. In Italy, in addition to the Handbook for COM management (National Seismic Survey and GNDT, 1998), the following tools have been developed and delivered:

- Software for the management of the inspections (National Seismic Survey, 2002).
- Software for the data computerisation and reports (National Seismic Survey, 2002).
- Software for economic loss estimate from dimensional, typological and damage data (Di Pasquale et al., 1998).

In all procedures, the judgement can be changed when effective measures have been taken to prevent collapse or other categories of danger or when the damage conditions have been changed or inspected in detail to have the original judgement changed.

Table 16.15. Forms and procedures in Italy, Greece, California, Japan and Turkey

	Usability and damage evaluation	Inspections	Results of usability inspection	Posting	Numb. of pages in the form
Italy	Simultaneous	On citizen demand	Compulsory if a Mayor decree is promulgated	No	1 form, 3 pages
Greece	Only Usability	Every building in epicentral area, on citizen demand in non epicentral area	Compulsory	Yes	1 page form, same form for quick and detailed inspection
California	Only usability	On citizen demand	Compulsory	Yes	1 page form for quick inspection, 2 pages form for detailed inspection
Japan	At different times	On previously selected buildings	Compulsory only if public safety is involved	Yes	2 forms, 1 page each
Turkey	At different times	On citizen demand			1 line

Data computerisation and validation are other important steps in inspection management. However, their analysis is beyond the scope of this book. We will just note that computerisation is crucial when buildings are inspected on request and no posting system is used, due to the fact that, in order to avoid repeated inspections on the same building, the selection of the buildings to be inspected should be done from an up-to-date building list. Validation is important when erroneous repeated inspections to the same buildings arise due to buildings with more than one entrance, to buildings with more than one request, to ineffective computerisation of the already inspected buildings, to inspections erroneously performed on dwellings instead of on buildings. Validation

takes a long time and it is usually performed with the aid of damage maps and making use, if possible, of the same inspectors used in the damage survey. Note that validation is required mainly because inspections are performed on request.

Procedures include also how to conduct inspections in order to guarantee the safety of evaluators. Here we list several suggestions taken from SAP Program (2003).

- Be aware and cautious.
- Always work in teams of at least two individuals.
- Always wear a hard hat.
- Do not enter obviously unsafe buildings, buildings located on potentially unstable slopes, buildings where falling hazards exist that can block exits, buildings leaning excessively or significantly out-of-plumb and buildings where a hazardous material spill or release has occurred.
- Be aware of hanging or exposed electrical wires.
- Visually assess from the exterior and evaluate potential for collapse.
- One member of the team remains outside while other members are inside.

Recent advances in procedures involve new technologies for computerisation and data transfer. Pre-event data-bases, palm computers, GIS systems and Satellite images are more and more used in the inspection management.

A detailed analysis of legal issue and responsibilities is beyond the scope of this book. Substantial differences are found among countries. In California any government entity that regulates building or lifeline construction and is responsible for facility safety has safety assessment responsibilities. In Italy the Mayor of the municipality is responsible for safety. In Japan the owner of the building is responsible for public safety. Evaluator's responsibility, again, differs from country to country. California Civil Code, Section 1714.5 states that "No disaster service worker who is performing disaster services ordered by lawful authority during a state of war emergency, a state of emergency, or a local emergency, ..., shall be liable for civil damages on account of personal injury to or death of any person or damage to property resulting from any act or omission in the line of duty, except one that is wilful". In other countries inspector's responsibility is not stated. As the term usable can have consequences on surveyor's responsibility, in some countries usable buildings are termed "inspected".

16.6. Statistics and predictive models

The large number of buildings to be inspected is the reason for I level accuracy data collection. Although I level data cannot be used for engineer assessment, they can be statistically processed. In Table 16.16 percentages of usability classification after recent worldwide earthquakes are reported. Usability percentages can be better related to damage and building type. Following Di Pasquale and Goretti (2001), the probability of a building to be unusable, given the suffered damage and the building constructional type, is defined as secondary vulnerability. Statistics after recent Italian earthquakes are reported in Figure 16.14, considering the damage to vertical bearing components and several building types. (Masonry MasA, B and C refers to masonry buildings of poor, medium and good quality, while RC refers to reinforced concrete structures).

Table 16.16. Results of usability classification after recent worldwide earthquakes

Earthquake	Country	Year	Number of inspected buildings	Inspected, Safe, Usable	Restricted use, Limited entry, Usable after countermeasures, Partially usable	Unusable, unsafe, to be re-inspected, unusable due to external risk
Konitsa	Greece	1996	925	59,0%	25,0%	16,0%
Athens	Greece	1999	62,650	55,9%	41,2%	2,9%
Molise	Italy	2002	20,000	60,0%	15,0%	25,0%
Etna	Italy	2002	5,065	59,4%	19,3%	21,3%
Kobe	Japan	1995	46,610	66,1%	20,0%	13,9%
Northridge	USA	1994	114,000	83,0%	27,0%	

Unusable buildings in Figure 16.14 include 100% of the buildings classified unusable, unusable due to external risk and to be re-inspected plus 50% of the buildings classified partially usable, after 1997 Umbria Marche and 1998 Pollino earthquakes.

Primary vulnerability is defined as the probability to observe a damage grade, given seismic intensity and building constructional type. Once performed the convolution between primary and secondary vulnerability, one gets the total vulnerability, which is the probability to be in an unusable state, given seismic intensity and building type. It is reported in Figure 16.15 (Goretti, 2001), when primary vulnerability is obtained from 38,000 buildings damaged by 1980 Irpinia earthquake (Braga et al., 1982).

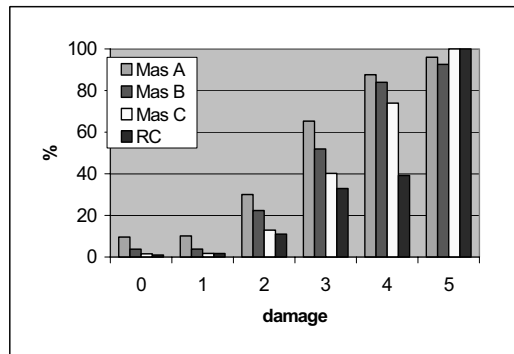


Fig. 16.14. Probability of unusability conditional upon damage to vertical components and building type (Di Pasquale and Goretti, 2001)

With few additional hypotheses it is possible to condition the building unusability on the epicentral intensity (Goretti, 2001). Assuming the probability to perceive an intensity, given an epicentral intensity, as the ratio of the area affected by that intensity and the total affected area, a uniform building density and an attenuation law of the form $I=I_0-k\log[1+(D/h)^2]^{0.5}$ with $k=4$ and $h=10$ km, one gets the total vulnerability reported in Figure 16.16. From Figure 16.15 about 65% of buildings belonging to vulnerability class A are expected to be unusable when affected by intensity $I=X$ MCS. However, only 30% of class A buildings are expected to be unusable in all the area affected by an earthquake of epicentral intensity $I_0=X$ MCS (Figure 16.16). Note also that unusability, except for class A buildings, does not vary so much with epicentral intensity. Obviously the number of buildings in the affected area will vary significantly.

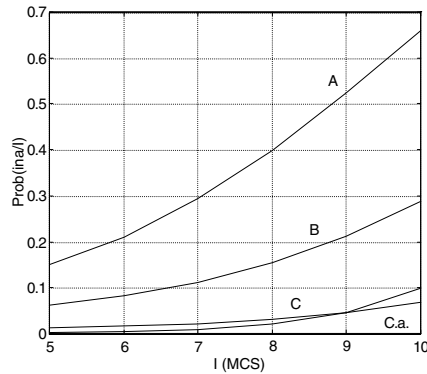


Fig. 16.15. Probability of unusability given building constructional type and felt seismic intensity, I (Goretti, 2001)

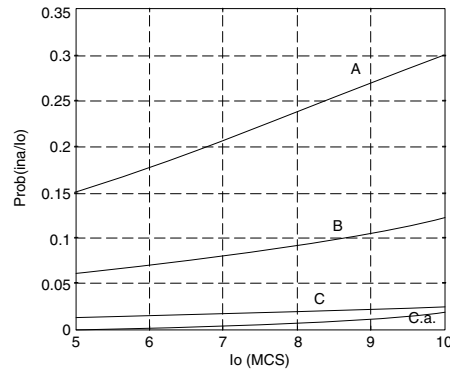


Fig. 16.16. Probability of unusability given building constructional type and epicentral intensity, I_0 (Goretti, 2001)

16.7. Special buildings

Special buildings require special procedures, instruments and technical skills to be evaluated shortly after an earthquake. Among them hospitals and historical churches represent two important cases: hospitals because of their complexity and the need of uninterrupted operating in order to assist population and churches because of their unusual structure and their religious and artistic value. Both types have social and economic importance and specific aspects have been introduced in order to assess safety in the most effective way. In the following main Italian features are summarised.

16.7.1. HOSPITALS

After the 1997 Umbria-Marche earthquake survey teams (Civil Protection, Hospital staff and University personnel) reported in detail the observed damage, the building vulnerability, the status of plant and the emergency provisions, including also plans and photographs (Biondi et al., 2000). At the same period a preliminary form to inspect the non- structural components, equipment and plan, was set up and experimented in the vulnerability census of Public Buildings in Southern Italy (GNDDT et al., 1999). After 2002 Molise earthquake specific teams used both the residential building form (in order to have a complete electronic database) and a written report addressed to the hospital direction. In recent times an effort has been made to organize in a systematic way the hospital safety inspections in cooperation with Applied Technology Council.

In Italy many hospital facilities were built prior to the adoption and enforcement of strict seismic resistant design and construction practices. In this situation a specific plan for emergency response and post-earthquake inspection has been recognized, in the "U.S.-Italy Collaborative Recommendations for Improving the Seismic Safety of Hospitals in Italy" (ATC-51, 2000), as a short term objective to reduce seismic risk. The Italian Ministry of Health recognised the importance of emergency planning in a recent guideline (Department of Civil Protection and Ministry of Health, 1998). While the mitigation of seismic structural and non-structural risk (e.g., by seismic rehabilitation or

replacement of buildings or individual components) is one of the most important, preparations in planning for earthquakes, earthquake emergency planning cannot wait until all hazards are mitigated. Improved planning for emergency response and post-earthquake inspection needs to be developed immediately and must consider the hazards and vulnerabilities that currently exist in Italian hospitals.

The topic has been addressed in a second phase of the program, the ATC-51-1 project (ATC-51-1, 2002), considering current practices for emergency response planning in the United States and available information on Italian hospitals and regulations pertaining to hospital emergency response planning in Italy. The report covers emergency management organizational structure, organization of building and system documentation and information, earthquake performance levels and scenarios, seismic vulnerability, early damage intervention, evacuation plans and routes, post-earthquake inspection, training, and mitigation of seismic hazards by upgrading structural and non-structural components or by reorganizing health systems.

Many of the above items have been addressed with the help of a Post-earthquake Inspection Notebook, derived by similar protocols adopted in California (Kaiser, 1997). The notebook is to be used by hospital technicians immediately after the earthquake. It contains all of the key information needed by inspectors in order to assess earthquake damage, including:

- Post-earthquake emergency procedures for the Hospital Engineering Department, to be coordinated with the overall hospital emergency response plan.
- Summarised information on hospital seismic vulnerability.
- Building-specific information including description of the structural components and their functions, contents, and identified deficiencies.
- Overall floor plans of the hospital, and building floor plans that point out suspected areas of particular vulnerability.
- Placards for posting in all areas of the hospital: open (green posting), restricted use (yellow posting), or closed (red posting).

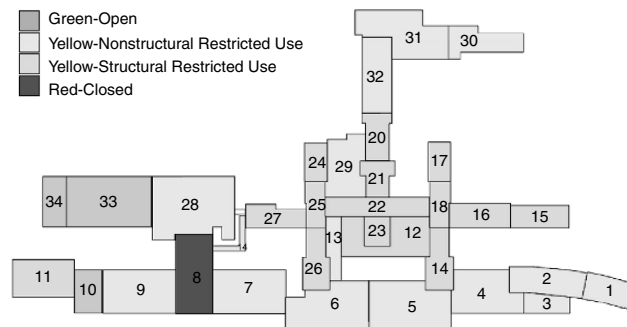


Fig. 16.17. Hospital plan showing expected performance for each building for a MCS Intensity VIII (MCS) scenario. (ATC-51-1, 2002)

The idea is to provide the maximum amount of information in normal time (location of components and systems, vulnerability, hazardous areas, essential equipments, zones of expected damage and areas expected to be damaged after the earthquake) in order to

speed up the damage recognition at the moment of the earthquake. As the official inspectors will arrive after several hours or days after the earthquake, a damage survey has to be taken, at a first stage, by internal technical teams on the basis of the above mentioned information and through direct quick recognition of the structural and non-structural components, medical equipment and plant. It is also necessary to integrate the safety procedures with the health management in emergency (Morra et al., 2002, San Mateo County EMS, 1998).

16.7.2. CHURCHES

Monuments may have unusual structural typologies that significantly differ from ordinary buildings. This is generally the case of historic churches in Italy and in many other European countries, where these constructions are an important part of the cultural heritage. Particular skill has been used in their construction, and particular skill and protocols are needed for their post-earthquake safety assessment.

In Italy the methodology for quick inspection of churches dates back to after the 1976 Friuli Earthquake (GNDT, 1994), when an extensive observation of damage suffered by churches led to identify the most frequent damage failure modes. Other studies were performed and results were later synthesized in a methodology (Lagomarsino, 1999) extensively applied in the years from 1996 to 2002. After the 1997 Umbria–Marche earthquake more than 1000 churches were surveyed in Umbria Region and the field observations led to an upgrade of the methodology (see Chapter 7).

The form used in the safety assessment of churches is more complex than the one used in building assessment. It is made up by a general identification section reporting name, age, maintenance state, localization, site and use, plus 7 specific sections devoted to:

1. Typology, description and dimensions of each structural component (roof, façade, transept, nave, chapel etc).
2. Damages to artistic contents (frescoes, paints, statues, furniture...).
3. Damage and vulnerability factors in 17 possible failure mechanisms; the damage and the vulnerability index are then computed on the basis of the number of activated mechanisms and their damage level.
4. Masonry features for each structural component, including thickness.
5. Usability assessment with five possible cases a) usable, b) usable after emergency intervention, c) partially usable, d) to be checked again, e) unusable.
6. Notes (emergency countermeasures, damage conditions, contents to be safeguarded).
7. Graphical sketches.

From the structural point of view the most interesting section is the one devoted to the description of the failure mechanisms. In the form recently adopted by the Department of Civil Protection (2001), all sections have been revised: typology and economic damage sections are placed in the first page, while vulnerability and structural damage sections are placed in a separate page, with only 11 failure mechanisms. Cost models for the church repair have been also set up.

Church evaluator teams are generally made of experts from the Ministry of Cultural Heritage and experts in seismic engineering.

16.8. Training and preparedness

The efficiency of the safety inspections rely primary on a homogeneous and non - conservative assessment. This is achieved by special training programs. One of them is the Safety Assessment Program established by OES California (SAP, 2003). It provides resources (volunteer and mutual aid) to local governments in order to perform safety assessments of buildings and infrastructures as quickly as possible in the aftermath of a disastrous event.

SAP utilizes volunteering professional structural and civil engineers, licensed architects, and mutual aid certified building inspectors. They are divided in two resource pools: Volunteers and Public Resources. The latter one is divided in Local and State government employees. Volunteers are individuals from the private sector who are registered as Disaster Service workers-Volunteers (DSW-V). They provide services without compensation for a period of 3 days. Local Government Employees (DSW-L) and State Government Employees (DSW-S) are provided to the requesting jurisdiction for a period of 3 days or more (in practice as long as needed) and are provided salary by their home jurisdiction while deployed for safety assessment, by OES of recognized training. For all of them is issued a different identification card by State OES. All of them must be deputized as Deputy Building Inspectors by the requesting jurisdiction to post official jurisdiction placards. They are reimbursed for all housing, meals, travel and other related expenses. Additionally SAP Evaluators must have general knowledge of construction, ability to inspect any framing system and rapidly identify how the system works and the corresponding load paths, professional and practical experience working with various framing systems, and ability to make a judgment of the ability of that system to withstand seismic events. It is explicitly stated that SAP Evaluators will not (i) provide cost estimates for buildings they have evaluated, (ii) perform evaluation based on code compliances and (iii) provide escort or property retrieval for owners or occupants of buildings.

OES designs and monitors the training for SAP facility Evaluators and Coordinators, registers individuals into the program, issues registration IDs for volunteers, and deploys volunteering licensed professionals and mutual aid building inspectors after disasters. In order to be registered, one is requested to complete a one-day standardised training program presented by a certified trainer. The training program is different for trainers, evaluators and for the people that will manage the inspections. In the past, identification cards expired at different intervals, now all cards expire on a 5-year cycle. Refresher courses are planned to be available on the Internet.

All volunteers and public resources must be activated by State OES through the State Operations Centre (SOC) utilizing the Incident Command System (ICS) structure of the Standardized Emergency Management System (SEMS). Field responders coordinate with the local agency to secure additional resources needed on-scene. If the request exceeds local capabilities, the requested is forwarded to the Operational Area and then to the Regional or state Operations Centre. The Statewide SAP Coordinator will facilitate the deployment of the SAP Evaluators through the appropriate professional organization Disaster Contacts. To this end, SAP includes partner organizations such as American Society of Civil Engineering, Structural Engineers Association of California, American Institute of Architects. All the partners agree to provide contacts 24 hours a

day and to deploy individuals at the request of the State OES. In addition they organize SAP Evaluator training periodically, update annually the list of registered individuals and manage the internal organizational deployment procedures.

In Greece, similarly, a training course on earthquake emergency operations for engineers working in the public sector is organised on a regular basis by the Institute of Training of the National Centre for Public Administration. The training courses takes 5 days and one is devoted to building usability assessment.

Also the Italian safety assessment training program is devoted only to engineers, architects and surveyors working in the (Local, Regional and State) public sectors. The program, organised in 2000 by the National Seismic Survey, takes 5 days and is addressed, at the same time, to evaluators and managers of inspections. A field manual is delivered to participants (Baggio et al., 2000). During the training virtual safety assessment is performed with Medea software (Zuccaro and Papa, 2002b) and virtual inspection management is performed with SET software (National Seismic Survey, 2002). An expert system on usability assessment has been published by Masiani (1999). A similar expert system called PEDAB has been delivered a few years before by Anagnostopoulos, together with a field manual (Anagnostopoulos, 1996).

In Japan, training courses on post-earthquake safety assessment (Hirosawa et al., 1995) are also organised for foreign people at International Institute of Seismology and Earthquake Engineering (ISEE).

Similarly to national training programs, local training programs have been developed all around the world, in order to have at disposal more technicians in case of emergency. Regions, Counties, Provinces, Municipalities, depending on the local administrative structure, are in charge of local training programs.

Regarding preparedness on safety assessment, the Building Occupancy Resumption Program (BORP) in San Francisco, CA, should be mentioned. The program allows San Francisco building owners to pre-certify private post-earthquake inspection of their buildings by qualified engineers upon acceptance of a written inspection program. The purpose of a pre-certified emergency inspection program is to allow a quick and thorough evaluation of possible damage to a structure by qualified persons familiar with the structural design and life-safety systems of the building. This private emergency inspection could facilitate rapid decisions regarding the closure or re-occupancy of building areas. Prearranged emergency inspection could reduce inspection delays, as City inspection personnel typically are dispatched first to areas of greatest damage or public hazard, which may not include the building in question. Building owners who wish to participate in the program should select an emergency inspection team, obtain building plans, write an inspection plan, develop building information, an evacuation plan, inspector response requirements, equipment and drawing locations and submit a written building emergency inspection program, including an inspection plan.

16.9. Short term countermeasures

Just after an earthquake short term countermeasures are needed in order to reduce risk for citizens and for the restoration of the normal everyday city life. It should be pointed

out that the organisation of the short term countermeasure and emergency technical intervention is equally important with the intervention itself and the better organised and planned the better outcome reflects during the time of the crisis. Short term countermeasures include risk elements removal, temporal support and temporal propping (Fringas and Kyriazis, 2000). Short term countermeasures depend on building constructional type, building failure modes and damage grade and extension.

Risk elements removal is required when unstable or likely-to-fall buildings or parts of buildings result in a hazard. They are mainly roof tile hanging on roof edge, decoration tiles, chimneys, glass windows, non -structural light components, balconies, architectural decoration. In case of heavy damage the whole building can be hazardous. Such buildings must be distinguished from the buildings that have to be demolished as their repair is not economically convenient. In this case there is no urgency of demolishing. The aim of the risk element removal is the fastest possible removal of risk elements which may fall down from the building facade and the securing of vehicle and pedestrian passing. The same goal is achieved by means of barriers or protected crossing. The risk element removal is classed as first priority for the main road arteries, central roads, city entrances and access to strategic buildings as Hospitals, Fire Brigade Stations, Prefectures, Schools, etc. In these cases removal should be completed within a few days after the events. Elements at risk in less important roads can be removed within a few weeks f after the event.

Temporal supports are inserted to bear the vertical loads of the damaged structure, due mainly to gravity. They are used in case of damage to vertical components (walls and columns) or to horizontal components (beams, slabs).

Temporal propping is inserted to bear the horizontal loads of the damaged structure, due mainly to strong aftershocks. They are used in case of insufficient lateral stability. Temporal supports and propping will rescue the buildings in the damaged area and reduce the collapse risk. Priority is given to strategic buildings and to a less extent to monumental historical buildings.



Fig. 16.18. Wooden propping (Etna 2002)

Fig. 16.19. Wooden protected passage (Molise 2002)

Fig. 16.20. Steel tightening of the church façade (Molise 2002)

Each one of the above countermeasures must be carried out urgently and with rough calculations, based also on the building constructional type and observed damage. There should be no intention to return to the initial safety level of the building. As pointed out in Fringas and Kyriazis (2000), *“It is certain that any kind of temporal support or*

propping after a catastrophic event is definitely more preferable than lack of such intervention”.

Temporal supports and propping have to satisfy some requirements, often contrasting: easy to be found near the affected area; easy to be assembled; low cost; durability; stiffness; easy to wedge; small size; easy to be included in the long term intervention and possibly ability to act as bilateral support. The first requirement implies using wood, in form of tree trunk or timber beams, or steel, in form of shores, industrial scaffolding and normal profiles.

Vertical loads can be supported by means of:

- Single metal column of adjustable height.
- Metal industrial scaffolding, usually to form towers with stiffening bracing. Wedging is made by special bolts at the top or bottom of the scaffolding.
- Steel sections, as normal profiles, at the sides of damaged columns.
- Tightening, with angular elements at the column corners, connected with welded transverse elements, once preheated or tightened together with bolt and wires.
- Timber beams in case of small loads. Sometimes they can be assembled in the form of a tower. Wedging is made with triangular wooden wedges. Tree trunks can be used if straight, in one piece, with constant diameter, without nodes and obtained from hard and healthy timber such as beech and oak.

Horizontal loads can be supported by means of:

- Single raking shores, of timber or metal sections. In case of a long raker, braces should be introduced in order to reduce slenderness. Rakers should be placed at floor levels. In order to avoid horizontal sliding, sufficient anchorage should be achieved in the ground. Possibly connect the vertical part of the shore to the building in order to prevent relative sliding.
- Diagonal braces inside the structural frames, of timber or metal sections. They are constructed with rectangular additional frames, stiffened by diagonal braces, placed preferably at the building perimeter and symmetrically. In comparison with single raking shores, it saves space outside the damaged building.
- “Flying” shore, when limitation of space does not permit inserting a single raking shore. They are inserted typically between two buildings at a given height in order to allow a clear passage of personnel or vehicles. In case of long distances, vertical and diagonal braces are inserted to reduce slenderness.
- Tension rods and rings. To connect orthogonal walls and transfer forces perpendicular to the wall to walls parallel to the force.

In general propping should be applied at a small distance away from the damaged elements. Wedging of the propping is also an essential ingredient, due to the dynamic building behaviour in case of aftershocks. Propping to more than one floor is recommended but it is costly and time consuming. When the final repair or strengthening takes place, it can be difficult to intervene due to the presence of the propping. However, their removal prior to the intervention should be adequately investigated.

Statistics concerning short term countermeasures after 2002 Molise earthquake, initially presented in Galanti et al. (2004a), are reported in the following. Figure 16.21 highlights

the percentage of different types of short term countermeasures. The term “Other” has to be considered mainly as temporal propping or support, as they were not included in the form. Percentages sum up to 42.5%. However in the same buildings more than one type of countermeasure can be present. Figure 16.22 illustrates the number of buildings with countermeasure in relation to the usability classification. A stands for usable, B usable after countermeasures, C partially usable, D to be re-inspected, E unusable and F unusable only for external risk. It can be seen that most countermeasures can be ascribed to buildings usable after countermeasures (B) and unusable (E). The high number of countermeasures in usable buildings (A) is not compatible with the concept of usable building. They refer to small importance countermeasures that do not require the building to be classified as restricted use, questioning the limit of intervention in case of usable building and restricted use building.

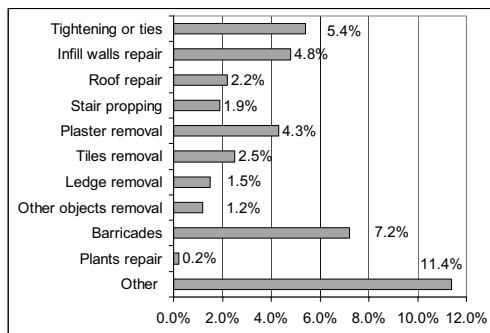


Fig. 16.21. Short term countermeasures as percentage of total inspected buildings after 2002 Molise earthquake

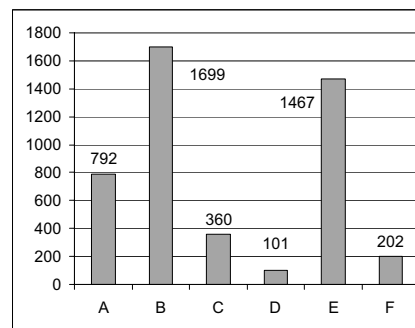


Fig. 16.22. Number of buildings with short term countermeasures versus usability classification after 2002 Molise earthquake

Finally it should be pointed out that, due to the huge number of buildings involved and to the urgency of the countermeasures, the organisation of short term countermeasures and emergency technical intervention is equally important with the intervention itself and the better organised and planned, the better outcome will be reflected during the time of the crisis.

Acknowledgements

We are grateful to Miranda Dandoulaki (Greece), Polat Gulkan (Turkey), Mizuo Inukai (Japan) and Michael Sabbaghian (California) for the information they provided on concepts, methodologies, procedures and forms used in their respective countries in the field of post-earthquake safety assessment. Without their invaluable contribution this chapter would not have been possible.

PART IV: MANAGING EARTHQUAKE RISK

CHAPTER 17 CIVIL PROTECTION MANAGEMENT

E. Galanti¹ A. Goretti¹, B. Foster² and G. Di Pasquale¹

1. *Civil Protection Department - USSN, Rome, Italy*

2. *Foster & Associates, California, USA*

17.1. Introduction

The suddenness of an earthquake and its devastating impact on the victims preclude the improvisation of relief more than any other kind of disaster. It is therefore necessary to prepare the earthquake response in advance, taking into account the probability of occurrence, and, operating to safeguard life and property immediately following the event. Afterwards, recovery operations should be extended to ensure a speedy return to normal life.

Earthquakes in some regions have the potential to cause widespread destruction, so it would be impossible to address the event with only the resources of the stricken region. Consequently, a tiered response is often implemented, whereby all of a country's resources are available to assist those impacted, from local, to regional, to national government levels.

Public authorities in seismic-prone states are typically responsible for assessing and mitigating public earthquake hazards, protecting public safety, and coordinating emergency response and reconstruction. In order to optimise the user of available funds, personnel and equipment, a standardized emergency response structure is usually employed by all public and private sector groups. Such an organizational approach promotes integration and coordination within and between all response groups and is of particular importance when the size of the disaster grows, in terms of victims, damages, and impact areas.

Responding to earthquakes can be a very difficult task if nothing has been done to prepare for such events in advance. Therefore, preventive and preparedness actions should be carried out to reduce risks and facilitate emergency response. In addition to implementing measures to protect life and property, preparedness measures should be taken to provide social and psychological support to the impacted population, including those who have been displaced from their homes and need to be comforted, reassured and sheltered.

Procedures should also be developed to ensure that objective, clear, timely and accurate information concerning the event is provided by official announcements and press conferences.

Finally, preparedness measures should also address the conditions necessary for the transition from emergency response to the subsequent phase in which normal activities of daily living are restored through recovery and reconstruction. This phase generally is not simply a return to past conditions, it is a long term phase in which the likelihood of damage and discomfort from future earthquakes is reduced through upgrades to previous land use policies, building codes, and similar matters.

Emergency response, as well as reconstruction, is generally the responsibility of public authorities.

In most States, authority is delegated to various levels - local, provincial, regional and State authorities - each assuming a share of responsibility proportionate to its political responsibility and economic and financial resources. Consequently, obligations should be similarly apportioned in the event of a disaster. The way in which task and responsibility should be shared between the various authorities cannot be fixed by a general all-embracing formula. However some fundamental principles can be highlighted.

As a matter of fact, emergency management has been performed for many years (in some States for centuries), both by government and private agencies, but only recently the concept of managing emergencies has been developed, which has led to Comprehensive Emergency Management (CEM).

The goal of Emergency Management is to coordinate a unified response to a crisis; to prevent or minimise the threat when possible; and to respond quickly and effectively when prevention is not possible. This is based upon three interrelated components:

- Capacity to be used for all types of hazards : Many types of man - made and natural disasters have similarities between them, so many of the same management strategies can apply to all such emergencies.
- An emergency management partnership : The disaster management burden, and the associated resources, require a close working partnership among all levels of government and the private sector.
- An emergency lifecycle (Figure 17.1) : Disasters do not just suddenly occur. Disasters exist throughout time and they have a lifecycle of occurrence which must be matched by a series of management phases. These phases include strategies to mitigate hazards, prepare for, respond to, and recover from the effects of the emergencies.

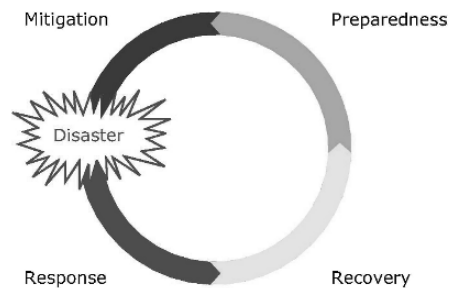


Fig. 17.1. The emergency cycle

Realising that disasters exist throughout time, leads to organising emergency management in parallel with the disaster life cycle: foreseeing a series of phases that include strategies to mitigate the hazards, prepare for and respond to emergencies and finally to recover from their effects. These phases are integrated with each other, hence, the Emergency Management Cycle is an open ended process. The four phases

comprising the cycle begin and end with mitigation, the on-going attempt to limit or prohibit the effects of a disaster. Often the four phases are grouped as before, during and after the earthquake, with the former including mitigation and preparedness, the second addressing response, and the latter, recovery.

Mitigation refers to activities which actually eliminate or reduce the chance of occurrence or the effects of a disaster, either natural or man made, through some instruments such as: Building and Safety Codes, Disaster Insurance, Land Use Management, Monitoring / Inspection, Public Education, Research, Risk Mapping, Statutes / Ordinances, Tax Incentives, and Tax Disincentives.

Preparedness is planning how to respond in case an emergency or disaster occurs and working to increase the resources available to wage an effective response effort. Emergency preparedness involves activities like: developing emergency policies, plans and procedures; conducting and evaluating drills and exercises; and providing training and public education.

Response activities occur during and immediately following a disaster. The goal of the responder is to save lives, minimise property damage and facilitate the beginning of recovery from the incident. Police, fire and rescue services are the primary responders during the response phase.

Recovery is the final phase of the emergency management cycle, which continues until all systems return to normal, or near normal. Short-term recovery returns vital life support systems to minimum operating standards. Long-term recovery from a disaster may go on for years, until the entire disaster area is completely redeveloped, eventually improving upon past conditions. Short term recovery activities include: Damage Assessment, Debris Removal, Disaster Assistance Centres, Crisis Counselling, and Long-Term Care/Unmet Needs. Long term recovery comprises rebuilding and upgrading and is generally an activity carried out by local authorities under the local Building Department.

17.2. Civil protection organization

The first step in emergency management planning is to establish which agency or discipline will have the task of providing protection after a disaster, usually called Civil Protection Service. The organisation of a specialised service of this kind can be conceived in accordance with different guiding principles and within different administrative framework; in (Unesco, 1978) three different alternatives are proposed.

- The protection of the population is entrusted to a special functional ministry, similar to the other ministries. It allows the Minister of Civil Protection to have very wide administrative and operational functions, but is a costly solution that absorbs large numbers of personnel.
- Civil Protection Service is attached to the Prime Minister's Office. Civil Protection retains some advantages of a normal Ministry, but, in addition, Prime Ministry confers executive power on Civil Protection and gives its decisions an authority which reduces possible objections or protests on the part of ministerial services.

- Civil Protection Service is attached to a Ministry Office. Several choices are possible for the Ministry, as several are called on to participate in civil protection action: Public Works, Public Health, Economy and Finance, Defence, Interior. In any case, Civil Protection runs the risk of seeing its essential functions subordinated to the technical functions of the ministry concerned. If Civil Protection is made an integral part of a Ministry, the best choice is probably in favour of the Ministry of Interiors, as it will have the most authority for action, particularly when obtaining the co-operation of other ministries.

The experience gained by various nations which have already established cohesive Civil Protection Services indicate that Civil Protection machinery should consist of a national headquarters and area offices for the different provinces, districts and other territorial divisions. These services must be established on a permanent footing.

Following the emergency management cycle, three sectors are essential: Prevention, Operations, and Reconstruction. The importance attached to each of these functions depends on whether the functions of the Civil Protection are conceived in a broad or restrictive manner.

If Civil Protection is restrictively conceived, studies and research in support of Prevention are left to external technical bodies. In this case, Civil Protection should be able to individuate the need for these studies and translate them into operative instruments, like: guidelines, procedures, regulations, predictive models, organizational schemes and so on.

The competence of Civil Protection in reconstruction is usually limited to the relief measures implemented during the initial stage of reconstruction: organising rest centres and temporary shelters, distributing meals, transporting families being accommodated by relatives and friends, recovering valuable personal goods from the ruins, organising centres for tracing missing persons, and performing damage surveys. Other aspects of reconstruction are normally managed by pre-existing services, which deal with them during non-emergency periods.

The Operations function fulfils the essential mission of a Civil Protection Service, the one which it will always have even if Preventive Action and Reconstruction are taken completely out of its hands. The main responsibilities of the Operations function are to:

- Monitor status of the situation and its evolution.
- Maintain order in the stricken zone, to prevent panic and repress looting;
- Rescue victims and administer first aid to the injured.
- Limit the disaster's consequences.
- Provide food and shelter for a prescribed period of time for homeless persons.
- Arrange transport facilities.
- Continue the most urgent work required to restore communication, lifelines and sanitary systems.

The above tasks can be divided into a number of services, different from one State to another. One possibility is to arrange the tasks among six services: 1) Liaison-Transmission; 2) Police-Information; 3) Rescue-Relief; 4) Medical; 5) Welfare-Temporary Shelter; and 6) Transportation-Public Works.

Time is a key factor in emergency management, so every effort has to be made to operate as quickly and efficiently as possible, in order to limit the number of victims and to prevent further damage. To this end, the organisation of relief must be planned in advance, with activities organised following pre-established protocols and field operations properly coordinated. The following rules are key for the successful operation of civil protection:

- Unified command.
- Ongoing exchange of information between central and peripheral systems.
- Rational use of available human and material resources.
- Tasks assigned to the fewest number of operational services needed.
- Personnel pre-assigned to each service according to their respective skills.

The organisation of Civil Protection Service must have sound legal backing, with its structure and its operation based on a law and its attendant regulations. The study, drafting and distribution of legislative and/or administrative texts, such as laws, regulations, decrees, orders, instructions, and circular letters, is another important sector function of Civil Protection, in order to establish the organisation of relief at various government levels, and to define required preventive actions.

In the following section, the Californian and Italian emergency management systems are presented. Emergency management during the 2002 Molise earthquake in Italy is then discussed.

17.3. SEMS, California

The Standardized Emergency Management System, commonly referred to as SEMS, establishes and standardizes the principles and methods employed for emergency response in California. Public agencies are required to use SEMS when responding to multi-agency and multi-jurisdictional emergencies in California and is intended to facilitate and improve:

- Communications and the flow of information within and between the operational levels of the system.
- Coordination among all responding agencies.
- The mobilisation, deployment, utilisation, tracking, and demobilisation of resources.

The use of SEMS greatly enhances intelligence gathering and sharing capabilities and ensures that requests for mutual aid, and the sharing of damage assessment and situation status information is accomplished in a timely fashion.

SEMS consists of five organisational levels, which are activated as required by the scope of the emergency: 1) Field Response, 2) Local Government, 3) Operational Area, 4) Regional, and 5) State. The Regional and State levels are under the jurisdiction of the Governor's Office of Emergency Services, also known as State OES.

Under SEMS, all jurisdictions within the geographical boundaries of a county are considered a single Operational Area organisation during declared emergencies. The Operational Area is not a formal political subdivision of the State, rather, a special

purpose organisation created to accomplish specific tasks during times of emergency. In accordance with SEMS regulations, County governments serve as the lead agency in the development and operation of each Operational Area. The Local Government level is comprised of the political subdivisions within the boundary of a county, including municipalities and special districts (e.g., water, sanitary, school). Each of these entities is responsible to carry out its defined functions within its respective jurisdictional boundaries. The Field Response level is comprised of first line responders, including law enforcement, fire and rescue, emergency medical services, public works, and similar personnel representing their respective agencies.

SEMS requires the standardization of management methods at all levels of operations. The Incident Command System (ICS) is used by all Field Response level personnel, while Local Government, Operational Area, Regional and State levels use either ICS or a Multi- Agency Coordination System (MACS) in their emergency management environment, which is usually an Emergency Operations Centre (EOC). ICS provides standardised procedures and terminology, a unified command structure, a manageable span-of-control, and an action planning process which identifies overall incident response strategies and specific tactical actions.

An appropriate training course meets and maintains competencies of a specific target audience, including:

Orientation (All Employees):

- Field Course (Field Responders).
- Emergency Operations Centre (pre-assigned EOC Staff).
- Executive Course (Senior Administrators).

Every incident or event has certain major management activities or functions that must be performed. Even if the event is small, and only one or two people are involved, these activities will still apply to some degree. Five major management functions are the foundation upon which the ICS organisation develops. For small incidents, these major functions may be managed by one person, the Incident Commander (IC). Larger incidents usually require the five management functions to be set up as separate Sections within the organisation, as shown in Figure 17.2.

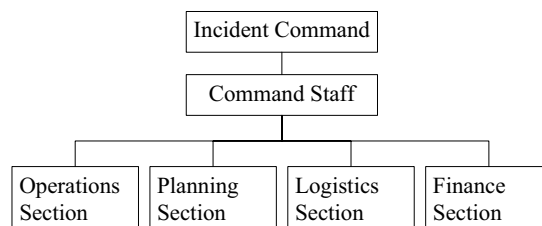


Fig. 17.2. ICS Sections and organisation

Each of the five primary ICS Sections may include sub-functions, termed Branches or Divisions, as needed. For example, the Operations Section may include Law Enforcement, Fire and Rescue, and Public Works Branches. The ICS organisation has the capability to expand or contract to meet the needs of the incident. Thus, organisational flexibility is obtained by activating only the branches that are needed.

A basic ICS operating guideline is that the person at the top of the organisation is responsible until the authority is delegated to another person. Thus, on smaller incidents, where additional personnel are not required, the Incident Commander directly manages all aspects of the incident organisation.

The five primary SEMS functions are performed in:

- Emergency Operations Centre (EOC): A location from which centralised emergency management is performed. EOC facilities are found at the Local Government, Operational Area, Regional, and State levels.
- Department Operations Centre (DOC): A location from which a specific department within a municipality, special district, county, regional or state agency coordinates its emergency activities and reports its status information to the central EOC. DOC facilities are found at the Local Government, Operational Area, Regional and State levels.

In Table 17.1 operations are grouped according to activities and location (Field, EOC or DOC).

Table 17.1. Operations grouped per activity and location

Activities	FIELD	EOC	DOC
COMMAND (Field) MANAGEMENT (EOC)	Sets objectives and priorities and has overall responsibility at the scene for the incident	Overall responsibility for establishing and implementing jurisdiction-wide policy and response strategy	Implements jurisdiction policy Established by the EOC and manages all departmental activities
OPERATIONS	Directs the tactical response of all operations at the scene of the incident	Coordinates all jurisdiction operations in support of response activities	Coordinates all department operations in support of the incident
PLANNING	Collects, processes and documents information for use at the scene of the incident	Collects, analyses, processes and documents jurisdiction-wide information; develops the action plan; maintains resource status	Collects, analyses, processes, documents and submits department information to the EOC
LOGISTICS	Provides services, personnel and equipment required at the scene of the incident	Provides services, personnel, equipment and facilities in support of all jurisdictional operations	Provides department services, personnel, equipment, and facilities as assigned or as directed by the EOC
FINANCE & ADMINISTRATION	Provides financial accounting and cost control at incident site	Overall responsibility for fiscal accounting, compensation and claims, and for jurisdiction's disaster survey report	Monitors and summarizes department costs related to incident

17.4. Augustus method, Italy

The Italian National Service of Civil Protection was created in 1992, but the emergency response as a contribution of a series of services coming from different local and State organizations dates back to the 1980's. The Parliament entrusted to the Civil Protection

Department (DPC) the development and implementation of a national program of disaster preparedness and response, giving to it the role of coordinating a number of public and private entities cooperating in the emergency response phase. Since 2001 DPC is headed by a chief reporting to the Prime Minister, who has the highest power in terms of policy and coordination in the Civil Protection Field.

The Civil Protection activities are: 1) risk assessment, 2) risk prevention/reduction, 3) response activities, and 4) recovery. From the scientific and technical side the DPC is supported by a National Commission for High Risks, subdivided into eight sections (Earthquakes, Volcanoes, Nuclear, ...), and by National Research Groups. Recently DPC funded a specific Research Centre for Seismic Engineering and a network of university laboratories working in the same field (RELUIS).

In the emergency management, three event levels are considered:

- a) Events (man made or natural), that can be managed by the responsible administration.
- b) Events that require the coordinated intervention of several administrations each responsible for a specific aspect.
- c) Events that require extraordinary means and powers.

When an event of level c) occurs, the Ministry Council declares a “state of emergency”, giving to the Prime Minister the power to issue special Ordinances to manage the disaster.

To explain how the Civil Protection System works it is necessary to summarize briefly the Italian administrative structure. Italy is divided into 20 administrative regions, each of which is divided into provinces. Each of the 104 provinces consists of numerous municipalities. Regions are responsible for adopting regulations consistent with national laws and guidelines, to ensure that civil protection activities are implemented at the local government (e.g., province and municipality level). Each province has a designated prefect who represents the national government and is responsible for disaster planning, response, and recovery for the province and the included municipalities.

Italy's emergency management organisation (EMO) includes three levels of response, depending on the impact of the disaster and on the capacity of the impacted jurisdiction to manage it: 1) municipal, 2) regional/provincial, and 3) national. During a disaster, the mayor serves as the municipal civil protection authority responsible for direction and coordination of local emergency response. An Operative Centre (Centro Operativo Comunale: COC) may be established in each affected town to direct local response activities and to serve as a central point of coordination and communication with other towns and higher levels of the emergency management organisation.

When the impact of the event cannot be managed by town resources alone, the mayor requests assistance from the prefect who declares a local emergency, and serves as the delegate of the Cabinet President or Minister of Civil Protection. A Mixed Operative Centre (Centro Operativo Misto: COM) is established to direct emergency response activities within the province and to provide a central point of coordination and communication with the DPC at the national level.

The emergency management approach employed by DPC establishes, according to the Augustus method (Galanti, 1997), 14 support functions within the COM and nine within the COC. The functions required to activate the immediate response to the emergency are activated first, while the remaining functions are activated later, when conditions warrant and personnel are available to staff each function.

Only those support functions required to address the specific emergency situation are activated in the COM and COC. The organisation may be expanded or contracted, based on the extent of the event. In addition, one person may be assigned to manage more than one function when a limited number of trained personnel are available.

Voluntary Organisations are an integral part of the EMO at every level of response. Since 1991 it is required, in the regional disaster planning and response regulations, to address the activation and deployment of recognised voluntary associations. These voluntary associations are typically connected to local civil protection offices, and employers are reimbursed for the time employees take off from work to volunteer during declared disasters.

Volunteers are divided into four categories:

- Research groups, including the Rescue Dogs Training Society.
- Technical rescue groups, such as the National Corps of Mountain and Speleological Rescue and Volunteer Fire Departments.
- Medical rescue groups, including the Red Cross and Misericordie.
- Technical logistics function groups, such as the Radio Emergency Group.

For events in which more than one COM is activated in the same Province, the COMs are coordinated by one Rescue Coordination Centre (Centro Coordinamento Soccorsi: CCS) at the Provincial level. CCS is where the intervention strategy is established, while in the COMs and COCs the strategy is implemented, depending on the field situation. For instance, CCS selects the location where the various COMs will be activated.

Table 17.2. COM & COC Functions

COM	COC	Functions
1	1	Technical and Planning Support
2	2	Health and Social Assistance, Veterinary Assistance
3		Mass Media and Information
4	3	Volunteers
5	4	Materials and Resources (Logistics)
6		Transportation and Traffic Control
7	5	Telecommunications
8	6	Lifelines and Schools Assistance
9	7	Damage Assessment
10		Search and Rescue
11		Assistance to Local Authorities
12		Dangerous Materials
13	8	Population Logistics
14	9	Operational Coordination

At the national level, an Emergency Coordination Room (EMERCOM) serves as a central location where representatives from all public and private entities involved in the emergency response are present to share information and coordinate response and recovery efforts.

17.5. Molise 2002 earthquake

The Molise earthquake received widespread attention within Italy (Galanti et al., 2004) and abroad (Foster and Kodama, 2004) because of its devastating impact on the residents and on the economy of the sparsely populated regions of Molise and Puglia. Overall, 91 municipalities requested government assistance, including 65 in the province of Campobasso and 26 in the province of Foggia. The most extensive damage occurred in the village of San Giuliano di Puglia, where 27 children and one teacher were killed in a collapse of the primary school and the entire town had to be relocated.

The Molise earthquake sequence began at 11:32 on October 31, 2002, with an Mw 5.7 shock. The earthquake affected a population of 370,000. The extent of damage varied among the impacted municipalities, with most structural damages, all 30 fatalities, and 61 of the total 173 serious injuries sustained immediately following the initial shock in the small village of San Giuliano di Puglia (population 1,163). In addition to the deaths in the collapsed school, two elderly women were killed in building collapses a few blocks from the school.

At 16:08 on November 1, an Mw 5.7 aftershock significantly worsened existing damage, causing several already weakened structures to collapse. In San Giuliano, the aftershock threatened rescuers and resulted in the mayor ordering the evacuation and closure of the entire town. The November 1st aftershock, together with the fear of further aftershocks, more than tripled the number of displaced persons needing emergency shelter. The number of shelter seekers increased from an estimated 1,100 on October 31, to 3,325 on November 1 and rose to almost 12,000 by the end of the first week. Emergency shelter operations continued for more than ten weeks, with the last shelter closing on January 15, 2003 (DPC, 2002).

The earthquake struck an area not previously classified as a seismic zone, with intensities of I=VIII-IX MCS (Figure 17.3.) felt in San Giuliano di Puglia. The towns surrounding San Giuliano di Puglia also suffered varying degrees of damage, with lower felt intensities, no fatalities, and relatively few injuries. Historic and culturally significant structures also suffered substantial damage throughout the affected region.

The emergency response phase began immediately following the initial Mw 5.7 shock on October 31 and continued for nearly three months, when the primary COM was deactivated on January 24, 2003. In addition to the Mw 5.7 aftershock, around 200 smaller shocks (M 2.5 to 3.5) occurred over the first 60 hours following the initial event (DPC, 2002). As a result, rescue operations and damage inspections were interrupted. Continuing aftershocks over the next several months required re-inspection of many structures, and many of the displaced were prevented from returning to damaged homes.

As is often the case following an earthquake, response to the event was both planned and emergent. Automatic response protocols were implemented by DPC and essential

service personnel were assigned at every level of the emergency organisation. Ambulances were dispatched to the affected area and local hospitals prepared to receive the injured. Fire Brigades initiated search and rescue and emergency shoring operations, State Police secured access into the impact area for emergency vehicles, and municipal technicians began damage inspections. At the collapsed primary school in San Giuliano di Puglia, bystanders dug through the rubble by hand, searching for survivors until the Fire Brigade and canine search and rescue teams arrived.

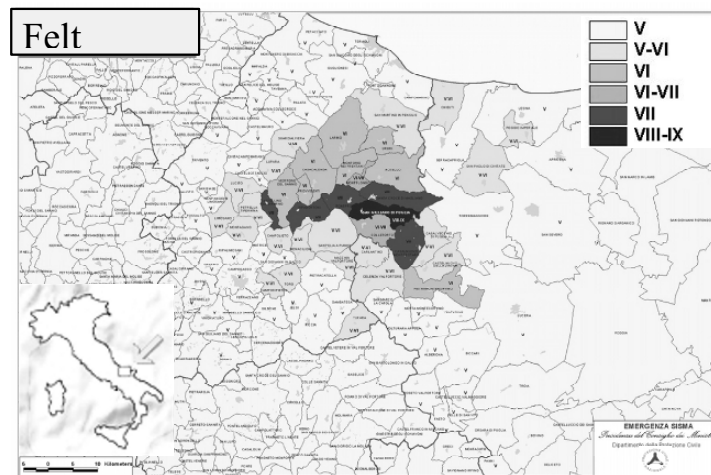


Fig. 17.3. 2002 Molise earthquake felt intensities (MCS scale)

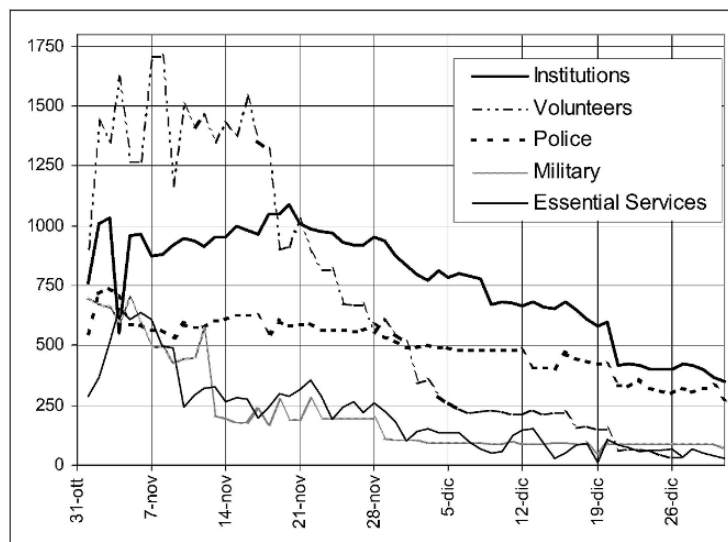


Fig. 17.4. Timing of personnel during Molise 2002 relief (Institutions: Civil Protection Department, Ministry of Interiors, Red Cross, Molise Region, Campobasso Province; Volunteers; Police: Police, Carabinieri, Custom Services, Foresters; Military: Army, Navy, Air Force; Essential Services: Electricity, Water, Telecommunications, Road)

While the closest emergency response agencies responded initially, the Minister of Interior directed teams outside the affected regions to respond on November 1 (DPC, 2002). An estimated 3,100 emergency responders and volunteers were available in the affected areas within 24 hours of the event. The total number of response personnel peaked at almost 5,000 between the first and second weeks (Figure 17.4), and gradually declined thereafter (DPC, 2002).

Response agencies included military personnel (Army, Air Force and Naval Force) who distributed emergency supply containers and pharmaceuticals, provided generators, lighting towers, and heavy machinery, and assisted the Italian Red Cross in setting up outdoor emergency shelters. Police agencies (Carabinieri, Police and Customer Services) provided traffic and access control and escorted heavy equipment into impacted towns. Rangers from the Corpo Forestale Italiano assisted police agencies and road maintenance technicians (Ente Nazionale Strade - ANAS), inspected roads, and bridges. The Italian Red Cross established and managed emergency shelters and a field hospital. Voluntaries Misericordie provided advanced mobile medical units, and amateur radio operators provided supplemental communications.

Emergency supplies and equipment were immediately available from stockpiles maintained throughout the country by the Interior Ministry. Chemical toilets, portable showers, and heavy equipment were provided by private firms under contract to the DPC, and private trucking companies assisted government agencies in transporting material resources to the impacted towns.

Within five hours of the earthquake, staff from the national DPC office in Rome (270 km away) arrived in Molise and activated the primary COM at a pre-designated location in Larino, the northern municipality where I=VI MCS intensities were felt (Figure 17.3.). The national DPC Chief of Volunteers and International Liaison became the designated Chief of this COM, which also served as the COC for the town of Larino. A second COM was established in Molise in a gymnasium on the outskirts of San Giuliano di Puglia to support intensive response and recovery operations in that extensively damaged town. This COM also provided logistical support to four nearby towns and served as the COC for the town of San Giuliano.

A local emergency was declared in the two impacted regions by the DPC Chief on November 1 and was ratified by Law 245 on November 4. One week following the initial earthquake, a COM was activated at Casalnuovo Monterotaro to provide logistical support to the impacted towns in Puglia. By November 12, a total of nine COCs were activated in towns with significant damage and emergency shelters. In addition to the COCs in Larino and San Giuliano, COCs were established in Bonefro, Casacalenda, Colletorto, Ripabottoni, Provvidenti, San Martino di Pensilis, and Toro, where each mayor served as the COC Chief. Upon activation, the Larino COM implemented initial support functions, including Technical and Planning Support (F-1), Health and Social Assistance (F-2) and Damage Assessment (F-9). Consistent with the Augustus Method of emergency management, additional support functions were activated over the first few days and, in addition to the 14 pre-designated support functions, a Cultural/Historical function was established to oversee inspection and restoration of damage to churches and monuments. Limited support functions were implemented in the COCs, based on the needs of each affected town.

The need to sustain emergency management operations on a 24-hour basis for almost three months would challenge any emergency management organisation. In this case, a dearth of local emergency management expertise increased the reliance on national DPC staff based in Rome, a three-hour drive from the impact area. Consequently, DPC staff assigned to the COMs and COCs worked extended hours for several days and stayed in local hotels. Over the prolonged emergency response phase, long work hours and separation from homes and families, added to the challenges confronting emergency managers.

Immediately following the main shock, local technicians conducted initial safety inspections to determine the scope and extent of damage. Requests for assessment of damaged structures were made by residents through the mayor to the local technical office (local building department), which referred those structures requiring a rapid inspection to the COM. It quickly became apparent that responding to individual resident requests was an inefficient approach to inspections and an exhaustive survey was performed in the epicentral area.

Damage is divided into five degrees of severity and those structures that are considered uninhabitable for any reason are termed "unusable". The mayor orders evacuation or limited use of damaged structures, based on a recommendation from technicians or engineers. An estimated 23,000 requests for structural damage inspections were received by the Larino COM. Fourteen percent of the total number of public buildings and 23% of private buildings were determined to be inaccessible immediately following the earthquake (Table 17.3). Another 5% required re-inspection before accessibility could be determined. Inaccessibility was due either to direct damage or to risk of collapse from an adjacent structure (Goretti and Di Pasquale, 2004). Although some of the displaced stayed with family or friends outside the impact area, the majority was housed in local emergency shelters.

Table 17.3. Percent of damaged public and private structures

Category	A	B	C	D	E	F
Public	65%	15%	3%	3%	13%	1%
Private	60%	11%	4%	2%	20%	3%

A=Safe and habitable, B=Partially or totally uninhabitable, but habitable with limited counter measures, C=Partially habitable, D=To be re-inspected, E=Unsafe uninhabitable to be demolished, F=Unsafe uninhabitable due to risk of collapse of adjacent structure(s).

For inspections managed at the Larino COM (Molise Region), the inspection timing is reported in Figure 17.5. After 4 months (120 days) from the event, almost 20,000 buildings were inspected. Inspection requests and building inspections started to slow down after 3-4 weeks. The timing of the inspected buildings reflects the request timing, similarly the timing of the unusable buildings reflects the inspection timing. Repeated requests and repeated inspections of the same buildings are not considered in Figure 17.5. As shown in another chapter of this book (see Chapter 16), the mode of daily inspections occurred at the end of the second week. The inspection timing showed a long tail, due to inspections in rural areas, to emigrant building owners that could not come back at the time of the earthquake, and to the validation of the collected data that required some inspections to be repeated. The average number of daily inspections per team turned out to be 8.6 inspections/day at the beginning of the survey and 6.5 at the

end of the survey. This again reflects the great difficulty in performing the final inspections.

All schools in the Region were closed following the earthquake for damage inspections and seismic evaluations, and remained closed for more than two weeks. Of the schools evaluated, 80% were found to have little or no damage. Requested temporary classrooms in each municipality are reported in Table 17.4, together with the requested temporary residences for homeless.

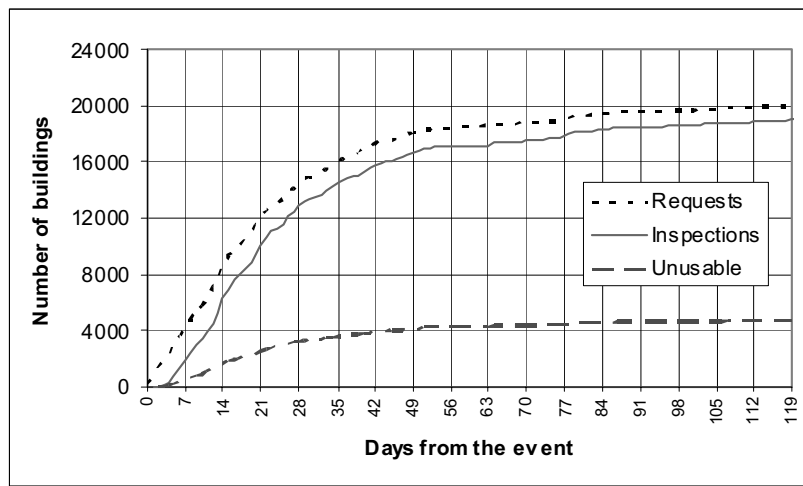


Fig. 17.5. Number of requests for inspections, inspections and unusable buildings at Larino COM for residential and public buildings (Molise Region)

Table 17.4. Requested temporary residences and classrooms per Municipality

Municipality	Requested residences	Requested classrooms	Municipality	Requested residences	Requested classrooms
Boiano		14	Montecilfone	2	
Bonefro	173	21	Montorio Nei Frentani	3	
Campodipietra	5	16	Morrone Del Sannio	8	
Campolieto	7		Pietracatella		4
Casacalenda	77	20	Provvidenti	8	
Castellino	22		Riccia	1	
Colletorto	18	13	Ripabottoni	13	
Gambatesa	1		Rotello	1	
Guardialfiera	12	20	San Giovanni in Galdo	1	
Guglionesi		14	San Martino in Pensilis	9	14
Jelsi		8	Santa Croce	19	24
Larino	48	29	Termoli		1
Lucito	12		Toro	8	9
Lupara	2		Ururi		10
Monacilioni	4				
Montagano	16		Total	470	217

A sequence of significant aftershocks (M3.8 to M4.2) over the first four days necessitated re-inspection of a number of damaged structures and dramatically increased the number of displaced persons in need of emergency shelter. Over time, people afraid

to return to their lightly damaged homes posed an ongoing challenge to emergency managers, who were attempting to return lightly or moderately damaged villages to normal operations. The sheltered population over time is reported in Figure 17.6.

From the fifth to the tenth day after the event, sheltered people were more than 10,000. The number decreased rapidly, but with a long tail, due to people who were unable or unwilling to support themselves (Galanti et al., 2004).

Most of the emergency shelters were located in outdoor tent communities (tendopoli) comprised of large tents for meals and socialising, numerous smaller six-bed tents for sleeping, and portable toilets and showers. The elderly and disabled were housed in four-bed campers located in the tendopoli, or in hotels outside the impact area. In some cases, single tents were erected next to individual homes so worried owners could protect their property and belongings. Additionally, as observed in other disasters throughout the world, some of the displaced chose to stay in hotels or with families and friends rather than in shelters. Ultimately, 31 tent camps (tendopoli) were established and a surplus of beds was available (Table 17.5).

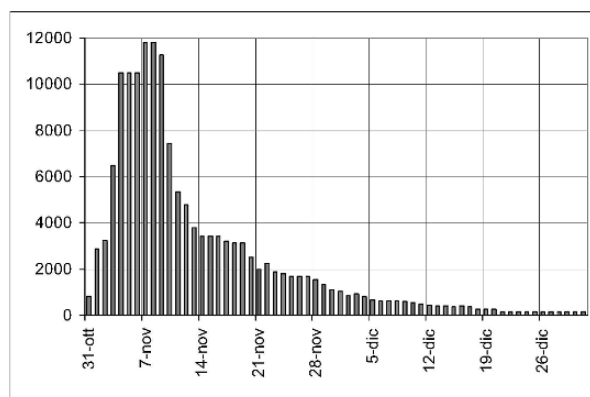


Fig. 17.6. Sheltered population along time

Table 17.5. Assistance to population in the stricken area

Number of inhabitants	370,839
Number of homeless	11,820
Number of tendopoli	31
Number of tents	2,737
Number of requested beds	15,720
Number of caravans	518
Number of chemical toilets	452
Number of field kitchens	14

Although the tents were relatively comfortable, with lighting, heating, and television powered by emergency generators, the advance of winter and the need to provide transitional housing for those whose homes were destroyed presented yet another challenge for emergency managers. While continuing to provide logistical support to the shelters, planning for some form of transitional housing had to be undertaken before recovery could commence. The central government provided those whose homes were destroyed or required major repairs with the option of living in prefabricated homes, or

accepting 500 Euro per month to arrange for independent temporary housing. For San Giuliano, where it will take a few years to rebuild the destroyed section of the town, an entire temporary village would need to be planned.

A total of 535 prefabricated homes were provided, 268 of which were constructed in the temporary village in San Giuliano, and the remainder constructed in numerous villages throughout the damaged region. The decision to build a temporary village for San Giuliano was made by the mayor and Town Council on November 12, just short of two weeks following the earthquake. The temporary village, comprised of a primary school, town hall, market, pharmacy, and social centre, is located approximately one kilometre from the damaged town. The site was chosen because it is less vulnerable to amplified ground shaking and provided enough space to keep the residents together as a community (Figure 17.7). The school and the first 30 of the planned 268 prefabricated homes in the temporary village were opened on December 1.

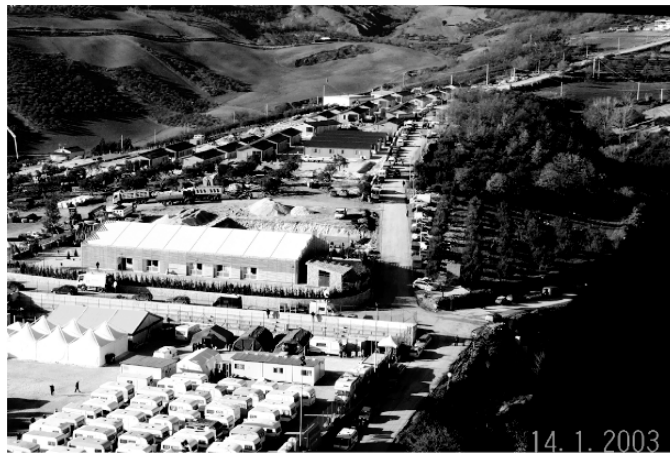


Fig. 17.7. Temporary village of San Giuliano

CHAPTER 18
EARTHQUAKE RISK AND INSURANCE

R. Spence¹ and A. Coburn²

1. *Cambridge University Department of Architecture, UK*

2. *RMS, Inc, California*

18.1. Insurance and earthquakes

Earthquake insurance is a means of transferring or sharing the risk of a catastrophic loss from an earthquake among a large number of individual risk-takers, all of whom contribute to a common pool by means of regular contributions or premiums. Different types of risk from earthquakes are commonly covered by different types of insurance policies – property and contents, life and health, workers compensation, and business interruption can all be covered. In most cases today the insurer is a commercial company which makes its business from selling policies and managing the risks involved, and also aims to make a profit to provide a return for its shareholders. There are limits to the risks covered by insurers and outside of these limits it has commonly fallen to governments to provide compensation of last-resort, so governments also have a stake in understanding the risk and assessing their likely role in compensating property-owners for their losses.

The largest volume of earthquake insurance premium is generated by commercial property, with private companies insuring their facilities, buildings and employee-related liabilities against earthquake losses. This plays a vital social role in protecting the commercial engines of a seismic region from long-term debilitation.

Individual homeowners can also protect themselves from the financial impacts that earthquake damage could cause through the purchase of homeowners' insurance. In some places, mostly those with a relatively low earthquake risk, earthquake coverage is included as a standard peril within an all-risks homeowners' policy covering fire, flood and other natural perils; in a few countries earthquake insurance is covered by a compulsory government-backed scheme (New Zealand, Turkey, Spain and France have different approaches). Most commonly in the areas of highest risk, earthquake coverage is offered as an optional add-on to the standard homeowners insurance policy for a premium which reflects both the seismicity of the location and the type of property.

Because an earthquake often causes damage to a very large number of properties in one region, householders policies are often written so that the insurer only pays for damage above a certain threshold, (known as a deductible or excess), which can often be as high as 15% of the sum insured; and sometimes co-insurance (a percentage of the damage above the deductible payable by the insured) is also required. Varying rates for location and type of building are commonly specified. In Turkey's highest-risk zone (comprising about 40% of the country) coverage under the Turkish Catastrophe Insurance Pool (DASK) will cost \$2.2 per \$1000 sum insured for a reinforced concrete or steel building, and \$3.85 per \$1000 sum insured for a masonry building, up to a maximum sum insured of about \$26,000; coverage beyond that is available from commercial companies at a higher rate. In California, earthquake insurance through the California Earthquake Authority is available at a rate varying from \$1.1 to \$5.25 per \$1000 sum

insured depending on the location and quality of building, with a 15% deductible. In Mexico City the typical range is higher, from \$0.28 to \$7.27 per \$1000, again depending on location and building type.

In spite of the availability of such insurance, take-up of optional policies has been very slow, and even in areas of high earthquake awareness like California and Japan, a relatively small number of homeowners are today covered by such policies, only 17% in California as a whole (RMS, 2004). Reasons for this, some of which will be discussed later, include: the relatively high deductible and high premium rate which makes many believe that their money is better spent on improving their own property; and the belief that government compensation will be available to meet their losses.

Another common form of earthquake insurance is 'facultative' insurance to cover businesses and their facilities; policies may cover buildings, manufacturing plant, stocks and inventories, and loss of business resulting from the earthquake. Premiums are worked out on an individual plant basis. A high proportion of larger manufacturing businesses are covered in this way (for example, 85% of industrial plants examined by RMS following the Kocaeli earthquake (Johnson et al., 2000). A few institutions are large enough, and have their risks spread over a wide enough area to be able to cover the risk themselves without purchasing insurance. However, at the other end of the scale, insurance take-up amongst small businesses is very low, partly because of the short business horizons of such businesses, and partly for reasons similar to those for homeowners.

18.1.1. CATASTROPHE REINSURANCE

Insurance companies calculate their premiums based on the expected claims rate and costs of claims, with an allowance for expenses, uncertainty and a margin for profit. This works well for the more routine perils such as fire and accidental damage, those with high frequency and low severity, because the insurer will be able to predict claims with some accuracy, the annual premiums can be calculated to be sufficient to meet these claims. Covering earthquake risk is more difficult for two reasons; first because earthquakes occur infrequently so there is no adequate database of claims experience for any region; and secondly because it takes a long period of time to accumulate the level of reserves based on premiums to cover the maximum loss which may occur in any one event. The latter difficulty is usually dealt with partly by reinsurance; the primary insurer passes on the risk of a loss higher than a certain amount to a reinsurance company, which has its risks diversified by covering only a part of the risk of any single loss, by covering risks in many parts of the world and among many different types of perils. Reinsurers are smaller in number and larger in size than primary insurers, and many have developed their own specialist teams for assessing earthquake risks and making information on losses more widely available (Munich Re, 1995-2004). Reinsurers need to have access to capital markets to ensure that their reserves are sufficient. All this makes earthquake insurance more costly than it would be based simply on the average annual rate of claims (Walker, 2000).

18.1.2. CATASTROPHE MODELLING

The second difficulty, that of calculating the expected average loss rate and “maximum probable loss”, is one for which the insurer’s usual source of data – the dataset of past claims – is likely to be inadequate, and assistance is needed from the scientific and engineering community. During the last 20 years, insurers have increasingly sought assistance from seismologists in identifying the likely magnitude, intensity and frequencies of earthquakes in any area, and of earthquake engineers in identifying the level of damage which is likely to result from any given level of ground shaking. This has grown into the technological field of catastrophe modelling, which makes use of GIS tools to simulate events, plot their consequences, and thus estimate losses from any insurance portfolio with a given probability of occurrence. Subsequent sections of this chapter will discuss particular issues in the development of an earthquake catastrophe model for a particular insurance application. Catastrophe modelling companies, too, have made considerable contributions to our knowledge of earthquake risks, producing detailed reports on the major events, and even looking ahead to consider the implications of some future events (RMS, 1995b, RMS, 2004)

18.1.3. INSURANCE AND EARTHQUAKE RISK MITIGATION

It is a well-established practice in many types of insurance that the premium paid is discounted if the insured can show that various protection measures have been taken – locks and alarm systems for theft insurance, and smoke alarms for fire insurance, for example – and the same approach could in principle be applied to earthquake insurance. In some earthquake insurance schemes a similar principle applies. A survey of various national insurance schemes (Spence, 2004) found that methods adopted have included:

- Relating the premium to the vulnerability of the building, for example considering the earthquake zone it is located in or the construction type or materials.
- Offering a discount on the premium if the building has undergone structural mitigation (i.e. retrofit).
- Enforcing minimum non-structural measures that must be met before insurance can be taken out.
- Supporting community mitigation activities.
- Offering insurance coverage that will pay the cost of bringing the building into compliance with building standards during repair or rebuilding of the building after substantial damage.
- Invalidating insurance if a building is altered contrary to the related design or in a way that will detrimentally affect the load-bearing system, therefore increasing vulnerability.
- Funding research into mitigation and supporting public education.

However, none of these various approaches is yet in general use, partly because of the difficulty of ensuring, for each of many thousands of properties at risk, that the measures have been taken, but also partly because of the difficulty in estimating the reduction in risk which would result from any particular measure. It remains a challenge for earthquake engineering to develop reliable methods to estimate the risk associated with various states of verifiable vulnerability reduction or risk mitigation techniques.

A further role for earthquake engineering in the future will be to incorporate designed levels of structural performance and vulnerability into new building designs so as to optimise long-term economic value (Walker, 2000). At present designed structural performance is based on minimum values set to ensure an acceptable life-safety; the design earthquake may nevertheless cause considerable physical damage and therefore loss. In many cases the long-term financial interest of the user of the building may be better served by setting a higher level of structural performance which ensures that the building remains useable throughout the worst expected earthquake. Such an approach can also be encouraged by tying insurance premiums more closely to the designed level of structural resistance.

18.2. Losses and insurance exposure in recent events

The monitoring of catastrophe losses by the reinsurance company Munich Re (1995-2004) shows that insured losses are increasing rapidly worldwide. For all natural catastrophes losses in the last complete decade, the 1990s, had grown to fifteen times those experienced in the 1960s.

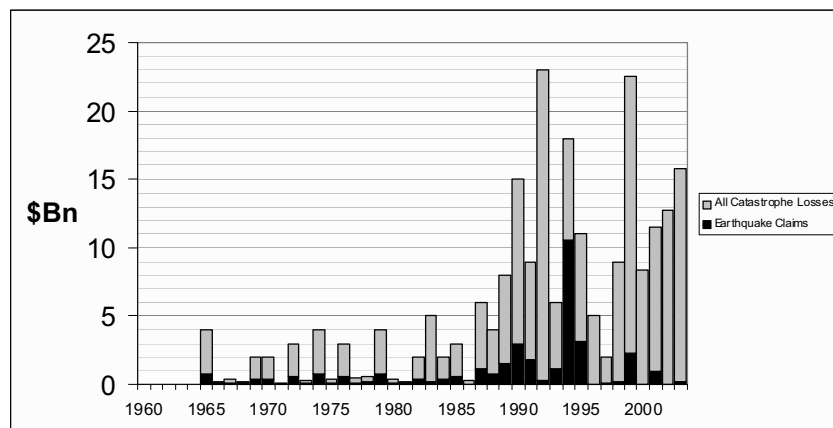


Fig. 18.1. The growth of insured losses from catastrophe in the last four decades of the 20th century. Sources: Munich Re (1995-2004)

The frequency with which natural hazards have become major insurance losses is also increasing. Records for the cost of a natural disaster are constantly being broken in each country of the world. This recognition has had wide-ranging implications for the reinsurance industry and has brought to prominence new techniques of risk management, successive waves of new capital being brought into the insurance industry, and a growing role for the capital markets in the transfer of catastrophe risk.

Earthquakes account for about 20% of insured catastrophe losses (and over a third of all economic losses from natural hazards). Figure 18.1 shows the increasing insured losses from catastrophe insurance and how earthquake losses have contributed to the growth. The statistics do not follow a precise trend because the losses are dominated by a small number of individual catastrophes, such as Hurricane Andrew in 1992 and the

Northridge earthquake in 1994, and yet the overall trend is clear: individual extreme events are occurring more frequently.

But it is not the frequency of the extreme events themselves which is increasing. In general, there have not been more strong earthquakes during the past quarter of a century than in other 25-year periods in history. The evidence suggests that the main driver for the increased cost is that the events that occur are causing higher losses than they did previously. The number of insured properties and the value of the property exposed to the events that occur is very much larger today than it was a generation ago. The values at risk are increasing. The population of the planet has doubled in a generation. Increasing numbers of people and businesses have their assets insured. And the pattern of insured assets is changing in the areas of the world where earthquakes occur. The severity, locations and types of losses suffered in the past are no longer very good guides to the losses that will occur in the future.

Those who live in the countries where insurance is a way of life are becoming wealthier and expecting to have their increasing assets covered, largely within existing insurance arrangements. Although there is little growth in premium income from property insurance in the OECD countries (averaging less than 2% growth during the price-competitive 1990s) there is little doubt that the insured values at risk are increasing rapidly. Economists show that more wealth was created in the United States in the last ten years of the twentieth century than in the first sixty. A large proportion of this wealth turns into property and find its way into the insurance industry's portfolio. The average householders are far better off than their parents' generation and today own houses and contents of far greater value. Commercial operations have more (and different) property, liabilities and dependencies than ever before.

The demographics of risk have also changed. For example, population movement has meant that the state of California and the earthquake-prone regions of the United States have grown by 50% since the 1970s, and similar shifts towards more earthquake-prone regions can be observed elsewhere, for example in Turkey and the Andean countries of Latin America.

Increasingly, developing countries are developing their own insurance industries. Insurance premium growth in the newly emerging economies is averaging 10% a year. India and China, representing a third of the world's population, ended the 1990s more than twice as rich as they started it. As countries become more prosperous, they buy insurance to protect that wealth. The types of property in these regions are more vulnerable to the prevailing hazards, being built to lower and less rigorously controlled construction standards, so relative to the developed world they suffer higher proportional losses when disaster does strike.

The early 1990s saw a sequence of catastrophic events that put unprecedented pressure on the reinsurance industry. Even though the second half of the 1990s and the first years of the present century proved less eventful and catastrophe reinsurance pricing slumped to low levels afterwards, the sequence of sizeable losses in the first half of the 1990s had significant consequences for catastrophe reinsurance as an industry. Fifteen of the worst twenty catastrophe events in history, ranked by insured loss, occurred in the early 1990s. These included Hurricane Andrew in Florida, 1992 (\$16.5 bn), the Northridge

Earthquake in California, 1994 (\$15 bn); Typhoon Mireille in Japan, 1991 (\$5.2 bn) and Storm 90A in Northern Europe, 1990 (\$3.2 bn).

But the possibility of even higher losses in the future needs to be considered by insurers and reinsurers. Reports by RMS (1995a, b) have suggested that, in spite of huge investment in earthquake risk mitigation, a repeat of the 1906 San Francisco earthquake would today result in economic losses between \$170 and \$220 billion, compared with the \$50 billion loss which actually occurred then (estimated at today's prices); and that a repeat today of the 1923 Great Kanto Earthquake in Japan would cost between \$1,000 billion and \$1,600 billion in property losses, and perhaps an equal amount in business interruption, with a consequent but unquantifiable additional loss to worldwide trade and financial markets. Proper modelling of such risks is therefore vital to ensure that earthquake insurance is financially viable.

18.3. Modelling of earthquake risks for insurance

The main objective of modelling earthquakes for insurance risk management is to ensure the financial viability of operations. Insurance is based on the principle of diversification of risk – spreading the risk over a sufficiently large number of policy-holders to create a premium flow that will comfortably cover the losses. Predicting the losses from earthquakes requires modelling the probability, location and likely costs of all potential events. The modelling process essentially creates a simulated history of several hundreds of years of earthquake losses to the portfolio of properties insured by that company.

In the modelling, the probability of events occurring (the 'frequency' of loss) is as important as how much damage they will cause when they occur (the 'severity' of loss). A probabilistic model has to be comprehensive in its coverage and as accurate as possible. Earthquake occurrence is of course an uncertain process and there are gaps and probably errors in the estimations, so this is taken into account by adding safety margins (uncertainty or risk loadings) to the financial calculations.

18.3.1. UNDERWRITING RESULTS

The insurance company balances the premiums it receives from all its policy-holders against all the losses that could occur to their properties. Over a long enough period of time, the total rate of losses (the 'burning rate') should be less than the total premium earned. Insurers also need to cover their operating costs, which can be a substantial part of the premium, ensure that they have a good safety margin and a profit margin to ensure that they can provide an attractive return to their shareholders. Insurers make a lot of their income from investing the money they receive as premiums, but their underwriting results (the profitability of premium against claims) is fundamental to the long-term viability of the business and becomes more critical in times of lower interest rates. Complicating this further is the fact that pricing for catastrophe risk is cyclical. After a big insurance loss, premium rates rise across the board (the market 'hardens') and over time prices fall again (the market 'softens') but maintaining a viable business through these cycles requires a long term view of risk, such as one provided by modelling.

18.3.2. CAPITAL ADEQUACY

Insurance companies maintain capital reserves to pay out their claims. If the company insures a lot of properties in one seismic area, then a large earthquake in that area could require a major call on that capital. Models are used to assess the likelihood of large catastrophe claims. The probability of the company experiencing a loss of a certain size can be assessed from the model output, usually expressed as an ‘exceedance probability’ (EP) curve. Larger losses occur with lower probability than smaller losses. Each company has its own metrics, but most monitor particular loss levels, for example their ‘250-year return period loss’ (i.e. the loss that has a 0.004 probability of occurring in a year). They ensure that their capital reserves are adequate to cover this level of loss. Government regulators, credit rating agencies and other external parties are also interested in ensuring that insurance companies have sufficient funds to pay their obligations, so insurers are increasingly obliged to demonstrate their modelled losses to other people.

Insurers are not obliged to maintain capital reserves to pay for the largest loss imaginable – for example a massive magnitude earthquake with a 10,000 year return period that could cause losses many times higher than their 250-year capital adequacy benchmark. There may be potential catastrophe losses large enough to force an insurer into bankruptcy (in which case policy-holders would find themselves unable to get all of their claim paid). The costs of maintaining reserves large enough to pay for the extreme events would be an inefficient use of shareholders’ capital. The ‘risk of ruin’ – the probability of events larger than the capital reserves – can be computed from the modelled EP curve.

18.3.3. REINSURANCE

Most primary insurance companies find it efficient to protect themselves from larger losses by purchasing catastrophe reinsurance from a reinsurance company. Reinsurance companies operate by selling protection to many different insurance companies across the world. A reinsurance contract ensures that if an earthquake occurs causing a loss above a certain threshold (‘the deductible’), then the reinsurance company will pay a proportion of those losses up to a maximum level (‘the limit’). These reinsurance contracts are commonly renegotiated on an annual basis, evaluating how the portfolio has changed during the year and other factors. Modelling of earthquake losses is an important part of the risk assessment that goes in to pricing negotiations. An insurance company, usually advised by its reinsurance broker, will model how much protection it requires – the optimum layers of a reinsurance program – and the broker will place this program in the market, negotiating with several reinsurance companies to have them participate in the program.

Reinsurance companies also model the contracts they are offered, taking the exposure data of the cedant insurance company and running their own analysis of their loss exceedance probability. This output can be used to assess a ‘pure premium’ (the modelled average annual loss) to a layer as an input into pricing discussions.

18.3.4. PORTFOLIO MANAGEMENT

Reinsurers and primary insurance companies try to manage their portfolios to ensure that they are spreading the risk, and that they don't end up with large concentrations of exposure in areas where they could have a major earthquake that would cause an unmanageable loss. A property portfolio tends to be highly concentrated in cities, so the modelling process looks at the frequency and severity of losses in each city region. If cities are far enough apart – San Francisco and Seattle for example – the chances of a single earthquake affecting both is remote, so these can be treated as separate 'accumulation zones', areas where losses can be considered independently. Insurance companies will decide the maximum they are prepared to lose in each of their accumulation zones (for example a 250-year loss of \$100m in Seattle and \$200m in San Francisco) and allocate their capital reserves across the zones they do business in. The portfolio management operation involves assessing which policies to write that will maximize their return (i.e. produce most premium income for the minimum losses) against the capital allocation they have in that zone. Once they have written policies up to their limit in a particular zone, a prudent insurance company refuses to write any more business in that area, but will instead seek to fill up its remaining zones. The monitoring of the portfolio against capital allocation and for accumulation zones is a key part of the use of earthquake modelling in insurance.

18.3.5. UNDERWRITING POLICIES

The addition of a new insurance policy into an insurer's portfolio is examined within the context of the existing portfolio, the capital allocation in the accumulation zones, and the likely profitability of that policy. Large commercial insurance accounts, which tend to be the major contributors of many insurance companies' earthquake premiums, may include hundreds of different buildings across a country (for example most large companies have operations in many different cities). A model is used to analyse how these many different buildings and locations would add to the insurer's loss potential for each of its accumulation zones. Two insurance companies with different concentrations of business in a certain city may offer a prospective client different prices depending on how they view that addition to their existing portfolio.

Since earthquake insurance coverage is often an additional supplement to the insurance coverage for fire and other perils, an insurer has to balance earthquake risk as just one of several components of the attractiveness of the client, in deciding whether to write that business. And if an insurer does decide that they will underwrite the policy, there are a number of variable terms and conditions they can offer the client. They can negotiate the deductible (the threshold at which the insurer will start to pay losses), a limit (the maximum loss payout) and coinsurance (the proportion of the loss between those bounds). These can all be modelled for a particular account or location, and insurers are using increasingly sophisticated modelling systems that price, assess loss potential and monitor accumulations in zones in their underwriting processes.

18.3.6. MODELLING ATTRIBUTES FOR INSURANCE APPLICATIONS

For insurance applications earthquake models need to be comprehensive in the hazard that they include – an unknown fault or an unexpected magnitude could be very

financially damaging to an insurance company. The overall rates of occurrence of earthquake events and the seismicity they encompass has to be state-of-the-art: more earthquakes than expected would undermine the long-term viability of the business, but this can be kept in review and insurance business can usually adapt within the pace of new scientific developments in understanding seismic activity. The loss estimated by an event needs to be fairly accurate; particularly in aggregate: i.e. the losses to large numbers of buildings should be correct. Models benefit from the laws of large numbers. Models also need to be consistent in their relativities between the risks assessed to different locations and, importantly, different types and construction qualities of the buildings likely to be affected. Insurance applications do not normally require a precise prediction of loss to an individual structure under earthquake loading in the way that an engineering design of critical infrastructure might do. Instead insurers deal with the uncertainties inherent in real-world building performance in an earthquake by pricing for that uncertainty in the modelling process. It is important that the uncertainties are well understood and are properly quantified so that uncertainty loadings can be adequately calculated.

18.3.7. REWARDING MITIGATION ACTIVITIES

Because insurers deal with large numbers of buildings they are limited in the ways they can act to reinforce the mitigation measures that society is seeking. Insurers have a strong self-interest in reducing their own earthquake losses and are often keen participants in action programmes to promote mitigation. However as a recent study has found (Spence, 2004), few insurance companies have implemented schemes for discounted premiums for properties with earthquake-resistant measures in place. This is largely because the premium is only partially assessed on the quality of the individual property – mainly it is derived from the assessment of the volume of risks across the whole portfolio – and also because the margin that might be reducible would be only a small part of the premium and insufficient to provide the level of financial incentive for a property-owner to invest in costly building improvements. Other reasons include the uncertainty around the performance of individual buildings and the costs of carrying out the inspections and verifications required to implement such a scheme. Insurers are generally reluctant to reduce their premiums (their ‘cash in hand’) but they may be more flexible about more generous deductibles and limits that would affect the amount of claims paid to provide incentives that would contribute to mitigate activities.

18.3.8. LIMITATIONS TO THE ROLE OF PRIVATE INSURANCE

The private insurance industry is motivated to provide substantial capital to participate in risk where market rates provide a return on their capital. Private insurers need to be able to diversify their risk and offset one area of risk against another, and to benefit from volumes of business. In many countries commercial property owners are able to benefit from the private insurance industry by providing the volume, diversity and being willing to pay premiums for their insurance coverage that insurance companies find attractive. In some countries and sectors, this does not occur: the price of insurance may be considered too expensive for the majority of property-owners and this in turn means that there is insufficient volume or diversity of business to attract insurers and for them to offer lower prices. This is the case for some areas of homeowner insurance, even in

some of the richest areas of the world like California and Japan, as discussed above. The rates for earthquake insurance offered in these seismic areas appear too expensive to the consumer, compared to their perception of their risk (and there may also be some contributing element of fatalism by consumers who assume that in last resort, they would receive government aid to offset their losses). In these cases, the government may choose to intervene and provide subsidies to insurers (like the California Earthquake Commission) or to establish a national catastrophe pool in which the government acts as reinsurer of last resort (such as those operating in France, Spain and several other countries) or to set up its own insurance program. A government insurance scheme to encourage property-owners to participate in their own protection is described in the next section.

18.4. Modelling earthquake risk for the Turkish Catastrophe Insurance Pool

Turkey is situated in one of the most seismically active regions of the world with a large part of the country at significant risk of major catastrophe. Historically, the Government of Turkey has had a legal liability to fund the costs of reconstructing buildings after an earthquake under Disaster Law 7269. This exposure of the Government to catastrophe risk has significant adverse implications for the Government's budget, financing and its anti-inflationary targets. In 1999 the Government of Turkey launched an ambitious project to tackle this national catastrophe risk by firstly privatising the risk through offering insurance through the Turkish Catastrophe Insurance Pool (TCIP) and then exporting large parts of the risk to the world's reinsurance markets.

At the time of writing the TCIP has been in operation for 4 years. Some 2 million policy-holders have their property covered for earthquake damage, and benefit from a very low-cost premium structure because of the large size of the pool, its dispersion across the country and the fact that it is extensively reinsured on the international reinsurance market. In just over 3.5 years of operation payments totalling 7,900 billion Turkish Lire (around \$5 billion) have been made to 4660 policy-holders whose properties were damaged in more than 70 separate earthquakes. The Disaster Law has not however been repealed, and the Turkish Government has continued to compensate those who were not insured.

During the initial stages of the scheme, a consulting project undertaken by a UK consortium formed an essential part of the work to establish TCIP and reinsure the risk. The principal objectives of the project were to develop an advanced earthquake risk model to quantify the risks facing the nation, to develop an economic model to establish the impact on the Turkish economy of catastrophe risk, and to design an insurance pool to carry the risk. The elements of the earthquake risk model developed will be summarised. These elements were:

- The hazard model.
- The building stock inventory.
- The vulnerability model.
- The earthquake loss integration model.

18.4.1. THE HAZARD MODEL

As is common in catastrophe risk modelling, the approach used was to generate a large number of independent event scenarios, each with a location, a set of physical consequences and an annual occurrence probability, in order to derive average annual losses (AAL) for each zone of the territory. A set of synthetic scenarios was created to simulate credible earthquake events.

The basic input for the definition of the synthetic earthquake catalogue was the historical earthquake catalogue, location of major active geological faults, seismic source zones, recurrence relationships, estimates of maximum magnitude (M_{max}), fault mechanism and average dip angle for each source zone. In each source zone the earthquake activity was modelled according to the Gutenberg-Richter recurrence relationship and the assumption was made that the seismicity follows a Poisson process. In order to ensure that high population areas are captured by the areas of strong shaking due to the scenario events, some (large) zones were split into several sub-zones.

No earthquake was triggered that had magnitude greater than the value of M_{max} for the source zone with which it is associated. For a given magnitude of earthquake, M , the frequency of events of this size was obtained directly from the recurrence relationship. Each event was triggered with an epicentral location chosen completely randomly; anywhere within a source zone for magnitude < 7 and along a fault of a certain minimum length for magnitude ≥ 7 . It was assumed that all the earthquakes with $M \geq 7$ are associated with mapped faults, and rupture propagation direction from the epicentre is bi-lateral. The estimated length of fault rupture for a given magnitude decides the selection of available faults within a zone; it was assumed that the rupture does not exceed the mapped fault length.

The ground motion at each location was modelled in the form of a displacement response spectrum, the parameters for which were derived for each scenario earthquake using ground-motion attenuation relationships derived for the Western USA (Boore et al., 1997); only later, did curves developed specifically from Turkish data become available (Gülkan and Kalkan, 2002); each location was assigned a soil class according to the NEHRP soil classification, and appropriate amplification factors were adopted (FEMA, 1997a) to define the demand spectrum.

Collateral hazards were also considered. Liquefaction was modelled by assuming damage in areas where the soil was known to be liable to liquefaction would be equivalent to that which would have been caused by NEHRP soil class E. Damage directly associated with the fault rupture, earthquake-induced landslides, tsunamis and fire were not considered, on the basis of investigation of historical events in Turkey, likely to make a significant contribution to overall damage. The hazard model is discussed in detail by Bommer et al. (2002).

18.4.2. BUILDING STOCK INVENTORY

The system of classification used for the building stock was developed in order to distinguish building types according to their known earthquake performance, taking into account the need to make use of inventory data available, and considering the geographical resolution needed for the earthquake loss modelling. The geographical

resolution of the earthquake loss model was constrained by the resolution of the data regarding the exposed building stock. The basic administrative regions in Turkey are province (il), districts (ilce) and municipalities (mahalle); building stock data from census reports was available at district level, hence this was adopted as the basic geographical reference (geo-code) for the loss model.

To distinguish construction classes by vulnerability, a list of 38 construction classes was initially drawn up, based on expected differences in earthquake response. However, the inventory data available distinguished buildings by height and major construction material only. Other distinctions had to be inferred. Both for this reason, and to limit the computer run-time needed, the buildings type classification was finally limited to the 14 types shown in Table 1. Subdivisions of RC framed buildings by height and design quality presented a special challenge. "Poor" seismic design was eventually assumed to include any of the following: weak ground floor, evidence of poor construction quality, or built before 1975; any buildings with none of those features were assumed to be of "good" seismic design.

During the lifetime of the project the 2000 Turkish Building Census, became available providing the total number of buildings in a number of use categories numbers of dwelling units, and a breakdown of the proportion of buildings in each of a number of construction classes for each district and municipality in the country. To map these construction classes onto the chosen vulnerability classes, use was initially made of several localised building surveys carried out in different parts of Turkey, either in post-earthquake damage or vulnerability surveys (EEFIT, 1993; Boğazici University, 1992; Aydinoğlu, 2000b; Akbar, 1989). The distribution of the building stock between these categories in each locality was to some extent a matter of experienced local judgement.

Table 18.1. Turkish Building Stock Classification used, and estimates of typical distributions in urban and rural areas

Structural Type	Urban	Rural
Timber frame	< 1	< 1
Weak Masonry (adobe, rubble masonry)	7	9
Brick/block Unreinforced Masonry with timber floors	19	26
Brick/block Unreinforced Masonry with concrete floors	17	21
RC frame with masonry infill – 1 to 3 storeys, Poor Seismic Design	44	36
RC frame with masonry infill – 4 to 7 storeys, Poor Seismic Design	4	3
RC frame with masonry infill – 8 or more storeys, Poor Seismic Design	6	1
RC frame with masonry infill – 1 to 3 storeys, Good Seismic Design	1	< 1
RC frame with masonry infill – 4 to 7 storeys, Good Seismic Design	< 1	0
RC frame with masonry infill – 8 or more storeys, Good Seismic Design	< 1	0
RC shear wall – 4 to 7 storeys	1	< 1
RC shear wall – 8 or more storeys	2	1
Single storey industrial shed with light steel truss roof pinned to cantilever RC or steel stanchions	0	0
Single storey industrial shed with pre-cast concrete roof	0	0

18.4.3. THE VULNERABILITY MODEL

The approach adopted for the estimation of the physical losses to buildings followed, in its general form, that proposed by Kircher et al. (1997) and incorporated in the HAZUS methodology (NIBS 1997, 1999 and 2002). For any given scenario earthquake, the loss modelling process involves the following steps:

1. For each geo-code define
 - Soil type and conditions.
 - Liquefaction and other collateral hazard potential.
 - Number of individual dwellings.
 - Distribution of dwellings among building classes.
2. Use attenuation relationships to define key parameters of ground motion for standard soil conditions (i.e. NEHRP class B, which corresponds to rock).
3. Use these parameters to construct a set of elastic demand spectra for the site, corresponding to various levels of damping.
4. For each building class define:
 - A mean capacity curve – i.e. a curve of inertial force against expected displacement.
 - Fragility curves for a number of different damage states. Each fragility curve expresses the distribution of displacement within a group of buildings of the same class having the same damage state.
 - Reduction factor values as a function of earthquake shaking duration, reflecting the reduction of hysteretic energy absorbed by a structure as it degrades in strength and stiffness during an earthquake.
5. For each building class, a given spectral displacement implies a given level of damping, depending on the level of inelastic deformation and the reduction factor. The spectral acceleration of the input motion at the appropriate level of damping is then plotted at this displacement, to form a demand curve.
6. Find the ‘performance point’ for the building class at intersection of the demand and capacity curves.
7. From the appropriate fragility curve, determine the expected damage distribution to that building class.
8. Use inventory data to determine loss to that building class.
9. Integrate losses over all building classes.
10. Integrate losses over all geo-codes.

The process is illustrated in Figure 18.2. In this process the building vulnerability is characterised by two sets of curves: (1) fragility curves that describe the probability of reaching or exceeding different states of damage given peak building response, and (2) building capacity curves that are used, with the damping-modified demand spectra, to determine the peak building response.

The approach used to defining the values of the critical parameters was a composite one. In part the figures were modified from those proposed for US building and given in

the HAZUS manual (NIBS, 1997, 1999 and 2002) using expert judgement, based on a knowledge of both Turkish and US design and construction practices; in part alternative values proposed for these parameters by researchers from countries outside the US were considered (Griffith and Pinto, 2000; Aydinoglu, 2000b; Faccioli et al., 1999); and in part, loss estimates derived from this approach were used to calibrate parameters so as to match the relative damage levels of different building types and the distributions of damage which are characteristic of observed damage in Turkey. The testing of the resulting loss estimates against those actually observed in the 1999 earthquakes is discussed below.

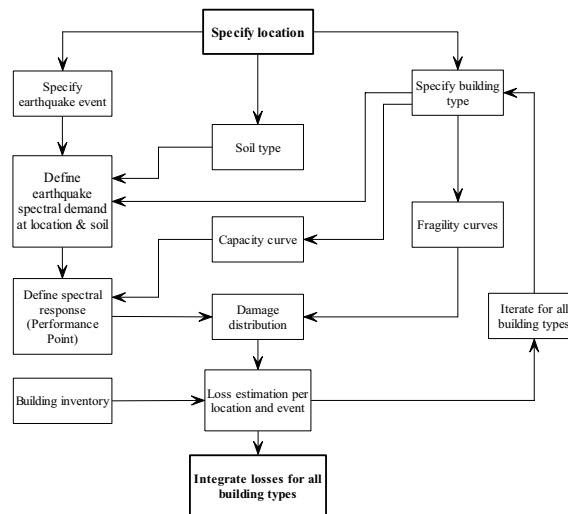


Fig. 18.2. Overview of the loss estimation methodology for a given scenario (for ground shaking only)

18.4.4. THE EARTHQUAKE LOSS MODEL

For calculating loss in any geocode, the summation of Eq. (18.1) was carried out.

$$L = \sum_i \frac{V_i}{N_i} \times (N_i P_i) \times dr_i \quad (18.1)$$

where L is the total monetary value of the loss in the geo-code, V_i is the total reconstruction cost of buildings of class i , N_i is the total number of buildings of class i , P_i is the proportion of buildings of class i affected, and dr_i is the mean damage ratio (expected cost of loss / rebuilding cost) for buildings of class i . V_i/N_i gives the average reconstruction cost per building and $N_i P_i$ gives the number of affected buildings.

N_i for each class derives from the building inventory data; the P_i are calculated by the loss modeller for each geo-code and earthquake. Values V_i were derived from recent construction values for several Turkish cities (and vary between classes of buildings). The dr values depended on the damage state: zero for zero to slight damage; 2% for

slight to moderate; 10% for moderate to extensive; 50% for extensive to complete; and 100% for complete.

The results of loss calculations from all events in the synthetic earthquake catalogue were used to calculate annual average loss (AAL), which is the statistical expectation of loss per year. The AAL varies by area and is governed by three factors, the seismicity, the quantity of building stock (measured in terms of rebuilding cost), and the distribution of building classes. Figure 18.3 shows the Annualised Earthquake Damage Ratio (AEDR) for residential buildings by province level, and is calculated by dividing AAL by total rebuilding cost. It illustrates the level of seismic risk in relation to the replacement value of property in a given province. High AEDRs are concentrated in the south-western parts of Turkey and provinces which were affected by the 1999 Kocaeli and Duzce events.

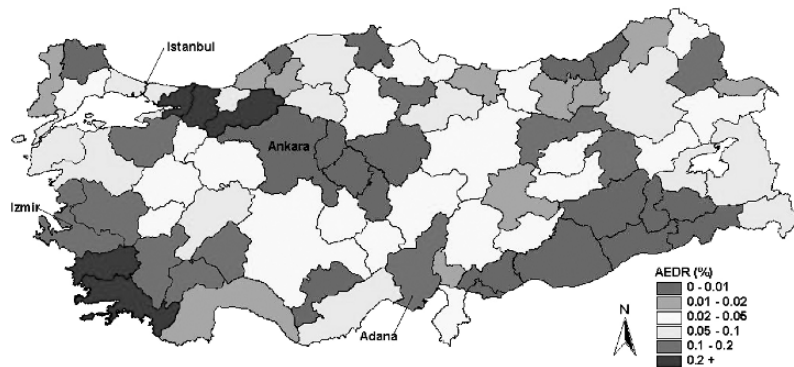


Fig. 18.3. Annualised Earthquake Damage Ratio shown in province level

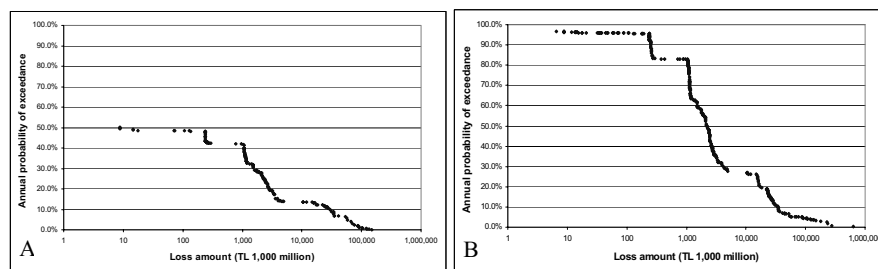


Fig. 18.4. Loss exceedance curves for (A) Adana and (B) Izmir

Figure 18.4 shows the loss exceedance curves for the province of Adana and Izmir. The annual probability of exceedance for Adana only reaches about 50%, implying that there is a 50% chance of the Province being affected by a damaging earthquake in each year. Izmir Province on the other hand can be seen to have a high annual probability of being affected by a damaging earthquake, with an estimated >90% annual probability of at least one loss exceeding about \$50,000.

18.4.5. COMPARISON OF THE MODEL RESULT WITH OBSERVED DAMAGE

Testing of earthquake loss models against actual observed losses is an important means to develop them and test their credibility. A detailed study on observed damage due to the August 1999 Kocaeli earthquake was carried out shortly after the earthquake by a Turkish-Japanese team and subsequently published by the Architectural Institute of Japan (AIJ, 2001). This detailed loss inventory provided an ideal opportunity to test the validity of the approach to loss modelling developed for the Turkish Catastrophe Insurance Pool (TCIP). The model developed was used to compute losses due to the occurrence of a scenario event represented by the Kocaeli earthquake and the results were compared with the observed damage distribution. For comparison, an intensity-based loss model was also used. This model is described elsewhere (Spence et al., 2003).

A comparison between losses estimated by the two methods and observed losses are shown for one site and for mid-rise RC frame buildings in Figure 18.5. The figures show the estimated losses in 5 damage bands (from undamaged to complete), and a composite measure of damage or mean damage ratio, MDR, calculated by assuming 2% loss for slight damage, 10% loss for moderate damage, 50% loss for extensive damage and 100% loss for complete damage (Bommer et al., 2002).

For the RC framed buildings, comparing first the spectral displacement and intensity models, the figures show that the intensity model predicts fewer buildings with moderate and extensive damage, but more with complete damage compared with the spectral displacement model, but these two models predict overall damage (MDR) at about the same level, 45-65% for "good" buildings, and 65-75% for "poor" buildings, at this site.

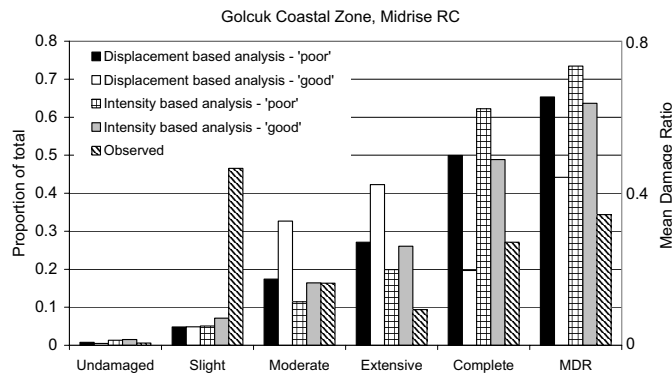


Fig. 18.5. Kocaeli earthquake: results and comparison with damage data – Midrise RC, Gölcük, Coastal Zone. The first five groups show the proportion of the total in each damage category. The final group shows the mean damage ratio (MDR), a composite damage measure using damage ratios of 0.02 for slight damage, 0.1 for moderate, 0.5 for extensive and 1.0 for complete

However, both models over-predict damage compared with the damage measured from the field surveys. The observed mean damage ratio derived from the damage survey data was 37% at this site, indicating an over-prediction by 20 to 50%. Study of Figure

18.5 indicates that in both cases, many more buildings were observed to have slight or moderate damage, and fewer to have extensive damage and collapse, compared with the predicted loss distributions from the two models.

Some possible reasons for the over-prediction of damage by the spectral displacement model include the following:

- The spectral response for the site has been overestimated by the ground motion equations.
- The soil amplification has been overestimated or the soil non-linearity has been underestimated.
- The effective damping in the degrading structural system has been underestimated.
- The assumed failure mechanism is incorrect.
- The capacity curve has been underestimated.
- The drift ratios to cause each damage state have been underestimated.
- The whole spectral displacement model is inappropriate in these conditions.

In addition, overprediction in either model could also be the result of incorrect identification of building classes or damage states in the surveys at the two sites.

A sensitivity analysis was used to test whether these sources of error were sufficient to explain the differences between observed and estimated damage. This concluded (Spence et al., 2003) that incorrect values of the parameters in the model was unlikely in itself to be the explanation for the discrepancy. However evidence from the damage surveys on the site indicated that, rather than behaving as bare moment-resisting frames as the model assumed, the infill walls in fact played an important part in the failure behaviour of the mid-rise concrete buildings, and that adjustments to the model to take this extra resistance into account would have been adequate to explain the discrepancy. Further recent analytical study has confirmed this as a likely explanation (Booth et al., 2004).

18.5. Conclusion

This Chapter has reviewed the approach of the insurance industry to understanding and modelling earthquake risks, and has identified ways in which earthquake engineering has contributed to this understanding. Three general points are offered in conclusion.

1. Large losses to the insurance industry in the 1990s, especially those associated with the 1994 Northridge earthquake, have stimulated a great deal of research into the causes of building vulnerability and the methods of estimating losses. One benefit of this has been the development of spectral displacement models of building performance, which provide a much more realistic estimate of likely losses than earlier approaches based on macroseismic intensity. This work has implications for earthquake mitigation beyond the insurance industry, in devising national and city earthquake mitigation programmes, and preparing emergency services.
2. Although businesses are today quite widely covered by insurance, there remains a surprisingly low rate of take-up of earthquake insurance among homeowners, even in some high-risk locations. High deductibles and the expectation that catastrophic

damage will eventually be compensated by governments seem to be factors contributing to low take-up.

3. The insurance industry has the opportunity to be active in earthquake risk mitigation through establishing preconditions for insurance or offering better rates for better-protected risks. However to date this opportunity seems to have been little realised; premiums are largely based on location and use-types or broad construction features. One reason for this is that expensive expert assessment of individual properties might be needed to make this work. But a clear identification of the reduction in losses which building modifications would lead to could stimulate better rating structures, to the benefit of both property-owners and insurers. Better interaction between earthquake engineers and insurance underwriters will be needed to bring this about, and this remains a challenge for both professions in the future.

Acknowledgements

The authors gratefully acknowledge the assistance of Julian Bommer, Oliver Peterken, Shigeko Tabuchi, Nuray Aydinoglu, Edmund Booth, Juliet Bird, Domenico del Re in the preparation of this Chapter, or the work on which it is based.

CHAPTER 19
STRENGTHENING AND REPAIRING EARTHQUAKE DAMAGED
STRUCTURES

A. G. Costa
University of Porto, Oporto, Portugal

19.1. Introduction

To preserve the architectural and structural value of existing constructions, detailed and thoughtful understanding of their structural behaviour, including modifications in the construction layout that may have been carried out over the years, must be accomplished before strengthening and repairing damaged structures. In the case of seismic repair, strengthening should consider and preserve the initial materials whenever possible. This implies the need for a deep comprehension of the construction processes that may be involved and for a reliable definition of the mechanical properties of materials. Experimental tests are, therefore, required. The end results of these experimental studies are, mainly, an adequate assessment of the mechanical properties of the materials and of the dynamic characteristics of the constructions. Calibration of the numerical analysis of constructions based on the available experimental data may then be performed to assess the quality of the analytical modelling. After this operation, several numerical analyses can be accomplished to identify critical zones in the construction, to correlate analytical damage measures to the real damage patterns and to obtain necessary information for the final repair strategy, like internal forces and displacements. In the case of earthquake repair, it is also important to have reliable information about the seismic hazard of the region where the construction is located. To withstand future earthquakes without damage, adequate knowledge about the type of earthquake activity is fundamental to define an efficient and lasting structural solution that enhances the ductility, stiffness and strength of the construction.

19.2. Historical survey

The purpose of the historical survey is to gather as much information as possible regarding the construction under analysis. This stage is fundamental to fully understand what has happened during the life cycle of the construction up to the point of the need for repair. More precisely, modifications in the construction layout that may have been carried out over the years need to be identified, as well as the possible causes for the present state of damage. Such a survey was carried out in the study to assess the safety and suitability of the upper deck of the Luiz I bridge in Oporto (Costa et al., 1998) for integration into a light metro network, thus subjecting the bridge to more severe load conditions. This research led to finding most of the original design plans, details about the construction and also details regarding the various changes carried out in the structure between its inauguration in 1881 up to the year of the study in 1996. Another case where an adequate historical survey was fundamental is the one regarding the safety assessment of the 1596 Serra do Pilar Monastery, (Almeida, 2000), Figure 19.1. During the survey, researchers were able to gather important information about changes carried out in the structure over the years, especially those regarding the construction of

a reinforced concrete beam at the base of the church dome which, otherwise, would not be included in the analysis, Figure 19.2.

19.3. Defining the constructions

Structural and architectural surveys and inspections of the constructions must be accomplished. If original design plans are available they should be used to determine if the actual construction is, currently, as originally designed. A good knowledge of the original building materials and construction techniques is essential to fully understand how the construction works. This stage of the global strengthening and repairing process may also be used to create databases of material and construction techniques that will prove to be a valuable help when studying similar constructions. As an example of such a work, the definition of the existing constructions in the Faial Island of the Azores is presented in the following. This survey was carried out following the July 1998 earthquake.



Fig. 19.1. Church of the Serra do Pilar Monastery: (a) main entrance; (b) interior; (c) dome



Fig. 19.2. Damage state of the church of the Serra do Pilar Monastery: (a) overall view; (b) dome retrofit works previously carried out

Since original design plans were not available, the survey involved around 400 houses along the wards of Matriz, Praia de Almozarife and Cedros in Faial Island. Three types

of construction were essentially identified: single-storey houses generally more modest and located in flat rural areas, Figure 19.3; two-storey houses more common in the wards' urban centres, Figure 19.4; and buildings with two and three storeys located in urban quarters, Figure 19.5.

Often it was difficult to determine the precise construction date as many houses were altered during their lifetime. Many were rebuilt or modified due to previous earthquakes.



Fig. 19.3. Rural house



Fig. 19.4. House in the ward's centre



Fig. 19.5. Urban house

Different forms of constructing exterior walls, i.e. the main structural members, were also identified, depending on the location (urban or rural) and on the owner's economic resources. The following types of walls are commonly found on the island (Correia Guedes and Oliveira, 1990): higher quality masonry, built with regular trimmed stone (trachyte, basalt, volcanic tuff or andesite) in alternating rows (or supports), placed parallel to the wall, and of cross-beams perpendicular to the wall, Figure 19.6; masonry of irregular stone, consisting of the same material as in the above item plus "burnt stone" which is placed and treated with greater or lesser care, mostly depending on the builder. The stones are interlocked to guarantee good performance, and the voids are filled with material of smaller granulometry or sometimes with clay, Figure 19.7, which may have "beds" (wall layer) and "battens." Even if well built, this masonry work generally does not perform well under seismic action; masonry of two leaves or "double-wall," Figure 19.8, made of selected stones slightly longer than half of the wall's thickness. The stones are interlocked and form well defined and spaced layers less than 1 m high.

In the rural areas of the Faial Island, houses have mostly exterior walls of the second and third types, which are about 65 to 70 cm thick. Usually, house interiors have double-leaf plaster walls, either with a hollow interior or filled with 2.50 cm thick boards, comprising a latticework that is plastered with lime, sand and clay mortar, and sometimes including also cow hair or even human hair. In some cases, interior walls may be found to be used also for structural purposes, Figure 19.9.

Most houses have the same type of roof structure, commonly called "scissor roof," Figure 19.10. These have sloping joists (i.e. in the water flow direction) of various sizes, from 14x5 cm² to 19x7 cm², spaced at about 35 cm and supporting the roof lining. These joists are supported by a 10x10 cm² main beam (a size which also varies from house to house) which is embedded in the wall crowning. The opposing walls supporting the main beam are connected by braces, which may be made of tree trunks

of irregular shape, with a circular cross section and trimmed ends, or with a rectangular cross section. The roof frame is covered by a lining or dust guard of overlapping boards that support the regional barrel tile. The roof finishes the façade with simple eaves, and frequently with double or even triple eaves, supported on the coping which is salient from the wall.



Fig. 19.6. Masonry of regular trimmed stones

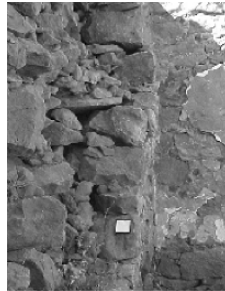


Fig. 19.7. Masonry of irregular stones



Fig. 19.8. Double-wall masonry

19.4. Observation and surveyed damages

The nature of earthquake damage is closely related to the structural material, the type of masonry and to the structural solution. The careful observation of the damages that occurred during an earthquake is fundamental to fully understand the origin of the structural deficiencies and, therefore, to develop adequate and efficient repairing techniques. The majority of the houses damaged by the Azores earthquake had the following most significant structural damages: one of the gables or façades collapsed, Figure 19.9; corner walls collapse due to defective connection between them, Figure 19.11; and total collapse, Figure 19.12.



Fig. 19.9. Aspect of the building's interior



Fig. 19.10. Structural roof solution ("scissor" roof)



Fig. 19.11. Collapsed corner

Besides these types of damage, most houses experienced general wall cracking, with substantial relative displacements in stones, which shows that the roof provided some support to the walls in various houses, Figure 19.9. Some single-storey houses exhibited cracks where the electricity wiretap frame was mounted, Figure 19.13, while in others the end wall (normally without support at the top) experienced large displacements and fell to the exterior, causing a 45° crack in the main façade, Figure 19.14.



Fig.19.12. Total collapse



Fig. 19.13. Cracks where the electricity wiretap frame is mounted on the wall



Fig. 19.14. 45° crack in the main façade caused by the displacements of the end wall

This type of construction is considerably vulnerable to ground motions with small focal distance and possessing a very important vertical component. One of the most important effects of this vertical component is the counterbalance of the self-weight of the walls. However, this effect may be far worse, leading to the collapse of the walls, since the dominant frequency of this component, between 6 to 7 Hz, is of the order of magnitude of the fundamental frequency of the walls. An adequate knowledge of the earthquake characteristics in the construction's location is of paramount importance when interpreting the damage and will lead to the development of more reliable strengthening design options. In a simplified way, ground motions with small focal distance can be expected to have more influence in constructions possessing higher stiffness, like masonry or adobe constructions, while ground motions with large focal distance can be expected to influence constructions that are more flexible, like reinforced concrete or steel structures. The strengthening and repair options should also be different from one case to the other. In masonry or adobe constructions, the strengthening options should favour provisions to increase the stiffness and strength of the walls and to improve the connections between them, tying the structural elements with efficiency and making them work as a continuous unit. In addition, wood floors should try to provide adequate bracing of the walls along their height and distribute the external forces to the structural elements. On the other hand, in reinforced concrete or steel structures the strengthening options should favour provisions to increase the ductility of the structural elements. In this case, the repair of the structure must be carried out accounting for the development of inelastic behaviour in specific zones of the construction and following a prescribed hierarchy. In the end, the repair solutions of structures with higher stiffness are usually defined to provide additional stiffness and strength to support the earthquake forces while in more flexible structures the repair solutions aim to improve the deformation capacity of the structural elements in order to dissipate the energy of the earthquake in a stable form.

19.5. Material mechanical characterization

19.5.1. INTRODUCTION

Knowledge about the mechanical properties of the structural materials is essential for a reliable numerical modelling of the structures under consideration. Any type of strengthening solution which does not include adequate knowledge about the mechanical properties of the structural materials may comprise potentially serious errors that can jeopardise the reliability and safety of the final construction. A reliable knowledge about the stiffness and the mass of the construction is essential to perform even the simplest analysis. The stiffness depends essentially on the modulus of elasticity while the mass depends on the density of the materials. When speaking of existing structures, these parameters, as well as many others, cannot be selected as in the case of the design of new constructions. Therefore, they will have to be defined based on experimental data. In many cases, the experimental tests required to obtain the necessary mechanical properties are relatively simple and common and are carried out on site or in laboratory facilities. For example, in the case of reinforced concrete structures, tests on concrete and steel samples extracted from the structure allow for the knowledge of most of the required mechanical properties (modulus of elasticity, Poisson coefficient, and compressive, tensile and shear strengths). In the case of constructions with irregularly constructed masonry, like the one found in the previously cited houses in the Azores, only in-situ tests can give accurate enough results of the mechanical properties due to the heterogeneous material of the walls.

Some non-destructive tests, as well as others partially destructive, commonly used to obtain the mechanical properties of the structural materials will be presented in the following. Also in many cases, such tests allow foreseeing the effectiveness of different repairing and strengthening options.

19.5.2. TESTS ON STONE MASONRY CONSTRUCTIONS

In this type of structure, samples of stone or stone and joint material can be extracted to perform laboratory tests to obtain the tensile and the compressive strength of the stone, or to define the sliding properties of the joint. On the other hand, in-situ tests should also be performed to obtain the dynamic characteristics of the structure (natural frequency and vibration modes), like dynamic identification tests, measurements of the velocity of propagation of ultrasonic pulses or dilatometric tests.

19.5.2.1. *In-situ tests*

In-situ tests should be performed whenever possible due to the amount of information they give about the construction under analysis and also due to the impossibility of obtaining laboratory samples that accurately reproduce on site conditions. Among the many available types of tests described in the literature, some of those that were performed in the scope of previous repairing and strengthening projects will be presented hereon.

In the case of the previously cited Azores masonry houses, in-situ tests were performed to characterise the materials and to test some repairing solutions. Several houses representing the region's typical construction methods and materials were selected. These houses normally had two or more openings and, therefore, at least three spandrels where it would be possible to apply two types of strengthening, thus leaving one intact, (Costa, 2002a). Each of the spandrels was subjected to cyclic loading in order to obtain

displaced shapes along the height. Correlations with the modulus of elasticity could then be obtained.

To estimate the masonry's mechanical property values, relations were established between the measured parameters and the properties of the structural materials. It was also necessary to obtain a better knowledge of the wall's interior filling material in order to estimate the mass of the wall. The mass was determined by extracting specimens from each wall in order to allow for mass density estimation, for visual inspection of the actual wall core and for some laboratory testing. The mass density of each wall was determined based on the quotient between the weight of the sample and the volume of the extraction hole. In addition, various vibration records representing different load stages after impact loadings with a sledge-hammer normal to the face of the wall were obtained by an accelerometer placed on top of the wall. These vibration records and the respective analyses are an indirect technique of estimating the mechanical elasticity properties of a given structure. Based on the analysis of all the data, the range of predominant frequencies and damping ratios of the walls was obtained. The value of the modulus of elasticity may also be quantified based on the fundamental frequency values for the various walls (Costa, 1999).

Measuring the velocity of propagation of ultrasonic pulses is another type of test that has been used in masonry constructions. With this test it is possible to find defective zones of the construction, like cracks or the existence of cavities and voids in the structural elements, based on the measurement of the velocity of waves propagating throughout the material. Also good estimates of the values of the modulus of elasticity and of the compressive strength can be obtained (Almeida, 2000). In previous studies, this test was performed on samples extracted from the constructions and also directly on masonry walls. The results obtained from the tests performed on the samples were found to be in agreement with the expected values. On the other hand, the results from the tests performed on the walls were not satisfactory, probably due to the highly heterogeneous material of the infill of the walls. For this reason, application of this test to masonry constructions is still limited.

Another type of test that has been used in previous works is the dilatometric test. Using this test it is possible to assess the deformation characteristics of the materials. After drilling a hole through the wall under analysis, a hydrostatic pressure is applied to the inner walls of the hole through a membrane (Figure 19.15). The deformations resulting from the applied pressure are then measured and, subsequently, the modulus of elasticity of the tested zone may be calculated (Almeida, 2000).



Fig. 19.15. Dilatometric test: (a) the equipment; (b) setting the equipment; (c) performing the test

19.5.2.2. Laboratory tests

These tests are usually carried out on samples of the structural materials extracted from walls using a drilling machine, Figure 19.16. During the extraction of the samples and after careful analysis of the holes in the walls, it is possible to have a general good description about the arrangement of the stones within the walls and the existence of cavities and voids. Therefore, it is possible to know how the external walls of the constructions are organized. For example, in the case of church walls, (Moreira et al., 2001), they usually comprise double-leap stone walls around 0.60 m thick near the buttresses, which have an internal filling composed of small size stones and mortar.

During the operation of extracting the core samples, it was observed that some of these samples are only composed of stone while others comprise both stone and joint material.

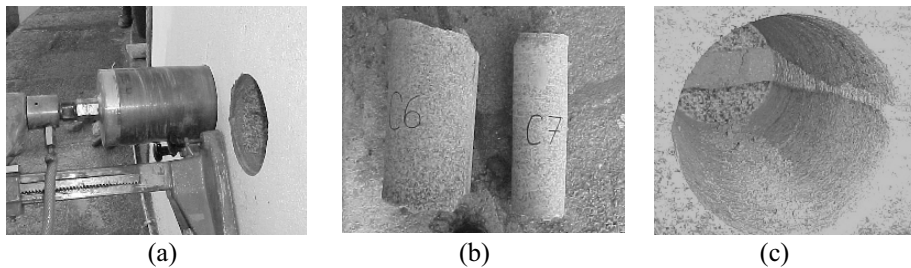


Fig. 19.16. (a) Extracting the core samples; (b) sample of the material; (c) interior of the hole

The definition of the properties of the stone blocks, from the extracted samples composed only of stone should be subjected to tests in order to obtain parameters like the compressive, tensile and shear strengths, or the modulus of elasticity. Figure 19.17 presents some of the tests performed on samples extracted from the church of the Serra do Pilar Monastery.

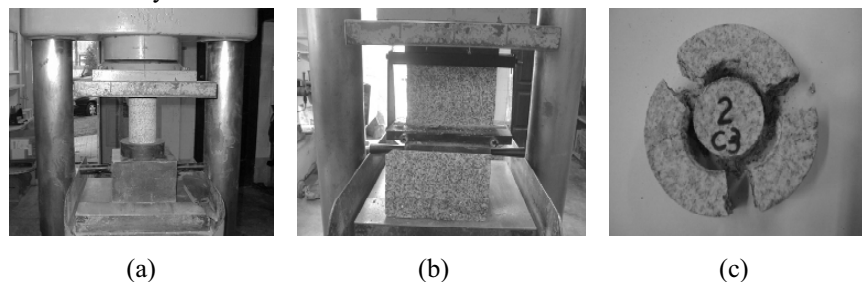


Fig. 19.17. Tests on the stone samples: (a) compression test; (b) tension test; (c) shear test

Tests were also performed on the extracted samples where both stone and joint material were present. Two types of joints were identified a dry joint and a mortar joint. These tests were carried out to assess the strength of the samples when subjected to loads normal to the joint and to sliding, Figure 19.18. From the results of these tests it is also possible to estimate the normal and sliding stiffness of the joints, thus enabling the definition of behaviour laws for this material (Almeida, 2000).

19.5.3. TESTS ON STEEL STRUCTURES

A series of experimental tests were performed by INEGI at the Mechanics Department of the Engineering Faculty of Universidade do Porto (FEUP) for the Metro do Porto S.A., (Coelho et al., 1996), concerning a study carried out by the Construction Institute of FEUP to assess the safety and suitability of the upper deck of the Luiz I bridge in Oporto for possible integration into a light metro network. These tests aimed to determine the remaining lifetime of the bridge due to material fatigue and to the potential fracture of critical elements for the current traffic conditions at that time as well as for the current urban load + light metro traffic conditions. The assessment was performed using standard methodologies, based on SN design plots, and fracture mechanics theory based methodologies. When considered appropriate, recommendations from international design codes were also taken into account.

The extraction of samples of the structure was performed by a specialized firm after authorization from the Junta Autónoma das Estradas, which is the regulating organism.

Samples were chosen based on the following criteria: samples were extracted from structural elements of the original construction of the bridge; the number of samples were as low as possible; samples should be representative of the more common structural shapes used in the bridge, steel equal leg angles, including their various thicknesses; samples should be extracted from structural members subjected to large as well as small internal forces.

The following tests were performed on the extracted samples: tension test, resilience test, the crack opening displacement test (COD), crack propagation test, material fatigue test, hardness test, macrographic test, impact test, chemical composition test, and tests to determine the elastic mechanical properties.

Based on the test results, it was possible to completely characterize the type of steel that was used in the construction of the bridge as well as to obtain an estimate of the maximum tensile strength to be used in the safety assessment of the bridge (Costa et al., 1998).

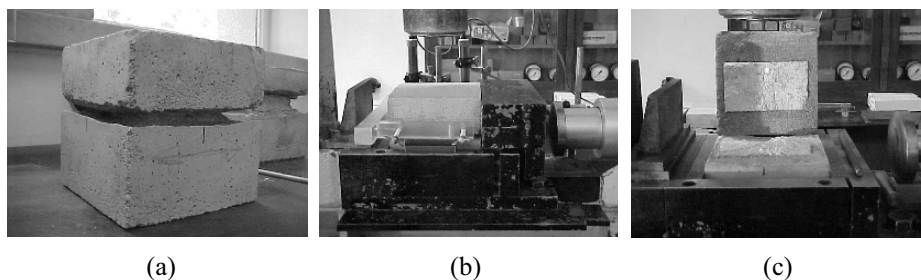


Fig. 19.18. Tests on the joints: (a) the joint sample; (b) beginning of the test; (c) the joint sample after the shear test

19.5.4. TESTS ON REINFORCED CONCRETE STRUCTURES

In order to illustrate some of the possible tests that may be conducted on reinforced concrete structures, a brief description of the works carried out to assess the structural safety of a reinforced concrete building located in the city of Maputo, Mozambique, will

be presented in the following. The construction of the building began in 1974 but was interrupted after the structure of the building was completed and no additional protection for the damaging environmental agent effects was defined (Costa, 2001).

The need to retrofit and possibly strengthen the structure, accounting for its future use, led to the full geometric identification of the structural elements as well as of their reinforcement detailing, and to the assessment of the level of deterioration of the structural materials and of their strength characteristics. In addition, load tests were carried out in representative zones of the structure. This study was also complemented by a numerical analysis where the structural safety assessment of an elastic model of the structure was performed. Based on these results a specific retrofitting methodology was prescribed. The following tests were performed: tests for small duration static loads; surveys of bar arrangement; surveys to identify the type of foundation; carbonation tests; dynamic tests to identify the fundamental frequency of the building.

The tests for small duration static loads (Figures 19.19 and 19.20) may be performed in any type of construction (masonry, steel or reinforced concrete structures) and aim to verify the structure's suitability to safely support the loads in accordance with the specific use of the building.

Through this test, the deflections of the structure are measured for different loading cases in representative zones and at different times to account for creep effects. After removing the loads, residual deflections are also measured. If these exceed specified percentages of the maximum deflections this can be seen as an indicator that permanent cracking may have occurred and/or that the behaviour of the structure is no longer elastic.

The type of steel used in the reinforcement was identified by performing tests on samples with different diameters considered to be representative of the building's reinforcing steel and that were extracted from columns and beams of the structure. Tension tests were performed according to the Portuguese NP-105 norm and led to estimates of the yield and ultimate stresses and strains.

The surveys for bar arrangement can be carried out using radar scanning equipment, like the Microcovero (Figure 19.21).



Fig. 19.19. Static test on a reinforced concrete slab



Fig. 19.20. Loading of a slab with 1 kN/m^2 load



Fig. 19.21. Survey of bar arrangement using scanning equipment

Additional prospecting was also carried out in zones of higher reinforcement density to confirm its detailing.

Estimates of the compressive strength of the concrete and of its superficial hardness can be obtained using the Schmidt rebound hammer. The device consists of a spring loaded steel mass that is automatically released against a plunger when the hammer is pressed against the concrete surface.

The level of carbonation of the reinforced concrete was obtained by several tests with a phenolphthalein solution performed on several structural elements.

19.5.5. DYNAMIC CHARACTERIZATION OF STRUCTURES

The dynamic characterization of constructions plays an essential role in repairing and strengthening damaged structures, hence it should always be performed for any kind of structure (masonry, steel or reinforced concrete structures). In some cases, these tests can be used to identify only the first vibration frequency (Costa and Oliveira, 1997), while in other cases a full modal identification of the construction can be conducted (Neves et al., 2004), therefore enabling the calculation of a range of frequencies and of vibration modes.

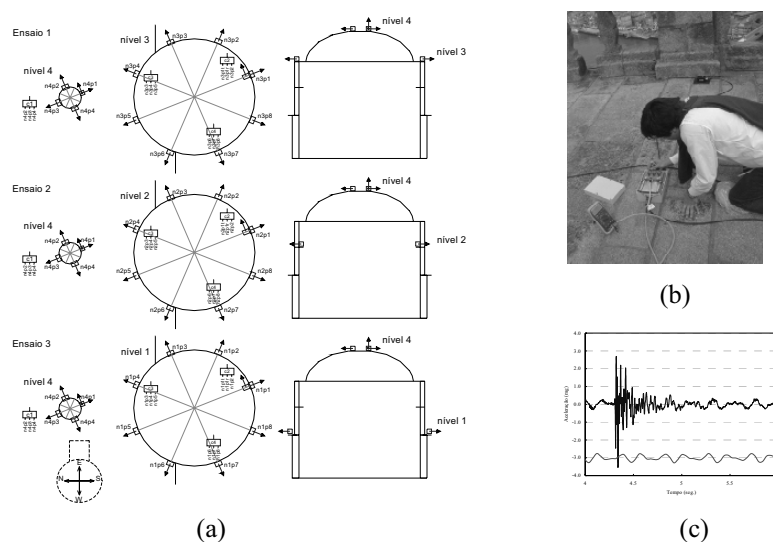


Fig. 19.22. Dynamic tests: (a) test setup; (b) data acquisition system; (c) sample of the record from the explosions of low power detonators

Besides the obvious dynamic characteristics that can be defined by such tests, other structural properties may also be obtained. Based on the dynamic tests results, it is possible to obtain estimates of the modulus of elasticity of the structural materials. On the other hand, the same results may provide a valuable help to calibrate numerical models trying to represent the behaviour of the construction.

A series of dynamic tests were carried out at the church of the Serra do Pilar Monastery. These tests were performed with the collaboration of the National Laboratory of Civil Engineering. The testing campaign (Almeida et al., 2002) consisted in the measurement of accelerations induced in the church structure by ambient sources of excitation (like

wind and traffic in nearby roads) and by explosions of low power detonators buried in the area surrounding the church (Figure 19.22). From these measurements, a full identification of the dynamic behaviour of the structure was carried out from which the natural frequencies and their vibration modes were obtained.

Based on the test results, the material property values were calibrated. A numerical computation of the frequencies and vibration modes was done using the computer code CASTEM 2000 (CEA, 1990) using the material property values obtained from the tests, Figure 19.23, (Arède et al., 2002).

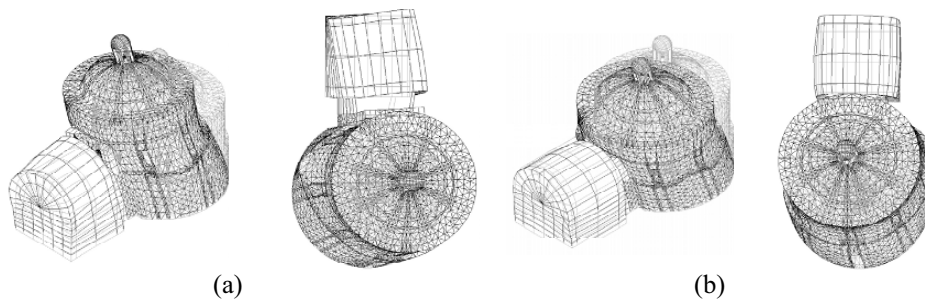


Fig. 19.23. Views of the numerical vibration modes: (a) first mode; (b) second mode

19.6. Numerical analysis

19.6.1. INTRODUCTION

The numerical modelling of the buildings is a fundamental operation for an adequate understanding of the structural behaviour and to obtain the internal forces necessary for the redesign of the members to repair or strengthen. In many cases it is also possible to simulate the actual behaviour of the structure when subjected to a real earthquake that may have been recorded at the site of the structure. Such simulations allow the identification of the critical zones of the construction enabling, in a following stage, the numerical modelling of the repaired structure and the comparison of the efficiency of different repair strategies.

19.6.2. SELECTING THE ANALYSIS PROGRAM

The selection of the analysis program to perform the numerical simulation of the structure must be carried out with much care and understanding of each program's limitations. Depending on the type of results that are needed, benefits can be found in many cases when the program allows some degree of interaction with the user in order to simplify the comprehension of the results. When large structures are analysed the number of results provided by the software may be of little use if not previously filtered or efficiently displayed. Some of the existing commercial analysis software can account for this type of special need from the user, many other programs don't. Therefore, the use of in-house developed analysis programs is favoured in many situations since they allow the user to change and adjust all the parameters of the analysis, especially those regarding the output of results in order to suit them to each specific situation. As an

example of this type of problem, reference is made to the study of the Luiz I bridge previously referred. As formerly stated, the study aimed to determine the suitability and safety of the upper deck for integration into a light metro network. During this study, it was necessary to verify if the internal forces of the structural members exceeded their strength capacity for the light metro traffic conditions. This task would have been extremely hard if a specific script to filter the output results hadn't been previously introduced in the program. This script performed the simple task of comparing the internal forces of the members with their corresponding strengths, generating after this a coloured graphical output of the corresponding demand/capacity ratios (Figure 19.24). Although the tasks were simple, the main problem was the high number of load combinations (more 1400) since it involved moving loads and also the fact that more than 4200 structural elements were present. After implementing this script, the analysis of the results was greatly improved and the decision making process of where and how to repair or retrofit was greatly enhanced.

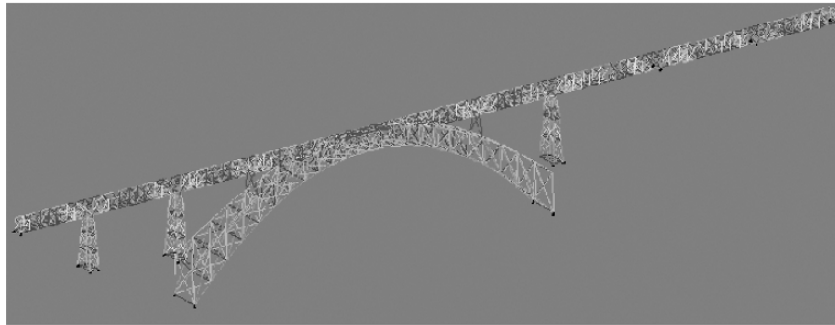


Fig. 19.24. Coloured graphical output of the demand/capacity ratios of the structural

In most of the cases analysed by the author, structural analyses were performed using software developed at FEUP that allows both static and dynamic analysis of structures, including the possibility of modelling materials with linear or nonlinear behaviour. For instance, the numerical modelling of the previously cited Azores masonry houses was performed using the software NLDYNA (Faria, 1995). In the case of the Luiz I bridge the analysis was performed using the software FEMIX (Azevedo and Barros, 1995). The software that has been most used in modelling masonry constructions, stone masonry arch bridges (Costa, 2002b), churches (Moreira et al., 2001; Almeida, 2002) and houses (Neves et al., 2004) is CASTEM. Although not developed at FEUP, CASTEM allows the definition of scripts that allow for the previously stated interaction with the user. In addition, this program allows also the user to improve the computer code by adding new modelling features. This program is available at FEUP through a protocol with the European Laboratory for Structural Assessment (ELSA) at Ispira, Italy. For reinforced concrete structures the program PNL has been widely used over the last years (Costa, 1989; Varum, 1995; Romão, 2002) allowing for the automatic design and performance evaluation of reinforcement concrete structures accounting for the nonlinear behaviour of the materials and the current Portuguese (RSA, 1983; REBAP, 1983) and European (EC2, 2001, EC8, 1994) design codes, (Romão et al., 2002). A more recent development of this program includes the redesign of structures needing retrofitting as well as the safety assessment of the retrofitted members (Rocha et al., 2004).

19.6.3. NUMERICAL ANALYSES

The first stage of the analysis process is calculation of the fundamental frequencies, and corresponding vibration modes, of the construction using the material properties obtained from the experimental tests previously cited. By comparing the numerical frequency results with the ones obtained by the dynamic experimental tests, it is possible to calibrate the numerical structural model. A sample of the first vibration mode configuration numerically obtained is presented in Figure 19.25.

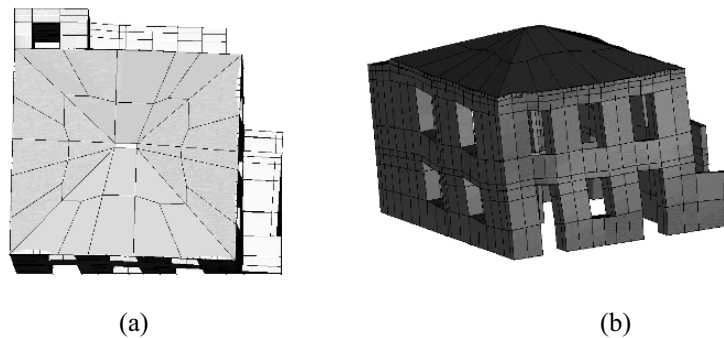


Fig. 19.25. Layout view (a) and perspective (b) of the first vibration mode (5.7 Hz)

In the second stage of the analysis process, a time-history analysis of the structure should be performed. This analysis should consider the three components of the ground motion. The ground motion can be defined by real earthquake records when such records are available, otherwise, artificial accelerograms matching the design code response spectrum must be defined (Oliveira et al., 1998).

These calculations generated time-history results in terms of displacements at various zones of the structures, and stresses and internal forces over several locations of the walls. In addition, maximum values of the principal stresses, internal forces and displacements are also obtained all over the structures. Samples of these results are presented in Figures 19.26, 19.27 and 19.28.

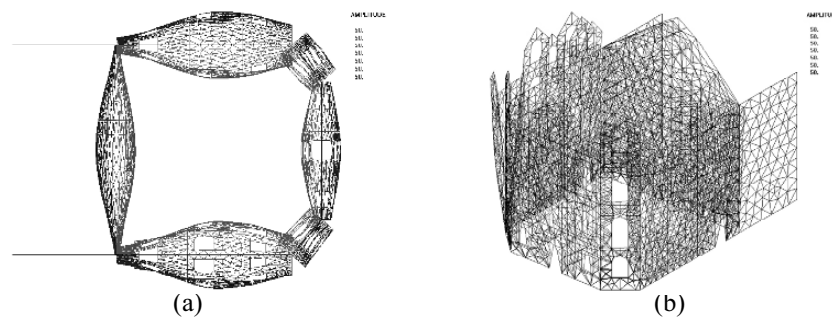


Fig. 19.26. Maximum out of plane displacements of the walls (amplification of 50x): (a) in plane; (b) perspective

Figure 19.26 presents the maximum displacements in the out of plane direction of the walls of the urban house, Figure 19.25 (Costa et al., 2001), while Figure 19.27

illustrates the distribution of maximum axial forces and bending moments on the main façade wall.

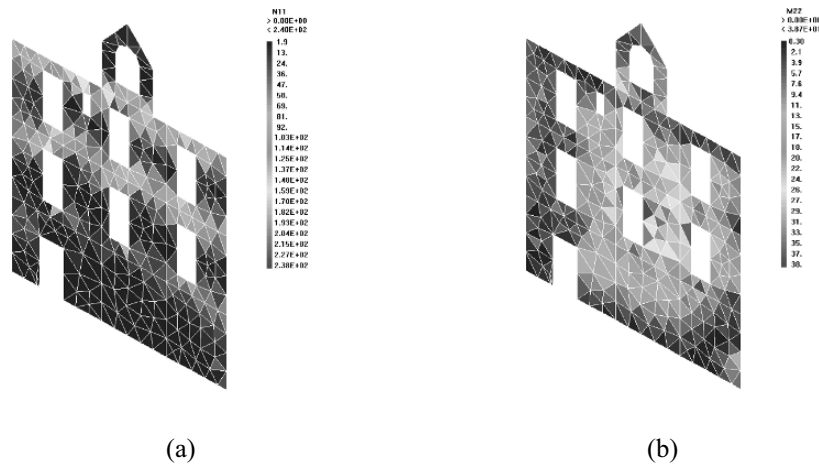
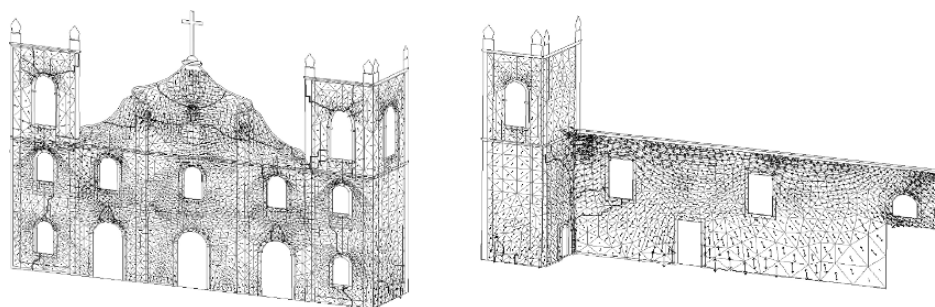


Fig. 19.27. Maximum internal forces in the main façade wall: (a) axial forces; (b) bending moments



(a) Façades and towers (b) Right tower and right lateral wall
 Fig. 19.28. Principal tensile stress directions and real cracking pattern

Two perspective views of the patterns of the principal tensile stresses for the Bandeiras Church, at the Pico Island, Azores (Neves et al., 2001) are displayed in Figure 19.28. These were obtained during the analysis which included the whole front wall (including the towers) and the right side longitudinal wall (including also the lateral rear part of the right side tower). The pattern of the principal stress directions, particularly for the tension ones, enables determination of the formation of cracks (perpendicularly to the tensile stress directions) in several locations that may be compared with the real cracks.

Finally, Figure 19.30 presents the results of the numerical analysis of a substructure of the church of the Serra do Pilar Monastery (Almeida, 2000). This substructure included the arches and corresponding supports, while the analysis considered the nonlinear behaviour of the joints between the stone masonry blocks.

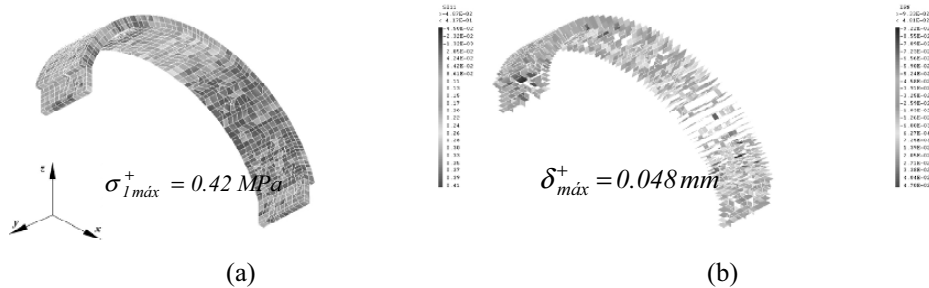


Fig. 19.29. Results of the linear analysis in arch no. 5 for the earthquake loading: (a) principal tension stresses of the stone blocks; (b) maximum opening in the joints between stone blocks

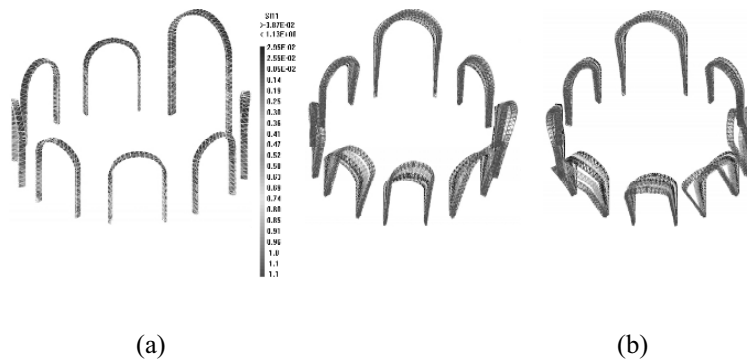


Fig. 19.30. (a) Maximum tensile stresses; (b) maximum displacements in the arches

Figure 19.29 presents the results of a linear analysis of one of the arches from a Roman stone bridge, the Lagoncinha bridge (Costa, 2002b) for the earthquake loading.

19.7. Strengthening solutions and application conditions

19.7.1. INTRODUCTION

Before carrying out a structural intervention on an earthquake damaged construction, the extent of the damages and the value of the construction must be taken into account in order to ponder if the repairing and strengthening operations are still possible and justifiable. Factors such as the patrimonial value of the construction, the economical interests of the owners or the simple location of the construction (whether it is or not located in a high seismic risk zone) must therefore be carefully pondered before deciding the final course of action.

From the structural point of view, and in particular regarding earthquake safety, the main purpose of the strengthening operations is not only to repair the damage of the construction but also to improve their seismic strength concerning future earthquakes bringing it as close as possible to the seismic strength of a new construction. Nevertheless, the rehabilitation and strengthening techniques must take into account the

type of damages and must be based on a good understanding of what caused those damages in order to prevent them from reoccurring in the future.

19.7.2. STONE MASONRY STRUCTURES

In the case of the previously cited Azores houses and considering the construction typology of most of the buildings on the Faial Island, it was concluded that they were built according to traditional construction methods, and that is why most of the earthquake damages were also very similar.

In rural zones, the typical traditional construction is somewhat uniform. Houses have usually two floors, with around 100 m² per floor, with exterior walls made of low-resistance masonry and with wooden floors and roofs. Some urban buildings have higher quality masonry, and greater care in the construction methods was applied to most buildings. Usually, urban buildings were also made using wood of better quality.

Since the structural behaviour problems are similar, the repair and strengthening techniques should also be similar. An exception is made for some specific cases where different structural elements or construction processes were used or because of possible anomalies in structural elements calling for special treatment.

Due to the aforementioned, and by comparison with on-site findings, it was concluded that the damages were caused essentially from the main factors summarised in the following: construction processes resulting in weak wall stiffness and resistance. These problems are also aggravated due to the characteristics of earthquakes in the Azores (close range earthquake, with a strong vertical component and high frequencies); faulty (or even non-existent) wall bracing due to the lack of horizontal supports along the height of the walls; faulty (or even non-existent) horizontal wall bracing; lack of horizontal supports along the height of the walls; inadequate roof construction methods. Since the roofs don't contribute to the bracing of walls, they end up causing horizontal forces at their most critical point, the top end; vertical and horizontal stiffness discontinuity causing larger seismic forces in the connection zones.

The proposed rehabilitation methodologies to correct the aforementioned weaknesses consist essentially of strengthening the walls, floors and roofs. Whenever possible, the existing materials should be maintained. The solution also calls for banding the wood floors and roofs, especially the connections between the various types of structural elements, to guarantee a combined resistance to seismic action, making them work as a continuous unit (Costa and Arêde, 2004).

19.7.2.1. Walls

To ensure that masonry walls will withstand earthquakes, it is first necessary to know what they are made of. This knowledge can only be obtained by chipping and cleaning the surface on both sides, possibly using a water jet before applying any mortar.

The walls should be strengthened according to the scheme in Figure 19.31a according to which these walls merely need to be wetted and then repaired with plaster, followed by the application of a stainless steel mesh covered in plaster and a sanded finish ready for final painting. Free walls running parallel to floor beams and roof braces must be braced at the roof and floor levels as shown in Figure 19.31b.

19.7.2.3. Roofs

The roof structure plays an essential role in these buildings since it supports the crowning of the walls. Because of its shape, the roof may behave like a very rigid sub-structure, provided its elements are in good condition and firmly connected to the walls. The roof's various wood elements must be inspected and replaced when exhibiting inadequate structural or physical preservation characteristics. The procedure illustrated in Figure 33a must be applied to connect the truss braces to the exterior walls using angle plates running along the top of the walls and all around the building's interior perimeter, thereby providing continuity at the corners. Gable ends that are not adequately supported may be braced according to the detailed illustration in Figure 33b.

19.7.2.4. Other structural elements

In the structural system of the buildings under study, some of the interior walls must be strengthened in the zones of their connections to the exterior wall, as shown in Figure 19.34a. These connections will be strengthened by placing brackets or angle plates in the corners bolted to the exterior walls with steel anchors. In these circumstances it is also important to provide a higher stiffness to the interior walls by applying the same strengthening solution previously presented for the walls. The neighbouring partition wall that generally separates two contiguous buildings must also be properly strengthened using the same solution described for walls in item 19.7.2.1. The process illustrated in Figure 19.34b presents the connection of this partition wall to the exterior façade walls that must also be accomplished. This strengthening solution is similar to the one recommended in Figure 19.34a, but has strengthening brackets bolted to both walls and embedded in the reinforced plaster.

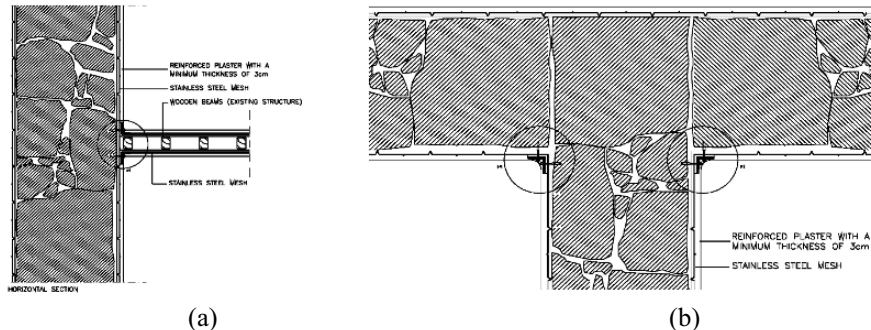


Fig. 19.34. Connections to exterior walls (ground plans): (a) interior wall to exterior wall; (b) neighbouring partition wall to exterior wall

19.7.2.5. Field applications of some of the strengthening options

The structural strengthening work described in the previous points was performed at two of the Azores houses previously cited: the rural house (single floor) and the house with a ground floor and first storey in the Cedros ward centre. Some details and photographs taken of the houses after the repair works are shown below.

Figure 19.35 illustrates the angle plate supporting the roof braces that is also part of the wall-crown band. Note how the plate is fastened to the wall using threaded rods crossing the walls, shown with more detail in Figure 19.36. Figure 19.37 shows a

reinforced plaster application stage, whereas Figure 19.38 shows the already plastered house.



Fig. 19.35. Angle plate supporting the roof braces



Fig. 19.36. Detail showing the brace support and the angle plate's connection to the wall



Fig. 19.37. Application of the reinforced plaster



Fig. 19.38. House with finished plastering operation

19.7.3. STEEL STRUCTURES

The strengthening of steel structures like the one of the Luiz I bridge previously cited implies many times the need to adequately brace some of the structural members. After performing the analysis of the structure, the existence of members that are unsafe due to buckling effects is a common situation in structures from the end of the XIX century. This situation arises from the fact that at the time of the original design the buckling effects were still pretty much unknown (Costeira and Costa, 2002).

When some of the structural members need strengthening, this situation is always related to the need to increase their cross section. The original structural shapes of the cross section are usually formed by steel angles or plates and their strengthening is in most cases performed by adding plates or other elements (Costa, 1996).

19.7.4. REINFORCED CONCRETE STRUCTURES

19.7.4.1. Introduction

Damage in reinforced concrete structures can come from many origins. Any type of structural strengthening or repairing operation must be carried out taking into account the origin of the damages in order to guarantee its efficiency.

Most damages in reinforced concrete structures may be attributed to the following causes: design or detailing errors; faulty construction practice related, for instance, to the use of inadequate materials, to the lack of qualified workmanship, or to the lack of proper inspection during the construction; structural degradation or alterations inadequately designed and executed as, for instance, the removal of interior walls, the change in the building functions, the increase of the number of storeys, the creation of unexpected openings in the exterior walls at ground floor level or in other walls of the construction.

If natural causes, such as earthquakes, are associated to these human errors, the necessary conditions for the collapse of the construction are then fulfilled. It is often said that an earthquake will identify all the errors of the construction and make use of those errors to cause its collapse.

The most common techniques to strengthen and to restore the structural integrity for reinforced concrete structures may be divided into two major groups: global level strengthening techniques and local level strengthening techniques (Pinho, 2000). Regarding the first group the following methods can be used (Varum, 2003): adding reinforced concrete shear walls; adding steel bracing elements and post-tensioned cables, associated or not with energy dissipation devices; base isolation; reduction of the mass of the construction; other techniques as, for instance, active control methods.

Regarding the second group of strengthening techniques the following methods can be used: epoxy injection resins; jacketing of the structural members with steel or FRP's, or reinforced concrete encasement of those members; jet-grouting; other techniques such as, for instance, prestressing existing members, or reducing or increasing the cross section of existing members.



Fig. 19.39. Steel bracing technique

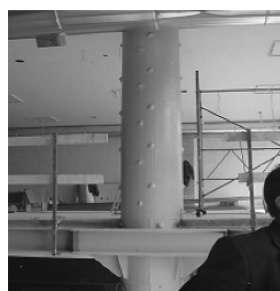


Fig. 19.40. Steel jacketing technique



Fig. 19.41. FRP jacketing technique

Some examples of these repairing techniques are presented in the following figures. Figure 19.39 presents the steel bracing technique (Varum, 2003), Figure 19.40 shows the steel jacketing of a column (Costa, 2003), Figure 19.41 displays an example of the

FRP jacketing of a column (Varum, 2003), Figure 19.42 presents the reinforced concrete encasement of a column (Costa, 2002) and Figure 19.43 shows an example of jet grouting on a wall (Varum, 2003). When the repairing technique only aims to increase the reinforcement area of the member due to its inadequate original design, the steel jacketing technique can also be accomplished using only some steel angle shapes and steel plates along the height of the column (Figure 19.44; Costa, 2004).



Fig. 19.42. Reinforced concrete encasement technique

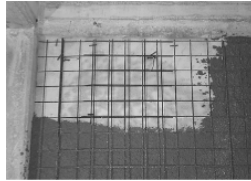


Fig. 19.43. Jet grouting technique



Fig. 19.44. Steel jacketing technique

19.7.5. OTHER EXAMPLES OF STRENGTHENING TECHNIQUES

The strengthening techniques referred to in the previous sections have been used by the author and his co-workers in several practical situations. Nonetheless, similar retrofit techniques can be found around the world. Some strengthening systems used in high seismic risk zones are highly intrusive, without any attempt to hide them. As examples of this situation, the reader is referred to retrofit and strengthening operations carried out on monuments in Sicily, Italy (Figures 19.45 to 19.47). In Figures 19.45 and 19.46 the strengthening techniques are clearly visible on the side of the buildings. Although the same situation also appears in Figure 19.47, some doubts still remain as to whether the strengthening system is fully completed or not. In masonry structures, it is also common to find walls strengthened by steel beams (Figure 19.48) and in some cases the full display of the strengthening system in the form of steel frames is found as a measure of seismic strengthening (Figures 19.49 and 19.50).



Fig. 19.45. Application of steel forks on the capital



Fig. 19.46. Corner wall confinement with steel plates



Fig. 19.47. Wall confinement with steel plates and bars



Fig. 19.48. Lateral wall strengthened by steel structure, Berkeley, California (2002)



Fig. 19.49. Building strengthening with exterior steel frame, Berkeley, California (2002)



Fig. 19.50. Building strengthening with exterior steel frame, Berkeley, California (2002)

19.8. Conclusions

The fundamental steps that must be incorporated into a structural strengthening and repair operation were addressed. Different types of constructions and structural materials were also considered and specific repairing methods were defined for each construction type. The experimental tests used to estimate the mechanical properties of the structural materials were also addressed.

Any type of structural repairing operation must account for the structural problems of the constructions and the type of selected repairing technique should be chosen to preserve as much as possible the existing constructions. Any kind of strengthening operation should be minimalist and the least invasive as possible. It should also make use of the existing structural elements by strengthening them and making them adequate to their final structural functions. After the repairing operation, the final construction must be able to safely survive future earthquake events.

The proposed strengthening solutions take advantage of existing structural members whenever possible. The connection between the existing members and the strengthening elements are efficiently performed and some of them were numerically simulated. Using this type of strengthening solutions, the fundamental frequencies of the

constructions and the range of dominant frequencies of earthquake activity must also be taken into account.

Adequately calibrated numerical analyses are valuable tools, not only to simulate earthquake effects, but also to allow for a more comprehensive knowledge of the observed damages and an easier design of the strengthening elements.

Careful observation of the damages that occurred during an earthquake is fundamental to fully understanding the origin of the structural deficiencies and, therefore, to eliminate them.

Detailed practical field applications of the several steps incorporated in a structural strengthening and repair operation are presented to allow for a clear comprehension of the selected strengthening solutions and to allow for the discussion of this subject which is of utmost importance for earthquake prone regions

Acknowledgements

For their valuable assistance, the author would like to thank all his colleagues who collaborated in this work.

CHAPTER 20
ADVANCED TECHNIQUES IN MODELLING, RESPONSE AND RECOVERY

L. Chiroiu¹, B. Adams² and K. Saito³

1. *Benfield Group, London, UK*

2. *Imagecat Inc, Long Beach, USA*

3. *The Martin centre, University of Cambridge, UK*

20.1. Introduction

Recent advances in the fields of geomatics and remote sensing are bringing significant benefits to the management of earthquake risk, in particular for loss estimation modelling and crisis response. Multidisciplinary approaches are emerging in response to the very high-resolution imagery offered by the new generation of optical satellites, and marked improvements in processing algorithms such as differential interferometry. As their value becomes established through successful implementation, scientific and disaster response communities are increasingly accepting remote sensing techniques as important tools for the assessment and the mitigation of natural hazards.

The value of remote sensing and geomatic technologies for emergency management is also increasingly recognized in national and international arenas (Kerle and Oppenheimer, 2002). Initiatives have been launched internationally by organizations including the United Nations (UN), European Commission (EC), Commission for Earth Observation Studies (CEOS), and various space agencies. Currently, research efforts are being spearheaded through the UN International Decade on Natural Disaster Reduction and its successor the International Strategy for Disaster Reduction (ISDR, 2003), the EC Natural Hazard Project (JRC, 2003), and the CEOS International Global Observation Strategy (IGOS, 2001). The European Space Agency now offers an Earth Watching Service, providing satellite disaster coverage acquired by Landsat, ERS and JERS sensors (ESA, 2003). The FEMA website posts also remote sensing coverage of recent events within the US (FEMA, 2003).

The development of building inventories prior to an earthquake, measurement of the ground displacement caused by the event, and rapid detection of damage once it has occurred, are important research thrusts. These fields make a valuable contribution to general loss estimation modelling. Satellite imagery can provide reliable information about the exposed infrastructure, which is necessary to define the site-specific vulnerability; vertical and lateral displacement provides data for the assessment of the seismic hazard; and the near real-time detection and mapping of affected areas, provides information for the calibration of fragility curves and loss estimation models, and critical support for crisis response and recovery operations. This final function is particularly important for lesser-developed nations, where emergency response is often hampered by poor communications and infrastructure. Relying on traditional ground-based methods of damage assessment, the full extent of damage may not be known for a number of days; an unacceptable delay given the criticality of the initial 48 hours for search and rescue efforts. In contrast, high-resolution satellite sensors such as Quickbird and IKONOS provide a remote regional perspective of the situation, coupled with the detailed visualization of damage sustained by individual buildings, often on a timescale

of less than 48 hours (Depending on various conditions, such as the current positioning of the satellite or the cloud coverage).

The following Chapter assesses the state of the art of these advanced technologies. Following an initial introduction to remote sensing data, emergent applications, methodologies, and tools are introduced and evaluated. Case studies are used to demonstrate their efficacy during a number of recent devastating earthquakes, including the 1999 Kocaeli, 2001 Bhuj, 2003 Boumerdes and 2003 Bam events. The chapter concludes with overarching perspectives and conclusions on the use of geospatial information for earthquake risk management.

20.2. Remote Sensing and Geomatic Technologies

'Remote sensing' is a general term describing the action of obtaining information about an object with a sensor that is physically separated from that object. As a technology, remote sensing dates back to photographs captured during the early nineteenth century. The photographic camera has served as a prime sensing device for more than 150 years, imaging features of interest by concentrating electromagnetic (EM) radiation (normally, visible light) through a lens, onto a recording medium.

The idea of photographing the Earth's surface from the air emerged during the 1860's, with pictures taken from a hot air balloon. However, as the science evolved, sensors have become increasingly sophisticated. After World War II, cameras were mounted on new platforms, such as military and meteorological spacecraft. During the 1960s, imaging sensors were incorporated into orbiting satellites. The first satellite specifically dedicated to the earth observation was designed and constructed by NASA and launched in 1972. ERTS-1 (Earth Resources Technology Satellite), later renamed Landsat, provided multispectral scenes covering a 185×185 km swath, with 30 m ground resolution (Depending on various conditions, such as the current positioning of the satellite or the cloud coverage). Since then, numerous earth observation satellites have been launched, with ever improving spatial and spectral resolution. The genre of data collected has also expanded from standard optical imagery, to include various types of radar.

Applications of remote sensing data for earth observation are diverse, and include geological and ecological applications, land-cover mapping, and urban growth modelling. From a disaster management perspective, landslides or subsidence monitoring, flood damage mapping, and hurricane tracking are common applications. In the case of earthquake, 1906 marks the first occasion where remote sensing technology was deployed. Aerial photographs recorded by G. R. Lawrence, captured widespread devastation throughout San Francisco (Lawrence, 1974).

Since the beginning of the 1990's, complementary geomatic technologies, such as the Global Positioning System (GPS) and Digital Elevation Models (DEM), have also been employed in the international disaster management arena for earthquake prevention, mitigation and modelling. The following sections provide an introduction to common remote sensing data types, together with prominent geomatic technologies.

20.2.1. OPTICAL IMAGERY

Today, earth observation and meteorological satellites as well as airborne sensors provide optical imagery. Satellite imagery is often preferred for natural hazard assessment applications, due to the large spatial coverage and relatively low commercial cost. Until recently, very high resolution imagery was the main advantage of the aerial data. However, satellite sensors are now able to offer submetric ground resolution in panchromatic mode. Table 20.1 lists the main commercial earth observation optical satellites. Currently, more than 15 sensors with a spatial resolution of between 2 km and 0.68 m, cover between 12×12 km and 400×400 km in a single scene.

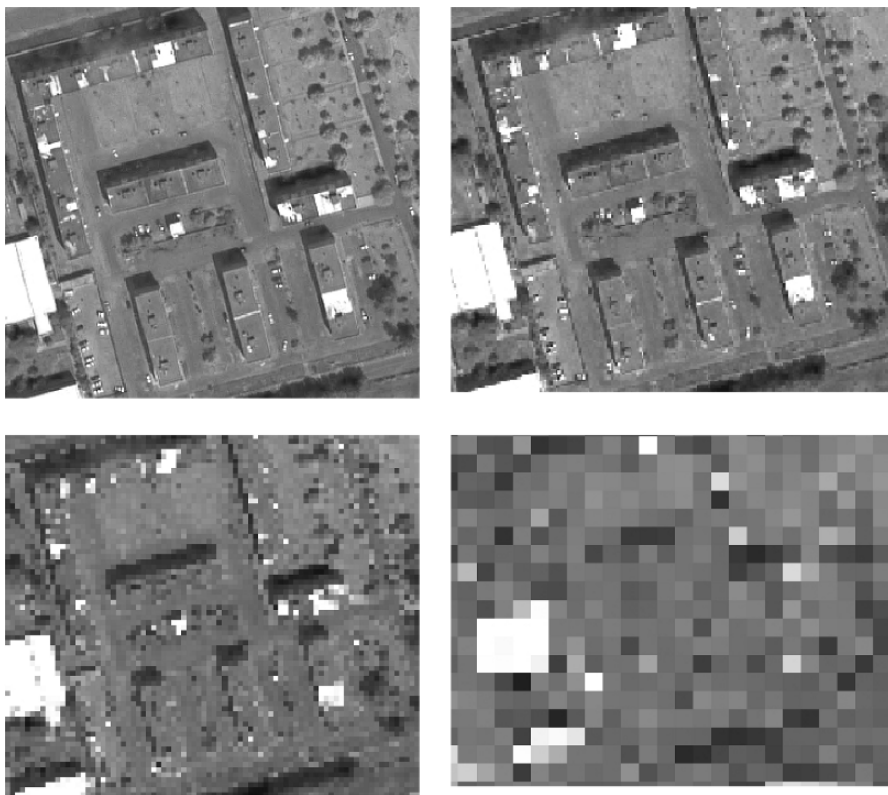


Fig. 20.1. Examples of different ground resolutions: 0.60 m (top left), 1 m (top right), 2.50 m (bottom left) and 10 m (bottom right)

The resolution of the data refers to the size of each pixel - the smallest element of an image. For example, at 100 m resolution (low resolution), objects smaller than 100m × 100m are difficult if not impossible to discern. At moderate 10 m resolution, individual structures are barely recognizable (see Figure 20.1). With 5 m high resolution data, medium multi-story buildings can be discerned, but not residential properties. At 1 m (very high resolution), objects covering an area in excess of 1m², such as cars and trees, can be identified.

Table 20.1. List of the main commercial earth observation optical satellites operational today, with some characteristics of the data provided

	Satellite	Resolution (m)		Swath width (km)	Starting year of operational activity
		Panchromatic mode (P)	Multispectral mode (XS)		
Low Resolution	AVHRR	-	1100	2400	1998
	MODIS	-	250 - 1000	10 - 2330	1999
	MERIS	-	300, 1200	650, 1150	2003
Medium Resolution	Landsat 7 TM	15	30	185	1999
	ASTER	-	15, 30, 90	60	2000
	SPOT 4	10	20	60	1998
	IRS	5.2	21.2	70	1995
High Resolution	SPOT5	2.5	5	60	2002
	KVR	2	-	40	1998
	EROS A1	1.8	-	14	2001
	IKONOS	1	4	11	1999
	ORBVIEW	1	4	11	2003
	QUICKBIRD	0,60	2,40	11	2001

In disaster management, the most common use of optical remote sensing data is for assessing the impacted area after the event. Various applications are documented for the detection and mapping of earthquake damage (Adams et al., 2003; André, 2003; Chiroiu et al., 2002; EDM, 2000; Estrada et al., 2001; Huyck et al., 2002b; Eguchi et al., 2002; Saito et al., 2004). For low and moderate resolution imagery, reconnaissance of affected areas is generally achieved through automatic or semi-automatic procedures. Where high-resolution data is available, these techniques may be augmented with photo interpretation (see § 20.3).

Other applications of optical imagery are related to mapping the earth's surface in 3D. Elevation models and topographic maps can be derived from satellite imagery, using specific techniques as stereoscopy. Recently, researches successfully employed similar techniques to quantify earthquake-related ground displacement (see § 20.3.2).

20.2.2. RADAR IMAGERY

An acronym for Radio Detection and Ranging, radar sensors operate in microwave regions of the electro magnetic spectrum. Unlike passive optical sensors that rely on illumination from the sun, radar is an active device that can function during night and day, without significant interference from atmospheric conditions (e.g. clouds). The technology is based on measuring the return time and the intensity of the microwaves emitted by the sensor and reflected back by the target. As shown in Figure 20.2, the radar beam is particularly sensitive to ground surface texture, the geometry of objects, and water content.

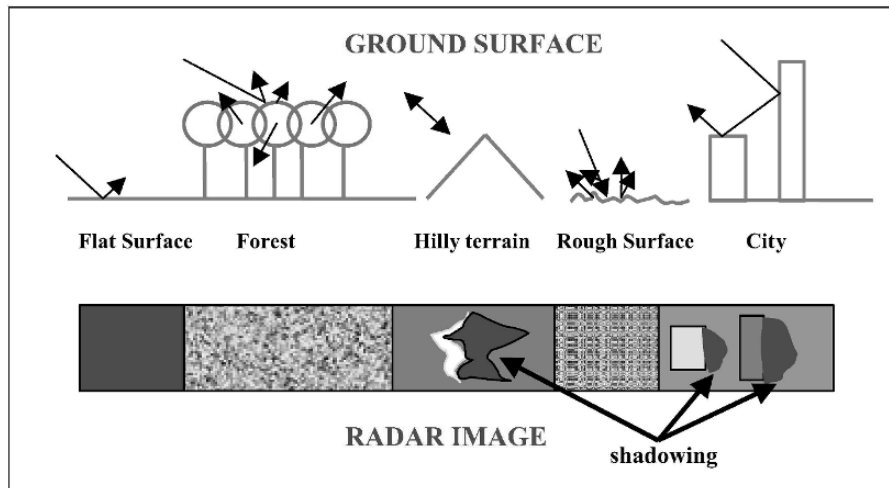


Fig. 20.2. Schematic representation of radar return from various ground surface features (image courtesy of ImageCat, Inc www.imagecatinc.com)

For airborne radar, the antenna may be mounted on the underside of the platform, from where it emits a sideways pointing beam in a direction normal to the flight path. This mode of operation is encapsulated by the acronym SLAR (Side Looking Airborne Radar). A second type of system, Synthetic Aperture Radar (SAR), is exclusive to moving platforms. It uses an antenna of much smaller physical dimensions, which sends forth its signals from different positions as the platform moves. It simulates a real aperture, by integrating the pulse "echoes" into a composite signal. Achieving an effective antennae length of up to 100 meters, the SAR technique produces higher resolution data. It also records both phase and amplitude information for the return beam, whereas SLAR records only the latter. Table 20.2 lists satellite platforms carrying SAR sensors.

Dating back to World War II, radar has been widely used for military applications, such as tracking aircraft and ships. Today, fixed and mobile radar application areas include telecommunications, oil exploration, agriculture and environmental monitoring. In terms of earthquake engineering, radar was originally used for quantifying ground displacement after earthquakes such as the Landers (Massonet et al., 1993), Northridge (Massonet et al., 1996), and Duzce (Burgmann et al., 2002) events. More recently, it has been implemented for post-earthquake urban damage assessment (Aoki et al., 1998; Eguchi et al., 1999; Matsuoka and Yamazaki, 2000) and for the development of urban inventories (Eguchi et al., 2000).

InSAR (interferometric SAR) is another radar-derived dataset. Airborne or satellite mounted InSAR systems acquire interferometric images, which are a pair of co-registered SAR images covering the same area, but taken from slightly different positions. An interferogram is computed, based on the phase difference between the two images. 3D topography is then derived from the interferogram (see § 20.3.3). DifSAR (differential SAR interferometry) is an extension of this technique, yielding differential interferograms. Oppose to simply topographic information, these provide very high precision information about ground displacement (see § 20.3.3).

Table 20.2. List of the main commercial earth observation optical satellites operational today, with some characteristics of the data provided

Satellite	Resolution (m)	Swath width (km)
Envisat (ASAR)	150 - 1000	100, 400
ERS	30	100
SRTM	30	225
SIR	10, 25, 40	50
RadarSat	8, 25, 30, 50, 100	50, 75, 100, 150, 300, 500
JERS-1	18	75

Airborne LIDAR (Light Detection And Ranging) is another active remote sensing technique being used for rapid topography mapping. LIDAR uses the same principles as RADAR, emitting a beam that bounces back from the target below. The transmitted wave interacts with the target and is returned to the sensor. The travel time is used to determine the range to the target, which is in turn converted to ground surface elevation. The main advantage of LIDAR data is the fast processing and high spatial resolution. Digital terrain models can be obtained with a precision between 10 cm and 1m.

20.3. Applications for earthquake risk management

The following sections introduce applications of remote sensing technology for pre-earthquake preparedness and post-earthquake response. The section is organized into four main research thrusts, namely: (1) building inventory development; (2) mapping ground surface displacement; (3) urban damage assessment; and (4) loss estimation modelling.

20.3.1. BUILDING INVENTORY DEVELOPMENT

Building inventories are a key element of disaster preparedness and response activities. The assessment of urban vulnerability is completed using loss estimation software, which in turn relies on an inventory of exposed elements. These elements include buildings, together with infrastructure such as bridges and tunnels (see §20.3.4). Loss estimation models generate quantitative information concerning the amount of damage. However, the distribution of damage is rarely provided, because urban vulnerability is generally evaluated at the city-wide scale. Current broad-scale methods of building vulnerability assessment are typically based on census information detailing the year of construction, square footage and building height. Other methods are based on visual inventory of a 'representative' sample of buildings, with generalization based on statistical extrapolation. Data obtained from both methods are typically integrated into a commercial GIS. However, these systems rarely span an entire urban area, at the building level.

Remote sensing data makes a valuable contribution to the development of building inventories. As described below, information concerning building occupancy and

structural type can be extracted from the high-resolution optical imagery, while radar imagery is a useful source of building height and square footage.

At present, construction material and structural building type (e.g. moment resisting frame or bearing walls) is not discernible from remote sensed data. However, different occupancy types residential properties, multi-story buildings (low rise, mid rise or high rise), industrial facilities and specific structures (e.g. architectural monuments, churches) (see. Figure 20.3), can be detected from the analysis of high-resolution optical imagery. Mapping occupancy type can be undertaken on a per structure basis, or at extended block or census tract scales. In the latter case, occupancy is characterized by the predominant structural type. From occupancy type, further assumptions can be made concerning the year of construction, a factor influencing vulnerability. A significant advantage of satellite imagery for inventory development is that large areas can be analysed without any supplementary information (e.g. Census data).

Researchers have recently developed methodological procedures through which building height and square footage can be obtained from a combination of IfSAR elevation data and optical imagery (Eguchi et al., 1999). Figure 20.4 shows the methodology of derivation of building heights, in terms of a normalized digital surface model (nDSM). Based on the method developed by Huyck et al. (2002a), this nDEM is obtained as the difference between a SAR-derived digital surface model (DSM) and a bare-earth digital terrain model (DTM).

The former DSM represents the apparent ground surface, as a composite of superimposed features, such as buildings and underlying bare earth topography. The latter DTM is solely topographic, obtained from the same base data via a sequence of filters. As shown by the flowchart in Figure 20.4, building heights are recorded as the local maxima within footprints delineated on high-resolution aerial photography. While the present set of building outlines were defined manually, research is progressing towards automated extraction procedures. The heights are then translated to storeys, using a conversion factor that corresponds with standard loss estimation software (NIBS 1997, 1999 and 2002).

Ground level square footage is also recorded on a per building basis, as the footprint area in pixel units. Using a scaling factor based on image resolution, this value is converted to single storey square footage. Finally, the total square footage for each structure is computed as the product of the number of storeys and ground level area.

The efficacy of this methodology has been tested for case study areas in Los Angeles. Results indicate that values for building height and square footage derived from remote sensing imagery correspond closely with independently derived tax assessor data.

Moving forwards, research efforts are focusing on using these results to update existing inventory data within US Federal Emergency Management Agency (FEMA) HAZUS programme. Within the international arena, inventories of this nature are scarce. However, using the techniques shown in Figure 20.4, building stock estimates of square footage and height could be recorded for urban areas around the world. Global inventories of these measurements could be posted online, and in the event of an earthquake applied in tandem with building damage detection methodologies described in the following section to yield a rapid estimate of the damage extent and associated

losses. Chiroiu and Andre (2001) and Chiroiu et al. (2002) similarly employ damage estimates for loss estimation, although in this instance, to quantify casualties arising from the Bhuj earthquake.



Fig. 20.3. a) Residential houses and b) high rise buildings, (image credit: DigitalGlobe.com (a) and SpaceImaging.com (b))

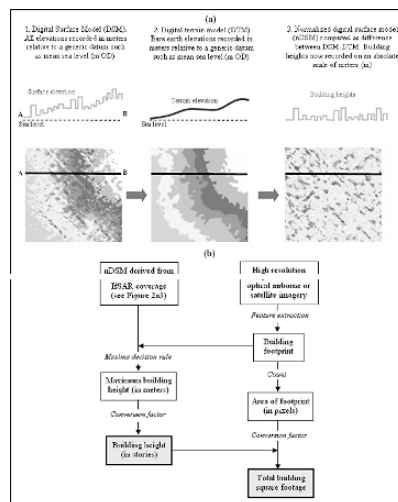


Fig. 20.4. Conceptual representation of methodological procedures used to obtain building inventory data from remote sensing imagery. (a) The derivation of a normalized digital surface model (nDSM) from IfSAR data. (b) Processing steps used to compute building height (in storeys) and coverage (in total square footage). (image courtesy of ImageCat, Inc www.imagecatinc.com)

The former DSM represents the apparent ground surface, as a composite of superimposed features, such as buildings and underlying bare earth topography. The latter DTM is solely topographic, obtained from the same base data via a sequence of filters. As shown by the flowchart in Figure 20.4, building heights are recorded as the local maxima within footprints delineated on high-resolution aerial photography. While the present set of building outlines were defined manually, research is progressing towards automated extraction procedures. The heights are then translated to storeys,

using a conversion factor that corresponds with standard loss estimation software (NIBS 1997, 1999 and 2002).

In addition to earthquake loss estimation modelling, building inventories could generate important information for the mitigation of other hazards, such as terrorism. Terrorism “loss estimation models”, which are used by civil protection and (re)insurance companies, are based on the assessment of the exposure accumulated in a given site. The consequence of an impact could be modelled relatively accurately through a spatial analysis applied to the building inventory data derived from sources such as LIDAR (Huyck et al., 2002a).

20.3.2. MAPPING GROUND SURFACE DISPLACEMENT

Since the early 1990s, post-earthquake ground surface displacement has been measured using radar interferometry (Massonet et al., 1993). SAR images acquired before and after an earthquake are compared using custom software, to produce a picture of ground movement. Changes between the images are represented as fringes, or contours of movement. Each fringe represents an additional increment of movement, which as shown in Figure 20.8, can be summed to give the total picture of ground distortion at a given point. The displacement represented by one fringe could be less than 10 cm, depending on the radar wavelength. Other unrelated sources of change that may introduce errors to IfSAR surface displacement measure, such as topography and meteorological conditions, can usually be identified and removed. However, the accuracy of results is inherently lower in dense urban zones, because the multitemporal radar signal may be distorted by numerous factors, such as the different humidity of buildings or vegetation, and changes in the urban elements. Near-fault zones are also less reliable, because large displacements induce low correlation between the images.

Today, seismic displacement is also being measured from optical imagery, whereby ground surface displacement is recorded using two SPOT 4 images of the same area, acquired before and after the earthquake (Van Puymbroeck et al., 2000; Michel and Avouac, 2002). Differences between these two images are attributable to a number of factors, of which earthquake-related ground displacement is one. By successively eliminating other influences, such as distance between the orbital pathways, variations in viewing angle, and geometry of the sensors, ground displacement may be quantified with an accuracy of 10 cm. This sub-pixel accuracy is impressive, given that the analysis employed 10 m resolution data.

The accuracy with which earth surface displacement is mapped from remote sensing data is generally enhanced through the integration of GPS information. This in turn improves the modelling of stress and fault interactions, with important outputs such as probabilistic time dependent models.

20.3.3. URBAN DAMAGE ASSESSMENT

Remote sensing technology is increasingly recognized as a valuable post-earthquake damage assessment tool. Recent studies have demonstrated that building damage sustained in urban environments can be readily identified using techniques including photo-interpretation and semi-automated change detection algorithms. The following sections introduce these respective methodologies.

20.3.3.1. *Damage detection based on photo-interpretation*

Visual interpretation of remote sensing imagery relies on the function of the human brain to recognize features, through its vision. Based on experience, the interpreter associates what can be seen in the image, with real objects on the ground. Characteristics such as size, shape, tone, colour and texture are some of the clues used to interpret features in the image. Specifically, photo interpretation is defined as the process in which the raw data in a photograph is processed by the human interpreter's brain so that it becomes information (Lillesand and Kiefer, 1994). This technique was widely used by military strategists during World War II, to identify targets and to assess damage caused by bombing raids. However, since WWII, photo interpretation has been widely used in civilian applications, ranging from agriculture, archaeology and geology, to wildlife management.

With the surge in digital (quantitative) techniques since the 1950's, the focus of the remote sensing community has shifted from visual interpretation to digital image processing techniques. However, this is not to say that one approach is superior to the other (Jensen, 1996); both have advantages and limitations. For instance, it is a well-known fact that computers are capable of distinguishing between more shades of grey than the human eye can, and that computers can process information far more quickly than a human interpreter. However, computers have to be "told" what to look for, whereas human interpreters are immediately able to extract information from the photograph, based on their experience.

With the latest generation of digital sensors providing images with very high-spatial resolution, there is a resurgence in the art and science of visual interpretation (Jensen, 1996). The current state-of-the-art optical satellite images, collected by systems such as Quickbird and IKONOS, have sub-meter spatial resolution. At this level of detail, individual buildings, cars and trees are readily distinguished. These high-resolution images look very much like a conventional aerial photograph, and as such, are considered to be of sufficient quality for post-earthquake damage assessment, using both qualitative and quantitative methods.

There are two basic approaches to photo-interpretation. The first 'mono-temporal' approach, involves the visual recognition of damaged elements within a single image collected after the event. The second 'multi-temporal' approach detects damage based on the comparative analysis of two images, collected before and after the event. Success of these approaches is directly related to image resolution and building type. For example, damage is difficult to detect for masonry or adobe traditional construction, while sub-meter resolution supports the recognition of damage to modern buildings (Chiroiu, 2004). Signature characteristics of building damage in optical imagery include radiometric heterogeneity of the roofs, geometric irregularities of contours, and the absence of shadows.

In terms of distinguishing the building damage state, complete collapse is consistently recognizable on remote sensing imagery. Limited damage is difficult to detect, because from overhead, the structure may retain the same outline profile and shape. However, changes in associated shadows within high resolution imagery, may point towards the presence of classical "soft story" damage (see Figure 20.5).

Instead of various uncertainties and limiting factors, photo-interpretation analysis is realized relatively fast, and brings interesting opportunities from a crisis management point of view. Large areas could be interpreted within a few hours, and damages maps could be prepared and transferred quickly to the rescue teams deployed after the earthquake (see §20.3.3).



Fig. 20.5. Examples of "soft story" damage detection on Boumerdes, Algeria, after May 21, 2003 earthquake. The comparison of the image before a) and the image after b) indicate clearly the collapse of a week story (image credit: Digitalglobe.com)

20.3.3.2. Damage detection based on semi-automated techniques

The use of remotely sensed data for assessing building damage offers significant advantages over ground-based survey. Where the affected area is extensive and access limited, it presents a low-risk, rapid overview of an extended geographic area. A range of assessment techniques are documented in the literature, including both direct and indirect approaches. In the former case, building damage is recorded directly, through its signature within the imagery (Yamazaki, 2001). Research by Matsuoka and Yamazaki (1998) and Chiroiu et al. (2002) suggests that collapsed and extensively damaged buildings have distinct spectral signatures. However, moderate and minor damage states are indistinguishable from non-damage. Damage is usually quantified in terms of the extent or density of collapsed structures. In the latter case, damage may also be determined using an indirect indicator, based on the theory that urban night-time lighting levels diminish in proportion to urban damage (CEOS, 2001). Further details of the respective methodologies are given in the Figure 20.6.

Direct approaches to building damage assessment may be categorized as multi- and mono-temporal. Multi-temporal analysis determines the extent of damage from spectral changes between images acquired at several time intervals; typically before and after an extreme event.

At a city-wide scale, comparative analysis of Landsat and ERS imagery collected before and after the 1995 Hyogoken-Nanbu (Kobe) earthquake, suggested a trend between spectral change and ground truth estimates for the concentration of collapsed buildings (Aoki et al., 1998; Matsuoka and Yamazaki, 1998; Tralli, 2000; Yamazaki, 2001). Similar qualitative and quantitative methods were used to evaluate damage in various cities affected by the 1999 Marmara earthquake in Turkey (Eguchi et al., 2002; Estrada et al., 2001; Huyck et al., 2002). The case study in Section 20.4 presents further details

of results obtained. This damage detection methodology has also been implemented for ERS SAR coverage (Eguchi et al., 2000), which offers advantageous 24/7, all weather viewing, and an additional index of change termed coherence. Matsuoka and Yamazaki (2002) have recently generalized this approach, to show consistency in the trend between building collapse and remote sensing measures for the 1993 Hokkaido, 1995 Kobe, 1999 Turkey, and 2001 Bhuj earthquakes.

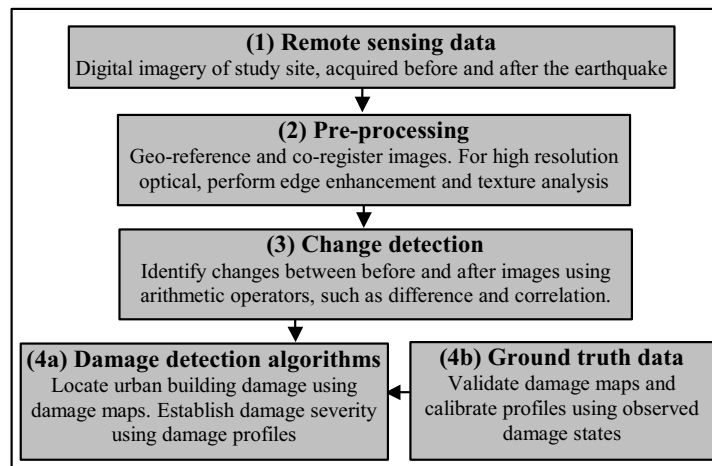


Fig. 20.6. Building damage detection methodology. (image courtesy of ImageCat, Inc www.imagecatinc.com)

Mono-temporal analysis detects damage from imagery acquired after a disaster has occurred. It is particularly useful where ‘before’ data is unavailable. The methodology relies on direct recognition of collapsed structures on high-resolution coverage, through either visual recognition or diagnostic measures. As with the multi-temporal approach, it is most effective for extreme damage states, where buildings have collapsed or are severely damaged (Chiroiu et al., 2002).

An indirect method of mono-temporal building damage assessment is also documented in the literature. Hashitera et al., (1999) compare night time lighting levels in US Defence Meteorological Satellite Program (DMSP) imagery acquired before and after the Marmara and Gujarat earthquakes. In both cases, areas exhibiting the greatest reduction in intensity corresponded with damaged settlements, supporting the hypothesis that fewer lights shine where buildings are severely damaged (Chiroiu and Andre, 2001). Operating under the cover of darkness, this damage assessment tool is a useful supplement to optically-based methodologies that are limited to daylight hours.

Current research is focusing on the refinement of semi-automated damage detection techniques to eliminate non-damage related changes due to sun angle and sensor look angle variations. The lack of pre-event data has also proved to be a limitation of mono-temporal studies, although as time passes since the launch of Quickbird and IKONOS, the volume of archival ‘before’ imagery is ever increasing. The presence of cloud cover is another limitation of optical data; while the small number of commercial systems and consequently low frequency of overpasses continues to limit the duration between the disaster occurrence and the delivery of remote sensing data.

20.3.3.3. Damage mapping for crisis management and recovery

During post-earthquake reconnaissance activities, mapping disaster-affected zones is typically based on the detection of damage sustained by individual buildings. Damage is usually separated into two or more classes, such as complete damage, extensive damage, moderate damage, etc. However, as noted previously, slight and moderate damage is quite difficult to recognize at the building level. Consequently, damage assessment based on remote sensing imagery is typically related to the spatial distribution or concentration of collapse.

The delay between an event and damage interpretation depends on the speed of image acquisition, which could vary between 24 and 72 hours. Where the results of image interpretation are provided in less than 3 days, they are useful for search and rescue efforts. Such data is particularly valuable for rural locations, since experience from the 2001 Algeria and 2004 February earthquakes suggest that there is often a significant delay in the delivery of damage state information to authorities (AFPS, 2003).



Fig. 20.7. Example of GIS database on a Quickbird background image on Boumerdes, Algeria, after May 21, 2003 earthquake

Results of the damage assessment are readily integrated into a Geographic Information System (GIS). In this format, digital data in vector or raster format can be readily transferred to emergency teams involved in relief operations (see Figure 20. 7). Following the 2003 Bam (Iran) earthquake, the Earthquake Engineering Research Institute (EERI) reconnaissance deployed the VIEWS (Visualizing Impacts of Earthquakes with Satellites) system as part of their damage assessment effort (Adams et al., 2004). The laptop-based VIEWS system directed the team to the hardest hit areas using a damage assessment map derived from remote sensing imagery. For more detailed damage information, collapsed buildings were easily identified on the high-resolution 'before' and 'after' Quickbird imagery. VIEWS also provided easy recall for observations made in the field. As team members comments such as building damage descriptions and photograph ID number, all information was linked back to their current GPS location. In the future, additional datasets such as accessibility (e.g. roads, railways, bridges), urban building types, and possible locations for relief camps could also be mapped and integrated into a GIS-based reconnaissance or emergency management system.

20.3.4. LOSS ESTIMATION

Loss estimation models represent a very important tool for risk mitigation; generally used by local authorities to anticipate the effects of an earthquake, and by insurance and reinsurance companies to manage its financial consequences. These models comprise four key modules: hazard assessment; exposure; damage curves; and direct and indirect losses. Remote sensing data analysis could be used for the vulnerability assessment for the pre-event models, and for the estimation of physical damage for post-event models. Imagery is also of value for model validation, and indirectly for the calibration of damage curves.

Casualty numbers can be derived from the physical damage to buildings, by associating the ratio of victims with damage levels detected in remote sensed data. Since the approach proposed by HAZUS (NIBS, 1997, 1999 and 2002) underestimates the real number of victims, an alternative statistical approach was developed by Chiroiu et al (2002; 2004). The proposed casualty ratios are based on engineering judgments and were tested and validated by the study of various earthquakes. These ratios, corresponding with the detection and mapping of two levels of damages (extensive and complete), are applied to the local density of population. It was supposed that for complete damage (defined as complete collapse), 80% of the occupants are dead and 20% injured; for extensive damage (defined as important damage including partial collapse), 5% of the occupants are dead and 60% are injured. An additional coefficient of 1.4 could be introduced for the estimation of injured persons, in order to account for the inability of remote sensing data to detect moderate and slight levels of damage.

Clearly, the estimation of casualties is critical information for the crisis management, providing a fast overview of the earthquake consequences, in terms of victims, and thereby determination the subsequent scale and coordination of relief operations. The only supplementary information required for this approach is the total population of the city.

The results obtained after Bhuj, Boumerdes and Bam earthquake indicate a relatively good accuracy, enabling the evaluation of the humanitarian consequences of the catastrophe, and dimensioning the international help.

20.4. Case studies

The following sections present a series of case studies of recent earthquakes, which detail the use of remote sensing and geomatic data for urban damage assessment. The studies include mono- and multi-temporal imagery from a range of different sensors, analysed using both image interpretation and semi-automated change detection techniques.

20.4.1. MARMARA (TURKEY) EARTHQUAKE, AUGUST 17th, 1999

Change detection algorithms were developed for the Turkish city of Golcuk, the most densely populated settlement in Kocaeli province. The city experienced extensive damage during the 17th August 1999 magnitude 7.4 earthquake. According to Coburn

et al. (1999, cited in Rathje, 2000), 30-40% of structures collapsed, due mostly to pancaking and the soft first story effect.

The performance of several change detection measurements was investigated. For the SPOT panchromatic data: (1) simple difference (dif); (2) sliding window-based (cor) correlation; and (3) modulated block correlation (bk_cor), were computed between the 'before' and 'after' images. In the case of SAR intensity and complex data, indices comprised: (1) simple difference between intensity values; (2) sliding window-based correlation; (3) modulated block correlation; and (4) coherence (coh) or complex correlation between complex images.

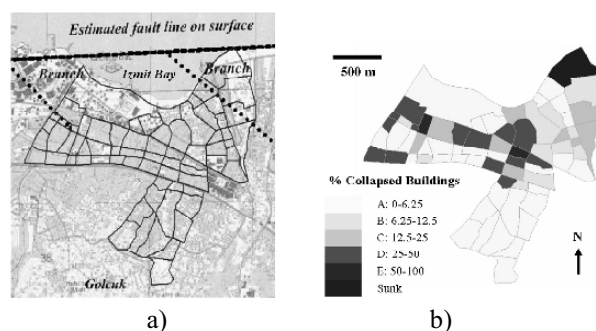


Fig. 20.8. a) Delineation of 70 sample zones in Golcuk. b) Ground observations of building collapse ((image courtesy of ImageCat, Inc www.imagecatinc.com))

The next methodological step compares indices of change with 'ground truth' damage data collected shortly after the earthquake by the Architectural Institute of Japan reconnaissance team (AIJ, 1999). The zone-based sampling strategy in Figure 20.8 was employed, using 70 administrative boundaries corresponding with the street network. Within each zone, damage states were recorded for a sample of buildings using the European Macro-seismic Scale (Grünthal, 1998) damage degrees.

Finally, damage maps and building damage profiles were generated to determine the location and severity of urban damage. For the profiles, average change was computed for each of the 70 zones, and these responses aggregated by damage state. The result is a central measure of tendency and standard deviation (plotted as error bars) for class A through class E.

The corresponding damage state map in Figure 20.8 expresses the percentage of collapsed structures (Grade 5) as a function of the total number of observations (sum of Grade 1 through Grade 5). For analytical purposes, these percentages are divided into the follow categories: A (0-6.25% of buildings totally collapsed); B (6.25-12.5%); C (12.5-25%); D (25-50%); and E (50-100%). The additional 'Sunk' zone corresponds with an area in northeast Golcuk experiencing significant subsidence.

Figure 20.9 depicts damage maps for Golcuk, obtained using the various measures of change. The difference scene (Figure 20.9 a) is classified to highlight regions of Golcuk exhibiting pronounced differences in reflectance. Changes are concentrated in the city centre, with strongly negative values suggesting a marked increase in reflectance following the earthquake. With reference to the damage map in Figure 20.9 b, these

areas correspond with zones of severe building damage (categories D-E). This result suggests that debris associated with collapsed buildings exhibits a higher spectral return than the standing structure. Although considerable damage was also sustained in western Golcuk, reduced differences may be due to suppressed reflectance values where smoke from the burning Tupras oil refinery was present in the upper atmosphere. Positive differences are limited to the ‘Sunk’ coastal stretch, where reflectance values have fallen following widespread inundation.

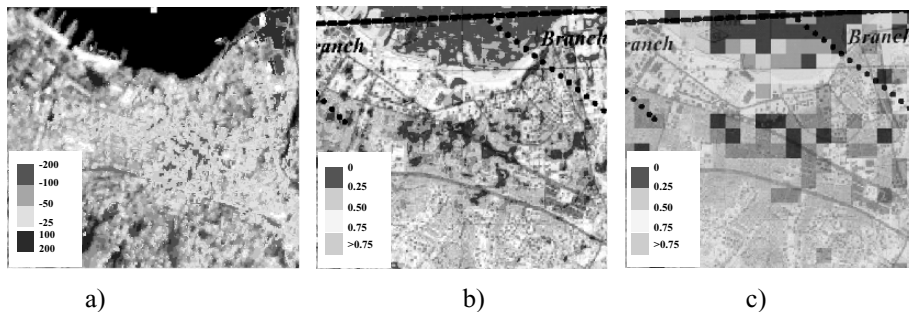


Fig. 20.9. SPOT damage maps: a) difference; b) correlation and c) block correlation. Areas of high positive difference and low correlation correspond with the Golcuk city centre, which from Figure b sustained severe and widespread building damage. (image courtesy of ImageCat, Inc. www.imagecatinc.com)

Results for the block and window-based correlation (Figure 20.9 b and Figure 20.9 c) are overlaid with a base map of Golcuk. For visualization purposes, all values are displayed as positive, since the magnitude rather than the direction of change is of interest. For both block and sliding window-based results, areas of low correlation (displayed in red) are concentrated in central Golcuk. As for the difference values, the damage map in Figure 20.9b confirms that building collapse was widespread. A low level of correlation around the subsidence zone is due to the change in reflectance following inundation. Low correlation offshore in the Izmit Bay is probably attributable to the random or chaotic patterns of surface reflectance associated with wind-driven wave action.

Intensity analysis of radar imagery from ERS sensor revealed the same tendency as SPOT data; mean correlation decreases as building damage escalates. Thus, correlation provides a consistent association between temporal changes on remote sensing imagery and urban building damage.

20.4.2. BHUJ (INDIA) EARTHQUAKE, JANUARY 26th, 2001

On the 26th of January, 2001, an Mw 7.6 earthquake shook the town of Bhuj in the Gujarat region of north-west India, causing significant losses. The epicentre of the earthquake was located approximately 20 km from Bhuj, which had a population of 150,000. According to statistics collected by Gujarat state one year after the event, the official death toll for the region stands as more than 13,800, with around 166,000 injured. Remote villages near the epicentre suffered extensive damage. A maximum intensity of X (MSK) was assigned by the local authorities.

We present here an application realized on the city of Bhuj, focused on its historical centre. A grid-based damage assessment was carried out in order to estimate the damage distribution pattern. A multispectral high resolution IKONOS image at 1 m resolution of the old city of Bhuj taken a week after the earthquake was used to carry out this application. The resulting grid-based damage map was compared with damage data collected on the ground by surveys of the buildings in Bhuj after the earthquake. The assessment using the satellite image was carried out by overlaying a grid consisting of 100 m by 100 m grid-squares on the satellite image and estimating the proportion of the number of buildings with damage level D4 or D5 according to EMS damage levels (EMS 98), i.e. partial or total collapse, among the total number of buildings within the grid-square. Four different damage levels were assigned to each grid-square according to the proportion of the partially or totally collapsed buildings among the number of buildings in the grid square i.e. $0 < 25\%$: damage level 1; $25 < 50\%$: damage level 2; $50 < 75\%$ damage level 3 and $75 = 100\%$: damage level 4. Comparison of the two datasets (experiment and ground truth data) revealed that the general damage distribution pattern can indeed be derived from the visual interpretation of the satellite image (see Figure 20.10).

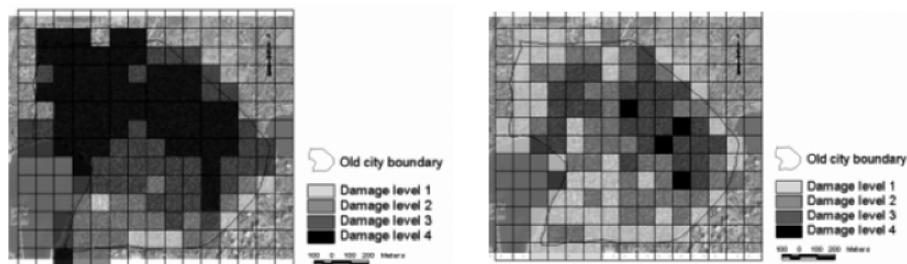


Fig. 20.10. Result of the ground damage survey (left) and the grid-based visual interpretation (right)

The analysis of the result indicated however that the detection of slight and moderate damage levels is more difficult, inducing a global underestimate of damages. The dense urban habitat of the old city, according to the traditional architectural type of buildings, was another factor constraining the interpretation. Instead of these limits, the entire application for the old city of Bhuj was realized relatively fast, within a few hours.

In order to validate results issues from photo – interpretation, a ground truth comparison was made in the frame of a damage detection after Bhuj (India) earthquake of January 26th, 2001. Ground photographs of 24 buildings in the town of Bhuj have been compared with a high-resolution optical satellite image showing the same buildings (see Figure 20.11). This comparison revealed the ability and limits of these satellite images to show damage to buildings using visual interpretation (Saito et al., 2004).

After this comparison study, it became clear that completely collapsed buildings together with severe structural damage to the buildings such as tilts, overturned buildings, splits, debris and failure to building appendages could be identified from a satellite image with this resolution, if the view is not obscured by shadows or the presence of nearby buildings.



Fig. 20.11. Photo a) and satellite image b) of a collapsed single building in the north of Bhuj. The remains of the building are visible in the satellite image. Note the difference between the building immediately to the left that is still standing and the others. The white arrow in the satellite image shows the look angle of the photo. The scale of the satellite images is approximately 1:1,500

20.4.3. BOUMERDES (ALGERIA) EARTHQUAKE, MAY 21st, 2003

On May 21 2003, at 7:44 pm, a strong earthquake of M6.8 hit the north of Algeria, causing important losses in the main urban zones of the Mediterranean coast. A 2 m run-up tsunami was produced, inducing damages as far as the harbours of Balearic Island. The most affected region was the province of Boumerdes, where various cities suffered widespread destructions, as Thenia, Zemmouri or Boumerdes.

We present here damage detection by photo-interpretation realized over the city of Boumerdes, located at around 20 km from the epicentre. Multi-temporal Quickbird imagery at 0.60 m was used for this application. The precision of the details provided by the high resolution images, and the characteristics of the buildings (majority of multi-story buildings) facilitated the detection of damages. In this case, the total collapse was visible with only a post-event recently acquired image; the post event images confirm the mono-temporal analysis (see Figure 20.12).

In addition to the complete damage with total collapse, relatively easy to detect, other types of damage were recognized in this case, through the comparison of changes before and after the earthquake. Soft-story damage, building rotation and torsion or partial collapse could be detected (see Figure 20.12).

The damage mapping was realized based on the reconnaissance of damaged buildings by photo-interpretation. The high precision of sub-metric resolution allowed mapping at the level of each building (see Figure 20.13); extrapolating, we can obtain a general view of the spatial extent of destruction, by mapping at the level of a zone or region. The fast estimation of casualties, based on the method presented in § 20.3.4, and applied to the damage mapping on Boumerdes provided relatively accurate results. We note that the mapping of the entire urban zone of Boumerdes was realized again within a few hours.

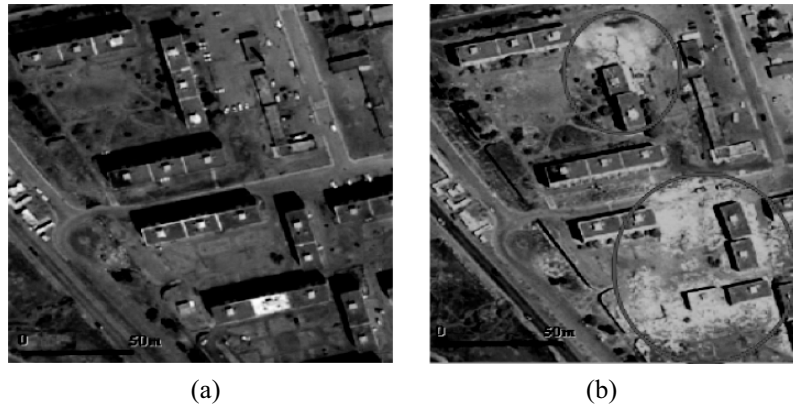


Fig. 20.12. Complete destruction of a few buildings at Boumerdes, after the May 21, 2003, earthquake. a) Pre-earthquake image and b) post-earthquake image. We note that damages are clearly recognizable with only the post-event image. (image credit: DigitalGlobe)



Fig. 20.13. Damage mapping at the level of a building, on Boumerdes, after the May 21, 2003 earthquake (image courtesy: DigitalGlobe)

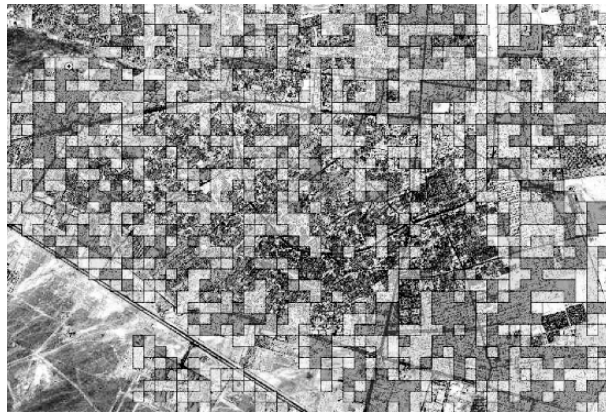
20.4.4. BAM (IRAN) EARTHQUAKE, DECEMBER 26th, 2003

At 05:26 on December 26 2003, a magnitude 6.6 earthquake struck the historic city of Bam, in the Iranian province of Kerman. The earthquake was centred approximately 10 km to the south-west of Bam. Damage was concentrated in a 16 km radius around the city, which is famed for its 2,500 year old citadel Arg-e-Bam.

In terms of human cost, the Bam earthquake ranks as the worst recorded disaster in Iranian history. According to recent reports, the death toll has reached 43,200, with a further 45,000 people displaced from their homes (USAID, 2004). Initial reports from aid organizations in Bam estimated that between 70-95% of buildings were destroyed.

The detection and the mapping of damages was based on multitemporal Quickbird imagery of Bam acquired by the University of California at Irvine, and the Earthquake Engineering Research Institute (EERI) as part of their Learning from Earthquakes

Program. The first image is dated approximately 3 months before the earthquake and the second was taken just over one week after. The city-wide damage map in Figure 20.14 a shows the widespread occurrence of extreme changes throughout Bam. The red and orange blocks correspond with the highest concentration of collapsed structures, are widespread through eastern areas of the city and the Arge-Bam citadel. Visual comparison with the USAID damage map published in early January, indicates that 80-100% of buildings were destroyed in these areas. Formal verification of the damage map against these ground-based observations is a subject for future research.



(a)

- Red** – Extreme change. *Complete building collapse*
- Orange** – Widespread change *Building collapse widespread*
- Yellow** – Some collapse *Localized pockets of collapse*



(b)

- 80-100% Destroyed
- 50-80% Destroyed
- 20-50% Destroyed

Fig. 20.14. a) Quickbird damage map for Bam (image courtesy of ImageCat, Inc. www.imagecatinc.com). Extreme textural changes caused by building collapse relate to a high average block standard deviation from the image mean. b) Distribution of building collapse in Bam (courtesy of USAID)

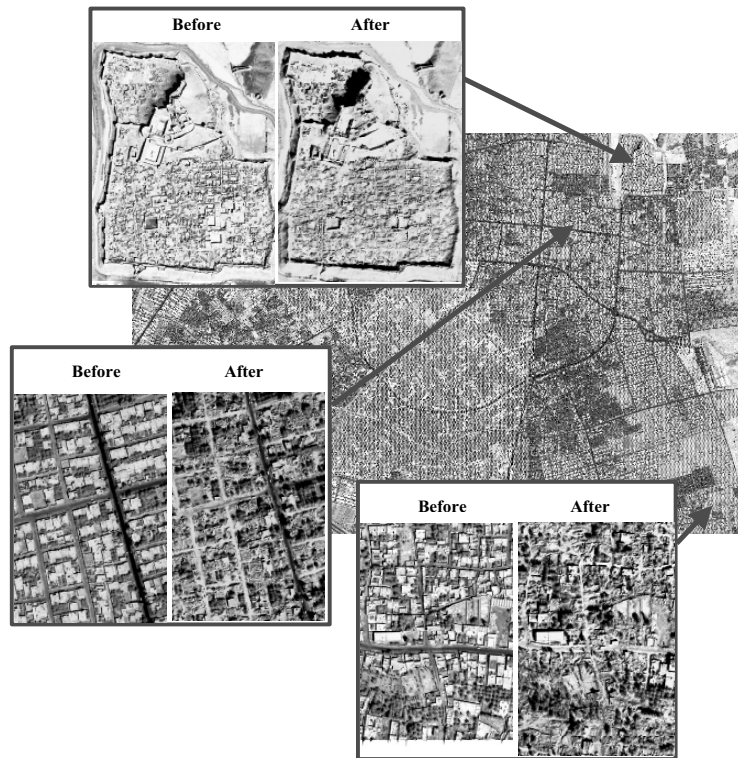


Fig. 20.15. Visualization of building collapse in Bam. The selected neighbourhoods were identified as regions of extreme damage (80-100% collapse) on the USAID damage map (Figure 20.14b) (image courtesy of ImageCat, Inc www.imagecatinc.com)

In terms of visual inspection, Figure 20.15 provides a close-up view of damage within a selection of areas on the damage map recording extreme changes. Collapsed buildings are evident throughout the ancient citadel. The eastern wall of the fortress appears to have collapsed. Many of the surrounding structures are no longer clearly defined as the walls and roofs have fallen in. In surrounding residential areas, building collapse is widespread; entire blocks of family homes have been destroyed. Their distinct footprint and white roofs in the before image, have been replaced by chaotic piles of brown rubble. Constructed from local material, the sand-coloured debris is difficult to distinguish from the surrounding sandy ground surface.

20.5. Conclusions

This chapter has provided an overview of the emerging role of advanced methodologies in earthquake modelling, response and recovery. For readers who are new to the field of remote sensing, key types of sensor have been introduced, and emphasis placed on the respective advantages associated with each dataset, such as realistic and detailed visualization from optical imagery, highly accurate GPS positioning, and the 24/7, all weather viewing offered by SAR. Building inventory development, mapping ground

surface displacement, urban damage assessment and loss estimation are presented as the principal applications for this imagery.

The impressive capabilities of very high resolution optical Quickbird and IKONOS imagery were illustrated through a series of case studies featuring recent earthquakes in Turkey, India, Algeria and Iran. From an emergency management standpoint, the semi-automated detection of regional damage extent and determination of building damage severity through visual inspection satisfies core response of recovery needs. Together with derived loss estimates, this information supports decision making, by directing first responders to the hardest hit locations, and indicating the required level of relief operations.

Looking to the future, from a technological perspective, a number of new satellites constellations are under development, which promise increased spatial resolution and temporal frequency for both optical and SAR data. However, tandem investment is required in the infrastructure for processing, displaying and disseminating the data, to ensure that it reaches the hands of emergency responders in near-real time. From an implementation viewpoint, one of the most significant challenges continues to be educating potential users about the capabilities that remote sensing and geomatic technologies offer for disaster modelling, response and recovery. Considering the large number of policy initiatives, and research programmes that have been launched worldwide, the outlook is promising.

CHAPTER 21
SEISMIC LOSS SCENARIOS BASED ON HAZARD DISAGGREGATION.
APPLICATION TO THE METROPOLITAN REGION OF LISBON,
PORTUGAL

A. Campos Costa, M. L. Sousa, A. Carvalho and E. Coelho
National Laboratory for Civil Engineering (LNEC), Lisbon, Portugal

21.1. Introduction

Reports on the effects of earthquakes that have occurred in the past in Portugal, the recognized moderate level of seismic hazard in the country and the existence of constructions not designed or built in accordance to modern earthquake-resistant codes indicate that a significant fraction of the Portuguese population is exposed to a considerable level of seismic risk.

Particularly, the 40 km radius Metropolitan Area of Lisbon (MAL), which is under study, has been historically stricken by scarce, though intense, earthquakes, such as the 1755 Lisbon earthquake estimated as M8.7. In Lisbon town, about 10 000 deaths and 14 000 buildings collapsed or damaged were reported, although these numbers are coloured by with natural historical uncertainty. In the last decade of the XXth century the MAL region experienced an intense construction rate. However, 27.3% of the existing buildings were constructed before the first Portuguese seismic code, enforced since 1960, and this percentage rises to 63.9% if we look at Lisbon town. Figure 21.1 presents the geographic location of the area under analysis and the geographic distribution of dwellings by parish.

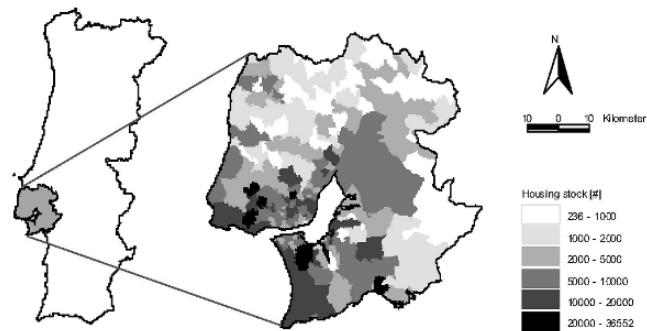


Fig. 21.1. Metropolitan Area of Lisbon and geographic distribution of dwellings according to Census 2001 (INE, 2003)

Due to this high concentration of elements at risk and to the potential of occurrence of destructive seismic events, Portuguese authorities motivated some studies intending to mitigate the seismic risk in this region and in the whole country. In the framework of those seismic risk mitigation projects, an automatic Seismic Scenario Loss estimate methodology (LNECloss) was developed, integrated on a Geographic Information System (GIS) initially designed as a tool to define a civil protection emergency plan for

the MAL region. Soon after, LNECloss was updated to estimate the seismic risk in the whole country and to identify earthquake protection strategies to reduce future losses.

In the context of disaster preparedness plans it is mandatory to select scenarios representative of the seismic activity of the MAL region, the customary choice being the most important historical earthquake affecting the region. The allocation of resources within an earthquake relief plan for an urban area is then performed following the results of detailed simulations of the consequences of occurrence of that specific event. However, there is no unique criterion for selecting that event and a rational design of resources for emergency planning based on the utility theory or cost-benefit analysis is clearly a difficult task in approaches based on the deterministic selection of the scenario. As an example, the allocation of resources based on the occurrence of the largest historical event may be deemed excessive given its extremely low probability of occurrence.

Besides, rather than identify the highest hazard scenario in a region, the main objective of civil protection emergency planning, should be to identify the event, or group of events, generating the worst loss scenario for a reference time interval and exceedance probability. An alternative approach is now presented where seismic risk scenarios are evaluated based on probabilistic seismic hazard disaggregation in order to complement deterministic approaches traditionally adopted in civil protection emergency management and planning.

21.2. Assessment of probability-based seismic loss scenarios

21.2.1. SEISMIC HAZARD DISAGGREGATION

A procedure to derive a dominating scenario event at a site from a probabilistic seismic hazard analysis (PSHA) involves the evaluation of hazard disaggregation at that site as described in chapter 2. This type of analysis has already been extensively discussed and applied specifically in Portugal, to Lisbon Metropolitan region (Campos Costa et al., 2002), Azores islands (Carvalho et al., 2001) and to a broader geographic region comprising the Portugal mainland (Montilla et al., 2002; Sousa, 2004).

In summary seismic hazard disaggregation consists of assessment of the hazard contributions in a space of bins of the random variables of the process. The most used bin space is bidimensional; that is, the relative contribution to the hazard is studied in terms of elementary bins of magnitude M , and source-to-site distance R . Therefore, hazard disaggregation represents the conditional probability that the exceedance of a specified ground motion level (hazard value) has been caused by a certain combination of M and R (McGuire, 1995).

Results of hazard disaggregation are often summarised into central statistics like means or modes. Discussion of whether an earthquake scenario should be defined by a pair of mean values or by modal values of magnitude and distance resulting from disaggregation, has already taken place (Harmsen et al., 1999; Bazzurro and Cornell, 1999).

Due to the seismicity pattern affecting Portugal (Figure 21.2, left) it was decided to follow a disaggregation scheme evaluating hazard marginal distributions in terms of latitude and longitude (x,y) and expected value of M. In this way, interplate and intraplate seismic scenarios can be independently assessed.

21.2.2. APPLICATION TO THE METROPOLITAN AREA OF LISBON

21.2.2.1. Seismic hazard scenarios

In practice, to evaluate seismic hazard scenarios the following four step procedure was implemented: (i) perform a PSHA for a site (parishes of MAL) and generate a hazard curve; (ii) determine the contribution factor of each geographic bin (x,y) for that particular site and intensity level; (iii) identify the geographic bin (x,y) with the modal value of the contribution and (iv) define the hazard consistent magnitude for that particular geographic bin. To perform a PSHA for a site a mixed model was used considering gross source zones to compute b values of the Gutenberg-Richter law, maximum magnitudes and annual rates in geographically uniform bins to obtain spatially seismic rates represented in Figure 21.2 right (Campos Costa et al., 1998).

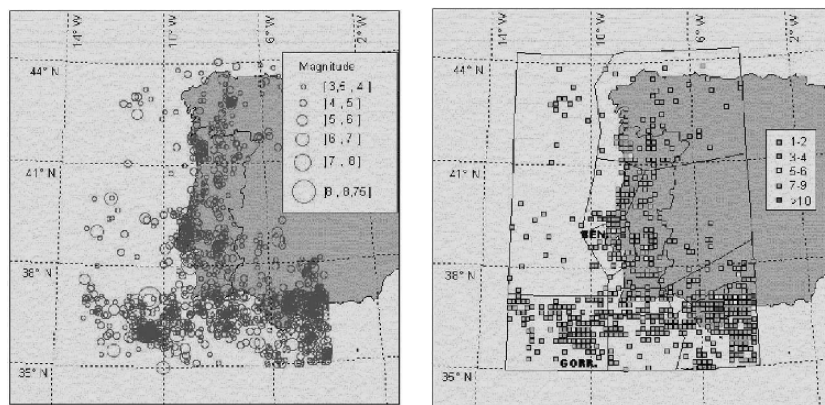


Fig. 21.2. Left: Earthquake epicentres, 33 AD – 1999; Right: Seismic source model and number of earthquake events ($M \geq 3.5$) for each geographic bin, since 1910. BEN. – Benavente source zone; GORR. – Gorringe source-zone

Figure 21.3 illustrates the above four steps for five parishes of MAL. It shows the contribution factors of the geographic bin, for three different annual probabilities, and the corresponding hazard seismic scenario. Parishes were chosen due to the relevance of their geographic localization: the northern, the eastern, the western and the southern ones, and one in the centre.

From the analysis of Figure 21.3, one may conclude that: (i) the local source-zone (Benavente zone, Figure 21.2) dominates for a return period of 10 years; (ii) for a 475 years return period the seismicity of the northern, western and southern parishes is dominated by the far distant offshore source (Gorringe zone, Figure 21.2). On the contrary, seismicity of the eastern parish and the one in the centre is still dominated by the local short distant source-area (Benavente zone); (iii) for the 1000 years return period seismicity is mainly controlled by the Gorringe area except for the one in the

centre whose seismicity is still dominated by the local source; there is also visible a dual characteristic in scenarios associated to the Gorringe zone. In fact, southern and eastern parish scenarios are closer than the ones to the north and west, reflecting the relative importance of magnitude and distance coefficients inherent to the attenuation law.

After repeating the same procedure for all the 277 parishes of MAL, theoretically, there will be 277 seismic hazard scenarios, each one characterized by a magnitude and a pair of geographic coordinates, for one specific probability level. However, due to the adopted methodology, a concentration of the geographic localization of scenarios in a few specific points within the limits of Benavente and Gorringe zones is expected.

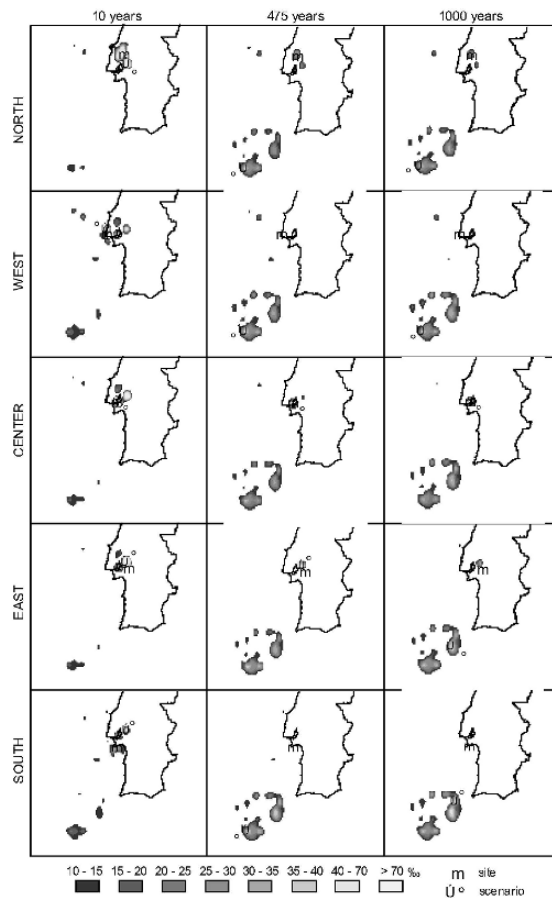


Fig. 21.3. Disaggregation (contribution factors) for five parishes of MAL (rows), for three different annual probabilities (columns)

The assumptions stated above are represented in Figure 21.4. This Figure and Table 21.1 present the location of the 277 seismic scenarios assessed for the above-mentioned three return periods. As shown, for each return period, one may determine only a few specific seismic scenario locations. Values of magnitude shown are the highest expected magnitudes assessed for each location. Pairs of location and magnitude identified in the procedure are defined as the hazard scenarios for the metropolitan region of Lisbon, for

the three different probability levels, once they convey the most likely locations with the maximum expected magnitude in those locations.

Table 21.1. Seismic hazard scenarios for Metropolitan Area of Lisbon for the three probability of exceedance (PE) considered (three return periods)

10% annual PE			PE 10% in 50 years			PE 5% in 50 years		
Lat.	Long.	Mag.	Lat.	Long.	Mag.	Lat.	Long.	Mag.
-9.5	38.9	4.3	-10.75	36.0	8.1	-10.8	36.0	8.2
-9.1	38.8	4.6	-9.8	36.6	7.8	-9.8	36.6	8.1
-9.1	39.1	4.3	-9.6	36.9	7.6	-9.6	36.9	7.9
-8.8	38.9	5.0	-9.1	38.8	5.7	-9.1	38.8	5.9
			-9.1	39.1	5.6	-9.1	39.1	5.7
			-9.0	39.3	5.4	-9.0	39.3	5.7
			-8.8	38.9	6.3	-8.8	38.9	6.4

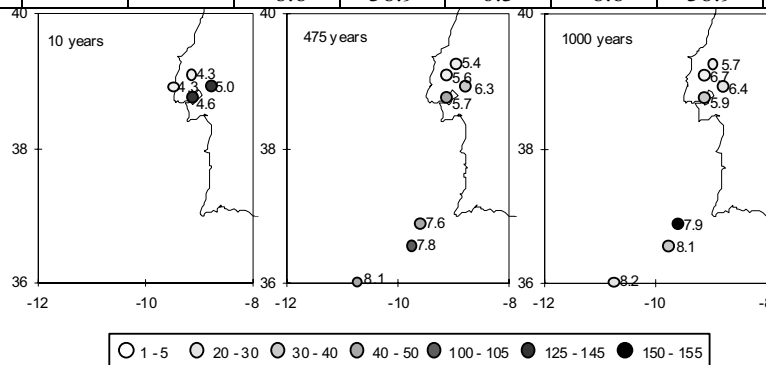


Fig. 21.4. Epicentre location of the 277 hazard seismic scenarios. Values of magnitude represented are the highest expected magnitudes assessed for each location. Circles represent the number of epicentres for each location

21.2.2.2. Seismic loss scenarios

Once the most likely scenarios that can affect the metropolitan area of Lisbon have been attained, seismic risk scenarios can be assessed by weighting those hazard scenarios with the geographic distribution of elements at risk in the region, implying as many seismic risk scenarios as the number of seismic hazard scenarios plotted in Figure 21.4. In the present context the final risk scenario was the one that conducted to the highest losses for the region, in each considered return period (bold signed in Table 21.1).

Losses were computed using the Seismic Scenario Loss estimate methodology integrated on a GIS as it is described in the following section.

21.3. A seismic loss methodology integrated in a Geographic Information System

21.3.1. OVERVIEW

The automatic Seismic Scenario Loss estimate methodology, integrated on a GIS (ArcGIS, or other) comprises several modules to perform seismic risk analyses that are

developed in a high level programming language and compiled in DLL (Dynamic Link Library-DLL) that may be accessed rather efficiently by any Windows program environment (ArcView, EXCEL, MathLab, etc.). The several modules are schematically represented in Figure 21.5 and are the following:

Bedrock Seismic Input - Given a seismic scenario (magnitude and epicentral location) it computes the Power Spectral Density Function (PSDF) of the strong ground motions at bedrock level of any site at a given epicentral distance.

Local Soil Effects - Given a stratified soil profile unit it computes the new PSDF for any location at the surface level, taking into account the nonlinear behaviour of the stratified geotechnical site conditions.

Vulnerability Analysis - Giving the PSDF at surface level, it computes the response of building typologies following a displacement-based methodology based on capacity curves.

Fragility Analysis - For a particular site, taking into account damage observed in each typology, the number of existing buildings in each typology (inventory) and respective occupancy, it computes number of buildings in each damage state.

Human Losses - Taking into account damages in each typology and the occupancy per typology it computes human casualties and homeless.

Economic Losses - Taking into account damages in each typology and damage state it computes building floor lost areas, that can be multiplied by the repair and replacement cost to obtain economic losses.

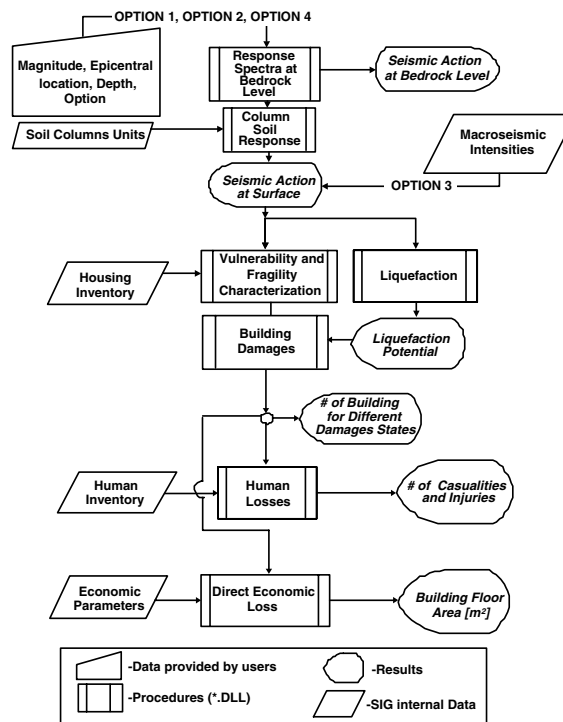


Fig. 21.5. Diagram of LNEC automatic Seismic Scenario Loss methodology

Due to lack of recent damaging earthquakes affecting the Portugal mainland, LNECloss was calibrated with historical data, namely 1755 and 1909 earthquakes, for which statistics of damages and victims are known for a few regions. The older typologies of the housing inventory were used in this calibration and estimates were compared in proportional terms with historical data.

21.3.2. INPUT DATA

The required input data to LNECloss operation includes:

Shallow Geology – Data Base containing information on stratified soil profile units for the region under analysis. Each record comprises the thickness of shallow layers, shear waves velocity, density and plasticity index.

Building stock – Residential building database, geographically organized by small administrative divisions (parishes), surveyed in the Portuguese 2001 Census (INE, 2003) and classified by epoch of construction, building construction materials and number of floors.

Population at risk - Inhabitants database, with the same level of geographic organization, surveyed in the Portuguese 2001 Census (INE, 2003). This database settles accounts for the number of inhabitants living in buildings classified according to their age, structural elements and height.

Economic parameters - Average floor areas, repair and replacement costs by parish and typology.

The user should provide the following information: (i) x, y coordinates of the scenario's epicentre in a rectangular (planar) coordinate system, (ii) the scenario magnitude and (iii) the option to evaluate seismic intensities in each site (see the following section).

21.3.3. PROCEDURES AND RESULTS

21.3.3.1. *Seismic action at bedrock level*

Such tools require equally refined approaches for seismic input simulation reflecting the seismotectonic environment of the urban area under study.

Given a seismic scenario (magnitude and location) it computes the PSDF of the strong ground motions at bedrock level of any site. Spectral characteristics can be computed using different approaches that are the following:

Option 1 – uses Boomer et al. (1998) empirical spectral attenuation relationship;

Option 2 – uses Sousa (1996) attenuation model based on macroseismic intensities. These models were achieved by integrating intensity data concerning the events of the Portuguese catalogue. Intensity results are then converted into response spectra after Trifunac and Brady (1975);

Option 3 – uses real macroseismic intensities of a specific earthquake, which are, then converted into response spectra after Trifunac and Brady (1975); the seismic action is evaluated not at a bedrock level but at the surface. User is required to provide a file with intensities;

Option 4 – uses seismological models. It performs non-stationary stochastic finite – fault modelling. Carvalho et al. (2004) describe theoretical aspects of this approach.

An application to the MAL was performed for the worst loss scenario estimated for 1000 years return period. As this scenario corresponds to a 7.9 magnitude (see table 21.1), the utilization of a finite-fault source geometry model is justified. Figure 21.6 presents the source geometry used to simulate the chosen scenario and the peak ground acceleration at bedrock level for MAL.

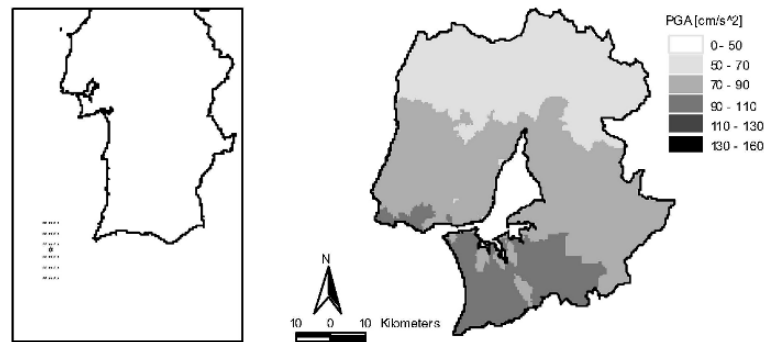


Fig. 21.6. Left: Surface projection of the fault source geometry. Points show the center of the subfaults. The big circle shows localization corresponding to the chosen scenario and considered as the initial point of rupture. Right: Peak Ground Acceleration at bedrock

21.3.3.2. *Seismic action at surface*

Given the stratified soil profile units, we compute the new PSDF for any location at the surface. The computer algorithms now developed and implemented take into account site effects due to soil dynamic amplification in a rather efficient way. These effects are also evaluated by means of an equivalent stochastic nonlinear one-dimensional ground response analysis of stratified soil profile units designed for the region.

Figure 21.7 presents the soil units for MAL and the peak ground acceleration at the surface for the worst loss scenario for an exceedance probability of 5% in 50 years.

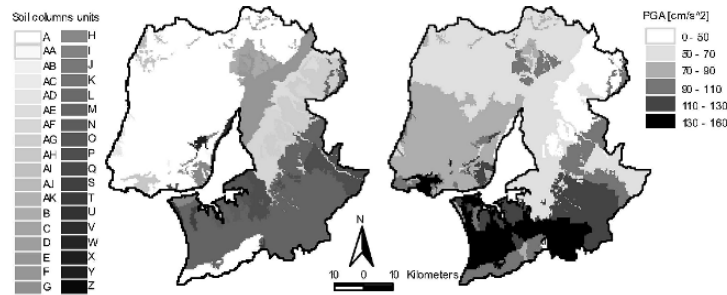


Fig. 21.7. Left: Soil columns units for MAL (after Carvalho et al., 2002). Right: Peak Ground Acceleration at surface for MAL

21.3.3.3. Vulnerability and fragility characterization

Methodologies using hysteretic displacement-based assessment and fragility analysis for building loss estimation are novel approaches in seismic risk analysis of urban areas. Damage procedures require a previous classification of the vulnerability of the building stock.

Sousa (2004) analysed the 2001 Portuguese Census with three main purposes: (i) to build the statistics of the number of buildings and inhabitants on the Portuguese mainland, (ii) to characterize their geographic distribution and (iii) to identify the most representative and frequent building types by region.

In the Building Questionnaire of that Census there were identified some variables representing structural characteristics that are expected to influence a building's performance when stricken by an earthquake: epoch of construction; resisting elements; number of floors. Table 2 presents the classes of those variables available in Census 2001.

Table 21.2. Classes of vulnerability variables obtained in Portuguese Census 2001

<i>Epoch of construction</i>	<i>Building structure</i>	<i>Number of floors</i>
Before 1919	Reinforced concrete	1
1919 to 1945	Masonry with RC floors	2
1946 to 1960	Masonry without RC floors	3
1961 to 1970	Adobe rubble stone	4
1971 to 1980	Others (wood, steel, etc)	5 to 7
1981 to 1985		8 to 15
1986 to 1990		+ 15
1991 to 1995		
1996 to 2001		

Carvalho et al. (2002) established a typological classification of Portuguese building stock taking into account a first analysis of Portuguese Census 1991 and expert opinion. Experts gave information on the most relevant building practices in the Country, materials and technologies employed in construction, their evolution over time and space. The history of building seismic upgrade in Portugal is mainly related to the occurrence of earthquake disasters (e.g. 1755 earthquake) or to the building codes enforcement.

The authors identified seven typological classes allowing for the two Census 1991 variables, *Epoch of construction* and *resisting elements*. Each of those classes was further subdivided in seven categories, considering building height, leading to forty-nine building types with similar seismic response characteristics. For those 49 typologies of buildings, the authors proposed capacity (pushover) and fragility curves, and those 49 typologies were now updated taking into account the new features included in Census 2001, namely a more reliable classification of the building structure.

Fragility curves allow evaluation of the probability of exceeding the threshold of a given damage state. As required by HAZUS 99 (NIBS, 1997, 1999 and 2002) five damage states were considered: No damage, Slight, Moderate, Severe and Complete

Damage. The thresholds of those damage states are established in terms of global drift for each typology.

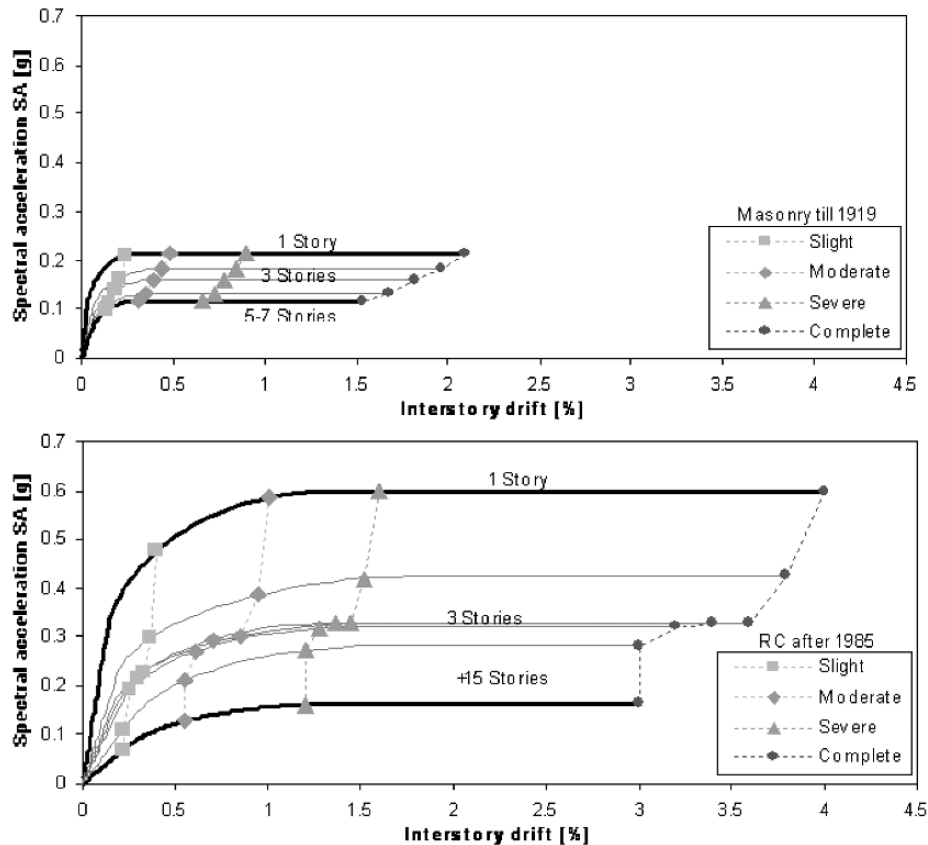


Fig. 21.8. Capacity curves and thresholds of damage states for two typologies identified in 2001 Portuguese Census

21.3.3.4. Building damage

The evaluation of peak response for each type of building relies on the intersection of its capacity curve with the seismic spectral demand at the site. This technique is called the “capacity spectrum method” ATC-40 (1996) and the HAZUS loss estimation methodology (NIBS, 1997, 1999 and 2002) has been adopted worldwide.

The capacity spectrum method is based on performance-based procedures for the design of new buildings and on a reduction of the initial elastic response spectra to the so-called demand spectra, taking into account the degradation of the building exposed to seismic motion.

An innovative technique was introduced in the LNECloss taking into account an iterative procedure that estimates sequential demand spectra, with increasing damping, reflecting structure degradation during its cyclic response. While in HAZUS the modifications of spectral demand are represented by reduction factors, in LNECloss

those modifications were performed through an iterative equivalent non-linear stochastic methodology, similar to that presented in the section entitled “seismic action at bedrock level”. Progressive building responses are obtained over the demand spectra till the convergence with the median capacity curve is achieved. The so-called performance point obtained this way corresponds to the peak of the dynamic response of a structure idealized by a single degree of freedom system.

The evaluation of damages is obtained multiplying the relative frequencies of the buildings in each damage state by the number of buildings for each typology in a given geographic unit.

Figure 21.9 presents the number of buildings in MAL in *Severe* and *Complete* damage states for the 1000 years return period worst loss scenario.

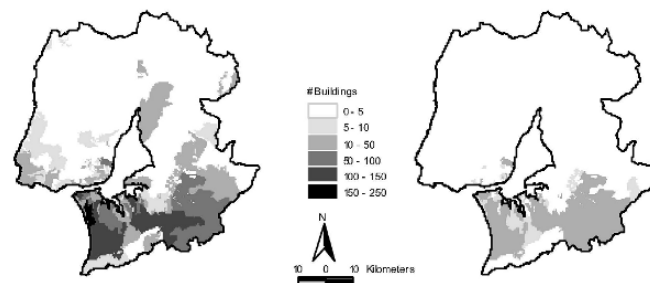


Fig. 21.9. Number of damaged buildings in MAL for the chosen scenario. Severe (left) and Complete (right) damage state

21.3.3.5. Human losses

Most methods to estimate human casualties as a consequence of earthquakes are based on the correlation between building damages and the number of people killed, injured or homeless. A great level of uncertainty always affects those estimations, because the same seismic intensity causes a heterogeneous number of victims in different countries and regions. In addition, the statistics following an earthquake are poor turning the casualty estimation into a rather difficult task (Coburn and Spence, 2002).

For a seismic scenario similar to the 1755 earthquake affecting existing housing stock in MAL, the LNECloss estimates 12 448 deaths using Tiedemann’s method and 919 if option HAZUS 99 was chosen.

The LNECloss routine for casualty estimation implemented two methods to evaluate death rate and injuries as a consequence of earthquakes: option Tiedemann (Tiedmann, 1992) and option HAZUS 99 (NIBS, 1997, 1999 and 2002).

If option Tiedemann is chosen, the LNECloss routine on human losses estimates for each geographic/soil unit, and for each building typology, the Death Rate for a given seismic scenario. On the other hand, if HAZUS 99 option is chosen the LNECloss routine on human losses estimates for each geographic/soil unit, and for each building

typology, the casualties for four levels of injury severity: Light injuries, Hospitalisation, Life threatening and Death.

Figure 21.10 presents the number of death victims for Tiedemann and HAZUS 99 methodologies. The scattering of results is notorious.

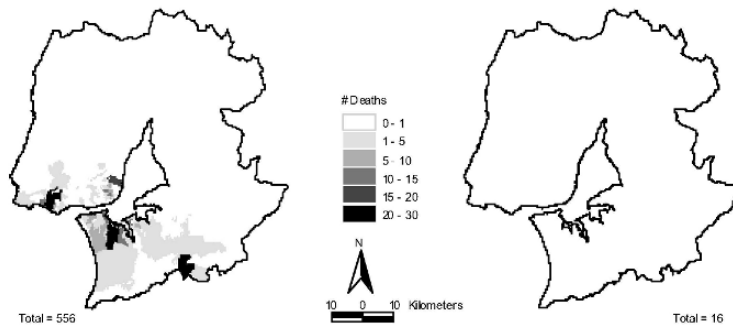


Fig. 21.10. Number of death victims in MAL for the chosen scenario. Left: Tiedemann method; right: HAZUS 99 method

21.3.3.6. Economic losses

The module of economic losses computes the lost area of building floors (Figure 21.11.) obtained by a weighted linear combination of the probability of the building type being in a given damage state summed over all the elements at risk. To obtain economic losses the lost area is simple multiplied by the replacement cost of a square meter, by parish and typology.

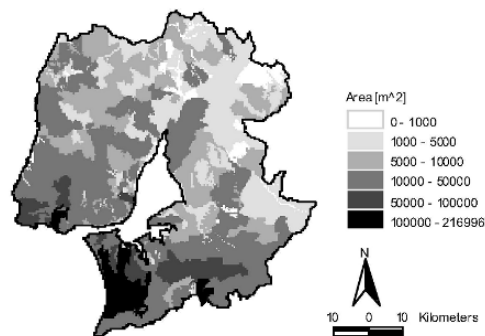


Fig. 21.11. MAL Building floor lost area for the chosen risk scenario

21.3.4. SEISMIC RISK ANALYSIS

A seismic risk analysis in terms of economic losses was performed considering near (intraplate) and far (interplates) distant scenarios. The former covers a range of magnitude between 4.0 and 7.2 whereas the latter covers a range of magnitude between 4.0 and 8.5. The annual probability for each scenario (x,y,M) was computed considering the gross source zones and the corresponding Gutenberg-Richter laws as described in

the PSHA (section 21.2.2.1). Figure 21.12 presents the economic losses for each return period of the interplates and the intraplate scenarios, based on an indicative value of 500€ per square meter.

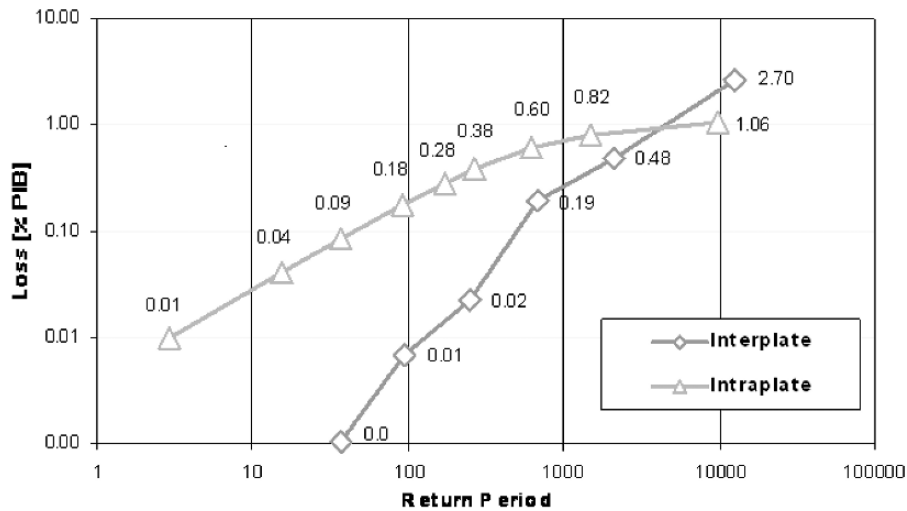


Fig. 21.12. Probability loss distribution for interplates and intraplate scenarios

21.4. Conclusions

A methodology was presented to assess seismic loss scenarios for a metropolitan region based on seismic hazard disaggregation. The methodology was illustrated for the metropolitan region of Lisbon simulating the worst loss scenario, obtained for an exceedance probability of 5% in 50 years.

The developed automatic Seismic Scenario Loss methodology, integrated on a GIS, was a key instrument to bridge the gap between seismic hazard disaggregation and risk analysis.

Being a modular structure, the LNECloss is constantly being updated in a very simple way, both in terms of data and methodologies. For instance, an important new feature was included in LNECloss since seismic action and damage algorithms were based on non-linear (or equivalent linear) non-stationary stochastic analysis. Besides, a methodology was developed (Sousa, 2004) aiming to calibrate the parameters of the capacity spectrum method with the statistics of European earthquakes (SSI, 2003; Zuccaro and Papa, 2002a) and with the fragility inherent to EMS-98 (Giovinazzi and Lagomarsino, 2003). Also the sensitivity analysis of results is being performed focusing on the parameters of seismic rupture, on the classification of building stock vulnerability and on the modelling of human losses. A third methodology to evaluate human losses as a consequence of earthquakes is included in LNECloss (Coburn and Spence, 2002).

The LNECloss is also an important tool to achieve significant progress in seismic risk mitigation in Portugal, being useful for several issues, such as: (i) decision support for

the establishment of rational emergency planning, since it operates in real time, (ii) definition of policies for seismic retrofitting of the building stock, allowing the study of the influence of interventions by geographical areas and by type of construction, and the subsequent identification of the most efficient intervention strategies by means of a cost-benefit study, (iii) definition of technical insurance premiums for insurance policy.

This tool should be supplied to local and regional authorities to provide a decision support system to evaluate seismic risk and to found mitigation programs.

Acknowledgements

The initial code of the LNECloss was developed in the framework of two Portuguese research projects funded by the Fundação para a Ciência e a Tecnologia (FCT) and the Serviço Nacional de Protecção Civil (SNPC).

Further developments in LNECloss and the present study was supported by LESSLOSS - A European Integrated Project on Risk Mitigation for Earthquakes and Landslides under the 6th Framework program of the EU.

The authors are grateful to Dr. Cansado Carvalho for valuable scientific advice and Dr. Anabela Martins for her help in processing data and computer graphics.

CHAPTER 22

LOSS SCENARIOS FOR REGIONAL EMERGENCY PLANS: APPLICATION TO CATALONIA, SPAIN

T. Susagna¹, X. Goula¹, A. Roca¹, L. Pujades², N. Gasulla³ and J. J. Palma³.

1. *Institut Cartogràfic de Catalunya, Barcelona, Spain*

2. *Universitat Politècnica de Catalunya, Barcelona, Spain*

3. *Direcció General d'Emergències i Protecció Civil, Barcelona, Spain*

22.1. Introduction

The organization of human and material resources to face up to an earthquake crisis is established through emergency plans at different scales (national, regional and local). National plans often establish the criteria for preparing regional and local plans mainly based on intensity of ground shaking. However, in order to decide which counties or municipalities need to prepare a specific emergency plan, vulnerability and risk should be assessed and damage scenarios generated.

The emergency plans include various levels of intervention, bringing out an adequate amount of resources, depending on the severity of the event.

An approach was developed for the area of Catalonia, Spain, in which earthquake risk and damage scenarios are estimated. Activation levels for plans are defined in function of the focal parameters of the seismic event and on population distribution at that time.

These activation levels take into account not only ground shaking but also many other factors related to physical, human and societal vulnerability, such as the number of uninhabitable dwelling buildings, the number of homeless and the direct economic losses. All these parameters can be estimated for a regional damage scenario previously developed for an earthquake occurring at any point of the territory with any magnitude.

In order to generate damage scenarios, several methodologies exist, some of which have been developed in different chapters of this book, including those which provide detailed vulnerability and damage assessment at local scale. The example presented here corresponds to a simplified statistical approach for regional-scale assessment. This type of methodologies are useful for helping the preparation of national and regional emergency plans and other applications at this scale which do not require a very detailed analysis of building characterization. One can also apply these methods when preliminary results are required in a short time, when budget for detailed and costly studies is not available and when detailed data on buildings can not be obtained, as is particularly the case in developing countries.

22.2. Risk assessment

Catalonia is considered to be in general a region of moderate seismicity. However, there are some areas in which the probability of occurring situations of seismic emergency is higher. The studies to identify these zones are presented in the SISMICAT, the Seismic

Emergencies Plan of Catalonia (DGEiSC, 2003), covering the following three main aspects:

- 1) The seismic hazard assessment gives an estimation of the intensity of the seismic action that can be reasonably expected in each municipality of Catalonia.
- 2) The seismic vulnerability assessment gives an estimation of the damages that the seismic action can cause on the exposed structures considered in each municipality: dwelling houses and buildings with other uses for the population, essential services for the community, and constructions that, due to their activities, could significantly increase the damage and even induce catastrophic effects.
- 3) Through the combination of these two components, hazard and vulnerability, risk scenarios for each municipality of Catalonia can be elaborated and therefore the populations at higher risk can be identified.

22.2.1. SEISMIC HAZARD ASSESSMENT

With the purpose of preparing the necessary information to carry out a correct evaluation of the seismic hazard (see Chapter 2 of this book) the Cartographic Institute of Catalonia (ICC) elaborated a new earthquake catalogue (Susagna and Goula, 1999) that collects and unifies seismic information from various existing sources and from new researches. Also a new seismotectonic zonation based on geologic and seismic criteria was made (Fleta et al., 1996). The seismic hazard assessment was then carried out combining deterministic and probabilistic methods that consider these new data (Secanell et al., 2004).

The map that determines the different areas of the territory based on its seismic hazard, considering the soil effect, is the map of seismic zones, which is presented in Figure 22.1 in terms of intensity values for an annual probability of 2×10^{-3} (equivalent to a return period of 500 years)

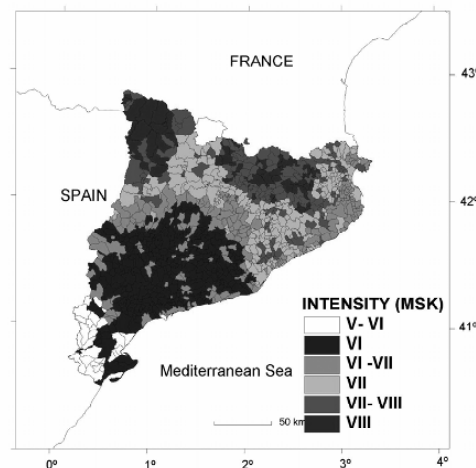


Fig. 22.1. Seismic hazard map for 500 years return period taken into account soil effects

22.2.2. VULNERABILITY ASSESSMENT

For the evaluation of seismic vulnerability, different methods have been considered, depending on the type of elements at risk: for dwelling or similar buildings (hospitals, firemen stations) methods are based on their constructive and structural properties (see Chapter 6); for lifelines (gas and electricity conductions, electric transforming stations, etc.) methods are based on their specific technical characteristics (see Chapter 9). A detailed local-scale vulnerability assessment requires a previous collection of detailed data of each element at risk. This is always a very hard and costly task that can not be carried out in a first approach for a general, regional level, emergency plan. Instead, for a first regional-level evaluation simpler techniques, of a general statistical character, have to be used. Therefore, the methods used here have in common that they consider damages to be caused by seismic actions expressed in terms of macroseismic intensity based on the new scale of intensities EMS-98 (Grünthal, 1998) which completes the definition of the scale of intensity MSK, considered for the seismic zones map in Figure 22.1 The present construction typologies can be expressed without too many difficulties in terms of the typologies defined in EMS-98 and the expected damages for a certain intensity can be deduced from a matrix of probability of damages in agreement with this scale.

The methodology applied to dwelling buildings has a statistical character to make use of easily available statistical data, without needing a hard search for detailed information on individual buildings that requires intense fieldwork. This implies that the results obtained for each municipality, which is the selected unit of work, always refer to global values, without giving detailed results for individual buildings.

A first approach to the vulnerability assessment of hospitals and firemen stations was also required. The same approach for dwelling buildings has been applied introducing the concept of a probabilistic individual building assessment, as presented in 22.2.4. It is clear that when knowledge about the seismic behaviour of a specific building is required, as is the case of those with essential services for the community, further detailed analysis would be needed, but as a first approach, the “probable” response of some individual building can be assessed, associating to this individual building the statistical vulnerability distribution of the class of buildings it belongs to.

The classification of the dwelling buildings of Catalonia (near a million), according to the defined classes of vulnerability in the EMS-98, has been elaborated from data from the buildings census made in 1990 by the Institute of Statistics of Catalonia (IEC); the available information is the age, the height and the geographic location of the buildings.

The age and the height are clearly associated to the seismic vulnerability of the buildings. The age not only has importance by its effect on the process of loss of the resistance of the building but is indicative of constructive techniques, variable throughout time. According to information collected by specialists it has been possible to make three groups of buildings according to the period of construction: previous to 1950, between 1950 and 1970 and after 1970. On the other hand, the height influences the response of the buildings to a seismic action. In the case of the buildings of Catalonia, that have been constructed to hold gravitational loads solely, this parameter has served to differentiate buildings that have a safety margin with respect to which they are in the resistance limit. Buildings were classified by height in three ranges: low,

up to 12 m (less than 5 plants), high more than 18 m (more than 5 plants) and the buildings of intermediate heights (5 plants, 15 m). The fact that buildings are in an urban or rural area is also considered. Table 22.1 shows the distribution of the dwelling buildings of Catalonia (aprox. 935,000) according to the three indicated groups.

Table 22.1. Distribution of dwelling buildings of Catalonia by height, age and location

Date of Construction		Pre – 1950		1951-1970		Post - 1970	
Geographic Situation		Urban	Rural	Urban	Rural	Urban	Rural
Height	< 5 stories	232740	31119	212070	16304	315504	37346
	= 5 stories	7065	9	14083	24	11937	22
	> 5 stories	12699	2	21963	33	22028	44

As it is shown in Table 22.1, most of the buildings of Catalonia, around 90%, are located in urban nuclei. A similar percentage is observed for the low rise buildings (less than 5 stories). When looking at the age of the buildings, a large percentage of the construction has taken place since 1970, as 41% of the buildings were built after that date.

The different building structural typologies existing in Catalonia were identified by age of construction. Additional knowledge on state of conservation of the building stock in the study region has also been considered. Weighing all the information available, within the criteria of the EMS-98 and the judgment of experts allowed a classification of the buildings of Catalonia into 18 Typologies described, by Chávez (1998) as percentages of vulnerability classes A, B, C and D of the EMS-98, in function of the three above mentioned parameters: age, height and location in urban or rural area (Table 22.2).

Table 22.2. Classification of buildings in Catalonia in vulnerability classes, according to EMS-98

	< 1950		1951-1970		> 1970	
	Urban	Rural	Urban	Rural	Urban	Rural
< 5 plants	20% A + 80% B Typology 1	30% A + 70% B Typology 4	5 % A + 50% B + 45% C Typology 7	15 % A + 70% B + 15% C Typology 10	85% C + 15% D Typology 13	5% A + 20% B + 65% C + 10% D Typology 16
= 5 plants	20% A + 80% B Typology 2	40% A + 60% B Typology 5	10% A + 60% B + 30% C Typology 8	20% A + 70% B + 10% C Typology 11	5% A + 20% B + 65% C + 10% D Typology 14	10% A + 30% B + 55% C + 5% D Typology 17
> 5 plants	40% A + 60% B Typology 3	60% A + 40% B Typology 6	15 % A + 70% B + 15% C Typology 9	30% A + 65% B + 5% C Typology 12	8% A + 27% B + 60% C + 5% D Typology 15	15% A + 45% B + 40% C Typology 18

22.2.3. LOSS ESTIMATION

An estimation has been carried out of the damages that can afflict buildings in the different municipalities for the intensities of the map of seismic zones presented in Figure 22.1. In addition, as a result of the damage caused in the buildings, a scenario of the consequences for the population of each municipality has been made.

22.2.3.1. Loss estimation to dwelling buildings

The estimation of the damage has been made by means of probability damages matrices that have been determined for the classes of vulnerability A, B, C, D, E and F, the degrees of damages of 0 (no damage) to 5 (total collapse) and the degrees of intensity (VI to X) of the EMS-98 scale (Chávez, 1998; Chávez et al., 1998). An example for intensity VIII is presented in Figure 22.2.

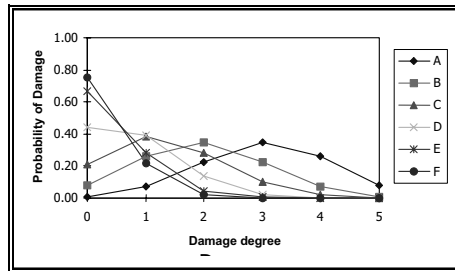


Fig. 22.2. Probability damages matrix for intensity VIII

As a result of the evaluation of the physical damage, the number of buildings of each municipality distributed according to the different damage degrees is obtained. From the damage experienced by the buildings has been elaborated an estimation of how many of them could stay in uninhabitable conditions, considering those that undergo the degrees of damages 4 and 5 to be in this state as well as 50% of those that experience damage 3. These results are of maximum importance for the evaluation of the possible number of homeless after occurrence of the earthquake.

The estimation of the number of buildings for each municipality that would be uninhabitable, considering the seismic action defined in Figure 22.1 is shown in Figure 22.3.

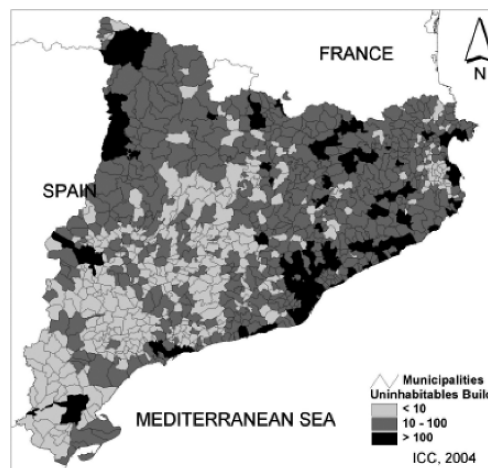


Fig. 22.3. Map with the estimation of the number of uninhabitable buildings for each municipality for the degrees of intensity considered in the map of Figure 22.1

The results of these estimations show that a great number of municipalities, near 400, would not be much affected, i.e., would have less than 10 uninhabitable buildings; approximately a half of municipalities of Catalonia would have between 10 and 100 uninhabitable buildings and less than 100 municipalities would have more than 100 uninhabitable buildings.

22.2.3.2. Estimation of human casualties

The possibility of having human victims as a result of the action of an earthquake is directly related to the number of buildings damaged and to the number of persons that live there. But it also depends on other circumstances such as the season, the day of the week and the hour of the earthquake occurrence and the preparedness of the people in charge of Civil Protection and the citizens requiring face first aid.

In a first approach the number of victims of different severity can be estimated using damage data from past earthquakes (Coburn and Spence, 1992) considering the results of damaged buildings that have been previously obtained together with data of the population census.

The result obtained is that in most of the municipalities, more than 800, the average number of people by building is less than 5 and only some municipalities, such as Barcelona and others of their zone of influence, arrive at average values of almost 30 inhabitants per building. A map with the estimation of the number of homeless due to the non-inhabitability of their houses, for each municipality, is shown in Figure 22.4.

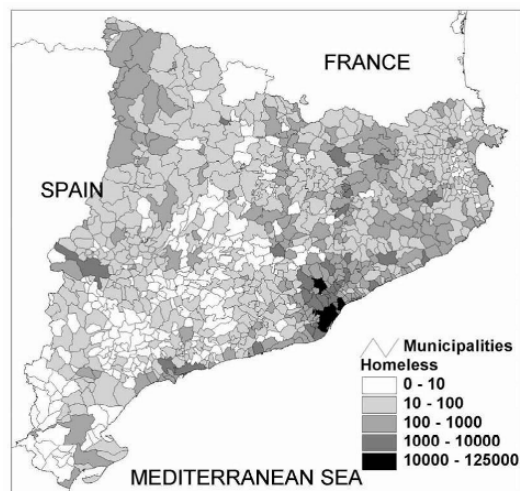


Fig. 22.4. First estimation of the distribution of the number of homeless in the different municipalities for the intensities given in the hazard map

The inhabitants of almost two thirds of the total number of municipalities of Catalonia would not be much affected by an earthquake (less than 100 people per municipality). The upper bound corresponds to the city of Barcelona with a total of more than 100,000

people that could become homeless, in case of occurrence of the intensity indicated in this municipality in the map of seismic zones of Figure 22.1.

22.2.4. DAMAGE ESTIMATION AT HOSPITALS

An estimation of the damages that the hospitals could suffer, considering the intensities of the map of seismic zones presented in Figure 22.1 and the classification of the buildings in the 18 defined typologies (Table 22.2) has been carried out. Each typology has a characteristic behaviour that has been calculated using the probability damages matrices and the distribution of the buildings in vulnerability classes. The percentage of each damage degree (from damage 0, to damage 5, collapse of the building) that can undergo the building by different intensities has been obtained (González et al., 2002).

For each typology the distribution of the probability of damages for each degree of damage and each intensity has been plotted. Also the different behaviours of the buildings have been grouped on the basis of the morphology of the curves of probability of damages (Figure 22.5). Four classes of behaviour are defined as a response to the seismic action:

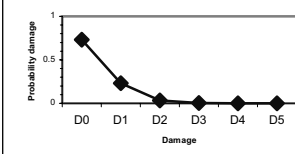
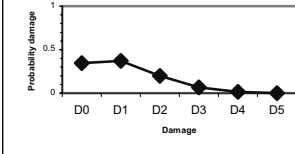
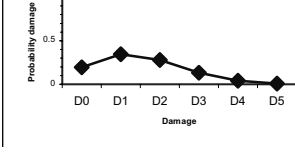
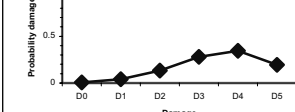
BEHAVIOUR BUILDINGS	FEATURES	INSTALLATIONS
	<p>BEHAVIOUR 1 Less than 10% of damage > D2</p>	<p>Undamaged</p>
	<p>BEHAVIOUR 2 Between 10-40% of damage >D2 Between 0-15% of damage >D3</p>	<p>Operative</p>
	<p>BEHAVIOUR 3 40% or more of damage >D2 Between 15-40% of damage >D3</p>	<p>Not Operative Inhabitable</p>
	<p>BEHAVIOUR 4 More than 50% of damage >D3 More than 20% of damage >D4</p>	<p>Not Operative Uninhabitable</p>

Fig. 22.5. The different behaviour of the hospitals based on the curves of probability of damages

- Behaviour 1 means that after the earthquake the building would be undamaged and stay able to continue with its functions.
- Behaviour 2 means that after the earthquake the installation is still operative, but an inspection of all the facilities is recommended.
- Behaviour 3 means that after the earthquake the installation would be out of service, although the building continues being inhabitable. An inspection of the building is recommended in this case.
- Behaviour 4 means that it will be necessary to evacuate the building.

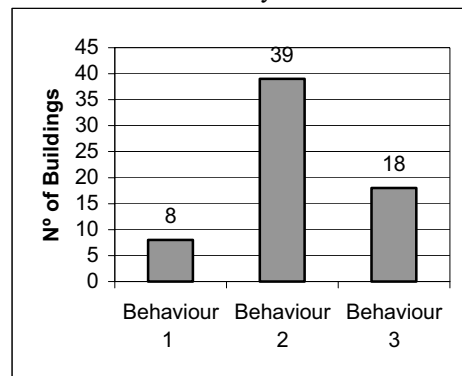


Fig. 22.6. Number of hospitals for each type of behaviour

The number of hospitals corresponding to each behaviour type is shown in Figure 22.6: 8 hospitals would have Behaviour 1, 39 would have Behaviour 2, 18 would have Behaviour 3 and no hospital would have Behaviour 4.

Further developments concerning analysis of hospital systems have been discussed in Chapter 12.

22.2.5. LOSS ESTIMATION IN LIFELINES

The lifelines are constituted of those infrastructures that are essential for the normal development of human activity and, in general, include lines that make possible the mobility of merchandise and people (transport), great lines of energy and basic elements provision, as for example, water, electricity, gas and fuels and, finally those that ensure communications (see Chapter 9).

In order to consider the damages in the lifelines, the methodology proposed by the "Applied Technical Council" (ATC), from California and in particular, methods ATC-13 (1985) and ATC-25 (1991) developed under the sponsorship of the Federal Emergency Management Agency (FEMA) have been applied. These methods are of easy use if the data on the elements to be analysed are available; this aspect is very important due to the great number of elements to be considered. It is necessary to say that the obtained results are of statistical nature and that allow only to give a first plot of the most vulnerable points of the lifelines in the study region. More detailed specific studies will have to be carried out in the elements of highest vulnerability or of highest strategic importance.

With this methodology the following lifelines have been analysed: road network, railway transport, electrical system, water supply, gas network and dams.

Each lifeline is considered to be constituted by basic elements: walls, bridges, highways, electrical lines, mechanical equipment, electrical equipment, etc. Each basic element has a vulnerability function that relates the intensity of the earthquake to the proportion of damage that the basic element will undergo. From the determination of the damage of each one of the basic elements that compose the lifeline the damage of this line can be assessed.

The classic scales of intensity profit from the experience of a great number of earthquakes and, for example, scale MSK refers to damages to lifelines only from intensity degree VIII (sometimes the rupture of some joints of pipelines takes place). For intensity IX the scale indicates considerable damages in deposits of liquids, partial breaking of underground canalisations and, in some cases railroad bending and interruption of highways service. For intensity X dangerous damages in dams, serious damages in bridges, railroads turned aside and, sometimes, waved, underground conductions turned or broken, and pavement of the streets and asphalt suffering great undulations are envisaged. Therefore, it is not very probable that damages on lifelines in areas with intensity VI or VII appear.

The obtained results show that, in general, lifelines have a good behaviour for the levels of intensity associated to a return period of 500 years (always lower than or equal to VIII). The more significant damages would take place mainly in the mechanical and electrical equipment and in those of high technology that form part of the transport and communications nets of electricity, gas and water, of the great networks of transport like for example freeways and railroads and those of the communication systems (telephone, radio, television, among others). It is therefore in the pumping stations, the transforming stations and substations and the communications centres or other centres equipped with equipment of high technology where it can be expected that incidences arise in case of earthquakes of intensity VII-VIII and VIII.

22.3. Damage scenario mapping: a tool for emergency preparedness

A methodology has been proposed to generate damage scenarios that gives an estimation of the possible effects of a given earthquake for the preparation of emergencies. The method can also be used to give a first damage estimation, immediately after the occurrence of an earthquake.

The main objective of the simulation of damage scenarios is to carry out a quick evaluation of the possible intensities that could have been felt in each municipality of the region, the number of persons that could have felt the earthquake with each intensity degree and the surface (km²) of the affected area for each intensity degree. If the earthquake has an intensity high enough to produce damages, the method gives an estimation of damages to buildings, human casualties and economic losses.

This methodology can be also used to simulate the damages of historical damaging earthquakes if they would occur today. The simulation of damages corresponding to an

earthquake scenario similar to that of one of the largest earthquakes that occurred in the Pyrenees in historical times will be shown in 22.3.2.

Another application of the methodology is the zonation of the territory in order to establish the criteria for activation of different levels of the earthquake emergency plan according to the severity of the estimated consequences of the events.

22.3.1. METHODOLOGY

The methodology consists of three steps:

- 1) Estimation of epicentral intensity. If the epicentre depth and magnitude of the earthquake are known, it is possible to estimate the epicentral intensity from a correlation between magnitudes and intensities felt by the population in the last years.
- 2) Intensity attributed to each municipality. It is necessary to adopt a law of attenuation of the intensity versus the distance. The relationship used for Catalonia has been fitted to the intensity data points contained in the database of felt earthquakes (Susagna et al., 1996; 2001).
- 3) Estimation of damage in buildings, assessment of the human casualties and evaluation of economic losses. In the case of intensities greater than V these computations are carried out following the methodology presented in 22.2. The number of uninhabitable buildings, the number of homeless, and the damages to the people are also computed. Data on building occupancy (inhabitants / building) for each municipality and average surface of the houses are used. The economic losses produced by the damage to the buildings are estimated and, finally, are expressed in terms of the Gross National Product (GNP). The surface that could be covered by debris is also estimated.

A Geographical Information System (GIS) is used in this application - *ESCENARIS V1.00* (RSE, 2003) - to visualise the results together with different information layers. An example of a scenario map and list of municipalities is shown in Figure 22.7.

22.3.2. DAMAGE SCENARIO FOR AN EARTHQUAKE SIMILAR TO AN HISTORICAL ONE

The earthquake that occurred in 1428 in the *Ripollès* (Girona) near the border between Spain and France is one of the greatest seismic events that the region has suffered in the past. Chronicles and other documents contemporary to the event report effects in a quite extensive way, including destruction of towns, churches, castles, etc., and the death of 800 people (Banda and Correig, 1984; Olivera et al., 2005). This is the reason for the interest in the simulation of a scenario of the possible effects of an earthquake like this one of 1428 if it occurred at the present time.

In this case, the attenuation of the intensity with the distance has been fitted with the values of epicentral intensity and intensities in several localities given by Banda and Correig (1984). A map with the simulation of intensities possibly felt in each of the present day municipalities of Catalonia is shown in Figure 22.8 (González et al., 2001).

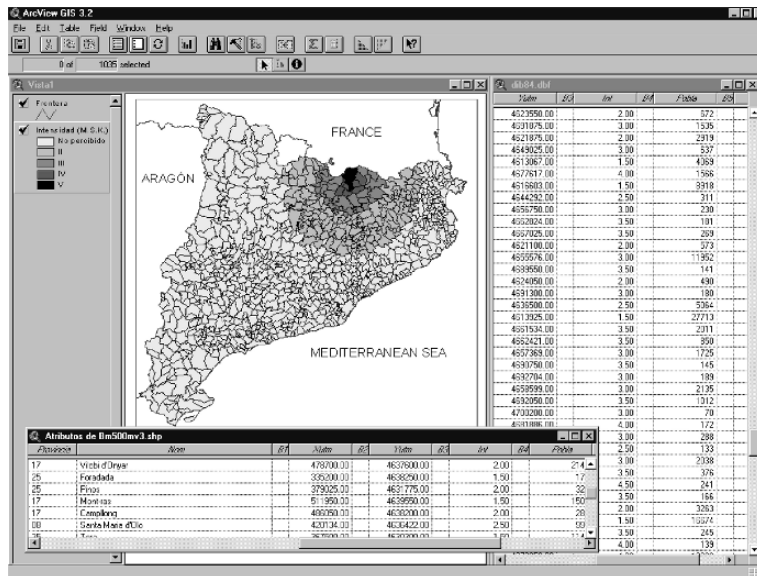


Fig. 22.7. Example of a scenario map with the list of municipalities for an earthquake of M=4.0 in the Pyrenees

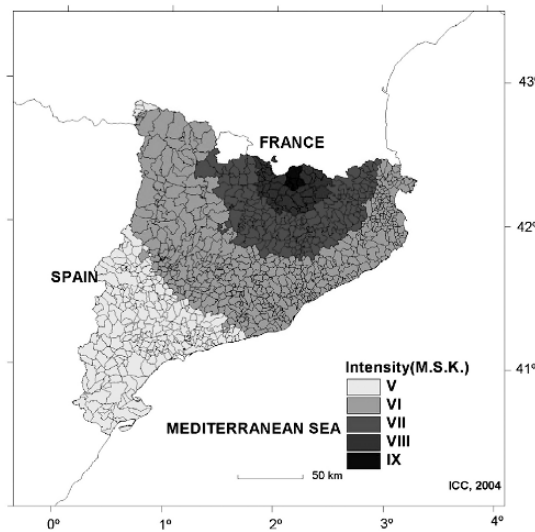


Fig. 22.8. Probable felt intensity map for the earthquake that occurred in the Ripollès in 1428, I_{max} = IX

An estimation of the different damage grades, affecting the dwelling buildings of each municipality as well as the number of homeless and victims has been done. A summary of damages for the whole of Catalonia has been completed. The results are shown in Table 22.3. The estimated *destroyed area* refers to the probable surface with debris. The direct economic cost of the resulting damage - only referred to the dwelling buildings -

is about 8% of the annual GNP of this community. Other direct costs related to installations other than dwellings and indirect costs (e.g. related to the interruption of services and interruption of economic activities) are not considered.

22.3.3. CRITERIA OF ACTIVATION OF THE PLAN OF SEISMIC EMERGENCIES IN CATALONIA (SISMICAT)

22.3.3.1. Present situation

The emergency plans include various levels of intervention (ALERT, EMERGENCY 1 and EMERGENCY 2), bringing out the adequate amount of resources, depending on the severity of the event.

Table 22.3. Earthquake scenario simulation for an earthquake in the Ripollès of $I_{max}=IX$

Uninhabitable buildings	Homeless	Economic losses (M€)
23 570	136 901	4 978
Economic losses (%GNP of Catalunya)	Destroyed Area (m ²)	
8	207 712	

These activation levels are defined in the current plan (SISMICAT) taking into account the ground shaking and the population density.

Three types of zones are distinguished, according to their population density: Zone A, Zone B and Zone C, constituted by municipalities with population density (inhabitants per km²) greater than 100, between 10 and 100 and less than 10, respectively (Figure 22.9).

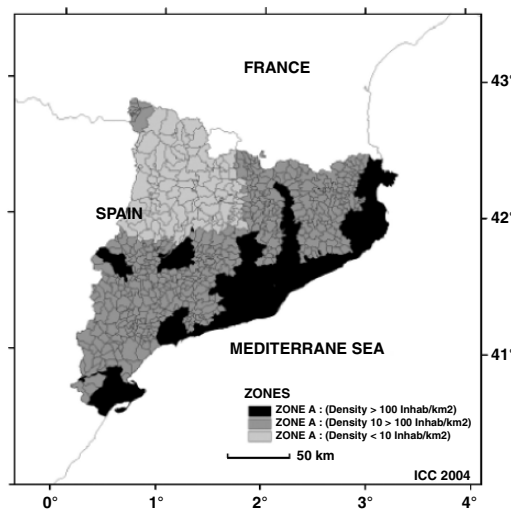


Fig. 22.9. Map of zones according to their population density

The activation levels are defined as follows:

- *Alert*: The Alert level is activated when wide preventive and control measures are required. The activation in this phase of alert implies a warning to the acting groups, information to the involved organisms and services, information to the population if requested, and follow-up of the tasks to be done. Actions from Security and Intervention groups are only considered in a preventive way.
- Emergency 1: It entails putting into operation of the organizational structure of emergency management with the general or partial mobilization of the tools and means assigned to the plan. The SISMICAT plan is activated in emergency 1 when a seismic event with important, but local and limited effects on the territory takes place. This situation will be evaluated from the information available at the moment of the emergency considering the following criteria: the degree of affect on the population and the kind of actions required (e.g. information, evacuation, etc.), the geographical extension of the crisis (e.g. number of affected municipalities) and the tools needed.
- Emergency 2: The plan is activated in Emergency 2 when the seismic effects affect an important extension of the territory on the basis of the same criteria above mentioned.

A synthesis of the criteria adopted in the SISMICAT Plan for triggering the above defined activation levels, for each zone of the territory, from felt intensity and complementary data is shown in Figure 22.10 and in Table 22.4. The Pre-Alert level corresponds, as it is indicated by its name, to a non-activation of Civil Protection Services.

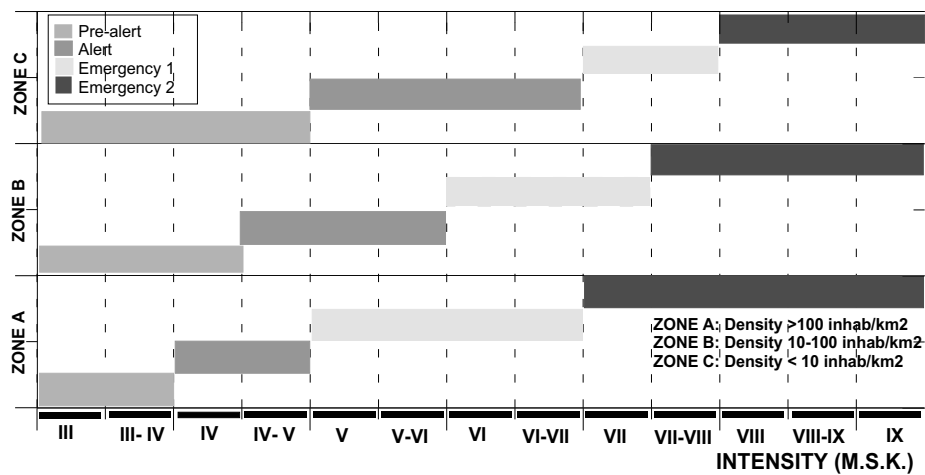


Fig. 22.10. Different level of activation of the emergency plan, depending on the intensity of the seismic action and the population density (zones A, B and C)

Table 22.4. Criteria of activation of the different levels on the basis of population density, macroseismic intensity and other additional criteria from information on effects. (* *comarca* is an administrative division comprising a number of municipalities)

Activation evels	Intensity			Other criteria
	Zone height density populate (A)	Zone medium populate (B)	Zone low populate (C)	
ALERT	IV to IV-V	IV-V to V-VI	V to VI-VII	Some people with minor injuries 1-10 homeless
EMERGENCY 1	V to VI-VII	VI to VII	VII to VII-VIII	1-10 dead people 10-100 homeless Panic Failure of basic services (local level) Possibility of dominoes effect
EMERGENCY 2	≥VII	≥VII-VIII	≥VIII	>10 dead people >100 homeless Failure of basic services (at the scale of <i>comarca</i> *) Domino Effect ,with activation of other special plans.

22.3.3.2. A tool for the definition of the level of activation

These activation levels can be defined taking into account not only the estimation of ground shaking but also other factors related to physical, human and societal vulnerability, such as the expected number of uninhabitable dwelling buildings, the number of homeless or the direct economical losses. All these parameters can be estimated for a regional damage scenario developed previously for an earthquake occurring at any point of the territory with any magnitude.

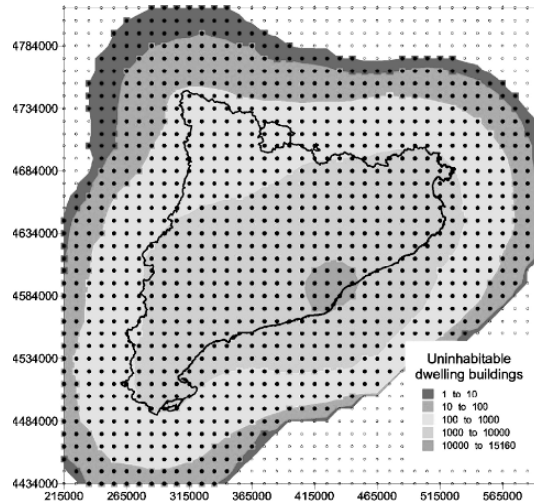


Fig. 22.11. Number of uninhabitable dwelling buildings after an earthquake of M5.5, occurring at each point of the grid

The methodology proposed is based on a graphical representation that concentrates all the regional damages estimated for an earthquake on its epicentre. Then, each point of the territory can be characterized by the severity of damages caused by an earthquake with epicentre in this given point, for each possible magnitude. The same methodology explained in the preceding sections has been applied to compute damages. As an example of the method, the number of uninhabitable dwelling buildings that would be observed after an earthquake of M5.5 is shown in Figure 22.11.

If the value of one parameter of damage is fixed, it is possible to construct new maps with the magnitude of the earthquake needed at any point of the grid to produce this damage.

A seismic zonation proposed for an emergency plan activation is shown in Figure 22.12 and in Table 22.5 (Reinoso et al., 2003). In this table the ranges of magnitude are defined for each zone and for each level of activation, indicating the grades of damages expected (Figure 22.12).

With the aid of the zonation established on this basis, immediately after an event detected by the seismological network, the preliminary level of intervention can be quickly decided.

This procedure will then be implemented in connexion with the real-time VSAT transmissions based regional seismological network of the ICC to provide the Civil Protection authority with fast information to trigger adequate levels of activation of the Seismic Emergency Plan.

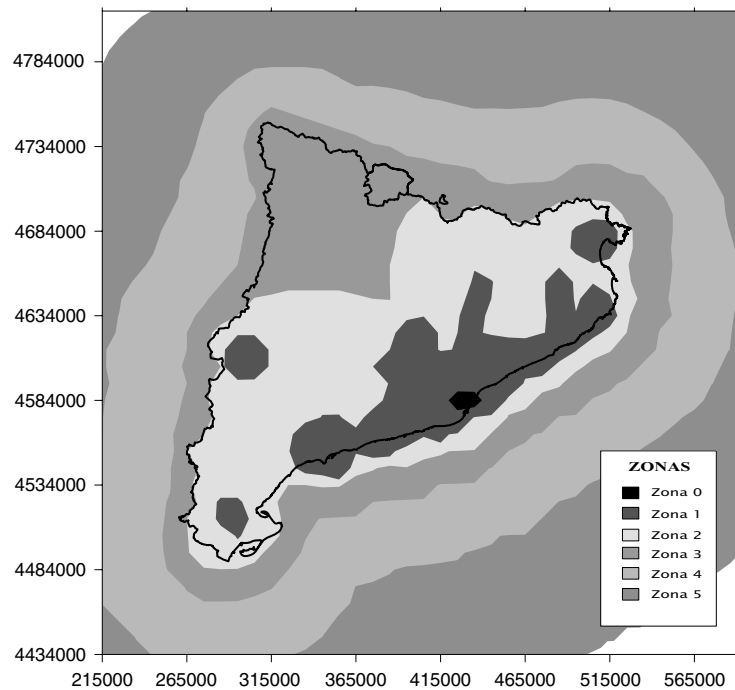


Fig. 22.12. Seismic zonation proposed for activation of the emergency plan

Table 22.5. Ranges of values of magnitude for each zone and for each level of activation

Seismic criteria for emergency plan activation			
ZONES	Alert	Emergency 1	Emergency 2
	More than 25 000 inhabitants feel an earthquake with intensity \geq IV	Uninhabitable dwelling buildings: < 500 Homeless: < 2.000 Losses: < 180 M€	Uninhabitable dwelling buildings: > 500 Homeless: > 2.000 Losses: > 180 M€
0	Magnitude 3.8 to 4.3	Magnitude 4.3 to 4.6	Magnitude > 4.6
1	Magnitude 3.8 to 4.3	Magnitude 4.3 to 4.8	Magnitude > 4.8
2	Magnitude 4.0 to 4.6	Magnitude 4.6 to 5.1	Magnitude > 5.1
3	Magnitude 4.3 to 4.8	Magnitude 4.8 to 5.4	Magnitude > 5.4
4	Magnitude 4.6 to 5.1	Magnitude 5.1 to 5.9	Magnitude > 5.9
5	Magnitude 5.1 to 5.6	Magnitude 5.6 to 6.1	Magnitude > 6.1

Aknowledgements

The methodology for damage assessment was developed by Justina Chávez in her PhD Thesis. She had the support of Josep Presmanes and Fructuós Mañá for the classification of vulnerability typologies. Marta González adapted the algorithms to the application of damage scenarios, which was automated by Núria Romeu in the ESCENARIS v1.1 code. Edwin Reinoso developed the methodology for the seismic zonation for activation levels. We are grateful to all them for the help provided.

CHAPTER 23

RISK-UE PROJECT: AN ADVANCED APPROACH TO EARTHQUAKE RISK SCENARIOS WITH APPLICATION TO DIFFERENT EUROPEAN TOWNS

P. Mouroux and B. Le Brun

Bureau de Recherches Géologiques et Minières, Marseille, France.

23.1. Introduction

The European RISK-UE project was launched in 1999, at the end of the International Decade for Natural Disaster Reduction (IDNDR). The project started in January 2001 and ended in September 2004.

The project itself involved the assessment of earthquake scenarios based on the analysis of the global impact of one or more plausible earthquakes at city scale, within a European context. The primary aim of these scenarios was to increase awareness within the decision-making centres of a city, of the successful appropriation of the problems caused by a seismic risk and of the implementation of *Management Plans* and *Plans of Action* to effectively reduce this risk.

No such global programme, as HAZUS and RADIUS, was launched in Europe and this has proved to be an urgent requirement, particularly in light of the political impact of the earthquakes in Izmit, Turkey, in Athens, Greece and in ChiChi, Taiwan, by the end of 1999.

Structured around European cities, the RISK-UE project, first and foremost, developed a *Modular Methodology* for creating earthquake scenarios concentrating on the distinctive features of European cities with regard to current and historical buildings, as well as on their functional and social organisation, in order to identify weak points within the urban system.

This approach has been applied to the following 7 European cities: Barcelona, Bitola, Bucharest, Catania, Nice, Sofia and Thessaloniki (Figure 23.1).



Fig. 23.1. Cities of RISK-UE Project

Before going into details for the RISK-UE project, we present two among the most world-wide cited cases dealing with seismic scenario studies: HAZUS, produced by FEMA (USA) and RADIUS, developed for cities in developing countries (UN-ISDR).

23.2. Previous case studies

23.2.1. HAZUS

23.2.1.1. Introduction

Earthquakes pose a threat to life and property in 45 states and territories of the United States. As they have become more urbanized, more frequent smaller earthquakes in the 6.5 to 7.5 magnitude range now have the potential of causing damage equal to or exceeding the estimated 40 millions of dollars from the 1994 Northridge Earthquake.

FEMA (Federal Emergency Management Agency) is committed to mitigation as a means of reducing damages and, both, the social and economic impact from earthquakes. FEMA, in agreements with the National Institute of Building Sciences, has developed HAZUS (NIBS, 1997, 1999 and 2002), a standard, nationally applicable methodology for assessing earthquake risk. HAZUS was first released in 1997, followed by three subsequent releases.

23.2.1.2. HAZUS overview

Purpose. As explained in the technical manual (see HAZUS website) and in H. Shah different presentations (see RISK-UE ftp and website), the purpose of HAZUS is multiple:

- It is an integrated GIS tool for performing comprehensive natural hazard assessment studies on any region within the United States.
- Its results encompass several disciplines that are useful in risk assessment, emergency preparedness, response planning and recovery, decision-making and mitigation.
- It assists in understanding hazard, inventory, vulnerability and response.
- It is a useful tool for assessing the fragility of the general inventory components and for pinpointing deficiencies in the existing infrastructure.
- It provides the knowledge necessary for the design and implementation of plans and strategies which reduce the negative impact of future natural disasters.

The general framework for the model is represented in Table 23.1.

FEMA loss Estimation Methodology. The primary purpose of HAZUS is to develop guidelines and procedures for making earthquake loss estimates at a regional scale. This would be used primarily by local, state and regional officials to plan and stimulate efforts to reduce risks from earthquakes and to prepare for emergency response and recovery. A secondary purpose of HAZUS is to provide a basis for assessing nationwide risk of earthquake losses.

Overall approach and framework of methodology. The methodology should be both flexible, accommodating the needs of a variety of different users and applications, and

able to provide the uniformity of a standardized approach. The framework of the methodology includes each of the components shown in Figure 23.2.

Table 23.1. HAZUS: General framework for model

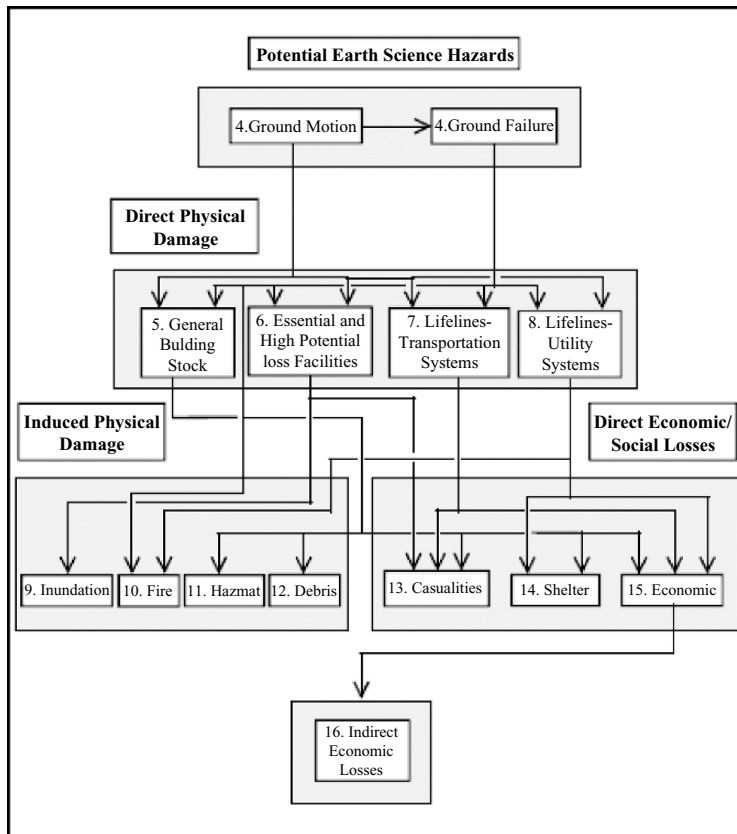
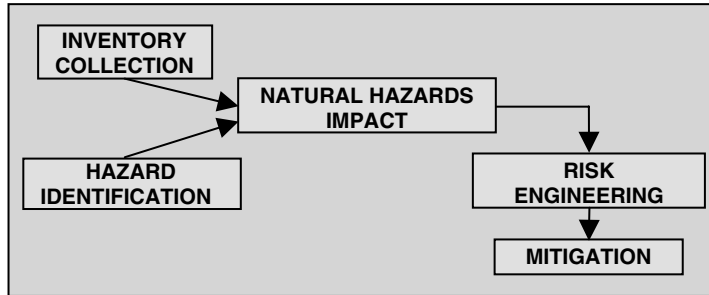


Fig. 23.2. HAZUS: Flowchart of the earthquake loss estimation methodology

Technical tools - HAZUS software. A technical manual and a user's manual are available for application of the methodology by different (experts and non- technical) users. The last manual addresses important implementation issues, such as:

- 1) Selection of scenario earthquakes and hazard inputs
- 2) Selection of appropriate methods to meet different user needs
- 3) Collection of required inventory data
- 4) Costs associated with inventory collection
- 5) Presentation of results including appropriate terminology, etc.
- 6) Interpretation of results including consideration of all uncertainties.

23.2.1.3. HAZUS risk assessment

It is implemented as explained in the technical manual, from the knowledge of all components described in Figure 23.2 and a specific methodology using the following main elements: Building structure types, deterministic and/or probabilistic ground motion and ground failure, performance based design approach for the buildings, allowing the evaluation of direct physical damage of general building stock, essential and high potential loss facilities, transportation systems, utility systems and then, direct social losses (casualties and displaced households), direct and indirect economic losses. The influence of potential collateral effects (inundation, fire following earthquake, hazardous material release, debris, etc...) are also considered.

23.2.1.4. HAZUS as a decision making tool

HAZUS estimates the type and the amount of resources needed to assist affected areas and organizes and sets priorities for recovery based on damage pattern. It provides a basis for planning, zoning, building codes and development of regulations and policy to reduce risk from natural disasters. HAZUS can help in the following aspects:

Preparedness:

- Transportation: ranking of roads and bridges based on risk with respect to hazard, capacity and vulnerability.
- Information and action plans, preparing alternatives to deal with potential damage to transportation and utility systems, therefore assuring faster post-disaster response and recovery.
- Resource support, identifying locations of key recovery facilities.
- Hazardous material, identifying potential sites for hazardous release and regulating future sites.
- Energy, identifying fuel and electrical power systems vulnerable to damage and preparing for fast restoration and recovery plans.

Response and Recovery:

- Real time situation assessment, identifying likely damaged areas and providing quick estimate of damage and casualties.
- Rapid response to reduce loss of life and expedite relief to victims.
- Rapid response leading to faster recovery.
- Numerous tools can be prepared in the following fields: Urban search and rescue, food storage and distribution, communications, fire fighting, health and medical services.

Mitigation, among numerous actions:

- Simulate long term effects of future natural disasters.
- Identify the critical and significant infrastructure components and links.
- Develop strategies to minimize the socio-economic impacts.
- Evaluate alternative mitigation strategies by performing cost-effectiveness analyses.
- Select feasible policies for allocating resources based on the most effective and efficient strategies.
- For long term mitigation plans, adjust the strategies based on additional risk studies that reflect regional future investments and projected inventory and exposure based on current growth trends.
- Different measures concerning Public works, Building code administration, Land-use planning.

23.2.1.5. *HAZUS Examples*

By 2004 numerous examples of HAZUS application exist as it has been used in many cities of the United States like those in Southern California.

We selected here the case study of New York City, because this area is not known as the most seismically dangerous in the US and, in spite of that, a very important and complete evaluation of seismic risk was done and is available on:

<http://www.nycem.org/default.asp>

This evaluation, still in progress, should allow authorities everywhere to achieve and implement a global action plan.

Some results of this application from Tantala et al. (2002) are shown from Figure 23.3 to Figure 23.8.

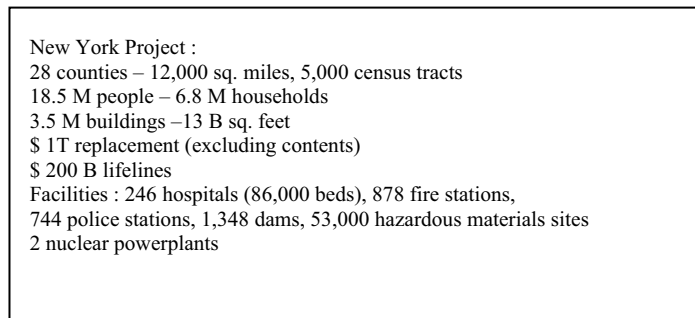


Fig. 23.3. New York - Value at risk

These figures show different scenarios: deterministic scenarios for Magnitudes: 5, 6 and 7, south of Brooklyn, at the same location of an historical earthquake and probabilistic scenarios for return periods of 100, 500 and 2500 years (Maximum considered earthquake). These scenarios show the important increase of seismic motion and building losses with the return period RP (6 billions \$ for RP = 500 years (PGA: 0.17g) and 63 billions \$ for RP = 2,500 years (PGA: 0.36g).

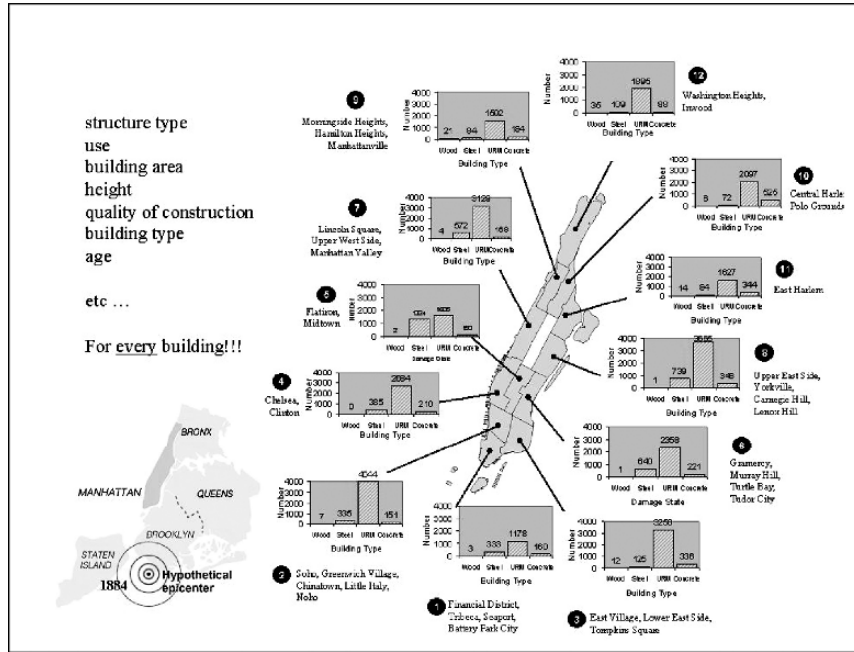


Fig. 23.4. New York - Manhattan : Collected Building Information

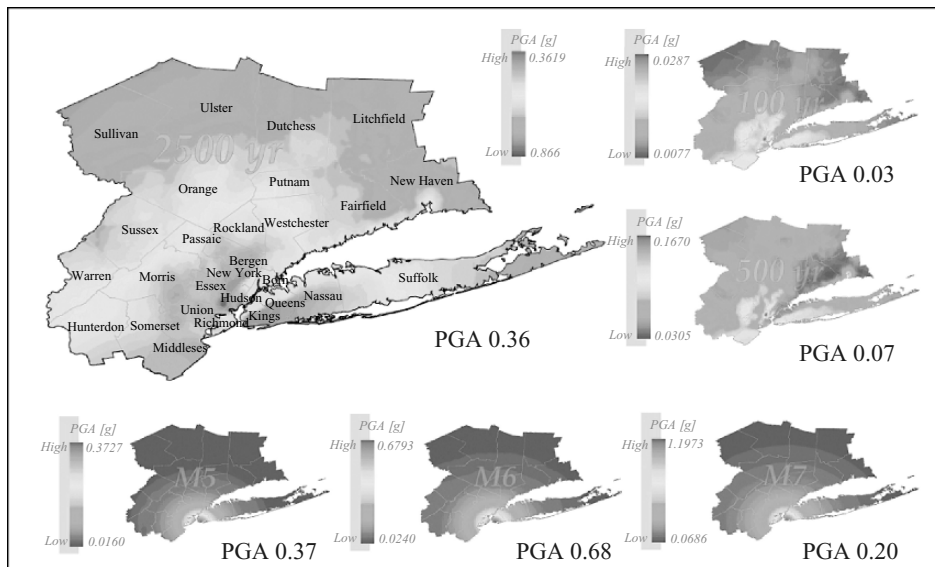


Fig. 23.5. New York: Peak ground acceleration for different scenarios

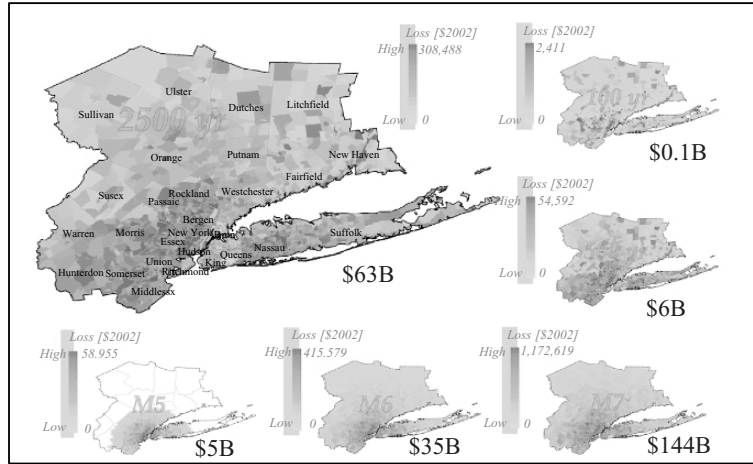


Fig. 23.6. Total building loss with different scenarios

Scenario	Building	Income	Total	Hospitalization [Death]	People requiring Shelter	Fires	Extensive or Complete Damage Buildings	Debris m-tons
M5	\$5.4B	\$0.5B	\$5.9B	24 [13]	2,911	589	967	1.8
M6	\$35.8B	\$12.1B	\$37.9B	2,296 [1,170]	197,705	864	71,926	36
M7	\$144.6B	\$57.6B	\$202.2B	13,171 [6,705]	766,746	1,156	802,484	141
100 yr return 50% in 50 yrs	\$0.1B	\$0.1B	\$0.2B	0 [0]	0	0	0	0.2
500 yr return 10% in 50 yrs	\$5.7B	\$1.8B	\$7.5B	28 [14]	575	48	2,102	3.1
2500 yr return 2% in 50 yrs	\$63.3B	\$18.3B	\$81.6B	1,430 [727]	84,626	906	154,123	32

Fig. 23.7. Total building loss and consequences

Awareness campaign:

- <http://www.nycem.org>
- Discovery Channel's program "Earthquake's in New York?"
- WNBC-News broadcast
- several articles in The New York Times

Developing specific vulnerability relationships for tall buildings
"uniquely metropolitan" infrastructure

Assisted 9/11 effort:
using NYCEM database to survey and map damage with SEAoNY
provide rapid, rough estimates to FEMA of the projected losses

Other work and other areas

Fig. 23.8. New York: Outreach/ additional work

23.2.2. RADIUS

23.2.2.1. *Introduction*

The United Nations General Assembly designated the 1990s, as the “International Decade for National Disaster Reduction (IDNDR)” to reduce loss of life, property damage and social and economic disruption caused by natural disasters. Then, the IDNDR secretariat launched the RADIUS initiative (Risk Assessment tools for Diagnosis of Urban Areas against Seismic Disasters) in 1996, with financial and technical assistance from the Government of Japan. It aimed to promote wordlist activities for the reduction of urban seismic risk, which is growing rapidly, particularly in developing countries. The primary goal of this initiative is to help people understand their seismic risk and raise public awareness as the first step towards seismic risk reduction.

23.2.2.2. *RADIUS overview*

As stated by Kenji Okazaki, Manager of the Initiative, the direct objectives of RADIUS (1999) were:

- A) To develop earthquake damage scenarios and action plans in nine case-study cities selected worldwide;
- B) To develop practical tools for seismic risk management, which could be applied to any earthquake-prone city in the world;
- C) To conduct a comparative study to understand urban seismic risk around the world;
- D) To promote information exchange for seismic risk mitigation at city level.

The tools resulting from this initiative are useful to decision makers and government officials who are responsible for disaster prevention and disaster preparedness in their respective cities:

- To decide priorities for urban planning, land-use planning, and building regulations;
- To prepare an improvement plan for existing urban structures such as reinforcement (retrofitting) of vulnerable buildings and infrastructure, securing of open spaces and emergency roads;
- To prepare for emergency activities such as life saving, fire fighting, and emergency transportation.

The results are also useful to communities, NGOs, and citizens:

- To understand the vulnerability of the area where they live;
- To understand how to behave in case of an earthquake;
- To participate in preparing plans for disaster prevention.

The results are useful to semi-public companies that maintain urban infrastructure to understand the necessity of prevention and preparedness. The results can also be useful to business leaders, building owners, developers, real estate agents, and

insurance/reinsurance companies so that they may minimize the damage on their human resources as well as properties for their business.

The implementation of RADIUS took place over 2 years, starting in 1997, with preliminary selections of cities, scientific and technical subcommittees and three international Institutes. It continued with the selection of 9 case-study cities, kick-off meetings, training seminars in Japan, launching of the 9 studies in 1998, and ended in 1999, with “Earthquake damage scenario” workshops, followed by “Action plans” workshops, a comparative study on “understanding urban seismic risk in the world”, a development of practical tools and finally an “International RADIUS Symposium”, Tijuana-Mexico, in October.

In 2000, the following publications were issued: 2 brochures – outline and outcome of RADIUS Initiative, a summary of RADIUS, with CD-ROM, full reports, including “Project document and the developed tools” and 9 case studies. See: <http://www.geohaz.org/radius/>

23.2.2.3. *RADIUS case studies*

Objectives. As stated in the final document, the direct objectives of the case studies were:

- A) To develop an earthquake damage scenario which describes the consequence of possible earthquakes;
- B) To prepare a risk management plan and propose an action plan for earthquake disaster mitigation.

The case studies aimed:

- A) To raise the awareness of decision makers and the public to seismic risk;
- B) To transfer appropriate technologies to the cities;
- C) To set up a local infrastructure for a sustainable plan for earthquake disaster mitigation;
- D) To promote multidisciplinary collaboration within the local governments as well as between government officers and scientists;
- E) To promote worldwide interaction with other earthquake-prone cities.

In order to develop earthquake damage scenarios, the physical damage to buildings and infrastructure, human losses in the city, as well as the effects on urban functions and activities were first estimated. The earthquake damage scenario describes the various stages of the city’s damage during and after a probable earthquake. Human loss was estimated, based on the damage of buildings and infrastructure, the efficiency of relief activities, and outbreaks of fires.

Based on the scenario, a risk management plan was prepared containing the following aspects:

- Urban development plan to mitigate seismic disasters;

- Improvement plan for the existing urban structures such as reinforcement (retrofitting) of vulnerable buildings and infrastructures, securing of open spaces and emergency roads, and designation of areas for evacuation;
- Emergency activities such as life saving, fire fighting, emergency transportation, and assistance to suffering people;
- Individual countermeasures for important facilities;
- Dissemination of information to, and training of, the public and private sectors.

Finally, a practical “Action Plan” was proposed. It prioritised the necessary actions so that they could be implemented soon after the project. It was a first small step for each community in the city. The scenario and action plan were disseminated to relevant organisations and the public.

Case-study cities A total of 9 cities were selected in 1998 (Figure 23.9 and Table 23.2) under consultation with assigned international institutes, namely INCED, Japan (International Center for Disaster Mitigation Engineering), BRGM, France (Bureau de Recherches Géologiques et Minières), GHI, United States (GeoHazard International). These 9 cities were:

For Asia: Bandung (Indonesia), Tashkent (Uzbekistan), Zigong (China),

For Europe and Africa: Addis-Ababa (Ethiopia), Izmir (Turkey), Skopje (Former Yugoslav Republic of Macedonia),

For Latin America: Antofagasta (Chili), Guayaquil (Ecuador), Tijuana (Mexico).

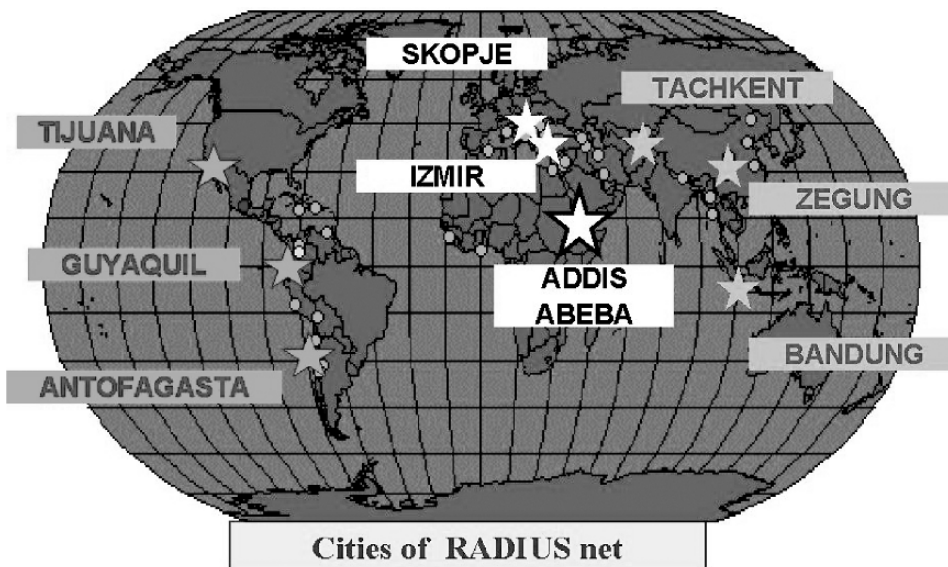


Fig. 23.9. Cities of RADIUS net

Table 23.2. Basic information on the nine RADIUS case-study cities

City	Addis Ababa	Antofagasta	Bandung	Guayaquil	Izmir	Skopje	Tashkent	Tijuana	Zigong
Area (km ²)	54	90	168	340	90	1,860	326	250	4,373
Population (in millions)	2.90	0.22	2.06	2.10	3.00	0.55	2.08	1.25	3.13
Population growth	3.80%	3.00%	3.48%	3.20%	3.00%	8.00%	2.00%	6.02%	0.74%

“Earthquake Damage Scenario” workshops.

All the case-study cities held Earthquake Damage Scenario workshops from October 1998 to March 1999, the end of the first phase of the case study. The workshops greatly raised public awareness through various coverage by mass media, such as newspapers, radio and TV. The common objectives of the workshops were to:

- Present the damage estimates to the city and ask for feedback from the participants;
- Estimate the impact of the estimated damage on the city activities;
- Produce ideas for actions that could reduce the impact of an earthquake on the city;
- Discuss the conditions needed to institutionalise the risk management activities.

“Action Plan” workshops.

In most of the nine case-study cities, the second workshop, the “Action Plan” workshop, was held from April to July 1999. The objectives of the workshops were to develop a Risk Management Plan, based on the evaluation of the earthquake damage scenarios and propose an Action Plan for immediate actions. Active discussions widely covered by mass media, such as TV and newspapers, greatly raised public awareness of disaster preparedness.

23.2.2.4. RADIUS development of practical tools

One of the major objectives of the RADIUS initiative was to develop two kinds of practical tools for urban seismic risk management, based on the experience of the nine case studies implemented worldwide. One of the tools is a set of Guidelines for Implementation of Risk Management Projects. These guidelines have the following aims:

- To explain the philosophy and methodologies adopted by RADIUS;
- To assist in reading, understanding, and interpreting the RADIUS case study reports, and
- To provide general guidelines on how RADIUS-type Risk Management Projects can be implemented in other cities.

GHI developed the guidelines, based on the experiences in Quito (Ecuador), Kathmandu (Nepal), and the nine RADIUS case studies. The emphasis was put on:

- A) How to involve decision makers, relevant organizations/institutions, communities, private sectors and scientists in a multidisciplinary way;

- B) How to practically transfer scientific data into decision making information;
- C) How to disseminate information and educate people, particularly through the mass media;
- D) How to prepare a risk management plan as well as an action plan; and
- E) What to do as the next step.

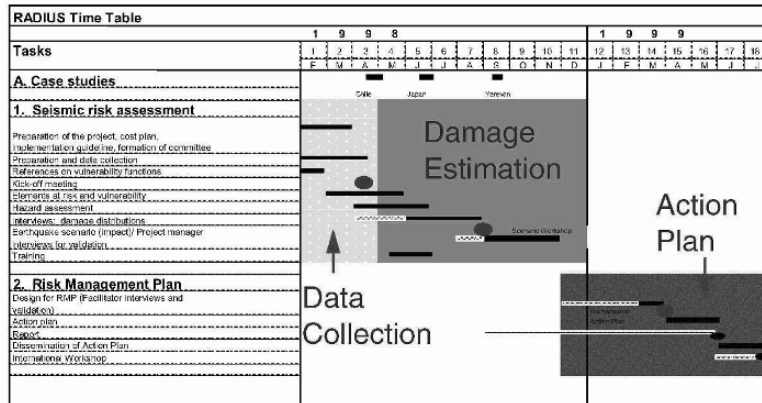


Fig. 23.10. RADIUS: Programme of activities for an earthquake risk management project

A computer programme for simplified Earthquake Damage Estimation was developed by the OYO Group (OYO Corporation and OYO International). It is intended that this programme will be used as a practical tool to aid users in understanding the seismic vulnerability of their own cities and encourage the start of disaster prevention programmes. The results of the application of the programme should be regarded as a preliminary estimation. The programme requires input of a simple data set and provides visual results with user-friendly prompts and help functions. Input data are population, building types, ground types, and lifeline facilities. Outputs are seismic intensity (MMI), building damage, lifeline damage and casualties, which are shown with tables and maps. Users can apply a historical earthquake such as Kobe (1995, Japan), Kocaeli (1999, Turkey) and Chichi (1999, Taiwan) as a hypothetical scenario earthquake. The programme is available on CD-ROM, along with other outcomes, including guidelines and reports of the RADIUS project (available near ISDR. See some outputs from Figure 23.10 to Figure 23.14.

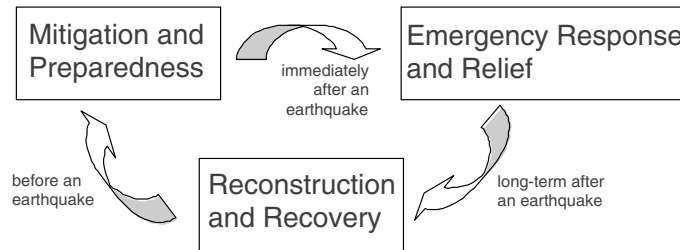


Fig. 23.11. The planning phase considers all the stages of the “disaster cycle”

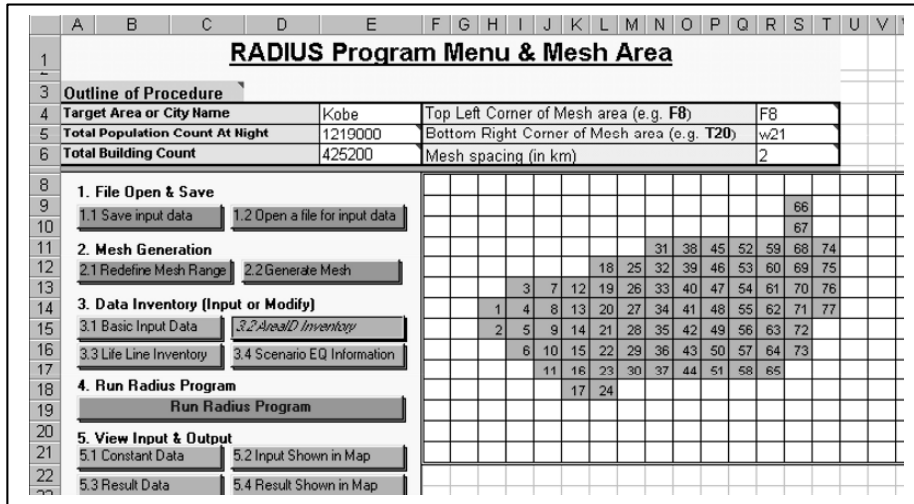


Fig. 23.12. RADIUS Main menu screen

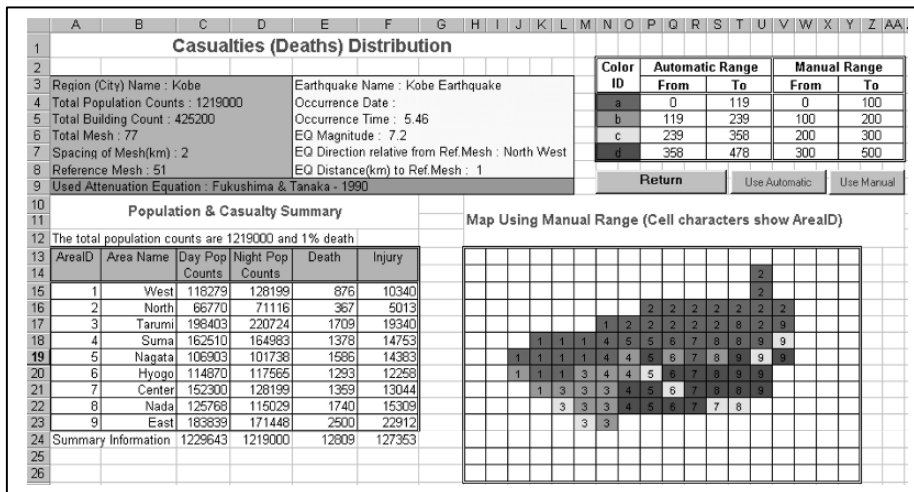


Fig. 23.13. RADIUS Casualties distribution map screen

23.3. The RISK-UE project

23.3.1. OBJECTIVES

The *strategic* objectives of the RISK-UE project were:

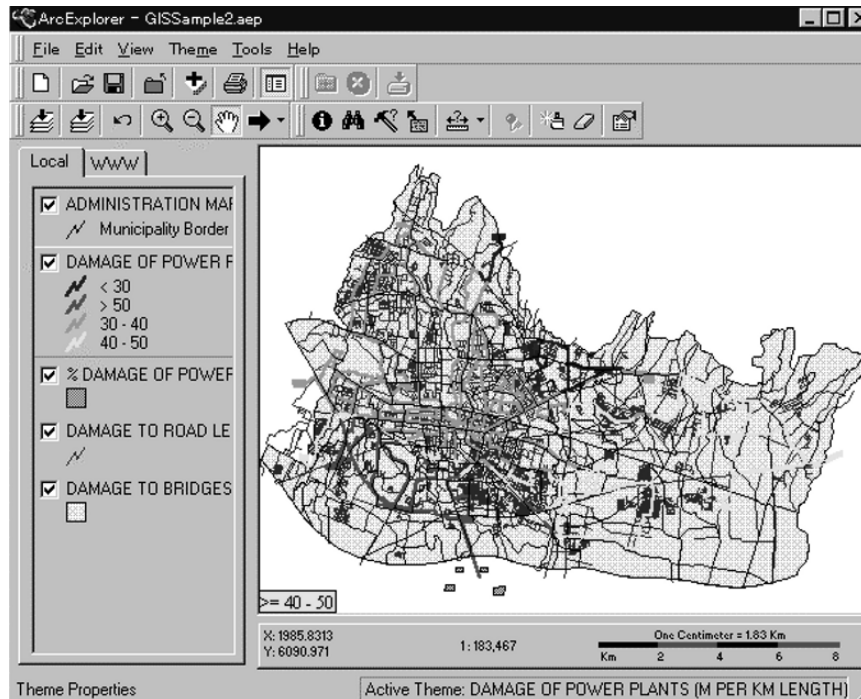


Fig. 23.14. RADIUS - An example of GIS map for lifeline damage distribution map of Bandung

- To create earthquake scenarios, validated by the decision-makers within each city, and enabling the direct (in terms of cost and victims) and indirect (in terms of failure of services within the city) consequences to be assessed.
- To develop the most comprehensive database possible, enabled within a GIS, and structured around the following key subjects: Natural phenomena (hazards) and the elements at risk (stakes, vulnerability and impacts). This database will be completely integrated into the standard GIS for the city.
- To introduce, by means of a web site, all the stages involved in implementing the different earthquake scenarios: www.RISK-UE.net, which will be available to all those concerned.
- To create synergy enabling a network of Euro-Mediterranean cities to be established, particularly in the Balkan region and Africa.

The *scientific* objectives were as follows:

- To establish a modular approach for creating earthquake risk scenarios on the consensus of several European institutions specialised in the field of seismic risk.
- To highlight the distinctive European features of the various urban systems including: urbanisation, old town centres, different building types, among them: monuments, lifeline facilities, and the general organisation of the city and its response to an earthquake.

- To homogenise the work already undertaken in other European projects.
- To apply the methodology to several European cities, in partnership with the various public services involved in planning, construction and national security.
- To validate this methodology in conjunction with other experts, in particular at the final summit taking place in Nice in 2004.

23.3.2. ORGANISATION OF THE RISK-UE PROJECT

Organisations: 10 scientific and technical organisations were taking part in the RISK-UE project, along with the 7 cities implicated in the methodology (in italics, hereafter)

Partners: Spain: ICC and CIMNE (Barcelona) for *Barcelona*, Italy : POLIMI (Milano) and UNIGE (Genoa) for *Catania*, Greece : AUTH (Thessaloniki) for *Thessaloniki*, FYROM : IZIIS (Skopje) for *Bitola*, Bulgaria : CLSMEE (Sofia) for *Sofia*, Rumania : UTCB (Bucharest) for *Bucharest*, France : BRGM and GeoTer (Marseille) for *Nice*.

23.3.3. DEFINITION OF THE METHODOLOGY DEVELOPED IN RISK-UE

In response to the objectives described above, 7 work packages (WP) have been drawn up in order to implement this methodology. This chapter summarises the work done in each technical workpackage (Mouroux et al., 2004). For further details, refer to the corresponding handbook available on: ftp.brgm.RISK-UE.

23.3.3.1. *Distinctive feature of European towns (WP1)*

The aim of Work Package 1 is to provide a methodology for collecting and classifying building and earthquake data for urban seismic risk assessment in Europe.

Therefore the 7 case-studies of European towns - *Barcelona, Bitola, Bucharest, Catania, Nice, Sofia and Thessaloniki* - were analysed in an effort to identify and classify European specific features: old monuments, specific building types, urban development rate during the 20-th century, risk management organisations, earth-science information, building vulnerability data, etc.

This analysis revealed that the most specific European distinctive feature related to seismic risk assessment is the very high value of historical patrimony exposed to earthquakes.

The main Objectives of WP1 are:

- *Objective 1, Distinctive features of European towns*, lists the most important information, data and indicators that characterise the town hazard, vulnerability, exposure and seismic risk. *Objective 1* is a kind of identification of the city and has a methodological meaning for collecting data that allow a focussed overview of all elements to be taken into consideration for urban seismic risk assessment.

- *Objective 2, Inventory database and typology*, presents the methodological frame for collecting physical data (buildings and lifelines). *Objective 2* focuses on classification of building occupancy and lifelines and suggests a matrix for building typology description (BTM).

23.3.3.2. Seismic hazard (WP2)

The primary purpose of this workpackage is to provide basic tools for estimating the earthquake ground-shaking hazard (and some related effects) in urban areas in Europe and elsewhere, and for producing suitable map representations. Such estimations and maps are intended as a basic input for developing relatively detailed earthquake damage scenarios for cities.

The document identifies and briefly describes the methods considered suitable for tackling the different tasks involved, and provides an illustration and discussion through practical applications to specific cities. The location of the cities involved in the project, in the context of a recent representation of seismic hazard distribution in Europe is illustrated in Figure 23.15.

The wide differences in earthquake hazard exposure, local geological and geotechnical characteristics, and urban and construction features of the cities has made it necessary to adopt at each step approaches sufficiently flexible to account for the basic factors in the different situations. For various reasons, but mainly due to the results of extensive previous projects and investigations, the work done for some cities, notably Catania and Thessaloniki, is more complete and detailed, which also befits the expected occurrence of higher levels of ground motion with respect to most of the other cities.

Keeping in mind the noted differences in exposure levels, and also the ongoing discussion among specialists on which methods are preferable for describing earthquake hazard in scenario studies, emphasis was placed on:

- a) adopting homogeneous, standard criteria in the quantitative description of seismicity and in the construction of ground-shaking scenarios, and
- b) trying to provide a practical grasp to end users through comparison and discussion of the results obtained for the different cities.

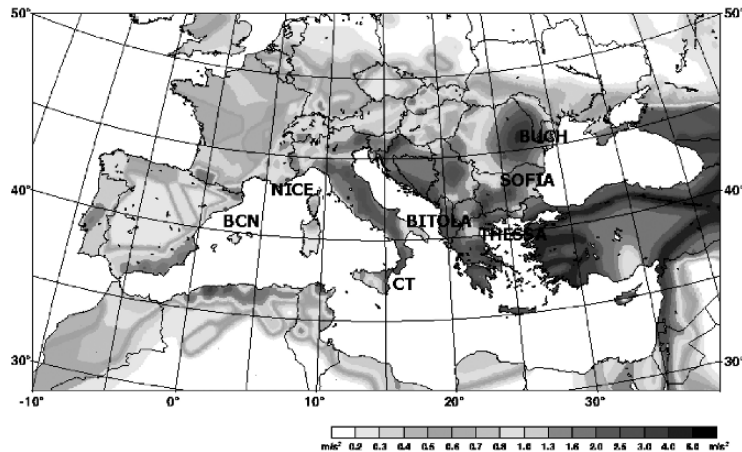


Fig. 23.15. Location of the 7 Risk EU Project cities on a seismic hazard map representing Horizontal Peak Ground Acceleration on stiff ground (in m/s^2) for a 10% in 50 years exceedance probability (map source: GSHAP Project <http://seismo.ethz.ch/gshap/>)

23.3.3.3. *Urban System Exposure (WP3)*

The Urban System Exposure methodology was developed as part of the GEMITIS research programme (1996-1999) with an application to the city of Nice in south-eastern France (See Chapter 11). This method was implemented into a global and integrated Risk Reduction Strategy for improving the risk-assessment effectiveness in urban areas, including the generation of crisis scenarios and medium to long term seismic-impact assessment.

The WP3 pursues three main objectives:

- The first one concerns the analysis of the urban system “*stricto sensu*”, which is necessary for the concrete analysis of the seismic risk. This leads to a rational organisation of the GIS.
- The second is a contribution to the identification of the main issues in the city and a *classification of elements at risk* through a value analysis, which allows identification of 3 classes of issues, in order to adapt the vulnerability analyses and the strategies of protection / prevention.

The third one concerns an important element of the vulnerability analysis of the urban system which is not treated in the other work packages (4, 5 and 6), that is the *Analysis of the social and functional vulnerability of the urban system*, the interdependences, the key points and weak points of the city. This analysis is important for the development of the crises scenarios and to estimate the conditions of recovery of the city (resilience) after occurrence of the seismic aggression.

23.3.3.4. *Vulnerability of current buildings (WP4)*

Current buildings refer to general multi-story building stock commonly used for the construction of contemporary buildings of various uses, dominantly residential, office, commercial and others. They have been designed and constructed during the last several decades, and their design dominantly complies with a certain level of seismic protection as specified by building codes and/or standards in effect at the time of their construction.

For a representative typology of the current building stock prevailing European built environment in general, and the RISK-UE cities in particular, the primary WP4 objectives are focused on:

- To develop vulnerability models describing the relation between potential building damage and the adopted seismic hazard determinant;
- To develop, based on analytical studies and/or expert judgement, corresponding fragility models and damage probability matrices expressing the probability of exceeding or, being in, a given damage state as a function of non-linear response spectral parameters;
- To develop and propose a standardised damage survey and building inventory form for rapid collection of relevant building data, building damage and post-earthquake building usability classification.

There are two main approaches for generating vulnerability relationships:

- *The first approach* (Level 1, statistical-macroseismic) is based on damage data obtained from field observations after an earthquake or from experiments. Level 1 is favoured as suitable for vulnerability, damage and loss assessments in urban environments having no detailed site specific seismicity estimates but adequate estimates on the seismic intensity.
- *The second approach* (Level 2, mechanical) is based on analytical studies of the structure, either through detailed time-history analysis or through simplified methods. Level 2, for urban environments possessing detailed microzonation studies expressed in terms of site-specific spectral quantities such as spectral acceleration, spectral velocities or spectral displacements.

Both methods, however have in common:

- Identification of suitable ground motion parameters controlling the building response, damage genesis and progress;
- Identification of different damage states based on either damage states systemized and deduced from past earthquake damage assessments or on suitable structural response parameters;
- Evaluation of the probability of a structure being in different damage states at a given level of seismic ground motion.

Some correspondences between the damage grades and the damage loss indices are proposed by partners, as summarized in Table 23.2.

Table 23.2. Damage grading and loss indices

Grade	Damage Grade Label			Description	Loss Indices			
	LM1	LM2	FEMA/ NIBS (HAZUS)		AUTH	IZIIS		UNIGE
						RC	M	
0 (D0)	None	None	None	No damage	0.0	0.0	0.0	0.0
1 (D1)	Slight	Minor	Slight	Negligible to slight damage	0-0.05	<0.15	<0.2	0.1
2 (D2)	Moderate	Moderate	Moderate	Slight structural, moderate nonstructural	0.05-0.2	0.15-0.25	0.20-0.30	0.2
3 (D3)	Substantial to heavy	Severe	Extensive	Moderate structural, heavy nonstructural	0.2-0.5	0.25-0.35	0.30-0.40	0.35
4 (D4)	Very heavy	Collapse	Complete	Heavy structural, very heavy nonstructural	0.5-1.0	0.35-0.45	0.40-0.50	0.75
5 (D5)	Destruction			Very heavy structural, total or near total collapse	-	>0.45	>0.50	1.00

23.3.3.5. Historical and monumental buildings in Europe (WP5)

Each European country shows a great interest in the preservation of the cultural heritage, being the historical memory of a country and an economic and cultural validation tool.

Several agencies promulgated specific rules to preserve a certain kind of structures. Actually all ancient buildings have their own intrinsic worth, as memory of the builders' crafts and as constitutive elements of the anthropic environment. In the past, only constructions built by famous architects or buildings of particular relevance were called "monuments". Nowadays the propensity for preservation of ancient buildings has increased in comparison with the past tendency. With the aim of a universal statement of the concept of "monument", we refer to each element of the built heritage for which preservation rules are activated.

All the European countries have several tools to make effective this kind of preservation: some rules provide different methodologies and the levels of analysis are not completely comparable. In many cases, the preservation desire clashes with the requirement of safety assurance, especially for public buildings. The idea of "preservation of a monument" may be marked by one of these two trends, depending on the awareness and cultural formation present in each country.

As proposed in WP4 methodology, two levels of analysis are suggested in WP5:

Level 1 is generally used when few or poor data are available; in this case the approach must necessarily be typological; the vulnerability is mainly connected to the kind of monument (palace, church, tower, castle, etc). The model individuated as the more effective and versatile is based on the attribution of a vulnerability index to each single building, defined as a function of the typology of the monument and corrected through modifier scores, that are correlated to some easily noticeable parameters (state of maintenance, material quality, structural regularity, etc).

In order to study the seismic vulnerability of monuments, Level 2 methodology presupposes that the vulnerability model can not propose capacity curves based only on a typological classification. The definition of a capacity curve that may be representative of a single monument is needed.

In order to define the capacity curve, we can use both refined and simplified methods (e.g. these could be validated through the previous ones).

The mechanical models may be based, for example, on different kinds of analyses:

1. non-linear analyses;
2. equilibrium limit analyses.

However, the procedure must maintain the characteristics of a simplified analysis. Only in this way could the method be automatically applicable to a meaningful number of buildings, even if fewer than the typical sample of the methods of level I, so as to respect the territorial approach of the vulnerability analyses.

23.3.3.6. *Vulnerability of lifelines and essential facilities (WP6)*

The objective of WP6 is to provide a preliminary methodological “handbook for vulnerability assessment of lifelines and essential facilities”, adapted to European contexts.

The application to each city should be performed based on this document. Lessons learned from applications and data collection will improve the final version of the methodological handbook, and the knowledge of European typologies.

Moreover, the difficulties to gather European post-earthquake experience have taught us the need to prepare investigation forms for lifelines.

The following systems and essential facilities are considered.

- four transportation systems: Roadway, Railway, Airport, Port.
- Five utility systems: Potable water, Waste water, Natural gas, Electric power, Telecommunication.

More attention is given to the utility and transportation facilities.

In order to produce even a preliminary version of a methodological handbook it was decided to apply an approach combining existing works, like HAZUS, bibliographic references, analytical/numerical studies in certain cases (i.e. vulnerability curves for certain elements at risk) and European expertise, whatever was available in the construction industry and lifeline owners and managers.

The steps to estimate losses and to propose post earthquake mitigation strategies and policies, in any kind of lifeline system and essential facility, were as follows:

1. To inventory and characterise elements of the system (location, classification of importance and typology) according to the specifications;
2. To describe synergies within system and interaction with other systems according to the reminder, interviews and data;
3. To define appropriate expression of losses;
4. To use seismic hazard and scenarios as basic input with appropriate vulnerability models to assess direct losses;
5. To use spatial networking models (hydraulic, transportation) within and between systems to assess/describe indirect losses;
6. To use direct losses and interactions with appropriate restoration models to assess recovery duration.

23.3.3.7. *Risk Scenarios (WP7)*

The direct objectives of the case studies were:

1. To develop an earthquake damage scenario which describes the consequence of a possible earthquake; and
2. To prepare a risk management plan and propose an action plan for earthquake disaster mitigation.

The case studies aim:

1. To raise the awareness of decision makers and the public to seismic risk;
2. To set up a local infrastructure for a sustainable plan for earthquake disaster mitigation;
3. To promote multidisciplinary collaboration within local governments as well as between government officers and scientists; and
4. To promote European interaction with other earthquake prone cities.

In order to develop earthquake damage scenarios, first, it is necessary to estimate the physical damage to buildings and infrastructure and human losses in the city as well as the effects on urban functions and activities.

The objective of WP7 is to *develop earthquake-risk model scenarios* for physical and human loss estimation in the member cities. The model should take into account the following components:

- Direct physical losses
- Human losses
- Direct economic losses
- Problems due to homeless, debris
- Handbook

Two types of earthquake-risk scenarios were considered within the analysis:

1. Type 1 - deterministic earthquake scenario, expressed in EMS 98 intensities, based on historical earthquakes with significant impacts on the concerned city. Level 1 approach is a minimum requirement for each city;
2. Type 2 – probabilistic-constant hazard scenario, selected on probabilistic basis, as uniform hazard acceleration spectra corresponding to a mean recurrence interval $MRI = 475 \text{ yr}$ (10 % probability of exceedance in 50 yr).

An evaluation method of the direct losses was developed using GIS technology enabling:

(i) Definition of contour maps of ground motion hazard according to earthquake scenario. The input information comes from:

- Earthquake-hazard maps, WP 2
- Surface geology data, WP 2;

(ii) Definition of state of damage for the elements at risk (buildings, infrastructures, lifelines) considering the local seismic hazard as well as induced hazards (slopes sliding, shore subsidence, liquefaction etc). The input information comes from:

- Vulnerability assessment, WP4, WP5, WP6
- Urban system analysis, WP 3;

(iii) Estimation of the human losses, based on: building damage, extent of damage and collapse patterns, escape and entrapment possibilities, rates of injury and casualty

indoor and outdoor, population exposure, infrastructure damage, efficiency of relief actions, outbreaks of fires (where appropriate);

(iv) Aggregation of physical building damage and human losses to get the global impact of the scenario earthquake at city scale, in terms of size and location:

- problems with the homeless relocation and temporary housing
- problems related to debris transportation and disposal
- overall economic and social impact
- functional and institutional impact

The input information comes from (i) + (ii) + (iii);

(v) Identification of the city functioning disruptions expected in a crisis situation;

(vi) Identification of the most vulnerable (weak) city sectors where preventive measures will take utmost priority, with special attention to important facilities such as hospitals, schools, government offices, water supply systems and power networks etc.

23.3.4. APPLICATION OF THE METHODOLOGY TO THE SEVEN CITIES

The methodology described in the workpackages 1 to 7 was then applied to the seven following cities. For each city, one picture is shown, describing only a small part of all the work that has been done.

Barcelona (Spain). With a total of 1,503,451 inhabitants, Barcelona, the capital of Catalonia, is located on the northeast coast of Spain. Bounded by the Collserola ridge and rivers Besós and Llobregat, the city has an area of almost 100 km² giving it a population density over 15,176 persons/km². Figure 23.16 shows some of the work performed in the application to Barcelona of the vulnerability and damage evaluation for the Church Santa Maria Del Mar. This figure is representative of what has been done inside the WP5.

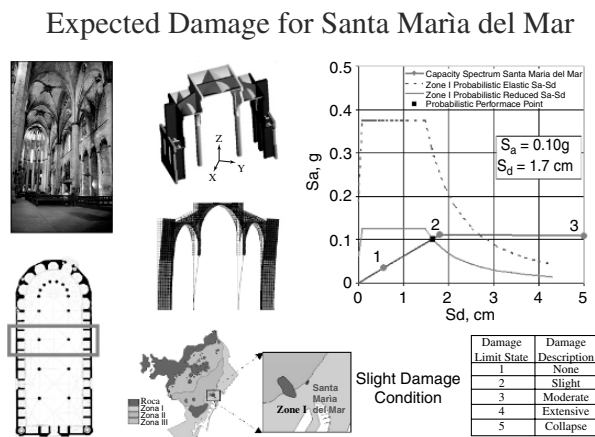


Fig. 23.16. Expected Damage for Santa María del Mar

Bitola (Former Yugoslavia Republic of Macedonia). The City of Bitola is situated in the southern part of Macedonia near the Greek border, in the western part of the Pelagonia Plain, between the Baba and the Nidze Mountains, at altitude of 660 meters (Figure 23.17). Often destroyed and set fire to, Bitola kept surviving, growing and developing into a large, beautiful and dignified town. Having over 110,000 inhabitants, it is the third largest town in Macedonia and the center of a wider region in south-western Macedonia with developed agriculture, industry, handicrafts, public-health service, transportation, and University. Figure 23.17 is representative of what has been done inside the WP1.



Fig. 23.17. Bitola Greater Region 3D Digital Modelling (WP1 – GIS)

Bucharest (Romania). Bucharest, capital city of Romania, is its main administrative, economic, social and cultural center.

Bucharest, because of its population, building stock, administrative and economic role, in combination with the seismic hazard induced by Vrancea source, can be ranked in Europe as one of the cities with highest seismic risk.

The number of inhabitants of Bucharest, on July 1, 1999 was 2,011,305 (Romanian Statistical Yearbook 2000, National Institute of Statistics). Mean population density in Bucharest is 10,806 persons/km² (1992 National Census). GDP per capita for Bucharest was 2988USD (1998 - Romanian Statistical Yearbook).

The city is located in the alluvial Romanian plain (South- East of Romania) half-way between the Danube and South Carpathian Mountains, The total urbanized area is about 228km².



Fig. 23.18. Old and new buildings in Bucharest (regarding WP1 – Building typology matrix, and importance to take into account old buildings)

The results of RISK-UE study combined with the seismic history of Bucharest led the authorities to launch large rehabilitation and retrofitting of many weakest constructions of the city (see Figure 23.18).

Catania (Italy). Catania is located in the middle of the Mediterranean, on Sicily's East coast, at the foot of the 3200 m high Etna volcano. It ranks ninth among Italian cities for population, and is the second largest city of Sicily. The most recent data, from the 1991 population census by the Italian National Institute of Statistics (ISTAT), indicate 333,075 inhabitants. Figure 23.19 shows the difference of the results obtained with 2 scenarios, during the day and during the night.

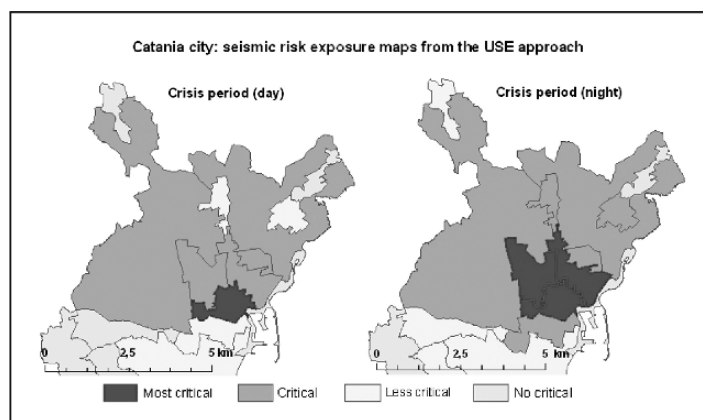


Fig. 23.19. Evaluation of seismic risk exposure in Catania. This figure is representative of what has been done in the WP3

Nice (France). Nice is the most important city of the French Riviera. The Nice township proper has a population of approximately 346,000, and its total metropolitan area, nearly 500,000. The population, and accordingly housing, are the first elements to be considered in the risk analysis. Figure 23.20 shows the results of microzonation study, in terms of response spectra for the 5 different zones which were determined thanks to a 3D geotechnical model of the city.

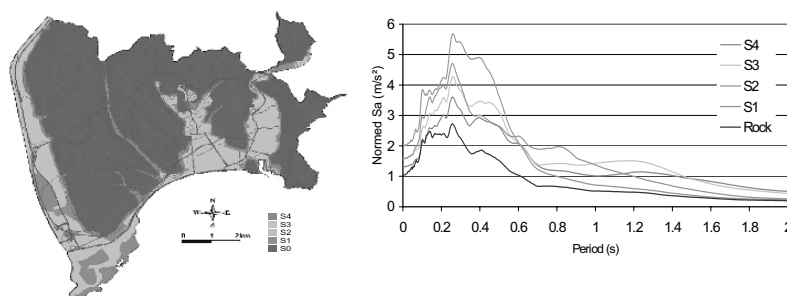


Fig. 23.20. Seismic microzonation of the city of Nice and associated response spectra (WP2)

Sofia (Bulgaria). Sofia extends over 1315 km² and its population was about 1177 thousand in 2000 (Statistical Year Book 2000, NSI). The urbanised territory is 242.2 km² (National Centre on Cadastre Balance, 1994). The administrative units of Sofia are 24 and one of them, TRIADITZA, is the region that was selected to be representative for the analyses within the frames of the project. TRIADITZA is about 9.3 km². The number of the housing units in it is 25717 with 55890 inhabitants. TRIADITZA administrative unit extends from the centre towards the Southern border of the urbanised area of Sofia.

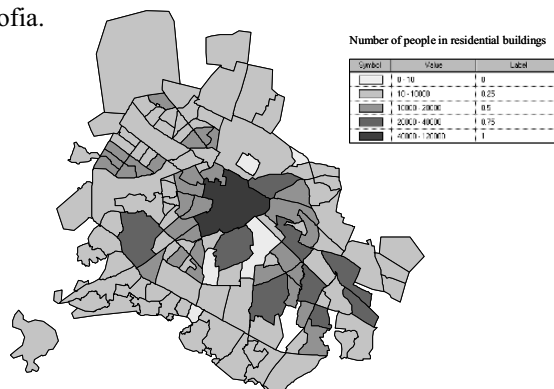


Fig. 23.21. “Population distribution” of Sofia (WP3)

Thessaloniki (Greece). The city of Thessaloniki is located in the eastern part of the Mediterranean in Northern Greece (Macedonia, Thrace) in a strategic geographical location, constituting a crossroad between Asia, Africa and Europe. It is the second city in population in Greece (1,048,151 people) after Athens and an important administrative, economic, industrial, academic and cultural centre at national scale. The urban area of Thessaloniki (Area of the city = 13130Ha, 1991) consists of 17 districts with the more important the municipality of Thessaloniki (Density: 216 people/ Ha), which includes the historical centre of Thessaloniki, the old town, the International Trade Fair, the two University campuses. Figure 23.22 shows the results of expected damage of buildings in the studied area, overlaid to the expected distribution of mean PGA.

The application in each city can be easily summarised in Tables 23.3 to 23.6 which allows a comparison between hazard, vulnerability and scenario results. These tables show the wide differences between the cities in term of regional hazard, site effects, vulnerability of current buildings, and then, in terms of damages. This indicates the important differences which may exist all over Europe, in terms of losses and consequences due to earthquakes which may affect European cities. It is then very significant that the problem of reducing seismic risk should be considered directly by the decision-makers of the city itself. All these results should therefore be reanalysed by them with the Mayor at the top, in order that they take them for their own use (step of “appropriation”).

This step is fundamental before the realisation of special “Risk Management and Action Plans”, for a future efficient mitigation of seismic risk.

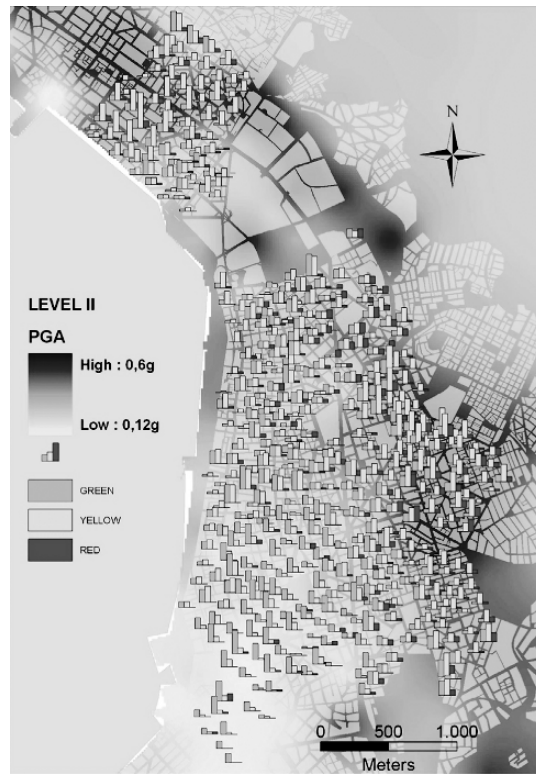


Fig. 23.22. Expected distribution of predicted tagging of buildings for the study area due to the Level II approach, overlaid to the expected distribution of mean PGA values of the Microzonation study (WP7 Thessaloniki)

Table 23.3. Seismic hazard characteristics for the different earthquakes scenarios

	Barc.	Buch.	Bitola	Catania	Nice	Thess.	Sofia
Earthq. 1 (deterministic, max historical earthquake)							
Magnitude	5.1	8.1	5.3	7.3	6.3	Ms=6.6	6.3
Distance	15 to 25 km	-	5.0 km	8 – 26 km	20 to 30 km	20km	10-30 km
Pga min rock	0.07g	-	-	0.21 g	0.08 g	0.12g	0.07 g
Pga max rock	0.07g	-	0.27 g	0.37 g	0.13 g	0.15g	0.18 g
Pga min site	0.07 g	-	-	0.19 g	0.11 g	0.13g	0.07 g
Pga max site	0.14 g	-	0.36 g		0.25 g	0.21g	0.23 g
Int. Min rock	VI	-	-	IX-X	VI - VII	VI - VII	VII
Int max rock	VII	-	-	IX-X	VII	VIII - IX	VII
Int. Min site	VI	IX	-	IX-X	VII	VII	VIII - IX
Int max site	VII-VIII	X	VII - VIII	IX-X	VIII	VII - VIII	VII
Probabilistic (T=475 yrs)							
Pga min rock	0.10 g	-	-	0.16 g	0.12 g	0.28g	0.15 g
Pga max rock	0.10 g	-	0.17 g	0.18 g	0.19 g	0.40g	0.25 g
Pga min site	0.10 g	0.35 g	0.18 g	0.24 g	0.15 g	0.34g	0.15 g
Pga max site	0.19 g	0.40 g	0.27 g	0.34 g	0.38 g	0.47g	0.32 g
Int. Min rock	-	-	-	-	VII - VIII	VII - VIII	VII - VIII
Int max rock	-	-	-	-	VIII	VIII	VIII - IX
Int. Min site	-	-	-	-	VII - VIII	VIII	VII - VIII
Int max site	-	-	-	-	IX	VIII - IX	IX

Table 23.4. Vulnerability analysis of current buildings for Level 1 method

	Barc.	Buch.	Bitola	Catania	Nice	Thess.	Sofia
Nb of buildings in the town	72,792	108,834	13,657	41,800	37,000	≈19,000*	3,865*
Nb of buildings in the studied zone	72,792	4,068	13,657	41,800	37,000	≈10,000	3,865
Nb of buildings for which analyse is performed.	63,291	4,068	13,657	41,800	3,328	5,047	-
Vi min masonry	0.48	0.202	0.623	0.509	0.301	-	0.3
Vi max masonry	1.000	0.365	0.825	0.804	1.02	-	1.02
Vi min RC	0.42	0.068	0.542	0.414	0.247	-	-0.02
Vi max RC	0.87	0.257	0.623	0.759	0.782	-	1.02

Table 23.5. Damage distribution in terms of percentage of buildings in the analysed area (Those damage distributions only concern residential buildings)

	Damage grade	Barc.	Buch.	Bitola	Catania	Nice	Thess.	Sofia
Total number of analysed buildings		63,358	4,068	13,657	41,800	37,000	5,047	3,647
Earthq. 1								
Max Rock Intensity		VII	VIII	VII	IX - X	VII	VII	VIII - IX
Level 1	D0	25.8 %	25.8 %	57.6 %	-	53.3 %	3.4 %	6.5 %
	D1	25.9 %	40.1 %	25.2 %	0.2%	25.7 %	35.5 %	27.2 %
	D2	24.7 %	25.0 %	13.1 %	14.1%	13.8 %	33.5 %	25.5 %
	D3	15.8 %	7.8 %	3.8 %	85.3%	5.6 %	15.7 %	26.0 %
	D4	7.3 %	1.3 %	0.3 %	0.4 %	1.5 %	6.3 %	12.8 %
	D5	0.5 %	-	-	-	0.1 %	5.6 %	2.0 %
Max Rock PGA		0.07 g	-	0.27 g	0.37 g	0.13 g	0.15 g	0.18 g
Level 2	D0	57.2 %	-	2.9 %	2.6 %	46.4 %	18.7%	-
	D1	20.8 %	-	7.7 %	13.5 %	17.6 %	40.4%	46.0 %
	D2	12.9 %	-	42.2 %	20.6 %	22.1 %	20.0%	25.2 %
	D3	8.1 %	-	44.7 %	25.5 %	9.6 %	11.0%	16.8 %
	D4	1.0 %	-	2.5 %	26.5%	3.3 %	3.8%	7.5 %
	D5	-	-	-	11.3 %	1.0 %	6.1%	4.5 %
Proba (T=475 yrs)								
Max Rock PGA		0.1 g	0.35 g	0.17 g	0.18 g	0.19 g	0.4 g	0.25 g
Level 2	D0	31.5 %	0.2 %	20.8 %	0.8 %	25.8 %	-	-
	D1	24.4 %	5.7 %	28.7 %	2.5 %	19.0 %	-	-
	D2	23.3 %	14.1 %	34.4 %	13.2 %	30.2 %	-	-
	D3	16.6 %	67.8 %	15.4 %	19.6 %	16.4 %	-	-
	D4	4.2 %	12.2 %	0.6 %	53.8 %	7.5 %	-	-
	D5	-	-	-	10.1 %	1.1 %	-	-

Table 23.6. Casualties and direct costs (The estimation was made only for current buildings during the night)

		Barc.	Buch.	Bitola	Catania	Nice	Thess	Sofia
	Number of inhabitants in the studied area	1,515,000	406,706	79,465	331,503	351,376	363,987	?
	Average repair cost/m ² of floor	707 €/m ²			650 €/m ²	950 €/m ²		
Earthq. 1					January 11, 1693	Type 1887		
Level 1	Injured	13,154	3918	37	3,874	990 / 2,170	711/1,000	800
	Death	4,198	1409	10	8,826	45 / 170	246 / 360	223
	Homeless	363,800	33893	344	78,223	10,500 / 22,700	-	-
	Direct cost	9,330	26.9	27.6 M€	4,000M€	1,600 / 2,250 M€	463 M€	-
Level 2	Injured	3,847	-	66	11,404	4,162	688/933	-
	Death	1,195	-	223		593	216/291	-
	Homeless	107,079	-	2,020	145,317	37,662	-	-
	Direct cost	3,962 M€	-	110.8 M€	-	3,500 M€	334 M€	-
Proba								
Level 2	Injured	11,192	36894	52	10,187	6,793	-	-
	Death	3523	13268	15		988	-	-
	Homeless	235,937	297922	1,279	232,457	61,700	-	-
	Direct cost	8,749 M€	1740	57.2 M€	-	5,750 M€	-	-

23.4. Comparison between HAZUS, RADIUS and RISK-UE

A comparison of study areas, data, methods and results for the three methodologies developed in HAZUS, RADIUS and RISK-UE is presented in Table 23.7

Table 23.7. Synthetic comparison between HAZUS, RADIUS and RISK-UE

Steps	HAZUS	RADIUS	RISK-UE
1) Area of application	United States and equivalent	Developing Countries	Euro-Mediterranean countries and equivalent
2) Basic Data			
• Collection and organisation	GIS	GIS or Excel	GIS
• Basic building typologies:	16	10 (basic)	23
- Masonry	3	or more,	10
- Reinforced Concrete	5	depending	7
- Steel	5	on the cities	5
- Wood	2		1
- Mobil home	1		-
3) Urban system Analysis , for the definition of main issues and priorities.	Not directly in the method	Not directly. Included in Risk Management Plan	YES, with Collaboration of City decision makers.
4) Seismic Hazard			
• Regional scale		[YES "reasonable" historical, earthquake]	YES
- Deterministic	YES		YES
- Probabilistic	YES		
• Local scale			
- site effects	YES	YES	YES
- liquefaction	YES	NO	YES
- mass movements	YES	NO	YES
5) Vulnerability			
• Current building , (normal + critical facilities)			
- Level 1 (statistical, macroseismic)	NO	YES	YES (with calibration of historical earthquakes)
- Level 2 (mechanical, performance based design)	YES	NO	YES (but no calibration yet)
• Historical buildings			
- Level 1	NO	NO	YES
- Level 2	NO	NO	YES
• Lifelines			
- Level 1	NO	YES	YES
- Level 2	YES	NO	YES
6) Scenario Loss estimation			
• casualties	YES	YES	YES
• homeless	YES	NO	YES
• direct losses	YES	YES	YES
• indirect losses	YES	NO	NO
• social impact	with 7)	with 7)	with 7)
7) Risk Management and Action Plan	YES, BUT DEPENDS ON AWARENESS OF CITY ACTORS	YES	YES, BUT DEPENDS ON AWARENESS OF CITY ACTORS
8) Appropriation by City actors		YES, BUT DEPENDS ON THE CITY ACTORS	

23.5. Final conclusions

All these methodologies (RISK-UE, HAZUS, RADIUS) leading to seismic scenarios allow a best understanding of what may happen during a plausible earthquake which may affect numerous cities in the European Union, the United States, or any developing countries.

These results are given in terms of different losses: casualties, direct and indirect financial costs, human and social consequences; In spite of great uncertainties, these results will allow the decision-makers and Mayors of cities to be more aware of the problems, to reanalyse the consequences (step of appropriation) and finally to launch themselves, with the whole population, more efficient “Risk Management and Action Plans”, for a systematic reduction of seismic risk in the future.

Acknowledgements

We are very grateful to all partners of RISK-UE Project for its finalization, and moreover to Xavier Goula, Antoni Roca, Zoran Milutinovic, Goran Trendafiloski, Dan Lungu, Alex Aldea, Ezio Faccioli, Sergio Lagomarsino, Myriam Bour, Etienne Bertrand, Philippe Masure, Christophe Martin, Olivier Monge, Antoaneta Kaneva, Marin Kostov, Andreas Kappos and Kyriasis Pitilakis.

We are also grateful to all partners of RADIUS Initiative and especially Kenji Okazaki, Etsuko Tsunozaki, Carlos Villacis, Cynthia Cardona, Rajib Shaw, Fumio Kaneko and Jichun Sun.

REFERENCES

- Abrahamson, N. A. and Shedlock, K. M. (1997). Overview. *Seis. Res. Letters*, 68, 9-23.
- Abrahamson, N. A. and Silva, W. J. (1997). Empirical response spectral attenuation relations for shallow crustal earthquakes. *Seis. Res. Letters*, 68, 94-127.
- Abrahamson, N. A. and Sommerville, P. G. (1996). Effects of the hanging wall and footwall on ground motions recorded during the northridge earthquake. *Bull. Seism. Soc. Am.*, 86, S93-S99.
- Adams, B. J., Huyck, C. K. and Eguchi, R. T. (2003). The Boumerdes (Algeria) earthquake of May 21, 2003: Preliminary reconnaissance using remotely sensed data. <http://mceer.buffalo.edu/research/boumerdes/default.asp> (consulted November 2004).
- Adams, B. J., Huyck, C. K., Mio, M., Cho, S., Ghosh, S., Chung, H. C., Eguchi, R. T., Houshmand, B., Shinozuka, M., and Mansouri, B. (2004). The Bam (Iran) earthquake of December 26, 2003: Preliminary reconnaissance using remotely sensed data and the VIEWS system, <http://mceer.buffalo.edu/research/bam/default.asp> (consulted November 2004).
- AFPS (1995). Guidelines for seismic microzonation studies. Association Française du Génie Parasismique.
- AFPS (2003). *Le séisme de 21 Mai, en Algérie*. Rapport préliminaire de mission. Paris, France.
- Afra, H., Argoul, P. and Bard, P.-Y. (1990). Identification of building structural behavior from earthquake records. *9th European Conference on Earthquake Engineering*, Moscow, USSR, Vol. 7-B, 3-12 p.
- AIJ (1999). *Report on the Damage Investigation of the 1999 Kocaeli Earthquake in Turkey*. Architectural Institute of Japan, Tokyo, Japan.
- AIJ (2001). *Report on Damage Investigation of the 1999 Kocaeli Earthquake in Turkey*. Architectural Institute of Japan, Tokyo, Japan.
- Akbar, S. (1989). *Urban housing in seismic areas: a computerised methodology for evaluating planning strategies to reduce risk*. PhD Dissertation, Cambridge University.
- Aki, K. (1993). Local Site Effects on Weak and Strong Ground Motion. *Tectonophysics*, 218, 93-111.
- Aki, K. (1998). Local site Effects on Strong Ground Motion. Earthquake Engineering and Soil Dynamics II-Recent Advances in Strong Motion Evaluation, *ASCE Geotechnical Special Publication*, 20, J. Lawrence Von Thul (Editor), 103-155.
- Aki, K. and Larner, L. (1970). Surface motion of a layered medium having an irregular interface due to incident plane SH waves. *Journal of Geophysical Research*, 75(5), 933-953.
- Akkar, S. and Gulkan, P. (2002). A critical examination of near-field accelerograms from the Sea of Marmara region earthquakes. *Bull. Seism. Soc. Am.*, 92, 428-447.
- ALA (2001a). *Seismic Fragility Formulations for Water Systems. Part 1 – Guideline*. American Lifelines Alliance (ALA). ASCE-FEMA, 104 p.
- ALA (2001b). *Seismic Fragility Formulations for Water Systems. Part 2 – Appendices*. American Lifelines Alliance (ALA). ASCE-FEMA, 239 p.
- ALA (2002). *Development of Guidelines to Define Natural Hazards Performance Objectives for Water Systems*. American Lifelines Alliance. Vol. I, Technical report prepared in by a public-private partnership between FEMA and ASCE, 138 p.
- Albini, P. and Stucchi, M. (1997). A basic European Earthquake Catalogue for the evaluation of long-term seismicity and seismic hazard (BEECD). In: A. Ghazi and M. Yeroyani (Editors), *Seismic Risk in the European Union*.
- Alesch, D., Nagy, R. and Taylor, C. (2002). Seeking Criteria for the Natural Hazard Mitigation Investment Decision. In: Taylor, C. and VanMarcke E. (Editors), *Acceptable Risk Processes. Lifelines and Natural Hazards*, Monograph No. 21, TCEE/ASCE, 160-184.
- Alexander, D. (1996). The health Effects of Earthquakes in the Mid-1990's. *Disasters* 20(3), 231-247.
- Alexoudi, M. (2004). *Seismic vulnerability assessment of utility systems*. PhD Thesis, Civil Engineering Department, Aristotle University of Thessaloniki, Greece (in progress).
- Alexoudi, M., Pitilakis, K., Hatzigogos, Th. and Anastasiadis, A. (2004). The Importance of Site Effects in the Damage Assessment, the Emergency Response and the Mitigation Strategy of Gas System. The Case of Thessaloniki. *Proceedings, 11th International Conference on Soil Dynamics and Earthquake Engineering and 3rd International Conference on Earthquake Geotechnical Engineering*, Berkeley, California.
- Allen, C. R. (1995). Earthquake Hazard Assessment: Has Our Approach Been Modified in the Light of Recent Earthquakes? *Earthquake Spectra*, 11, (3), 357-366.
- Allen, R. and Kanamori, H. (2003). The potential for earthquake early warning in South California. *Science*, 300, 786-789.
- Almeida, C. (2000). *Análise do comportamento da igreja do mosteiro da Serra do Pilar à ação dos sismos*. MSc Thesis on Civil Engineering Structures, Fac. Eng. Univ. Porto, Portugal.

- Almeida, C., Arêde, A. and Costa, A. (2002). Seismic analysis of the Serra do Pilar monastery church. *12th European Conference on Earthquake Engineering*, London, United Kingdom.
- Álvarez Rubio, S. (1999). El efecto local sobre el movimiento sísmico del suelo: fenomenología y resultados recientes. In: Benito, B. and Muñoz, D. (Editors), *Ingeniería Sísmica, Física de la Tierra*, 11, 141-173.
- Alves, E.I. (1994). *Uma Abordagem Coneccionista ao Problema da Previsão Sísmica*. PhD Thesis, Universidade de Coimbra, Coimbra.
- Ambraseys, N. N. and Bommer, J. J. (1995). Attenuation relations for use in Europe: an overview. *Proceedings 5th SECED Conf. On European Seismic Design Practice: Research and Applications*, Balkema, 67-73.
- Ambraseys, N. N., Simpson, K.A. and Bommer, J.J. (1996). Prediction of horizontal response spectra in Europe. *Earthquake Engineering and Structural Dynamics*, 25, 371-400.
- Amirbekian, R.V. and Bolt, B.A. (1998). Spectral comparison of vertical and horizontal seismic strong ground motions in alluvial basins. *Earthquake Spectra*, 14(4), 573-595.
- Anagnos, T., Rojahn C. and Kiremidjian, A. (1995). *NCEER-ATC joint study on fragility of buildings*. Report NCEER-95-0003, National Center for Earthquake Engineering Research, Buffalo, New York.
- Anagnostopoulos, S.A. (1996). *Post-earthquake Emergency Assessment of Building Safety*. Field Manual. European Commission DG XI Civil Protection, 61 p.
- Anastasiadis, M. Apeessou and Pitilakis, K. (2002). Earthquake-Hazard Assessment in Thessaloniki- Level II- Site Response Analyses. *Proceedings, International Conference on Earthquake Loss Estimation and Risk Reduction*, Bucharest, Romania. (In press).
- Andre, G. (2003). *Détection et la cartographie des dommages et des marqueurs de catastrophes naturelles par imagerie spatiale optique et radar*. PhD Thesis, Paris 7 University, France.
- Ansal, A., İyisan, R., and Güllü, H. (2001). Microtremor measurements for the microzonation of Dinar. *Pageoph*, 158(11), 2525-2541.
- Ansal, A. M., İyisan, R., Sengezer, B. S. and Gençoglu, S. (1993). The damage distribution in March 13, 1992 Erzincan earthquake and effects of geotechnical factors. In: Sêco e Pinto (Editors), *Soil Dynamics and Geotechnical Earthquake Engineering*, Balkema, Rotterdam, 413-434.
- Ansal, A., Laue, J., Buchheister, J., Erdik, M., Springman, S., Studer, J., and Koksall, D. (2004). Site characterization and site amplification for a seismic microzonation study in Turkey. *11th Int. Conference on Soil Dynamics and Earthquake Engineering and 3rd Earthquake Geotechnical Engineering*, San Francisco.
- Ansal, A., Şengezer, B.S., İyisan, R. and Gençoglu, S. (1993). The damage distribution in March 13, 1992 earthquake and effects of geotechnical factors. In: P.Seco e Pinto (Editors), *Soil Dynamics and Geotechnical Earthquake Engineering*, Balkema, Rotterdam, 413-434.
- Aoki, H., Matsuoka, M. and Yamazaki, F. (1998). Characteristics of satellite SAR images in the damaged areas due to the Hyogoken-Nanbu earthquake. *19th Asian Conference on Remote Sensing*.
- Araya, R., Der Kiureghian, A. (1988). *Seismic Hazard Analysis Improved Models, Uncertainties and Sensitivities*. Report no. UCB/EERC 90/11, University of California, Berkeley.
- Arêde, A., Almeida, C., Costa, A., Rodrigues, J. and Campos Costa, A., (2002). Dynamic Identification and Seismic Analysis of the Serra do Pilar Monastery Church. *Proceedings of the International Modal Analysis Conference, 2002*, Los Angeles.
- Argyroudis, S., Argyriou, N., Chatzis, I. and Pitilakis, K. (2005). Seismic Fragility Curves of Shallow Tunnels. *11th International Conference of International Association of Computer Methods and Advances in Geomechanics, Turin (submitted)*.
- ATC-13 (1985). *Earthquake damage evaluation data for California*. Applied Technology Council (ATC). Redwood City, California.
- ATC-20 (1989). *Procedures for post-earthquake safety evaluation of buildings*. Applied Technology Council (ATC), Redwood City, California.
- ATC-20-2 (1995). *Addendum to ATC-20*. Applied Technology Council (ATC), Redwood City, California.
- ATC-21 (1988). *Rapid Visual Screening of Buildings for Potential Seismic Hazard*. Applied Technology Council (ATC). Redwood City, California.
- ATC-25 (1991). *Seismic Vulnerability and Impact of Disruption of Lifelines in the Conterminous United States*. Applied Technology Council (ATC). Redwood City, California.
- ATC-40 (1996). *Seismic evaluation and retrofit of concrete buildings*. Applied Technology Council (ATC). Redwood City, California.
- ATC-51 (2000). *U.S.-Italy Collaborative Recommendations for Improving the Seismic Safety of Hospitals in Italy*. Applied Technology Council (ATC), Redwood City, California.
- ATC-51-1 (2002). *Recommended US-Italy Collaborative Procedures for Earthquake Emergency Response Planning for Hospitals in Italy*. Applied Technology Council (ATC), Redwood City, California.

- ATC-6-2 (1983). *Seismic Retrofitting Guidelines for Highway Bridges*. Applied Technology Council (ATC). Redwood City, California.
- Athanasopoulos, G.A., Pelekis, P.C. and Leonidou, E.A. (1999). Effects of surface topography on seismic ground response in the Egion (Greece) 15 June 1995 earthquake. *Soil Dynamics and Earthquake Engineering*, (18), 135-149.
- Atkinson, G. M. (2004). An Overview of Developments in Seismic Hazard Analysis. Keynote Lecture, *13th World Conference on Earthquake Engineering*, Vancouver, Canada.
- Aubry, D., Chouvet, D., Modaresi, A. and Modaresi, H. (1986). *GEFDYN, Logiciel d'analyse de comportement mécanique des sols par éléments finis avec prise en compte du couplage sol-eau-air*. Manuel scientifique, École Centrale Paris, LMSS-Mat.
- Aubry, D. and Modaresi, A. (1996). *GEFDYN*. manuel scientifique. École Centrale Paris, LMSS-Mat.
- Audigier, M. A., Kiremidjian, A.S., Chiu, S. S. and King S. A. (2000). Risk analysis of port facilities. *12th World Conference on Earthquake Engineering*. Auckland, New Zealand, CD-Rom, paper 2311.
- Ayala, G. (2004). Personal Communication.
- Aydinoğlu (2000a). *Chapter 7: Loss Estimation of Building Stock in Izmir Earthquake Master Plan*. Bogazici University Report for the RADIUS Project.
- Aydinoğlu (2000b). *Izmir Deprem Senaryosu*, Radius Report, Chapter 7, Binalar, <http://www.izmir-bld.gov.tr/izmirdeprem/chp7.html> (consulted November 2004).
- Azevedo, A. and Barros, J. (1995). *Manual de Utilização do Programa FEMIX - Versão 2.1*. Porto.
- Azzaro, R., Ferrelì, L., Michetti, A. M., Serva, L. and Vittori, E. (1998). Environmental hazard of capable faulting: the case of the Pernicana fault (Mt. Etna, Sicily). *Natural Hazards*, 17, 147-162.
- Bachmann, H. (2004). Political activities of earthquake engineers for seismic risk mitigation? *13th World Conference on Earthquake Engineering*, Vancouver, B. C., Canada, Keynote lecture, paper #5004.
- Baggio, C., Bernardini, A., Colozza, R., Corazza, L., Della Bella, M., Di Pasquale, G., Dolce, M., Goretti, A., Martinelli, A., Orsini, G., Papa, F. and Zuccaro, G. (2000). *Field Manual for the I Level Post-earthquake Damage, Usability and Emergency Measures Form*. National Seismic Survey and National Group for Defence against Earthquakes.
- Bak, P. and Tang, C. (1989). Earthquakes as a Self Organized Critical Phenomenon. *Journal of Geophysical Research*, 94, 1535-1539.
- Ballantyne, D. B. (2003). Water and Wastewater Systems. In: Chen, W. and Scawthorn, C. (Editors), *Earthquake Engineering Handbook*, CRC Press, Chapter 24.
- Ballantyne, D.B. and Heubach, W. (1991). *Earthquake Loss Estimation for the City of Everett Washington Lifelines*. K/J/C 906014.00, Federal Way, Washington: Kennedy/ Jenks/ Chilton.
- Ballantyne, D. B., Kennedy/Jenks/Clinton (1990a). *Earthquake Loss Estimation Modeling of the Seattle Water System*. K/J/C 886005.00 Federal Way, Washington Kennedy/ Jenks/ Chilton.
- Ballantyne, D. B., Kennedy/Jenks/Clinton (1990b). *Earthquake Loss Estimation of the Portland, Oregon Water and Sewage Systems*.-K/J/C 896015.00 report to USGS (Contract 14-08-0001-G1694) Federal Way, Washington Kennedy/ Jenks/ Chilton.
- Banda, E. and Correig, A. (1984). The Catalan earthquake of February 2, 1428. *Engineering Geology*, 20, 89-97 Elsevier Science Publishers B.V.
- Baptista, A. and Oliveira C. S. (2003). Análise Pseudo-Linear de um Pórtico de Betão Armado com e sem Alvenaria sujeito à Acção Sísmica. *Proceedings 3rd National Conf. on Seismic Engineering, AEIS, Málaga*.
- Barbat, A. H. (2003). *Vulnerability and holistic risk indices from engineering perspective and holistic approach to consider hard and soft variables at urban level*. IADB/IDEA Program of Indicators for Disaster Risk Management, Universidad Nacional de Colombia, Manizales. <http://idea.unalmz.edu.co> (consulted November 2004)
- Barbat, A. H., Yépez Moya, F. and Canas, J. A. (1996). Damage scenarios simulation for seismic risk assessment in urban zones. *Earthquake Spectra*, 12(3), 371-394.
- Bard, P.-Y. (1988). The importance of rocking in building motion: an experimental evidence. *9th World Conference on Earthquake Engineering*, Tokyo-Kyoto, August 2-9, 1988, VIII, 333-338.
- Bard, P.-Y. (1994). Effects of surface geology on ground motion, recent results and remaining issues. *10th European Conference on Earthquake Engineering*, Vienna, Balkema, Rotterdam, 305-323.
- Bard, P.-Y. (1998). Local effects on strong ground motion: Basic physical phenomena and estimation methods for microzonation studies. *Proceedings of the Advanced Course on Seismic Risk. "SERINA- Seismic Risk: An integrated seismological, geotechnical and structural approach"*. European Commission Directorate General for Science, Research and Development, 229-299.
- Bard, P.-Y. (1999). Strong motion and site effects: General Report. *2nd International Conference on Geotechnical Engineering, Lisbon*, 21-25 June 1999.

- Bard, P.-Y. (2004). The SESAME project: an overview and main results. *13th World Conference on Earthquake Engineering*, Vancouver, B. C., Canada, CDROM, paper #2207.
- Bard, P.-Y., Afra, H. and Argoul P. (1992). Dynamic behavior of buildings: experimental results from strong motion data. In: Davidovici V. (Editor), *Recent advances in earthquake engineering and structural dynamics*, Ouest-Editions, 441-478.
- Bard, P.-Y. and Bouchon, M. (1980a). The seismic response of sediment filled valleys. The case of incident SH waves. *Bull. Seism. Soc. Am.*, 70, 1263-1286.
- Bard, P.-Y. and Bouchon, M. (1980b). The seismic response of sediment filled valleys. Part II: The case of incident P and SV waves. *Bull. Seism. Soc. Am.*, 70, 1921-1941.
- Bard, P.-Y. and Bouchon, M. (1985). The two-dimensional resonance of sediment-filled valleys. *Bull. Seism. Soc. Am.*, 75, 519-541.
- Bard, P.-Y. and Gariel, J.C. (1986). The seismic response of two dimensional sedimentary deposits with large vertical velocity gradients. *Bull. Seism. Soc. Am.*, 76, 343-346.
- Barone, D., Macchi, G., Petrangeli, G., Pugliese, A., Ricchiuti, A. and Sanò, T. (1998). *Proposte di Linee guida per la verifica sismica di impianti a rischio di incidente rilevante esistenti*. Comitato Termotecnico Italiano, Sottocomitato 7: Gruppo "Tecnologie di Sicurezza", unpublished.
- Basoz, N. and Kiremidjian, A. S. (1993). Lifeline Network Analysis for Bridge Prioritization. *Proceedings, 2nd China-Japan-US trilateral Symposium on Lifeline Earthquake Engineering, Xian, China*, 239-247.
- Basoz, N. and Kiremidjian, A. S. (1995). *Prioritization of Bridges for Seismic Retrofitting*. Technical Report NCEER-95-0007, State University of New York, Buffalo.
- Basoz, N. and Kiremidjian, A. S. (1998). *Evaluation of Bridge Damage Data from the Loma Prieta and Northridge, California Earthquake*. Technical Report MCEER-98-0004, State University of New York, Buffalo.
- Bazzurro, P. and Cornell, C. A. (1999). Disaggregation of Seismic Hazard. *Bull. Seism. Soc. Am.*, 89, 501-520.
- Beauval, C., Bard, P.-Y., Moczo, P. and Kristek, J. (2003). Quantification of frequency-dependent lengthening of seismic ground motion duration due to local geology: application to the Volvi Area (Greece). *Bull. Seism. Soc. Am.*, 93, 371-385.
- Bender, B. and Perkins, D.M. (1987). *SEISRISK III: a Computer Program for Seismic Hazard Estimation*. U. S. Geological Survey Bulletin, no. 1772.
- Benedetti, D. and Petrini, V. (1984). Sulla vulnerabilità sismica di edifici in muratura i proposte di un metodo di valutazione. *L'industria delle Costruzioni*, 149, 66-74.
- Benjamin, J. R. and Cornell, C.A. (1970). *Probability, statistics and decisions for civil engineers*. McGraw-Hill, inc., USA.
- Bernard, P. and Herrero, A. (1994). Slip heterogeneity, body-wave spectra, and directivity of earthquake ruptures. *Annali di Geofisica*, 37, 6, 1679-1690.
- Bernardini A. (1999). Seismic Damage to masonry Buildings. *Proceedings of the Workshop of Seismic Damage to Masonry Buildings, Balkema, Rotterdam*.
- Bernreuter, D. L. (1981). *Seismic Hazard Analysis: Application of Methodology, Results and Sensitivity Studies*. Report NUREG/CR 1582, vols 1-5, prepared by Lawrence Livermore National Laboratory for the U.S. Nuclear Regulatory Commission.
- Bernreuter, D. L. and Chung, D.H. (1979). Development of Seismic Input for Use in the Seismic Safety Margins Research Program. *5th International Conference on Structural Mechanics in Reactor Technology*, vol. K (a), North-Holland.
- Bernreuter, D. L., Savy, J. B., Mensing, R. W. and Chen, J.C. (1989). *Seismic Hazard Characterization of 69 Nuclear Plants Sites East of the Rocky Mountains*. Report NUREG/CR 5250, vols 1-8, prepared by Lawrence Livermore National Laboratory for the U.S. Nuclear Regulatory Commission.
- Bianchi, A. and Accardo, G. (1998). The seismic risk map of Italian monuments. In: Benetti, D., Guccione, M. and Segnalini, O., (Editors) *Primo repertorio dei centri storici in Umbria: il terremoto del 26 settembre 1997*, Gangemi Editore, Rome, Italy.
- Biondi, D., De Sortis, A., Di Pasquale, G., Nuti, C., Orsini, G., Sanò, T. and Vanzi, I. (2000). Hospitals behavior during the September 1997 Earthquake in Umbria and Marche. *12th World Conference on Earthquake Engineering*, Auckland, January 30 – February 4, 2000.
- Boese, M., Erdik, M. and Wenzel, F. (2003). Artificial Neural Networks for Earthquake Early-Warning. *Proceedings AGU2003 Abstracts*, S42B-0155 Poster.
- Bogazici University. (1992). *The 13 March 1992 Erzincan earthquake: a preliminary report*. Bogazici University, Istanbul.
- Bolt, B. A. (2003). *Earthquakes*, 5th edition, W.H. Freeman, New York.

- Bolt, B. A and Abrahamson N. A. (2003). Estimation of strong seismic ground motions. In: Lee, W., Kanamori, H., Jennings, P. and Kisslinger, C. (Editors), *International Handbook of Earthquake and Engineering Seismology*, Chapter 59, Academic Press, 983-1001.
- Bommer, J. J., Elnashai, A. S., Chlimentzas, G. O. and Lee, D. (1998). *Review and development of response spectra for displacement-based design*. ESEE research Report, 98 – 3, Imperial College, London.
- Bommer, J. J., Spence, R., Erdik, M., Tabuchi, S., Aydinoglu, N., Booth, E., del Re, D. and Peterken, O. (2002). Development of an earthquake loss model for Turkish catastrophe insurance. *Journal of Seismology* 6(3), 431-446.
- Bonnefoy-Claudet, S. (2001). *Interaction site-ville: application à Mexico et à Nice*. Mémoire de DEA, Mécanique des Milieux géophysiques et Environnement, Université Joseph Fourier- Grenoble I, juin 2001.
- Boore, D. M. (1983). Stochastic simulation of high-frequency ground motions based on seismological models of the radiated spectra. *Bull. Seism. Soc. Am.*, 73, 1865-1894.
- Boore, D. M., Joyner, W. B. and Fumal, T. E. (1993). *Estimation of response spectra and peak accelerations from western North American earthquakes: an interim report*. U.S. Geological Survey Open-File Report, 93-509.
- Boore, D. M., Joyner, W. B. and Fumal, T. E. (1994). *Estimation of response spectra and peak accelerations from western North American earthquakes: an interim report, part 2*. U.S. Geological Survey Open-File Report, 94-127.
- Boore, D. M., Joyner, W. B. and Fumal, T. E. (1997). Equations for estimating horizontal response spectra and peak acceleration from western north american earthquakes: a summary of recent work. *Seismological Research Letters*, 68, 1, 129-151.
- Booth, E., Bird, J. and Spence, R. (2004). Building vulnerability assessment using pushover methods-a Turkish case study. In: Fajfar, P. and Krawinkler, H. (Editors), *Performance-Based Seismic Design Concepts and Implementation Proceedings of the International Workshop Bled, Slovenia, June 28-July 1, 2004*. Pacific Earthquake Engineering Research Centre (PEER), University of California, Berkeley.
- Borcherdt, R. D. (1970). Effects of local geology on ground motion near San Francisco Bay. *Bull. Seism. Soc. Am.*, 60, 29-61.
- Borcherdt, R.D. and Gibbs, J.F. (1976). Effects of local geological conditions in the San Francisco bay region on ground motions and the intensities of the 1906 earthquake. *Bull. Seism. Soc. Am.*, 66, 467-500.
- Borges, J.F., and Castanheta, M. (1968). *Structural Safety. Course 101*. Laboratório Nacional de Engenharia Civil, Lisbon, Portugal.
- Borzi B., Elnashai A., Faccioli E., Calvi G. M. and Bommer, J.J. (1988). *Inelastic spectra and ductility-damping relationships for displacement-based seismic design*. ESEE Research Report 98-4, Civil Engng. Dept., Imperial College, London.
- Bouchon, M. (1981). A simple method to calculate Green's functions for elastic layered media. *Bull. Seism. Soc. Am.*, 71, 959-971.
- Bouchon, M. (1985). A Simple, Complete Numerical Solution to the Problem of Diffraction of SH Waves by an Irregular Surface. *J. Acoust. Society of America*, 77, 1-5.
- Bouchon, M. and Aki, K. (1977). Discrete wavenumber representation of seismic source wave fields. *Bull. Seis. Soc. Am.*, 67, 259-277.
- Bouckovalas, G.D. and Kouretzis, G. (2001). Review of soil and topography effects in the September 7, 1999 Athens (Greece) earthquake. *Proceedings Fourth Intl. Conf. On Recent Advances in Geotechnical Earthquake Engineering and Soil Dynamics and Symposium in Honor of Prof. W.D. Liam Finn, SPL-10.3, 1-10*.
- Bouckovalas, G.D. and Papadimitriou, A.G. (2004). Numerical evaluation of slope topography effects on seismic ground motion. *Proceedings, 11th Intl. Conf. On Soil Dynamics and Earthquake Engineering and 3rd Intl. Conf. on Earthquake Geotechnical Engineering*, Berkeley, 329-335.
- Boutin, C. and Roussillon, P. (2004). Assessment of the urbanization effect on seismic response. *Bull. Seism. Soc. Am.*, 94-1, 251-268
- Bozzo, L. and Barbat, A. (1999). *Diseño sismorresistente de edificios. Técnicas convencionales y avanzadas*. Editorial Reverte, Barcelona.
- Braga, F., Dolce, M. and Liberatore, D. (1982). A Statistical Study on Damaged Buildings and an Ensuing Review of the M.S.K.-76 Scale. *7th European Conference on Earthquake Engineering*, Athens.
- Braga, F., Dolce, M. and Liberatore, D. (1983). Influence of different assumptions on the maximum likelihood estimation of the macroseismic intensities. *Proceedings of the 4th International Conference on Applications of Statistics and Probability in Soil and Structural Engineering*, Florence.
- BRI, Building Research Institute (2002). *Guideline for Damage Survey Methods of Earthquake Disaster Related with Buildings and Houses, Tsukuba, Japan*.

- Brownjohn, J. M. W. (2003). Ambient vibration studies for system identification of tall buildings. *Earthquake Engineering and Structural Dynamics*, 32, 71-95.
- Brunamonte, F., Michetti, A. M., Serva, L. and Whitney, R. E. (1995). Seismic hazard assessment from paleoseismological evidence in the Rieti Region (Central Italy). In: Serva, L. and Slemmons, D. B. (Editors), *Perspectives in Paleoseismology*, AEG Special Publication No. 6, Seattle, WA, USA, 63-82.
- Brune, J. N. (1970). Tectonic stress and the spectra of seismic shear waves from earthquakes. *J. Geophys. Res.*, 75, 4997-5009.
- Brune, J. N. (1971). Correction, *J. Geophys. Res.*, 76, 5002.
- Brune, J. N. (1984). Preliminary results on topographic seismic amplification effect on a foam rubber model for the topography near Pacoima dam. *8th World Conference on Earthquake Engineering*, 663-670.
- Buckle, I. (1991). Screening Procedures for the Retrofit of Bridges. *Proceedings, 3rd US Conference on Lifeline Earthquake Engineering*. Los Angeles, California, TCLEE/ASCE, Monograph No. 4, edited by M. A. Cassaro, 156-165.
- Buckle, I. and Cooper, J. (1995). Mitigation of Seismic Damage to Lifelines: Highways and Railroads. In: Schiff, A. and Buckle, I. (Editors), *Critical Issues and State-of-the-Art in Lifeline Earthquake Engineering*. Monograph No. 7, TCLEE/ASCE, October 1995, 70-87.
- Budnitz, R.J., Apostolakis, G., Boore, D.M., Cluff, L.S., Coppersmith, K.J., Cornell, C.A. and Morris, P.A. (1997). *Recommendations for Probabilistic Seismic Hazard Analysis: Guidance on Uncertainty and Use of Experts*. Report NUREG/CR 6372, vols 1-2, prepared by Lawrence Livermore National Laboratory for the U.S. Nuclear Regulatory Commission, U.S. Department of Energy and Electric Power Research Institute.
- Burgmann, R., Ayhan, M. E., Fielding, E. J., Wright, T. J., McClusky, S., Aktug, B., Demir, C., Lenk, O. and Turkezer, A. (2002). Deformation during the 12 November 1999 Duzce, Turkey, Earthquake, from GPS and InSAR Data. *Bull. Seis. Soc. Am.*, 92, 161-171.
- Bustamante, G., Chatelain, J. L., Fernández, J., Valverde, J., Yepes, H., Tucker, B., Villacis, C., Yamada, T. and Kaneko, F. (1995). An example in Quito, Ecuador, of the use of seismic microzoning for risk reduction in developing countries. *Proceedings of the 5th International Conference on Seismic Zonation, Nice, 1*, 683-690.
- Cahis, X., Torres, L.I. and Bozzo, L. (2000). An inovative elasto-plastic energy dissipator for the structural and non-structural building protection. *12th World Conference on Earthquake Engineering*; Auckland, New Zealand.
- Calderini, C. and Lagomarsino, S. (2004). The effect of the masonry pattern on the global behaviour of vaults. In: Modena, C., Lourenço, P.B and Roca, P., (Editors). *Structural Analysis of Historical Constructions, Proceedings of IV Int. Seminar SAHC*, Padova, Italy, A.A. Balkema, London (UK), Vol. 1, 619-628.
- Campbell, K. W. (2003a). Engineering Models of Strong Ground Motion. In: Chen, W. and Scawthorn, C. (Editors), *Earthquake Engineering Handbook*. CRC Press, Chapter 5.
- Campbell, K. W. (2003b). Strong-Motion Attenuation Relationships. In: Lee, W., Kanamori, H., Jennings, P. and Kisslinger, C. (Editors), *International Handbook of Earthquake and Engineering Seismology*. Academic Press, 1003-1012.
- Campbell, K. W. and Bozorognia, Y. (1994). Near-source attenuation of peak horizontal acceleration from worldwide accelerogram recorded from 1957 to 1993. *5th US National Conf. on Earthq. Engrg.*, Chicago.
- Campos-Costa, A. (1993). *A Acção dos Sismos e o Comportamento das Estruturas*. PhD Thesis, Universidade do Porto, Porto.
- Campos-Costa, A., Oliveira, C. S and Sousa, M.L. (1992). Seismic hazard-consistent studies for Portugal. *10th World Conference on Earthquake Engineering*, Madrid, Spain. Rotterdam: AA Balkema, 207-225.
- Campos-Costa, A. and Pinto, A. V. (1997). European Seismic Hazard Scenarios: Definition of input motions for testing and reliability assessment of civil engineering structures. (Personal communication).
- Campos Costa, A., Sousa, M. L., Carvalho, A., Bilé Serra, J. and Carvalho, E. C. (2002). Regional Seismic Risk Scenarios on hazard deaggregation. *12th European Conference on Earthquake Engineering*, London, paper 470.
- Campos Costa, A., Sousa, M. L. and Oliveira, C. S. (1998). Seismic risk: methods and application to Portugal. *11th European Conference on Earthquake Engineering*, Paris, France. Rotterdam: AA Balkema, CDROM.
- Cardenas, M., Bard, P.-Y. and Chavez-Garcia, F.J. (1999). Comportement dynamique des bâtiments sous fortes sollicitations: le cas de Mexico. *5ème Colloque National de l'Association Française de Génie Parasismique*, Cachan (France), 1, 181-188.

- Cardona, O. D. (2001). *Estimación holística del riesgo sísmico utilizando sistemas dinámicos complejos*. Universidad Politécnica de Cataluña, PhD thesis, Barcelona, Spain. <http://www.tdcat.cesca.es/TDCat-0416102-075520/> (consulted November 2004)
- Cardona, O. D. and Barbat, A. H. (2000). *El riesgo sísmico y su prevención*, Calidad Siderúrgica, Madrid, Spain.
- Carr, A. (2000). *Inelastic Dynamic Analysis Program: RUAUMOKO and Post-processor for RUAUMOKO*, Department of Civil Engineering, University of Canterbury, New Zealand.
- Carvalho, A., Campos Costa, A. and Oliveira, C. S. (2004). A stochastic finite-fault modeling for the 1755 Lisbon earthquake. *13th World Conference on Earthquake Engineering, London*. Elsevier Science Lt., DVD, paper 2194.
- Carvalho, E. C., Campos Costa, A., Sousa, M. L. and Martins, A. (2002). *Caracterização, Vulnerabilidade e Estabelecimento de Danos para o Planeamento de Emergência sobre o Risco Sísmico na Área Metropolitana de Lisboa e nos Municípios de Benavente, Salvaterra de Magos, Cartaxo, Alenquer, Sobral de Monte Agraço, Arruda dos Vinhos e Torres Vedras. Contribuição para uma Simulação Simplificada de Danos. Relatório final*. Report 280/02, G3ES, Proc. 037/1/13810, LNEC.
- Carvalho, A., Sousa, M. L., Campos Costa, A., Nunes, J. C. and Forjaz, V.H. (2001). Seismic hazard for the Central Group of the Azores Islands. *Bolletino di Geofisica Teorica ed Applicata*, 42, 1-2, 89-105.
- Carydis, P. and Mouzakis, H. P. (1986). Small amplitude vibration measurements of buildings undamaged, damaged, and repaired after earthquakes. *Earthquake Spectra*, 2 (3), 515-535.
- Caselles, J. O., Espinoza, F. Muñoz, F., Lana, X., Sánchez, J., Navarro, M., Chourak, M. and De La Cruz, S.T. (1999). Variabilidad del período propio de los edificios de hormigón armado según sus características constructivas. *Proceedings, 1st National Conf. on Seismic Engineering*, Murcia (Spain) April 12-16, 1999, 2, 619-624.
- Castro, G. and Poulos, J.J. (1977). Factors affecting liquefaction and cyclic mobility. *ASCE, Journal of Geotechnical Engineering*, 103 GT6,501-516.
- Catalan, A., Roca, A. and Goula, X. (1999). Predicción espectral de la acción sísmica a partir del modelo de Brune modificado. *Memorias del 1er Congreso Nacional de Ingeniería Sísmica, Murcia 12-16 abril, 1999*, 177-189.
- CEA (1990). *CASTEM 2000. Guide d'utilisation*. CEA, France.
- Celebi, M. (1987). Topographical and geological amplifications determined from strong motion and aftershocks records of the 3 March 1985 Chile earthquake. *Bull. Seism. Soc. Am.*, 77, 1147-1167.
- Celebi, M., Sanli, A., Sinclair, M., Gallant and S. Radulescu, D. (2004). Real-time seismic monitoring needs of a building owner – and the solution, cooperative effort. *Earthquake Spectra*, 20 (2), 333-346.
- Cello, G., Deiana, G., Mangano, P., Mazzoli, S., Tondi, E., Ferrel, L., Maschio, L., Michetti, A. M., Serva, L. and Vittori, E. (1998). Evidence for surface faulting during the September 26, 1997 Colfiorito (Central Italy) earthquakes. *Journal of Earthquake Engineering* 2, 122, Imperial College Press, U.K.
- CEOS (2001). *The Use of Earth Observing Satellites for Hazard Support: Assessments and Scenarios*. Final Report of the CEOS Disaster Management Support Group, http://www.oosa.unvienna.org/SAP/stdm/CEOS_DMSG_Final_Report.pdf (consulted November 2004).
- Chang, S. E. (2000). Transportation Performance, Disaster Vulnerability, and Long-Term Effects of Earthquakes. *Proceedings, 2nd EuroConference on Global Change and Catastrophe Risk Management, Luxemburg, Austria*.
- Chang, S. E. and Nojima, N. (1997). Highway System Performance Measures and Economic Impact. *Proceedings, 7th U.S.-Japan Workshop on Earthquake Disaster Prevention for Lifeline Systems, Seattle, Washington*.
- Chang, S., Shinozuka, M. And Svekla, W. (1999). Modeling Post-Disaster Urban Lifeline Restoration. *Proceedings, 6th US Conference on Lifeline Earthquake Engineering*, Seattle, Washington, TCLEE/ASCE, Monograph No.16, edited by Elliott W, McDonough, 602-611.
- Chapman, MC. (1995). A probabilistic approach to ground-motion selection for engineering design. *Bull. Seism. Soc. Am.*, 85(3), 937-942.
- Chávez, J. (1998). *Evaluación de la vulnerabilidad y el riesgo sísmico a escala regional: Aplicación a Cataluña*. Tesis Doctoral. Universidad Politécnica de Cataluña, Barcelona, 343 p.
- Chavez, M. and García-Rubio, L. (1995). Seismic vulnerability of the metropolitan zone of Guadalajara, México. *Proceedings of the 5th International Conference on Seismic Zonation, Nice, 1*, 33-40.
- Chávez-García, F.J. and Faccioli, E. (2000). Complex site effects and building codes: making the leap. *Journal of Seismology*, 4, 23-40.
- Chávez-García, F.J., Rodríguez, M. and Hatzfeld, D. (1996). Topographic site effects and HVSR. A comparison between observation and theory. *Bull. Seism. Soc. Am.*, 86, 1559-1573.

- Chávez-García, F.J., Rodríguez, M., Field, E.H. and Hatzfeld, D. (1997). Topographic site effects and HVSR. A comparison of two nonreference methods. *Bull. Seism. Soc. Am.*, 87, 1667-1673.
- Chazelas, J.-L., Guéguen, Ph., Bard, P.-Y. and Semblat, J.-F. (2003). Modélisation de l'effet site-ville en modèle réduit centrifuge (validation des techniques instrumentales). *Actes du 6e Colloque National de Génie Parasismique*, AFPS 2003, Palaiseau, Vol I, 245-252.
- Chen, W. and Scawthorn, C. (Editors) (2002). *Earthquake Engineering Handbook*, ICBO, 1350 p.
- Chen, W. W., Shih Ban-Jwu, Wu Chuan-Wei, Chen Yi-Chih (2000). Natural Gas Pipeline System Damages in the Ji-Ji Earthquake (the city of Nantou). *Proceedings, 6th International Conference on Seismic Zonation, Palm Springs, California*.
- Chin-Hsiung, L., Jeng-Yaw, H. and Tzay-Chyn, S. (1998). Observed variation of earthquake motion across a basin-Taipei city. *Earthquake Spectra*, 14(1), 115-134.
- Chiroiu, L. (2004). *Modélisation des dommages dus aux seismes. Extension a d'autres risques naturels*. PhD Thesis, Paris 7 University, France.
- Chiroiu, L. and Andre, G. (2001). *Damage assessment using high resolution satellite imagery: application to 2001 Bhuj, India earthquake*. www.riskworld.com (consulted November 2004).
- Chiroiu, L., Andre, G., Guillande, R., and Bahoken, F. (2002). Earthquake damage assessment using high resolution satellite imagery. *Proceedings of the 7th U.S. National Conference on Earthquake Engineering*, Boston.
- Chopra, A. K. and Goel, R. K. (2000). Building period formulas for estimating seismic displacements. *Earthquake Spectra*, 16(2), 533-536.
- Cid, J., Susagna, T., Goula, X., Chavariia, L., Figueras, S., Fleta, J., Casas, A. and Roca, A. (2001). Seismic zonation of Barcelona based on numerical simulation of site effects. *Pure and Applied Geophysics*, 158, 2559-2577.
- Clark, J. A., Lee, C. H and Savage, W. U. (1991). Seismic geologic risks as factors in prioritising gas pipeline system replacement. *Proceedings, 3rd US Conference on Lifeline Earthquake Engineering*, Los Angeles, California, TCLEE/ASCE, Monograph No. 4, edited by M. A. Cassaro, 206-215.
- Clouteau, D. and Aubry, D. (2001). Modifications of the ground motion in dense urban areas. *Journal of Computational Acoustics*, 9, 1659-1675.
- Cluff, L. (1978). Geologic Considerations for Seismic Microzonation. *Proceedings, 2nd International Conference on Microzonation, I*, 135-152.
- Coburn A. and Spence R. (1992). *Earthquake Protection*. John Wiley and Sons, 355 p.
- Coburn A. and Spence R. (2002). *Earthquake Protection*. Second Edition. John Wiley and Sons, 420 p.
- Cocco, M. (1998). Seismic Hazard Assessment: Rupture propagation modeling for ground motion prediction. *Proceedings of the Advanced Course on Seismic Risk*. "SERINA- Seismic Risk: An integrated seismological, geotechnical and structural approach". European Commission Directorate General for Science, Research and Development, 1998, 154-189.
- Coelho, A.G. and Marcelino, J. (1997). Falhas Activas. Avaliação Probabilística da Perigosidade Sísmica. O Programa de Cálculo PROSISM. *3th National Conference on Seismology and Earthquake Engineering*, 21-30, Instituto Superior Técnico, Lisbon, Portugal.
- Coelho, A. G., Mota Freitas, J., Azeredo, Costa, A., Santos, N., Cruz, J. S. and Lopes, D. (1996). *Estudo de Viabilidade de Utilização da Ponte Luiz I pelo Metro Ligeiro do Porto*. Relatório Técnico (Definitivo), Serviço de Estruturas do Instituto de Construção, Fac. Eng. Univ. Porto, Portugal.
- Cole, H.A. (1968). On-the-line analysis of random vibrations. *AIAA/ASME 9th Struct. Dyn. Materials. Conf.* Palm Spring, CA.
- Comartin, C. D., Niewiarowski, R. W., Freeman, S. A., and Turner, F.M. (2000). Seismic Evaluation and Retrofit of Concrete Buildings: A practical Overview of the ATC-40 Document. *Earthquake Spectra*, 16 (3), 241-261.
- Commissariat Général du Plan (1997). *La prévention des risques naturels, rapport d'évaluation*, La Documentation Française, Paris.
- Cooper, M. D. (1868). Editorial. In: *San Francisco Daily Evening Bulletin*, November 3.
- Cornell, C. A. (1968). Engineering seismic risk analysis. *Bull. Seism. Soc. Am.*, 58, 1583-1906.
- Cornell, C.A. (1971). Probabilistic Analysis of Damage to Structures under Seismic Load. In: Howell, D.A., Haigh, I. P. and Taylor, C. (Editors), *Dynamic Waves in Civil Engineering*, London, Interscience, 473-488.
- Cornell, C.A. and Merz, H. A. (1974). Seismic Risk Analysis of Boston. *ASCE, Journal of Structural Division*, 101, 2027-2043.
- Cornou, C., Bard, P.-Y., Dietrich, M. (2003). Contribution of dense array analysis to basin-edge-induced waves identification and quantification. Application to Grenoble basin, French Alps (II). *Bull. Seism. Soc. Am.*, 93-6, 2624-2648.

- Correia Guedes, J. H. and Oliveira, C. S. (1990). *Caracterização da Edificação de Alvenaria Tradicional. Elementos para o Estudo do Comportamento e verificação do Parque Habitacional aquando do sismo de 1/1/80 nos Açores. 10 anos Após o Sismo de 1 de Janeiro de 1980. Vol.2.* In: Oliveira, C. S., Lucas, R. A. and Correia Guedes, (Editors), J. H. S. R. H. O. P. LNEC.
- Correia, R. (1996). *Avaliação Probabilística da Perigosidade Sísmica.* Report 28/96 – NEGE, Laboratório Nacional de Engenharia Civil, Lisbon, Portugal.
- Corte, J. F. (Editor) (1988), Centrifuge 88. *Proceedings Int. Conf. on geotechnical centrifuge model.* Paris, 610p.
- Costa, A. (1989). *Análise Sísmica de Estruturas Irregulares.* PhD Thesis, Fac. Eng. Univ. Porto, Portugal.
- Costa, A. (1996). *Estudo do Reforço da Ponte Luiz I.* Structural Study for the Design and Construction of a Strengthening Solution for the Luiz I Bridge.
- Costa, A. (1999). Ensaaios de Caracterização de Alvenarias Tradicionais. *Trabalhos de Engenharia Civil, Lda,* Porto.
- Costa, A. (2001). Avaliação Estrutural de um Edifício de Betão Armado. Avenida Olaf Palme – Maputo – Moçambique. In: Barroso de Aguiar, J. L., Jalali, S., Camões, A. and Ferreira, R. M. *I Seminário de Materiais de Construção, Civil Engineering Department,* Guimarães, 71-114.
- Costa, A. (2002a). Determination of mechanical properties of traditional masonry walls in dwellings of Faial Island, Azores. *Earthquake Engineering and Structural Dynamics,* 7, 31, 1361-1382.
- Costa, A. (2002b). *Análise do Comportamento da Ponte da Lagoncinha sob a Acção do Tráfego Rodoviário.* MSc Thesis on Civil Engineering Structures, Fac. Eng. Univ. Porto, Portugal.
- Costa, A. (2003). A Qualidade na Construção/Reabilitação e Reforço de Estruturas. *1º Encontro Nacional sobre Patologia e Reabilitação de Edifícios,* Fac. Eng. Univ. Porto, Portugal., 18-19 March, 219-237.
- Costa, A. (2004). Técnicas de Reabilitação Aplicadas a Diferentes Construções. *2º Colóquio – Construção Civil. Reflexão pela Qualidade. Novos Desafios, 20-21 May, Instituto Politécnico de Tomar, Tomar.*
- Costa, A. and Arêde, A. (2004). Strengthening of Structures Damaged by the Azores Earthquake of 1998. *Actas do Sismica 2004, International Meeting of Masonry Walls and Earthquakes, 14-16 April, Guimarães, 57-70.*
- Costa, A., Arêde, A., Moreira, D. and Neves, N. (2001). Técnicas de Reforço a Usar numa Construção Tradicional Danificada pelo Sismo de 9/7/98 na Ilha do Faial, Açores. *Actas do Sismica 2001, 5th Meeting On Seismology and Seismic Engineering, 27-29 October, Azores, 607-618.*
- Costa, A., Coelho, A., Mota Freitas, J., Azeredo, M., Cruz, J., Santos, N. and Lopes, D. (1998). Análise da Ponte Luiz I com vista à utilização pelo Metro Ligeiro do Porto. *Revista Portuguesa de Engenharia de Estruturas, 43,* LNEC, Lisbon.
- Costa, A. and Oliveira, C. (1997). Caracterização Dinâmica de Pontes Metálicas através de Ensaios Expeditos. *I Encontro Nacional de Construção Metálica e Mista, 20 -21 November, Porto, 577-587.*
- Costa, R. (1989). *Modelação do Processo Estocástico Sísmico na Península Ibérica.* PhD Thesis, Instituto Superior Técnico, Lisbon, Portugal.
- Costeira, P. and Costa, A. (2002). Characterisation of the Dynamic Behaviour of Maria Pia's Bridge. *First International Conference on Bridge Maintenance, Safety and Management, IABMAS 2002,* Barcelona.
- Coupland, R. M. (1994). Epidemiological Approach to Surgical Management of the Casualties of War. *British Medical Journal, 308,* 1693-6.
- Crowley, H. and Pinho, R. (2000). Period-height relationship for existing European reinforced concrete buildings. *Journal of Earthquake Engineering, 8, Special issue, 93-119.*
- Dandoulaki, M., Panoutsopoulou, M. and Ioannides, K. (1998). An Overview of Post-earthquake Building Inspection Practices in Greece and the Introduction of a Rapid Building Usability Evaluation Procedure after the 1996 Kozitsa Earthquake. *11th European Conference on Earthquake Engineering,* Balkema, Rotterdam.
- De Boer, J. (1995). An Introduction to Disaster Medicine in Europe. *The Journal of Emergency Medicine 13(2), 212-216.*
- De Boer, J. (1997). Tools for Evaluating Disasters: Preliminary Results of Some Hundreds of Disasters. *European Journal of Emergency Medicine 4, 107-111.*
- De Boer, J., Brisbar, B., Eldar, R. and Rutherford, W.H. (1989). The medical severity index of disasters. *The Journal of Emergency Medicine, 7, 269-273.*
- De Bruycker, M. D., Greco, M. F., Lechat, I., Annno, de Rugiero, N. and Triassi, M. (1985). The 1980 earthquake in Southern Italy: Morbidity and Mortality. *International Journal of Epidemiology, 14(1), 113-17.*

- De la Barra, T. (1989). *Integrated Land Use and Transportation Modelling*. Cambridge University Press, Cambridge.
- Department of Civil Protection (2001). Forms for the damage survey to cultural heritage. *Official Gazzette n. 116, May 21*.
- Department of Civil Protection and Ministry of Health. (1998). *Guidelines for the intra-hospital planning of a large-scale emergency*.
- Der Kiureghian, A. and Ang, A. H.-S. (1977). A Fault Rupture Model for Seismic Risk Analysis. *Bull. Seism. Soc. Am.*, 67 (4), 1173-1194.
- DGEiSC (2003). Pla especial d'emergències sísmiques de Catalunya. Direcció General d'Emergències i Seguretat Civil. *Diari Oficial Generalitat de Catalunya no. 3912, 26 Juny 2003*.
- Di Pasquale, G. and Galli, P. (2001). The Damage in the Area West to Gualdo Tadino after the 3 April 1998 Earthquake. *Ingegneria Sismica*, 18, 3-12.
- Di Pasquale, G. and Goretti, A. (2001). Functional and Economic Vulnerability in Residential Buildings due to Recent Italian Seismic Events. *X National Conference on Seismic Engineering in Italy, Potenza-Matera, 9-13 September*.
- Di Pasquale, G., Orsini, G. (1997). Proposta per la valutazione di scenari di danno conseguenti ad un evento sismico a partire dai dati ISTAT. *Atti del 8° Convegno nazionale L'Ingegneria Sismica in Italia, Taormina, 1997, 477-486*.
- Di Pasquale, G., Orsini, G. and Serra, C. (1998). Assessment of the Economic Loss from the DPC-GNDT-SSN Safety Evaluation Forms. *Proceedings International Workshop on Measures of Seismic Damage to Masonry Buildings, Monselice, Italy, June 25-27, Balkema, Rotterdam*.
- Disaster Prevention Council of the Tokyo Metropolitan Area. (1997). *Report on the Damage Estimation in Tokyo by the Earthquake Right Under the Area*. (In Japanese).
- Dogliani, F., Moretti, A. and V. Petrini (1994). *The churches and the earthquake*. Edizioni LINT, Trieste, Italy.
- Doherty, K. T., Griffith, M. C., Lam, N. and Wilson, J. (2002). Displacement-based seismic analysis for out-of-plane bending of unreinforced masonry walls. *Earthquake Engineering and Structural Dynamics*, 31, 833-850.
- Dolce, M., Kappos, A., Zuccaro, G. and Coburn, A. W. (1994). Report of the EAEE Working Group 3: Vulnerability and risk analysis. *10th European Conference on Earthquake Engineering*, Vienna, 4, 3049-3077.
- Dong, W., Shah H. and Wong, F. (1988). *Expert System in Construction and Structural Engineering*. Chapman and Hall, London, 1988.
- DPC (2002). *Report to the European Community on 31 October 2002 Molise-Puglia Earthquake*. Technical Report, National Seismic Survey, Rome, Italy.
- DRM-World Institute for Disaster Risk Management (2004a). Seismic microzonation for municipalities: Manual. In: J.Studer and A.Ansal (Editors), *Republic of Turkey, Ministry of Public Works and Settlement, General Directorate of Disaster Affairs*, www.koeri.boun.edu.tr/deprenmuh/MERM Manual.pdf, 140 p.
- DRM-World Institute for Disaster Risk Management (2004b). Seismic microzonation for municipalities: Pilot Studies: Adapazarı, Gölcük, İhsaniye, and Değirmendere. A. Ansal and S. Springman (Editors), *Republic of Turkey, Ministry of Public Works and Settlement, General Directorate of Disaster Affairs*, www.koeri.boun.edu.tr/deprenmuh/MERM Pilot Studies.pdf, 270 p.
- Duarte, R. T., Oliveira, C. S., Costa, A. C. and Costa, A. G. (1990). A non-linear model for seismic analysis, design and safety assessment of reinforced concrete buildings. In *Earthquake Damage Evaluation and Vulnerability Analysis of Building Structures*, Editor A. Koridze, Omega Scientific, England, 133-160.
- Dubois D. and Parade H. (1980). *Fuzzy Sets and Systems*, Academic Press, New York.
- Dunand, F., Bard, P.-Y., Chatelain, J. L., Guéguen, Ph., Vassail, T. and Farsi, M. N. (2002). Damping and frequency from randomdec method applied to in situ measurements of ambient vibrations . Evidence for effective soil structure interaction. *12th European Conference on Earthquake Engineering*, London, Elsevier Science Ltd, Paper 869.
- Dunand, F., Bard, P.-Y., Duval, A.-M., Guéguen, Ph. and Vidal, S. (2003). Périodes et amortissement des bâtiments niçois à partir d'enregistrements de bruit de fond. *VI^{ème} Colloque National de l'AFPS, Ecole Polytechnique, 1-3 Juillet 2003, Vol. I*, 291-298.
- Durukal, E., Erdik, M., Avc, J., Yüzügüllü, Ö., Zulfikar, C., Biro, T. and Mert, A. (1998). Analysis of the strong motion data of the Dinar, Turkey earthquake, *Soil Dynamics and Earthquake Engineering*, 17, 557-578.
- EC2, Eurocode 2 (2001). Design of concrete structures - Part 1: General rules and rules for buildings. Comité Européen de Normalisation.

- EC8, Eurocode 8 (1994). Design provisions for earthquake resistance of structures, Part 1.1: General rules – Seismic actions and general requirements for structures; Part 1.2: General rules – General rules for buildings; Part 1.3: General rules – Specific rules for various materials and elements. Comité Européen de Normalisation.
- EC8, Eurocode 8 (2003). Design of structures for earthquakes resistance. Comité Européen, de Normalisation..
- EDM (2000). *Report on the Kocaeli Turkey Earthquake of August 17th 1999*. EDM Technical Report No. 6, EDM, Miki, Japan.
- EEFIT (1993). *The Erzincan earthquake of 13 March 1992*. EEFIT, Institution of Structural engineers, London
- EERI (1986). *Reducing Earthquake Hazards: Lessons Learned From Earthquakes*. EERI Publication No: 86-02, San Francisco, California
- EERI (1990). *Loma Prieta Earthquake Reconnaissance Report*. Earthquake Spectra. Supplement to Vol.6, Earthquake Engineering Research Institute, Oakland, CA.
- Eguchi, R. T., Goltz, J. D., Seligson, H. A., Flores, P. J., Blais, N. C., Heaton, T. H. and E. Bortugno, (1997). Real time loss estimation as an emergency response decision support system: The early post-earthquake damage assessment tool (EPEDAT). *Earthquake Spectra*, 13, 4, 815-832.
- Eguchi, R., Houshmand, B., Huyck, C., Shinozuka, M and Tralli, D. (1999). *A new application for remotely sensed data: Construction of building inventories using synthetic aperture radar technology*. MCEER research and Accomplishments 1997-1999, MCEER, Buffalo.
- Eguchi, R., Huyck, C., Adams, B., Mansouri, B., Houshmand, B., and Shinozuka, M. (2002). Earthquake damage detection algorithms using remote sensing data – Application to the August 17, 1999 Marmara, Turkey Earthquake, *Proceedings of the 7th U.S. National Conference on Earthquake Engineering, Boston*.
- Eguchi, R., Huyck, C., Houshmand, B., Mansouri, B., Shinozuka, M., Yamazaki, F., Matsuoka, M. and Ulgen, S. (2000). *The Marmara, Turkey earthquake: Using advanced technology to conduct earthquake reconnaissance*. MCEER research and Accomplishments 1999-2000, MCEER: Buffalo.
- Eidinger, J. (1993). Fire Conflagration and Post-Earthquake Response of Power and Water Lifelines. *Proceedings, 4th DOE of Energy Natural Phenomena Hazards Mitigation Conference, Atlanta, GA*.
- Eidinger, J. (1998). *Lifelines, Water Distribution System in the Loma Prieta, California, Earthquake of October 17, 1989, Performance of the Build Environment-Lifelines*. US Geological Survey Professional Paper 1552-A, edited by A. Schiff, A63-A80.
- Eidinger, J. and E. Avila (1999). *Guidelines for the Seismic Upgrade of Water Transmission Facilities*. Monograph No. 15, TCLEE/ASCE.
- ENEL (1998). *Elaborazioni delle principali registrazioni accelerometriche de la sequenza sismica Umbro-Marchigiana del settembre-ottobre 1997*. CD-ROM
- Enomoto, T., Lermo, J., Navarro, M., Abeki, N. and Masaka, K. (2004). Site Effect Characteristics of Damage Concentrated Area due to the 2003 Colima Earthquake (M7.6), Mexico. *13th World Conference on Earthquake Engineering*, August 1-6, 2004, Vancouver, Canada. Paper No. 2151.
- Enomoto, T., Navarro, M., Sánchez, F.J., Vidal, F., Seo, K. Luzón, F., García, J.M., Martín, J. and Romacho, M.D. (1999). Evaluación del comportamiento de los edificios en Almería mediante el análisis del ruido ambiental. *1^a Asamblea Hispano-Lusa. Aguadulce (Almería, Spain)*, 9-13 / Febrero de 1998. CD-ROM.
- Enomoto, T., Schmitz, M., Abeki, N., Masaki, K., Navarro, M., Rocavado, V. and Sanchez, A. (2000). Seismic Risk Assessment Using Soil Dynamics in Caracas, Venezuela, *12th World Conference on Earquake Engineering*, CD-ROM.
- ENSeRVES. (2000). European Network on Seismic Risk, Vulnerability and Earthquake Scenarios. *Proceedings International Workshop on Seismic Risk and Earthquake Scenarios of Potenza, University of Basilicata*.
- EPRI, Electric Power Research Institute (1989). *Probabilistic Seismic Hazard Evaluation at Nuclear Power Plant Sites in the Central and Eastern United States: Resolution of the Charleston Earthquake Issue*. Report NP-6395-D, prepared by Risk Engineering Inc., Yankee Atomic Power Company and Woodward Clyde Consultants.
- Erdik, M. (1994). Developing a comprehensive earthquake disaster masterplan for Istanbul. In: Tucker, B. et al. (Editors), *Issues in Urban Earthquake Risk*. Kluwer Academic Publishers, Netherlands.
- Erdik, M., Ansal, A., Aydinoglu, N., Barka, A., Yuzugullu, O., Birgoren, G., Swift, J., Alpaya, Y. and Sesetyan, K. (2000). Development of Earthquake Masterplan for the Municipality of Izmir. *Proceedings, Sixth International Conference on Seismic Zonation, Palm Springs, November 12-15, 2000, EERI, San Francisco*.

- Erdik, M., Aydinoglu, N., Fahjan, Y., Sesetyan, K., Demircioglu, M., Siyahi, B., Durukal, E., Ozbey, C., Biro, Y., Akman, H. and Yuzugullu, O. (2003b). Earthquake Risk Assessment for Istanbul Metropolitan Area. *Earthquake Engineering and Engineering Vibration*, V.2- N-1, 1-25.
- Erdik, M., Demircioglu, M. B., Sesetyan, K., Durukal, E. and Siyahi, B. (2003a). Earthquake Hazard in Marmara Region. *European Geophysical Society (EGS)-American Geophysical Union (AGU)-European Union of Geosciences (EUG) Joint Assembly, Nice-France, 06-11 April 2003*.
- Erdik, M., Demircioglu, M. B., Sesetyan, K., Durukal, E. and Siyahi, B. (2004b). Earthquake Hazard in Marmara Region, Turkey. *Soil Dynamics and Earthquake Engineering*, 24 (2004), 605-631
- Erdik, M., Doyuran, V., Akkas, P. and Gulkan, P. (1985). Assessment of the Earthquake Hazard in Turkey and Neighboring Regions. *Tectonophysics*, 117, 295-344.
- Erdik, M., Durukal, E., Siyahi, B., Fahjan, Y., Sesetyan, K., Demircioğlu, M. and Akman, H. (2004a). Earthquake Risk Mitigation in Istanbul. Chapter 7. In: Mulargia, F. and Geller, R.J. (Editors), *Earthquake Science and Seismic Risk Reduction*. Kluwer.
- Erlingssson, S. (1999). Three-dimensional dynamic soil analysis of a live load in Ullevi stadium, *Soil Dynamic and Earthquake Engineering*, 18, 373-386.
- Erlingssson, S. and Bodare, A. (1996). Live load induced vibrations in Ullevi stadium-Dynamic soil analysis, *Soil Dynamic and Earthquake Engenering*, 15, 171-188.
- ESA (2003). European Space Agency. www.esa.int (consulted November 2004).
- Escalier des Orres, P., Granier, T. and Mohammadioun, B. (1992). An overview of IPSN research on the evolution of the natural system in support of the French methodology for the safety evaluation of radwaste disposal in deep geological formations. *Proceedings, Third International Conference on "High Level Radioactive Waste Management, Las Vegas, USA, April 12-16, 1992*.
- Espinosa-Aranda, J., Jiménez, A., Ibarrola, G., Alcantar, F., Aguilar, A., Inostroza, M., and Maldonado, S. (1995). Mexico City seismic alert system. *Seism. Res. Lett.* 66, 42-53.
- Espinoza, F. (1999). *Determinación de las características dinámicas de estructuras*. Tesis Doctoral, Universitat Politècnica de Catalunya, Barcelona.
- Espinoza-Aranda, J., and Rodriguez-Cayeros F.H. (2003). The seismic Alert System of Mexico City. In: Lee, W. H. K., Kanamori, H., Jennings, P. C. and Kisslinger, C. (Editors), *International handbook of Earthquake and Engineering Seismology*, Academic Press, 1253-1260.
- Esteva, L. M. (1968). *Bases para la Formulación de Decisiones de Diseno Sismico*. Publicación no. 182, Instituto de Ingeniería, UNAM, Mexico.
- Estêvão, J. M. C. and Oliveira, C. S. (1999). Contribuição para a Avaliação do Risco Sísmico. Aplicação à Cidade de Faro. *4th National Conference on Seismology and Earthquake Engineering*, Universidade do Algarve, Faro.
- Estrada, M., Matsuoka, M. and Yamazaki, F. (2001). Digital damage detection due to the 1999 Kocaeli, Turkey earthquake. *Bulletin of the Earthquake Resistant Structure Research Center*, 34, 55-66.
- Estrella, H. F. and González, J. A. (2003). SPAC: An alternative method to estimate earthquake site effects in Mexico City. *Geofísica Internacional*, 42 (2), 227-236.
- Evernden, J. F., Kohler, W. M. and Clow, G. D. (1981). *Seismic intensities of earthquakes of Conterminous United States: Their prediction and interpretation*. U.S.G.S. Professional Paper 1223, 56p.
- Evernden, J. F. and Thomson, J. M. (1985). *Predicting seismic intensities in evaluating earthquake hazards in the Los Angeles region*. USGS Professional Paper No:1360, US Government Printing Office, Washington. 151-202.
- Faccioli, E., Pessina, V., Calvi, G. M. and Borzi, B. (1999). A study on damage scenario for residential buildings in Catania City. *Journal of Seismology* 3(3), 327-343.
- Faccioli, E. (1991). Seismic Amplification in the Presence of Geological and Topographic Irregularities. *Proceedings, 2nd International Conference on Recent Advances in Geotechnical Earthquake Engineering*, St. Louis, Missouri, State-of-art paper, 1779-1797.
- Faccioli, E. (Coordinatore) et al. (1997). *Scenari di danno da terremoto per il comune di Catania*. Gruppo Nazionale per la Difesa dei Terremoti. Italy.
- Faccioli, E. and Pessina, V. (2003). Use of Engineering Seismology Tools in Ground Shaking Scenarios. In: Lee, W., Kanamori, H., Jennings, P. and Kisslinger, C. (Editors), *International Handbook of Earthquake and Engineering Seismology*. Academic Press, 1031-1048.
- Faccioli, E., Paolucci, R. and Rey, J. (2004). Displacement Spectra for Long Periods. *Earthquake Spectra*, 20 (2), 347-376.
- Faeh, D., Kind, F., Lang, K. and Giardini, D. (2001). Earthquake scenarios for the city of Basel. *Soil Dynamics and Earthquake Engineering*, 21, 405-413.
- Fäh, D. (1994). *A hybrid technique for the estimation of strong ground motion in sedimentary basins*. Nr. 9767, eidg tech Hochschule, Zurich (ETHZ).

- Fajfar, P. (2000). A non linear analysis method for performance-based seismic design. *Earthquake Spectra*, 16(3), 573-5924.
- Faria, R. (1995). *Avaliação do Comportamento Sísmico de Barragens de Betão Através de um Modelo de Dano Contínuo*. PhD Thesis, FEUP, Porto.
- Farsi, M. N. (1996). *Identification des structures de génie civil à partir de leurs réponses vibratoires. Vulnérabilité du bâti existant*. Ph. D. Thesis, Université Joseph Fourier, Grenoble, France, 189 p.
- Farsi, M., and Bard, P.-Y. (2003) Estimation des périodes propres de bâtiments et vulnérabilité du bâti existant dans l'agglomération de Grenoble. *Revue Française de Génie Civil*, vol. 8, n. 2/3, 149-179
- Fawcett, W. and Oliveira, C.S. (2000). Casualty treatment after earthquake disasters: development of a regional simulation model. *Disasters*, 24(3), 271-287.
- FEMA (1994). *Assessment of the State-of-the-Art Earthquake Loss Estimation Methodologies*. Federal Emergency Management Agency (FEMA) Report 249, Washington.
- FEMA (1997a) *NEHRP Recommended Provisions for Seismic Regulations for New Buildings*. Federal Emergency Management Agency (FEMA) Report 273, Washington.
- FEMA (1997b) *NEHRP Recommended Provisions for Seismic Regulations for New Buildings and others structures*. Federal Emergency Management Agency (FEMA) Report 303, Washington.
- FEMA (1998). *Handbook for the Seismic Evaluation of Existing Buildings. A Prestandard*. Federal Emergency Management Agency (FEMA) Report 310, Washington.
- FEMA (2000). *Prestandar and commentary for the seismic rehabilitation of buildings*. Federal Emergency Management Agency (FEMA) Report 356, Washington.
- FEMA (2003) *Mapping and Analysis Center: Remote Sensing Information and Data*. Federal Emergency Management Agency (FEMA) <http://www.gismaps.fema.gov/rs.shtm> (consulted November 2004).
- Fernandez, J., Valverde, J., Yepes, H., Tucker, B., Bustamante, G., Chatelain, J. L., Kaneko, F., Villacis, C. and Yamada, T. (1994). The Quito, Equador, earthquake risk management project, an overview. *Geohazards International*, 34.
- Field, E. H., Hough, S.E. and Jacob, K.H. (1990). Using microtremors to assess potential earthquake site response: a case study in Flushing Meadows, New York City. *Bull. Seism. Soc. Am.*, 80, 1456-1480.
- Field, E. H., Jordan, T. H. and C. A. Cornell (2003) OpenSHA, a developing community-modeling environment for seismic hazard analysis. *Seis. Res Letters*, 74, 406-419.
- Figuerras, S. (1994). *Simulació numèrica del moviment del sòl produït per terratrèmols. Aplicació a moviments febles i forts*. PhD Thesis, Universitat Politècnica de Catalunya.
- Figuerras, S., Roca, A., Goula, X. and Blázquez, R. (1992). Larger Soil Amplification for Stronger Ground Motion from SMART-1 Records. *10th World Conference on Earthquake Engineering*, Madrid, 1043-1048.
- Fleta, J., Escuer, J., Goula, X., Olivera, C., Combes, Ph., Grellet and Granier, Th. (1996). Zonación tectónica, primer estadio de la zonación sismotectónica del NE de la península Ibérica (Catalunya). *Geogaceta*, 20, 853-856.
- Foster, B. and Kodama, S. (2004). Emergency Management, Recovery and Reconstruction Following the 2002 Molise, Italy, Earthquake. In: Bazzurro, P. and Maffei, J. (Editors), *Earthquake Spectra 20, Special Issue 1, 2002 Molise, Italy, Earthquake Reconnaissance Report*, S323-339.
- Frade, C., Graça, A., (1999). *Aplicações de Redes Neurais na Inferência de Características Sísmicas*. Projecto Final de Curso, Licenciatura em Matemática Aplicada e Computação, Instituto Superior Técnico, Lisbon, Portugal.
- Frankel, A. (1995). Mapping seismic hazard in the Central and Eastern United States. *Seismic. Res. Letts.*, 66, 8-21.
- Frankel, A., Mueller, C., Barnhard, T., Perkins, D., Leyendecker, E., Dickman, N., Hanson, S. and Hopper, M. (1996). *National seismic hazard mapping*. Documentation USGS Open- File Report 96-532. U.S. Government Printing Office, Washington. (<http://geohazrds.cr.usgs.gov/eq/>).
- Freeman, S. A. (1998a). Development and use of capacity spectrum method. *Proceedings of the 6th U.S. National Conf. Earthquake Engineering, Seattle, EERI, Oakland, California*.
- Freeman, S. A. (1998b). The Capacity Spectrum Method. *11th European Conference on Earthquake Engineering*, Paris.
- Freeman, S. A. (2004). Why properly code designed and constructed buildings have survived major earthquakes. *13th World Conference on Earthquake Engineering*, Vancouver, B. C., Canada, CDROM, paper #1689.
- Fringas, C., Kyriazis, E. (2000). *Risk Elements Removal, Temporal Support and Propping*. EPPO-ECPFE Handbook 2, Athens.
- Fukushima, Y. and Tanaka, T. (1990). A new attenuation relationship for peak horizontal acceleration of strong earthquake ground motion in Japan. *Bull. Seism. Soc. Am.*, 80, 757-783.

- Galanti, E. (1997). Augustus Method. *DPC Informa, Anno II, N. 4*, Tipo-Lito, Rome, Italy.
- Galanti, E., Albanese, V., De Sortis, A., Papa, F. and Sergio, S. (2004). 2002 Molise-Puglia earthquake: Emergency management, temporary shelters and short term countermeasures. *Ingegneria Sismica, Anno XX, Vol. 4*, Patron Editor, Bologna, Italy.
- Galasco, A., Lagomarsino, S. and Penna, A. (2002). *TREMURI Program: seismic analysis of 3D masonry Buildings*. University of Genoa, Italy.
- Galli, P., Orsini, G., Di Pasquale and G., Galadini, F. (2002). Testing damage scenarios. From historical earthquakes to silent active faults. *Proceedings XVII Gen. Ass. European Geophysical Society, Nice, April 22-24, 2002*.
- Gao S., Liu, H., Davis, P.M. and Knopoff, L. (1996). Localized amplification of seismic waves and correlation with damage due to the Northridge earthquake: evidence for focusing in Santa Monica, *Bull. Seism. Soc. Am., 86(2)*, S209-S230.
- García-Fernández, M. and Jiménez, M.J. (1997). *GSHAP Test Area VI: Ibero-Maghreb*. Summary Report. Institute of Earth Sciences Jaume Almera, Barcelona.
- Gavarini, C. (1985). Post-earthquake Building Usability: a Proposal. *L'Industria Italiana del Cemento*, n. 6.
- Gavarini, C. (1999). An Outline of Emergency Surveys: from Damage to Usability. Course on: *The Damage Survey and Post-Earthquake Usability Evaluation*. National Seismic Survey, University of Rome and Catania Municipality, Catania, 16 November.
- Gazetas, G., Dakoulas, P. and Papageorgiou, A. (1990). Local soil and source-mechanism effects in the 1986 Kalamata (Greece). *Earthquake Engineering and Structural Dynamics*, 19, 431-453.
- Geli, L., Bard, P.-Y. and Jullien, B. (1988). The effect of topography on earthquake ground motion: a review and new results. *Bull. Seism. Soc. Am.*, 78, 42-63.
- Geodeco, SpA (1998). (<http://www.geodeco.it/eng/gen/history.html>) (consulted Nov 2004)
- Giardini, D. (Editor) (1999). The Global Seismic Hazard Assessment Program (GSHAP) 1992-1999. Summary volume, *Annali di Geofisica*, 42, 957-1230.
- Giovinazzi, S. and Lagomarsino, S. (2003). *Seismic Risk Analysis: a method for the vulnerability assessment of built - up areas*. ESREL, Maastricht.
- Giovinazzi, S. and Lagomarsino, S. (2004). A macroseismic method for the vulnerability assessment of buildings. *13th World Conference on Earthquake Engineering, Vancouver, B.C., Canada*, Paper 896.
- GNDT Ministry of Labour and Civil Protection (1993). *Seismic Risk of Public Buildings. Part I. Methodology*. Tipografia moderna, Bologna.
- GNDT Ministry of Labour and Civil Protection (1994). *Churches and the earthquake*. Doglioni F., Moretti A., Pettrini V. editors, LINT edition, Trieste.
- GNDT Ministry of Labour and Civil Protection (1999). *Vulnerability survey of public, strategic and special buildings in Abruzzo, Basilicata, Calabria, Campania, Molise and Sicily Region*. Graphicpress srl, L'Aquila.
- Goel, R. K. and Chopra, A. K. (1998). Period formulas for concrete shear wall buildings. *Journal of Structural Engineering, ASCE*, 124(4), 426-433.
- Goltz, J. D. (2002). *Introducing earthquake early warning in California: A summary of social science and public policy issues*. Caltech Seismological Laboratory, Disaster Assistance Division, A report to OES and the Operational Areas.
- Gomes, R., Oliveira, C. S. and Correia, A. G. (1999). Analysis of the dynamic response of the Volvi Valley. *2nd International Conference of Earthquake Geotechnical Engineering*, LNEC, Lisbon, 1, 187-192.
- González, M., Chávez, J., Susagna, T., Goula, X. and Roca, A. (2001). Simulation des effets sismiques: application au séisme de 1428 dans les Pyrénées-Orientales. In archéosismicité et sismicité historique. Contribution à la connaissance et à la définition du risque. *APS. Perpignan*, 119-123.
- González, M., Safina, S. Susagna, T., Goula, X. and Roca, A. (2000). *Avaluació de la vulnerabilitat sísmica d'edificis essencials: hospitals i parcs de bombers*. Informe del Institut Cartogràfic de Catalunya - ICC. No. GS-138/00.
- González, M., Susagna, T., Goula, X., Roca, A. and Safina, S. (2001) Una primera aproximación de la vulnerabilidad sísmica de edificios esenciales: Hospitales y parques de bomberos. *Memorias del 2do Congreso Iberoamericano de Ingeniería Sísmica*, Madrid, España.
- González, M., Susagna, T., Goula, X., Roca, A. and Safina, S. (2002). A simplified approach to include essential facilities in risk scenarios for civil defence plans. *27 th General Assembly of the European Geophysical Society, Nice, April 2002*.
- Goretti, A. (2001). *Post-earthquake Building Usability Assessment*. Technical Report SSN/RT/01/03.
- Goretti, A. (2002). *Post-earthquake Usability and Damage Evaluation of Reinforced Concrete Buildings Designed Not According to Modern Seismic Codes*. JSPS Short Term Fellowship Final Report and Technical Report SSN/RT/02/01, March.

- Goretti, A. and Di Pasquale, G. (2002). An Overview of Post-Earthquake Damage Assessment in Italy. *EERI Invitational Workshop An Action Plan to Develop Earthquake Damage and Loss Data Protocols, 19-20 September, Pasadena*.
- Goretti, A. and Di Pasquale, G. (2004). Building Inspection and Damage Data of the Molise Earthquake Sequence of October 31-November 1, 2002. In: Bazzurro, P. and Maffei, J. (Editors), *Earthquake Spectra 20, Special Issue 1, 2002 Molise, Italy, Earthquake Reconnaissance Report*.
- Goretti, A. and Dolce, M. (2002). Site Effects Evaluation from Surveyed Typological and Damage Data. *12th European Conference on Earthquake Engineering*, London.
- Grecksch, G. and Kumpel, H. J. (1997). Statistical analysis of strong-motion accelerogram and its application to earthquake early-warning systems. *Geophys. J. Int.* 129, 113-123.
- Gregor, N. J. (1995). *The Attenuation of Strong Ground Displacements*. EERC Report No: UCB/EERC-95/02, Univ. of California at Berkeley.
- Griffith, M. C. and Pinto, A. (2000). Seismic retrofit of reinforced concrete buildings: a review and case study. *12th World Conference on Earthquake Engineering*, Auckland New Zealand, Paper 2327.
- Grossi, P., Cyr, C., Tao, W., Kunreuther, H., Lee, D. and Fuetter, T. (2002). Cost-Benefit Analysis: A tool to evaluate mitigation for lifeline systems. *Proceedings of 7th National Conference of Earthquake Engineering, Boston, Massachusetts*.
- Grünthal, G. (editor) (1993). European Macroseismic Scale 1992 (up-dated MSK-scale). *Cahiers du Centre Européen de Géodynamique et de Séismologie*, 15, Luxembourg, 79p.
- Grünthal, G. (editor) (1998). European Macroseismic Scale 1998. *Cahiers du Centre Européen de Géodynamique et de Séismologie*, 7, Luxembourg, 99p.
- Guéguen, Ph. (2000). *Interaction sismique entre le sol et le bâti: de l'Interaction Structure-Sol-Structure à l'Interaction Site-Ville*. Thèse, Université Joseph Fourier, Grenoble. 184 p.
- Guéguen, Ph., Bard, P. Y. and Chaves-García, F. J. (2002). Site-City seismic interaction in Mexico-city like environments: an analytic study. *Bull. Seism. Soc. Am.*, 92, 794-804.
- Guéguen, Ph., Bard, P. Y. and Oliveira, C. (2000). Distant motion from an isolated RC-building model: experimental and numerical approaches. *Bull. Seism. Soc. Am.*, 90-6, 1464-1479.
- Guéguen, Ph., Chatelain, J-L., Guillier, B., Yepes, H. and Egred, J. (1998). Site effect and damage distribution in Pujili (Ecuador) after the 28 March 1996 Earthquake. *Soil Dynamics and Earthquake Engineering*, 17, 329-334.
- Guidi, G.A., (1979). *Computer Programs for Seismic Hazard Analysis. A User Manual Stanford Seismic Hazard Analysis – STASHA*. Report no. 36. The John A. Blume Engineering Center, Stanford University.
- Guidoboni, E., Mariotti, D., Giammarinaro, M., S. and Rovelli, A. (2003). Identification of amplified damage zones in Palermo, Sicily (Italy) during the Earthquakes of the last Three Centuries. *Bull. Seism. Soc. Am.*, 93 (4), 1649-1669.
- Gülkan, P. and Kalkan, E. (2002). Attenuation modelling of recent earthquakes in Turkey. *Journal of Seismology* 6(3), 397-409.
- Gumbel, E.J. (1958). *Statistics of Extremes*. Columbia University Press, New York, 375p.
- Gunturi, S. K. V. (1993). *Building-Specific Earthquake Damage Estimation*. PhD. Thesis, Department of Civil Engineering, Stanford University.
- Gürpınar, A. (1997). A review of seismic safety considerations in the life cycle of critical facilities. *Journal of Earthquake Engineering*, 1, 57-76. Imperial College Press, London, U. K.
- Gutierrez, C. and Sing, S.K. (1992). A site effect study in Acapulco, Guerrero, México: comparison of results from strong motion and microtremor data. *Bull. Seism. Soc. Am.*, 82, 642-659.
- Hada, Y. and Meguro, K. (2000). Optimum restoration model considering interactions among lifeline systems-interactions among restoration activities of lifeline utilities. *12th World Conference on Earthquake Engineering*, New Zealand Society for Earthquake Engineering, Upper Hutt, NZ.
- Hanks, T. C. and Kanamori, H. (1979). A moment magnitude scale. *J. Geophys. Res.*, 84, 2348-2350.
- Harben, P.E. (1991). *Earthquake alert system feasibility study*. Lawrence Livermore National Laboratory, Livermore, CA, UCRL-LR-109625.
- Harmsen, S, Perkins, D. and Frankel, A. (1999). Deaggregation of probabilistic ground motions in the Central and Eastern United States. *Bull. Seism. Soc. Am.*, 89, 1-13.
- Hartzell, S., Carver, D. and Williams, R.A. (2001). Site response, shallow shear-wave velocity and damage in Los Gatos, California, from the 1989 Loma Prieta Earthquake, *Bull. Seism. Soc. Am.*, 91(3), 468-478.
- Hashitera, S., Kohiyama, M., Maki, N. and Fujita, H. (1999). Use of DMSP-OLS images for early identification of impacted areas due to the 1999 Marmara earthquake disaster. *Proceedings, 20th Asian Conference on Remote Sensing, Hong Kong*, 1291-1296.

- Haskell, N.A., (1953). The dispersion of surface waves on multilayered media. *Bull. Seism. Soc. Am.*, 43, 17-34.
- Hauksson, E., Jones, L. and Shakal, A., (2003). TriNet: A modern ground motion seismic network. In: Jennings, P., Kisslinger, C., Kanamori, H. and Lee, W. (Editors) *International Handbook of Earthquake and Engineering Seismology*, Academic Press, 1275-1284.
- Hauskov, J. and Alguacil, G. (2005). *Instrumentation in Earthquake Seismology*. Modern Approaches in Geophysics vol. 22, Springer, 360p.
- Heaton, T.H. (1985). A model for seismic computerized alert network. *Science*, 228, 987-990.
- Heyman, J. (1966). The stone skeleton. *International Journal of Solids and Structures*, 2, 249-279.
- Heyman, J. (1982). *The masonry arch*. Ellis Horwood Ltd., Chichester, UK.
- Hirosawa, M., Sugano S. and Kaminosono T. (1995). "Essentials of Current Evaluation and Retro Fitting for Existing and Damaged Buildings in Japan", Training Course in Seismology and Earthquake Engineering, International Institute of Seismology and Earthquake Engineering (ISEE).
- Hisada, Y. (1994). An efficient method for computing Green's functions for a layered half-space with sources and receivers at close depths (Part 1). *Bull. Seism. Soc. Am.*, 84, 1456-1472.
- Hisada, Y. (1995). An efficient method for computing Green's functions for a layered half-space with sources and receivers at close depths (Part 2). *Bull. Seism. Soc. Am.*, 85, 1080-1093.
- Honegger, D. G. and Eguchi, R. T. (1992). Determination of the Relative Vulnerabilities to Seismic Damage for Dan Diego Country Water Authority (SDCWA). Water Transmission Pipelines.
- Hoshiya, M. and Ohno, H. (1985). A system dynamic model in seismic performance assessment of electric power and water supply networks. *Proceedings, Trilateral Seminar – Workshop on Lifeline Earthquake Engineering*, Taipei, Taiwan, 181-189.
- Huyck, C. K., Eguchi, R. and Houshmand, B. (2002a) *Bare-earth algorithm for use with SAR and LIDAR digital elevation models*. MCEER-02-0004 Technical Report, MCEER, Buffalo.
- Huyck, C. K., Mansouri, B., Eguchi, R. T., Houshmand, B., Castner, L. and Shinozuka, M. (2002b). Earthquake damage detection algorithms using optical and ERS-SAR satellite data – Application to the August 17, 1999 Marmara, Turkey earthquake. *Proceedings, 7th U.S. National Conference on Earthquake Engineering*, Boston.
- IAEA (2002). *Evaluation of Seismic Hazards for Nuclear Power Plants*. IAEA Safety Guide NS-G-3.3, Vienna, Austria, 31 p.
- IAEA (2003). *Seismic Design and Qualification for Nuclear Power Plants*. IAEA Safety Guide NS-G-1.6, Vienna, Austria, 59 p.
- IASPEI (1993). The Practice of Earthquake Hazard Assessment. In: R. McGuire (Editor), *International Association of Seismology and Physics of the Earth's Interior*.
- ICC (1997). Butlletí sismològic 1996. Institut Cartogràfic de Catalunya, <http://www.icc.es>. (consulted November 2004).
- ICC (2000). Mapa Geotècnic de Barcelona. CD-Rom, Institut Cartogràfic de Catalunya, Barcelona.
- ICC (2001). Mapa de trànsit de Catalunya 2000. Direcció General de Carreteres. Institut Cartogràfic de Catalunya.
- Ichii, K. (2003). *Application of Performance-Based Seismic Design Concept for Caisson-Type Quaywalls*. PhD. Thesis, Civil Engineering Department, Kyoto University, Japan.
- Iglesias, J. (1988). Seismic Microregionalization of Mexico City after the 1985 earthquake. *9th World Conference on Earthquake Engineering*, 2,127-132.
- Iglesias, J. (1991). Seismic Zonation of Mexico City. *Proceedings, 4th Int. Conf. Seismic Zonation. Earthquake Engineering Research Institute*, Stanford, California, 3, 471-478.
- IGN (1999a). Base de datos de aceleración 1984 - 1997. CD - ROM.
- IGN (1999b). *Serie sísmica de Mula (Múrcia)*. Segundo informe general. Subdirección de Geodesia y Geofísica.
- IGOS (2001). What is IGOS? <http://www.igospartners.org/> (consulted November 2004).
- INE (2003). Censos 2001. Resultados Definitivos. Portugal. Instituto Nacional de Estatística, Lisboa.
- Irikura, K. (1983). Semi-empirical estimation of strong ground motions during large earthquakes. *Bull. Disaster Prev. Inst. Kyoto Univ.*, 33, Part 2, 298, 63-104.
- Irizarry, J., Goula, X. and Susagna, T. (2003). *Analytical formulation for the elastic acceleration-displacement response spectra adapted to Barcelona soil conditions*. Technical Report, Institut Cartogràfic de Catalunya, Barcelona.
- Irizarry, J., Goula, X., Susagna, T., Roca, A. and Maña, F. (2004). Earthquake risk scenarios for monuments in Barcelona, Spain. *13th World Conference on Earthquake Engineering*, Vancouver, BC, Canada, paper 2162 (CD-Rom).
- ISDR (2003). International Strategy for Disaster Reduction, <http://www.unisdr.org/> (consulted November 2004).

- Ishihara, K. (1997). Geotechnical aspects of ground damage during the Kobe-Awaji earthquake, Theme Lecture. *Earthquake Geotechnical Engineering*, Ishihara, K. ed., Balkema, Rotterdam, 1327-1331.
- Ishikawa, Y. and Kameda, H. (1988). Hazard-Consistent Magnitude and Distance for Extended Seismic Risk Analysis. *9th World Conference on Earthquake Engineering, II*, 95-100, Tokyo.
- Ishizawa, O., Clouteau, D., Lombaert, D. and Mezher, N. (2003). Caractérisation théorique et numérique de l'effet site-ville. Cas de la ville de Mexico. *6e Colloque National de Génie Parasismique, AFPS 2003, Palaiseau, 1-3 July 2003*.
- Isoyama, R., Ishida, E., Yune, K. and Shirozu, T. (1998). Seismic damage estimation procedure for water supply pipelines. *Proceedings, Water and Earthquake '98 Tokyo, IWSA International Workshop, Anti-Seismic Measures on Water Supply*, International Water Services Association and Japan Water Works Association, Tokyo, Japan.
- ISSMFE (1986). *Manual for Zonation on Seismic Geotechnical Hazards*. Technical Committee for Earthquake Geotechnical Engineering, TC4, The Japanese Society of Soil Mechanics and Foundation Engineering.
- ISSMGE (1999). *Manual for Zonation on Seismic Geotechnical Hazards (Revised Version)*. Technical committee for earthquake geotechnical engineering, TC4 of the International Society for Soil Mechanics and Geotechnical Engineers, The Japanese Geotechnical Society, 209 p.
- Iwasaki, T., Tatsuoka, F., Tokida, K. and Yasuda, S. (1978). A practical method for assessing soil liquefaction potential based on case studies at various sites in Japan. *2nd Int. Conference on Microzonation, San Francisco, 2*, 885-896.
- Japan Waterworks Association (1998). Seismic Damage Estimation Procedure for Water Pipes (in Japanese).
- Jeary, A. P. (1996). The description and measurement of nonlinear damping in structures. *Journal of Wind Engineering and Industrial Aerodynamics*, 59 (2-3), 103-114.
- Jeary, A. P. (1997). Damping in structures. *Journal of Wind Engineering and Industrial Aerodynamics*, 72 (1-3), 345-355.
- Jennings, P. (1970). Distant motions from a building vibration test. *Bull. Seism. Soc. Am.*, 60, 2037-2043.
- Jennings, P.C. (1997). Enduring Lessons and Opportunities Lost from the San Fernando Earthquake of February 6, 1971. *Earthquake Spectra*, 13(1), 25-53.
- Jensen, J. R. (1996). *Introductory Digital Image Processing: A Remote Sensing Perspective*. Prentice Hall Ed., NJ, USA.
- Jernigan, J. B., Werner S. D. and Hwang, H. H. M. (1996). Inventory of Bridges Using GIS for Seismic Risk Assessment of Highway Systems. *Center for Engineering Research and Information*, University of Memphis, Memphis TN.
- Jerry, A. P. (1986). Damping in tall buildings - A mechanism and a predictor. *Earthquake Engineering and Structural Dynamics*, 14, 733-750.
- JICA (2003). *The Study on A Disaster Prevention / Mitigation Basic Plan in Istanbul including Seismic Microzonation in the Republic of Turkey*. Report prepared for Istanbul Metropolitan Municipality, Japan International Cooperation Agency (JICA).
- Johnson, L., Coburn A, and Rahnama, M, (2000). Damage Survey Approach to Estimating Insurance Losses. In: Youd, T. L., J-P. Bardet and J. D. Bray (Editors), *The Kocaeli Turkey Earthquake of 17 August 1999 Reconnaissance Report*, Publication No 2000-03, EERI.
- Johnston, A., (1996a). Seismic Moment Assessment of Earthquakes in Stable Continental Regions. *I, Instrumental Seismicity. Geophysical Journal International*, 124,381-414.
- Johnston, A., (1996b). Seismic Moment Assessment of Earthquakes in Stable Continental Regions. *I, Historical Seismicity. Geophysical Journal International*, 125, 639-678.
- Jones, B. G. and Chang, S. (1993). Indirect methods for estimating the build physical environment for risk and damage assessment and relief, recovery and reconstruction planning. *Proceedings, 1993 National Earthquake Conference*, Memphis, Tennessee, 1, 593-602.
- Joyner, W. B. and Boore, D. M. (1988). Measurement, characterization, and prediction of strong ground motion. *Proceedings, Earthquake Engineering and Soil Dynamics II*. GT Div/ASCE, Park City, Utah, June, 27-30.
- Joyner, W.B. and Boore, D.M. (1981). Peak Horizontal Acceleration and Velocity from Strong-Motion Records Including Records from 1979 Imperial Valley, California Earthquake. *Bull. Seism. Soc. Am.*, 71, 2011-2038.
- JRC (2003). Natural Hazards Project, <http://natural-hazards.jrc.it/> (consulted Nov 2004).
- Kaas, J. E., Kates, R. W. and Bowden, M. J. (1987). *Reconstruction Following Disaster*. MIT Press, Cambridge, London.
- Kagami, H., Okada, S. and Ohta, Y. (1988). Versatile application of dense and precision seismic intensity data by an advanced questionnaire survey. *Proceedings, Ninth World Conf. on Earthquake Engineering*, 8, 937-942.

- Kagami, H., Okada, S., Shiono, K., Oner, M., Dravinski, M. and Mal, A.K. (1986). Observation of 1 to 5 second microtremors and their application to earthquake engineering. Part III. A two dimensional study of site effects in S. Fernando valley. *Bull. Seism. Soc. Am.*, 76, 1801-1812.
- Kagawa, T. (1996). Estimation of velocity structures beneath Mexico city using microtremor array data. *11th World Conference on Earthquake Engineering*, Acapulco, Mexico.
- Kaiser (1997). *Post-Earthquake Inspection Manual*. Kaiser Permanente report, Oakland, California.
- Kameda, H. (2000). Engineering management of lifeline systems under earthquake risk. *12th World Conference on Earthquake Engineering*, New Zealand Society for Earthquake Engineering, Upper Hutt, NZ.
- Kamiyama, M., Yoshida, M., Suzuki, T. (1999). Effects of Irregular Ground Structure on Earthquake Motions: a Comparison Between Observation and Numerical Simulation. *Proceedings, 2nd International Conference on Geotechnical Engineering*, Lisbon, 21-25 June 1999. Ed. Sêco Pinto, P., Balkema, Rotterdam, 255-260.
- Kanai, K. (1957). The requisite conditions for predominant vibration of ground. *Bull. Earthq. Res. Inst. Tokyo Univ.*, 31, 457.
- Kanamori, H. (2003). Earthquake Prediction an Overview. In: Lee, W. H. K., Kanamori, H., Jennings, P. C. and Kisslinger, C. (Editors), *International handbook of Earthquake and Engineering Seismology*, Academic Press, 1205-1216.
- Kanamori, H., Hauksson, E. and Heaton, T. (1997). Real-time seismology and earthquake hazard mitigation. *Nature*, 390, 461-464.
- Kanamori, H., Mori, J., Anderson, D. L. and Heaton, T. H. (1991). Seismic excitation by the space shuttle Columbia. *Nature*, 349, 781-782.
- Kappos, A., Ptilakis, K., Stylianidis K, and Morfidis, K. (1995). Cost-benefit analysis for the seismic rehabilitation of buildings in Thessaloniki, based on a hybrid method of vulnerability assessment. *Proceedings, 5th International Conference on Seismic Zonation*, Nice, 1, 406-413.
- Kareem, A. and Gurley, K. (1996). Damping in structures: Its evaluation and treatment of uncertainty. *Journal of Wind Engineering and Industrial Aerodynamics*, 59,131-157.
- Karim, K., and Yamazaki, F. (2001). Effect of earthquake ground motions on fragility curves of highway bridge piers based on numerical simulation. *Earthquake Engineering and Structural Dynamics*, 30,1839-1856.
- Katayama, T., Yamazaki, F., Nagata, S. and Isoyama, R. (1991). Fuzzy reasoning for earthquake damage assessment of large-scale city gas systems. *Proceedings, 3rd US Conference on Lifeline Earthquake Engineering, Los Angeles, California*, TCEE/ASCE, Monograph No. 4, edited by M. A. Cassaro, 639- 650.
- Kawase, H. (1998). The Cause of the Damage Belt in Kobe: 'The Basin Edge Effect', Constructive Interference of the Direct S-Wave with the Basin-induced Diffracted/Rayleigh Waves, *Seismological Research Letters*, 67, 25-34.
- Kawase, H. (2003). Site effects on strong ground motions. In: Lee et al. (Editors), *International Handbook of Earthquake and Engineering Seismology, Vol. 81B, Chapter 61*, Academic Press, 1013-1030.
- Kawashima, K. and Unjoh, S. (1990). An inspection method of seismic vulnerability of existing highway bridges. *Structural Eng./ Earthquake Eng.* 7, No 1, JSCE.
- Keilis-Borok, Kronrod, T.L. and Molchan, G.M. (1974). *Algorithm for Estimation of Seismic Risk. Computation Seismology*, 6, Nauka Publishing, Moscow.
- Kennett, B. L. N. and Kerry, N. S. (1979). Seismic waves in a stratified half space. *Geophys. Journal Royal Astron. Soc.*, 57, 557-583.
- Kerimidjian, A.S. and Anagnos, T. (1984). Stochastic Slip-Predictable Model for Earthquake Occurrences. *Bull. Seism. Soc. Am.*, 74 (2), 739-755.
- Kerle, N. and Oppenheimer, C. (2002). Satellite remote sensing as a tool in lahar disaster management. *Disasters*, 26(2), 140-160.
- Kham, M. (2004). *Propagation d'ondes sismiques dans les bassins sédimentaires: des effets de site à l'interaction site-ville*. Ph. D. thesis, Univ. Joseph Fourier, Grénoble, France.
- Kham, M., Semblat, J.-F., Bard, P.-Y. and Guéguen, P. (2003). Etude de l'interaction site-ville à l'aide d'un modèle de ville simplifié basé sur la méthode des éléments de frontière. *VI^{ème} Colloque National de l'AFPS, Ecole Polytechnique, 1-3 Juillet 2003, I*, 229-236.
- Khater, M., Scawthorn, C. and Johnson, J. J. (2003). Loss estimation. In earthquake engineering handbook. W.Chen and C. Scawthorn (Editors), CRC Press, Chapter 31.
- Kiimura, T., Kusakabe, O. and Takemura, J. (Editors) (1998). *Int. Conf. Centrifuge 98*. Tokyo, Balkema, 919 p.
- Kim, S. H. (1993). *A GIS Based Regional Risk Analysis Approach for Bridges Against Natural Hazards*. Ph.D. Dissertation, Civil Engineering Department, State University of New York at Buffalo.

- Kim, W. Y., Sykes, L. R., Armitage, J. H., Xie, J. K., Jacob, K. H., Richards, P. G., West, M., Waldhauser, F., Armbruster, J., Seeber, L., Du, W. X., and Lemer-Lam, A. (2001). Seismic waves generated by aircraft impacts and building collapses at World Trade Center, New York City. *EOS*, 82-47, 565 p.
- Kinoshita, S. (2003). Kyoshin Net (K-NET), Japan. In: Jennings, P., Kisslinger, C., Kanamori, H. and Lee, W. (Editors), *International Handbook of Earthquake and Engineering Seismology*, Academic Press, 1049-1056.
- Kircher, C. A., Nassar, A. A., Kustu, O. and Holmes, W.T. (1997). Development of building damage functions for earthquake loss estimation. *Earthquake Spectra*, 13, 4, 663-681.
- Kitada, Y., Kinoshita, M., Iguchi, M. and Fukuwa, N. (1999). Soil-structure interaction effect on an Npp reactor building. Activities of Nupec: achievements and the current status. In: M. Celebi and I. Okawa (Editors), *Proceedings, UJNR workshop on Soil-Structure Interaction*, September 22-23, 1998, Menlo Park, California, paper no 18.
- Kiureghian, A. (2002). Bayesian methods for seismic fragility assessment of lifeline components. In: C. Taylor and E. VanMarcke (Editors), *Acceptable Risk Processes. Lifelines and Natural Hazards*, Monograph No. 21, TCLEE/ASCE, 61-77.
- Ko, H. Y., and McLean, F. (Editors) (1991). *Int. Conf. Centrifuge 91*. Boulder, 13-14 June, Balkema. 616 p.
- Kobayashi, H., Midorikawa, S., Tanzawa, H. and Matsubara, M. (1987). Development of portable measurement system for ambient vibration test of building. *Journal of Structural and Construction Engineering* (Transactions of Architectural Institute of Japan), 378, 48-56.
- Kobayashi, H., Seo, K. and Midorikawa, S. (1986). Estimated Strong Ground Motions in México City. The México Earthquake-1985, Factors Involved and Lessons Learned. *ASCE*. 55-69.
- Kobayashi, H., Vidal, F., Feriche, D. Samano, T. and Alguacil, G. (1996). Evaluation of dynamic behaviour of building structures with microtremors for seismic microzonation Mapping. *11th World Conference on Earthquake Engineering*, Acapulco, México, June 23-28.
- Kobori, T., Miura, Y., Fukuzawa, E. Y., Yamada, T., Arita, T., Miyagawa, N., Tanaka, N. Y and Fukumoto, T. (1992). Development and application of hysteresis steel dampers. *Earthquake engineering, Tenth World Conference*; 2341-2346
- Komaru, Y., Yamada T, Segawa S and Villacis C (1995). Development of an earthquake damage estimation system. *10th European Conference on Earthquake Engineering*, Vienna, 1994.
- Kudo, K. (1991). Earthquake motions: given and blinded data. *Proceedings, International Symposium on the Effects of surface Geology on Seismic Motion, 1992*, Japan, 53-61.
- Kudo, K. (1995). *Practical Estimators of Site Response. State-of-art*. Report. 5th Int. Conf. Seis. Zonation, Nice, France, AFPS/EERI, Ouest Editions, 3, 1878-1907.
- Lachet, C. and Bard, P.Y., (1994). Numerical and theoretical investigations on the possibilities and limitations of the Nakamura's technique. *Journal Phys. Earth*, 42, 377-397.
- Lagomarsino, S. (1993). Forecast models for damping and vibration periods of buildings. *Journal of Wind Engineering and Industrial Aerodynamics*, 48,221-239.
- Lagomarsino, S. (1998). A new methodology for the post-earthquake investigation of ancient churches. *11th European Conference on Earthquake Engineering*, Paris, A.A. Balkema (CD-ROM), 67-78.
- Lagomarsino, S. (1999). Damage Survey of Ancient Churches: The Umbria-Marche Experience. In: Bernardini, A. (Editor), *Seismic Damage to Masonry Buildings*, Balkema, Rotterdam.
- Lagomarsino, S. and Podestà, S. (2004a). Seismic vulnerability of ancient churches. Part 1: damage assessment and emergency planning. *Earthquake Spectra*, 20(2), 377-394.
- Lagomarsino, S. and Podestà, S. (2004b). Seismic vulnerability of ancient churches. Part 2: statistical analysis of surveyed data and methods for risk analysis. *Earthquake Spectra*, 20(2), 395-412.
- Lagomarsino, S. and Podestà, S. (2004c). Damage and vulnerability assessment of churches after the 2002 Molise, Italy, earthquake. *Earthquake Spectra*, 20(S1), S271-S283.
- Lagomarsino, S., Podestà, S., Cifani, G. and Lemme, A. (2004a). The 31th October 2002 earthquake in Molise (Italy): a new methodology for the damage and seismic vulnerability survey of churches. *13th World Conference on Earthquake Engineering*, Vancouver, BC, Canada, paper 1366 (CD-Rom).
- Lagomarsino, S., Podestà, S., Resemini, S., Curti, E. and Parodi, S. (2004b). Mechanical models for the seismic vulnerability assessment of churches. In: Modena, C., Lourenço, P. B. and Roca, P. (Editors). *Structural Analysis of Historical Construction. Proceedings of IV Int. Seminar SAHC*, Padova, Italy, A.A. Balkema, London (UK), Vol. 2, 1091-1101.
- Lantada, N., Pujades L. G. and Barbat A. H. (2004). GIS techniques for seismic risk scenarios evaluation. application to Barcelona, Spain. *13th World Conference on Earthquake Engineering*, Vancouver, B.C., Canada , Paper 423.
- Lawrence, G. R. (1974). *Biography*. Encyclopedia of Photography. New York, Greystone Press
- Lebrun, B., Hatzfeld, D. and Bard, P.-Y. (2001). A site effect study in urban area: experimental results in Grenoble (France), *Pageoph*, 158, 2543-2557.

- Lee, H. K., Kanamori, H., Jennings, P. C. and Kisslinger, C. (editors) (2003). *International Handbook of Earthquake and Engineering Seismology*. Academic Press, Parts A and B, Elsevier, 1945 p.
- Lee, W. H. K. (1995). *A project implementation plan for an advanced earthquake monitoring system*. Research Report of the Central Weather Bureau, Taipei, Taiwan, R.O.C., No. 448, 411 p.
- Lee, W. H. K. and Espinosa-Aranda, J. M. (2003). Earthquake early warning systems: Current status and perspectives. In: Zschau, J. and Koppers, A. N. (Editors), *Early Warning Systems for Natural Disaster Reduction*, Springer, Berlin.
- Lee, W. H. K. and Espinosa-Aranda, J. M. (Conveners) (1996). Early warning and rapid response. *11th World Conference on Earthquake Engineering*, Acapulco, Mexico, 1437-1443.
- Lekkas, E.L. (1996). Pyrgos earthquake damages (based on E.M.S.-1992) in relation with geological and geotechnical conditions. *Soil Dynamics and Earthquake Eng.*, 15, 61-68.
- Lermo, J. and Chávez-García F. J. (1993). Site effect evaluation using spectral ratios with only one station. *Bull. Seism. Soc. Am.*, 83, 1574-1579.
- Lermo, J. and Chávez-García F. J. (1994). Are microtremors useful in site response evaluation?. *Bull. of Seism. Soc. of Am.*, 84, No. 5, 1350-1364.
- Leung, C F, Lee, F. H. and Ten, E. T. S. (Editors) (1994). *Int. Conf. Centrifuge 94*. Singapore, Balkema. 836 p.
- Leyendecker, E. V., Hunt, R. J., Frankel, A. D. and Rukstales, K. S. (2000). Development of maximum considered earthquake ground motion maps. *Earthquake Spectra*, Earthquake Engineering Research Institute, Oakland.
- Lillesand, T. M. and Keefe, R. W. (1994). *Remote Sensing and Image interpretation*. 3rd Edition, John Wiley and Sons, USA
- Lombaert, G., Clouteau, D., Ishizawa, O. and Mezher, N. (2004). The city-site effect: a fuzzy substructure approach and numerical simulations. *11th Int. Conf. on Soil Dynamics and Earthquake Engineering*, University of California at Berkeley, January 7-9, 2004.
- Lourenço, P. B., Borst, R. and Rots, J. G. (1997). A plane stress softening plasticity model for orthotropic materials. *Int. J. for Numerical Methods in Engineering*, 40, 4033-4057.
- Lutoff, C. (2000). *The Urban System at Nice face to earthquakes. Methodology for elements at risk and potential dysfunction analysis*. PhD thesis University of Savoie, France, 382 p.
- Maffei, J. (1995). A new method of prioritizing bridges for seismic upgrading. *Proceedings, 4th U.S Conference on Lifeline Earthquake Engineering, San Francisco California*, TCLEE/ASCE, Monograph No.6, edited by M.J O'Rourke, 501- 508.
- Mahaney, J. A., Paret, T. F., Kehoe, B. E., and Freeman, S. A. (1993). The capacity spectrum method for evaluating structural response during the Loma Prieta earthquake. *Proceedings, National Earthquake Conference*. Memphis Tennessee.
- Malheiro, A.M., Fraga, C.A. and Oliveira, C.S. (1999). Escorregamentos e Danos nas Vias de Comunicação Causados pelo Sismo de 9 de Julho de 1998 no Faial-Pico e São Jorge. *4th National Conference on Seismology and Earthquake Engineering*, Universidade do Algarve, Faro.
- Mallard, D.J., (1999). Learning to Cope with Faults. *International Conference on Hazard Determination in Areas with Moderate Seismicity*.
- Mander, J. and Basoz, N. (1999). Seismic fragility curve theory for highway bridges. In: M. Elliot and P. McDonough (Editors), *Proceedings, 5th US Conference on Lifeline Earthquake Engineering*, TCLEE/ASCE, Monograph No.16, 31-40.
- Manos, G. C., Demosthenous, M., Triamataki, M., Yasin, B. and Skalkos, P. (1995). Construction and instrumentation of a 5 storey masonry infilled RC building at the Volvi-Thessaloniki Euro-Seistest site. Correlation of measured and numerically predicted dynamic properties. *Proceedings of the Third International Conference on Earthquake Engineering*, Amman, 2, 857-866.
- Marcuson, W.F.III. (1978). Definition of terms related to liquefaction. *Journal of Geotechnical Engineering, ASCE*, 104 (9), 1197-1200.
- Martín Martín, A. J. (1984). *Riesgo Sísmico en la Península Ibérica*. Ph.D. Thesis, Universidad Politécnica, Madrid.
- Martín Martín, A. J. (1989). Problemas Relacionados con la Evaluación de la Peligrosidad en España. In: A. Udias and D. Muñoz (editors), *Movimientos Fuertes del Suelo y Riesgo de Terremotos, Física de la Tierra*, 1, 267-286, Ed. Universidad Complutense de Madrid, Madrid.
- Martín, A. J., Carreño, E. and Izquierdo, A., (1996). Análisis de la atenuación de aceleraciones de la serie de sismos de Adra de 1993 y 1994. *Avances en Geofísica y Geodesia*, 1., IGN, Madrid.
- Martin, C., Combes Ph., Secanell, R., Lignon, G., Firavanti, A., Carbon, D., Monge, O. and Grellet, B. (2002). *Revision du zonage sismique de la France. Etude probabiliste*. Rapport final GEOTER GTR/MATE/0701-150.

- Martin, G. R., Finn, W. D. L. and Seed, H. B. (1975). Fundamentals of liquefaction under cyclic loading, *Journal of Geotechnical Engineering, ASCE, 101 GT5*, 423-438.
- Masiani, R. (1999). SEAT (Expert System on Earthquake Usability). Course on: *The Damage Survey and Post-Earthquake Usability Evaluation*. National Seismic Survey, University of Rome and Catania Municipality, Catania, 16 November 1999.
- Massonnet, D., Feigl, K. L., Vadon, H. and Rossi, M. (1996). Coseismic deformation field of the M = 6.7 Northridge, California earthquake of January 17, 1994 recorded by two radar satellites using interferometry. *Geophys. Res. Lett.*, 23, 969-972.
- Massonnet, D., Rossi, M., Carmona, C., Adragna, F., Peltzer, G., Feigl, K. and T. Rabaute (1993). The displacement field of the Landers earthquake mapped by radar interferometry. *Nature*, 364, 138-142.
- Masure, Ph. (1996). *Preventive planning, condition for the sustainable development of cities*. Methodological bases of the GEMITIS programs, DHA News, N° 18.
- Masure, Ph. (1999). Urban networks for risk reduction : solidarity, exchanges and new forms of cooperation. *International Conference on Natural disasters reduction, territorial management and sustainable development*, Paris.
- Masure, Ph. (2000). *L'expert, le politique et l'opinion publique face aux risques naturels*. 5e Colloque transfrontalier CLUSE Risques majeurs: perception, globalisation et management. Université de Genève, Suisse
- Masure, Ph, and Lutoff, C. (2003). *Methodology on urban system exposure (USE) assessment to natural disasters*. BRGM Report, RISK UE project, Orléans, 82 p.
- Matsuda, E.N, Savage, W. U. Williams, K.K. Laguens, G.C. (1991). Earthquake evaluation of a substation network. *Proceedings, 3rd US Conference on Lifeline Earthquake Engineering*, Los Angeles, California, TCLEE/ASCE, Monograph No. 4, edited by M. A. Cassaro, 295-317.
- Matsuoka, M. and Yamazaki, F. (1998). Identification of damaged areas due to the 1995 Hyogoken-Nanbu earthquake using satellite optical images. *Proceedings, 19th Asian Conference on Remote Sensing*, Manila.
- Matsuoka, M. and Yamazaki, F. (2000). Interferometric characterization of areas damaged by the 1995 Kobe earthquake using satellite SAR images. *12th World Conference on Earthquake Engineering*, Auckland
- Matsuoka, M. and Yamazaki, F. (2002). Application of the damage detection method using SAR intensity images to recent earthquakes. *Proceedings of the IGARSS, Toronto*.
- Mayer-Rosa, D. and Jiménez, M.-J. (2000). *Seismic Zoning. State-of-the-art and Recommendations for Switzerland*. Swiss National Hydrological and Geological Survey, Geological Report No. 26, Bern.
- McGuire, R. K. (1976). *EQRISK, Evaluation of Earthquake Risk to Site*. Open File Report 76-67. United States Department of the Interior Geological Survey, USA.
- McGuire, R. K. (1993). *The Practice of Earthquake Hazard Assessment*. IDNDR Monograph, International Association of Seismology and Physics of the Earth Interior/European Seismological Commission, University of Colorado Department of Physics, Boulder, CO.
- McGuire, R. K. (1995). Probabilistic Seismic Hazard Analysis and Design Earthquakes: Closing the Loop. *Bull. Seism. Soc. Am.*, 85, 1275-1284.
- McGuire, R. K. (2004). *Seismic Hazard and Risk Analysis*. EERI, MNO-10, 221 p.
- Medvedev, J. (1962). *Engineering Seismology*. Academia Nauk Press, Moscow, 260 p.
- Medvedev, S. V. (1977). *Seismic Intensity Scale MSK 76*, Geophys. Pol. Acad. Sc. Inst. Publ., A-6 8117, Warsaw, 95-102.
- Méli, R., Faccioli, E., Muria-Vila, D., Quaas, R. and Paolucci, R. (1998). A study of site effects and seismic response of instrumented buildings in Mexico City. *Journal of Earthq. Engng.*, 2, 89-111.
- Merz, H. A. and Cornell, C. A. (1973). Seismic risk based on a quadratic magnitude-frequency law. *Bull. Seism. Soc. Am.*, 69, 1209-1214.
- Messele H. and Tadese K. (2002). The study of seismic behaviour buildings located on different site in Addis Ababa (Ethiopia) by using microtremors and analytical procedure. *Joint Study on microtremors and seismic microzonation in earthquake countries. Workshop to Exchange Research Information*, Hakone-Gora, Kanagawa, Japan.
- Mezher, N. (2004). *Modélisation numérique et quantification de l'effet sismique site-ville*. Ph.D. thesis, Ecole Centrale de Paris.
- Mezher, N. and Clouteau, D. (2003). Etude numérique de l'effet site-ville par homogénéisation périodique - Cas de la ville de Nice. *Actes du 6e Colloque National de Génie Parasismique, AFPS 2003, Palaiseau, 1-3 July 2003, I*, 237-244.

- Michel, R. and Avouac, J. P. (2001). Imaging Earthquake from Offsets Measured on Optical or Radar Images. Advances in Modelling of Deformation due to Earthquakes II. *AGU Fall meeting, San Francisco, USA*.
- Michel, R. and Avouac, J. P. (2002). Deformation due to the 17 August Izmit, Turkey, earthquake measured from SPOT images. *J. Geophys. Res.*, 107.
- Michetti, A. M., Brunamonte, F., Serva, L. and Vittori, E. (1996). Trench investigations along the 1915 Fucino earthquake fault scarps (Abruzzo, Central Italy): geological evidence of large historical events. *Journal of Geophysical Research*, 101, No. B3, 5921–5936.
- Michetti, A. M., Ferrelì, L., Esposito, E., Porfido, S., Blumetti, A. M., Vittori, E., Serva, L. and Roberts, G. P. (2000). Ground effects during the September 9, 1998, MW=5.6, Lauria earthquake and the seismic potential of the "aseismic" Pollino region in southern Italy. *Seism. Res. Letters*, January-February, 2000.
- Michetti, A. M., Ferrelì, L., Serva, L. and Vittori, E. (1997). Geological evidence for strong historical earthquakes in an 'aseismic' region: the Pollino case (Southern Italy). *Journal of Geodynamics* 24, No. 1-4, 67–86.
- Midorikawa, S. (1990). Ambient vibration tests of buildings in Santiago and Viña del Mar. *A Report on the Chile-Japan Joint Study Project on Seismic Design of Structures*. The Japan International Co-operation Agency.
- Midorikawa, S. (2004). Dense strong-motion array in Yokohama, Japan, and its use for disaster management, *International Workshop on Future Directions in Instrumentation for Strong Motion and Engineering Seismology*- NATO Meeting, May 17-21, Kusadasi, Turkey.
- Milutinovic, Z. V. and Trendafiloski, G. S. (2003). *Vulnerability of current buildings*. RISK-UE project, "An advanced approach to earthquake risk scenarios with applications to different European towns", Contract: EVK4-CT-2000-00014.
- Miyakoshi, J., Hayashi, Y., Tamura, K. and Fukuwa, N. (1997). Damage ratio functions of buildings using damage data of the 1995 Hyogoken-Nanbu earthquake. *ICOSSAR 1997*.
- Moczo, P. (1989). Finite-difference technique for SH-waves in 2D media using irregular grids-application to the seismic response problem. *Geophys. J. Int.*, 99, 321-329.
- Moczo, P., Kristek, J. and Ladislav, H. (2000). 3D Four-Order Staggered-Grid Finite-Difference Schemes: Stability and Grid Dispersion. *Bull. Seism. Soc. Am.*, 90 (3), 587-603.
- Mohammadioun, B., and Serva, L. (2001). Stress drop, slip type, earthquake magnitude-and seismic hazard. *Bull. Seism. Soc. Am.*, 91, 694–707.
- Molchan, G., T. Kronrod, and Panza, G. F. (1997). Multi-scale seismicity for seismic risk, *Bull. Seism. Soc. Am.*, 87, 5, 1220–1229.
- Monge, O., Alexoudi, M. and Argyroudis, S. (2003). *An advanced approach to earthquake risk scenarios with applications to different European towns. Vulnerability assessment of lifelines and essential facilities (WP06): basic methodological handbook*. Report n°GTR-RSK 0101-152av7, 71 p.
- Montesinos, F. G.; Camacho, A. G.; Nunes, J. C.; Oliveira, C. S. and Vieira, R. (2003). A 3-D gravity model for a volcanic crater in Terceira Island (Azores). *Geophysical Journal International*, 154, 393-406.
- Monti, G. and Nuti, C. (1996). A procedure for assessing the functional reliability of Hospital Systems. *Structural Safety*, 18, No. 4, 277-292.
- Monti, G., Nuti, C. and Santini, S. (1996). Seismic assessment of hospital systems. *Proceeding of the 11th Word Conference on Engineering Earthquake*, Paper No. 974, Acapulco, México.
- Montilla, J. A. P., Casado, C. L. and Romero J. H. (2002). Deaggregation in magnitude, distance, and azimuth in the South and West of the Iberian Peninsula. *Bull. Seism. Soc. Am.*, 92, 6.
- Moore, J., Chang, S., Gordon, P., Richardson, H., Shinozuka, M., Cho, S. and Dong, X. (1999). Integrating transportation and economic models. In: M. Elliot and P. McDonough (Editors), *Proceedings, 5th US Conference on Lifeline Earthquake Engineering*, TCEE/ASCE, Monograph No.16, 621-633.
- Moreira, D., Neves, N., Arêde, A. and Costa, A. (2001). Análise Sísmica da Igreja da Madalena na Ilha do Pico. *Actas do Sismica 2001, 5th Meeting On Seismology and Seismic Engineering*, 627–638, 27-29 October, Azores.
- Morra, A., Odetto, L., Bozza, C. and Bozzetto, P. (2002). *Disaster Management: Rescue and Medical Organization in Case of Disaster*. Civil Protection Department of Piemonte Region, Italy.
- Mouroux, P., Bertrand, E., Bour, M., Le Brun, B., Depinois, S. and Masure, P. (2004). The European RISK-UE project: an advanced approach to earthquake risk scenarios. *13th World Conference on Earthquake Engineering*, Vancouver, BC, Canada, paper 3329 (CD-Rom).
- MSK-81 (1981). Report on the ad-hoc panel meeting of experts on up-dating of the MSK-64 seismic intensity scale, Jena, 1981, Gerlands Beitr.Geophys., Leipzig.

- Mucciarelli, M, Monachesi, G. and Gallipoli, M. R. (2004). In-situ measurements of site effects and building dynamic behaviour related to damage observed during the 9/9/1998 earthquake in southern Italy. *Proceedings, ERES99 Conference*, Catania, Italy, 253-265.
- Mucciarelli, M., (1998). Reliability and applicability of Nakamura's technique using microtremors: an experimental approach. *Journal of Earthquake Engineering*, 2 (4), 625-638.
- Mucciarelli, M., Peruzza, L. and Caroli, P. (2000). Tuning of Seismic Hazard Estimates by Means of Observed Site Intensities. *Journal of Earthquake Engineering*, 2, 141-159.
- Muhlbauer, W. K. (Editor) (1996). *Pipeline risk management manual. a tested and proven system to prevent loss and assess risk*. Gulf Publishing Company, Houston, Texas.
- Mulas de la Pena, J. (2002). Microzonación de la respuesta sísmica del terreno por factores locales. In: Ayala and Olcina (Editors), *Riesgos Naturales*, Ariel Ciencia, Barcelona, 345-362.
- Munich Re. (1995-2004). *Topics Series*. Munich Re Group, Munchen, Germany.
- Murià Vila, D. and González Alcorta, R. (1995). Propiedades dinámicas de edificios de la Ciudad de México. *Revista de Ingeniería Sísmica*, 51, 25-45.
- Murphy, J.R. and Hewlett, R.A. (1975). Analysis of seismic response in the City of Las Vegas, Nevada: A preliminary microzonation, *Bull. Seism. Soc. Am.*, 65, 1557-1597.
- Naeim, F. (1997). *Performance of Extensively Instrumented Buildings during the January 17, 1994 Northridge Earthquake – An Interactive Information System*, California Division of Mines and Geology, JAMA Report no. 97-7530.68, John A. Martin and Associates, Inc. (www.johnmartin.com/research, consulted May 2004).
- Naeim, F. and Kelly, J. M. (1999). *Design of seismic isolated structures, From Theory to Practice*. John Wiley and Sons; New York.
- Nájera, A. (1999). *La catástrofes naturales y su cobertura aseguradora. Un estudio comparativo*. Consorcio de Compensación de Seguros, Madrid, 263 p.
- Nakamura, Y. (1988). On the urgent earthquake detection and alarm system (UrEDAS). *9th World Conference on Earthquake Engineering*, Tokyo-Kyoto, Japan.
- Nakamura, Y. (1989a). Earthquake alarm system for Japan Railways. *Japanese Railway Engineering*, 28, 4, 3-7.
- Nakamura, Y. (1989b). A method for dynamic characteristics estimation of subsurface using microtremor on the ground surface. *Quarterly Report of Railway Technical Research Institute (RTRI)*, 30.1.
- Nakamura, Y. (2000). Clear identification of fundamental idea of Nakamura's technique and its applications. *Proceedings, 12th World Conference on Earthquake Engineering*, CD-Rom, 2656.
- National Seismic Survey and GNDT (1998). *Handbook for the COM Management*, Civil Protection Department, Rome.
- National Seismic Survey (2002). S.E.T. Software to Manage the Inspections and the Data Collection in Post-earthquake Emergency. CD-ROM, Rome.
- Navarro, M. and Oliveira, C.S. (2004). Evaluation of dynamic characteristics of reinforced concrete buildings in the City of Lisbon. *4th Assembly of the Portuguese-Spanish of Geodesy and Geophysics*, Figueira da Foz, Portugal.
- Navarro, M., Sánchez, F.J., Enomoto, T., Vidal, F. and Rubio, S. (2000). Relation between the predominant period of soil and the damage distribution after Mula 1999 earthquake. *Proceedings, Sixth International Conference on Seismic Zonation (6ICSC)*, November 12-15, 2000, Palm Spring, California, USA.
- Navarro, M., Sánchez, F.J., Feriche, M., Vidal, F., Enomoto, T., Iwatate, T., Matsuda, I. and Maeda, T. (2002). Statistical estimation for dynamic characteristics of existing buildings in Granada, Spain, using microtremors. *Structural Dynamics, Eurodyn2002*, 1, 807-812, Balkema.
- Navarro, M., Vidal, F., Feriche, M., Enomoto, T., Sanchez, F.J. and I. Matsuda (2004). Expected Ground-RC Building structures resonant phenomena in Granada city (southern Spain). *13th World Conference on Earthquake Engineering*, Vancouver, Canada, Paper No. 3308.
- NEHRP (2000). *Recommended Provisions for Seismic Regulations for New Buildings and Other Structures, Part 1: Provisions*, FEMA 368, Building Seismic Safety Council of the National Institute of Building Sciences, USA.
- Neves, N., Costa, A. and Arêde, A. (2004). Identificação dinâmica e análise do comportamento sísmico de um quarteirão localizado na cidade da Horta-Ilha do Faial. *Actas do Sismica 2004, 6th Meeting on Seismology and Seismic Engineering*, 14-16 April, Guimarães.
- Neves, N., Moreira, D., Arêde, A. and Costa, A. (2001). Análise Sísmica da Igreja das Bandeiras na Ilha do Pico. *Actas do Sismica 2001, 5th Meeting On Seismology and Seismic Engineering*, 677-690, 27-29 October, Azores.

- NIBS, National Institute of Building Science. (1997, 1999 and 2002). *Earthquake loss estimation methodology. HAZUS*. Technical manuals. Federal Emergency Management Agency (FEMA), Washington, Vol. 1, 2, 3. (<http://www.fema.gov/hazus/>)
- NIBS, National Institute of Building Science. (1999). Direct physical damage to lifelines-transportation systems-utility systems. In: *Earthquake loss estimation methodology. HAZUS*. Technical manuals. Federal Emergency Management Agency (FEMA), Washington, Vol. 2.
- NIST (1996). The January 17, 1995 Hyogoken-Nanbu (Kobe) Earthquake. In: R. M Chung (Editor), *National Institute of Standards and Technology*, Bethesda, MD.
- NIST (1997). *Reliability and Restoration of Water Supply Systems for Fire Suppression and Drinking Following Earthquakes*. by D.B Ballantyne., C.B Crouse. GCR-97-730
- Nocevski, N. and Petrovski, J. T. (1994). Analytical vulnerability functions of earthquake resistant and non-resistant buildings. *10th European Conference on Earthquake Engineering 2*, Vienna, 1099-1103.
- Nogoshi, M. and Igarashi, T. (1970). On the propagation characteristics of microtremors. *J. Seism. Soc. Japan*, 23, 264-280 (in Japanese with English abstract).
- Nogoshi, M. and Igarashi, T. (1971). On the amplitude characteristics of microtremors. *J. Seism. Soc. Japan*, 24, 24-40 (in Japanese with English abstract).
- Nojima, N. and Kameda, H. (1991). Cross impact analysis for lifeline interactions. In: M. A. Cassaro (Editor), *Proceedings, 3rd US Conference on Lifeline Earthquake Engineering*, Los Angeles, California, TCLEE/ASCE, Monograph No. 4, 629- 638.
- NRC, Nuclear Regulatory Commission of U.S. (1973). *Title 10 of Code Federal Regulations, Part 100, Reactor Site Criteria. Subpart A - Evaluation Factors for Stationary Power Reactor Site Applications Before January 10, 1997 and for testing Reactors, and Appendix A - Seismic and Geologic Siting Criteria for Nuclear Power Plants*.
- NRC, Nuclear Regulatory Commission of U.S. (1977). *Title 10 of Code Federal Regulations, Part 100, Reactor Site Criteria. Appendix A - Seismic and Geologic Siting Criteria for Nuclear Power Plants, Amendment of Section V(a)(1)(iv)*.
- NRC, Nuclear Regulatory Commission of U.S. (1997a). *Regulatory Guide 1.165. Identification and Characterization of Seismic Sources and Determination of Safe Shutdown Earthquake Ground Motion*.
- NRC, Nuclear Regulatory Commission of U.S. (1997b). *Title 10 of Code Federal Regulations, Part 100, Reactor Site Criteria. Subpart B - Evaluation Factors for Stationary Power Reactor Site Applications on or After January 10, 1997*.
- NRC, Nuclear Regulatory Commission of U.S. (1997c). *Title 10 of Code Federal Regulations, Part 50, Domestic Licensing of Production and Utilization Facilities. §50.54(ff) - Conditions of Licenses, and Appendix S - Earthquake Engineering Criteria for Nuclear Power Plants*.
- Nuti C. and Monti, G. (1994). Evaluation of Vulnerability and Retrofitting Strategies for a Hospital Building. *Workshop on Collaborative European Research Activities Supported by the EC for Seismic Risk Prevention and Reduction*, Bergamo.
- Nuti, C. and Vanzi, I. (1998). Assessment of post-earthquake availability of hospital system and upgrading strategies. *Earthquake Engineering and Structural Dynamics. No. 27*, 1403-1423.
- Nuti, C. and Vanzi, I. (1999). *GHOST: A procedure and a program for the post-earthquake scenario and probabilistic analysis of a regional hospital's network performance*. Repporti No. 1/99, Universita' degli Studi Gabriele D'Annunzio de Chieti, Chieti, Italy.
- O'Rourke, M. J. (2003). Buried Pipelines. In *Earthquake Engineering Handbook*, W.Chen and C. Scawthorn (Editors), CRC Press, Chapter 23.
- O'Rourke, M. J and Ayala G. (1993). Pipeline damage due to wave propagation. *Journal of Geotechnical Engineering, ASCE, 119*, No.9.
- O'Rourke, T. D. (1989). *Compute assisted system engineering for water supply. Workshop on Serviceability Analysis of Water Delivery Systems*. Technical Report NCEER-89-0023, State University of New York, Buffalo.
- O'Rourke, T. D., Erdogan, F. H., Savage, W. U., Lund, L. V. and Manager, A. T. (2000). Water, gas, electric power, and telecommunications performance. *Earthquake Spectra*, Suppl. A to Vol.16, 1999 Kocaeli, Turkey, Earthq. Reconnaissance Rep., 377-402.
- Odeh, D. J, Khater M, Scawthorn Ch. R, Blackburn F. T.and Kubick K.S (1995). Reliability analysis of a dual use fire protection/ reclaimed water system, San Francisco, CA. In: M. J O'Rourke (Editor). *Proceedings, 4th U.S Conference on Lifeline Earthquake Engineering*, TCLEE/ASCE, Monograph No.6, San Francisco, California, 264-271.
- OES (1978). *Damage Assessment Plan for Volunteer Engineers*, State of California, Office of Emergency Services, Sacramento.

- Okumura, T., and Shinozuka, M. (1991). Serviceability analysis of Memphis water delivery system. In: M. A. Cassaro (Editor), *Proceedings, 3rd US Conference on Lifeline Earthquake Engineering*, TCLEE/ASCE, Monograph No.4, Los Angeles, California, 530-541.
- Okuyama, Y., Hewings, G. Kim, T., Boyce, D., Ham, H. and Sohn, J. (1999). Economic impacts of an earthquake in the New Madrid seismic zones: a multiregional analysis. In: W. Elliott and P. McDonough (Editors), *Proceedings, 6th US Conference on Lifeline Earthquake Engineering*, TCLEE/ASCE, Monograph No.16, 592-601.
- Oliveira, C. S. (1974). *Seismic Risk Analysis*. Report EERC 74-1, University of California, Berkeley.
- Oliveira, C. S. (1987). Probabilistic Models for Assessment of Strong Ground Motion. In: M. O. Erdik and M. N. Toksok (editors), *Strong Ground Motion Seismology*, NATO ASI Series, Serie C: Mathematical and Physical Sciences, vol. 204, 405-460.
- Oliveira, C. S. (2003). The influence of scale on microzonation and impact studies. In: A. Ansal (Editor), *Recent Advances in Earthquake Geotechnical Engineering and Microzonation*, Chapter 2, 27-65, Kluwer Academic Publishers, Dordrecht.
- Oliveira, C. S. (2004). Atualização das bases-de-dados sobre frequências próprias de estruturas a partir de medições expeditas *in-situ*. *Proceedings Sismica 2004, 5th Congresso Nacional de Sismologia e Engenharia Sismica*, Universidade do Minho, Guimarães.
- Oliveira C. S. and Guedes, J. H. C. (1996). *Contribuição para o Estudo do Comportamento Sísmico da Rede Hospitalar*. Final Draft, HOPE Project, Laboratório Nacional de Engenharia Civil, Lisbon.
- Oliveira, C. S.; Sousa, M. L.; Guedes, J. H. C., Martins, A. and Campos-Costa, A. (1998). A crise sísmica do Faial/Pico/São Jorge iniciada a 9 de Julho de 1998 Vista na Rede Acelerográfica dos Açores. *1st Symposium on Meteorology and Geophysics by APMG*, Lagos, 75-79.
- Olivera, C., Redondo, E., Lambert, J., Riera, A. and Roca, A. (2005). *Els terratrèmols dels segles XIV i XV a Catalunya*. Institut Cartogràfic de Catalunya (in press).
- OPS (1992). *Guía para la mitigación de riesgos naturales en las instalaciones de la salud de los países de América latina*, Washington, D.C.
- Ordaz, M. (1991). *CRISIS. Brief description of program CRISIS*. Institute of Solid Earth Physics, University of Bergen, Norway, Internal Report, 16 p.
- Ordoñez, D., Foti, D. and Bozzo, L. (2003). Comparative study of the inelastic response of base isolated building. *Earthquake Engineering and Structural Dynamics*, 32, 315-342.
- Orsini, G. (1999). A Model for Buildings Vulnerability Assessment using the Parameterless Scale of Seismic Intensity (PSI). *Earthquake Spectra*, 15, No.3, 463-483.
- Oyo Corporation (1988). Special Publication for Seismic Microzoning Techniques: A Case Study for Kawasaki City, Japan.
- Ozbeý, C. (2001). *Empirical peak horizontal acceleration attenuation relationship for Northwestern Turkey*. M.Sc. Thesis, KOERI, Bogazici University.
- Özel, O., Cranswick, E., Meremonte, M., Erdik, M. and Safak, E. (2002). Site effects in Avcilar, West of Istanbul, Turkey, from strong-and weak-motion data. *Bull. Seism. Soc. Am.*, 92(1), 499-508.
- Panoussis, G. (1974). *Seismic Reliability of Lifeline Networks*. Report no. R74-57, MIT, Massachusetts Institute of Technology.
- Panza, G. F. (1993). Synthetic seismograms for multimode summation – theory and computational aspects. *Acta Geod. Geoph. Mont. Hynq*, 28, 197-247.
- Panza, G. F., Romanelli, F. and Vaccari, F. (2001). Seismic wave propagation in laterally heterogeneous anelastic media: theory and application to the seismic zonation. *Advances in Geophysics* 43, 1-95, Academic Press.
- Paolucci, R. (1993). Soil-structure interaction effects on an instrumented building in Mexico City. *European Earthquake Engineering*, 3, 33-44.
- Paolucci, R. (1999). Fundamental vibration frequencies of 2D geological structures. *Proceedings, 2nd International Conference on Geotechnical Engineering*, Lisbon, 21-25 June 1999. Ed. Sêco Pinto, P., Balkema, Rotterdam, 255-260.
- Paolucci, R., Colli, P. and Giacinto, G. (2000). Assessment of seismic site effects in 2-D alluvial valleys using neural networks. *Earthquake Spectra*, 16 (3), 661-680.
- Papaoannou, Ch. A., Theodulis, N. P., Demosthenus, M., Klimis, N. and Dimitriou, P. (1997). The Konitsa (NW Greece) Earthquake of August 5, 1996: Strong Motion Data and Structural Response. *Abstracts of the 29th General Assembly of the International Association of Seismology and Physics of the Earth's Interior. Thessaloniki, Greece*.
- PARI (2003). Annual report on strong-motion earthquake records in Japanese ports (2002). *Independent Administrative Institution Part and Airport Research Institute*. Cd-ROM

- Pascalis, A., Raptakis, D., Roumelioti, Z. and Pitilakis, K. (2004). Determination of S-wave velocity structure using microtremors and spac method applied in Tessaaloniki (Greece). *Soil Dynamics and Earthquake Engineering*, 24, 49-67.
- Paula, A. O. and Oliveira, C. S. (1996). Evaluation of 1947-1993 Macroseismic Information in Portugal Using the EMS-92 Scale. *Annali di Geofisica*, 39, no.5, 989-1003.
- Pedersen, H., Le Brun, B., Hatzfeld, D., Campillo, M. and Bard, P.-Y. (1994). Ground motion amplitude across ridges. *Bull. Seism. Soc. Am.*, 84, 1786-1800.
- Pergalani, F., Romeo, R., Luzi, L., Petrini, V., Pugliese, A. and Sano, T. (1999). Seismic micozonation of the area struck by Umbria-Marche (Central Italy) MS 5.9 earthquake of 26 September 1997. *Soil Dynamics and Earthquake Engineering*, 18, 279-296.
- Phillips, R., Guo, P. J. and Popescu, R. (Editors) (2002). *Physical modelling in Geotechnics. ICPMG'02*. Balkema, 1025 p.
- Phillips, S. H, and Jvirostek, K. (1990). Natural gas disaster planning and recovery: The Loma Prieta Earthquake. Pacific Gas and Electric Company, San Francisco, California.
- Phillips, S.W. and Aki, K. (1986). Site amplification of coda waves from local earthquakes in Central California. *Bull. Seism. Soc. Am.*, 76, 627-648
- Pinho, R. (2000). *Selective Retrofitting of RC Structures in Seismic Areas*. PhD Thesis, Faculty of Engineering of the University of London, Imperial College.
- Pinto, P. E., Giannini, R. and Franchin P. (2004). *Seismic reliability analysis of structures*. Istituto Universitario di Studi Superiori di Pavia, IUSS Press.
- Pitilakis, K. D. and Anastasiadis, A. J., (1998). Soil and site characterization for seismic response analysis. *11th European Conference on Earthquake Engineering*, Paris, Balkema, 65-90.
- Pitilakis, K. D., (2004). Site Effects. Chapter 5. In: A. Ansal, (Editor), *Recent Advances in Earthquake Geotechnical Engineering and Microzonation*, Kluwer Academic Publishers, 139-197.
- Pomonis, A., Coburn, A. W. and Spence, R. J. S. (1992). *Strong Ground Motion and Damage to Masonry Buildings, As Revealed by Damage Surveys near Recording Instruments*. The Martin Centre For Architectural And Urban Studies, Internal Report, April 1992.
- Porter, K. (2003). Seismic Vulnerability. In *Earthquake Engineering Handbook*. W. Chen and C. Scawthorn (Editors), CRC Press, Chapter 21.
- Prevost, J. H. (1993). Non-linear dynamic response analysis of soil and soil-structure interacting systems. In Sêco Pinto, P. (Editors.), *Soil Dynamics and Geotechnical Earthquake Engineering*, Balkema, Rotterdam, 49-126.
- Priolo, E., Michelini, A. and Hutchings, L. (Editors) (2001). Site response estimation from observed ground motion data. *Special issue, Bolletino di Geofisica Teorica ed Applicata*, 42, 163-359.
- RADIUS (1999). **R**isk Assessment Tools for **D**iagnosis of Urban Areas Against Seismic Disasters. Involved cities: Tijuana-Mexico, Guyaquil-Ecuador, Antofagasta-Chile, Skopje-FYROM, Izmir-Turkey, Addis Ababa-Ethiopia, Tachkent-Ouzbekistan, Bandung-Indonesia, Zigong-China. Report United Nations Initiative towards Earthquake Safe Cities, 1999, <http://www.geohaz.org/radius/>, (consulted November 2004).
- Rassem, M, Heidebrecht, A.C. and Ghobarah, A. (1995). A simple engineering model for the seismic site response of alluvial valleys. *Soil Dynamics and Earthquake Engineering*, 14, 199-210.
- Rathje, E. (2000). Strong ground motions and site effects. In Youd, T.L., Bardet, JP and Bray, J.D. (Editors.), *1999 Kocaeli, Turkey, Earthquake Reconnaissance Report, Earthquake Spectra Supplement A to Volume 16*, 65-96.
- Rayleigh, Lord (J. W. Strutt). (1896). *The Theory of Sound*, 2, 2nd edition, section 272, Macmillan, London.
- REBAP (1983). Regulamento de Estruturas de Betão Armado e Pré-Esforçado. Imprensa Nacional, Casa da Moeda, Lisbon.
- Reinoso, E. and Ordaz, M. (1999). Spectral ratios for Mexico city from Free Field Recordings. *Earthquake Spectra*, 15(2), 273-295.
- Reinoso, E., Susagna, T. and Goula, X., (2003). *Contribución a la zonación sísmica de Cataluña, según criterios de emergencia sísmica*. Report nº 182/03. Institut Cartogràfic de Catalunya, 79 p.
- Reinoso, E., Wrobel, L.C. and Power, H. (1997). Three-dimensional scattering of seismic waves from topographical structures. *Soil Dynamics and Earthquake Engineering*, 16, 41-61.
- Reiter, L. (1990). *Earthquake hazard analysis*. New York, N.Y., Columbia University Press.
- Restrepo-Vélez, L. F. and Magenes, G. (2004). Experimental testing in support of a mechanics-based procedure for the seismic risk evaluation of unreinforced masonry buildings. In: Modena, C., Lourenço, P. B. and Roca, P. (Editors). *Structural Analysis of Historical Construction. Proceedings of IV Int. Seminar SAHC*, Padova, Italy, A.A. Balkema, London (UK), Vol. 2, 1079-1089.
- Ribeiro, A. (1997). Sismo Característico. *Proceedings, 3th National Conference on Seismology and*

- Earthquake Engineering*, 9-10, Instituto Superior Técnico, Lisbon, Portugal.
- Richter, C. (1958). *Elementary seismology*, W. H. Freeman, San Francisco, CA, 768 p.
- Richter, C. (1935). An instrumental earthquake magnitude scale. *Bull. Seism. Soc. Am.*, 25, 1-32.
- Risk Engineering, Inc. (1997) *EZ-Frisk™ Version 4.0, Users Manual*, Boulder, Colorado, 92 p.
- RMS (1995a). What if a major earthquake strikes the Los Angeles Area?, Risk Management Solutions, www.rms.com (consulted November 2004).
- RMS (1995b). What if the 1923 Earthquake Strikes Again? Risk Management Solutions, www.rms.com (consulted November 2004).
- RMS (1999). The Chi-chi Taiwan earthquake. Event Report, Risk Management Solutions, www.rms.com (consulted November 2004).
- RMS (1999). The Kocaeli, Turkey Earthquake, Event Report Risk Management Solutions, www.rms.com (consulted November 2004).
- RMS (2004). Catastrophe, Injury and Insurance, Risk Management Solutions, www.rms.com (consulted November 2004).
- Roca, A. and Oliveira, C.S. (Editors) (2002). *Earthquake Microzoning. Pageoph Topical*, 158, Birkhäuser, Berlin.
- Roca, A., Goula, X. and Susagna, T. (1999). Zonación sísmica a diferentes escalas. microzonación. *Física de la Tierra*, 11, 203-236.
- Rocha, P., Delgado, P., Costa, A. and Delgado, R. (2004). Seismic Retrofit of RC Frames. *Computer and Structures*, 82, Issues 17-19, 1523-1534.
- Rodgers, J. and Mahin, S.A. (1999). *Earthquake Resistant Design Interactive Homepage*. Pacific Earthquake Engineering Research Center, University of California, Berkeley, <http://peer.berkeley.edu/~jrodgers/index.htm?c227top.htm&227cont.htm&DesPhil/desphil5.htm>
- Rodrigues, M.C.M. (1999). *Modelação de um Sistema de Alarme Sísmico para a Península Ibérica*. PhD Thesis, Universidade Nova de Lisbon, Caparica, Portugal.
- Romão, X., (2002). *Novos modelos de dimensionamento sísmico de estruturas*. MSc Thesis on Civil Engineering Structures, Fac. Eng. Univ. Porto, Portugal.
- Romão, X., Costa, A. and Delgado, R.. (2002). Non Linear Analysis Based Seismic Design. *12th European Conference on Earthquake Engineering*, London.
- Rose, A. (2002). Model Validation in Estimating Higher-Order Economic Losses from Natural Hazards. In: C. Taylor and E. VanMarcke (Editors), *Acceptable Risk Processes. Lifelines and Natural Hazards*, Monograph No. 21, TCLEE/ASCE, 105-131.
- Rose, A. and Liao, S.Y. (2004). Modeling regional economic resilience to disasters: a computable general equilibrium analysis of water service disruptions. *13th Annual Conference of The European Association of Environmental and Resource Economists (EAERE)*, Budapest, Hungary (accepted).
- Ross T. J. (1995). *Fuzzy Logic with Engineering Applications*. McGraw Hill, New York.
- RSA (1983). *Regulamento de Segurança e Acções para Estruturas de Edifícios e Pontes*. Imprensa Nacional, Casa da Moeda, Lisbon.
- RSA (1985). *Regulamento da Segurança e Acções em Estruturas de Edifícios e Pontes*, Imprensa Nacional, Casa da Moeda, Lisbon.
- RSE (2003). *Manual d'utilització del programa de càlcul i representació d'escenaris de danys*, Internal Report, Institut Cartogràfic de Catalunya, Barcelona, 56 p.
- Rutenberg, A. (1994). *Earthquake Engineering*. Rotterdam, Balkema.
- Rutenberg, A., Jennings, P. C. and Housner, W. G. (1982). The response of veterans hospital building 41, in the San Fernando earthquake. *Earthquake Engineering and Structural Dynamics*, John Wiley and Sons, Ltd., Volumen 10.
- Sabetta, F. and Pugliese, A. (1996). Estimation of response spectra and simulation of nonstationary earthquake ground motions, *Bull. Seism. Soc. Am.*, 86, 2, 337-352.
- Sadigh, K., Chang, C. Y., Egan, J.A., Makdisi, F. and Youngs, R. R. (1997). Attenuation relationships for shallow crustal earthquakes based on California strong motion data. *Seismological Research Letters*, 68, 180-189.
- Safina, S. (2003). *Vulnerabilidad sísmica de edificaciones esenciales. Análisis de su contribución al riesgo sísmico. Tesis Doctoral*. Universidad Politécnica de Cataluña, Barcelona, 271 p.
- Safina, S., Pujades, L. and Roca, A. (2002). Respuesta sísmica del sistema sanitario regional. Aplicación al sistema sanitario de Cataluña. *Memorias del III Coloquio sobre Microzonificación Sísmica*, Caracas, Venezuela.
- Saito, K., Spence, R. J., Going, C., and Markus, M. (2004). Using high-resolution satellite images for post-earthquake building damage assessment: a study following the 26.1.01 Gujarat earthquake. *Earthquake Spectra*. (To be published).

- Samardjieva, E. and Badal, J. (2002). Estimation of the expected number of casualties caused by strong earthquakes. *Bull. Seism. Soc. Am.*, 92, 2310-2322.
- San Mateo County EMS (1998). *Hospital Emergency Incident Command System, San Mateo County Emergency Medical Services Agency*. Redwood City, California.
- Sánchez, F. J., Navarro, M., García, J. M., Enomoto, T. and Vidal, F. (2002). Evaluation of seismic effects on buildings structures using microtremor measurements and simulation response. *Structural Dynamics, Eurodyn2002*, 2, 1003-1008, Balkema.
- Sánchez-Sesma, F. J. (1983). Diffraction of elastic waves by three-dimensional surface irregularities. *Bull. Seism. Soc. Am.*, 73, 1621-1635.
- Sánchez-Sesma, F. J. (1985). Diffraction of elastic SH waves by edges. *Bull. Seism. Soc. Am.*, 75, 1435-1446.
- Sánchez-Sesma, F. J. and Campillo, M. (1991). Diffraction of P, SV and Rayleigh waves by topographic features: a boundary Integral formulation, *Bull. Seism. Soc. Am.*, 81, 2234-2253.
- Sánchez-Sesma, F. J., Campillo, M. and Irikura, K. (1989). A note on the rayleigh hypothesis and the Aki-Larner Method. *Bull. Seism. Soc. Am.*, 79, 1995-1999.
- Sanchez-Silva, M. and Garcia, L. (2001). Earthquake damage assessment based on fuzzy logic and neural network. *Earthquake Spectra*, 17(1), 89-112.
- Sandi, H. and Floricel, I. (1995). Analysis of seismic risk affecting the existing building stock. *10th European Conference on Earthquake Engineering*, 3, 1105-1110.
- SAP, Safety Assessment Program (2003). California Governor's Office of Emergency Services. Internet Site: www.oes.ca.gov. (consulted November 2004)
- Satake, N., Suda, K., Arakawa, T., Sasaki, A. and Tamura, Y. (2003). Damping evaluation using full-scale data of buildings in Japan, *Journal of Structural Engineering, ASCE*, 129(4), 470-477.
- Sato, R., Shinozuka, M. (1991). GIS-based interactive and graphic computer system to evaluate seismic risk on water delivery networks. In: M. A. Cassaro (Editor), *Proceedings, 3rd US Conference on Lifeline Earthquake Engineering*, Los Angeles, California, TCLEE/ASCE, Monograph No. 4, 651-660.
- Sato, T. and Toki, K. (1991). Seismic reliability analysis of large scale lifeline networks. In: M. A. Cassaro (Editor), *Proceedings, 3rd US Conference on Lifeline Earthquake Engineering*, Los Angeles, California, TCLEE/ASCE, Monograph No. 4, 673-682.
- Scawthorn, C. (1992). Lifeline interaction and post- earthquake functionality. *Proceedings, 5th U.S.- Japan Workshop on Earthquake Disaster Prevention for Lifeline Systems*, 441-450.
- Scawthorn, C. (1996). Reliability-based design of water supply systems. In: H. Hamada and T. O'Rourke (Editors), *Proceedings, 6th Japan-U.S Workshop on Earthquake Resistant Design of Lifeline Facilities and Countermeasures Against Soil Liquefaction*, Tokyo, Japan, 711-726.
- Scawthorn, C. (2003). Fire Following Earthquake. In: W. Chen and C. Scawthorn (Editors), *Earthquake Engineering Handbook*, CRC Press, Chapter 29.
- Schiff, A. J. (2003). Electrical Power Systems. In: W.Chen and C. Scawthorn (Editors), *Earthquake Engineering Handbook*, CRC Press, Chapter 25.
- Schiff, A. J. and Tang, A. (1995). Policy and General Technical Issues Related to Mitigating Seismic Effects on Electric Power and Communication Systems. In: A. Schiff and I. Buckle (Editors), *Critical Issues and State-of-the-Art in Lifeline Earthquake Engineering*, Monograph No. 7, TCLEE/ASCE, 1-29.
- Schnabel, P. B., Lysmer, J. and Seed, H. B. (1972). *SHAKE: a Computer Program for Earthquake Response Analysis of Horizontally Layered Sites*. Report EERC 72-12, Earthquake Engineering Research Center, University of California, Berkeley.
- Scholl, R. (1993). Fundamental design issues for supplemental damping applications. *Earthquake Spectra*, 9(3), 627-636.
- Scholz, C. H. (2003). *The Mechanics of Earthquakes and Faulting*. Second edition, corrected 2003, Cambridge University Press, Cambridge, England, 471 p.
- Schwartz, D. and Coppersmith, K. (1984). Fault Behaviour and Characteristic Earthquakes: Examples from the Wasatch and San Andrea Faults. *Journal of Geophysics Research*, 89, 5681-5698.
- SCS, (1996a). *Una red sanitaria de calidad para todos*. Fullletó informatiu del Servei Català de la Salut. D.L. B-1.680-96. Barcelona.
- SCS, (1996b). *La salut, més a prop Barcelona*. Fullletó informatiu del Servei Català de la Salut. D.L. B-41.969-96, Barcelona.
- SEAOC (1995). *Performance based seismic engineering of building*. VISION 2000 Committee. Structural Engineering Association of California, Sacramento.
- Secanell, R., Goula, X., Susagna, T., Flea, J. and Roca, A. (2004). Seismic hazard zonation of Catalonia, Spain, integrating random uncertainties. *Journal of Seismology*, 8, 25-40.

- Seed, H. B. and Idriss, I. M. (1969). Influence of soil conditions on ground motion during earthquakes. *Proceedings American Society of Civil Engineers*, 94, SM 1, 99-137.
- Seed, R. B., Dickenson, S.E. and Idriss, I.M., (1991). Principal geotechnical aspects of the 1989 Loma Prieta earthquake. *Soils and Foundations*, 31(1), 1-26.
- Seligson, H. A. and Shoaf, K. I. (2003). Human Impacts of Earthquakes. In: W.Chen and C. Scawthorn (Editors), *Earthquake Engineering Handbook*, CRC Press, Chapter 28.
- Semblat, J. F., Duval, A. M. and Dangla, P. (2000). Numerical analysis of seismic wave amplification in Nice (France) and comparisons with experiments, *Soil Dynamics and Earthquake Engineering*, 19, 5, 347-362,
- Semblat, J. F., Kham, M., Guéguen, P. and Bard, P.-Y. (2004). Could "site-city interaction" modify site effects in urban areas ? *13th World Conference on Earthquake Engineering*, Vancouver, Paper # 1978.
- Seo, K., Samano, T., Yamanaka, H., Hao, X., Koyama, S., Takeuchi, M., Fujioka, K., Kishino, Y., Kawano, K., Asano, K., Nakajima, N., Murai, M., Mualchin, L. and Hisada, Y. (1991). Microtremor measurements in the San Francisco Bay area. Part 1: Fundamental characteristics of microtremors. *Proceedings, 4th Conf. on Seism. Zonation*; Eng. Res. Inst., Stanford, California, 2, 417-424.
- Serva, L. (1993). An analysis of the major regulatory guides for NPP seismic design (a guideline for high risk facilities). *Energia Nucleare, Anno 10, No. 2*, May-August, 1993, 77-96, Roma.
- Serva, L., Blumetti, A. M., Guerrieri, L. and Michetti, A. M. (2000). The Apenninic intramountain basins: the results of repeated strong earthquakes over a geological time interval. *Mem. Soc. Geol. It. Atti del Convegno: Evoluzione geologica e geodinamica dell'Appennino – in memoria del Prof. Giampaolo PIALLI*, Foligno, February 16-18, 2000.
- Sevaduray, G. (2003). Hazardous Materials. In *Earthquake Engineering Handbook*. W.Chen and C. Scawthorn (Editors), CRC Press, Chapter 30.
- SGP (1988). *Carta Geotécnica do Concelho de Lisboa à Escala 1:10000*. Serviço Geológico de Portugal, Lisboa.
- Shimizu, Y. and Yamazaki, F. (1998). Real-time city gas network damage estimation system-SIGNAL. *11th European Conference on Earthquake Engineering*, Balkema, Rotterdam.
- Shin, T. C. and Teng, T. L. (2001). An overview of the 1999 Chi-Chi, Taiwan, earthquake. *Bull. Seism. Soc. Am.*, 91, 895-913.
- Shing, T. C., Tasi, Y. B., Yeh, Y. T., Lin, C. C. and Wu, Y. M. (2003). Strong motion instrumentation programs in Taiwan. In: Jennings, P., Kisslinger, C., Kanamori, H. and Lee, W. (Editors), *International Handbook of Earthquake and Engineering Seismology*, Academic Press, 1057-1062.
- Shinozuka, M. (Editor) (1995). *The Hanshin-Awaji Earthquake of January 17, 1995: Performance of Lifelines*. Technical Report NCEER-95-0015, State University of New York, Buffalo.
- Shinozuka, M. and Tanaka, S. (1996). Effects of lifeline interaction under seismic conditions. *11th World Conference on Earthquake Engineering*, Paper No. 348.
- Shinozuka, M., Feng, M. Q., Kim, H.-K., Uzawa, T. and Ueda, T. (2003). *Statistical Analysis of Fragility Curves*. Technical Report MCEER-03-0002, State University of New York, Buffalo.
- Shinozuka, M., Hwang, H. and Tanaka, S. (1993). GIS - Based assessment of the seismic performance of water delivery system. In: K. Kawashima, H. Sugita and T. Nakajima (Editors), *Proceedings, 5th US-Japan Workshop on Earthquake Disaster Prevention for Lifeline Systems*, PWRI 3198, Public Works Research Institute, Tsukuba, Japan, 233-249.
- Shinozuka, M., Rose, A. and Eguchi, R. (Editors) (1998). *Engineering and Socioeconomic Impacts of Earthquakes: An analysis of Electricity Lifeline Disruptions in the New Madrid Area*. Monograph MCEER-98-MN02, State University of New York, Buffalo.
- Shoaf, K. I., Nguyen, L. H., Sareen, H. R. and Bourque, L. B. (1998). Injuries as a Result of California Earthquakes in the past Decade. *Disasters* 22(3), 218-235.
- Shome, N., Cornell, C.A., Bazzurro, P. and Carballo, J. E. (1998). Earthquakes, records, and nonlinear responses *Earthquake Spectra* 14(3), 469-500
- Sinclairian, M., and Oliveira, C. S. (2002). A 2-D Sensitivity study of the dynamic behavior of a Volcanic Hill in the Azores islands: comparison with 1-D and 3-D Models. In: Roca, A. and Oliveira, C.S. (Editors) 2002, *Earthquake Microzonning. Pageoph Topical Volume, Birkhäuser, Berlin*, 158, 2431-2450.
- Singhal, A. and Kiremidjian, A. S. (1996). Method for probabilistic evaluation of seismic structural damage, *Journal of Structural Engineering ASCE*, 122(12), 1459-1467.
- Sokolov, Y. V., Loh, C. H. and Wen, K. L. (2001). Empirical models for site- and region-dependent ground motion parameters in the Taipei Area: A Unified Approach. *Earthquake Spectra*, 17 (2), 313-332.

- Somerville, P. and Y.Moriwaki (2003). Seismic Hazards and Risk Assessment in Engineering Practice. In W.Lee, H. Kanamori, P. Jennings and C. Kisslinger (Editors), *International Handbook of Earthquake and Engineering Seismology*, Academic Press, 1065-1080.
- Sousa, M. L. (1996). *Modelos Probabilistas para a Avaliação da Casualidade Sísmica em Portugal Continental*. Master Thesis, IST, Universidade Técnica de Lisboa.
- Sousa, M. L. (2004). *Risco sísmico em Portugal Continental*. PhD thesis, IST, Lisboa, in press.
- Sousa, M. L. and Oliveira, C. S., (1997). Hazard Mapping Based on Macroseismic Data Considering the Influence of Geological Conditions. *Natural Hazards*, 14, 207-225.
- Spence, R. (2004). Risk and regulation: can better laws prevent worse natural disasters. *Special Issue on Managing the Risks from Natural hazards*, Building Research and Information.
- Spence, R., Bommer, J., del Re, D., Aydinoglu, N. and Tabuchi, S. (2003). Comparing loss estimation with observed damage: a Study of the 1999 Kocaeli Earthquake in Turkey. *Bulletin of Earthquake Engineering I*, 83-113.
- Spence, R. J. S., Coburn, A. W. and Pomonis, A. (1992). Correlation of ground motion with building damage: the definition of a new damage-based seismic intensity scale. *10th World Conference On Earthquake Engineering*, Balkema, Rotterdam, 551-556.
- Spudich, P., Hellweg, M. and Lee, W.H.K. (1996). Directional topographic site response at Tarzana observed in aftershocks of the 1994 Northridge, California, Earthquake: Implications for mainshock motions. *Bull. Seism. Soc. Am.*, 86, 139-208.
- SSHAC (1995). *Recommendations for Probabilistic Seismic Hazard Analysis: Guidance on uncertainty and use of experts*. SSHAC, Senior Seismic Hazard Analysis Committee. (NUREG/CR-6372, 1995).
- SSI (2003). <http://www.serviziosismico.it> (consulted November 2004).
- Staeclin, W. (1997). Seismic design and performance of nonstructural components in hospitals. *Proceedings of Seminar on Seismic Design, Retrofit, and Performance of Nonstructural Components*, ATC-29-1, 469-473.
- Steidl, J. H., Tumarkin, A.G. and Archuleta, R. J. (1996). What is a reference site?. *Bull. Seism. Soc. Am.*, 86, 1733-1748.
- Streeter, V.L., Wylie, E.B., Benjamin, E. and Richart, F.E. (1974). Soil motion computations by characteristics method. *J. Geotech. Eng. Div. Amer. Soc. Civil Engineers* 100, GT3, 247-263
- Su, F., Anderson, G., Ni, S.D. and Zeng, Y. (1998). Effect of site amplification and basin response on strong motion in Las Vegas, Nevada. *Earthquake Spectra*, 14 (2), 357-376
- Suhadolc, P., Panza, G.F., (1985). Some applications of seismogram synthesis through the summation of modes of Rayleigh waves. *Journal of Geophysics*, 58, 183-188.
- Susagna, T. and Goula, X. (1999). *Catàleg de Sísmicitat*. Vol I Atlas Sísmic de Catalunya, Institut Cartogràfic de Catalunya, 436 p.
- Susagna, T., Goula, X. and Roca, A. (1996). Conception of a macroseismic catalogue for Catalonia (Spain). *Annali di Geofisica*, 39, 5, 1049-1054.
- Susagna, T., Goula, X. and Roca, A. (2001). A new macroseismic catalogue for Catalonia, in T. Glade, P. Albini and F. Francés (editors), *The Use of Historical Data in Natural Hazard Assessments*, Kluwer Academic Publishers, 71-79.
- Takada, S., Sub, J.S., Ogawa, Y. and Oka, S. (1991). An expert system for diagnosis of earthquake proof for underground lifelines. In: M. A. Cassaro (Editor), *Proceedings, 3rd US Conference on Lifeline Earthquake Engineering*, Los Angeles, California, TCLEE/ASCE, Monograph No. 4, 737-746.
- Tanaka H., Iwai, A., Oda, J., Kuwagata, Y., Matsuoka, T. Shimazu, T. and T. Yoshioka, Y. (1998). Overview of evacuation and transport of patients following the 1996 Hanshin-Awaji Earthquake. *Journal of Emergency Medicine*, 16(3), 439-44.
- Tantala, M.W., Dargush, A., Deodatis, G., Jacob, K., Nordenson, G.J.P., O'Brien, D. and Swiren, B. (2002). Earthquake loss estimation for the New York City Area. *7th National Conference on Earthquake Engineering*, Boston, MA, July 21-25.
- Teleb-Agha, A. and Whitman, R.V. (1975). *Seismic Risk Analysis of Discrete Systems*. Report no. 23, MIT-CE-R75-48, Order 523. Massachusetts Institute of Technology.
- Teng, T. L., Wu, Y. M., Shin, T. C., Tsai, Y. B. and Lee, W. H. K. (1997). One minute after: strong-motion map, effective epicenter, and effective magnitude. *Bull. Seism. Soc. Am.*, 87, 1209-1219.
- Tertulliani, A. (2000). Qualitative effects of local geology on damage pattern. *Bull. Seism. Soc. Am.*, 90(6), 1543-1548.
- Thenhaus, P. C. and Campbell, K. W. (2003). Seismic hazard analysis. In *Earthquake Engineering Handbook*. W.Chen and C. Scawthorn (Editors), CRC Press, Chapter 8.
- Theodulidis, N. and Bard, P.Y. (1995). Horizontal to vertical spectral ratio and geological conditions: an analysis of strong motion data from Greece and Taiwan (SMART1). *Soil Dyn. and Earthq. Engng*, 14, 177-197.

- Thompson, W.T. (1950). Transmission of elastic waves through a stratified solid medium. *J. Appl. Phys.*, 21, 89-93.
- Tiedemann, H. (1992). *Earthquakes and Volcanic Eruptions: A Handbook on Risk Assessment*. Swiss Re. Editor. Zurich.
- Topozada, R. T., Bennett, J. H., Borchardt, G., Saul, R. and Davis, J. F. (1988). *Planning sceanario for a major earthquake on the Newport-Inglewood fault zone*. Special Publication No.102, California Dept. of Conservation-Division of Mines and Geology, Sacramento, CA.
- Topozada, R. T., Borchardt, G. and Hallstrom, C. L. (1993). *Planning sceanario for a major earthquake on the San Jacinto Fault in the San Bernardino Area*, Special Publication No.102, California Dept. of Conservation-Division of Mines and Geology, Sacramento, CA.
- Topozada, R. T., Borchardt, G., Hallstrom, C. L. and Youngs, L. G. (1994). *Planning sceanario for a major earthquake on the Rodgers creek fault in the Northern San Francisco bay area*, Special Publication No.112, California Dept. of Conservation-Division of Mines and Geology, Sacramento, CA.
- Toprak, S. (1998). *Earthquake Effects on Buried Lifeline Systems*, PhD Thesis, Cornell University.
- Tralli, D. M. (2000). *Assessment of advanced technologies for loss estimation*. MCEER, Buffalo Univeristy, Ney Jersey.
- Trifunac, M. D. and Brady, A. G. (1975). On the correlation of seismic intensity scales with the peaks of recorded strong ground motion. *Bull. Seism. Soc. Am.*, 65.
- Trifunac, M. D., Ivanović, S. S. and Todorovska, M. I. (2001). Apparent periods of a building: II Time-Fourier analysis. *Journal of Structural Engineering, ASCE*, 127(5), 527-537.
- Trifunac, M.D. and Lee, V.W. (1989). Empirical Models for Scalling Pseudo-relative Velocity Spectra of Strong Earthquake Accelerations in Terms of Magnitude, Distance an Site Intensity and Recording Site Conditions. *Soil Dynamics and Earthquake Engineering*, 8, 126-144.
- Tsai Y.-B. and Lee C.-P. (2004). Strong Motion Instrumentation Programs in Taiwan - Past and Present -, *International Workshop on Future Directions in Instrumentation for Strong Motion and Engineering Seismology- NATO Meeting*, May 17-21, 2004, Kusadasi, Turkey.
- Tsai, Y. B. and Wu, Y. M. (1997). Quick determination of magnitude and intensity for seismic early warning. *29th IASPEI meeting, Thessaloniki, Greece*.
- Tsogka, C. and Wirgin, A. (2003). Seismic response of a set of blocks partially embedded in soft soil. *C. R. Mécanique*, 331(3), 217-224.
- Tsurugi, M., Tai, M., Kowada, A., Tatsumi, Y. and Irikura, K., (2000). Estimation of empirical site amplification effects using observed records. *12th World Conference on Earthquake Engineering*, CD-Rom, 1243.
- Turcotte, D. (1997). *Fractal and Chaos in Geology and Geophysics*. 2nd edition, Cambridge University Press.
- UBC-97 (1997) *Structural Engineering Design Provisions*. Uniform Building Code (UBC). International Conference of Building Officials, Whittier, California (USA).
- UNDP/UNIDO (1985). *Post Earthquake damage Evaluation and Strength Assessment of Buildings under Seismic Condition*. UNDP, Project RER/79/015, 4.Vienna.
- UNESCO (1978). *The Assessment and Mitigation of Earthquake Risk*. NICI, Ghent.
- USAID (2004) Iran Earthquake Fact Sheet #10, <http://www.usaid.gov/> (consulted November 2004)
- USNRC (1978). *Seismic and geologic siting criteria for nuclear power plants*. Appendix A of 10 CFR 100, Wahington D. C., U. S. A.
- Vacareanu, R., Lungu, D., Aldea, A. and Arion, C. (2004). *WP7 Report Seismic Risk Scenarios Handbook*. RISK-UE project: An advanced approach to earthquake risk scenarios with applications to different European towns. Contract No. EVK4-CT-2000-00014. 50 p.
- Van Puymbroeck, N., Michel, R., Binet, R., Avouac, J. P. and Taboury, J. (2000). Measuring earthquakes from optical satellite images. *Applied Optics*, 39, No. 20, Optical Society of America.
- Vanzi, I. (1996). Seismic reliability of electric power networks: methodology and application. *Structural Safety, Elsevier Science Ltd*, 18, n.4, 311-327.
- Vanzi, I. (2000). Structural upgrading strategy for electric power networks under seismic action. *Earthquake Engineering and Structural Dynamics*, 29, (7), 1053-1073.
- Varum, H., (1995). *Modelo numérico para a análise sísmica de pórticos planos de betão armado*. MSc Thesis on Civil Engineering Structures, Fac. Eng. Univ. Porto, Portugal.
- Varum, H., (2003). *Seismic assessment, strengthening and repair of existing buildings*. PhD Thesis, University of Aveiro, Portugal.
- Vieira, V., C. S. Oliveira, B. C. Costa (2000). A methodology to evaluate the strategic importance of bridges and tunnels considering seismic vulnerability: application to Lisbon. *Proceedings, 2nd EuroConference on Global Change and Catastrophe Risk Management, Earthquake Risks in Europe*, IIASA Luxemburg, Austria.

- Vittori, E., Deiana, G., Esposito, E., Ferrel, L., Marchegiani, L., Mastrolorenzo, G., Michetti, A. M., Porfido, S., Serva, L., Simonelli, A. L. and Tondi, E. (2000). Ground effects and surface faulting in the September-October 1997, Umbria-Marche (Central Italy) seismic sequence. *Journal of Geodynamics*, 29.
- Wald, D. J. and Graves, R. W. (1998). The response of the Los Angeles basin, California, *Bull. Seism. Soc. Am.*, 88(2),337-356.
- Wald, D. J., Heaton, T. H. and Hudnut, K. W., (1996). The slip history of the 1994 Northridge, California, earthquake determined from strong-motion, teleseismic, GPS, and levelling data. *Bull. Seism. Soc. Am.*, 86, S49-S70.
- Walker, G. (2000). Earthquake Engineering and Insurance: Past Present and Future. *12th World Conference on Earthquake Engineering*, Auckland New Zealand, Paper 1472.
- Wang, L., Ishibashi, I. and Wang, J. (1991). Inventory and seismic loss estimation of portland water/ sewer systems-GIS application to buried pipelines. In: M. A. Cassaro (Editor), *Proceedings, 3rd US Conference on Lifeline Earthquake Engineering*, Los Angeles, California, TCLEE/ASCE, Monograph No. 4, 490-499.
- Wang, L., Li, H. and Ishibashi, I. (1995). Prioritization for rehabilitation of buried lifelines. In: M.J. O'Rourke (Editor), *Proceedings, 4th U.S Conference on Lifeline Earthquake Engineering*, San Francisco California, TCLEE/ASCE, Monograph No.6, 588-595.
- Wang, Z., Woolery, E. W., Shi, B. and Kiefer, J. D. (2003). Communicating with Uncertainty: A Critical Issue with probabilistic seismic hazard analysis. *EOS Transactions, American Geophysical Union*, 84 (46), 501, 506, 508.
- Wells, D. L., and Coppersmith, K. J. (1994). New Empirical relationships among magnitude, rupture length, rupture width, rupture area and surface displacement. *Bull. Seism. Soc. Am.*, 84, 974-1002.
- Wen, K. L., Peng, H. T. and Lin, L. F. (1995). Basin effects analysis from a dense strong motion observation network. *Earthquake Engineering and Structural Dynamics*, 24, 1069-1083
- Wenzel, F., Lungu, D. and Novak O. (Editors) (1998). *Vrancea Earthquakes: Tectonics, Hazard and Risk Mitigation*, selected papers of the First International Workshop on Vrancea Earthquakes, Bucharest, November 1-4, 1997, Kluwer Academic Publishers, Dordrecht, Netherlands, 374 p.
- Wenzel, F., Baur, M., Fiedrich, F., Ionescu, C. and Oncescu, M. C. (2001). Potential of Earthquake Early Warning Systems. *Natural Hazards* 23, 407-416.
- Wenzel, F., Oncescu, M. C., Baur, M. and Fiedrich, F. (1999). An early warning system for Bucharest. *Seism. Res. Lett.*, 70, 2, 161-169.
- Werner, S. D., Taylor, C. E., Moore, J. E., Walton, J. S. and Cho, S. (2000). *A risk-based methodology for assessing the seismic performance of highway systems*. Technical Report MCEER-00-0014, State University of New York, Buffalo.
- WGCEP-Working Group on California Earthquake Probabilities (1988). *Probabilities of large earthquakes occurring in California on San Andreas Fault*, USGS Open-File Report, 88-393.
- WGCEP-Working Group on California Earthquake Probabilities (1995). Seismic Hazards in Southern California: Probable Earthquakes, 1994-2024. *Bull. Seism. Soc. Am.*, 85, 379-439.
- WGCEP-Working Group on California Earthquake Probabilities (2002). *Earthquake probabilities in the San Francisco Bay Region, 2000-2030*. USGS Circular 1189.
- Whitman, R. V. and Lagorio, H. J. (1999). The FEMA-NIBS methodology for earthquake loss estimation. (<http://www.fema.gov/hazus/hazus4a.htm>). (consulted November 2004).
- Whitman, R. V., Reed J. W. and Hong S. T. (1974). Earthquake damage probability matrices. *5th European Conference on Earthquake Engineering*, Rome 1974, 2531.
- Wilson, R. C. and Keefer, D. K. (1985). *Predicting areal limits of earthquake induced landsliding: in evaluating earthquake hazards in the Los Angeles region*. 317-346, USGS Professional Paper No1360, US Government Printing Office, Washington.
- Wirgin, A., and Bard, P.-Y. (1996). Effects of buildings on the duration and amplitude of ground motion in Mexico City. *Bull. Seism. Soc. Am.*, 86, 914-920.
- Wu, Y. M. and Teng, T. L. (2002). A virtual sub-network approach to earthquake early warning. *Bull. Seism. Soc. Am.*, 92, 2008-2018.
- Wu, Y. M., Chung, J. K., Shin, T. C., Hsiao, N. C., Tsai, Y. B., Lee, W. H. K. and Teng, T. L. (1999). Development of an integrated seismic early warning system in Taiwan - case for the Hualien area earthquakes. *TAO* 10, 719-736.
- Wu, Y. M., Shin, T. C. and Tsai, Y. B. (1998). Quick and reliable determination of magnitude for seismic early warning. *Bull. Seism. Soc. Am.*, 88, 1254-1259.
- Yamazaki, F. (2001). Applications of remote sensing and GIS for damage assessment. *Proceedings, Joint Workshop on Urban Safety Engineering*, Asian Institute of Technology, Bangkok.

- Yamazaki, F., Hamada, T., Motoyama, H. Yamauchi, H. (1999). Earthquake damage assessment of expressway bridges in Japan. In: W. Elliott and P. McDonough (Editors), *Proceedings, 6th US Conference on Lifeline Earthquake Engineering*, TCLEE/ASCE, Monograph No.16, 361-370.
- Yamazaki, F. and Murao, O. (2000). Vulnerability functions for Japanese buildings based on damage data from the 1995 Kobe earthquake, Implication of Recent Earthquakes on Seismic Risk. *Series on Innovation and Construction, 2*, Imperial College Press, 91-102.
- Yang, J.C.S., Aggour, M.S. and Al-sanad, H. (1982). Application of the Random Decrement Technique in the determination of damping of soils. *7th European Conference on Earthquake Engineering*, Athens, Greece, September 1982.
- Yang, J.C.S. and Caldwell, D. W. (1976). Measurement of damping and the detection of damages in structures by the Random Decrement Technique. *46th Shock and Vibration Bulletin*, 129-136.
- Yang, J.C.S. and Dagalakis, N.G. (1980). Detection of incipient failure in structure using random decrement technique. *Proceeding, Fall Meeting of Society of Experimental Stress Analysis (SESA)*, Ft Lauderdale, Florida, 43 p.
- Youd, T. L. (1991). Mapping of earthquake-induced liquefaction for seismic zonation. *Proceedings 4th Int. Conf. On Seismic Zonation*, EERI, Stanford, CA.
- Youd, T. L., Idriss, I. M., Andrus, R.D., Arango, I., Castro, G., Christian, J.T., Dobry, R., Finn, W.D.L., Harder, L.F.Jr., Hynes, M.E., Ishihara, K., Koester, J.P., Liao, S.S.C., Marcuson, W.F.III., Martin, G.R., Mitchell, J.K., Moriwaki, Y., Power, M.S., Robertson, P.K., Seed, R.B. and Stokoe, K.H.II. (2001). Liquefaction resistance of soils: summary Report from the 1996 NCEER and 1998 NCEER/NSF Workshops on evaluation of liquefaction resistance of Soils, *Journal of Geotechnical Engineering, ASCE, 127(10)*, 817-833.
- Youd, T. L. and Perkins, D. M. (1978). Mapping of Liquefaction Induced Ground Failure Potential. *Journal of Geotechnical Engineering, ASCE, 104*, No.4, 433-446.
- Youd, L. T., Tinsley, J. C., Perkins, D. M., King, E. J. and Preston, R. F. (1979). Liquefaction Potential Map of San Fernando, California. *Seismic Zonation in the San Francisco Bay Region*, USGS Circular No. 807.
- Zeng, Y., Anderson, J. G. and Yu, G. (1994). A composite source model for computing realistic synthetic strong ground motions. *J. Res. Lett.*, 21, 725-728.
- Zhang, B., Papageorgiou, A. S. and Tassoulas, J. L. (1998). A hybrid numerical technique, combining the finite-element and boundary-element methods, for modelling the 3D response of 2D scatterers. *Bull. Seism. Soc. Am.*, 88, 1036-1050.
- Zhao, C. and Valliappan, S. (1993). Seismic wave scattering effects under different canyon topographic and geological conditions. *Soil Dynamics and Earthquake Engineering, 12*, 129-143.
- Zuccaro, G. and Papa, F. (2002a). Method of seismic vulnerability and exposure assessment at national scale – the Italian case. *12th European Conference on Earthquake Engineering*, London, paper 698.
- Zuccaro, G. and Papa, F. (2002b). *Multimedial Handbook for Seismic Damage Evaluation and Post-event Macroseismic Assessment*. 50th Anniversary of the European Seismological Commission, XXVIII General Assembly, Genoa, Italy.
- Zuccaro, G., Papa, F. and Baratta, A. (2000). Revision of the National Map of Residential Building and Seismic Vulnerability. In: Bernardini, A. (Editor), *La Vulnerabilità degli Edifici: Valutazione a Scala Nazionale della Vulnerabilità Sismica degli Edifici Ordinari*, CNR-GNDT, Rome.

FIGURES ACKNOWLEDGEMENTS

Figure #	Courtesy of
3.6	Seismological Society of America
3.7	Seismological Society of America
4.3	Elsevier
5.5	Seismological Society of America
5.14	Seismological Society of America
9.11	John Wiley & Sons, Ltd.
9.12	John Wiley & Sons, Ltd.
14.1	Seismological Society of America
19.1	John Wiley & Sons, Ltd.
19.2	John Wiley & Sons, Ltd.
19.4 to 19.10	John Wiley & Sons, Ltd.

GEOTECHNICAL, GEOLOGICAL AND EARTHQUAKE ENGINEERING

1. A. Ansal (ed.): *Recent Advances in Earthquake Geotechnical Engineering and Microzonation*. 2004. ISBN: 1-4020-1827-4
2. C.S. Oliveira, A. Roca, X. Goula (eds.): *Assessing and Managing Earthquake Risk*. Geoscientific and Engineering Knowledge for Earthquake Risk Mitigation: developments, tools, techniques. 2006, 2008. ISBN: 978-1-4020-3524-1
3. To be published.
4. To be published.
5. To be published.
6. K.D. Pitilakis (ed.): *Earthquake Geotechnical Engineering*. 4th International Conference on Earthquake Geotechnical Engineering - Invited Lectures. 2007 ISBN: 978-1-4020-5892-9